Demonstration of Innovative Applications of Technology for Cost Reductions to the CT-121 FGD Process

DOE ICCT PROJECT DE-FC22-90PC89650

FINAL REPORT

Volume 6-A of 6: Appendices

Project Sponsors

Southern Company
US Department of Energy
Electric Power Research Institute

Issue Date: January 1997

Demonstration of Innovative Applications of Technology for Cost Reductions to the CT-121 FGD Process

Volume 6-A of 6: Appendices

Final Report, January 1997

Contents

"Design and Development of the Liquid Collectors for the 100 MW CT-121 FGD Duct and Stack at Plant Yates, Unit 1"
DynaFlow Systems

"Particulate Sampling of Chiyoda CT-121 Jet Bubbling Reactor Georgia Power Company Plant Yates Unit 1 - ESP Operational Test Phase"
Southern Research Institute

"Particulate Sampling of Chiyoda CT-121 Jet Bubbling Reactor Georgia Power Company Plant Yates Unit 1 - Increased Mass Loading Test Phase"
Southern Research Institute

"Particulate Testing Around the Yates CT-121 Scrubber, While Simulating a Marginally Performing ESP"
Radian Corporation

Project Manager

David P. Burford
Southern Company
Southern Company Services, Inc.
44 Inverness Center Parkway
Suite 230
Birmingham, Alabama 35242

Project Sponsors

Southern Company
US Department of Energy
Electric Power Research Institute

"Design and Development of the Liquid Collectors for the 100 MW CT-121 FGD Duct and Stack at Plant Yates, Unit 1"

DynaFlow Systems

DRAFT

DynaFlow Systems

A Division of Acentech Incorporated

DESIGN AND DEVELOPMENT OF THE LIQUID COLLECTORS FOR THE 100 MW CT-121 FGD DUCT AND STACK AT PLANT YATES, UNIT 1

DynaFlow Systems, Project No. SCS-1
DynaFlow Systems, Report No. 2504
Southern Company Services Contract C-90-000292

Submitted to:

Southern Company Services
P.O. Box 2625
Birmingham, AL 35202

Attn: Mr. David Burford

Prepared by:

Gerald B. Gilbert
Lewis A. Maroti

November 1996

Submitted by:

DynaFlow System Inc.
Div. of Acentech Incorporated
99 Erie Street
Cambridge, Massachusetts 02139

Telephone: (617) 499-8030

DESIGN AND DEVELOPMENT OF THE LIQUID COLLECTORS FOR THE 100 MW CT-121 FGD DUCT AND STACK AT PLANT YATES, UNIT 1

DynaFlow Systems, Project No. SCS-1
DynaFlow Systems, Report No. 2504
Southern Company Services Contract C-90-000292

Submitted to:

Southern Company Services
P.O. Box 2625
Birmingham, AL 35202

Attn: Mr. David Burford

Prepared by:

Gerald B. Gilbert
Lewis A. Maroti

November 1996

Submitted by:

DynaFlow System Inc.
Div. of Acentech Incorporated
99 Erie Street
Cambridge, Massachusetts 02139

Telephone: (617) 499-8030

TABLE OF CONTENTS

TABLE OF CONTENTS (Continued)

LIST OF FIGURES

LIST OF FIGURES (Continued)

LIST OF TABLES

Section 1

INTRODUCTION AND OBJECTIVES

Under a DOE Clean Coal II Project, Southern Company Services is installing a 100 MW Chiyoda Thoroughbred 121 Flue Gas Desulfurization Demonstration Unit at the Yates Plant of Georgia Power Company, Unit 1. The Chiyoda Jet Bubbling Reactor will be connected to a horizontal gas flow two stage mist eliminator and a fiberglass stack supported by an open steel girder support tower. The outlet ducts and stack liner will be operated wet without reheat of the flue gas. The purpose of the program at DynaFlow Systems, described in this report, is to develop a liquid collector and drainage system for the wet duct and stack to minimize the potential for stack liquid droplet discharge when the scrubber is operating.

The objectives of the program were the following:

(1) Develop a velocity profile into the mist eliminator with a RMS flow uniformity of no larger than 0.25.

(2) Develop liquid collectors for the duct and stack downstream of the mist eliminator that will collect and drain liquid from the walls to prevent reentrainment and stack liquid droplet discharge large enough in diameter to reach ground level.

(3) Measure the duct and stack system pressure loss with and without required liquid collectors.

The results of the experimental and analytical work to satisfy these objectives are presented in the sections that follow, including the recommendation of geometry for internal vanes, liquid collectors and drains that must be installed in the field unit to satisfy the objectives of the study.

The gas flow patterns and liquid flow patterns without and with liquid collectors in the model were recorded and edited with voice comments on a VHS video tape. Appendix A1 gives a list of titles for the video recording. Five copies of the video tapes were sent with the design drawings of the liquid collectors for construction.

The original duct and stack designs were reviewed to assure that the geometry is suitable for wet operation. Appendix A2 gives the brief evaluation report prepared before the flow modeling work.

The duct design leading from the main plant to the JBR has also been reviewed for fluid flow considerations. The comments and the report furnished at the beginning of this project are reproduced in Appendix A3.

The field installation of the liquid collectors was inspected near completion while the scaffolding was still in place so the changes and corrections found necessary were completed prior to start up. The Unit 1 liquid collection system has also been inspected after several months of operation to define how well the liquid collectors are operating and to assess the expected long term performance.

Section 2

EXPERIMENTAL TEST SYSTEM

The model to satisfy the objectives of the study must be designed and operated to simulate gas flow patterns and wet operation.

2.1 Modeling Considerations and Criteria

To properly model the behavior of gas and liquid in a power plant duct system, geometric similarity, the important ratios of fluid dynamic forces acting on the gas, and the ratio of forces acting on liquid droplets and films must be maintained the same between the model and field units. Geometry similarity is maintained by using a constant geometric scale factor (SF = 8.91 for this project) to convert most field dimensions into model dimensions. The gas flow and liquid behavior modeling criteria are discussed in the subsections that follow.

2.1.1 Gas Flow

For similar gas flow characteristics in a duct system, the model must operate in the same flow regime (laminar or turbulent) as the field unit though not necessarily at the same Reynolds number. The flow Reynolds number (Re), which is the ratio of inertia to viscous forces acting on the gas, is defined as:

1. $Re = \rho V D_h / \mu$

where: ρ = gas density (lb_m/ft^3);
V = gas velocity (ft.s);
D_h = hydraulic diameter (ft); and
μ = absolute viscosity (lb_m/ft.s).

The field value of Reynolds number in the stack liner just above the top of the breeching duct is 3.3×10^6. The equivalent model value is 4.5×10^5. For internal flow with Re greater than 2×10^4, the inertia forces dominate, the flow is turbulent, and the flow behavior (flow patterns, velocity profiles, pressure loss coefficient) is not influenced significantly by the Reynolds number. Therefore, model and field gas flow similarity is maintained.

The velocity level in the main ducts can be set at a range of values as long as the above criteria are met. The usual model velocity values used are either matching the field velocity or the field velocity head.

Because of the gas dynamic and geometric similarity, the total pressure loss coefficient (C_L) can be assumed identical for the model and field unit:

where: C_L = delta P_T/VH (dimensionless);
delta P_T = total pressure loss (inches of water); and
VH = gas velocity head (inches of water).

2.1.2 Modeling Criteria for Wet Operation

The gas /liquid flow in power plant duct systems involves different types of two-phase flow patterns which must be observed somewhat independently of each other. These are: (1) droplet trajectories and deposition in the turns and vaned sections of the system; (2) liquid motion along the walls and floor of the duct work due to the gas shear forces and gravitational forces; (3) reentrainment of the deposited liquid from the walls and floor of the duct work and from the internal duct components (struts, mounting plates, turning vanes, dampers, and thermal expansion joints); (4) liquid collection at the liquid collector; and (5) draining patterns at and through gravity drains placed at selected locations.

Gas-Liquid Ratio

The maximum value of liquid load, or ratio of liquid volume flow rate to gas volume flow rate (Q_L/Q_g) expected due to mist eliminator carryover, is selected for gas-liquid operation of the model. This liquid load is used for model testing purposes to observe gas-liquid flow behavior and to size the liquid collectors for worst case conditions. The maximum liquid load in the horizontal duct expected is 0.11 gr/acf or about 0.77 gpm with the design gas flow rate from the absorber of 406,400 acfm in the field. The maximum liquid load in the vertical liner is 4.0 gpm.

Liquid Entrainment

An important aspect of gas liquid flow modeling is to simulate the gas-shear driven liquid flow and reentrainment in the model. These flow mechanisms are controlled by the following three major forces:

1. Gas Shear Forces

$$F_f \alpha f \frac{\rho_g V_g^2 A}{2g_o}$$

where: ρ_g = gas density (lb_m/ft^3);
V_g = gas velocity (fps);
A = surface area (ft^2);
f = friction coefficient and
g_o = 32.2 ($lb_m ft/lb_f sec^2$).

2. Gravitational Forces

$$F_g = \frac{At\rho_L g}{g_o}$$

where:
- A = surface of liquid layer (ft^2)
- t = thickness of liquid layer (ft);
- ρ_L = liquid density (lb_m/ft^3);
- g = 32.2 (ft/sec^2); and
- g_o = 32.2 ($lb_m ft/lb_f sec^2$).

3. Surface Tension Forces

$$F_s = d\sigma$$

where:
- d = drop diameter (ft); and
- σ = liquid surface tension (lb_f/ft).

To simulate the effect caused by gas drag on liquid flowing on the duct walls, where gravitational forces are the same between model and field unit, the field value of gas velocity head is duplicated in the model. That is, $VH_M = VH_P$. The field value in the stack (cross-section K, Figure 2-2) is 0.51 inches of water at the 100% design flow condition.

Droplet Trajectory

Another important factor that can influence liquid deposition and collection is liquid droplet trajectory.

To simulate the ratio of centrifugal accelerational force to gravity force of a droplet suspended in the gas and moving through a bend of radius R, we set:

$$V_M = V_F \left(\frac{R_M}{R_F}\right)^{1/2} = V_F / SF^{1/2}$$

This equation and droplet drag relationships were used to set the model flow condition to define the liquid deposition patterns occurring in the field on turning vanes and curved duct surfaces or where the gas flow is swirling.

2.2 Field and Model Operating Conditions

Table 2-1 summarizes the field and model flow conditions that meet the modeling criteria in Section 2.1. The model velocity and pressure loss tests were conducted by matching the field velocity. The reentrainment tests were conducted by matching the gas velocity head over a range of conditions. The 100% load condition is the primary test condition for the model study.

The flow rate and gas pressures and temperatures for the 100% load operating conditions are listed below and on Table 2-1.

	100% Load One Absorber
Volume flow rate (acfm)	406,400
Gas temperature, °F	126
Gas density (lb_m/ft^3)	0.0653
RH (saturated)	100%

Table 2-2 presents flow rate, velocity, and velocity head values at five duct locations identified on Figure 2-2 for the following operating conditions:

1. field unit - 100% load;

2. model unit with model velocity equal to field velocity;

3. model unit with model velocity head equal to field velocity head; and

4. model unit with model velocity equal to field velocity divided by the square root of the scale factor.

Item 2 is the approximate condition at which the model was run for model tests to measure velocity profiles and pressure loss. Item 3 is the approximate condition at which the model was run to evaluate liquid film behavior and liquid reentrainment. Item 4 is the approximate condition at which the model was run to evaluate droplet impingement regions. See Section 2.1.1 for further discussion.

2.3 Model Geometry and Construction

The model was constructed to a scale factor of 8.91 with the following start and end points:

1. The model starts in the absorber in the outlet plenum at the upper tube sheet.

2. The model ends in the stack liner about 3.0 stack liner diameters above the top of the breeching duct.

The geometry of the absorber-outlet duct system is shown on Figure 2-1, with dimensions given for field geometry on the top and the equivalent model geometry on the bottom. The scale factor of 8.91 was selected to keep the model ducts large enough for satisfactory modeling observations and to match a plexiglass tube size of 17.5" inner diameter. Two pictures of the assembled model are presented on Figure 2-3. The curved dome of the top of the absorber vessel was approximated with a truncated cone with a plexiglass roof as shown on Figure 2-1.

The following comments apply to the model absorber outlet duct and stack liner system:

1. Material Selection

   - All components of the model were constructed from plexiglass except the absorber outlet plenum.

   - The stack liner entrance 90° mitered elbow and bottom section were fabricated from a plexiglass tube.

2. Flange Locations

   - Flanges are located at damper or expansion joint locations where possible and practical.

   - Other locations are selected so as not to interfere with liquid collectors to be installed and developed.

3. Expansion Joints and Dampers

   - All slide gate dampers are left out of model since nothing protrudes into the duct.

   - The expansion joint between the mist eliminator and the stack elbow is included in the model. It is constructed oversize to dimensions of 0.375 inches depth x 2.0 inches long all around the circular duct so that the water behavior in the joint can be evaluated. The scaled size would have been 0.22" inches x 1.35" inches which is too small.

   - All other expansion joints are not included in the model.

4. Mist Eliminator Simulation

   - Two perforated plates were used to simulate the scaled value of mist eliminator pressure loss. Because perforated plates would interfere with the droplet flow carried into the model during the wet tests, the model was separated at the mist eliminator outlet for wet tests to develop liquid collectors.

2.4 Instrumentation

The following instrumentation was used to measure data and make observations on the model:

1. **Flow Measurement**

   - A 20 inch diameter orifice system was used to measure total stack flow rate.

2. **Velocity Profiles and Static Pressure**

   - A standard "L" shaped Prandlt type pitot tube was used for both measurements. Both were connected to one or more pressure transducers, a data acquisition system, and a computer for on-line data recording, reduction, and tabular printout.

   - A hot-wire anemometer is used to measure the velocity profile at traverse location V2 on Figure 2-2.

3. **Observations**

   - Smoke filament and tufts of yarn were used to visualize the gas flow in the ducts.

   - A rotating disk type aerosol generator was used to provide a 30 μm water droplet spray to the model inlet for evaluation of droplet trajectory, deposition, and reentrainment.

The location of the measurement stations for velocity and pressure are shown on Figure 2-2 for the absorber ducts and stack. The measurements taken at each station and the number of data points are also specified on Figure 2-2.

2.5 Data Reduction and Scaling

1. **Orifice Flow Rate**

   Orifice flow calculations are carried out using equations and orifice coefficients developed by ASME and documented in their publications.

2. **Velocity Values**

   Velocity is calculated from the velocity head sensed by the pitot tube, measured by the pressure transducer, and recorded by the computer. The velocity head is:

$$VH = \frac{\rho V^2}{2g_o (5.21)}$$

where:

VH	=	velocity head (inches of water);
V	=	velocity data point (fps);
ρ	=	air density (lb_m/ft^3); and
g_o	=	32.2 ($ft \cdot lb_m/lb_f s^2$).

The density is calculated from the measured barometric pressure, local static pressure, and the gas temperature using the perfect gas equation.

3. <u>RMS Velocity Uniformity</u>

The root mean square velocity uniformity value listed on the velocity data reduction sheets is similar to a standard deviation. It is defined as follows:

$$\left[\frac{\sum\left[\frac{V}{V_{AVG}} - 1\right]^2}{N}\right]^{1/2}$$

where

V	=	velocity data point in fps;
V_{AVG}	=	average of all velocity values in fps; and
N	=	number of data points.

In effect, it is the standard deviation of velocity about an average velocity, expressed as a fraction of the average velocity. For a value of zero, the flow would be perfectly uniform with all data points equal.

4. <u>Stagnation Pressure Loss</u>

Static pressure data is measured in inches of water at six or eight points in each cross-section using a pitot tube and a pressure transducer. The average flow velocity head for a cross-section is determined by:

$$VH = \frac{\rho V_o^2}{2g_o (5.21)}$$

where

VH	=	velocity head (inches of water);
ρ	=	air density (lb_m/ft^3);
V_o	=	volume flow rate divided by the cross-sectional area (fps); and
g_o	=	32.2 ($ft \cdot lb_m/lb_f s^2$).

Total pressure at each cross-section is calculated as:

$$P_T = P_S + VH$$

where: P_T = total pressure (inches of water);
P_S = measured static pressure (inches of water); and
VH = velocity head (inches of water).

The field value of total pressure loss between two cross-sections is calculated as:

$$(\text{delta}P_T)_{FIELD} = (\text{delta}P_T)_{MODEL} \times \frac{(VH)_{FIELD}}{(VH)_{MODEL}}$$

2.6 Test Program

All quantitative testing conducted during the program was for the simulation of 100% unit load. The velocity profile and pressure measurement locations are identified on Figure 2-2.

The model is connected to the laboratory orifice and blower facilities so that the total flow from the top of the model stack is drawn through an orifice by a single large blower. Air flows into the model absorber from the laboratory. All tests are run in this manner. The approximate model flow rates for quantitative measurements and wet tests are presented on Table 2-2 for the 100% load condition and discussed in Section 2.2.

Table 2-1

LIST OF FLOW PARAMETERS FROM JBR TO STACK FOR FIELD AND MODEL CONDITIONS

INPUTS VALUES	
S.F.=	8.914
FIELD DENSITY=	0.065
MODEL DENSITY=	0.0742
FOR FLOW PARAMETER CHART ONLY	
Plane loc. =	K
Geo. code =	0
Dim. a or ID =	0
Dim. b or OD =	156
Abs.viscos. f [lbm/ft	1.33E-05
Abs.viscos. m [lbm/ft	1.22E-05
Dh f =	156.000
Dh m =	17.501
DIA.=0,RECT.=1: ENTER CODE IN UPPER PLANE LOCATION	
[C9,C16,C23,C30,	,C37,C44,C51]
NOTE: STORE UNDER NEW NAME	CALCLATIONS ME

PARAMETER	UNITS	FIELD	MODEL		
			Vm = Vf	Vm = Vf/SF^.	VHm = VHf
Scale Factor	-	8.914	8.914	8.914	8.914
m gas	lbm/hr	1,586,400	22,714.00	7,607.77	21,259.27
Operating range	% of m gas	[25 - 100]			
T gas	Deg. F	126	70	70	70
P gas	psia	14.7	14.7	14.7	14.7
Density gas	lbm/ft^3	0.065	0.0742	0.0742	0.0742
Q gas	acfm	405,400	5,101.98	1,708.84	4,775.22
MW wt gas	lbm/lb mole	27.93			
Kgas = (Cp/Cv)	-		1.40	1.40	1.40
Gas Velocity at plane loc. K	ft/sec	50.9	50.90	17.05	47.76
Reynolds Number at plane loc. K	-	3.23E+06	4.51E+05	1.51E+05	4.24E+05
Gas Velocity Head at plane loc. K	IN. H2O	0.50	0.574	0.064	0.503

Table 2-2

LIST OF GEOMETRIC PARAMETERS, FLOW RATES, VELOCITIES, AND VELOCITY HEADS FROM JBR TO STACK FOR FIELD AND MODEL

PLANE LOCATION (See Sketch) 1	MODELING CONDITIONS	PASSAGE DIMENSIONS a I.D. (IN.)	x ;	b O.D. (IN.)	FLOW AREA (IN.^2)	VOLUME FLOWRATE (ACFM)	AVERAGE VELOCITY (FT/SEC)	AVERAGE VELOCITY HEAD (IN. H2O)
G	Field	0.000	;	22.000	380.133	8,626	54.46	5.76E-01
	Model	0.000	;	2.468	4.784			
	Vm = Vf					109	54.46	6.57E-01
	Vm = Vf/(SF)^.5					36	18.24	7.37E-02
	VHm = VHf					102	50.97	5.76E-01
H	Field	0.000	;	504.000	199503.700	405,400	4.88	4.62E-03
	Model	0.000	;	56.540	2510.763			
	Vm = Vf					5,102	4.88	5.27E-03
	Vm = Vf/(SF)^.5					1,709	1.63	5.91E-04
	VHm = VHf					4,775	4.56	4.62E-03
I	Field	264.000	X	84.000	22176.000	405,400	43.87	3.74E-01
	Model	29.616	X	9.423	279.086			
	Vm = Vf					5,102	43.87	4.27E-01
	Vm = Vf/(SF)^.5					1,709	14.70	4.79E-02
	VHm = VHf					4,775	41.06	3.74E-01
J	Field	375.250	X	156.000	58539.000	405,400	16.62	5.36E-02
	Model	42.097	X	17.501	736.716			
	Vm = Vf					5,102	16.62	6.12E-02
	Vm = Vf/(SF)^.5					1,709	5.57	6.87E-03
	VHm = VHf					4,775	15.56	5.36E-02
K	Field	0.000	;	156.000	19113.450	405,400	50.90	5.03E-01
	Model	0.000	;	17.501	240.544			
	Vm = Vf					5,102	50.90	5.74E-01
	Vm = Vf/(SF)^.5					1,709	17.05	6.44E-02
	VHm = VHf					4,775	47.64	5.03E-01

Figure 2-1

DIMENSIONS OF JBR AND OUTLET DUCTS FOR MODEL DEVELOPMENT OF LIQUID COLLECTORS

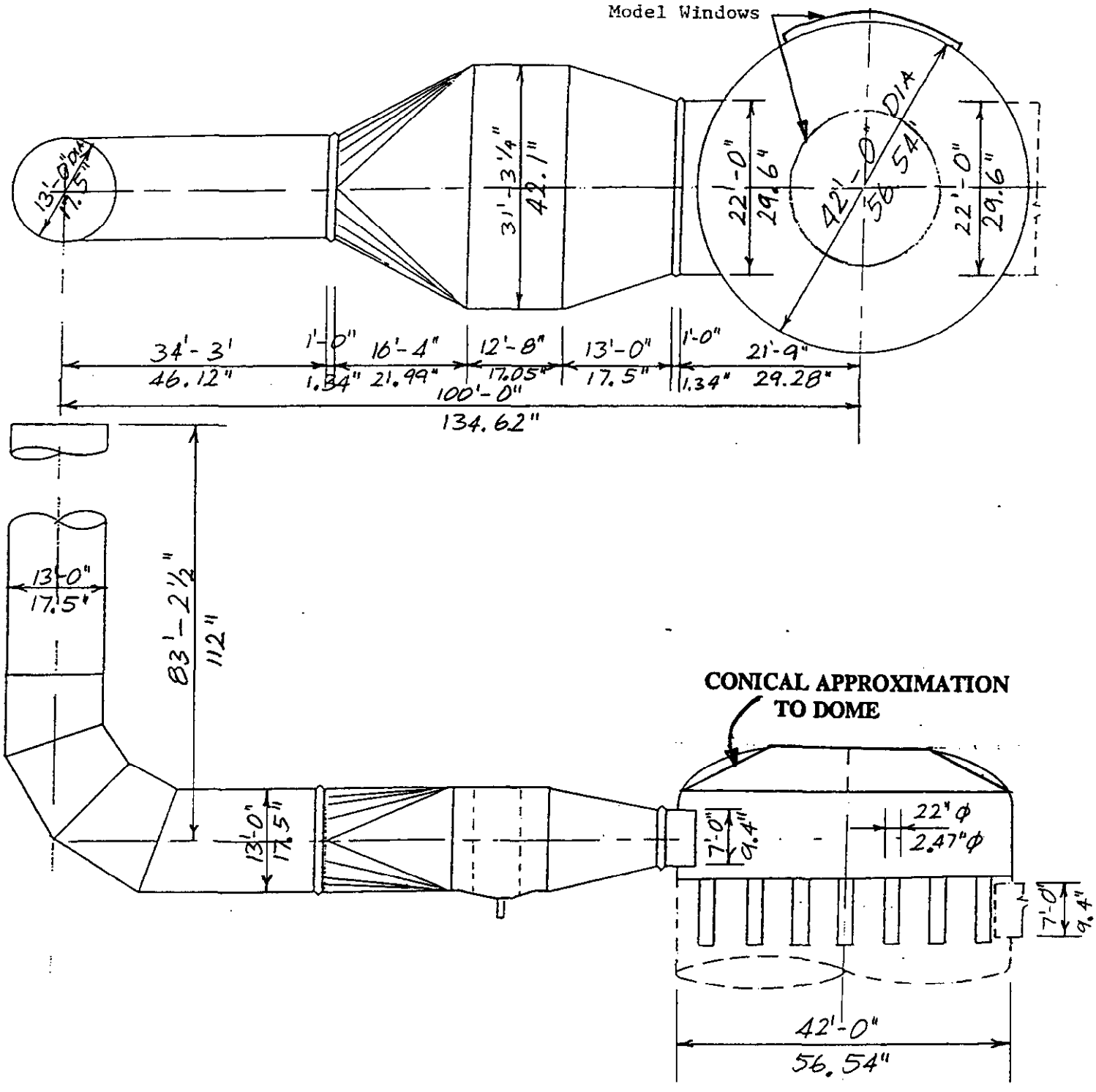

Notes:

1. Scale factor = 8.91.
2. Dimensions above line are field values and below line are model values.
3. 33% open perforated plates are used to simulate two mist eliminator modules.

Figure 2-2

INSTRUMENTATION ON MODEL OF JBR OUTLET DUCTS
(Scale Factor = 8.91)

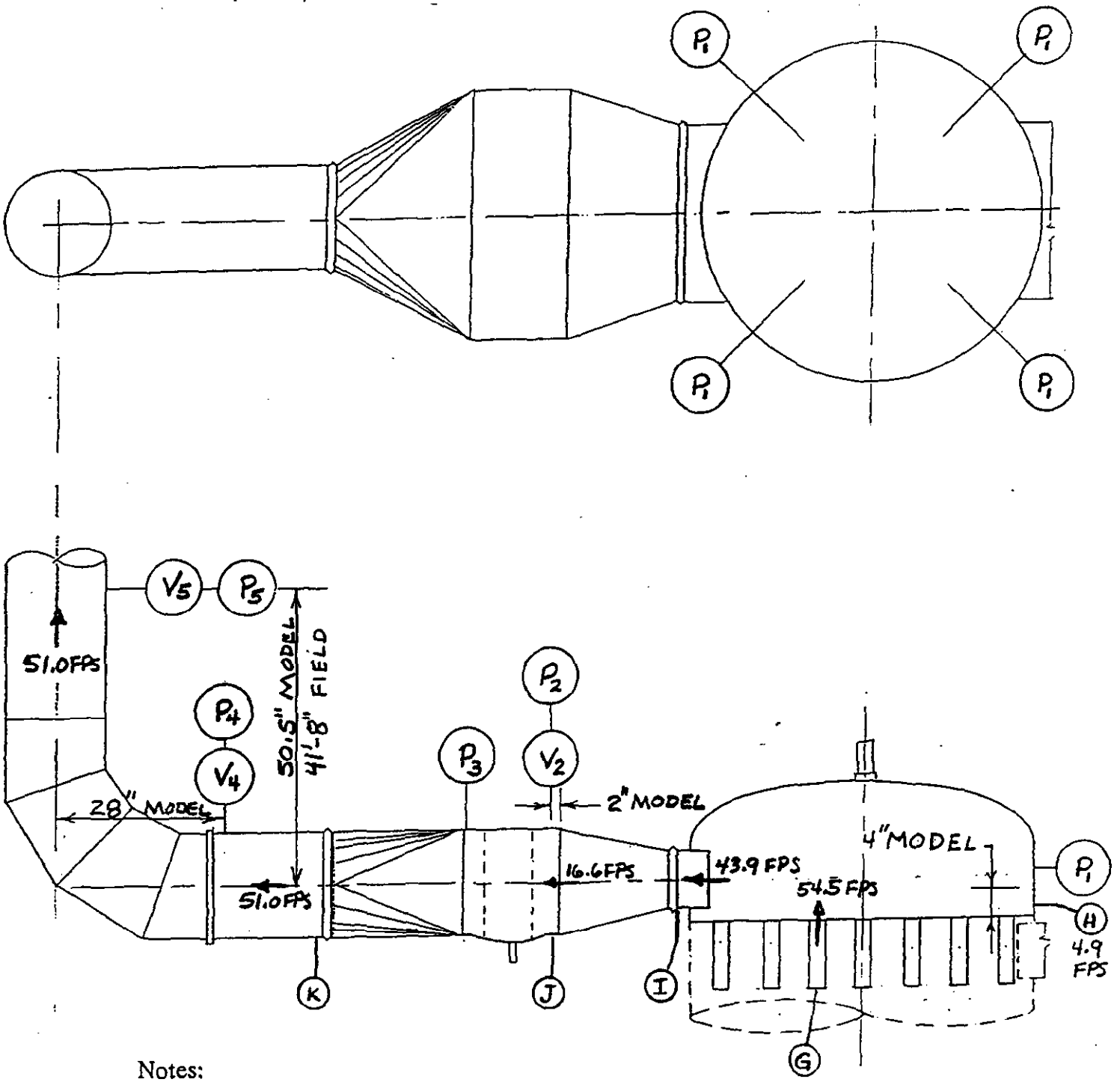

Notes:

1. All pressures taken by pitot tube, 4 in each cross-section.
2. V_2 measured by hot wire anemometer (21 across by 8 vertically).
3. V_3 and V_4 measured by pitot tube (40 points, 5 points on 8 radii).
4. Velocities shown above are field values at 100% flow rate.
5. Lettered circles are cross-sections where field and model velocity values are presented on Table 2.

Figure 2-3

PHOTOGRAPHS OF MODEL FROM
JBR TO STACK LINER

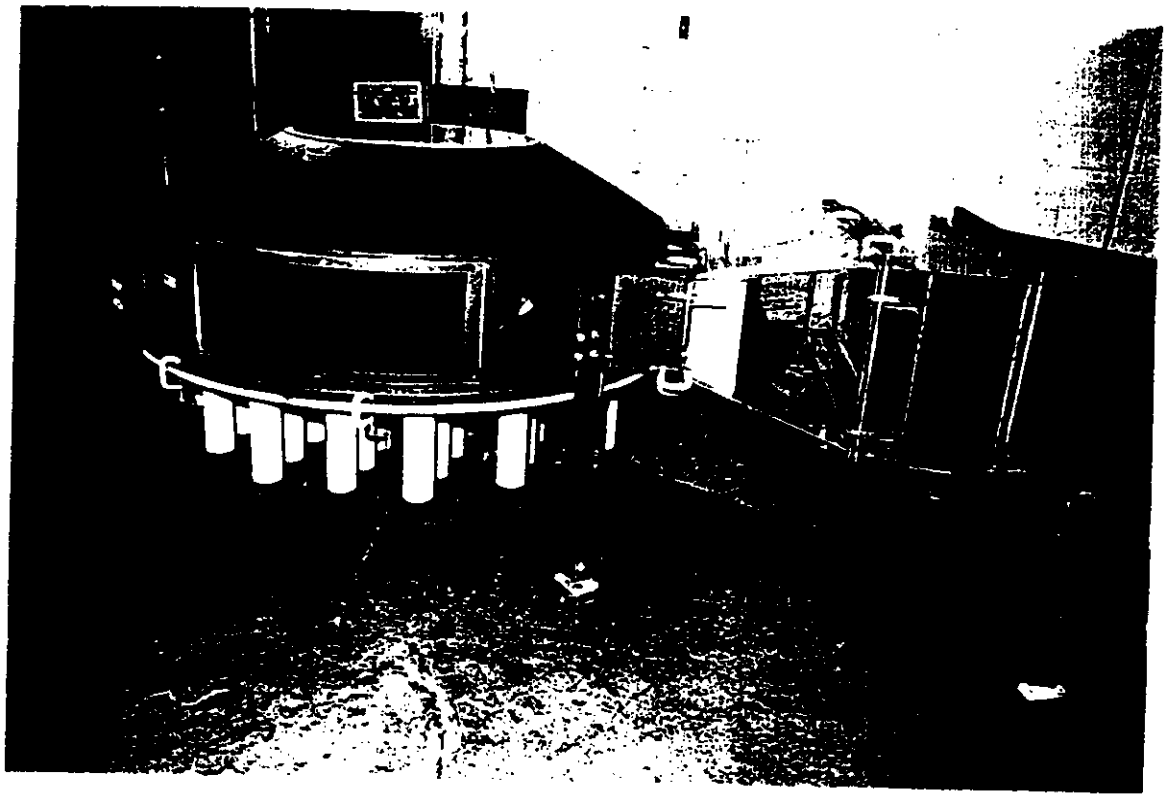

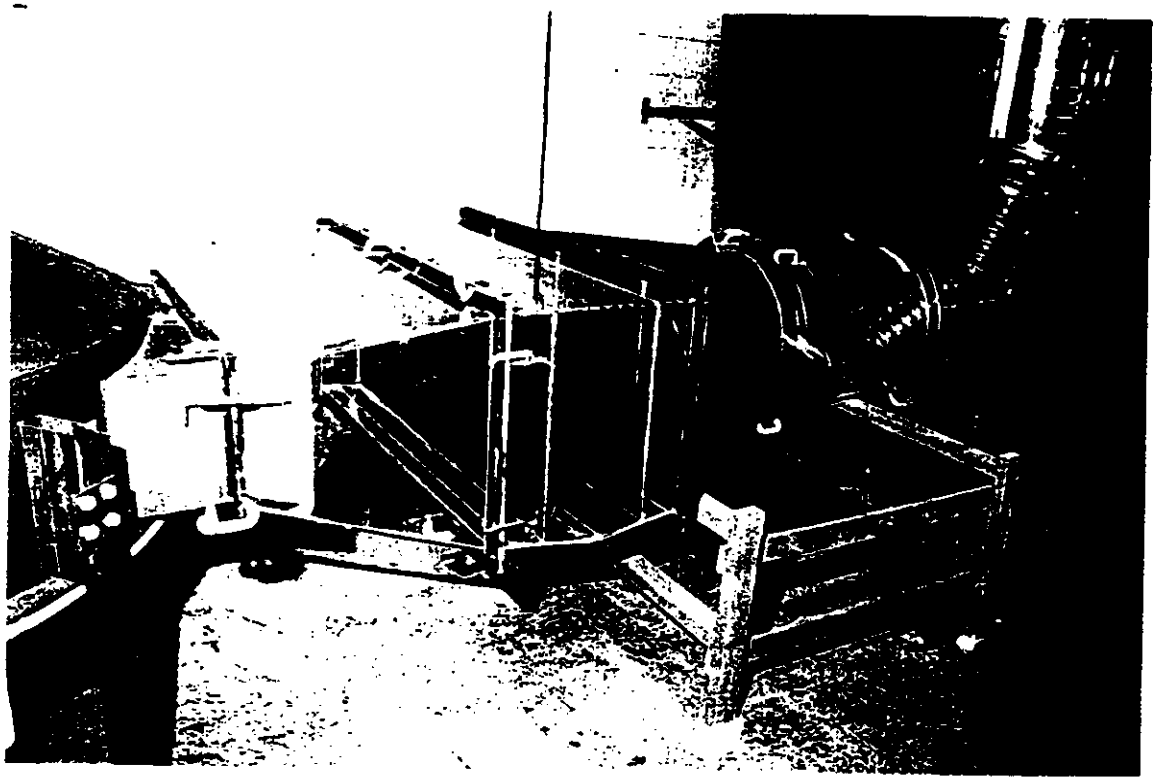

Section 3

EVALUATION OF THE ABSORBER OUTLET DUCT SYSTEM WITHOUT LIQUID COLLECTORS

3.1 Velocity Profiles

Visual observations of flow patterns using smoke and tufts of yarn were carried out first before any quantitative velocity profiles were measured. The results of these observations are shown on Figure 3-1. The flow pattern coming out of the absorber outlet plenum into the transition duct leading to the mist eliminator was significantly distorted with large reverse flow regions as shown. The other flow pattern, which will influence liquid collection, is the swirling gas flow patterns set up in the 90° mitered elbow.

Since the mist eliminator inlet velocity profile was so grossly distorted, the first design of absorber outlet vanes shown on Figure 3-2 was installed in the model before measuring the velocity profiles and pressure loss at the locations identified on Figure 2-2. The vane design consisted of 3 full width straight horizontal vanes in the absorber outlet port and two full width vanes inclined upward in the diffuser inlet to eliminate the reverse flow region on the diffuser roof (see Figure 3-1). Single full height vanes were installed on both sides of the diffuser to eliminate the side wall reversed flow regions. Flow observations with smoke showed significant improvement but quantitative velocity profiles for Test 1 showed that the velocity uniformity did not achieve the objective of 0.25 RMS. The velocity profile data ahead of the mist eliminator (Location V2) is shown on Figure 3-3 as isovelocity contours and on Table 3-1 as tabulated data showing both a velocity array and a % of average velocity array. The RMS for the traverse was 0.444 with low regions of velocity along the top of the diffuser duct and along the left side. All the traverse data is presented as though you are standing downstream at the mist eliminator looking back toward the scrubber. All of the numbers on the isovelocity plot on Figure 3-3 are local velocities as a percent of average velocity. On Table 3-1, the data array at the top is local velocity data points recorded with a hot-wire anemometer. The data array at the bottom is the ratio of local velocity divided by average velocity times 100 to express the number in % of average velocity. Each array has a column of numbers to the far left that is the average value for each row. At the bottom of each array is a row of numbers that is the average value for each column. Several uniformity values are listed in the lower left corner of Table 3-1. Discussion of improved vane designs and reduced RMS flow uniformity are discussed in Section 4.

Figures 3-4 and 3-5 show isovelocity contours for test locations V4 and V5 on Figure 2-2 in the 13' diameter pipe upstream and downstream of the 90° mitered elbow. The velocity profile entering the elbow (V4 on Figure 3-4) is a good profile with an RMS of 0.086 and a reasonably symmetrical profile except that the sides near the wall are about 25% below average as compared to near average velocity at the top and bottom of the inlet pipe. This could be due to the contraction transition upstream that contracts in dimension significantly from the sides but has no change in dimension top to bottom. The velocity profile at the elbow outlet (V5) is more distorted as shown on Figure 3-5. The low velocity region occurs over the inside of the elbow located below. The swirl pattern sketched on Figure 3-1 helps to bring

flow into the wall region just above the sharp inner corners of the miter joints and at the same time pushes the lowest velocity zone about a quarter of the diameter out toward the pipe centerline. This low flow region causes elevated velocities in the rest of the cross-section of about 10% above average. Unfortunately, these elevated velocity levels occur near the wall at the outside of the bend where liquid will impinge and can be reentrained if not collected and drained.

The field total pressure loss for three sections of the duct system with Vane Set 1 and no liquid collectors is listed on Table 3-2 for the 100% load condition specified on Tables 2-1 and 2-2. The field unit gas velocity head in the 13' diameter pipe and stack is 0.51 inches of water. The largest pressure loss occurs from the JBR outlet header to the inlet of the ME. The biggest portion of this loss may be due to the high gas velocity head in the upflow pipes discharging and diffusing into the large header (0.577" water) and then reaccelerating into the outlet port. The 90° long radius mitered elbow has a relatively low pressure loss (0.15" water) which is very close to the value of 0.168 inches of water that was estimated using loss coefficients from published literature ($\Delta P_T/VH = 0.33$). These pressure loss values will be compared to the final geometry pressure loss values in Section 8.2.

Table 3-1

VELOCITY TRAVERSE DATA AT LOCATION 2 AT INLET TO MIST ELIMINATOR WITH VANES ON FIGURE 3-2 INSTALLED AT JBR OUTLET

TRAVERSE LOCATION: T1-V1-1

DENSITY = .0746(LB/FT^3)

ORIFICE FLOWRATE = 5146ACFM

FLOW OUT OF PAPER

MODEL STATIC PRESSURE= -1.6 IN. H2O

NUMERICAL AVE. VELOCITY = 934. FT/MIN

Q/A= 1005. FT/MIN

VELOCITYFT/MIN

ROW AVG								
547.	375.	275.	378.	521.	991.	1002.	570.	267.
982.	385.	650.	886.	1109.	1484.	1749.	1250.	342.
1073.	862.	1214.	1425.	1545.	1459.	1206.	591.	285.
1012.	882.	1362.	1486.	1570.	1265.	786.	516.	229.
884.	940.	1169.	1333.	1374.	1011.	735.	298.	214.
849.	1071.	1142.	1209.	1063.	1073.	686.	338.	210.
852.	949.	1210.	1051.	986.	1188.	903.	329.	201.
1001.	1064.	1177.	1095.	1315.	1486.	1360.	302.	212.
1046.	898.	924.	1176.	1382.	1629.	1475.	654.	232.
1115.	1067.	1124.	1196.	1380.	1542.	1581.	810.	221.
1101.	1140.	1119.	1252.	1308.	1581.	1511.	685.	213.
1094.	1170.	1322.	1286.	1312.	1378.	1196.	836.	251.
1013.	1128.	1216.	1069.	1158.	1260.	1151.	861.	260.
1049.	1033.	1282.	1237.	1258.	1277.	1182.	847.	279.
936.	978.	1314.	1199.	1145.	1172.	1050.	416.	211.
884.	963.	1310.	1307.	1154.	967.	783.	349.	238.
806.	867.	1179.	1366.	1236.	911.	467.	223.	196.
899.	875.	1191.	1429.	1495.	1048.	540.	341.	272.
902.	918.	1275.	1381.	1329.	1055.	616.	368.	274.
897.	876.	1142.	1149.	1317.	1106.	856.	430.	302.
677.	466.	731.	984.	1041.	926.	649.	369.	248.
COL AVG	900.	1111.	1185.	1238.	1229.	1023.	542.	246.

VELOCITY(% OF NUM. AVE.)

ROW AVG								
58.6	40.1	29.4	40.4	55.8	106.1	107.3	61.1	28.6
105.1	41.3	69.6	94.8	118.7	158.8	187.3	133.8	36.6
114.9	92.2	130.0	152.6	165.4	156.2	129.1	63.2	30.5
108.3	94.4	145.7	159.1	168.1	135.4	84.1	55.2	24.5
94.7	100.6	125.2	142.7	147.1	108.3	78.6	31.9	23.0
90.9	114.7	122.3	129.4	113.8	114.9	73.4	36.2	22.5
91.2	101.5	129.5	112.5	105.5	127.1	96.6	35.2	21.5
107.2	113.8	125.9	117.2	140.8	159.0	145.5	32.3	22.7
112.0	96.2	98.9	125.8	147.9	174.4	157.9	70.0	24.8
119.4	114.2	120.3	128.0	147.7	165.1	169.2	86.7	23.7
117.8	122.0	119.8	134.0	140.0	169.3	161.7	73.3	22.8
117.1	125.2	141.5	137.7	140.5	147.5	128.0	89.4	26.8
108.4	120.7	130.1	114.5	123.9	134.9	123.2	92.1	27.8
112.3	110.5	137.2	132.3	134.6	136.7	126.5	90.6	29.9
100.2	104.7	140.7	128.4	122.6	125.5	112.4	44.5	22.6
94.6	103.0	140.2	139.9	123.5	103.5	83.8	37.4	25.5
86.2	92.7	126.2	146.3	132.3	97.5	50.0	23.9	21.0
96.2	93.6	127.5	152.9	160.0	112.2	57.8	36.5	29.1
96.5	98.3	136.5	147.8	142.2	112.9	65.9	39.4	29.3
96.0	93.7	122.2	123.0	140.9	118.4	91.7	46.1	32.3
72.4	49.9	78.2	105.3	111.5	99.1	69.5	39.5	26.5
COL AVG	96.4	118.9	126.9	132.5	131.6	109.5	58.0	26.3

Bottom of Duct

Top of Duct

BANDSIZE PERCENT	VRANGE FT/MIN	COUNT	PERCENT
10	841.-1028.		14.9
15	794.-1074.		23.2
25	701.-1168.		33.9
40	561.-1308.		56.5

RMS=0.444 DEV. OF MAX=0.873 DEV. OF MIN=0.790

Table 3-2

SUMMARY OF FIELD PRESSURE LOSS FOR TWO COMBINATIONS OF VANES AND LIQUID COLLECTORS FOR 100% LOAD CONDITION ON TABLE 2-1

Section of Duct	Vane Set 1 (Figure 3-2) No Liquid Collectors Total Pressure Loss Inches Water	Vane Set 3 (Figure 4-2) Final Liquid Collectors Total Pressure Loss Inches Water
JBR (1) to ME Inlet (2)	0.40	0.33
ME ΔP (2-3)	Use Actual Pressure Loss From ME Manufacturer	
ME Outlet (3) to Elbow Inlet (4)	0.08"	0.11"
Elbow ΔP (4-5)	0.15"	0.44"
TOTAL JBR TO LINER*	0.63 + Δp (ME)	0.88 + ΔP (ME)

*The measuring point in the liner is 37'-6" above the horizontal centerline of the elbow inlet.

Figure 3-1

GAS FLOW PATTERN OBSERVATIONS FOR ORIGINAL DUCT AND STACK WITHOUT VANES OR LIQUID COLLECTORS

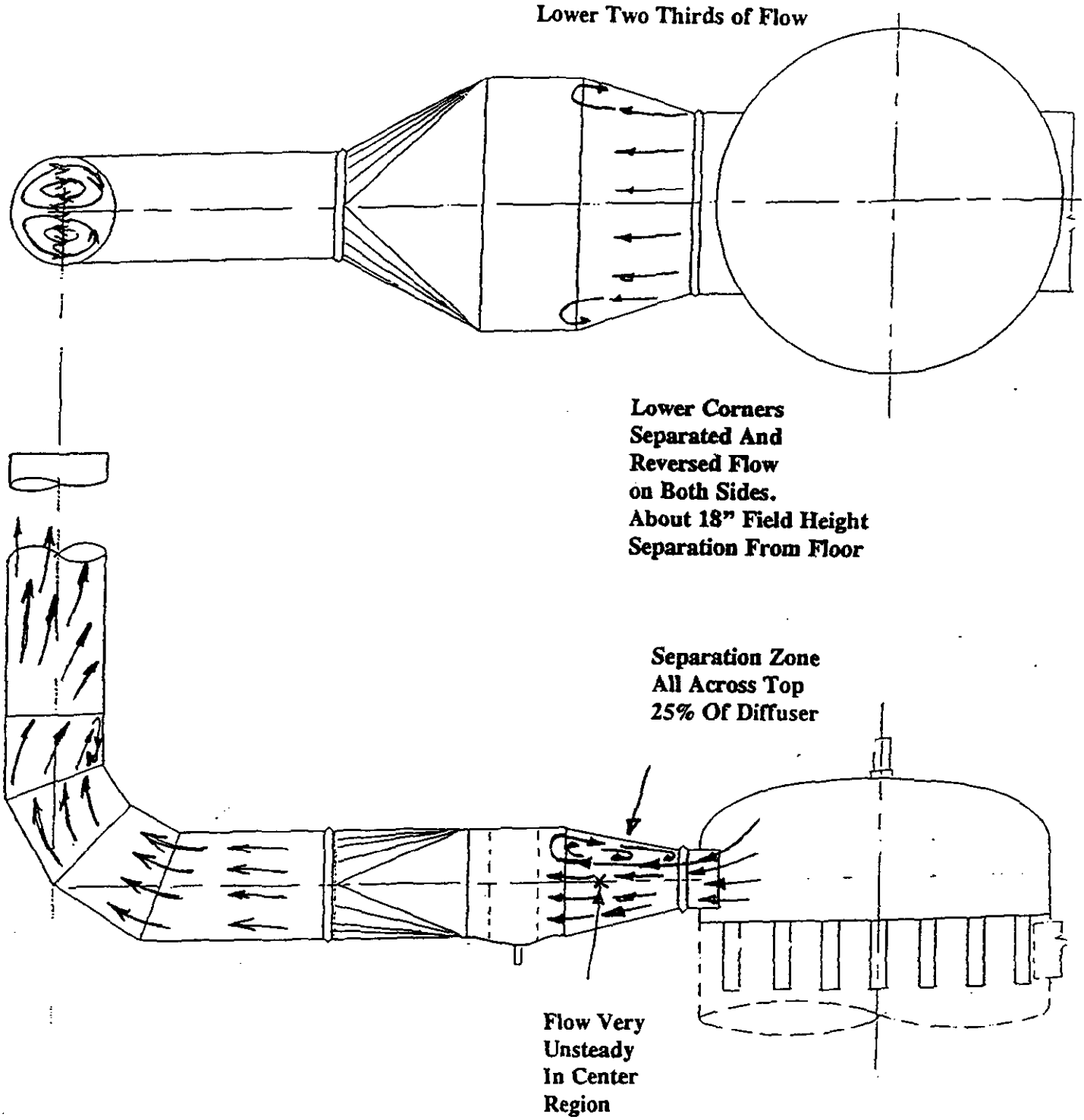

Figure 3-2 FIELD DIMENSIONS FOR DESIGN NO. 1 FOR VANES IN JBR OUTLET

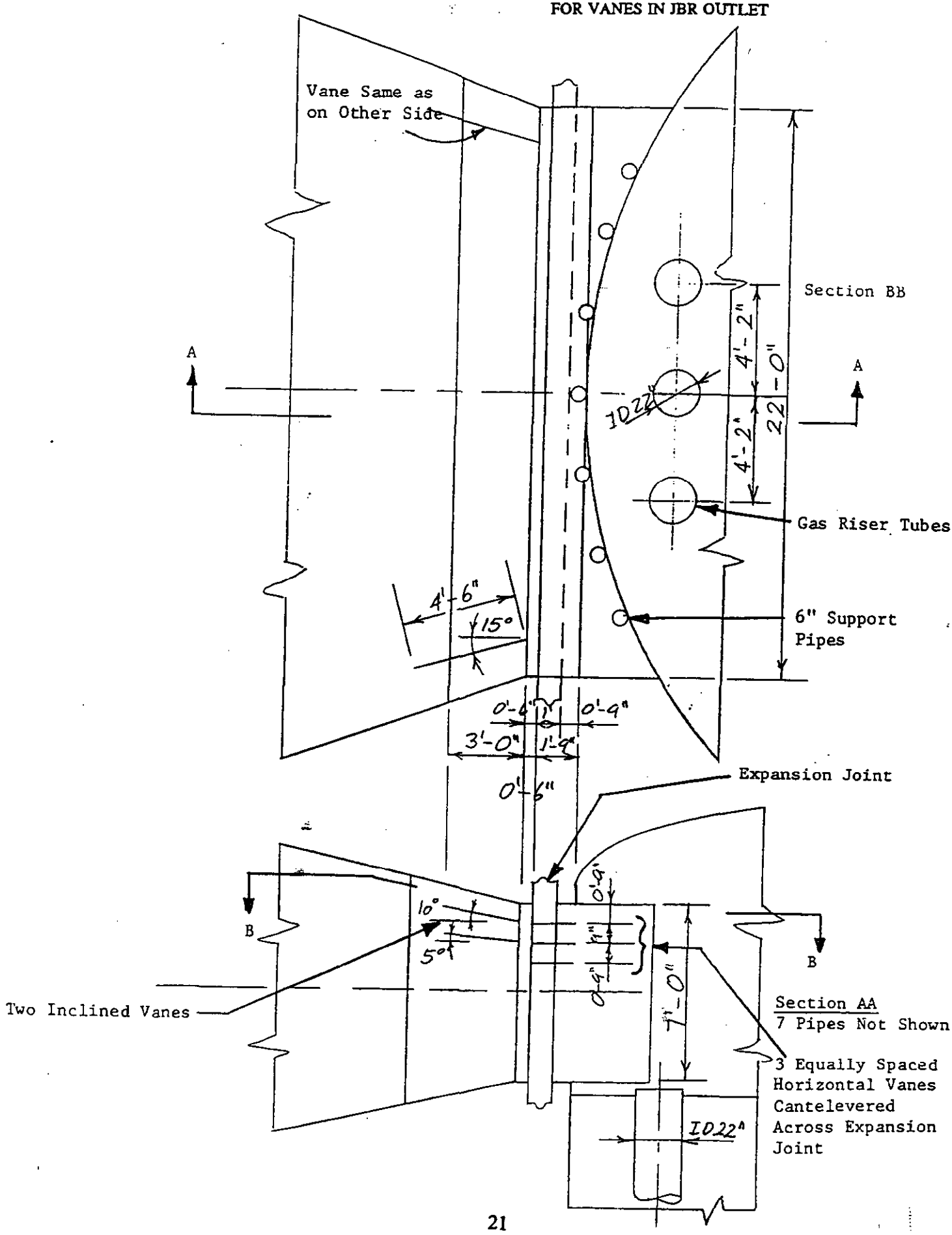

FIGURE 3-3 TEST No. 1 ISO-VELOCITY CONTOURS
JBR PILOT PLANT MODEL TEST
TRAVERSE LOCATION: V2 MIST ELIMINATOR INLET
CONFIGURATION DESCRIPTION: VANES INSTALLED AT JBR OUTLET AS SHOWN ON FIGURE 3-2

Percent of Average Velocity
Flow Out of Paper

RMS = 0.444

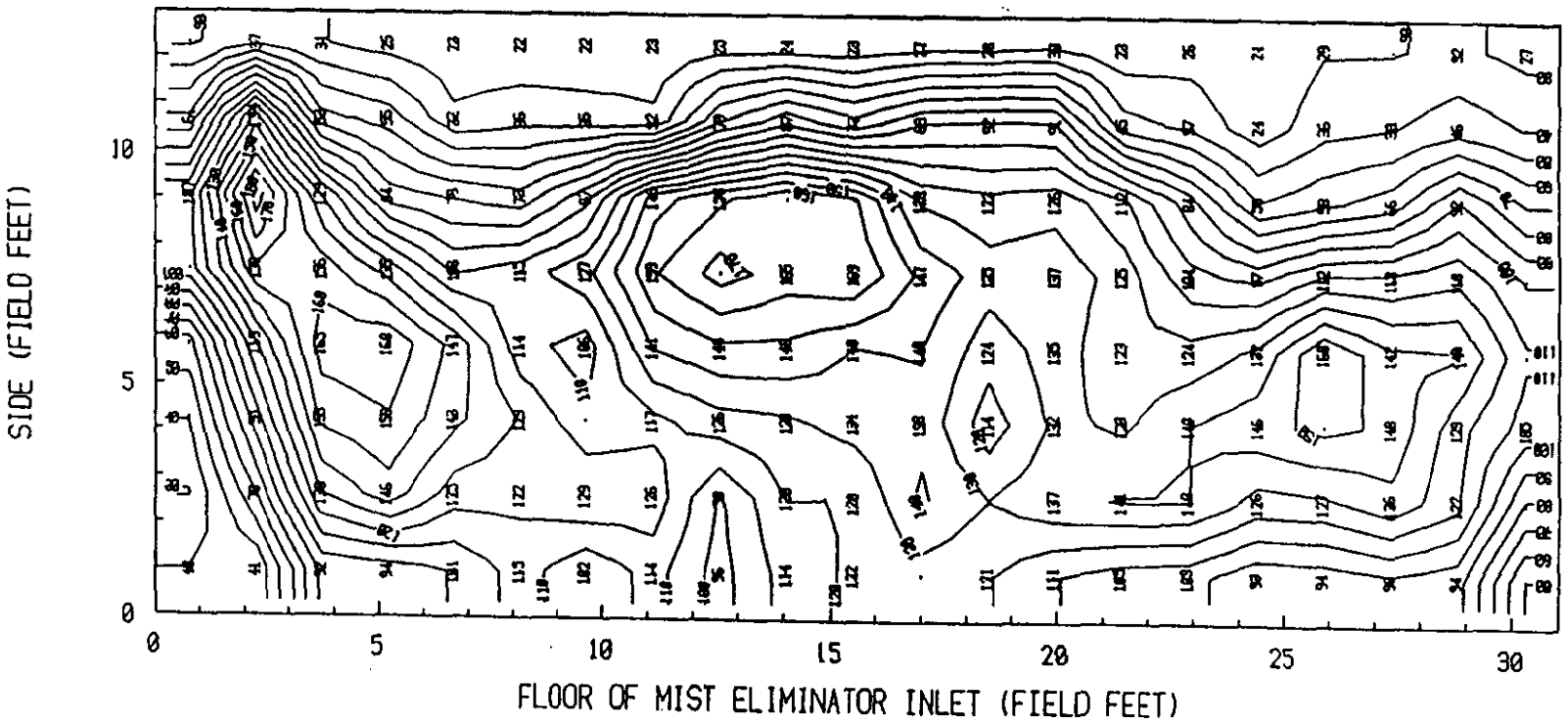

Figure 3-4
ISOVELOCITY CONTOUR IN 13' DIAMETER STACK INLET
JBR PILOT PLANT MODEL TEST
TRAVERSE LOCATION: V4 STACK INLET
CONFIGURATION DESCRIPTION: VANES IN JBR OUTLET (FIGURE 3-2)
OPEN DUCT AND STACK OF 13' DIAMETER

Percent of Average Velocity
Flow Out of Paper
TOP OF DUCT

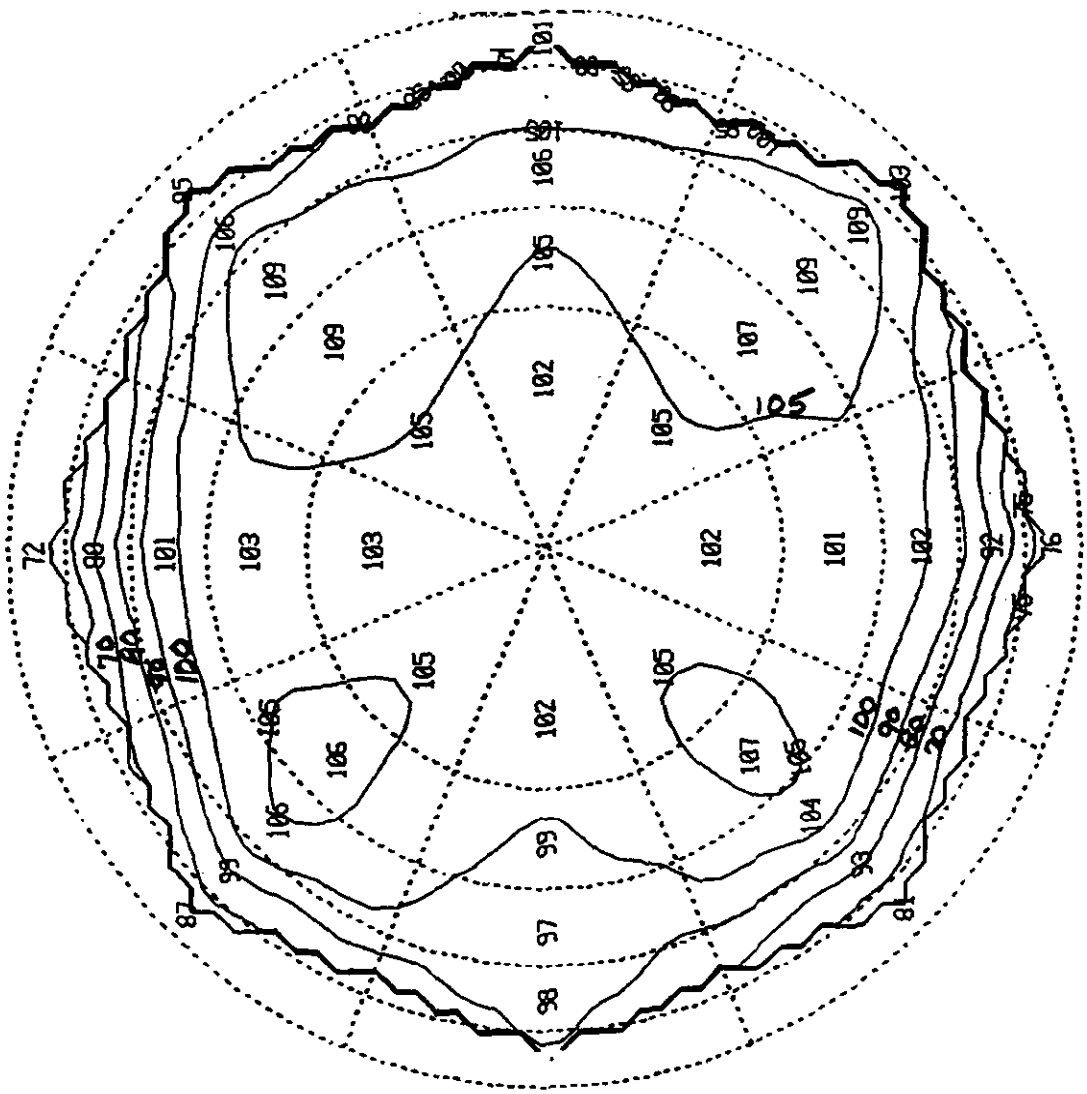

40 points measured at center of equal area segments
% of data within bands
87.3% within ±10% of Vavg
92.5% within ±15% of Vavg
97.5% within ±25% of Vavg
RMS= 0.086

Figure 3-5

ISOVELOCITY CONTOURS IN 13' DIAMETER STACK ELBOW OUTLET
JBR PILOT PLANT MODEL TEST
TRAVERSE LOCATION: V5 IN STACK LINER
CONFIGURATION DESCRIPTION: VANES IN JBR OUTLET (FIGURE 3-2)
OPEN DUCT AND STACK OF 13' DIAMETER

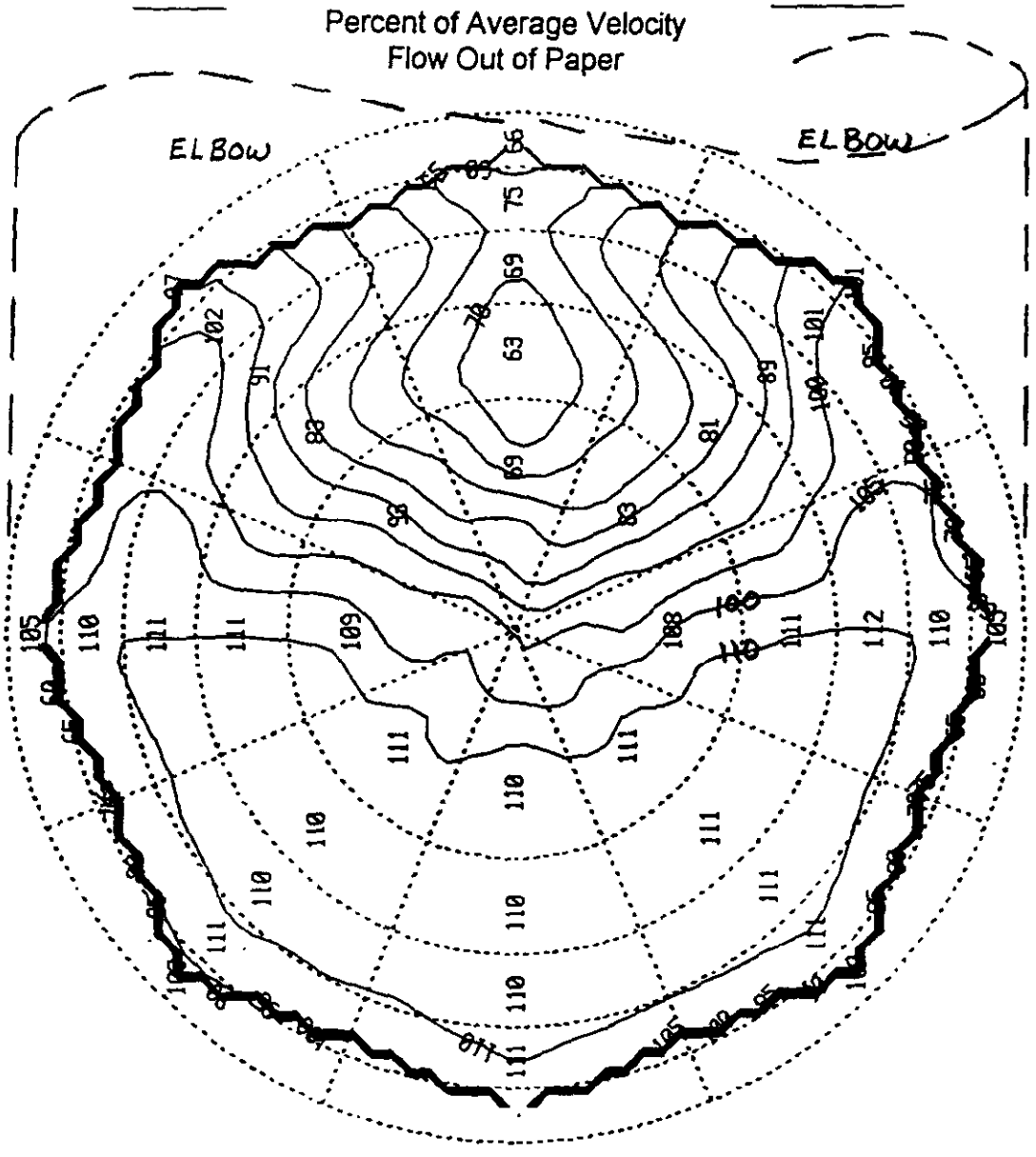

40 points measured at center of equal area segments
% of data within bands
37.5% within ±10% of Vavg
80.0% within ±15% of Vavg
87.5% within ±25% of Vavg

RMS= 0.147

Section 4

DEVELOPMENT OF ABSORBER OUTLET VANES

Vane Set 1 (Figure 3-2) did not have enough flow in the top part of the diffuser. Flow visualization showed that the downward flow from the roof of the absorber outlet plenum was not intersecting the horizontal vanes sufficiently. To improve the capture of flow by these three horizontal vanes, they were constructed to conform to the curvature of the plenum shell and have a 1'-9" radial depth field dimension (See Figure 4-1 for Vane Set 2). No changes were made to the side of the diffuser. Evaluation by flow visualization did not show sufficient improvement to warrant a velocity profile measurement.

Vane Set 3 shown on Figure 4-2 included the following changes compared to Vane Set 2.

(1) The three curved horizontal vanes were moved slightly out into the plenum to intersect more of the downward angled flow. The top vane was moved 4-1/2" inward from the shell and the bottom two vanes were moved inward by 9" from the shell. The dimensions and locations were otherwise the same as Vane Set 2.

(2) In the diffuser inlet, the two full width vanes near the top of the duct and inclined upward plus two full height single vanes on each side of the diffuser were kept as they had been in Vane Sets 1 and 2. (See photograph on Figure 4-4).

(3) In both lower corners, one partial height vertical vane and two partial width nearly horizontal vanes were added as shown on Figure 4-2 and on photograph on Figure 4-4).

The visual flow pattern observations showed sufficient improvement to warrant a detailed velocity traverse. The profile just reached the required flow uniformity of RMS = 0.25. The data is shown as isovelocity contours at the mist eliminator inlet on Figure 4-3 and as tabulated data on Table 4-1. The Vane Set 3 geometry specified on Figure 4-2 was therefore selected as the final design to be recommended for field installation and the design was used for all further testing to develop liquid collectors for the duct and stack.

Table 4-1

VELOCITY TRAVERSE DATA AT LOCATION 2 AT INLET TO MIST ELIMINATOR WITH VANES ON FIGURE 4-2 INSTALLED AT JBR OUTLET

TRAVERSE LOCATION: T3-V2-1

VANE SET 3 — DENSITY= .0740(LB/FT^3) — ORIFICE FLOWRATE= 5168ACFM

FIGURE 4-2

**FLOW OUT OF PAPER ** — MODEL STATIC PRESSURE= 1.5 IN.H2O

NUMERICAL AVE. VELOCITY= 1051. FT/MIN — Q/A= 1009. FT/MIN

VELOCITYFT/MIN

ROW AVG									
	735.	319.	618.	1030.	1063.	922.	373.	556.	999.
	1106.	567.	1089.	1466.	1561.	1254.	850.	880.	1181.
	1042.	602.	1250.	1571.	1406.	1051.	826.	771.	855.
	1091.	854.	1323.	1408.	1467.	1042.	776.	782.	1079.
	1205.	903.	1190.	1297.	1348.	1514.	1314.	938.	1138.
	1168.	955.	1062.	1104.	1229.	1336.	1358.	1040.	1259.
	1020.	735.	987.	927.	971.	1185.	1216.	988.	1147.
	947.	471.	830.	846.	959.	1220.	1229.	878.	1144.
	1136.	841.	1004.	1044.	1354.	1457.	1340.	872.	1173.
	1127.	957.	1145.	1091.	1322.	1484.	1233.	786.	999.
	1111.	1102.	1164.	1233.	1276.	1419.	1104.	638.	950.
	1196.	1027.	1117.	1343.	1330.	1428.	1323.	818.	1178.
	1117.	998.	1140.	1163.	1296.	1311.	1108.	770.	1153.
	1044.	972.	1057.	1146.	1243.	1234.	957.	754.	992.
	1089.	979.	1143.	1185.	1149.	1135.	935.	956.	1227.
	1188.	1126.	1227.	1267.	1214.	1172.	1194.	982.	1323.
	1109.	893.	1220.	1400.	1277.	1177.	925.	828.	1156.
	1018.	691.	1093.	1333.	1342.	1136.	785.	768.	995.
	1001.	561.	955.	1223.	1356.	1211.	995.	843.	862.
	984.	442.	595.	993.	1207.	1361.	1217.	748.	1306.
	633.	316.	372.	461.	729.	1029.	647.	542.	965.
COL AVG		777.	1028.	1168.	1243.	1242.	1034.	816.	1099.

Top

VELOCITY(% OF NUM. AVE.)

ROW AVG.									
	69.9	30.4	58.8	98.0	101.2	87.7	35.5	52.9	95.1
	105.3	54.0	103.6	139.5	148.6	119.3	80.9	83.8	112.4
	99.1	57.3	119.0	149.5	133.8	100.0	78.6	73.4	81.3
	103.8	81.2	125.9	134.0	139.6	99.1	73.9	74.5	102.6
	114.7	86.0	113.2	123.4	128.2	144.0	125.1	89.3	108.3
	111.1	90.9	101.0	105.0	117.0	127.2	129.3	99.0	119.8
	97.0	70.0	94.0	88.2	92.4	112.8	115.8	94.0	109.1
	90.1	44.8	79.0	80.5	91.3	116.1	117.0	83.5	108.9
	108.1	80.0	95.5	99.3	128.8	138.7	127.5	83.0	111.7
	107.3	91.1	108.9	103.8	125.8	141.3	117.4	74.8	95.1
	105.7	104.9	110.7	117.3	121.5	135.1	105.1	60.7	90.4
	113.8	97.8	106.3	127.8	126.6	135.9	126.0	77.9	112.1
	106.3	95.0	108.5	110.7	123.3	124.8	105.4	73.3	109.8
	99.4	92.5	100.6	109.0	118.3	117.5	91.1	71.8	94.4
	103.6	93.2	108.8	112.8	109.4	108.1	88.9	91.0	116.7
	113.1	107.2	116.8	120.6	115.5	111.6	113.7	93.4	125.9
	105.6	84.9	116.1	133.3	121.5	112.0	88.0	78.8	110.0
	96.9	65.8	104.0	126.9	127.7	108.1	74.7	73.1	94.7
	95.3	53.4	90.9	116.4	129.0	115.3	94.7	80.3	82.0
	93.6	42.1	56.6	94.5	114.9	129.6	115.8	71.2	124.3
	60.2	30.1	35.4	43.8	69.4	97.9	61.5	51.6	91.9
COL AVG		73.9	97.8	111.2	118.3	118.2	98.4	77.7	104.6

Top

BANDSIZE PERCENT	VRANGE FT/MIN	COUNT PERCENT
10	946. - 1156.	31.5
15	893. - 1208.	42.9
25	788. - 1313.	66.7
40	630. - 1471.	89.3

RMS= 0.250 — DEV. OF MAX= 0.495 — DEV. OF MIN= 0.699

Figure 4-1

FIELD DIMENSIONS FOR DESIGN NO. 2
FOR VANES IN JBR OUTLET

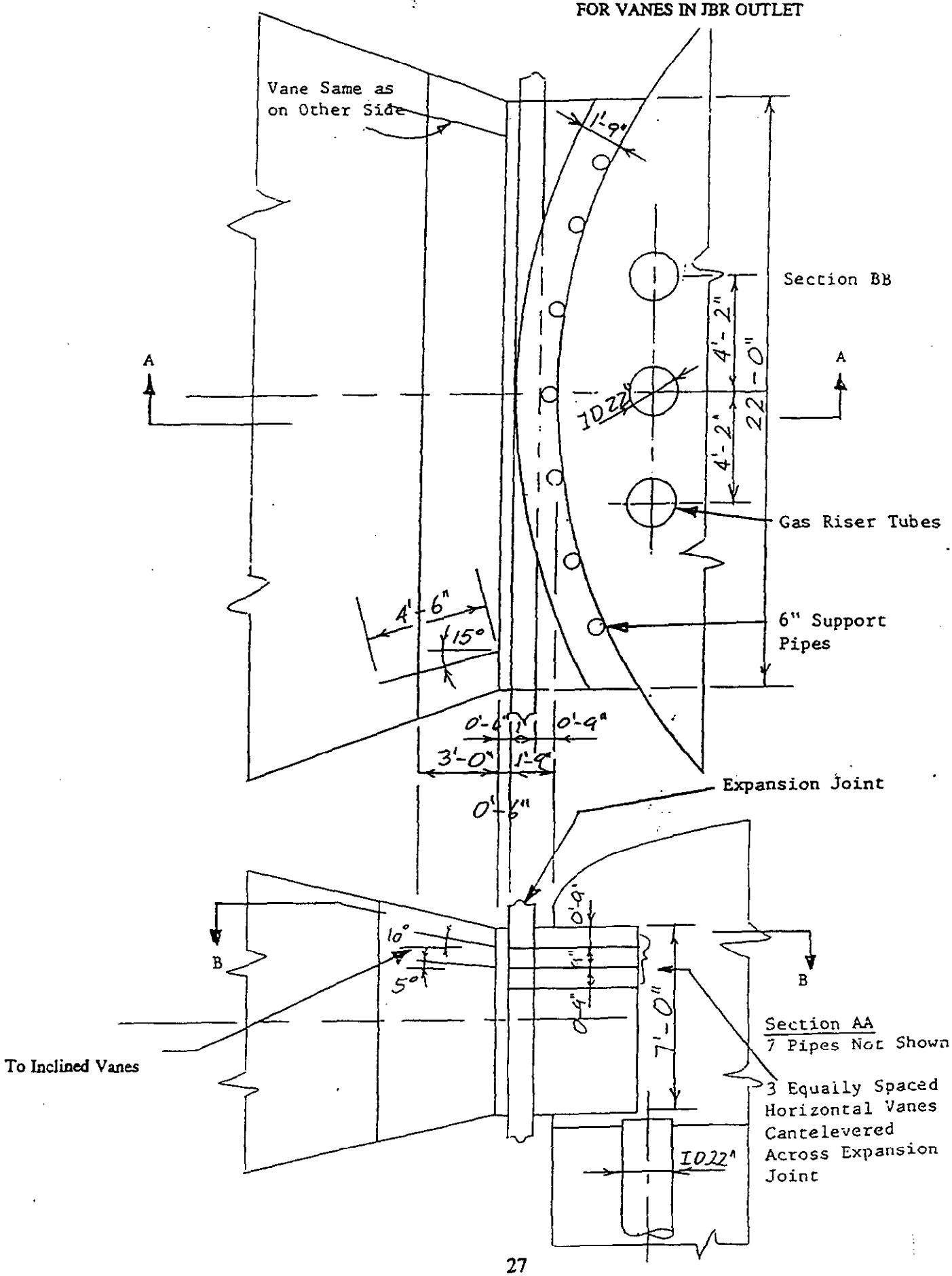

Figure 4-2 FIELD DIMENSIONS FOR DESIGN NO. 3
FOR VANES IN JBR OUTLET
RMS = 25% (0.25) Proposed Final Design

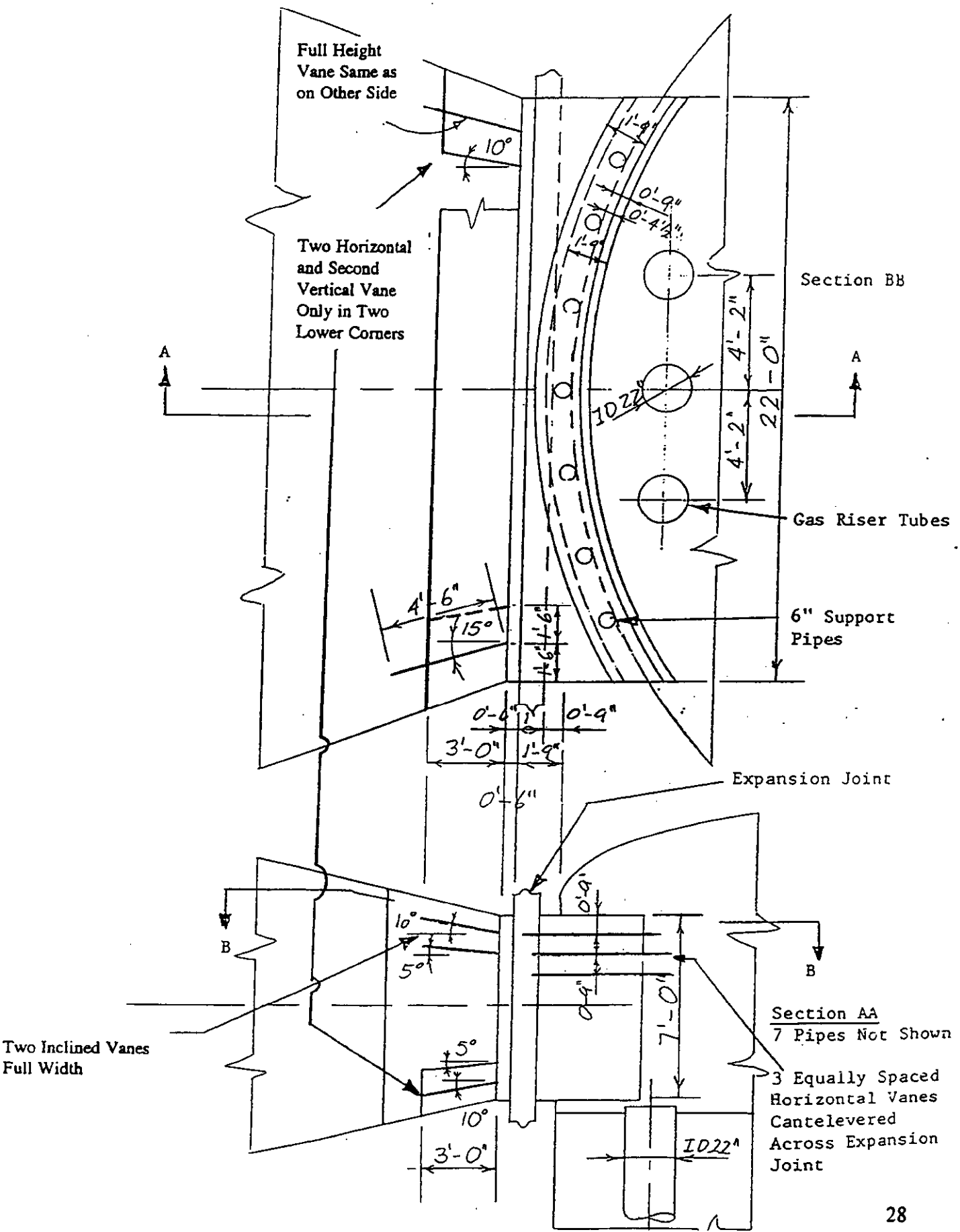

FIGURE 4-3 TEST No. 3 ISOVELOCITY CONTOURS
JBR PILOT PLANT MODEL TEST
TRAVERSE LOCATION: **V2 MIST ELIMINATOR INLET**
CONFIGURATION DESCRIPTION: **VANE SET 3 INSTALLED AT JBR OUTLET AS SHOWN ON FIGURE 4-2**

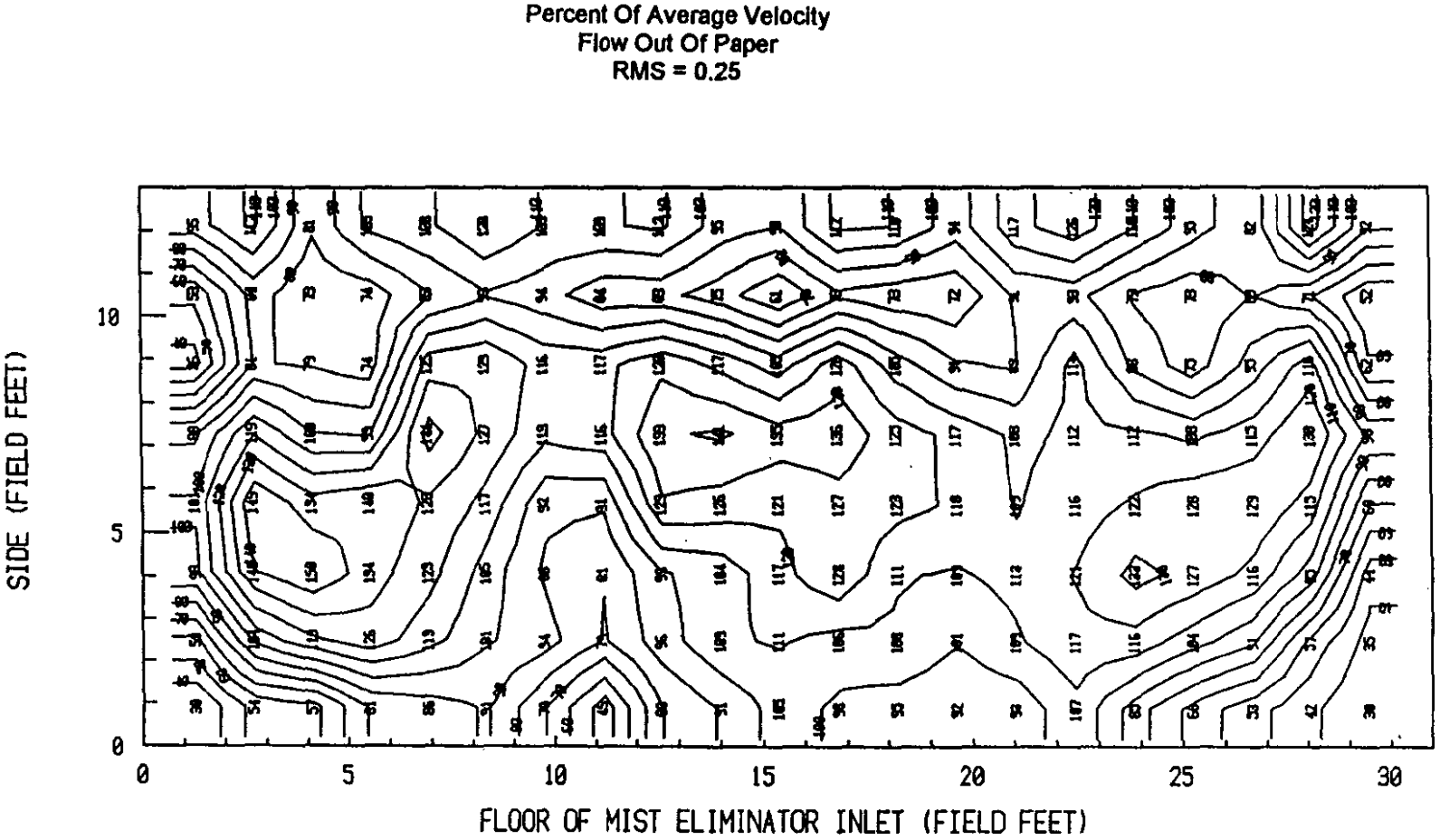

Figure 4-4

PHOTOGRAPHS OF VANES IN DUCT
BETWEEN JBR AND MIST ELIMINATOR

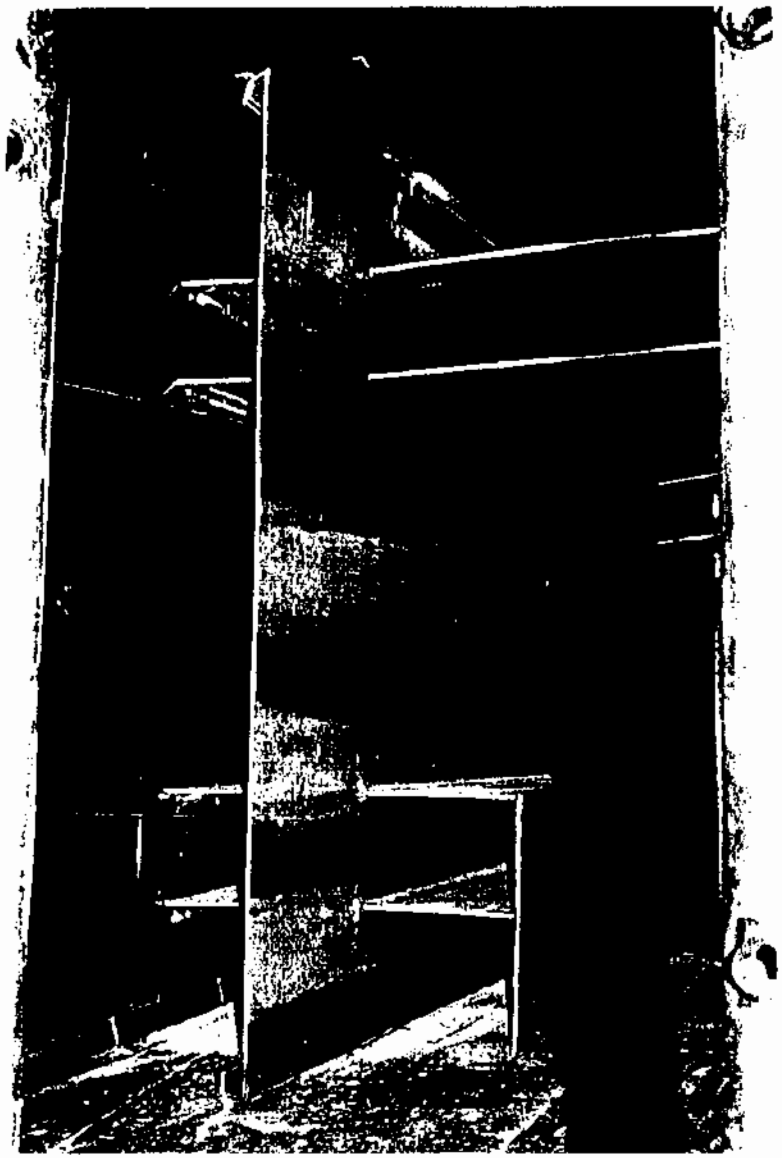

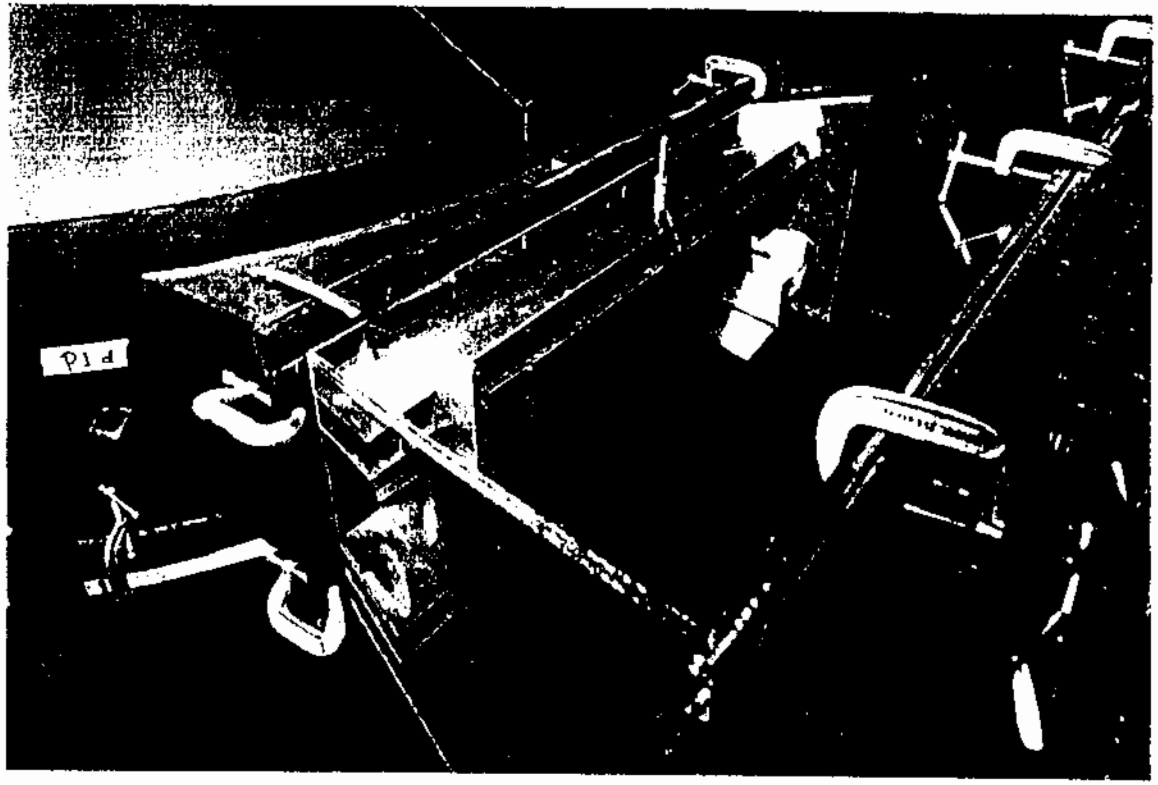

Section 5

DEVELOPMENT OF LIQUID COLLECTORS AND DRAINS

5.1 Evaluation Techniques Used

To select liquid collector designs and locations for a specific power plant duct system and stack geometry, the gas flow patterns and the behavior of liquid droplets and motion of liquid films must be evaluated in an experimental model.

Gas flow patterns are visualized using smoke filaments from a moveable injector tube attached to a smoke generator. By positioning the end of the tube anywhere in the duct, flow direction, swirl patterns, and flow separations can be identified. Small tufts of yarn mounted on movable rods are also used to look at small scale flow features.

Liquid injection into the model in the following ways is used to evaluate droplet trajectories, impingement locations, liquid motion on surfaces, drainage patterns, and reentrainment sites.

1. An aerosol generator that produces a cloud of small droplets (about 30 microns) is used to introduce droplets into the model inlet. They are carried through the duct and stack system by the gas flow and will deposit on the surfaces of the ducts and stack. By operating the model at a velocity level equal to the field velocity divided by the square root of the scale factor (8.91), impingement locations will be modeled (see Section 2.1.2).

2. Liquid is introduced onto surfaces by the aerosol generator, by a small spray nozzle, or by a syringe and long injection tube. The liquid motion on the surfaces can then be observed to determine, if the water naturally drains, where reentrainment occurs, where to put liquid collectors to intercept moving liquid, and where to install drains to remove the liquid from the duct system. This testing is carried out at the model flow condition that duplicates the field gas velocity head.

3. Liquid collectors and drains are then designed, installed, and evaluated in the same way as described above.

Liquid collectors and drains are added, changed, and modified until a design is achieved that is both effective for collecting and draining liquid and practical to install and maintain.

5.2 Description of the Gas Flow Patterns

The gas velocity profile entering the horizontal circular duct is fairly uniform after a 3 to 1 area contraction in the discharge manifold of the mist eliminator section (Figures 2-3 and 5-1) but within a short distance the gas velocity profile is distorted with a high value at the top of the horizontal duct due to the flow entering the 90° mitered elbow at the stack entrance.

The gas flow patterns show a fully developed double vortex pattern by the third miter cut of the elbow. This pattern is typical of 90° circular cross-section bends.

The qualitative velocity profile above the 90° mitered elbow shows a peak value in Figure 5-1 at the outside wall and a small reversed downflow at the inside of the elbow. The maximum measured velocity is 111% of the average near the outside as shown in Figure 3-5. Figure 3-1 shows a time average value of 66% of average velocity for the minimum velocity at the inside of the bend. Closer to the inside of the mitered bend the flow is unsteady and reversed under detailed observation.

The video recording (5 copies) supplied to Southern Company Services earlier shows the three dimensional gas flow patterns and the unsteady region in the FRP elbow very vividly. Appendix 1 gives a list of video titles of the video recording.

5.3 Liquid Behavior and Flow Patterns Without Liquid Collectors

Most droplets suspended in the gas flow will deposit on the outside of the 90° mitered bend (see Figure 5-2), except the very fine droplets. The deposited liquid moves to the inside of the bend under the shear action of the double gas flow vortexes. At the inside of the elbow, the liquid flows down to the third and second miter cuts and nearly all liquid is reentrained by the gas flow at the second miter cut. Most of the reentrained drops are carried out of the chimney.

These liquid flow patterns are shown in the video recording (see the list of video titles in Appendix 1).

5.4 Testing and Development of Liquid Collectors

Based on the gas and liquid flow observations in the liner, we reached the conclusion that liquid collectors are necessary to minimize the liquid discharge from the chimney.

A variety of liquid collectors were designed and discussed with Southern Company Services. Several jointly selected liquid collector concepts were experimentally evaluated in the wet duct-stack flow model. The best performing liquid collector concepts were modified and tested to optimize performance while trying to minimize cost and pressure loss.

The details of the development work are not described in this report. The final and recommended set of liquid collectors are described in full details in Section 6.0 and their performance is documented on the videotape.

Figure 5-1

BASIC GAS FLOW PATTERNS IN THE MITERED FRP ELBOW

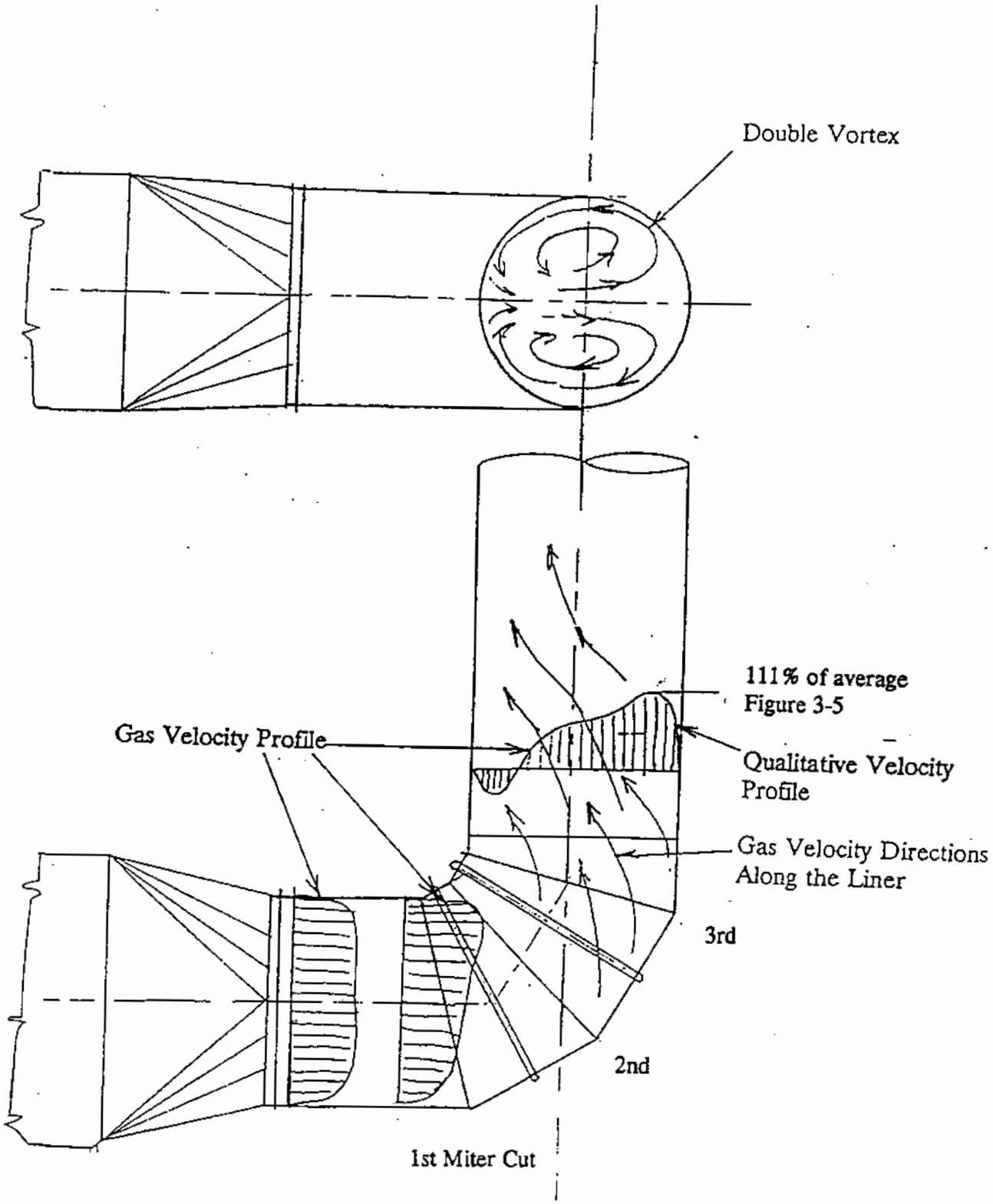

Figure 5-2

BASIC LIQUID FLOW PATTERNS IN THE MITERED FRP ELBOW

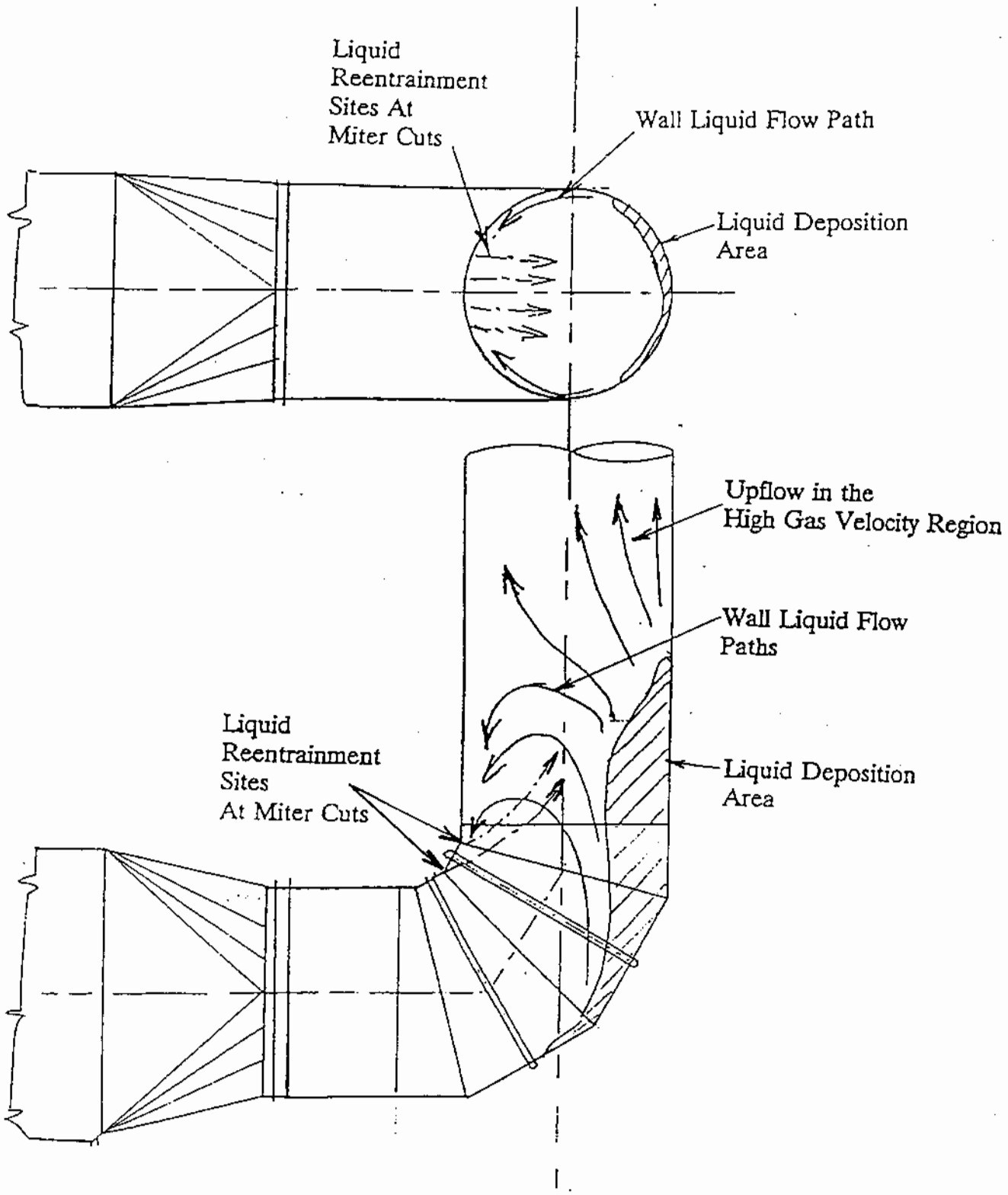

Section 6

GEOMETRY OF FINAL RECOMMENDED LIQUID COLLECTORS

6.1 The Final Recommended Liquid Collection System

The final liquid collectors (LC's) are numbered and described on Table 6-1. Also included on these tables is the purpose for each collector and comments on the size and installation. The geometry of the liquid collector assemblies and their individual pieces is presented on Figures 6-1 through 6-8 which are also listed on Table 6-1 opposite the appropriate collectors. Figure 6-1 shows the liquid collection system and the location of each liquid collector. Figure 6-10 is a photograph of the model liquid collection system.

The liquid collection system has only one drain pipe (LC2). It is important to prevent blockage of this drain, therefore, the installation of the drain cage (LC3) is necessary.

The liquid collection starts in the horizontal duct downstream of the mist eliminators with a drain fence (LC1) which guides liquid to the drain (LC2). The two side flow guides (LC4) prevent the liquid flow from the outside of the elbow to the inside of the elbow from where it can reentrain.

The major liquid deposition area (Figure 5-2) is covered with liquid collector grating. The grates between the second and third miter cuts (LC5) are above and below the lower collector ring (LC8). The grates in the vertical section of the liner (LC7) are tilted down from the center (Figure 6-5) to lead the liquid to the two sides of the grating.

Most of the liquid collected flows through the lower collector ring (LC8). It leads the liquid to the outside center of the elbow where it can flow under the grates (LC6 and LC5) to the drain. The upper collection ring (LC9) is the last of the liquid collectors in the liner. The liquid collected in the upper ring is directed through the vertical drain duct (LC10) to the lower collector ring. The connection between the upper ring and the vertical drain duct has to be sealed to prevent gas flow into the duct.

The slant flow guides (LC11 and LC12) guide the liquid towards the two sides of the vertical drain duct, (LC10). The slant angle of the flow guide (LC12) is lower due to the manhole location.

Photographs in Figures 6-9 to 6-13 show the final recommended liquid collection system installed in the 1:8.9 scale model of the absorber, duct, and stack.

The liquid collectors can handle a lot of liquid carryover and a nominal amount of solid carryover from the mist eliminators of the absorbers. The proper washing of the mist eliminators can prevent damaging the mist eliminator modules and reduce excessive solid carryover which is essential for good operation of the wet duct and stack system.

The liquid collectors should be inspected during scheduled and unscheduled outages and cleaned as needed during the first year. After experience is gained on the need for cleaning, the schedule and techniques for cleaning can be established. Normally, a once a year inspection and cleaning is sufficient.

The combined performance of all the liquid collectors provides a satisfactory liquid collection at all plant load levels. The tendency for liquid deposition and for reentrainment is high at high operating load levels. The opposite is true at lower operating loads, therefore, a larger percent of very small droplets will be discharged from the stack at low load operation contributing to the familiar white plume of the wet operation.

Using the geometry of the liquid collection system specified in Figures 6-1 to 6-8 and Table 6-1 Composit Construction & Engineering, Inc. prepared installation drawings for the liquid collectors. These drawings were reviewed and the final geometry for the liquid collectors was approved for installation by DynaFlow Systems.

Table 6-1A

LIST OF LIQUID COLLECTORS FOR YATES PLANT UNIT 1
JBR OUTLET DUCTS AND CHIMNEY

Collector Number (LC)	Figure	Description	Purpose	Comments
1	6-1 6-2	Drain Fence	To divert gas flow from the drain	12 in. high equal-sided triangle shape (optional)!
2	6-1 6-2	Drain Pipe	To drain liquid from chimney	6" pipe I.D.
3	6-1 6-2	Drain Cage	To prevent plugging of drain pipe	Cage is 10" dia. x 10" high wire construction with 2" x 2" openings
4	6-1 6-3 6-4	Side Flow Guides	Guide liquid to the drain pipe	T-shape 2" wide; 3" up 3" down. On both sides of the elbow.
5	6-1 6-4	Floor-grate in first miter	Promote deposition and protect drain liquid	MMFG DURADEK T-5000-2" Outside edges contact liner
6	6-1 6-4	Floor-grate in second miter	Promote deposition and protect drain	MMFG DURADEK T-5000-2" Outside edges contact liner
7	6-1 6-5	Floor-grate in vertical liner	Promote deposition and protect drain	MMFG DURADEK T-5000-2" Angled down 9.6° from horizontal. Outside edges contact liner.

Table 6-1B

LIST OF LIQUID COLLECTORS FOR YATES PLANT UNIT 1
JBR OUTLET DUCTS AND CHIMNEY

Collector Number (LC)	Figure	Description	Purpose	Comments
8	6-1 6-6	Lower Collector Ring	Collect and lead liquid to the outside of the bend.	3" wide x 10" high with seven 3" x 7" ribs on both halfs.
9	6-1 6-7 6-8	Upper Collector Ring	To guide liquid underneath, collect draining liquid from above and drain into lower ring.	3" wide 4" up and 4" down. Slopes 4.4° towards the inside of the bend. 2 1/2" x 6" cutout for liquid.
10	6-1 6-7 6-8	Vertical Drain Duct	To drain liquid from the top of LC8 into LC9.	Inside 7 1/2" x 2 1/2".
11	6-1 6-7	Slant Flow Guide	Guides liquid into circumferential motion.	2" wide x 3" up and 3" down. 30° slope.
12	6-1 6-7	Slant Flow Guide (Manhole Side)	Guides liquid into circumferential motion.	2" wide x 3" up and 3" down. Top edge is tangent to manhole cutout at a 10° slope.

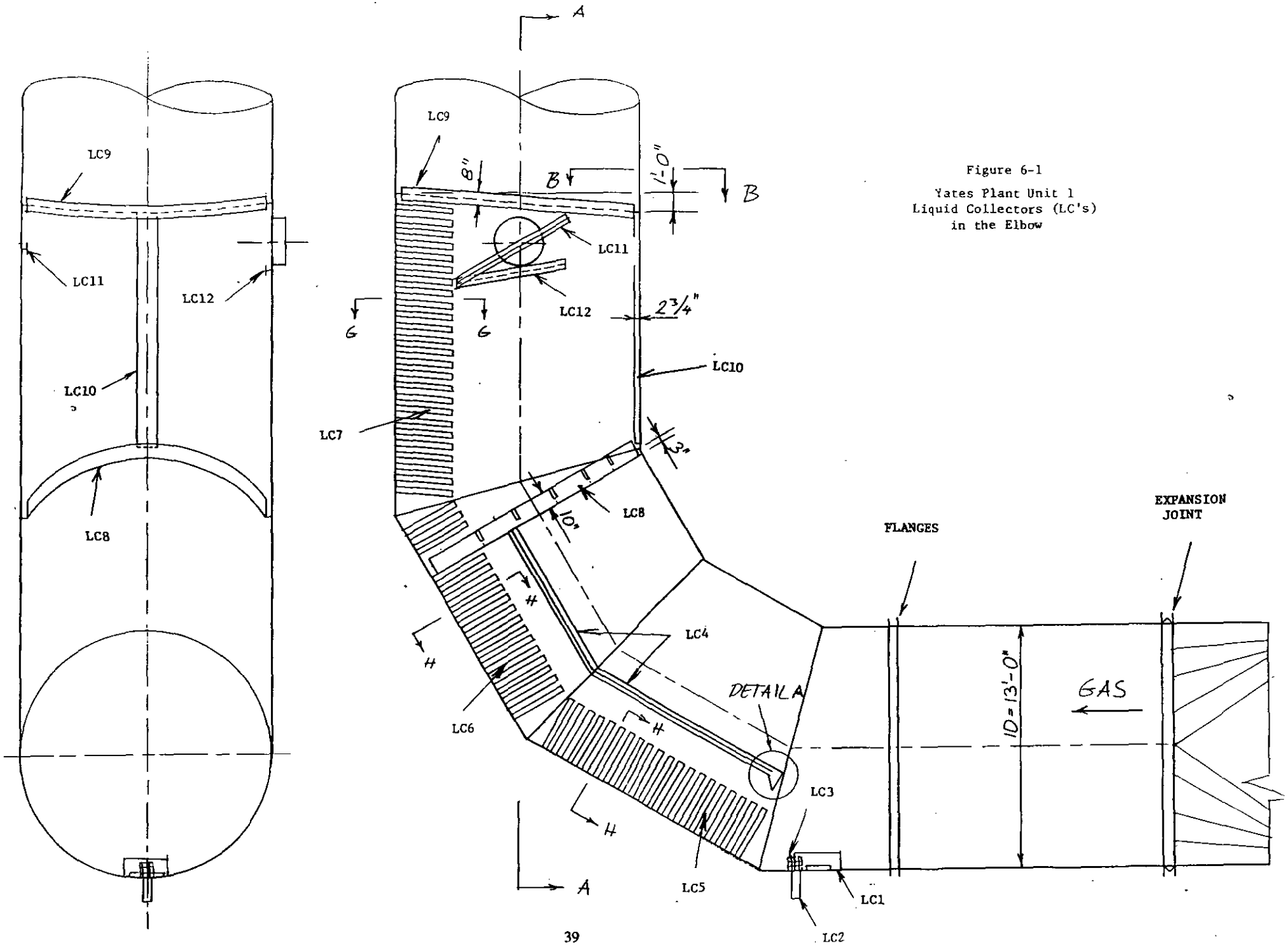

Figure 6-1

Yates Plant Unit 1
Liquid Collectors (LC's)
in the Elbow

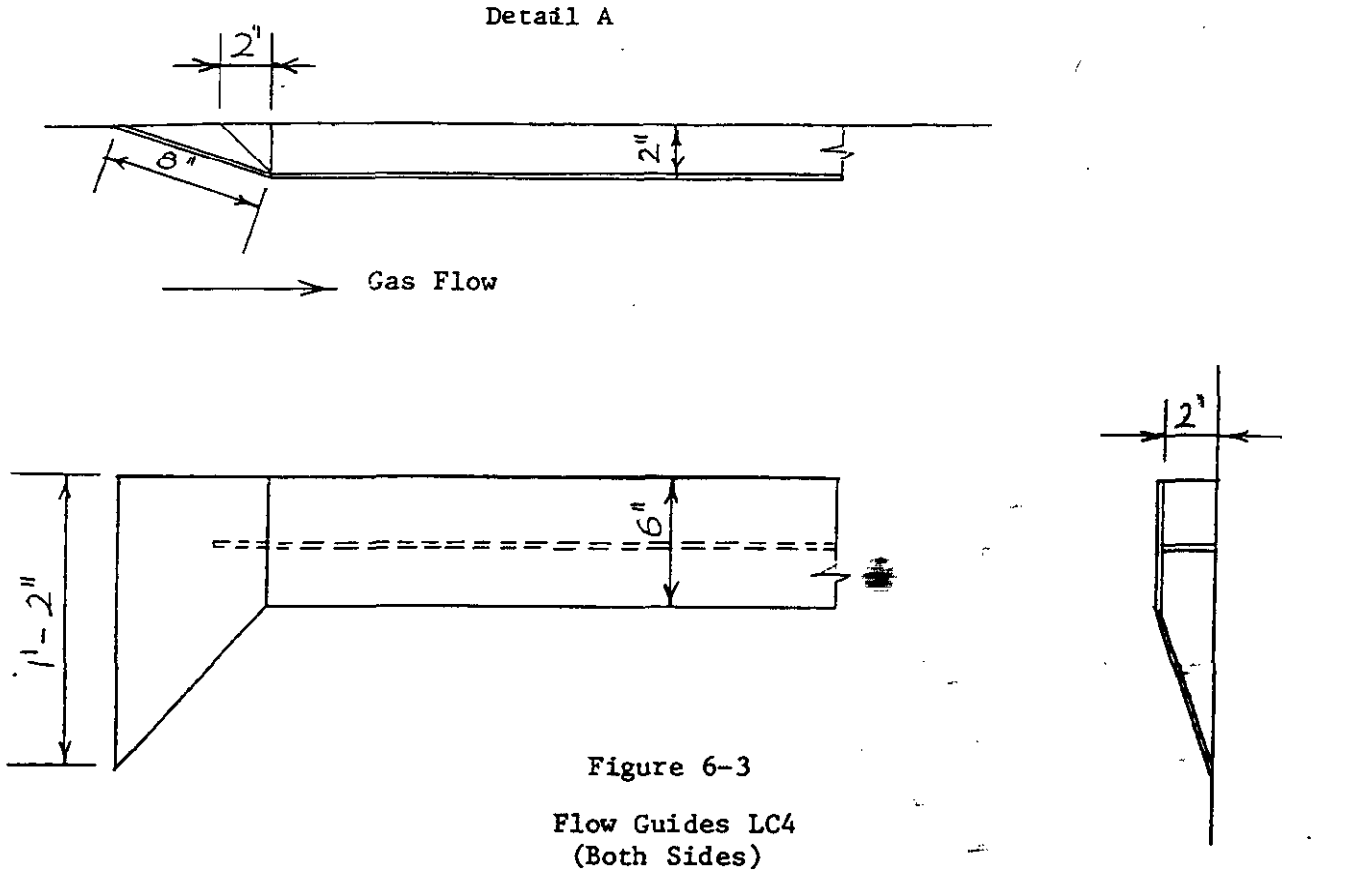

Figure 6-3

Flow Guides LC4
(Both Sides)

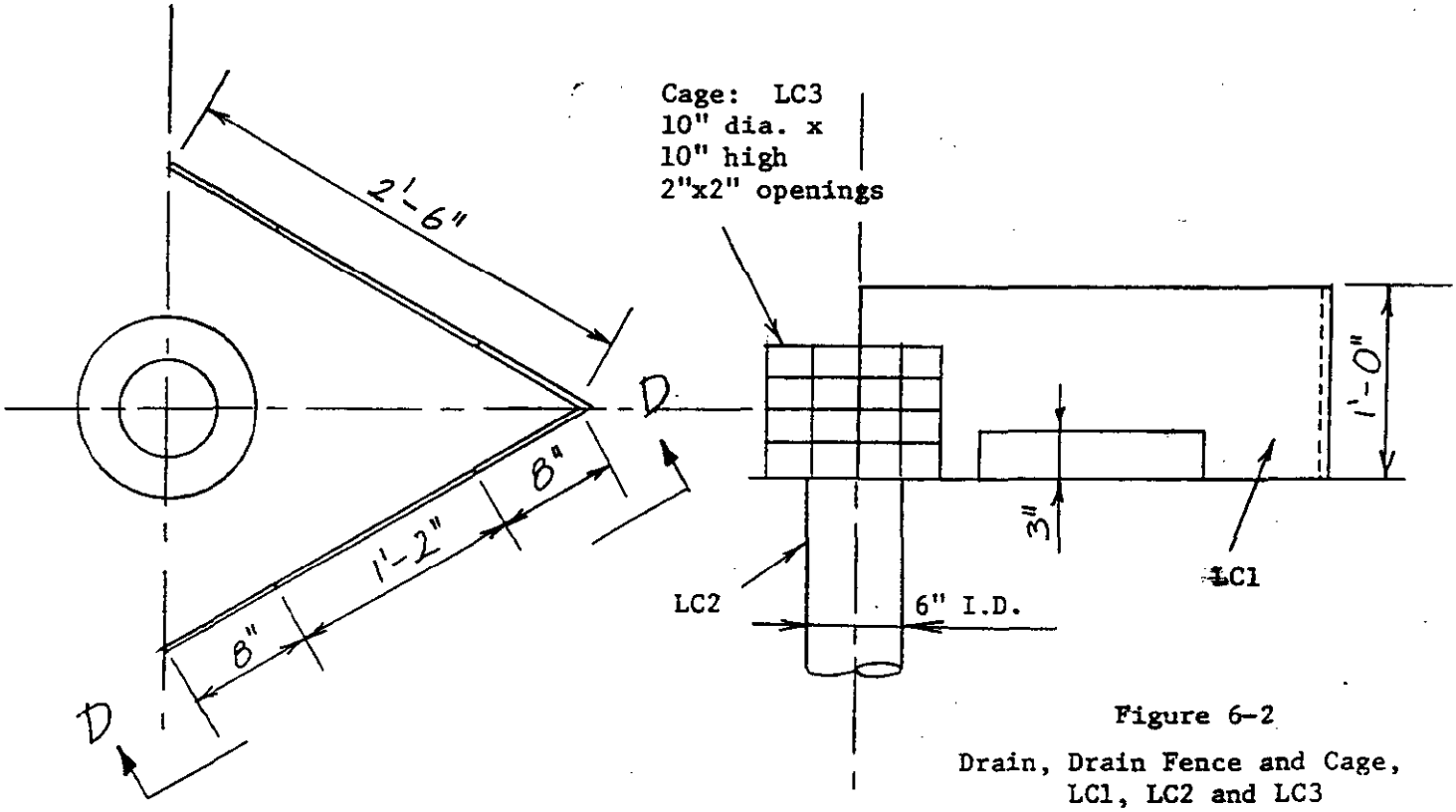

Figure 6-2

Drain, Drain Fence and Cage,
LC1, LC2 and LC3

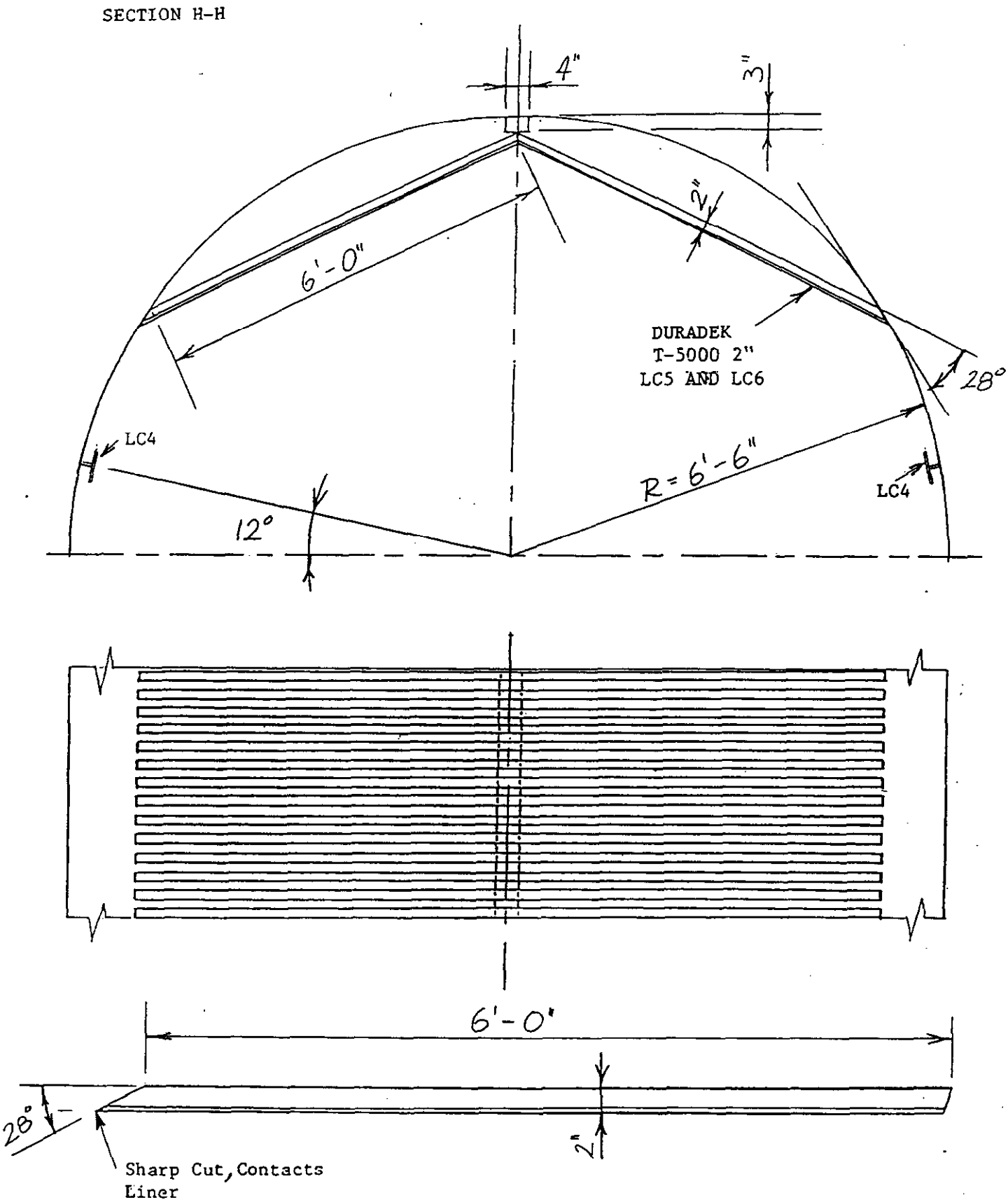

Figure 6-4

Grates in the Two Miters
LC4, LC5 and LC6

SECTION G-G

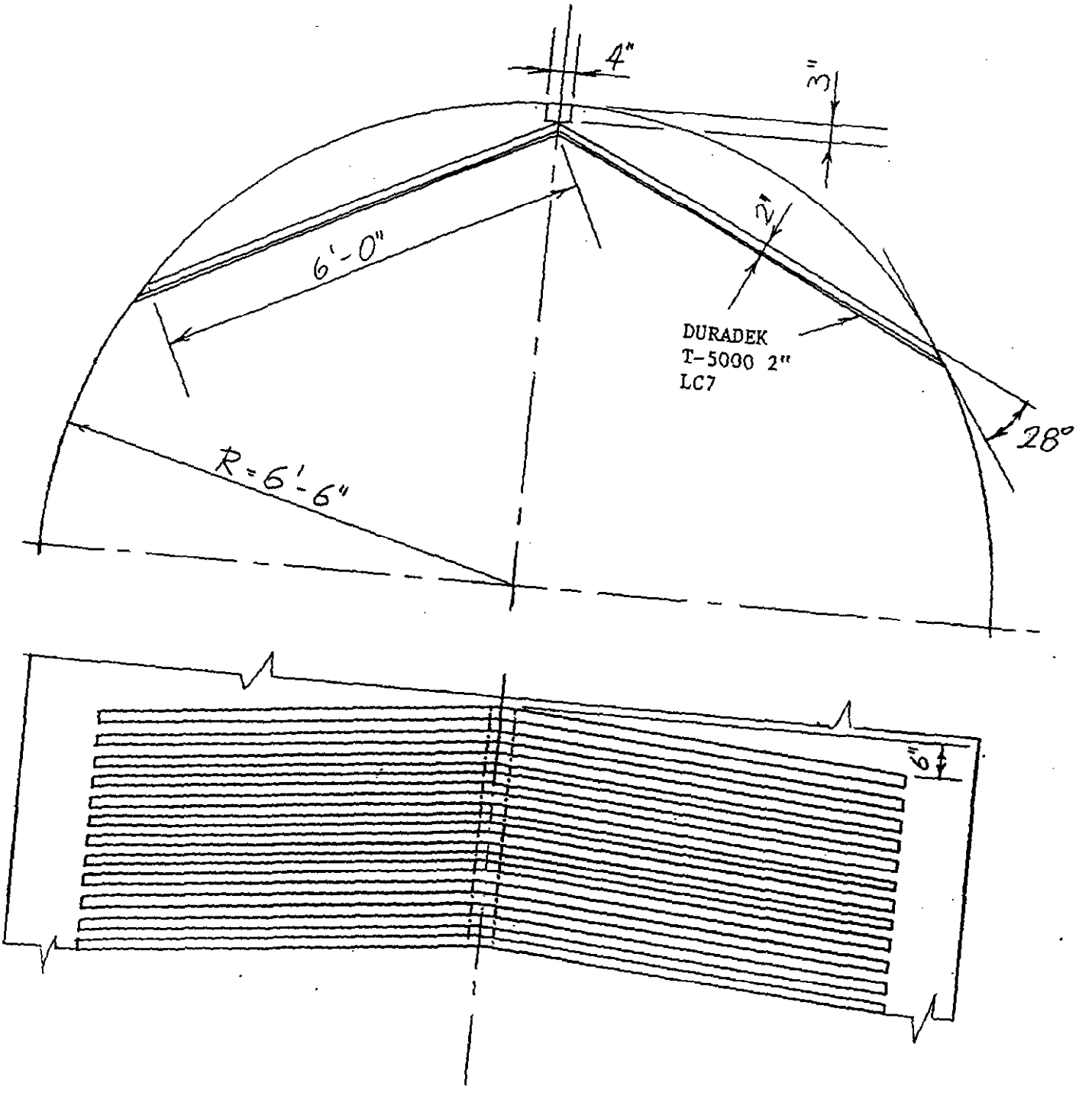

Figure 6-5

Grates in the Vertical Liner Section
LC7

Figure 6-6

Lower Collector Ring
LC8

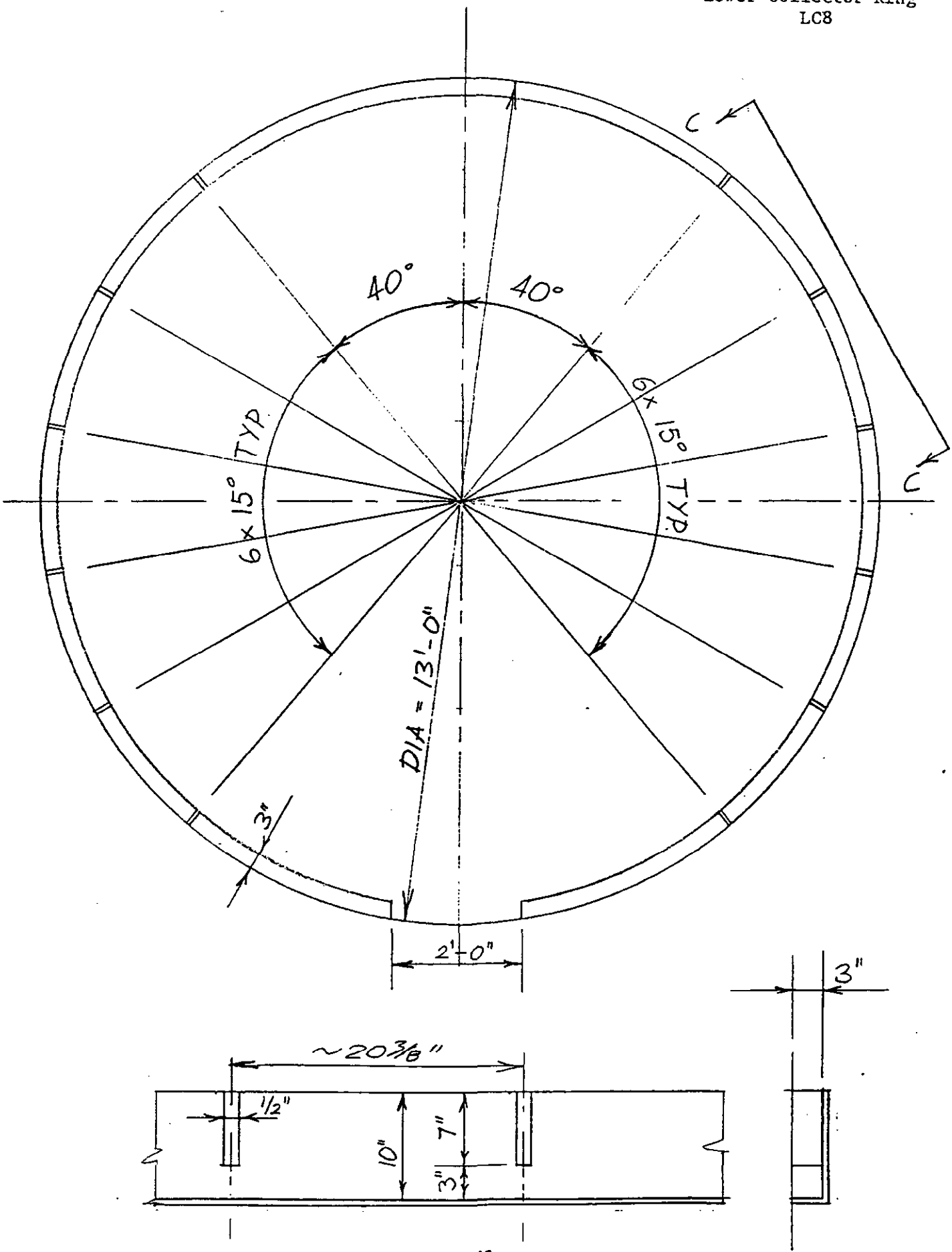

SECTION B-B

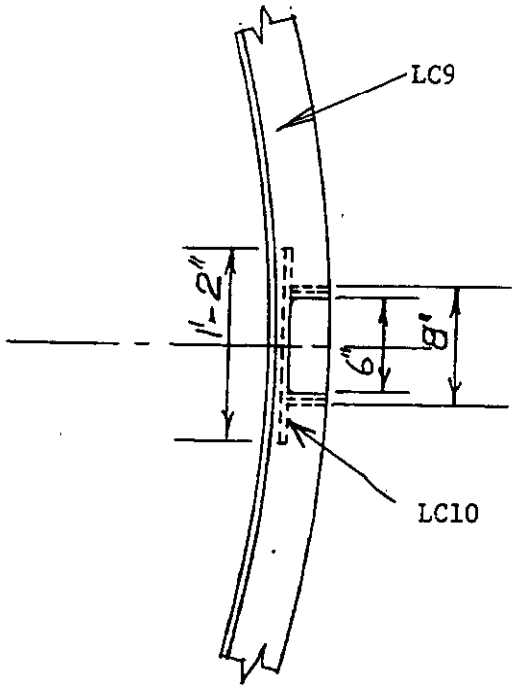

Figure 6-7

Upper Collector Ring and Vertical Drain Duct
LC9 and LC10

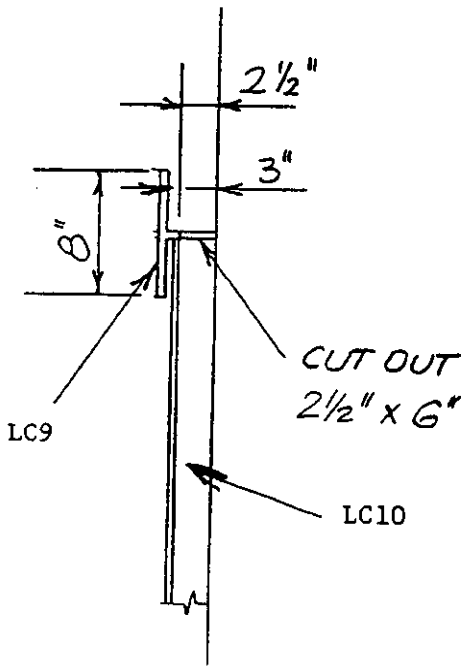

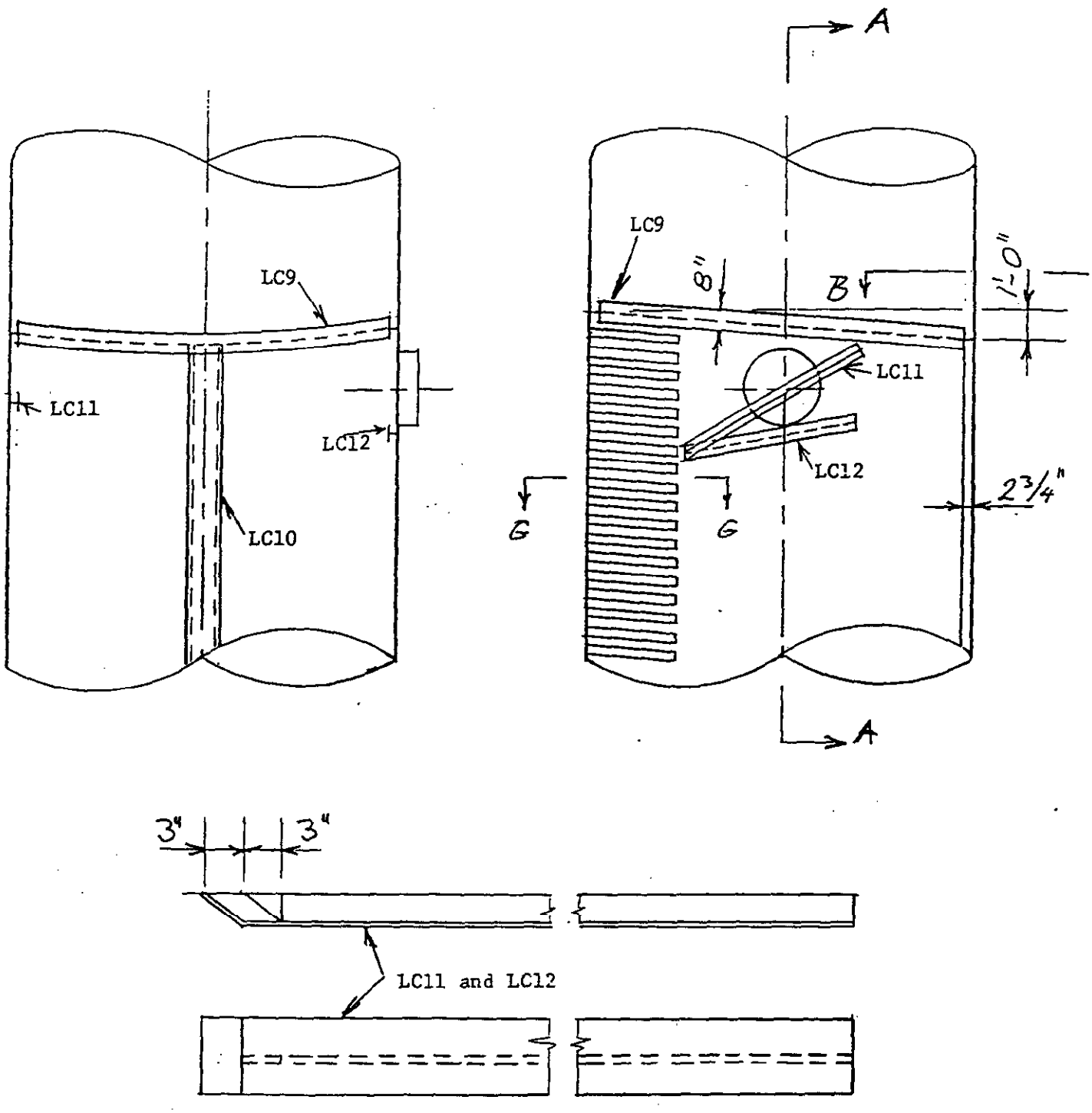

Figure 6-8

Upper Collector Ring, Vertical Drain Duct and
Slant Flow Guides
LC9, LC10, LC11 and LC12

Figure 6-9

VIEW OF THE MODEL LC'S FROM THE MIST ELIMINATORS

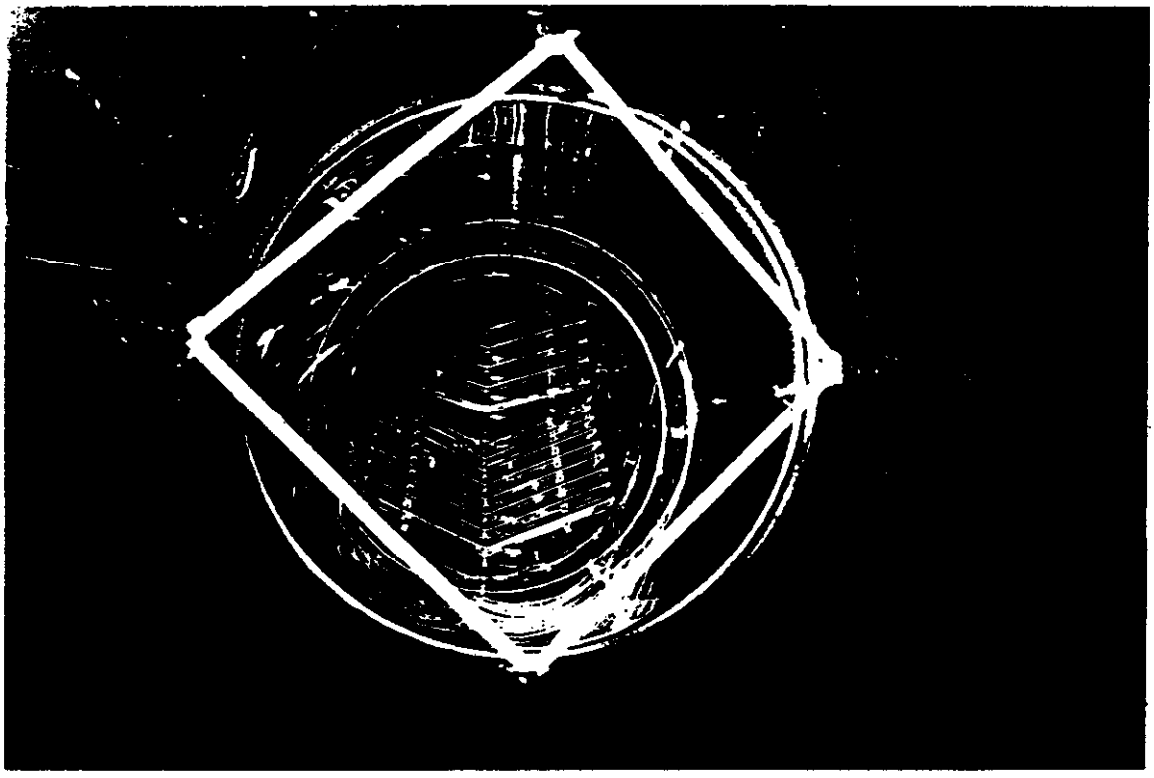

Figure 6-10

LIQUID COLLECTION SYSTEM IN THE MODEL

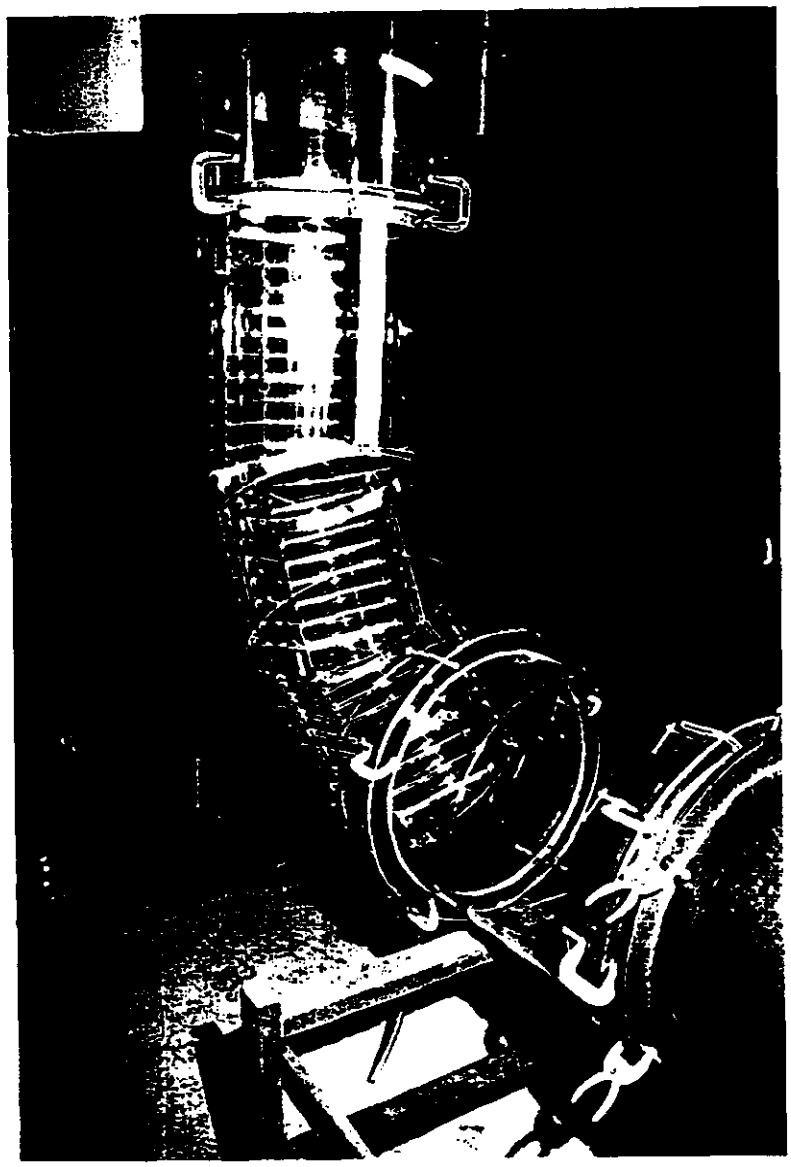

Figure 6-11

LOWER HALF OF THE LIQUID COLLECTION SYSTEM

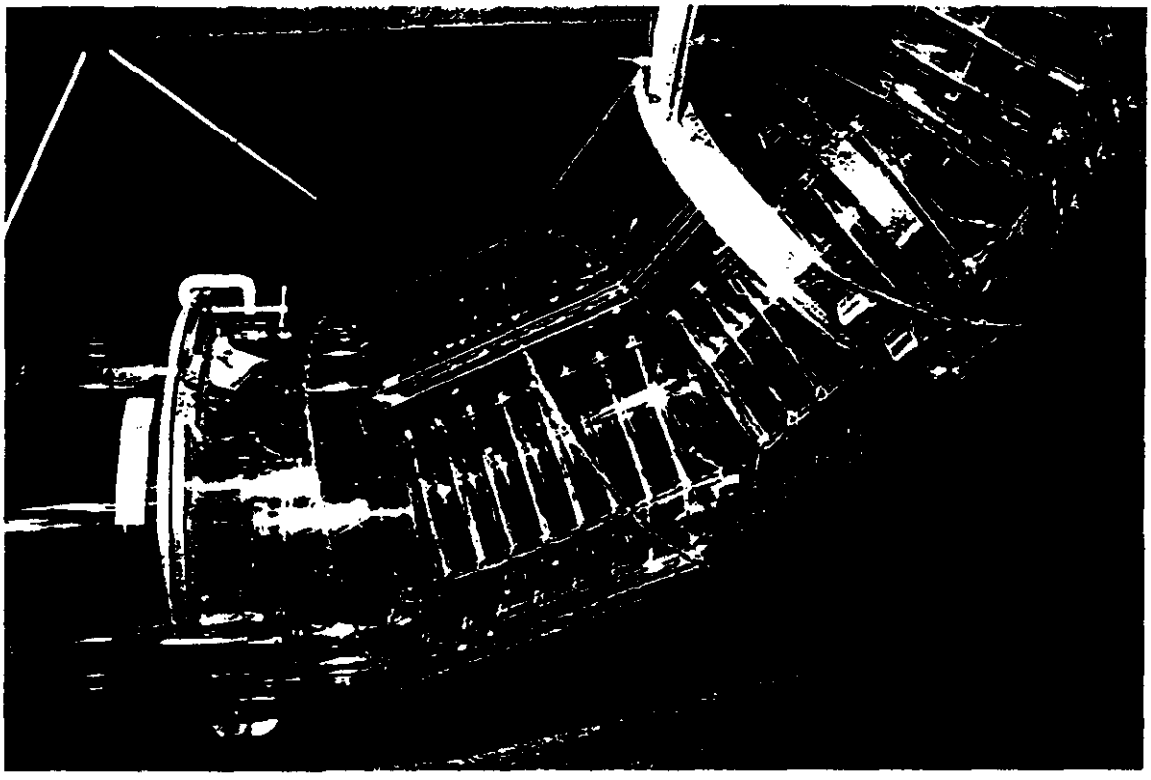

Figure 6-12

UPPER HALF OF THE LIQUID COLLECTION SYSTEM

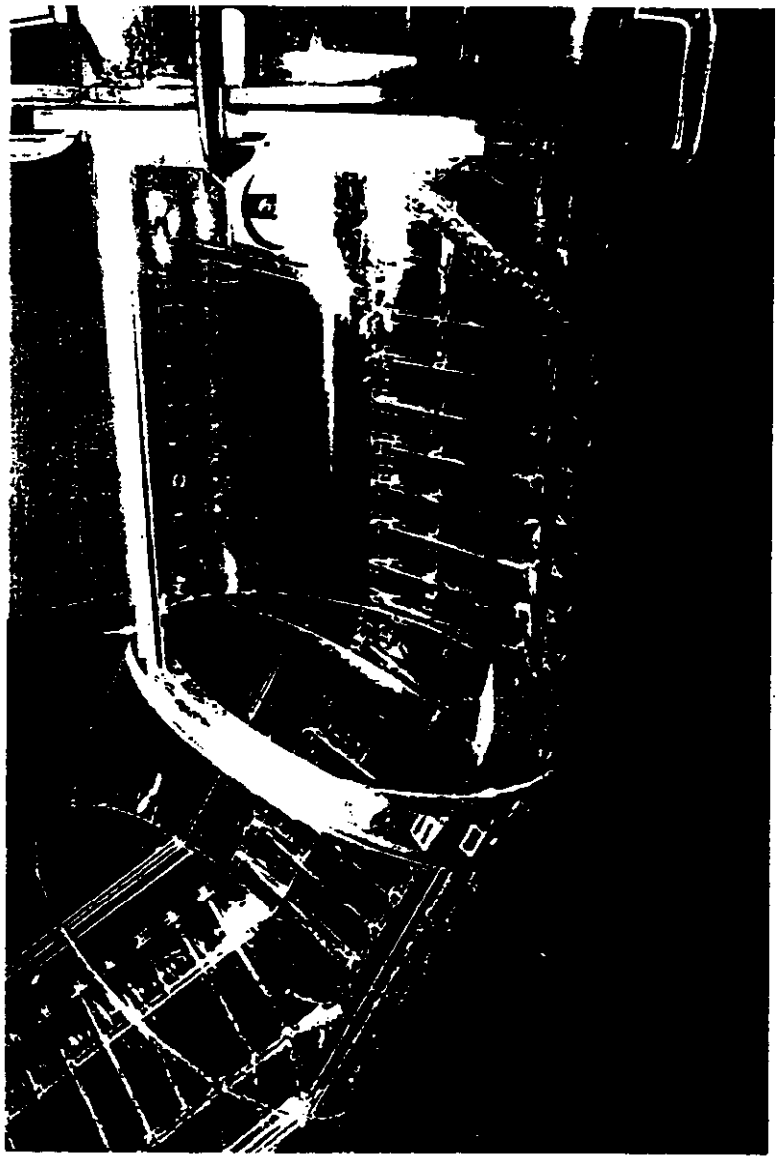

Figure 6-13

SIDE FLOW GUIDE (LC4) IN THE MODEL AND IN THE FIELD ELBOW

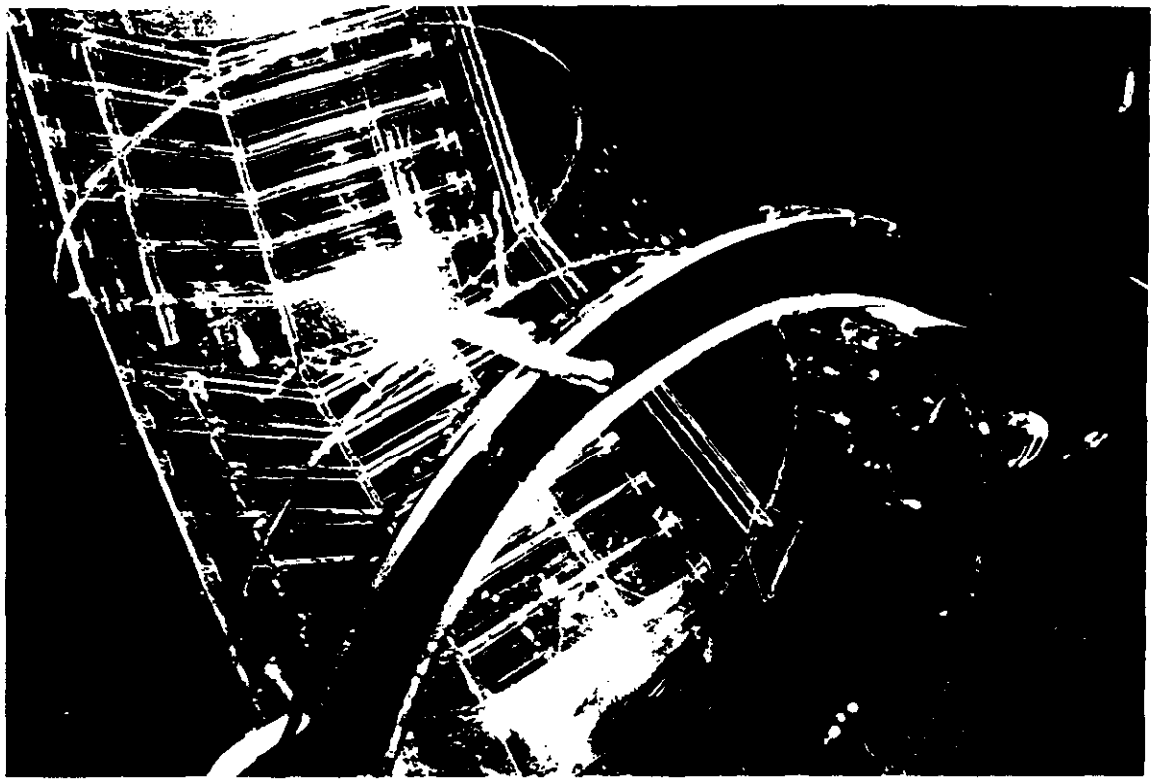

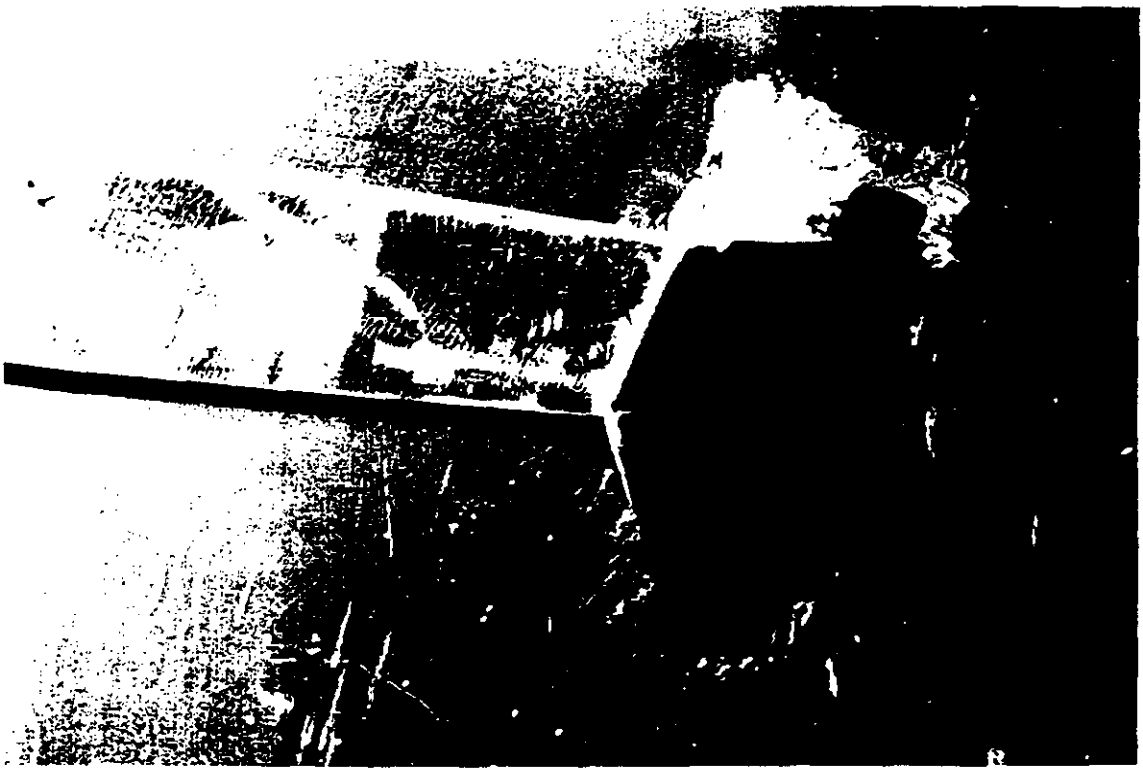

Section 7

EVALUATION OF CONDENSATION IN THE STACK LINER OF THE 100 MW CT-121 FGD SYSTEM AT PLANT YATES

One of the sources of liquid in the stack system is condensation from the saturated gas on the duct and stack liner surfaces. The rate of heat transfer and thermal condensation on the liner surfaces is a function of the chimney construction, the internal gas flow conditions, and the atmospheric air temperature and wind velocity. The other mode of liquid condensation is by adiabatic expansion along the height of the stack. The elevation difference from the breaching duct to the top of the stack produces an appreciable amount of liquid condensation in the bulk of the gas flow caused by the temperature and pressure drop from adiabatic expansion. A fraction of this liquid deposits on the stack liner surface by turbulent deposition and the rest will discharge from the top of the stack as very small droplets in the plume of the gas stream.

Analytical calculations were carried out using our computer program to estimate the rate of liquid condensation on the liner wall and in the bulk of the flue gas along the height of the stack from the horizontal duct to the top of the stack liner.

The total liner height of 231.5 ft. was divided into ten sections of selected heights according to the geometry of the stack design for the numerical calculations. The chimney is an uninsulated FRP liner with a constant internal diameter of 13'-0". A 90° mitered elbow connects the horizontal duct to the liner as shown in Figure 2-1.

An assumed "reasonable worst" cold ambient condition and selected plant operation conditions at which the condensation calculations were carried out are the following:

100% MCR Flow Condition at the Stack Entrance

Volume Flow Rate	:	406,400 ACFM
Temperature	:	126°F

Ambient Conditions (selected "reasonable worst")

Barometric Pressure at Ground Level	:	14.30 psia
Air Temperature	:	10°F
Wind Velocity	:	58.65 fps 40 mph

Detailed input and output data listings are given in Tables 7-1 and 7-2.

The results of the calculation are given on the output sheet as functions of the stack height.

The adiabatic bulk condensation rate is 0.69 gpm which is relatively low due to the short height of this stack. But the thermal wall condensation is 3.79 gpm, which is high compared to typical power plant stacks with thermal insulation and concrete shell surrounding the liner.

These condensation rates are conservative and close to the maximum at this site. The thermal condensation rate is lower at higher ambient temperatures, (e.g. it is half at 70°F ambient air temperature, about 1.9 gpm.) The thermal condensation is uniformly distributed along the height of the stack. At the average gas velocity of 51 fps in the liner at 100% load the condensed liquid is expected to flow down on the liner surface to the upper collector ring without reentrainment if the liner inside surface does not have larger than 1/8 inch sharp discontinuities.

Table 7-1

```
CONDENSATION IN CHIMNEY - PROGRAM INPUTS
========================================
RUN NUMBER                  DATE    8-7-91
PROJECT NUMBER SCS-1   BASIC CONDITIONS:
     Relative Humidity=100%, Load=100% MCR
     Wet mode of operation
     Liner only, no shell

DESIGN PARAMETERS:
==================
VOLUME FLOW RATE OF FLUE GAS      = 4.0640E+05     CFM
INLET TEMPERATURE OF FLUE GAS     =   126.0000     F
AMBIENT AIR TEMPERATURE           =    10.0000     F
WIND VELOCITY                     =    58.7000     FT/SEC
ATM.PRESS. AT BASE OF STACK       =    14.3000     PSIA

FLUE GAS PROPERTIES:
====================
SPECIFIC HEAT OF FLUE GAS         =     0.2400     BTU/LBM F
DENSITY OF FLUE GAS               =     0.0651     LBM/FT3
THERMAL CONDUCTIVITY OF FLUE GAS  =     0.0163     BTU/HR FT F
KINEMATIC VISCOSITY OF FLUE GAS   = 1.7200E-04     FT2/SEC
SPECIFIC VOLUME OF WATER VAPOR    =   173.5750     FT3/LBM
PRANDTL/SCHMIDT NUMBERS           =     1.0000     ------
PRANDTL NUMBER OF GAS             =     0.7000     ------
MOL. WEIGHT OF DRY FLUE GAS       =    30.2300     LBM/LB MOLE
MOL. WEIGHT OF WET FLUE GAS       =    28.6388     LBM/LB MOLE

AMBIENT AIR PROPERTIES:
=======================
SPECIFIC HEAT OF AIR              =     0.2390     BTU/LBM F
THERMAL CONDUCTIVITY OF AIR       =     0.0130     BTU/HR FT F
DENSITY OF AIR                    =     0.0822     LBM/FT3
KINEMATIC VISCOSITY OF AIR        = 1.3200E-04     FT2/SEC
PRANDTL NUMBER OF AIR             =     0.7200     ------

LINER AND SHELL PROPERTIES:
===========================
THERMAL CONDUCTIVITY OF LINER     =     0.1300     BTU/HR FT F
EMISSIVITY OF THE LINER           =     0.8600     ------
STACK ENTRANCE LOSS COEFFICIENT   =     0.3000     ------
BREACHING DUCT X-SECTIONAL AREA   =   132.7000     FT2

GEOMETRY - MAJOR INTERNAL DIMENSIONS:
=====================================
TOTAL STACK HEIGHT                    231.50 FT
NUMBER OF SECTIONS                      8
LINER AT BOTTOM OF BREECHING   ID =    13.00 FT
                                H =     0.00 FT
LINER AT TOP OF STACK          ID =    13.00 FT
                                H =   231.50 FT
```

Table 7-2

CONDENSATION IN CHIMNEY - SUMMARY OF PROGRAM OUTPUT

RUN NUMBER 47 DATE 8-7-91
PROJECT NUMBER SCS-1 BASIC CONDITIONS:
Relative Humidity=100%, Load=100% MCR
Wet mode of operation
Liner only, no shell

CONDENSATION RESULTS (Values at Section Exit)

Section No. (-)	Length (ft)	Stack Height (ft)	Condensed Bulk Liquid (lbm/min)	Condensed Bulk Liquid (lbm/min ft)*1000	Wall Condensation (lbm/min)	Wall Condensation (lbm/min ft)*1000
1-3	20.96	20.96	0.43	20.48	2.80	133.39
4	25.46	46.42	0.63	24.64	3.18	124.94
5	30.00	76.42	0.75	25.06	4.24	141.36
6	30.00	106.42	0.75	25.11	4.24	141.18
7	30.00	136.42	0.75	25.12	4.23	141.00
8	30.00	166.42	0.75	24.92	3.98	132.60
9	30.00	196.42	0.74	24.74	3.73	124.17
10	35.08	231.50	0.88	25.07	4.93	140.45
TOTALS	LBM/MIN		5.68		31.31	
GR/ACF	EQUIVALENT		0.0979		0.5394	
GPM			0.69		3.79	

TEMPERATURES (Values at Section Center)

Section No. (-)	Length (ft)	Stack Hgt(ft)	Liner I.D. Temp. (F)	Gas Temp. (F)
1-3	20.96	10.48	121.45	125.96
4	25.46	33.69	121.66	125.87
5	30.00	61.42	120.97	125.78
6	30.00	91.42	120.86	125.67
7	30.00	121.42	120.75	125.56
8	30.00	151.42	120.93	125.46
9	30.00	181.42	121.13	125.36
10	35.08	213.96	120.42	125.25

VELOCITY AND PRESSURE INSIDE LINER (Values at Section Exit)

Section No. (-)	Length (ft)	Stack Hgt(ft)	Static Pressure (in H2O absolute)	Static Pressure * (in H2O)	Q/A (ft/sec)
0	0.00	0.00	395.434	-0.447	51.04
1-3	20.96	20.96	395.006	-0.875	51.07
4	25.46	46.42	394.669	-1.212	51.09
5	30.00	76.42	394.272	-1.609	51.12
6	30.00	106.42	393.876	-2.005	51.15
7	30.00	136.42	393.480	-2.401	51.17
8	30.00	166.42	393.084	-2.797	51.20
9	30.00	196.42	392.689	-3.193	51.23
10	35.08	231.50	392.226	-3.655	51.26

* Static pressure relative to ambient barometric pressure at breaching duct floor level.

Section 8

FINAL DRY TESTS WITH LIQUID COLLECTORS INSTALLED

8.1 Velocity Traverse Results

With the required final liquid collectors installed in the mitered elbow, the flow separations off of miter corners and liquid collectors coupled with a reduction in open area due to the liquid collectors have combined to make the velocity profile more distorted than the original open mitered elbow. The isovelocity contour plot is presented on Figure 8-1. It compares to the original open mitered elbow as follows.

	Mitered Elbow With Final Liquid Collectors	Open Mitered Elbow
RMS	0.30	0.147
% Within ± 10% $V_{avg.}$	20%	37.5%
% Within ± 15% $V_{avg.}$	25%	80.0%
% Within ± 25% $V_{avg.}$	40%	87.5%
Lowest % $V_{avg.}$	42%	63%
Highest % $V_{avg.}$	136%	112%

Even though the final velocity profile is more distorted, the extensive liquid collectors will collect the liquid, protect the liquid from reentrainment, and allow the liquid to drain thereby minimizing the potential for stack liquid droplet discharge.

The final liquid collector tests also included Vane Set 3 (Figure 4-2) installed at the JBR outlet. The velocity profile at the ME inlet was not repeated since no changes were made upstream of the stack inlet elbow that could affect the flow patterns upstream of the mist eliminator. The mist eliminator velocity profile shown on Figure 4-3 and Table 4-1 represent the final geometry results which were discussed in Section 4.

8.2 Pressure Loss Due to Liquid Collectors

The results of the pressure loss test with Vane Set 3 and the final liquid collectors installed is tabulated on Table 3-2 in the righthand column. The data for both the initial design with no liquid collectors and the final design with liquid collectors are compared side by side for field total pressure loss value in inches of water at 100% load.

The pressure loss from the JBR outlet plenum to the mist eliminator inlet has reduced slightly to a value of 0.33 inches of water due to the installation of the turning vanes. The pressure loss in the mitered elbow with the final liquid collectors installed increased from 0.15" of water to 0.44" of water. The actual field pressure loss is expected to be slightly less than the 0.44" water value because some of the model liquid collectors had to be made larger than scaled size to operate correctly from a liquid behavior standpoint.

Figure 8-1

ISOVELOCITY CONTOURS IN 13' DIAMETER STACK ELBOW OUTLET
JBR PILOT PLANT MODEL TEST
TRAVERSE LOCATION: V5 IN STACK LINER
CONFIGURATION DESCRIPTION: VANES IN JBR OUTLET (FIGURE 4-2)
FINAL LIQUID COLLECTORS IN DUCT AND STACK ELBOW

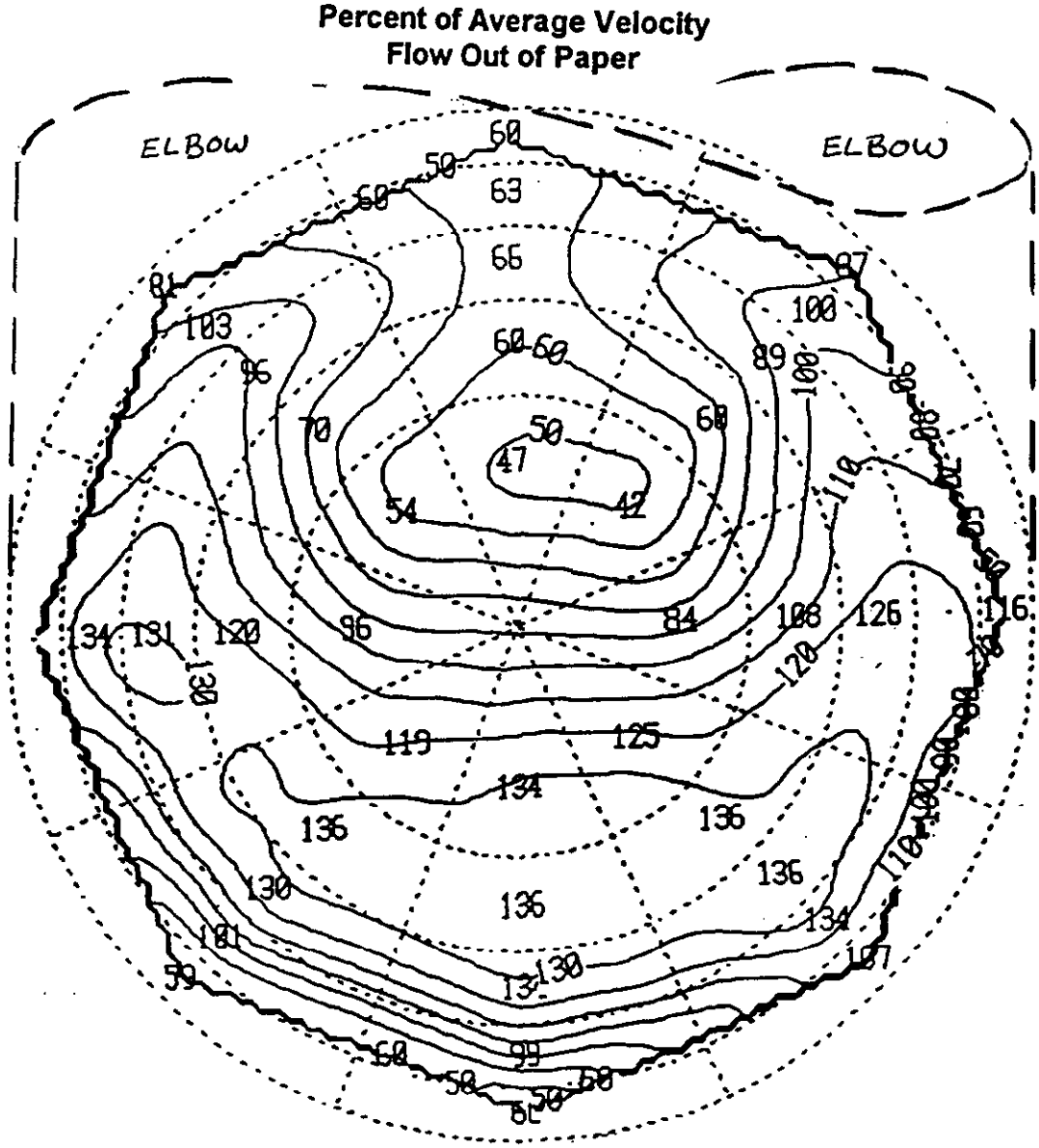

40 points measured at center of equal area segments
% of data within bands
20% within ±10% of Vavg
25% within ±15% of Vavg
40% within ±25% of Vavg

RMS = 0.30

APPENDIX

Appendix A1

LIST OF TITLES FOR VIDEO RECORDING

APPENDIX A1

LIST OF TITLES FOR VIDEO RECORDING

- CLEAN COAL TECHNOLOGY
  DEMONSTRATION PROGRAM
  CT-121 FGD Process

- SPONSOR:
  SOUTHERN COMPANY
  SERVICES INC.

- AT PLANT YATES
  GEORGIA POWER COMPANY

- GAS AND LIQUID FLOW
  CONTROL DEVELOPMENT
  By: Gerald B. Gilbert
  Lewis A. Maroti
  DynaGen, Inc.
  April 1992

- LABORATORY FLOW MODEL
  ABSORBER TO STACK LINER
  Scale 1:9

- MODEL INSTALLATION
  WITHOUT VANES AND
  LIQUID COLLECTORS

- GAS FLOW PATTERNS IN JBR
  DISCHARGE DUCT

- GAS FLOW IN FRP
  ELBOW AND LINER

- GAS-LIQUID FLOW PATTERNS
  IN FRP ELBOW
  100% LOAD

- MODEL INSTALLATION
  WITH VANES AND
  LIQUID COLLECTORS

- GAS FLOW PATTERNS IN JBR DISCHARGE DUCT WITH VANES
- LIQUID COLLECTORS IN THE FRP ELBOW
- MAJOR LIQUID COLLECTORS
- GAS FLOW IN FRP ELBOW WITH LIQUID COLLECTORS
- GAS-LIQUID FLOW PATTERNS IN FRP ELBOW WITH LIQUID COLLECTORS
- THE END

Appendix A2

COMMENTS ON DUCT DESIGN FROM THE JBR OUTLET TO THE STACK LINER FOR THE CHIYODA CLEAN COAL TECHNOLOGY PROJECT AT PLANT YATES UNIT 1

APPENDIX A2

COMMENTS ON DUCT DESIGN FROM THE JBR OUTLET TO THE STACK LINER FOR THE CHIYODA CLEAN COAL TECHNOLOGY PROJECT AT PLANT YATES UNIT 1

Task 1B, SCS Contract No. 195-89-015

Lewis A. Maroti
Gerald B. Gilbert
DynaGen, Inc.

May 29, 1991

1. JBR to Mist Eliminator

   a. The velocity variation along the ducts is acceptable for the geometry selected although it could be improved. There is about 20% reduction in velocity from the 47 riser gas tubes to the 7' x 22' vessel outlet port although in between the gas velocity drops lower in the discharge header and then reaccelerates into the outlet duct. Then there is a 2.64 discharge to inlet area ratio through the diffuser from the JBR outlet to the mist eliminator inlet. The equivalent cone angle of the diffuser is 37.2° which would result in separated diffuser flow even with a uniform flow out of the JBR port.

   b. In the model tests, we will measure the mist eliminator inlet face velocity profile, compare it to the velocity uniformity required by the mist eliminator manufacturer, and design internal flow distribution devices required to achieve the specified flow uniformity.

   c. The basic duct geometry in this section is an acceptable design for the limited space available (100' from JBR to stack) and no changes are required. However, the design could be improved by using a JBR outlet duct width equal to the mist eliminator module width (31'-3 1/4") to reduce the JBR outlet velocity level and reduce the diffuser area ratio.

2. Mist Eliminator Housing (13' high x 31'-3 1/4" wide x 12'-8" long)

   a. The location of the two mist eliminator stages in the housing and the spacing between them is good.

   b. One potential problem is the drainage of liquid from the bottom of the two mist eliminator stages to the two drains between them. It is unclear on drawing EC-1216 where the blades will sit vertically in the lower support U-channels that have the drain slots out the bottom. Is this a field proven design?

c. Pressure drop across the second stage mist eliminator and the gas velocity produced in the slot under the mist eliminator may drag the collected liquid up the incline toward the mist eliminator housing outlet and stack.

d. The common vertical drain duct of all the mist eliminator modules located in the upper half of the housing has a 6" high and 5" wide cut-out at the floor (Drawing EC-1216, Detail "I"). Some of the liquid draining out of the drainage port will be dragged out of the second stage mist eliminator drain towards the stack by the gas flow through this cut-out due to the stage pressure drop.

3. Mist Eliminator Outlet Contraction Transition

a. The sharply converging side walls (63.6° equivalent flat wall diffuser) will promote droplet impingement on the side walls of the transition. Liquid collectors will be developed in the model tests to collect this liquid and guide it to a drain before entering the cylindrical duct.

b. The 3" pipe internal supports shown on Sections F-F and G-G will be liquid droplet deposition and reentrainment sites. Droplets generated here will be carried directly into the mitered elbow and stack liner. Are they necessary downstream of the mist eliminator?

4. Stack Entrance Mitered Elbow

Mitered elbows for stack entrances are a low pressure loss component and produce a reasonably good velocity profile in the stack liner. However, for operation with a saturated gas flow, it may create a difficult to solve liquid reentrainment situation in the following ways:

a. Entrained droplets will tend to impinge on the outside surface of the elbow on surfaces that are vertical or nearly vertical and where gas velocities are significantly above average.

b. Liquid that condenses on the vertical liner wall above the elbow will flow downward into the mitered elbow or must be collected and drained out of the liner before reaching the elbow.

c. Both sources of liquid on the liner and elbow surfaces must be collected and drained out of the elbow where velocities are high and space for collection areas and drains is minimal.

d. The inclusion of liquid collectors and drains will decrease the flow area and increase gas velocities.

These potential problems led to the questions asked in our fax on May 24, 1991 to determine the amount of flexibility for change to this stack entrance section.

Within the next few weeks, we will be testing a smaller radius to diameter ratio mitered elbow for another project. At that time, we will begin quantifying the degree of severity of this reentrainment problem and whether it can be solved with reasonable internal additions or whether modifications must be made to the elbow design.

We have also developed conceptual designs for stack entrances to substitute for a mitered elbow that will make liquid collection easier and more efficient. These designs will adapt from a circular or rectangular inlet duct shape to a circular stack liner in a compact volume. It may be less expensive than the elbow but its pressure loss is expected to be somewhat higher. If your construction schedule permits time to consider such a change, we can send you the conceptual designs for review. If your schedule does not permit such a change, we will limit our changes to the basic mitered elbow design you now have.

5. <u>Manhole Recess</u>

Just above the mitered elbow built into the liner wall is a circular manhole of 30" diameter and 8" depth. This is a potential liquid collection and reentrainment site that we will include in the model. This recess will either have to be filled with a plug attached to the cover or it will have to have an edge built into part of the circumference of the hole and a drain installed in the recess. Liquid collectors or diverters may also be needed on the inside of the liner to prevent liquid flowing on the liner from entering the manhole or splashing off of it. These items will all be developed in the model study work.

We believe it would be better to position the manhole cut-out 90° from where it is to locate it over the inside of the elbow bend. Lowering the elevation may also be desirable. If these changes are possible, we will look at the manhole recess effect on the model to optimize its location and size.

6. <u>DynaGen Actions</u>

We are proceeding to construct a model from the JBR vessel to the stack liner about 3 diameters above the elbow outlet using your current design. The mist eliminators will be simulated for flow distribution using perforated plates to model the mist eliminator stage pressure losses. The mitered elbow will be built and installed for initial tests and liquid collectors will be developed to prevent liquid reentrainment with as few changes to the basic elbow envelope as possible. Before making changes to the mitered elbow envelope or proceeding with exploration of design changes, we will discuss our test results and recommendations with you.

7. SCS Actions

Provide answers to the May 24, 1991 fax to Mr. Looney according to our requested schedule or sooner if possible.

Let us know if we can move the liner entry manhole as discussed earlier in item 5.

Let us know if you will consider a change from a mitered elbow to a design more compatible with liquid collection and drainage as discussed in item 4 as soon as possible.

GBG/cak

Appendix A3

COMMENTS ON DUCT DESIGN FROM THE MAIN PLANT DUCT TO THE JBR INLET FOR THE CHIYODA CLEAN COAL TECHNOLOGY PROJECT AT PLANT YATES UNIT 1

APPENDIX A3

COMMENTS ON DUCT DESIGN FROM THE MAIN PLANT DUCT TO THE JBR INLET FOR THE CHIYODA CLEAN COAL TECHNOLOGY PROJECT AT PLANT YATES UNIT-1

Task 1A-SCS Contract No.: 195-89-015
Lewis A. Maroti
Gerald B. Gilbert

June 28, 1991
Project SCS-1

(1) Take Off Duct From Main PLant Duct in the Horizontal Plane

This sharp corner 90° take off will produce pressure losses and flow distortions similar to a 90° sharp corner elbow. To cut the pressure loss about in half and improve the downstream velocity profile significantly in the duct leading to the JBR, the upstream corner should be rounded with a radius of about 5 feet and the expansion joint and damper moved away from the main plant duct far enough to accommodate this corner radius. This will save about 0.35 inches of water pressure loss when the duct velocity head is about 0.60 inches of water. Figure 1 shows velocity and velocity head values for on assumed flow rate of 480,000 ACFM upstream of the JBR booster fan.

(2) Two 16° Bends in Series in the Vertical Plane

These elbows are satisfactory without vanes as specified on your drawings. If the 5 foot radius is incorporated into the upstream duct, then these two elbows will move closer together and the angle will increase to about 20° which will still be satisfactory without vanes.

(3) 90° Vaned Elbow in the Horizontal Plane

The vanes in the 90° elbow and the rounded inner and outer duct corners are satisfactory as designed. If any improvement were to be made it would be to shorten the vane leading edges by one foot and lengthen the trailing edges by one foot. The center plate vane stiffener is a good design to prevent vane vibration with low pressure loss.

(4) Pipe Trusses for Duct Stiffening

From the main duct take off to the entrance to the 7' x 22' fiberglass duct near the JBR inlet, there are about 22 pipe trusses for internal duct stiffening. These trusses will cause about 1.25 inches of water pressure loss all together or an average of 0.057 inches of water pressure loss per truss. The calculated truss blockages in the 22 duct cross-section range from 6.5% to 9.86% of the cross-section and the assumed velocity head

is about 0.60 inches of water. The pressure loss per truss is proportional to the percent blockage and the gas velocity head. The above estimate does not include the blockage of gusset plates. By scaling your detail H, a typical gusset would be about 6.3" x 22.4" or about one square foot per gusset. Since only about half of this is additional blockage and assuming four gussets to a cross-section, this amounts to about 2 ft^2 additional blockage per cross-section or about 1.7%. This gusset blockage could increase the truss pressure loss of about 20% equivalent to 0.25 inches of water more loss.

It is acceptable to leave these trusses installed in the duct system, but you must make sure that you have accounted for this 1.50 inches of water pressure loss in the fan pressure rise requirements. The gusset plate pressure loss amount could be reduced by installing the gussets parallel to the gas flow.

(5) A 37° Elbow in the Horizontal Plane and a 60° Elbow in the Vertical Plane Both with 3 Sharp Angle Vanes

For each elbow vaned with sharp corner vanes and a sharp inner elbow corner the pressure loss is estimated to be approximately 0.07 (37°) and 0.17 (60°) inches of water larger than for curved vanes and a curved inner corner. Assuming a gas velocity head of 0.60 inches of water. The flow distribution downstream of the elbows with sharp corner vanes will be satisfactory within about eleven feet (about 4 vane spaces) from the vane discharges where the separation zones from the sharp corners will be reasonably well smoothed out.

The sharp corner vane designs can be used satisfactorily in this system provided that the extra 0.24 inches of water pressure loss has been included in the calculation of the fan head requirements.

(6) Transition From Common Duct to Two Fan Inlet Flanges

This split transition duct with small angle turns and nearly constant velocity level is a good design and should produce satisfactory flow balance and velocity uniformity at the two fan inlet flanges. No vanes are needed in this duct component.

(7) Fan Outlet Diffuser

The flow profile out of this diffuser will probably be highly distorted for the following reasons:

(a) The fan discharge flow entering the diffuser is usually highly distorted and unsteady.

(b) The diffuser as shown on the drawing has an equivalent conical cone angle of 23° with an area ratio of 1.82 (outlet area over inlet area). This diffuser would probably be separated even with a uniform inlet flow profile and most certainly is separated as designed.

(c) The diffuser is nonsymmetrical followed by a duct bend. The large diffuser wall angle is on the same side of the duct where the fan outlet velocity profile is usually very low in velocity or separated.

This duct geometry and diffuser outlet flow profile could be improved in two ways. First and easiest would be to change the diffuser by using four flat sides between the two expansion joints. This will more than triple the diffuser length and reduced the equivalent cone angle by a factor of about 3. We recommend this approach.

Secondly, the nonsymmetrical diffuser and duct band could be vaned to produce a reasonably good velocity profile leading into the JBR. How to design these vanes without knowing the fan outlet velocity profile will be a guess. Also the vanes close to the fan could cause increased fan noise levels. You could select one of the following ways to design these vanes:

(a) Obtain the fan outlet profile estimate from the fan manufacturer and select a vane design based on the assumed fan outlet profile. We can assist you with this if you want us to.

(b) Using the same assumed fan outlet velocity profile, we could build a duct flow model from the fan outlet to the JBR and experimentally optimize the required vanes and measure pressure loss. This is outside the cost scope of our current contract.

(c) When the field unit is operational with or without vanes installed in the fan outlet diffuser, field velocity profiles should be measured at the fan outlet flange, at the end of the 11'-4" x 11'-4" straight duct downstream of the fan outlet diffuser, and at the JBR inlet. This data can then be used to determine whether flow profiles are acceptable or whether changes are needed.

With the diffuser and duct band located so close to the fan outlet, there will probably be some added pressure loss called "System Effect" factor. Without knowing the details of the fan design or the fan outlet velocity profile, we can not estimate the magnitude of this added loss. If this was not considered in the duct pressure rise requirements, an additional 0.5 to 1.0 inches of water may be needed on the fan head rise.

(8) Transition Diffuser Upstream of the JBR

The gradual transition diffuser upstream of the JBR has the following geometry:

Inlet Dimensions	11'-4" x 11'-4"
Outlet Dimensions	7' x 22'
Area Ratio (Outlet/Inlet)	1.20
Length of Transition	39'-6"
Equivalent Cone Angle	1.8°
Actual Side Wall Included Angle	15.4°

If the inlet velocity profile is reasonably uniform, the outlet velocity profile will also be reasonably uniform. If a flow distortion is caused by the fan outlet component, the flow distortion will pass through this transition with some improvement because of the reduction is vertical duct height and the length of the transition.

This transition diffuser is a good design and needs no changes.

(9) Fiberglass Spray Saturator Duct (7'x22')

This duct section should operate satisfactorily. The first 2 spray sections are pointed in the same direction as the gas flow. As long as the flow profile has no separated zones as it enters the sprays there should be no significant problem with a wet/dry line build up. The 6° floor slope should allow a smooth flow of liquid into the duct drain trough. The depth of the trough is two feet at the center and zero at the side walls. We recommend to change the depth at the side walls to one foot for better capture of the liquid running on the floor. The drain diameter of 30 inches I.D. is more than adequate for the drainage flow rate expected.

(10) Actions by SCS

(a) You should review your pressure loss estimates to make sure they include adequate margin for the pressure losses identified in this memo that may be more than allowed in your calculations.

(b) You should decide what alternate path you will take to insure that the fan outlet close coupled diffuser and turn do not produce a distorted flow into JBR inlet duct spray zone. If you want our assistance, please call.

(11) Actions by DynaGen

No further work on Task 1A is planned unless there are specific requests by SCS.

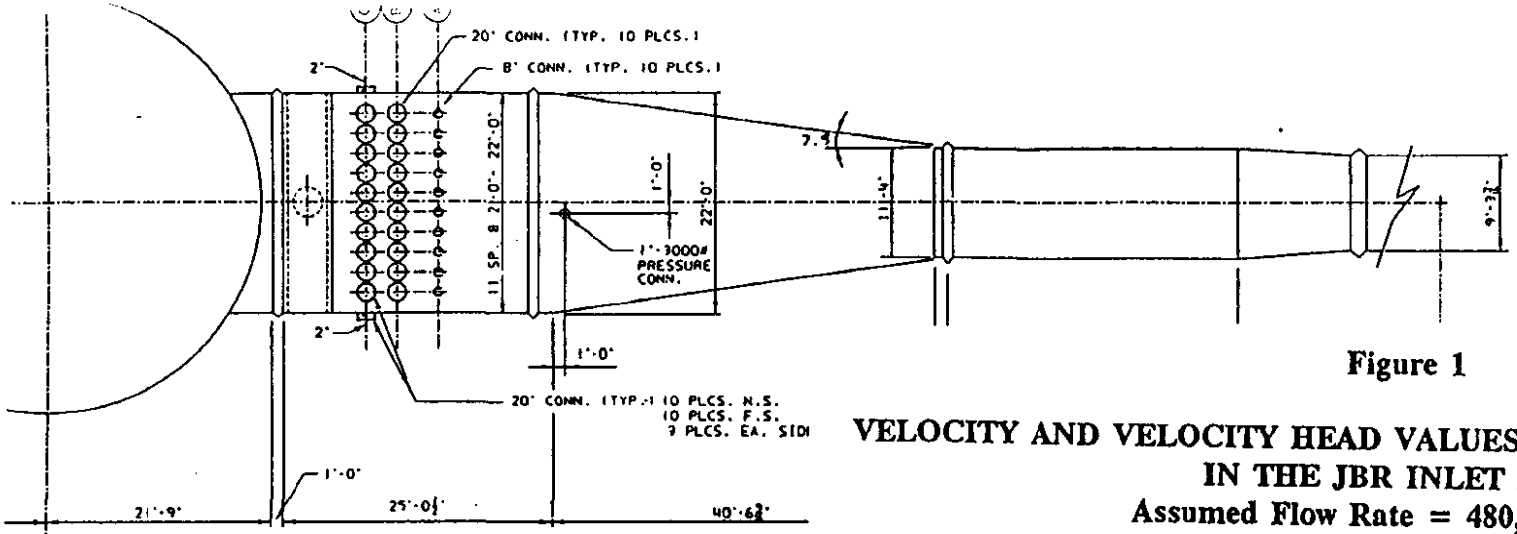

Figure 1

VELOCITY AND VELOCITY HEAD VALUES AT FIVE CROSS-SECTIONS IN THE JBR INLET DUCT
Assumed Flow Rate = 480,000 ACFM
Upstream of Fan

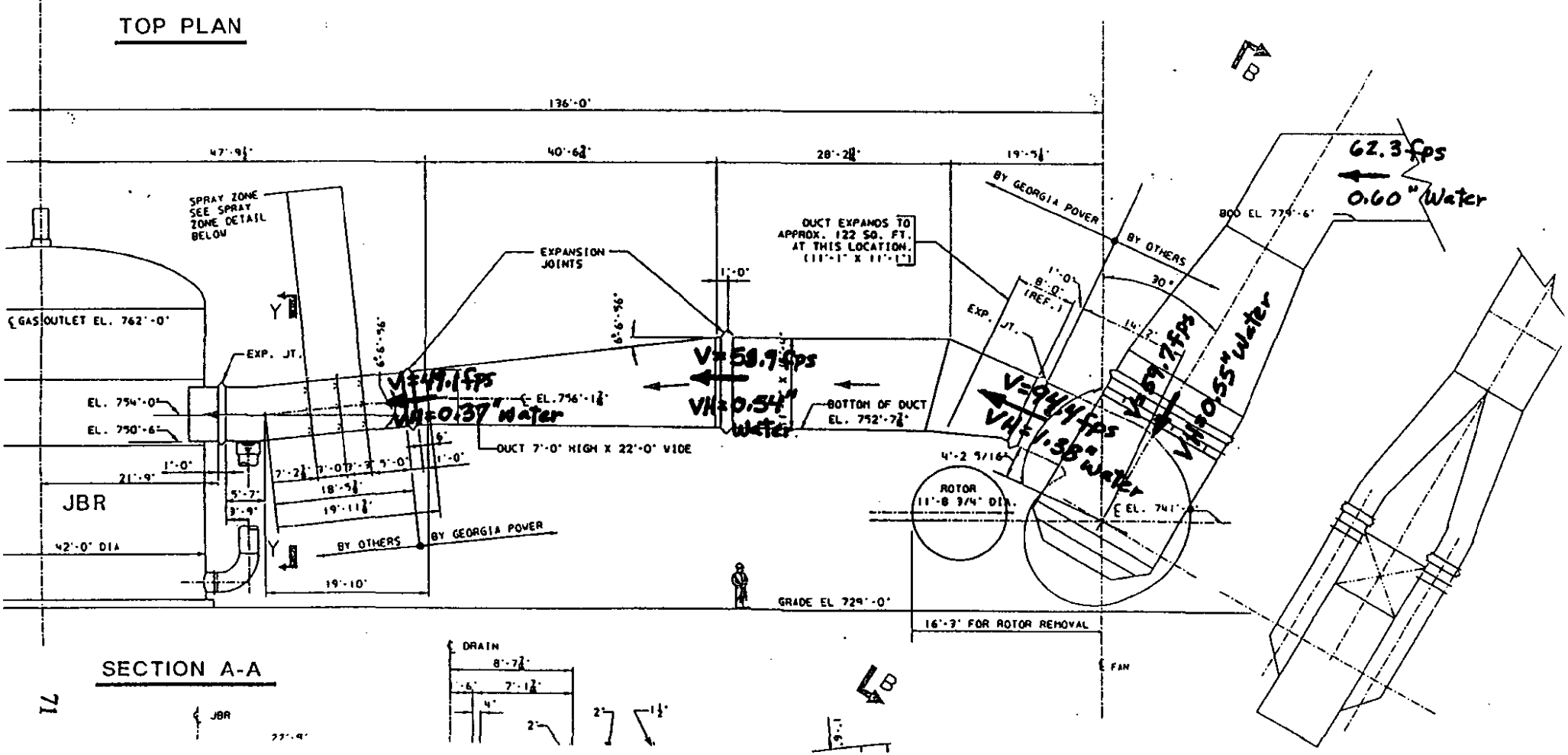

"Particulate Sampling of Chiyoda CT-121 Jet Bubbling Reactor
Georgia Power Company Plant Yates Unit 1 - ESP Operational Test Phase"

Southern Research Institute

PARTICULATE SAMPLING OF CHIYODA CT-121 WET SCRUBBER GEORGIA POWER COMPANY PLANT YATES UNIT 1

ESP OPERATIONAL TEST PHASE

JANUARY 21 THROUGH 31, 1993 TESTS

PREPARED BY

SOUTHERN RESEARCH INSTITUTE
2000 NINTH AVENUE SOUTH
BIRMINGHAM, ALABAMA 35205

FOR

SOUTHERN COMPANY SERVICES
800 SHADES CREEK PARKWAY
BIRMINGHAM, ALABAMA 35209

MARCH 19, 1993

SRI-ENV-93-317-7872.1F

INTRODUCTION

As part of the Innovative Clean Coal Technology (ICCT) program, funded primarily by Southern Company Services and the U. S. Department of Energy, a Chiyoda CT-121 Jet Bubbling Reactor (JBR) was installed at Georgia Power Company's Plant Yates Unit 1. As part of the two year demonstration of this innovative process for Flue Gas Desulfurization(FGD), Southern Research Institute was contracted to determine the particulate mass removal efficiency, particle fractional collection efficiency and SO_3/H_2SO_4 mist removal efficiency of the JBR. The test program, which this report covers, was conducted with an energized electrostatic precipitator installed ahead of the JBR.

The test program was designed to evaluate the scrubber under nine test conditions. Table 1 presents the conditions for each test. During each test day, three measurements were obtained at the inlet and outlet sampling locations for total mass loading, particle size distribution and SO_2/SO_3.

MEASUREMENTS

Mass Measurements

EPA Method 5B-Determination of Nonsulfuric Acid Particulate Matter From Stationary Sources (40CFR60, Appendix A) was used at the inlet and stack sampling locations for determination of overall mass collection efficiency of the JBR. On each test day, three Method 5B traverses were completed at each sampling location. Tables 2 and 3 present the inlet and outlet Method 5B data obtained during the 100 megawatt operating conditions. Tables 4 and 5 present these data for the 75 megawatt operating conditions, while Tables 6 and 7 present the data from the 50 megawatt conditions.

Particle Size Measurements

University of Washington (UW) Cascade Impactors were operated at the inlet and outlet sampling locations during each test day. The inlet impactors traversed the inlet sampling plane at an average isokinetic flow rate for the inlet location. Each impactor sampled at four points in each of the six ports. "Blank impactors" (an impactor preceded by a filter) were operated at the inlet sampling location each test day to evaluate weight gains or losses for the impactor substrates. The three impactors operated at the inlet each day were averaged together for the inlet size distribution reported for that test condition.

UW impactors were also used at the stack sampling location to determine the outlet particle size distribution. The impactors at the outlet were heated to approximately 300 °F and each impactor traversed one port at the average isokinetic flow rate for that port. The outlet impactors from each test day were averaged together to produce the outlet size distribution for the stated test condition. After the data for each impactor run were reduced and groupings determined, the data were input into a cascade impactor data reduction system (CIDRS) developed for the EPA by SRI. This program calculates the size distributions for the respective locations as cumulative mass, cumulative percent, differential mass per differential log diameter (dM/dlogD) and differential number per differential log diameter (dN/dlogD) verses particle

diameter. The CIDRS program was also used to calculate the fractional collection efficiency of the JBR using the dM/dlogD data for the assigned inlet and outlet groupings.

Figures 1 through 9 present the cumulative mass vs particle size data from the inlet for each of the nine test conditions, while Figures 10 through 18 present these data for the JBR outlet. Figures 19 through 27 present the fractional collection efficiency for each test condition, 1 through 9, respectively. The remaining size distribution curves are in the appendix.

SO_2/SO_3 Measurements

The Controlled Condensation Method was used at each sampling location for the determination of sulfur dioxide and sulfur trioxide. Tables 8, 9 and 10 present these data for the test program.

DISCUSSION OF RESULTS

Mass Measurements and Chemical Analyses

Figures 28 through 34 were prepared from the data in Tables 2 through 10 to assist in the interpretation of the Method 5B results.

Figures 28 and 29 display the Method 5B mass loadings at the scrubber inlet and outlet as an average per test condition and as individual sampling runs, respectively. These graphs indicate that the outlet mass loading from the scrubber remained low (always less than 0.015 lb/MBtu) and relatively constant, even though there was considerable variation in the inlet dust concentration. With the exception of spikes in concentration that occurred during test condition 3 and 7, the inlet mass loadings show a general decrease as the unit load was decreased from 100 MW to 50 MW. This indicates the upstream precipitator was collecting at higher efficiency as the gas flow decreased, as would be expected.

The penetration of particulate matter through the scrubber as determined by Method 5B is presented as an average per test condition and as determinations from each run in Figures 30 and 31, respectively. These graphs illustrate that the variations in penetration do not show a clear trend caused by either pressure drop through the scrubber or by changes in plant load. However, the last test series indicates an increased penetration, but this results from decreased inlet loadings rather than increased outlet mass concentrations.

Another observation on the effect of inlet loading can be made concerning the spike in inlet loading which occurred on Test Number 20. This spike is not reflected in increased outlet mass concentrations, suggesting the transient event consisted primarily of large particles which were easily collected by the scrubber.

Figure 32 compares inlet and outlet mass loadings determined by the cascade impactors and by the Method 5B sampling system. The agreement between these two sampling systems is considered relatively good in view of the fact that impactor sampling is performed at an average gas velocity instead of with a point-to-point isokinetic traverse.

Sulfuric acid vapor present in the flue gas is expected to condense as it is cooled in the scrubbing system. If the condensation occurs and a fine mist is formed before the acid gas can be absorbed in the scrubbing liquid, the condensed mist will pass through the scrubber as an aerosol. Figure 33 presents SO_3 concentrations determined at the scrubber inlet and outlet for the nine test conditions. As with the Method 5B measurements, there is no consistent trend of sulfur trioxide concentration with load or scrubber pressure drop. In all cases, however, a substantial amount of SO_3 was found at the scrubber outlet. For conditions 4, 5, and 6, the SO_3 measured at the outlet was slightly greater than the values determined for the inlet. These differences, however, are interpreted as reflecting normal variations in the measurements at these concentration levels rather than any actual indication of SO_3 generation in the scrubbing system.

Figure 34 compares outlet mass loadings determined by the impactors and by the Method 5B trains on an expanded scale. These are the same data that are presented in the lower portion of Figure 32. With the exception of Test Condition 6, the Method 5B train indicates higher total outlet loadings than the impactors. Both systems, however, are indicating relatively low total mass concentrations.

Also shown in Figure 34 is the SO_3 concentration in Figure 33 converted to a mass loading. These data illustrate that, if the SO_3 were collected in either of these sampling systems as particles, the mass of SO_3 would in most cases dominate the total particulate catch.

Table 11 summarizes results of chemical analyses performed on the Method 5B filters in an effort to determine if the collected mass consisted of sulfuric acid mist. These data show that the fraction of soluble sulfate increased by factors of two or more from inlet to outlet filters. The fraction of soluble sulfate on the outlet filters is highly variable, ranging from a low of 20% to a high of 91%. The percentages are based on the particulate catch on the filters. The relatively low amounts of calcium present on the outlet filters suggest that sulfuric acid is likely the predominant compound at the outlet. However, there is some enrichment of calcium from inlet to outlet, suggesting the presence of some scrubber solids.

Since the Method 5B System was maintained at 320 °F, the sulfuric acid mist concentrations measured at the scrubber outlet would vaporize at this temperature if equilibrium were achieved, since SO_3 dew point correlations indicate flue gas with 10% H_2O vapor at 320 °F can sustain a vapor concentration of SO_3 of 85 ppm by volume. However, the analytical data clearly indicate a substantial fraction of the acid mist did not vaporize before it was collected and retained on the Method 5B filter.

Particle Size Measurements

Since the scrubber is operating downstream from an energized precipitator, the inlet mass loading to the scrubber is much reduced from the values expected from the furnace without an upstream control device. This reduction in particle loading is also reflected in the fine particle measurements obtained by the impactors. For example, Figure 1 indicates the cumulative mass below 2 microns particle diameter for the 100 MWe, 8 inch delta P condition was about 12 mg/acm at the scrubber inlet. In contrast, similar measurements on an ESP inlet would be expected to produce a cumulative loading below two microns in the range of 200-300 mg/acm.

The effect of reduced load and the resulting increase in precipitator performance is indicated by the reduction in fine particle loading at the scrubber inlet for the 50 MW_e test condition. Cumulative mass loadings below two microns at this condition ranged between 1 and 2 mg/acm.

Figures 19 through 27 present the efficiency of the scrubber as a function of particle size. Although these graphs indicate large confidence intervals, it is clear the scrubber is relatively ineffective in collecting particles smaller than one micron in diameter. Negative collection efficiencies are also indicated on some of the graphs, especially for the 50 MW_e test condition where the inlet fly ash concentration was reduced because of the improved performance of the precipitator at the lower gas flow rates. The negative efficiencies are probably the result of acid mist formation in the scrubber. The SO_3 would be in the vapor state in the inlet impactors, condense to form an aerosol in the scrubber, and then be collected on the lower stage substrates of the impactors as fine particles at the scrubber exit.

Figures 35 and 36 present the cumulative outlet mass loadings as mg/dscm at 3% oxygen for comparison purposes. It is apparent that the outlet cumulative loadings show only relatively small variations with test condition. In other words, the scrubber outlet particle size distribution and mass emissions were relatively insensitive to changes in pressure drop or plant load. The variability observed in calculated efficiency vs particle size in the scrubber is therefore caused primarily by changes in the inlet particle loading vs particle size.

Figures 35 and 36 also contain for comparative purposes a plot of cumulative mass vs particle size obtained for a spray dryer-reverse gas fabric filter combination. This data set illustrates that the Chiyoda Scrubber emits a cumulative mass concentration at 1.5 microns diameter which is about an order of magnitude greater than the fabric filter-spray dryer combination.

In view of the apparent formation of an acid aerosol within the scrubber by condensation of sulfuric acid vapor, an effort was made to analyze selected outlet impactor substrates with the objective of qualitatively establishing whether fly ash or acid aerosol was the dominant constituent on these substrates. Results from this effort are presented in Table 12. These data indicate that, while sulfate was a significant component of all of the stage catches, it did not dominate on the stages which contained the largest total mass. Note that this particular run was performed at high load with the greatest fine particle concentration exiting the precipitator. Calcium as a very minor component on all stages. These analytical results and the photomicrographs in Figure 37 indicate fly ash was also a significant component on the outlet impactor stages. Figure 38 presents the Energy Dispersive X-Ray Analysis for each of the impactor stages in Figure 37. The higher percentage of Silicon in the Stage 2 is due to the substrate material which was in the scanning electron microscope field of view.

In conclusion, these data indicate that the scrubber produced very consistent and low outlet total mass concentrations over the entire range of test conditions examined. However, the scrubber was relatively ineffective in the collection of fine particles and in the collection of sulfuric acid. A comparison of these results with others obtained with similar instrumentation at the outlet of a spray dryer fabric filter system indicated the latter system emitted cumulative mass emissions smaller than 1.5 microns diameter which are about a factor of ten lower than those observed in this test program.

TABLES

TABLE 1 CHIYODA TEST SCHEDULE			
Condition	Date	Unit Load, MW_e	JBR ΔP, in. H_2O
1	1/21/93	100	8
2	1/22/93	100	12
3	1/23/93	100	16
4	1/25/93	75	8
5	1/26/93	75	12
6	1/27/93	75	16
7	1/29/93	50	8
8	1/30/93	50	12
9	1/31/93	50	16

Table 2

CHIYODA SCRUBBER, 100 MEGAWATTS

INLET Method 5B Mass loading

Run ID	IMT-1-1	IMT-1-2	IMT-1-3	IMT-2-1	IMT-2-2	IMT-2-3	IMT-3-1	IMT-3-2	IMT-3-3
Date	1/21/93	1/21/93	1/21/93	1/22/93	1/22/93	1/22/93	1/23/93	1/23/93	1/23/93
Sample time	1119-1237	1410-1325	1631-1744	0741-0851	0950-1103	1221-1332	0731-0845	1004-1124	1235-1350
Gas analysis, %									
O2	8.4	8.2	8.4	8.0	8.0	8.0	8.4	8.4	8.6
CO2	10.5	10.5	10.5	11.0	11.0	11.0	10.4	10.0	11.0
H2O	6.0	7.6	6.4	8.9	7.4	8.6	6.0	7.8	7.6
Ambient pressure, in Hg	29.44	29.44	29.44	29.40	29.40	29.40	29.40	29.40	29.40
Static pressure, in H2O	-11.1	-10.8	-11.1	-11.2	-11.1	-11.2	-11.5	-11.4	-11.6
Stack Temprature, F	261	265	267	261	268	271	257	267	266
Velocity, ft/sec	58.7	60.4	59.7	58.7	59.0	60.3	60.4	60.9	60.2
Gas volume flow,									
Kacfm	452	465	460	452	454	465	466	469	464
Kdscfm	298	300	299	298	292	293	308	300	297
Mass loading,									
gr/acf	0.0216	0.0200	0.0256	0.0216	0.0250	0.0251	0.0333	0.0297	0.0310
gr/dscf	0.0328	0.0310	0.0394	0.0328	0.0390	0.0397	0.0504	0.0464	0.0483
lb/MBtu	0.077	0.073	0.092	0.077	0.089	0.090	0.118	0.109	0.115

Table 3

CHIYODA SCRUBBER, 100 MEGAWATTS

OUTLET Method 5B Mass loading

Run ID	OMT-1-1	OMT-1-2	OMT-1-3	OMT-2-1	0MT-2-2	OMT-2-3	OMT-3-1	OMT-3-2	OMT-3-3
Date	1/21/93	1/21/93	1/21/93	1/22/93	1/22/93	1/22/93	1/23/93	1/23/93	1/23/93
Sample time	1116-1233	1518-1639	1636-1758	0737-0845	0952-1103	1219-1426	0730-0838	1022-1128	1238-1343
Gas analysis, %									
O2	9.0	8.2	9.0	9.0	8.8	8.2	9.2	8.0	8.4
CO2	9.0	10.8	9.0	11.5	9.0	11.0	10.0	11.0	11.0
H2O	12.0	11.1	12.2	13.2	12.8	13.1	12.0	12.0	12.0
Ambient pressure, in Hg	29.37	29.37	29.37	29.33	29.33	29.33	29.32	29.32	29.32
Static pressure, in H2O	-0.5	-0.5	-0.5	-0.5	-0.5	-0.5	-0.6	-0.6	-0.5
Stack Temprature, F	119	118	119	119	122	121	124	119	120
Velocity, ft/sec	47.3	48.1	48.1	47.3	47.9	48.0	48.7	48.0	47.5
Gas volume flow,									
Kacfm	377	383	383	377	381	383	388	382	379
Kdscfm	300	305	301	300	295	296	299	302	298
Mass loading,									
gr/acf	0.0034	0.0025	0.0025	0.0034	0.0038	0.0031	0.0026	0.0048	0.0030
gr/dscf	0.0043	0.0032	0.0032	0.0043	0.0049	0.0040	0.0034	0.0061	0.0038
lb/MBtu	0.011	0.007	0.008	0.011	0.012	0.009	0.008	0.014	0.009

Table 4

CHIYODA SCRUBBER, 75 MEGAWATTS

INLET Method 5B Mass loading

Run ID	IMT-4-1	IMT-4-2	IMT-4-3	IMT-5-1	IMT-5-2	IMT-5-3	IMT-6-1	IMT-6-2	IMT-6-3
Date	1/25/93	1/25/93	1/25/93	1/26/93	1/26/93	1/26/93	1/27/93	1/27/93	1/27/93
Sample time	0800-0916	1107-1217	1328-1443	0804-1052	1200-1316	1409-1520	0706-0820	0916-1026	1208-1319
Gas analysis, %									
O2	9.4	9.4	9.2	10.0	9.8	9.6	9.3	9.4	9.4
CO2	10.4	10.4	10.6	9.2	9.4	10.0	9.5	10.2	10.0
H2O	7.2	7.0	8.0	6.5	7.2	6.9	6.7	6.0	7.4
Ambient pressure,in Hg	29.44	29.44	29.44	29.37	29.37	29.37	29.34	29.34	29.34
Static pressure, in H2O	-7.2	-7.4	-7.3	-7.5	-7.7	-7.6	-7.6	-7.5	-7.6
Stack Temprature, F	245	250	252	261	259	256	249	251	254
Velocity, ft/sec	47.3	47.0	48.3	58.7	50.1	48.6	48.8	47.8	47.6
Gas volume flow,									
Kacfm	364	362	372	452	386	374	376	368	367
Kdscfm	245	242	245	298	253	247	251	247	242
Mass loading,									
gr/acf	0.0337	0.0227	0.0184	0.0216	0.0167	0.0181	0.0113	0.0108	0.0107
gr/dscf	0.0502	0.0339	0.0279	0.0328	0.0254	0.0274	0.0169	0.0160	0.0163
lb/MBtu	0.128	0.087	0.070	0.077	0.067	0.071	0.043	0.041	0.041

Table 5

CHIYODA SCRUBBER, 75 MEGAWATTS

OUTLET Method 5B Mass loading

Run ID	OMT-4-1	OMT-4-2	OMT-4-3	OMT-5-1	OMT-5-2	OMT-5-3	OMT-6-1	OMT-6-2	OMT-6-3
Date	1/25/93	1/25/93	1/25/93	1/26/93	1/26/93	1/26/93	1/27/93	1/27/93	1/27/93
Sample time	0829-0937	1110-1219	1331-1439	0808-1108	1205-1312	1404-1511	0704-0811	0917-1027	1132-1250
Gas analysis, %									
O2	9.0	9.0	9.2	9.4	9.4	9.2	10.6	9.2	9.2
CO2	10.0	10.0	10.4	10.2	10.2	10.4	10.2	10.4	10.4
H2O	12.0	12.0	12.2	11.0	10.6	11.2	10.9	11.7	11.6
Ambient pressure, in Hg	29.36	29.36	29.36	29.29	29.29	29.29	29.26	29.26	29.26
Static pressure, in H2O	-0.4	-0.4	-0.4	-0.6	-0.6	-0.6	-0.4	-0.4	-0.4
Stack Temprature, F	124	132	120	119	118	118	118	117	118
Velocity, ft/sec	39.5	39.1	39.2	47.3	38.7	37.6	38.3	38.1	37.5
Gas volume flow,									
Kacfm	315	311	312	377	308	299	305	303	299
Kdscfm	248	242	245	300	246	237	242	240	236
Mass loading,									
gr/acf	0.0031	0.0030	0.0036	0.0034	0.0023	0.0024	0.0013	0.0018	0.0018
gr/dscf	0.0039	0.0039	0.0046	0.0043	0.0028	0.0030	0.0016	0.0023	0.0023
lb/MBtu	0.010	0.010	0.011	0.011	0.007	0.007	0.005	0.006	0.006

Table 6

CHIYODA SCRUBBER, 50 MEGAWATTS

INLET Method 5B Mass loading

Run ID	IMT-7-1	IMT-7-2	IMT-7-3	IMT-8-1	IMT-8-2	IMT-8-3	IMT-9-1	IMT-9-2	IMT-9-3
Date	1/29/93	1/29/93	1/29/93	1/30/93	1/30/93	1/30/93	1/31/93	1/31/93	1/31/93
Sample time	0722-0832	0946-1054	1215-1324	0708-0819	0934-1043	1213-1328	0658-0808	0900-1009	1107-1217
Gas analysis, %									
O2	10.8	10.4	10.4	10.2	10.6	10.6	10.2	10.6	10.2
CO2	8.8	9.0	9.2	9.4	9.0	9.0	9.6	9.0	9.4
H2O	6.9	6.9	6.6	7.2	7.9	7.8	5.5	6.4	6.4
Ambient pressure, in Hg	29.41	29.41	29.41	29.61	29.61	29.61	29.47	29.47	29.47
Static pressure, in H2O	-5.0	-4.7	-4.8	-4.8	-4.8	-4.6	-5.1	-5.0	-5.1
Stack Temprature, F	241	240	241	234	238	241	234	234	239
Velocity, ft/sec	34.2	34.6	37.3	34.0	33.6	34.2	34.5	33.8	33.8
Gas volume flow,									
Kacfm	264	267	287	262	259	264	266	261	260
Kdscfm	179	181	196	181	176	179	186	181	179
Mass loading,									
gr/acf	0.0077	0.0422	0.0132	0.0054	0.0079	0.0036	0.0055	0.0043	0.0045
gr/dscf	0.0114	0.0620	0.0193	0.0078	0.0116	0.0052	0.0079	0.0062	0.0065
lb/MBtu	0.033	0.173	0.054	0.021	0.033	0.015	0.022	0.018	0.018

Table 7

CHIYODA SCRUBBER, 50 MEGAWATTS

OUTLET Method 5B Mass loading

Run ID	OMT-7-1	OMT-7-2	OMT-7-3	OMT-8-1	OMT-8-2	OMT-8-3	OMT-9-1	OMT-9-2	OMT-9-3
Date	1/29/93	1/29/93	1/29/93	1/30/93	1/30/93	1/30/93	1/31/93	1/31/93	1/31/93
Sample time	0723-0831	0946-1114	1217-1330	0709-0817	0942-1057	1222-1331	0657-0805	0902-1011	1144-1252
Gas analysis, %									
O2	10.0	10.2	10.2	10.2	10.4	10.6	10.4	10.2	10.6
CO2	9.4	9.4	9.4	9.4	9.4	9.2	9.4	9.4	9.0
H2O	9.0	11.8	9.6	11.3	10.9	10.9	10.9	10.2	10.9
Ambient pressure, in Hg	29.34	29.34	29.34	29.54	29.54	29.54	29.40	29.40	29.40
Static pressure, in H2O	-0.3	-0.3	-0.3	-0.4	-0.4	-0.4	-0.3	-0.3	-0.3
Stack Temprature, F	113	113	112	115	116	113	115	113	113
Velocity, ft/sec	28.4	27.8	28.1	27.6	27.4	28.2	28.8	29.0	29.4
Gas volume flow,									
Kacfm	226	221	224	220	218	225	229	231	234
Kdscfm	186	176	183	177	176	182	187	187	189
Mass loading,									
gr/acf	0.0030	0.0017	0.0027	0.0022	0.0024	0.0011	0.0022	0.0014	0.0014
gr/dscf	0.0037	0.0021	0.0033	0.0027	0.0030	0.0013	0.0027	0.0017	0.0018
lb/MBtu	0.010	0.006	0.009	0.007	0.008	0.004	0.008	0.005	0.005

TABLE 8

CHIYODA SCRUBBER TEST PROGRAM
UNIT 1; 100 MEGAWATT

DATE	TIME	ppm SO2	ppm SO3	% O2	% H2O	FLUE GAS TEMP. F	@3% O2 SO2	@3% O2 SO3
1/21/93								
INLET	1052-1105	1578	2.4	8.2		254	2224	3.4
	1128-1142	1572	3.1	8.4		255	2251	4.4
	1332-1345	1620	2.6	8.6		257	2358	3.8
	1408-1421	1614	2.3	8.4		257	2311	3.3
	1435				7.4	260		
AVERAGE		1596	2.6	8.4		257	2286	3.7
OUTLET	1052-1107	369	1.9	8.6		122	537	2.8
	1128-1142	358	1.9	8.5		121	517	2.7
	1332-1347	355	1.9	8.4		120	508	2.7
	1408-1413	407	1.9	8.5		121	588	2.7
	1435				12.4	120		
AVERAGE		372	1.9	8.5		121	537	2.7
1/22/93								
INLET	0825-0838	1614	2.9	8.2		260	2275	4.1
	0901-0914	1657	2.3	8.2		261	2335	3.2
	0934-0947	1614	2.3	8.1		260	2257	3.2
	1103-1116	1647	2.3	8		261	2285	3.2
	1129				7.8	265		
AVERAGE		1633	2.5	8.1		261	2288	3.4
OUTLET	0825-0838	157	1.9	8.3		121	223	2.7
	0901-0915	145	1.9	8.4		123	208	2.7
	0934-0948	136	1.9	8.4		124	195	2.7
	1103-1116	138	1.8	8.1		122	193	2.5
	1132				13.5	122		
AVERAGE		144	1.9	8.3		122	205	2.7
1/23/93								
INLET	0821-0834	1585	2.3	8.6		256	2307	3.3
	0858-0911	1598	2.2	8.4		255	2288	3.2
	0936-0949	1592	2.3	8.2		258	2244	3.2
	1106-1119	1580	2.5	8.2		258	2227	3.5
	1134				6.7	260		
AVERAGE		1589	2.3	8.4		257	2266	3.3
OUTLET	0821-0840	62	1.5	8.7		120	91	2.2
	0859-0919	46	1.6	8.6		120	67	2.3
	0936-0954	46	1.6	8.6		120	67	2.3
	1106-1123	42	1.7	8.4	12.3	119	60	2.4
	1133					119		
AVERAGE		49	1.6	8.6		120	71	2.3

TABLE 9

CHIYODA SCRUBBER TEST PROGRAM
UNIT 1, 75 MEGAWATT

DATE	TIME	ppm SO2	ppm SO3	% O2	% H2O	FLUE GAS TEMP. F	@3% O2 SO2	@3% O2 SO3
1/25/92								
INLET	0916-0929	1452	1.5	9.3		241	2241	2.3
	0952-1005	1474	1.6	9.2		242	2255	2.4
	1025-1038	1481	1.7	9.3		241	2285	2.6
	1212-1225	1500	1.8	9.4		244	2335	2.8
	1239				6.8	244		
AVERAGE		1477	1.7	9.3		242	2279	2.5
OUTLET	0917-0931	240	1.7	9.3		117	370	2.6
	0953-1007	271	1.7	9.4		117	422	2.6
	1025-1039	245	1.8	9.5		116	385	2.8
	1212-1226	240	1.4	9		117	361	2.1
	1103				10.8	117		
AVERAGE		249	1.7	9.3		117	384	2.6
1/26/93								
INLET	1049-1102	1426	1.8	9.5		243	2239	2.8
	1122-1135	1425	1.9	9.1		243	2162	2.9
	1154-1207	1413	1.9	9.2		244	2162	2.9
	1220				6.2	245		
AVERAGE		1421	1.9	9.3		243	2187	2.9
OUTLET	1049-1103	79	2.2	9.3		116	122	3.4
	1122-1136	91	2.2	9.3		116	140	3.4
	1154-1208	78	2.2	9.4		115	121	3.4
	1215				11	116		
AVERAGE		83	2.2	9.3		116	128	3.4
1/27/93								
INLET	0752-0805	1489	1.7	9.3		237	2298	2.6
	0829-0842	1502	1.7	9.3		239	2318	2.6
	0904-0916	1499	1.8	9.5		238	2354	2.8
	1054-1107	1520	2.0	9		242	2286	3.0
	1120				6.5	244		
AVERAGE		1503	1.8	9.3		239	2314	2.8
OUTLET	0752-0810	32	2.0	9.1		116	49	3.0
	0829-0846	32	2.0	9		117	48	3.0
	0904-0922	32	2.0	9.1		118	49	3.0
	1054-1111	33	1.9	8.8		117	49	2.8
	1115				11.8	117		
AVERAGE		32	2.0	9.0		117	49	3.0

TABLE 10

CHIYODA SCRUBBER TEST PROGRAM
UNIT 1, 50 MEGAWATT

DATE	TIME	ppm SO2	ppm SO3	% O2	% H2O	FLUE GAS TEMP. F	@3% O2 SO2	@3% O2 SO3
1/29/93								
INLET	0807-0819	1400	1.3	10.3		235	2364	2.2
	0839-0852	1406	0.9	10.2		236	2352	1.5
	0912-0925	1406	1.1	10.3		237	2374	1.9
	1047-1059	1416	1.2	10.4		239	2414	2.0
	1113				6.1	240		
AVERAGE		1407	1.1	10.3		237	2376	1.9
OUTLET	0807-0821	159	0.9	11.5		115	303	1.7
	0840-0854	164	0.9	11.5		115	312	1.7
	0913-0926	163	0.9	11.6		114	314	1.7
	1048-1100	163	0.8	11.6		115	314	1.5
	1105				10.1	115		
AVERAGE		162	0.9	11.6		115	311	1.7
1/30/93								
INLET	0756-0809	1428	1.2	10.5		237	2458	2.1
	0832-0844	1411	1.1	10.5		237	2429	1.9
	0906-0919	1420	1.2	10.4		239	2421	2.0
	1046-1054	1489	2.0	10.1		242	2468	3.3
	1108				5.6	242		
AVERAGE		1437	1.4	10.4		239	2444	2.3
OUTLET	0756-0814	57	0.9	10.8		114	101	1.6
	0832-0849	61	0.9	10.6		114	106	1.6
	0906-0923	64	0.7	10.6		115	111	1.2
	1047-1104	61	1.0	10.7		115	107	1.8
	1108				9.5	115		
AVERAGE		61	0.9	10.7		115	106	1.5
1/31/93								
INLET	0741-0753	1394	2.0	10.6		239	2423	3.5
	0823-0835	1401	2.2	10.5		239	2411	3.8
	1003-1015	1397	2.3	10.6		241	2428	4.0
	1127				5.7			
AVERAGE		1397	2.2	10.6		240	2421	3.8
OUTLET	0742-0804	27	1.3	10.6		112	47	2.3
	0824-0845	25	1.4	10.5		112	43	2.4
	1004-1025	27	1.4	10.1		114	45	2.3
	1030				10.5	114		
AVERAGE		26	1.4	10.4		113	45	2.4

Table 11
Analysis of Method 5B Filters

Date	1/21/93	1/21/93	1/23/93	1/23/93	1/29/93	1/29/93	1/30/93	1/30/93	1/31/93	1/31/93
Sample	In	Out	In	Out	In	Out	In	Out	In	Out
Acid Digestion										
Na, %	1	0.64	0.96	0.65	0.63					
K, %	2.6	1.9	2.5	1.7	2		1.8		1.5	
Ca, %	1.5	2.7	1.5	3.4	1.2		1.1		1.7	
Mg, %	0.73	0.8	0.73	0.62	0.58		0.09		0.08	
Fe, %	5.8	4.7	5.3	5.4	6.4		8.6		7.2	
Water Extraction										
Soluble SO_4, %	7.7	20.3	9.1	41.6	17.6	51.8	7.6	90.8	8.5	67.3
Soluble SO_3, %	<0.21	<0.48	<0.17	<0.66						
Soluble Ca, %	0.76	2.2	0.79	3.5	0.91	7.5	0.36	14.3	0.71	10.6
ph	3.9	3.5	3.2	3.1	3.2	3.3	3.4	3.2	3.2	3

Table 12
Analysis of Impactor Substrate
Test Condition 2

Stage No.	Stage Weight, mg	Run 89 mg, SO_4	Soluble %SO_4	%Ca
2	0.84	0.53	63.1	2.4
3	0.83	0.53	63.9	2.9
4	2.14	0.61	28.7	1.9
5	3.22	0.78	24.2	2.5
6	1.44	0.66	45.9	4.4

FIGURES

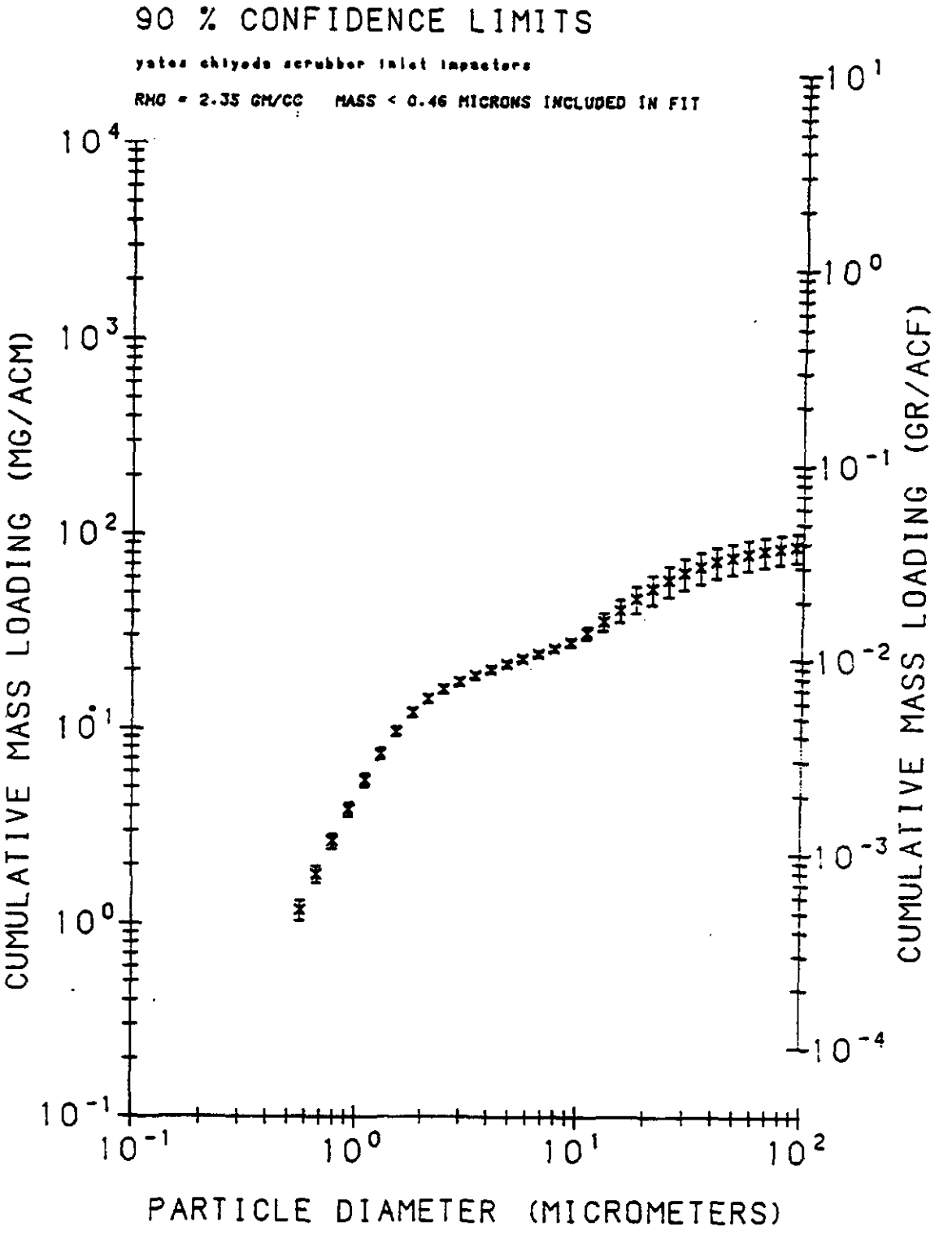

Figure 1. Inlet Cumulative Mass vs Particle Diameter for Chiyoda Scrubber, 100 MW, at 8" ΔP, January 21, 1993.

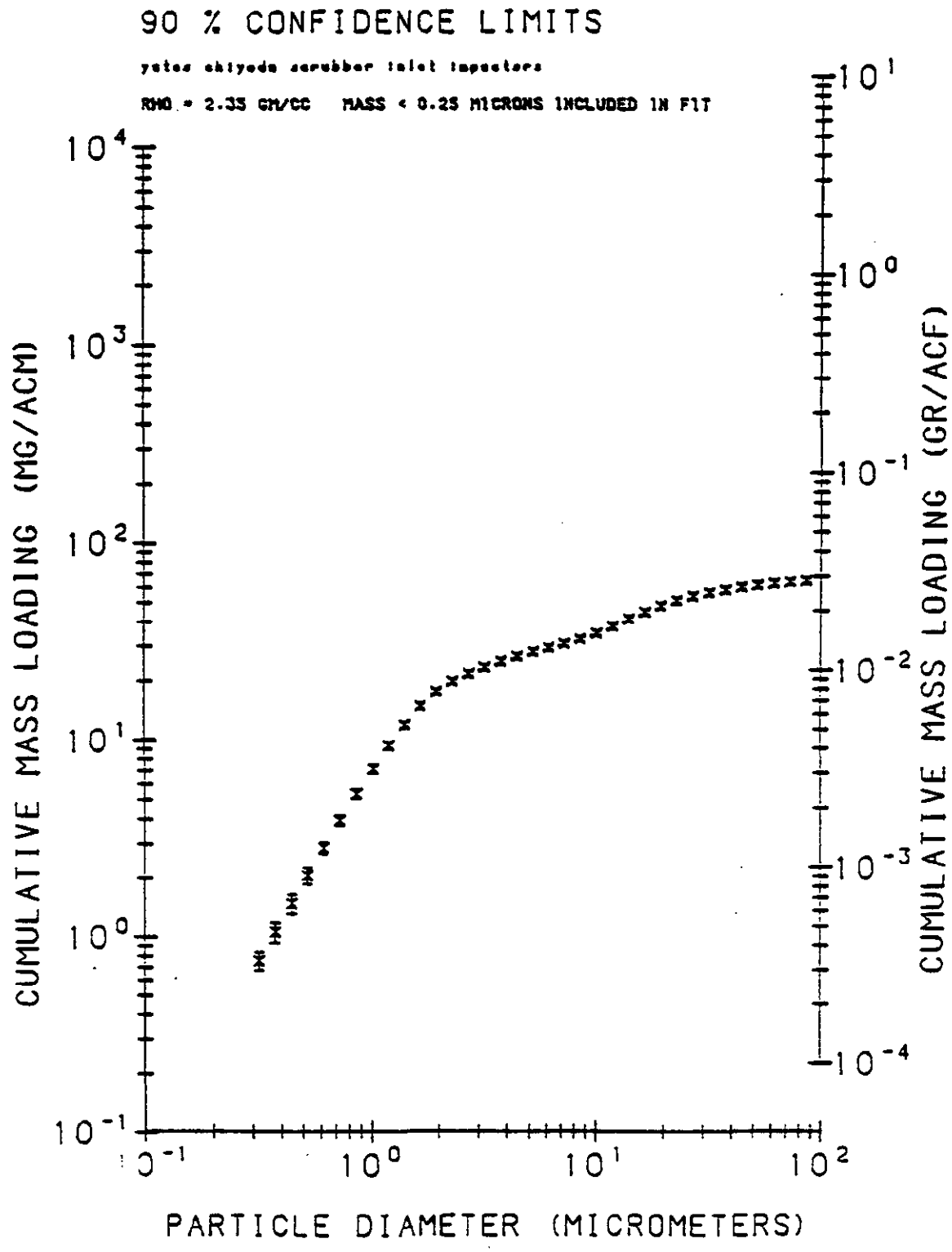

Figure 2. Inlet Cumulative Mass vs Particle Diameter for Chiyoda Scrubber, 100 MW, at 12" ΔP, January 22, 1993.

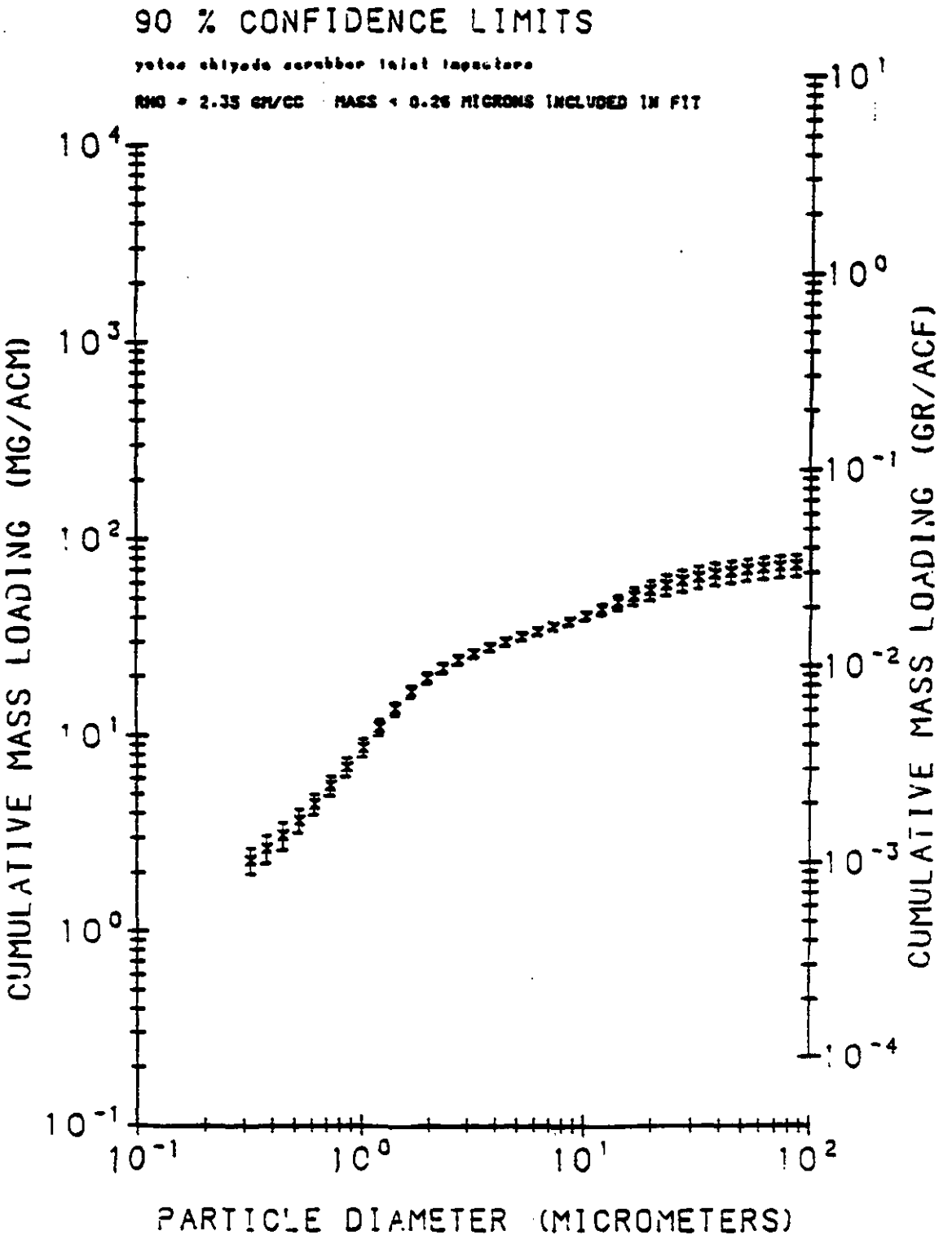

Figure 3. Inlet Cumulative Mass vs Particle Diameter for Chiyoda Scrubber, 100 MW$_e$ at 16" ΔP, January 23, 1993.

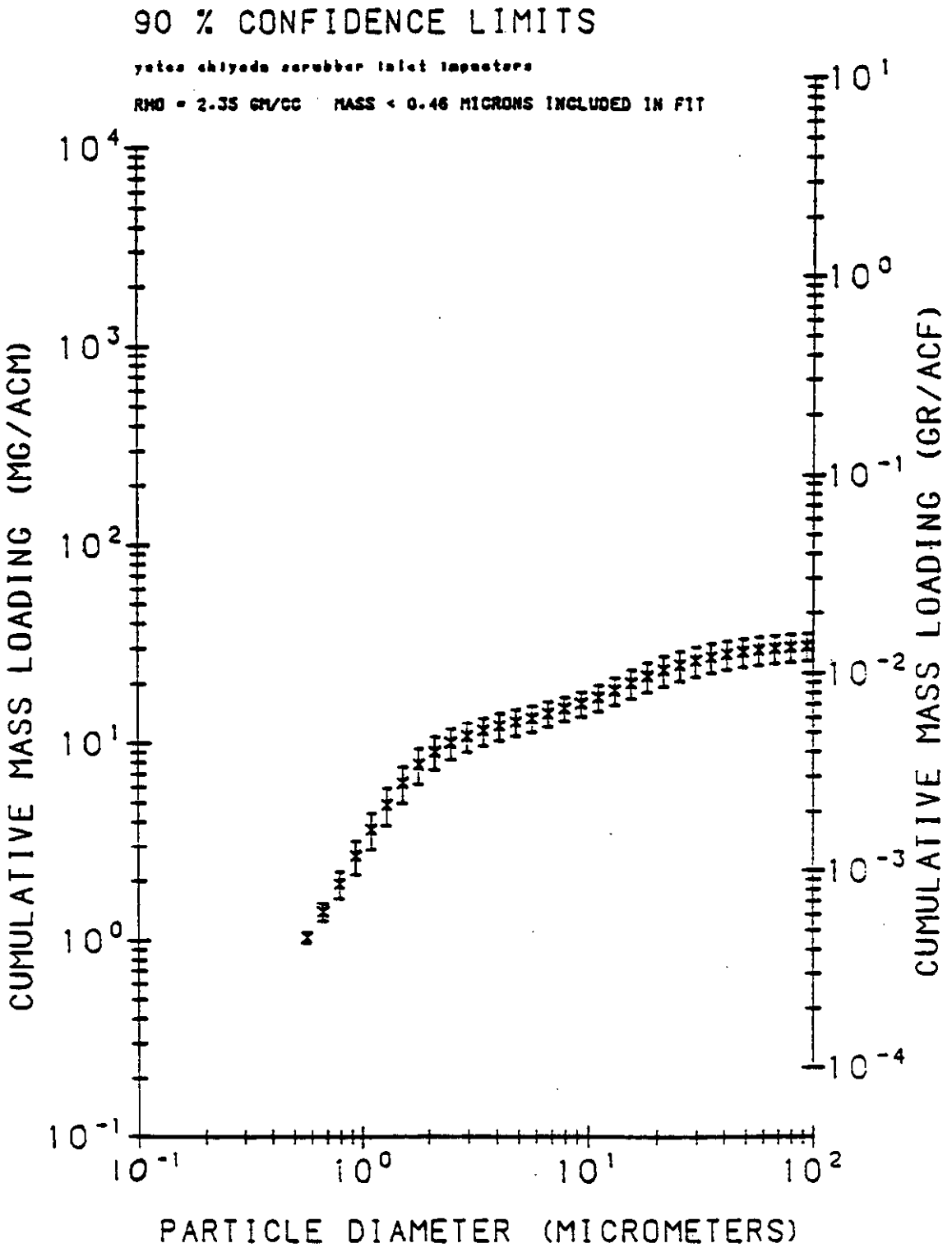

Figure 4. Inlet Cumulative Mass vs Particle Diameter for Chiyoda Scrubber, 75 MW, at 8" ΔP, January 25, 1993.

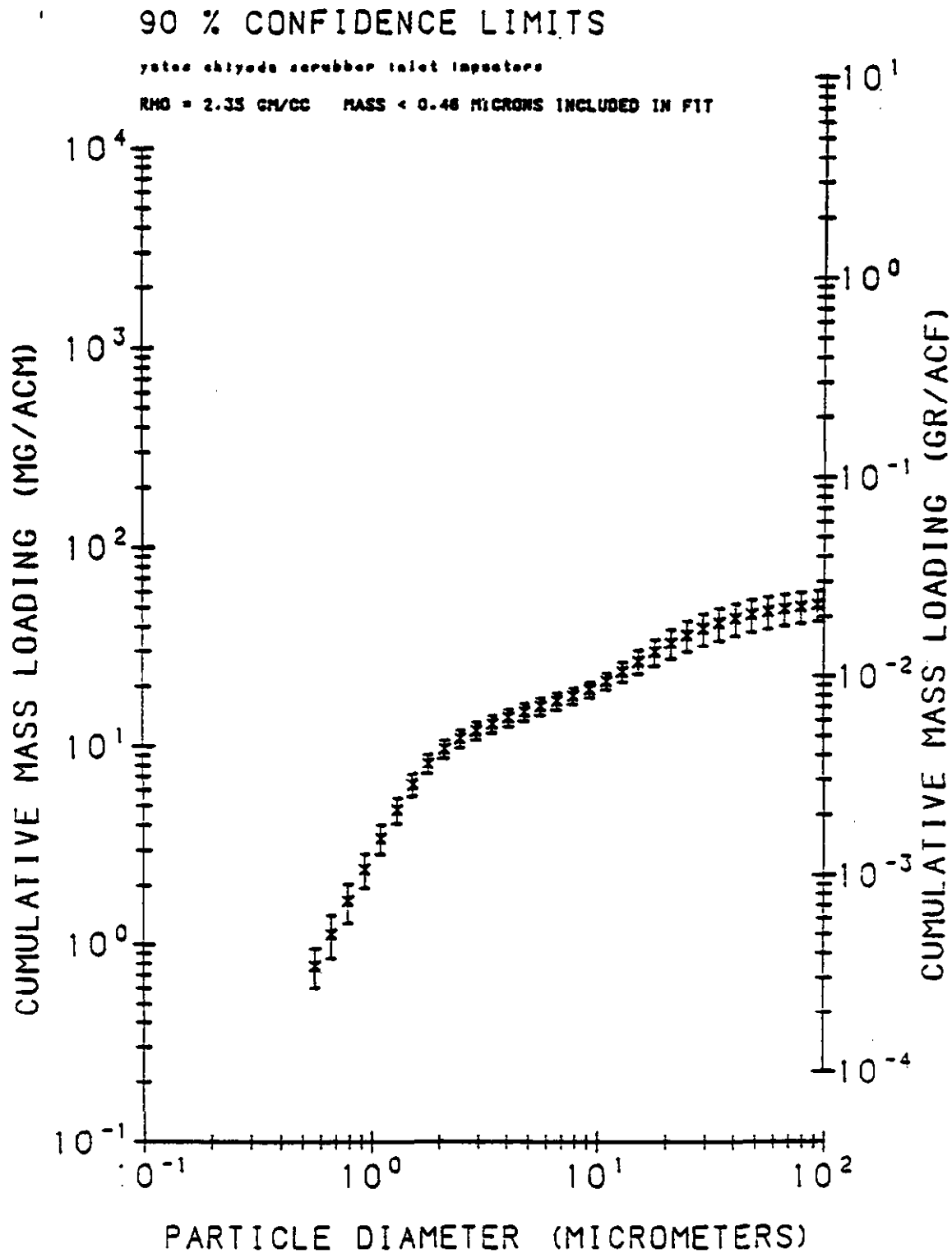

Figure 5. Inlet Cumulative Mass vs Particle Diameter for Chiyoda Scrubber, 75 MW, at 12" ΔP, January 26, 1993.

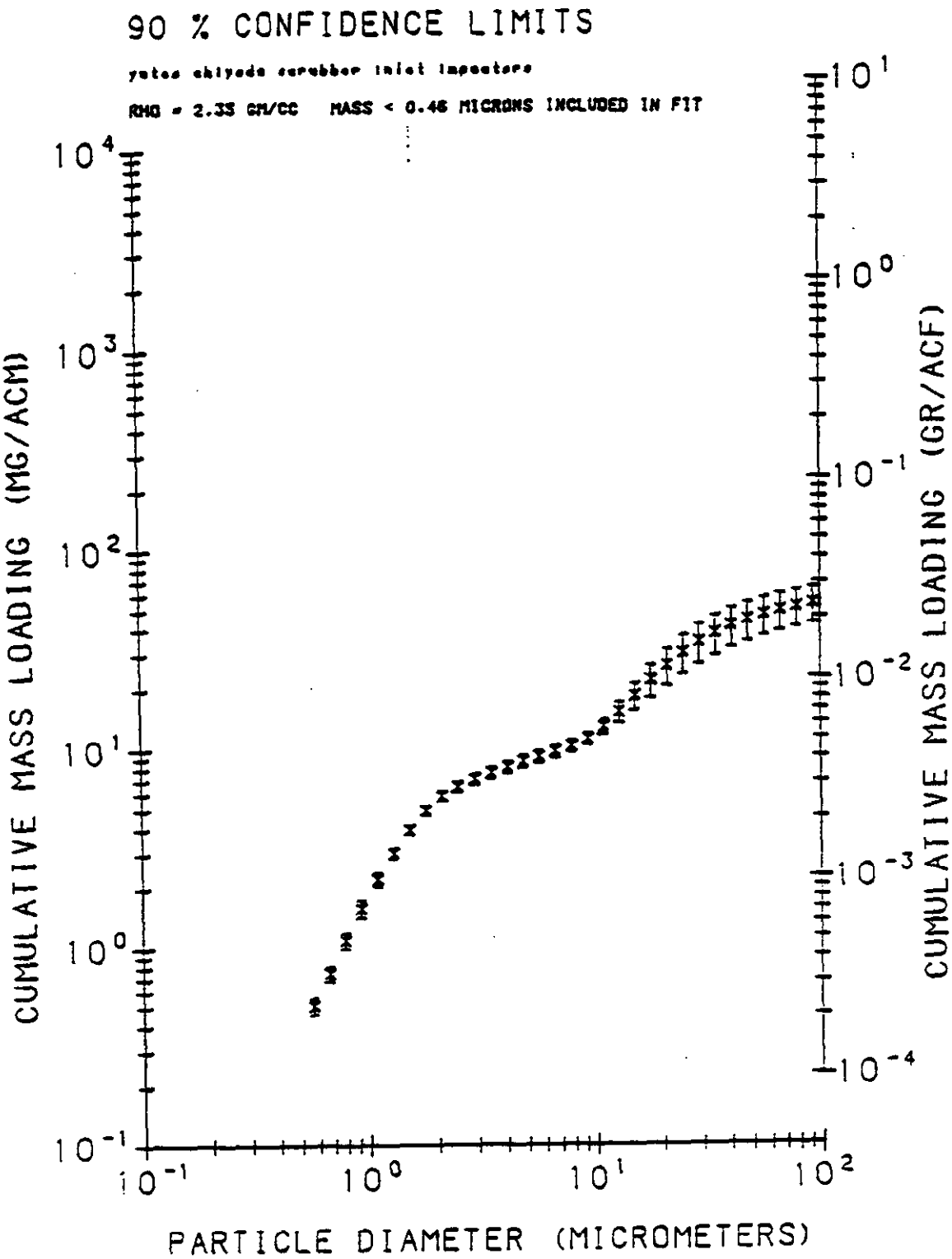

Figure 6. Inlet Cumulative Mass vs Particle Diameter for Chiyoda Scrubber, 75 MW, at 16" ΔP, January 27, 1993.

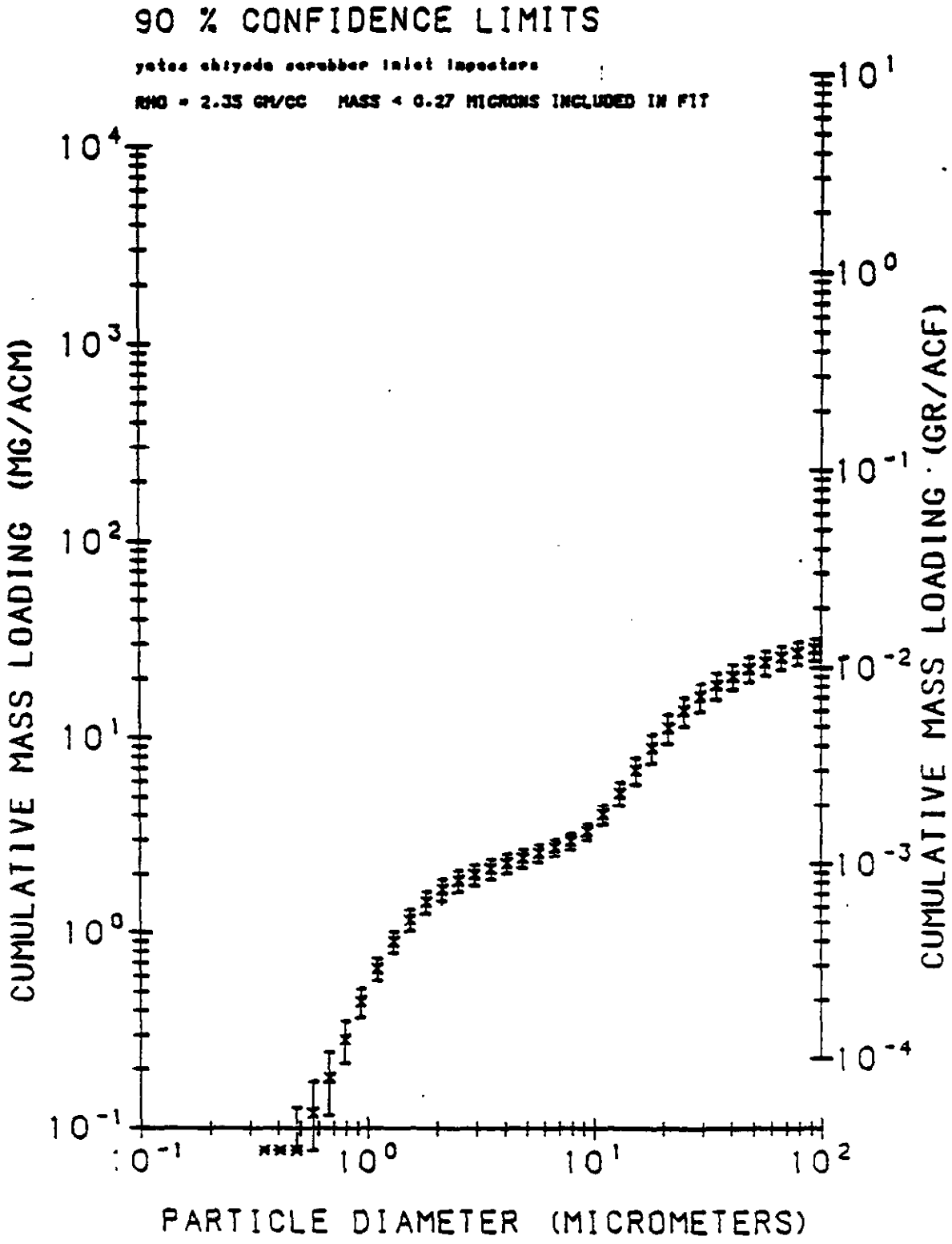

Figure 7. Inlet Cumulative Mass vs Particle Diameter for Chiyoda Scrubber, 50 MW, at 8" ΔP, January 29, 1993.

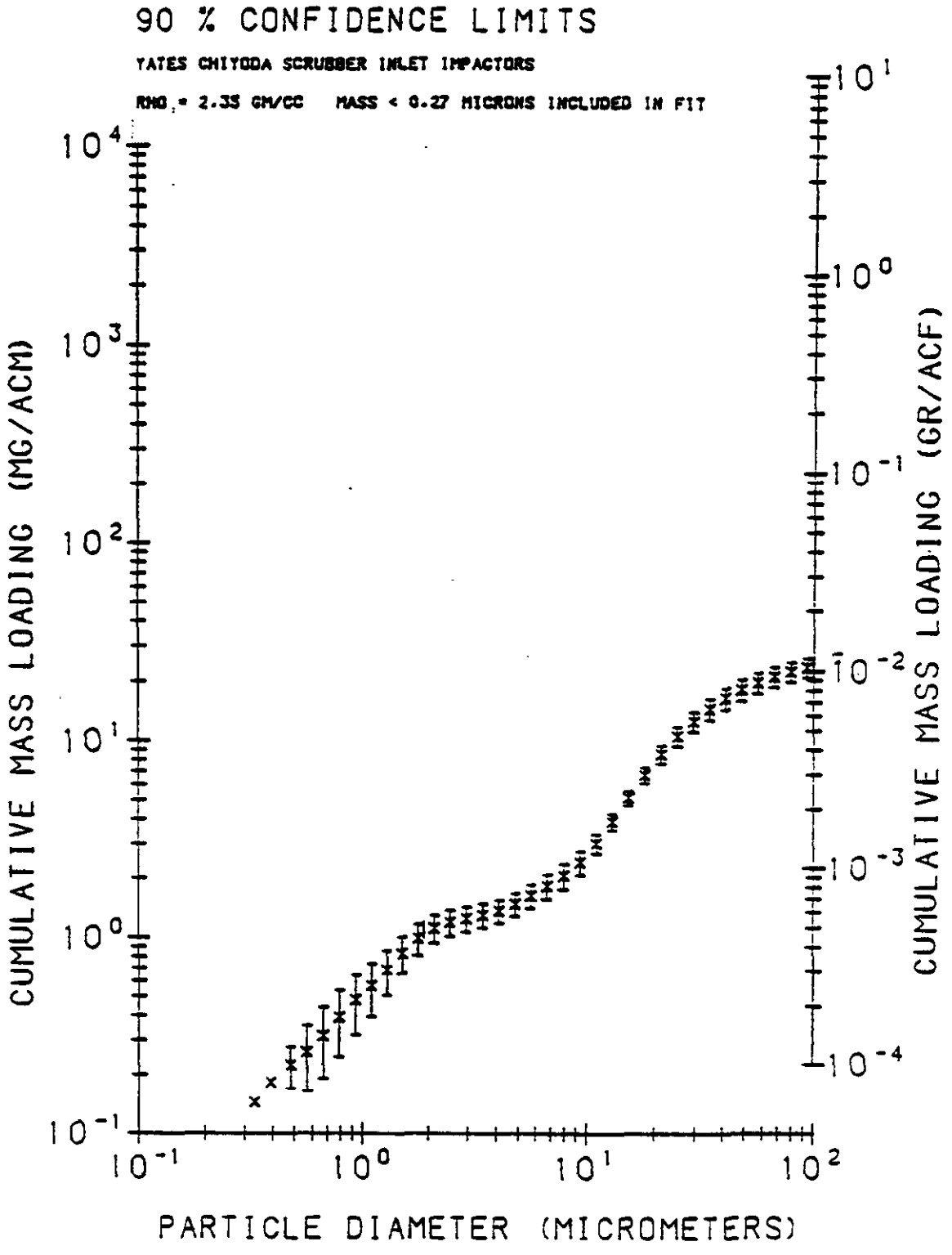

Figure 8. Inlet Cumulative Mass vs Particle Diameter for Chiyoda Scrubber, 50 MW_e at 12" ΔP, January 30, 1993.

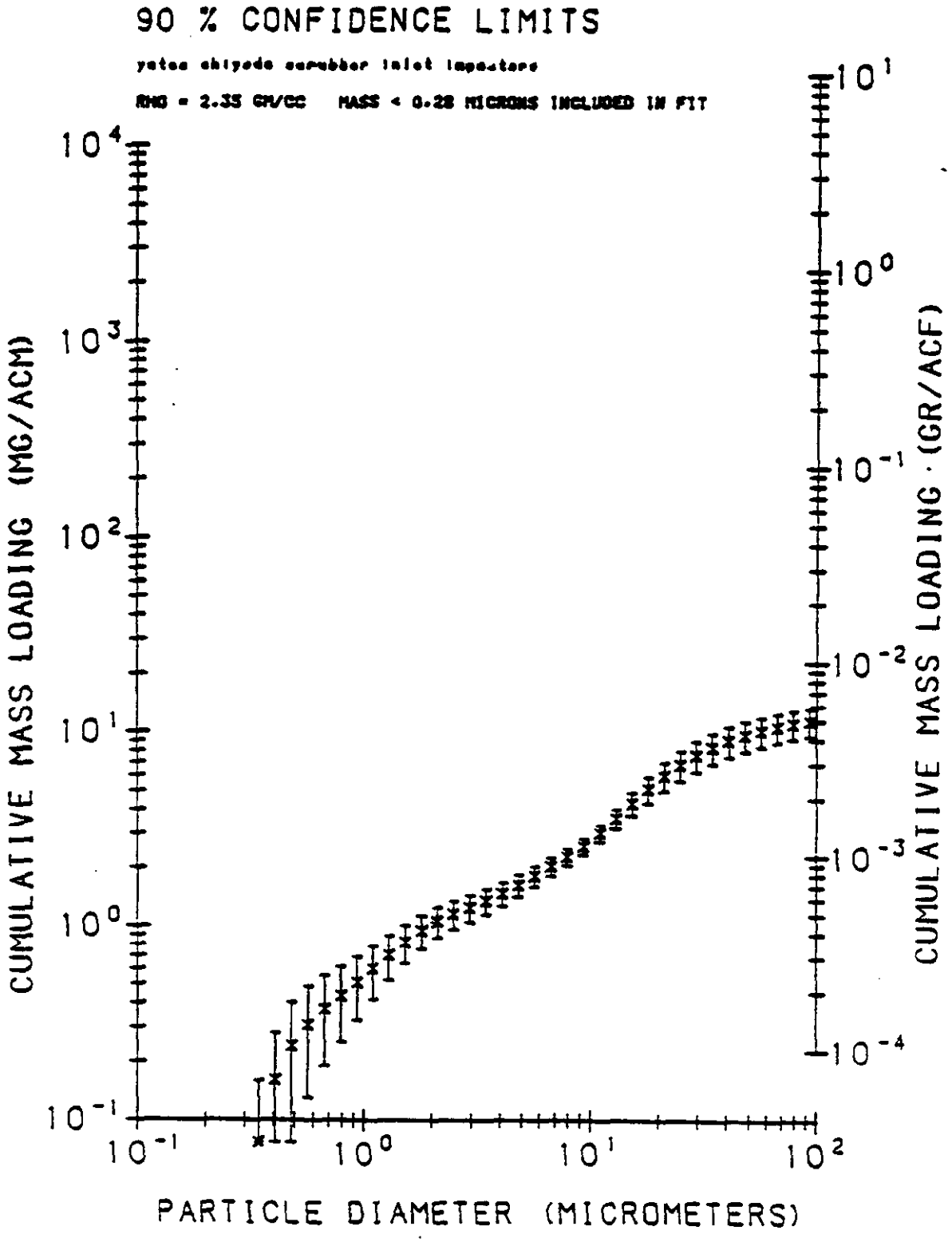

Figure 9. Inlet Cumulative Mass vs Particle Diameter for Chiyoda Scrubber, 50 MW, at 16" ΔP, January 31, 1993.

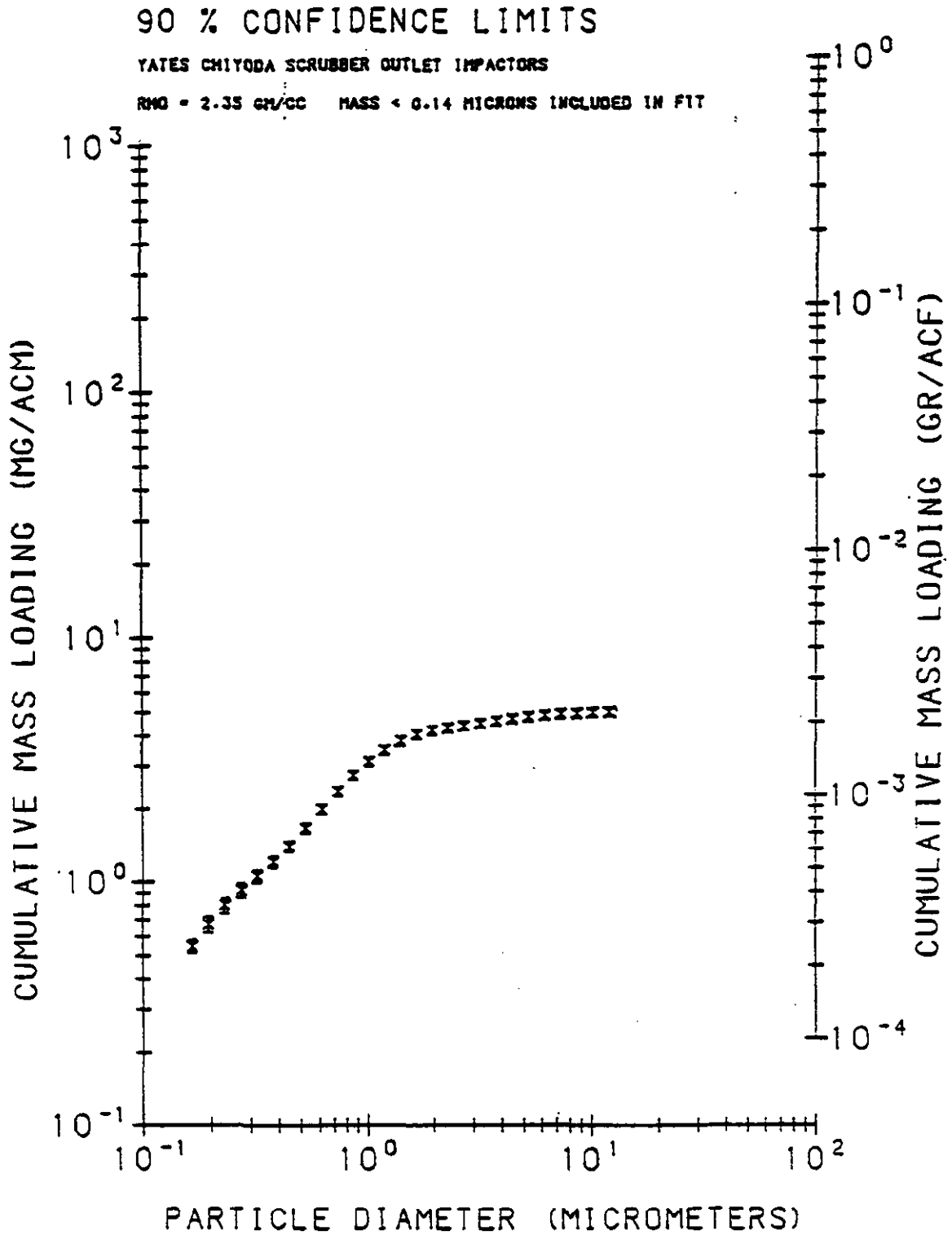

Figure 10. Outlet Cumulative Mass vs Particle Diameter for Chiyoda Scrubber, 100 MW_e at 8" ΔP, January 21, 1993.

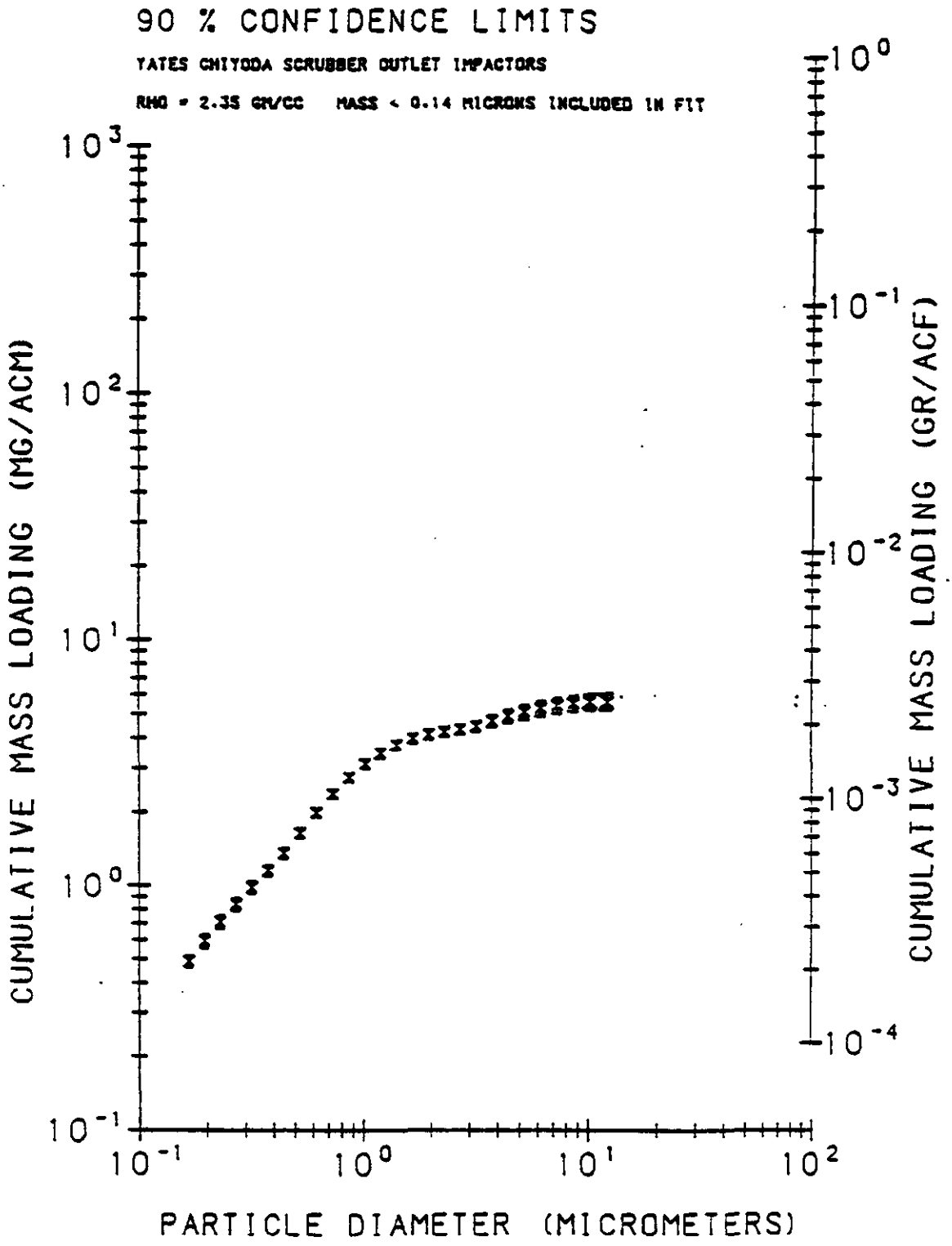

Figure 11. Outlet Cumulative Mass vs Particle Diameter for Chiyoda Scrubber, 100 MW$_e$ at 12" ΔP, January 22, 1993.

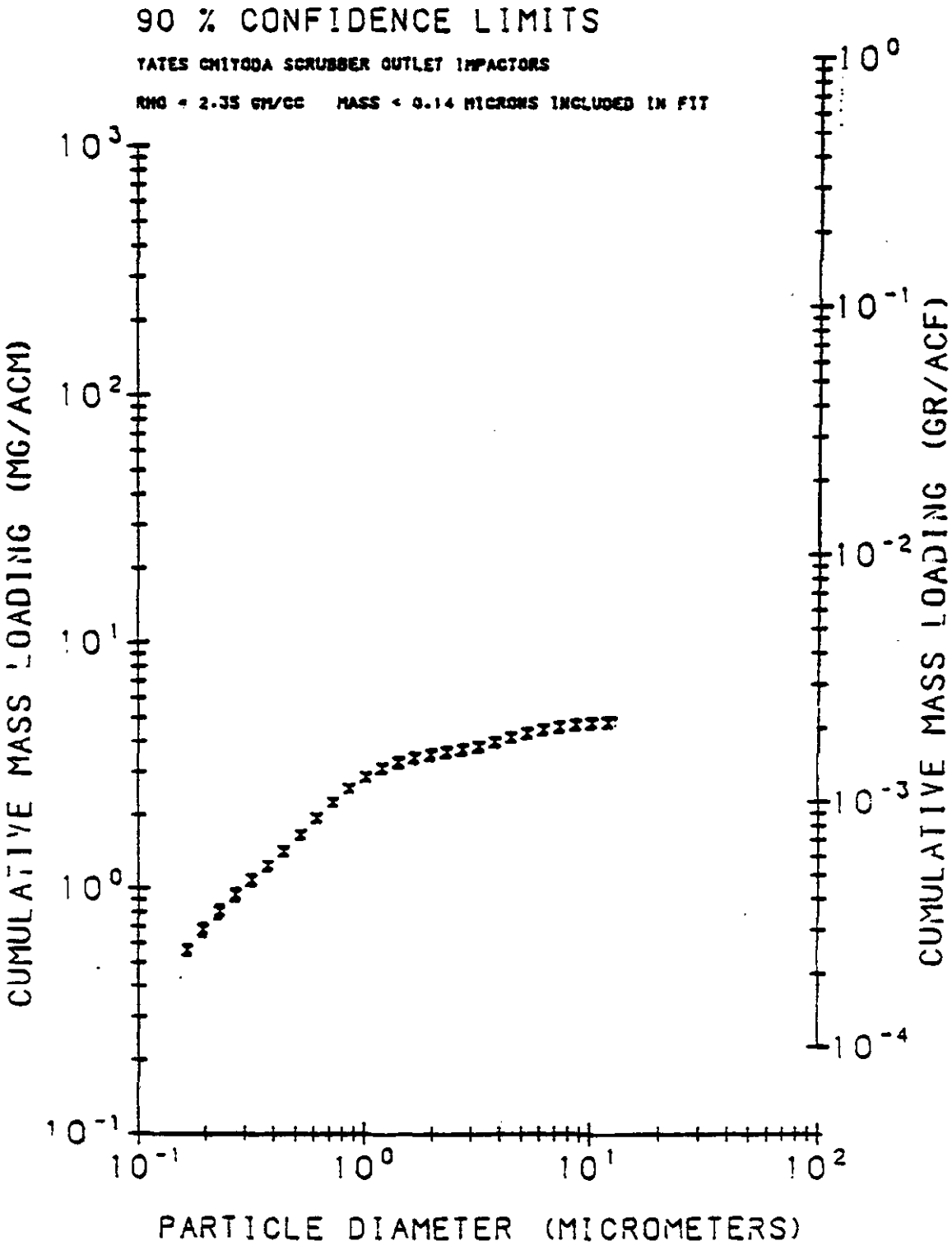

Figure 12. Outlet Cumulative Mass vs Particle Diameter for Chiyoda Scrubber, 100 MW, at 16" ΔP, January 23, 1993.

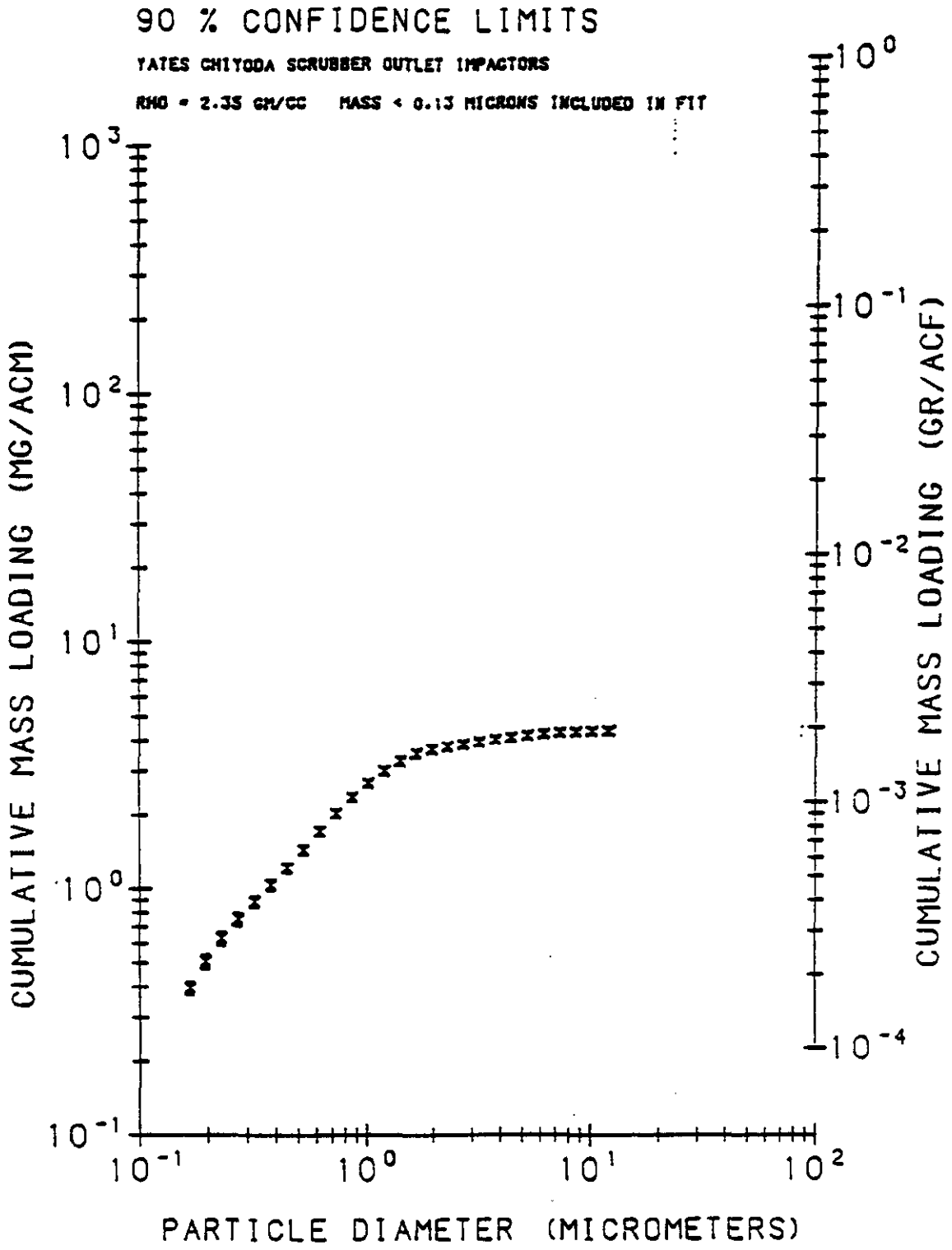

Figure 13. Outlet Cumulative Mass vs Particle Diameter for Chiyoda Scrubber, 75 MW_e at 8" ΔP, January 25, 1993.

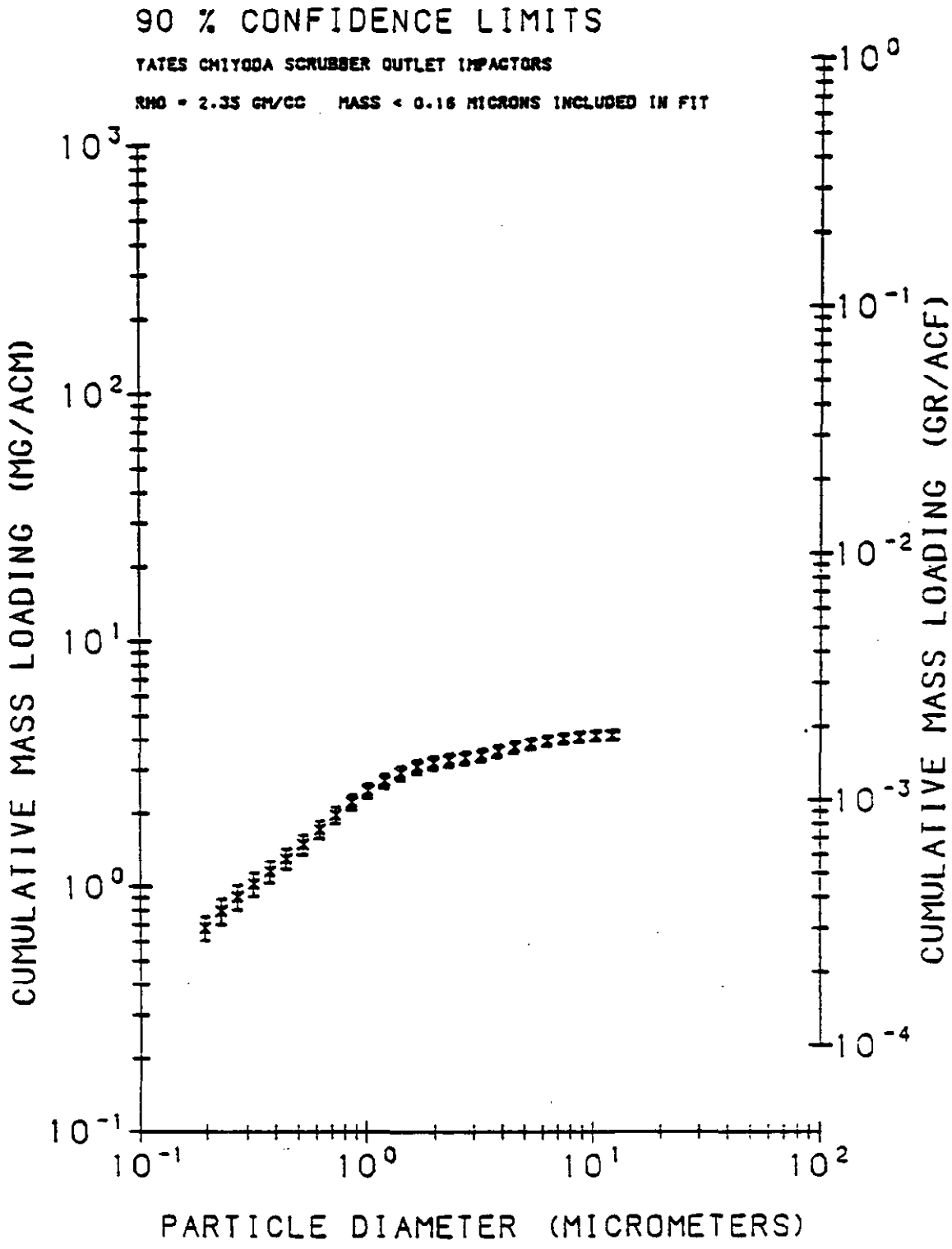

Figure 14. Outlet Cumulative Mass vs Particle Diameter for Chiyoda Scrubber, 75 MW_e at 12" ΔP, January 26, 1993.

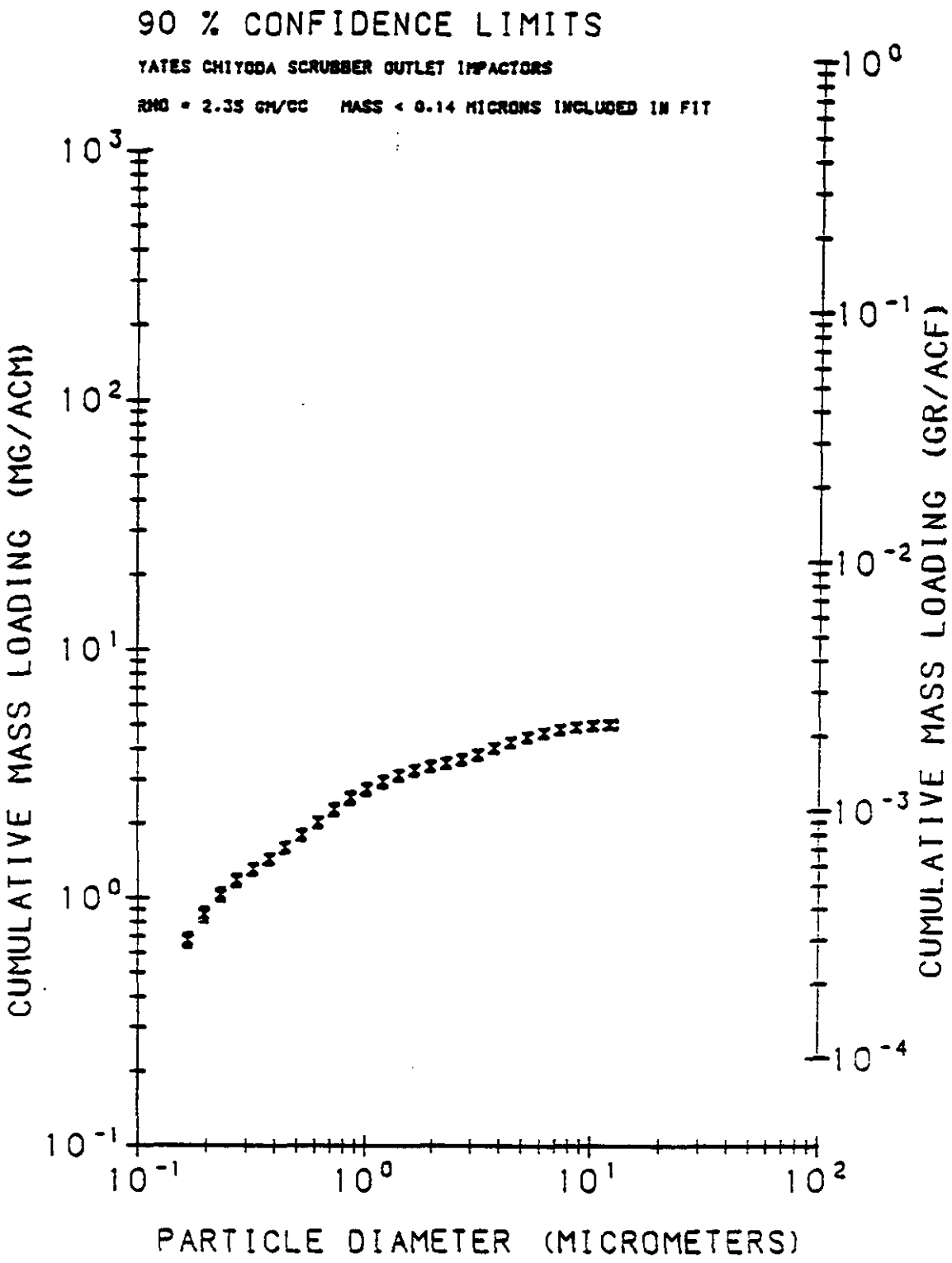

Figure 15. Outlet Cumulative Mass vs Particle Diameter for Chiyoda Scrubber, 75 MW, at 16" ΔP, January 27, 1993.

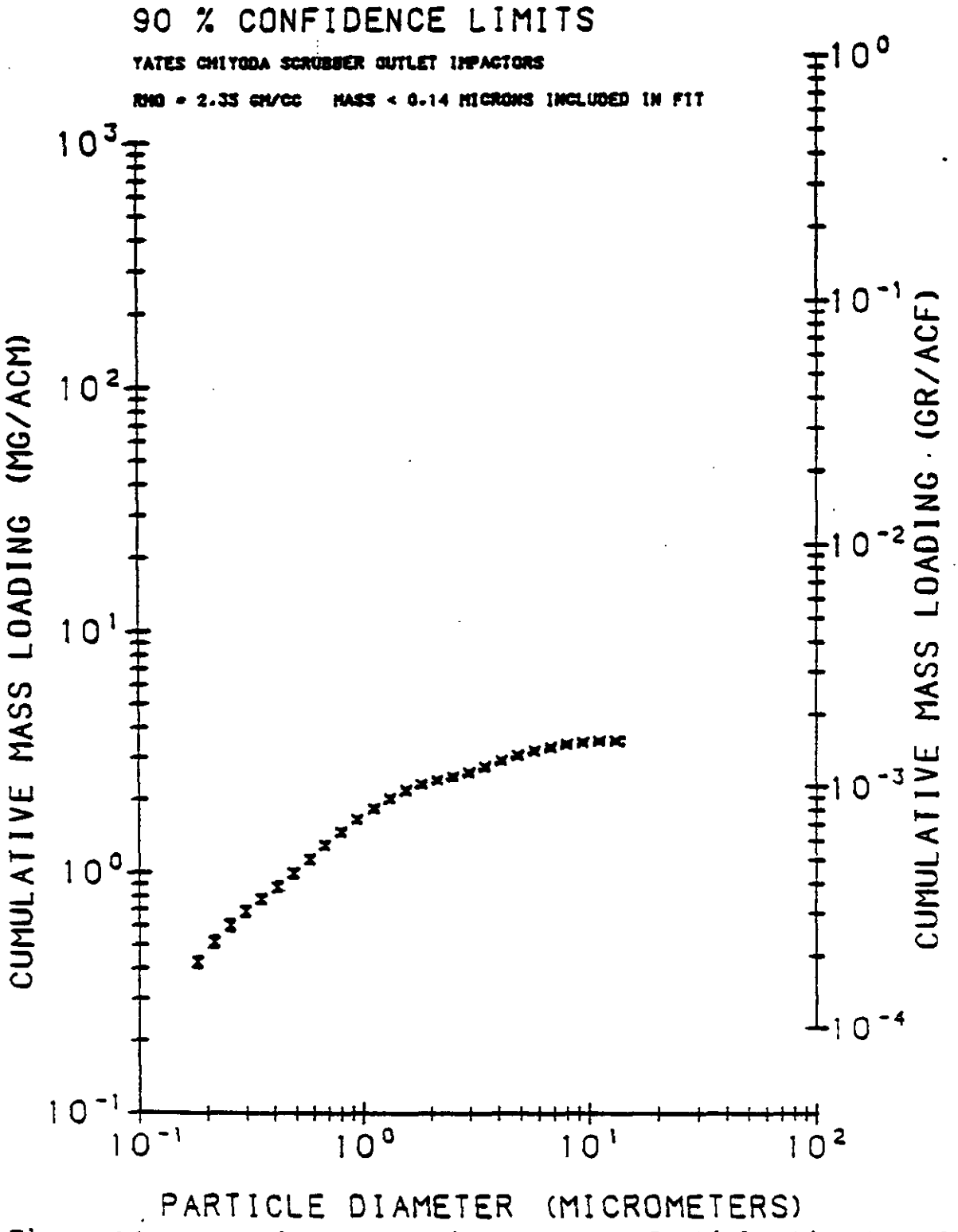

Figure 16. Outlet Cumulative Mass vs Particle Diameter for Chiyoda Scrubber, 50 MW, at 8" ΔP, January 29, 1993.

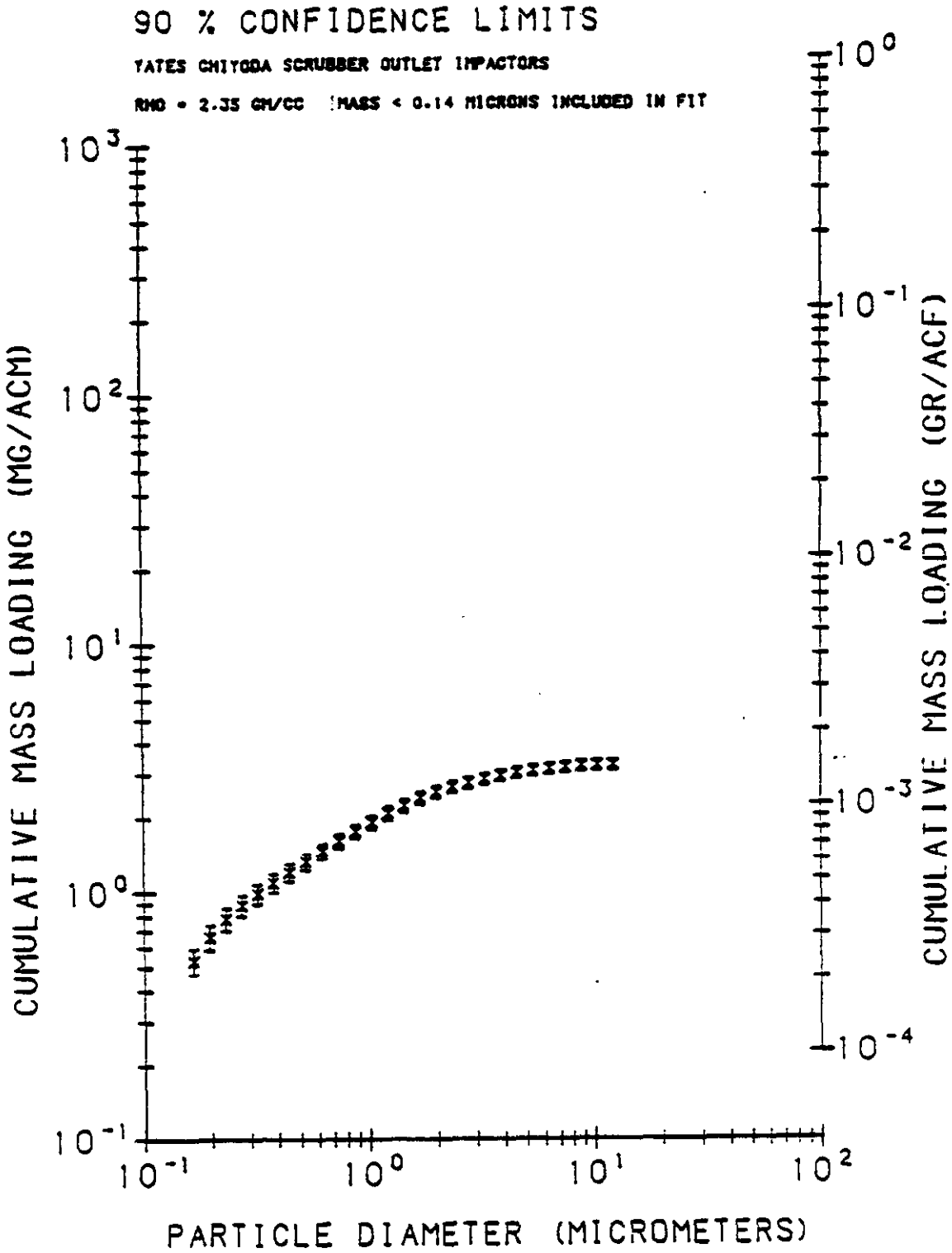

Figure 17. Outlet Cumulative Mass vs Particle Diameter for Chiyoda Scrubber, 50 MW, at 12" ΔP, January 30, 1993.

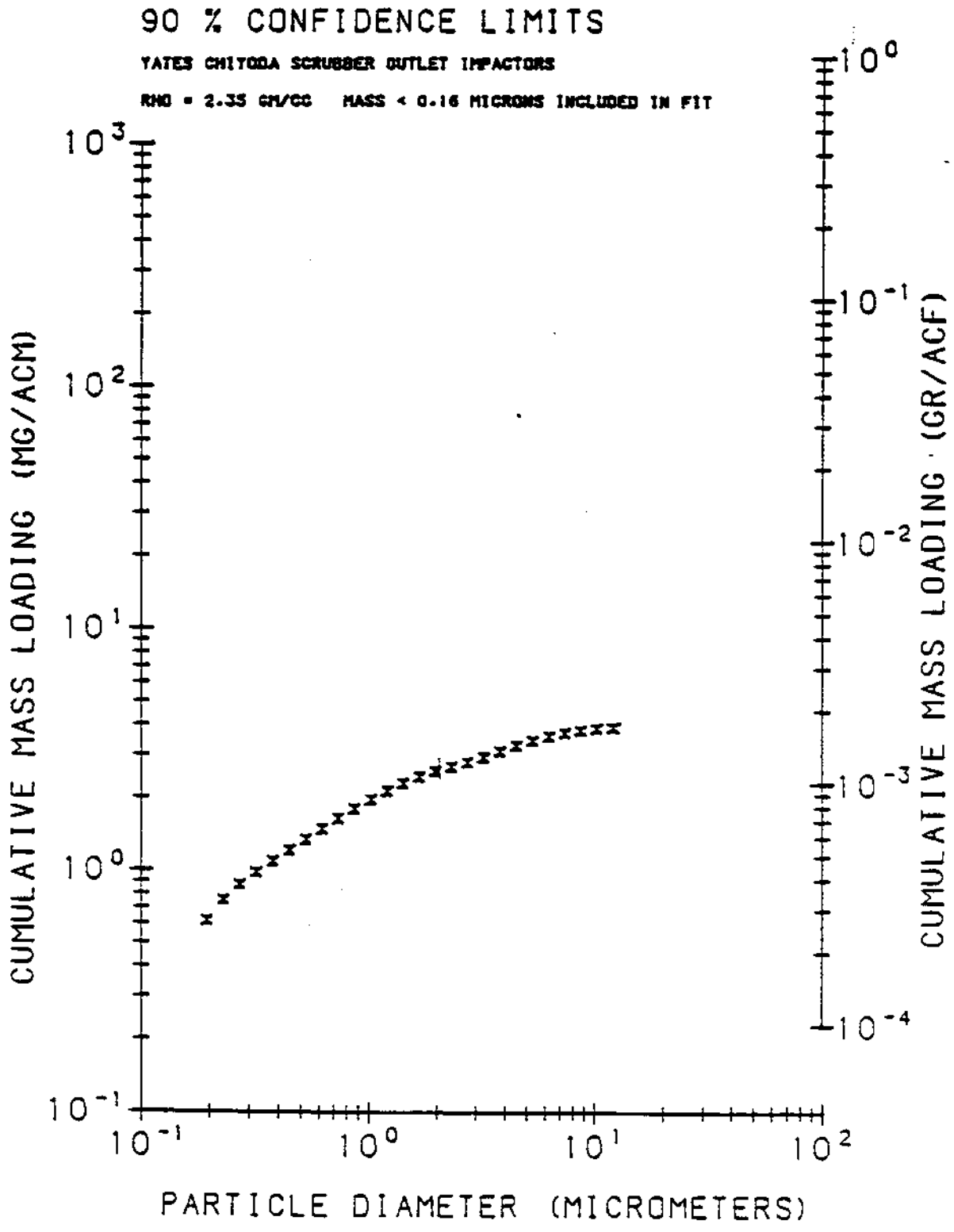

Figure 18. Outlet Cumulative Mass vs Particle Diameter for Chiyoda Scrubber, 50 MW$_e$ at 16" ΔP, January 31, 1993.

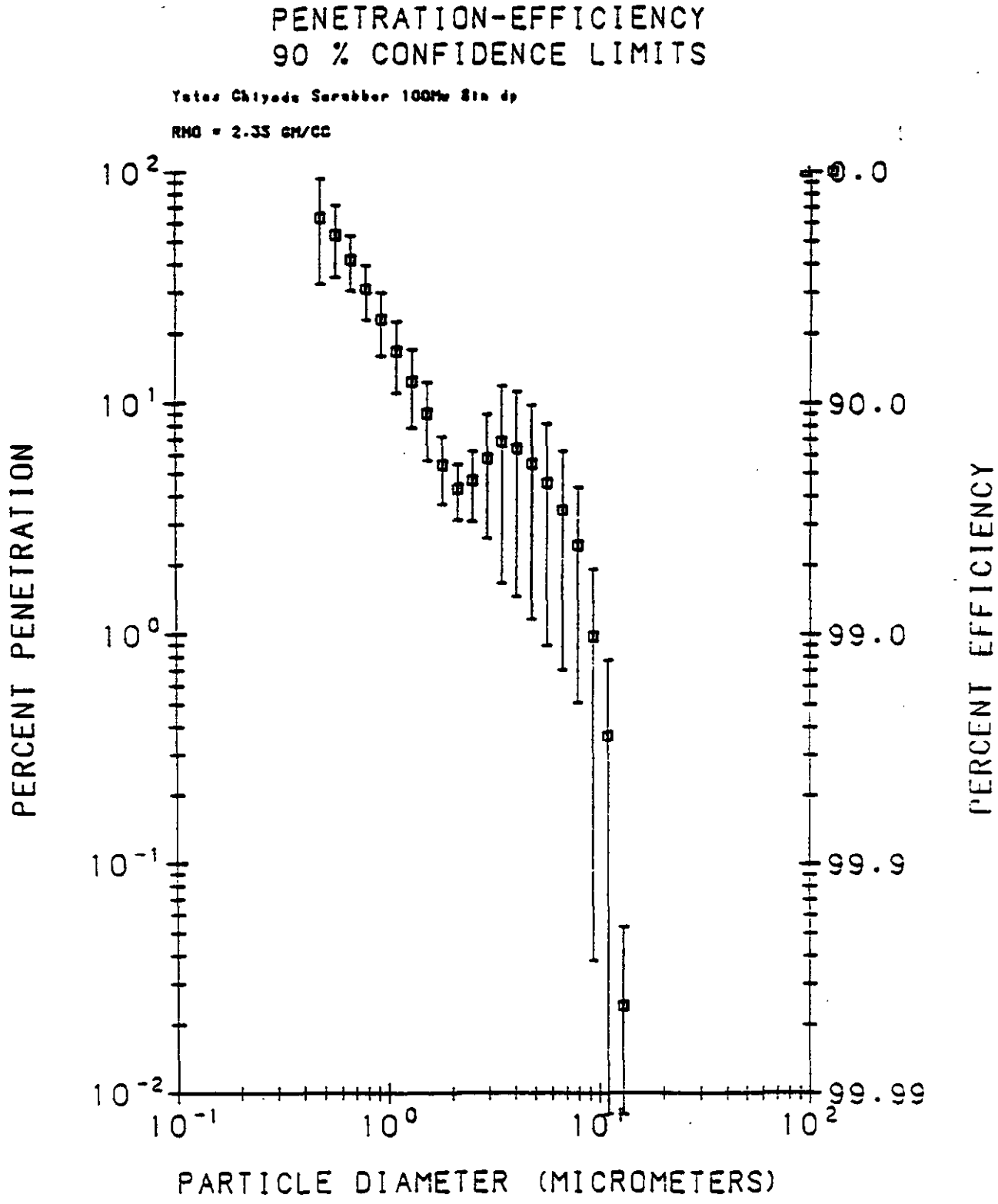

Figure 19. Fractional Collection Efficiency of Chiyoda Scrubber, 100 MW, at 8" ΔP, January 21, 1993.

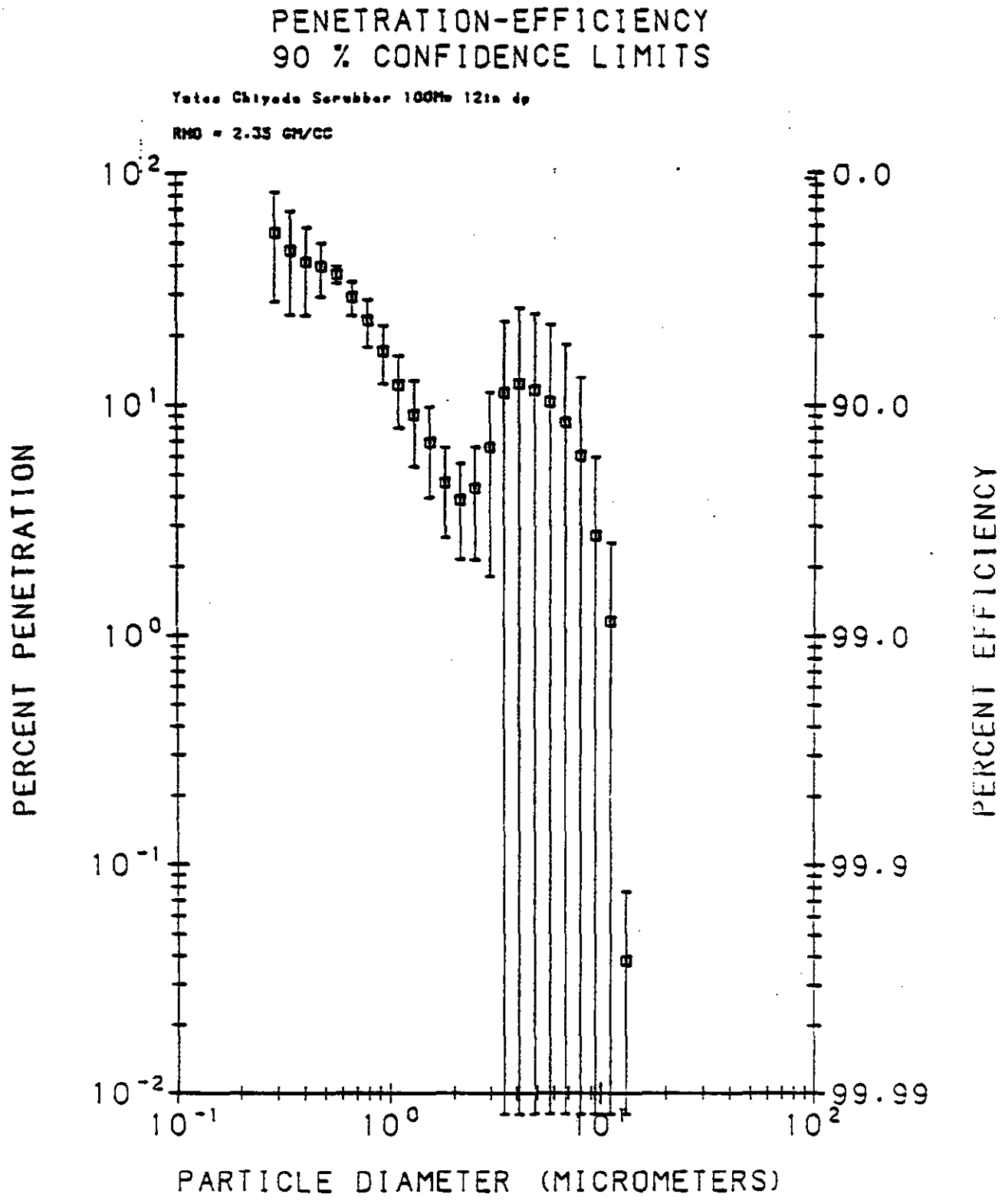

Figure 20. Fractional Collection Efficiency of Chiyoda Scrubber, 100 MW_e at 12" ΔP, January 22, 1993.

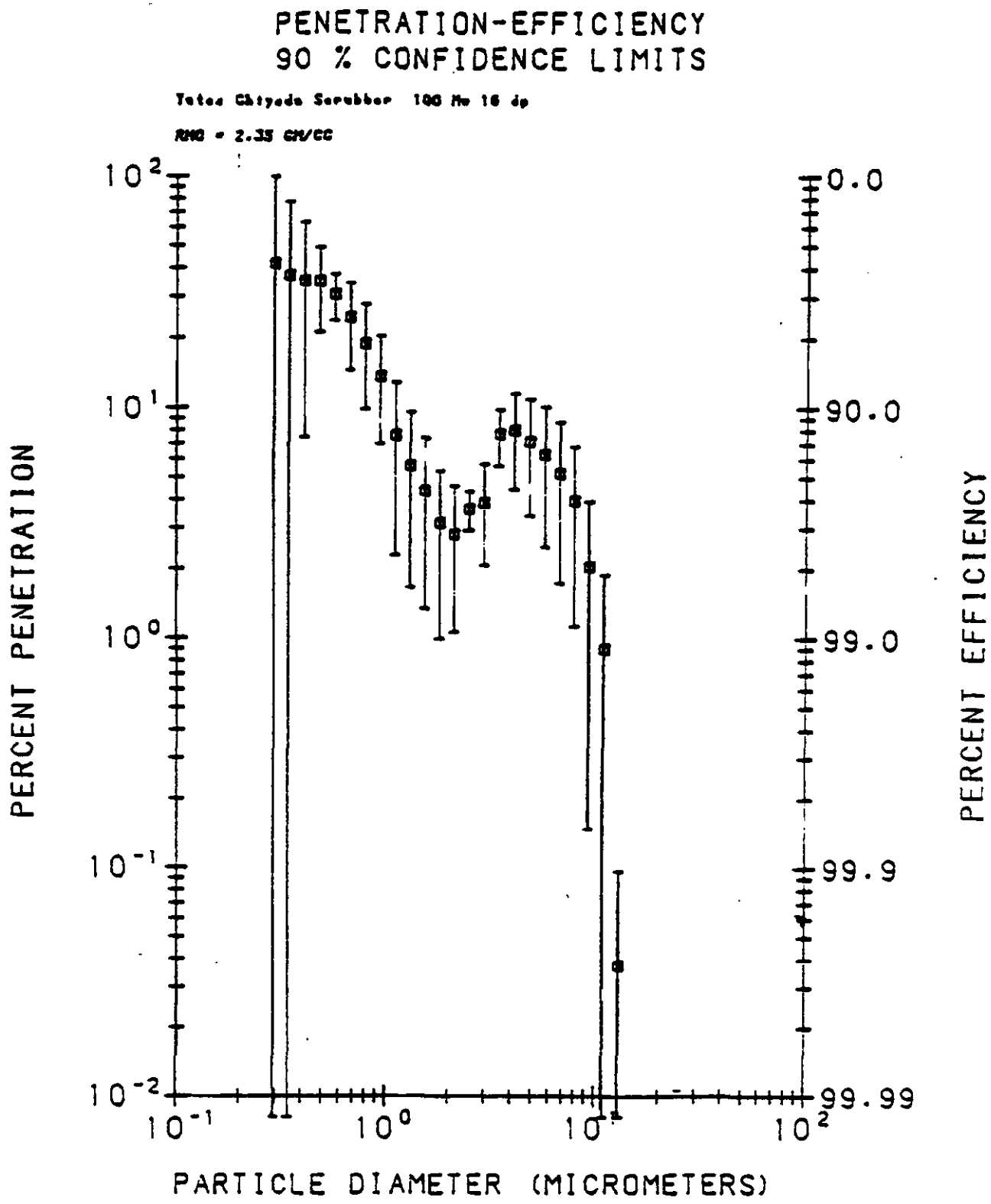

Figure 21. Fractional Collection Efficiency of Chiyoda Scrubber, 100 MW, at 16" ΔP, January 23, 1993.

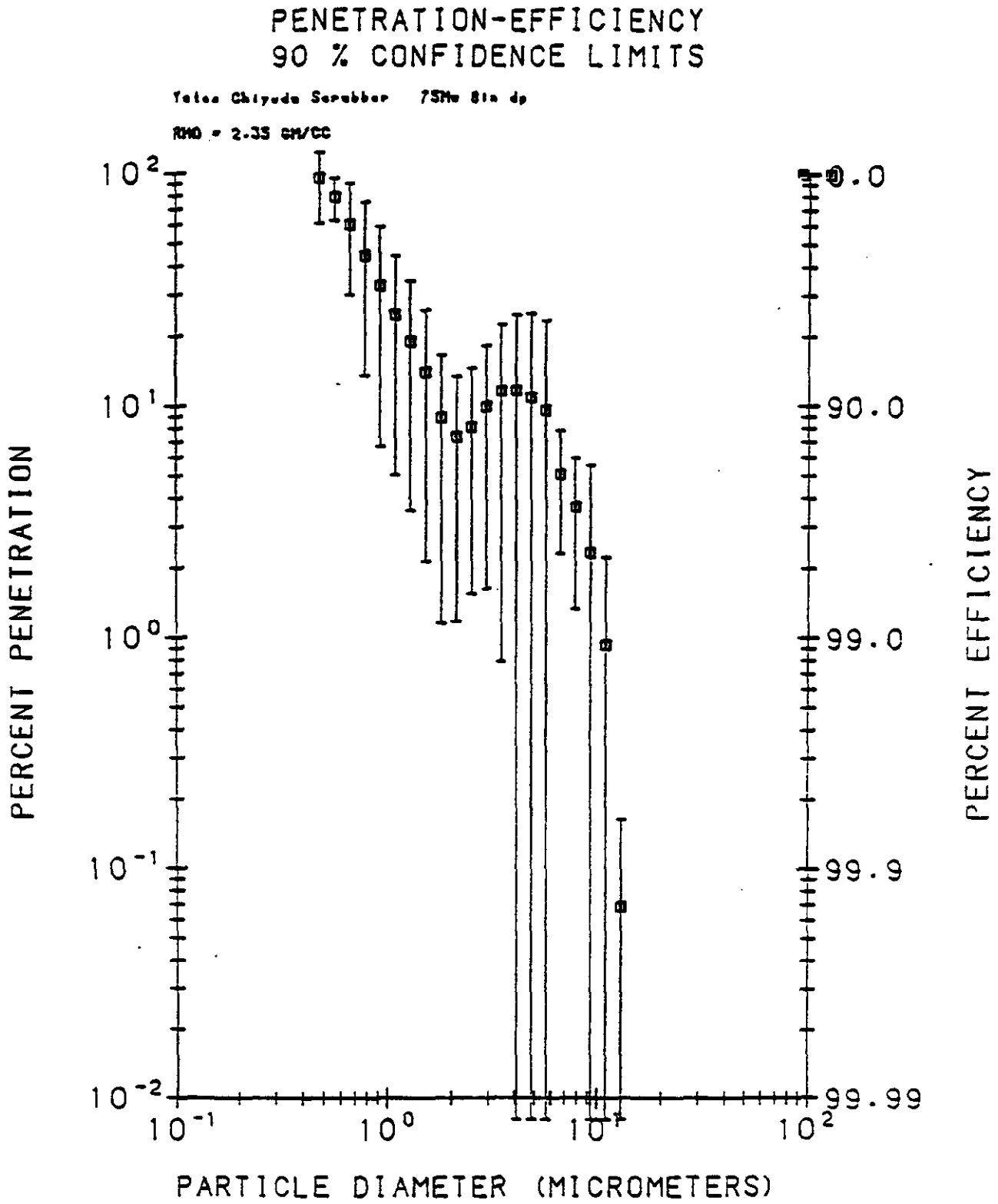

Figure 22. Fractional Collection Efficiency of Chiyoda Scrubber, 75 MW, at 8" ΔP, January 25, 1993.

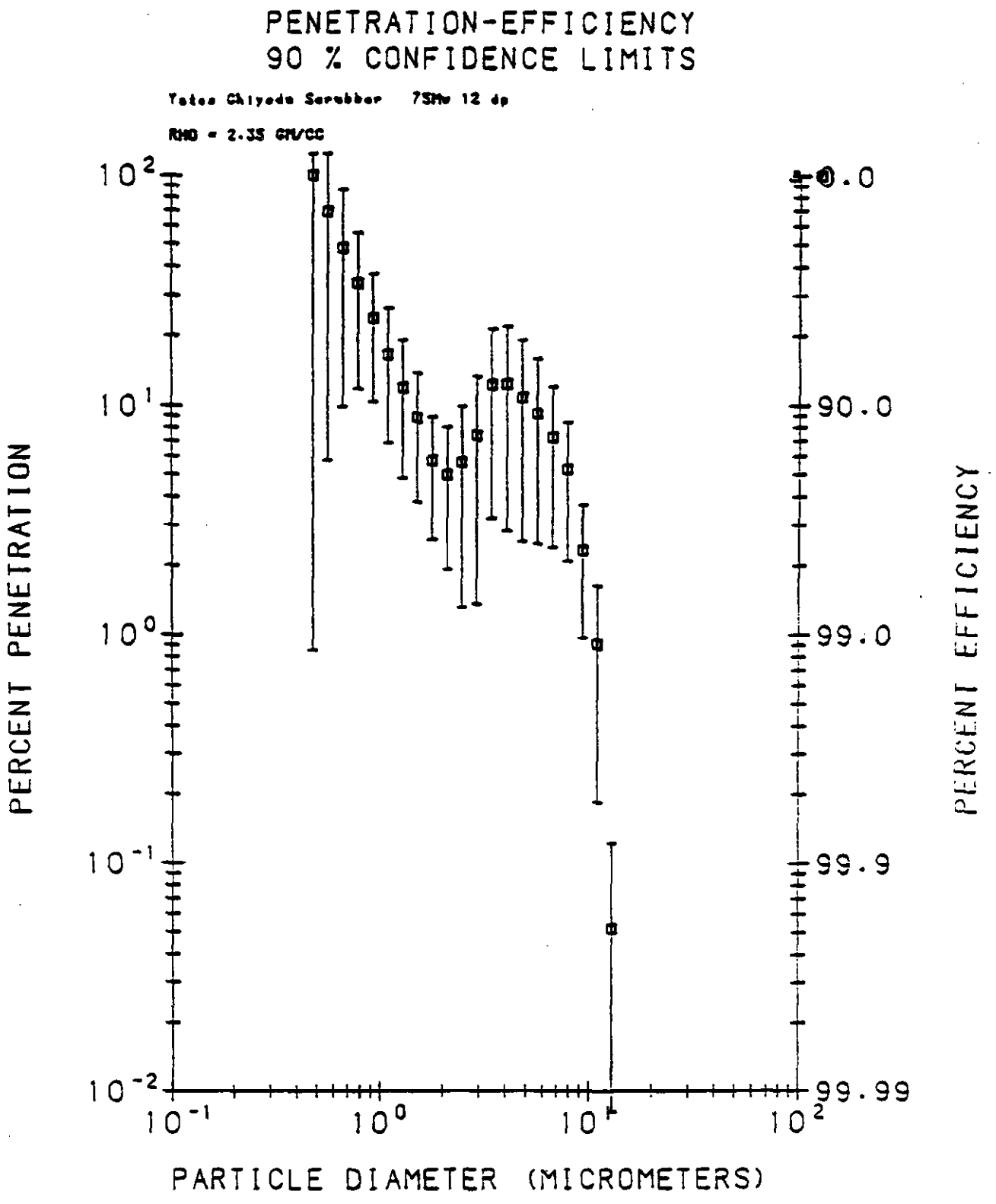

Figure 23. Fractional Collection Efficiency of Chiyoda Scrubber, 75 MW, at 12" ΔP, January 26, 1993.

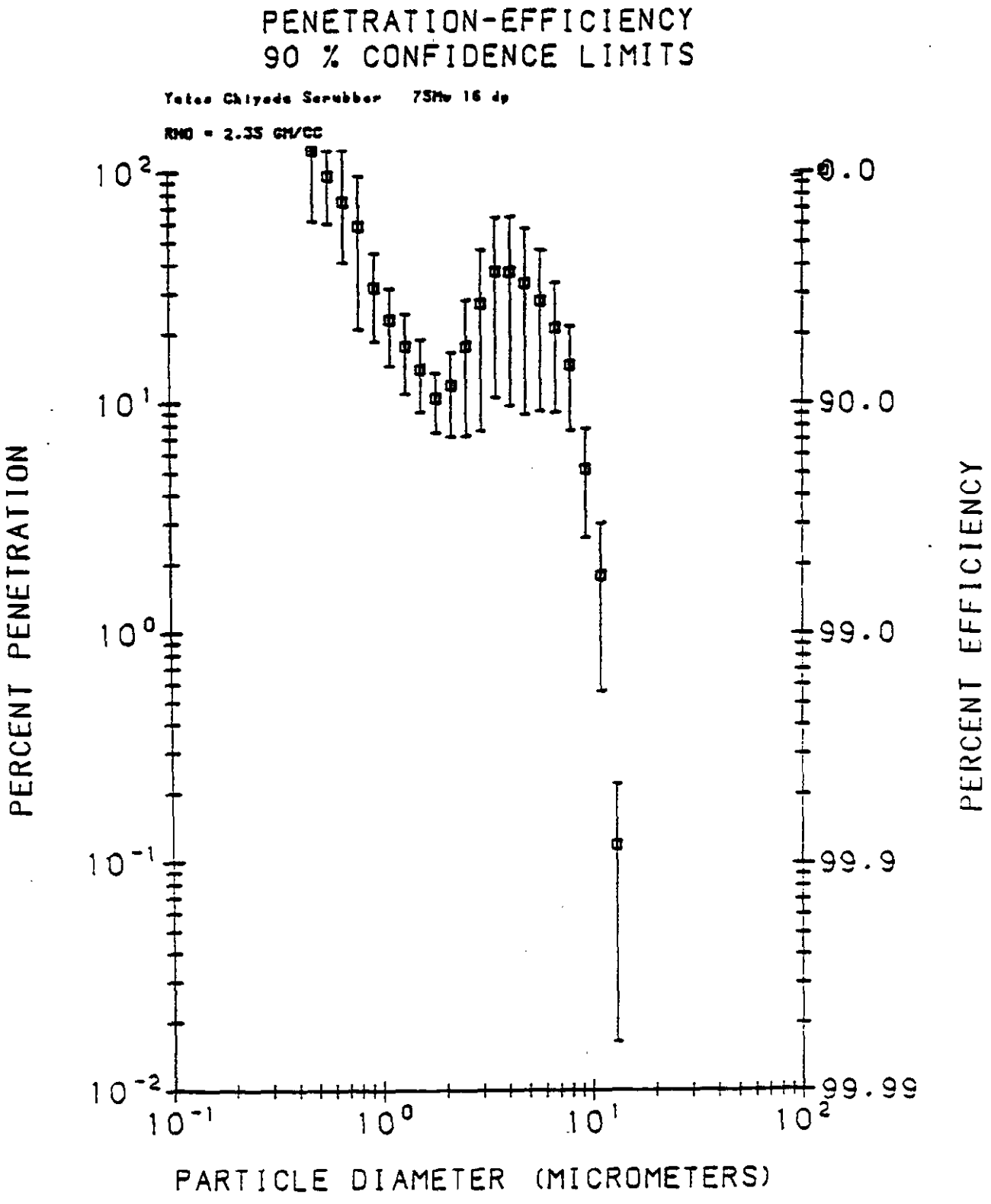

Figure 24. Fractional Collection Efficiency of Chiyoda Scrubber, 75 MW$_e$ at 16" ΔP, January 27, 1993.

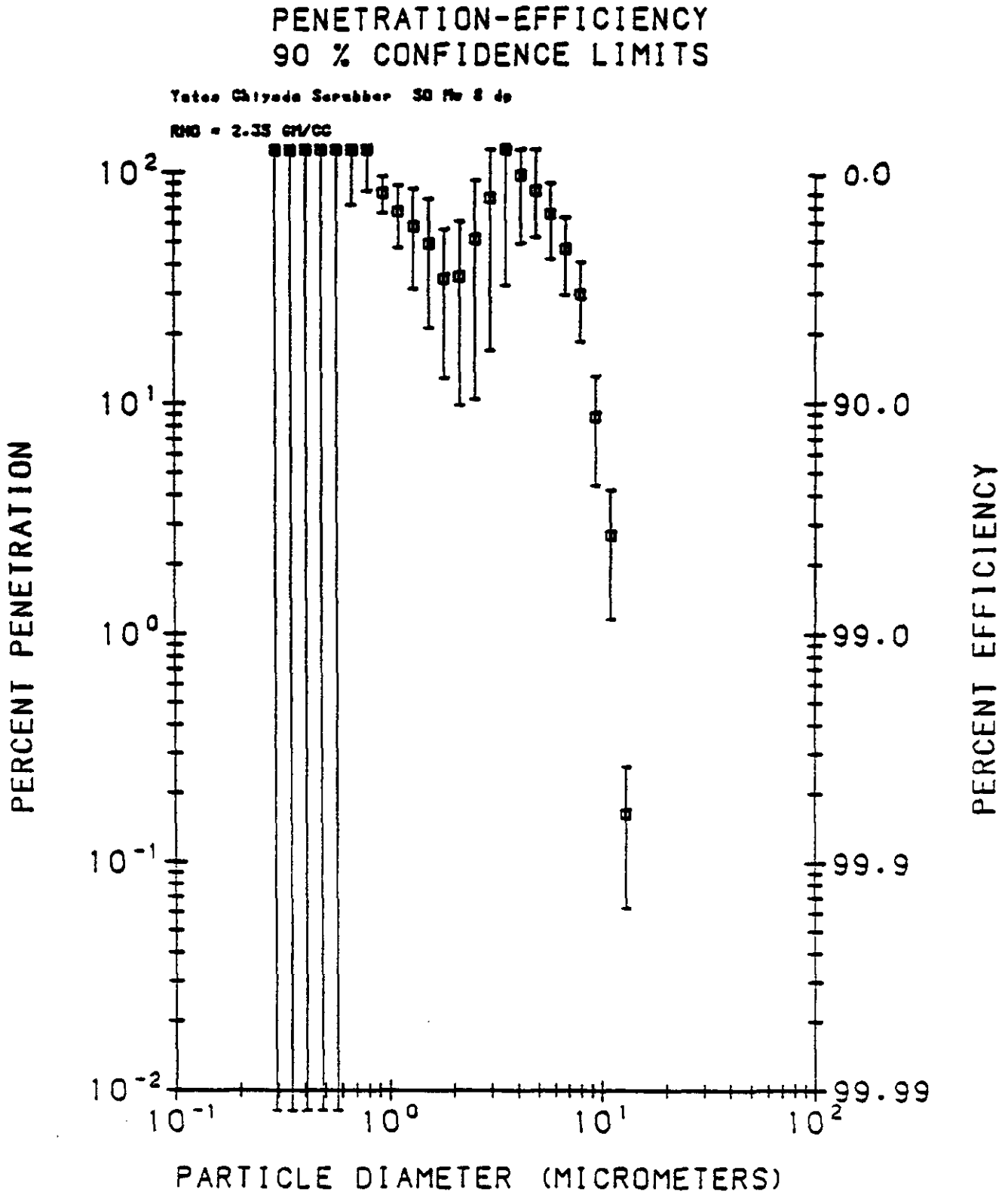

Figure 25. Fractional Collection Efficiency of Chiyoda Scrubber, 50 MW, at 8" ΔP, January 29, 1993.

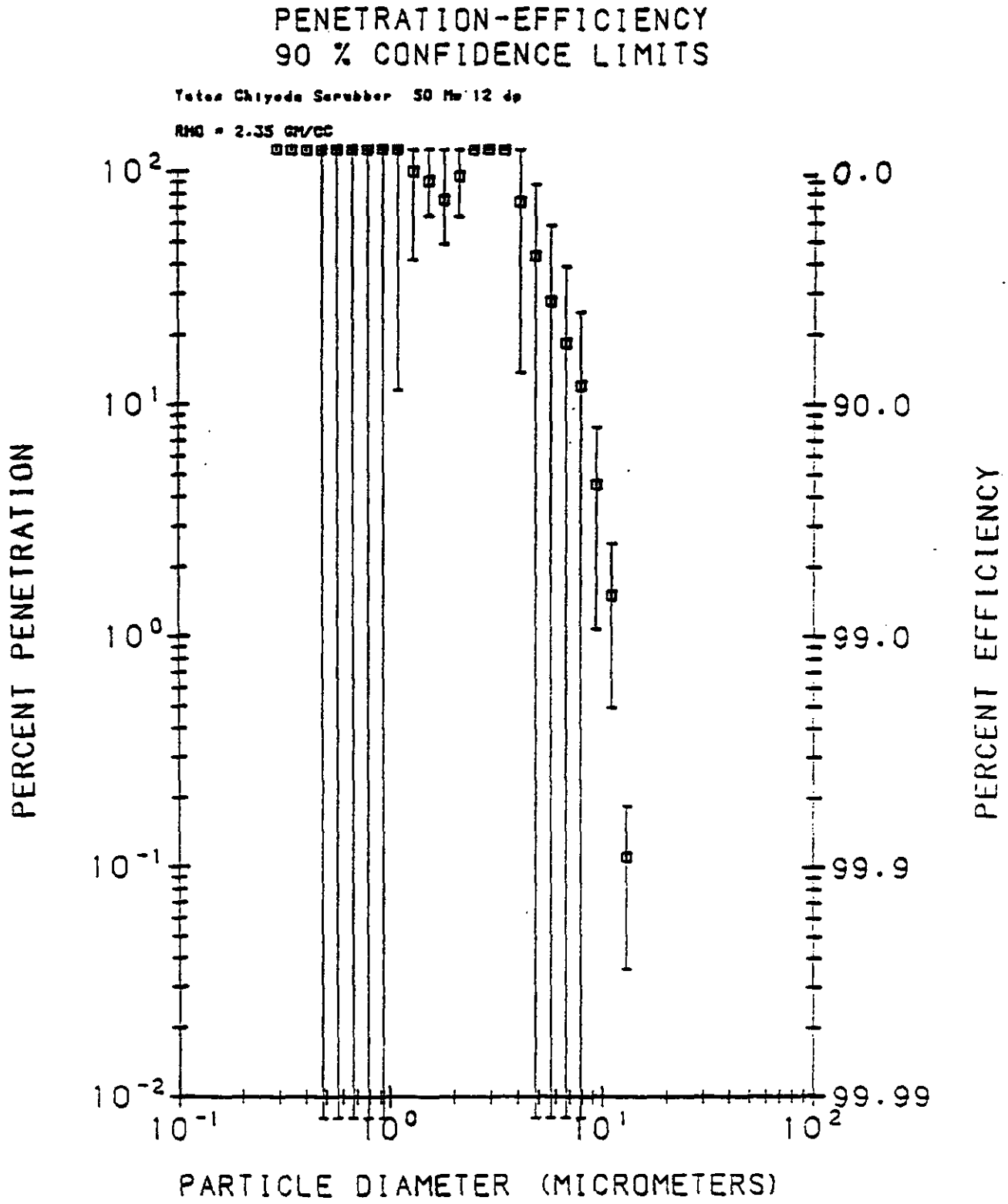

Figure 26. Fractional Collection Efficiency of Chiyoda Scrubber, 50 MW, at 12" ΔP, January 30, 1993.

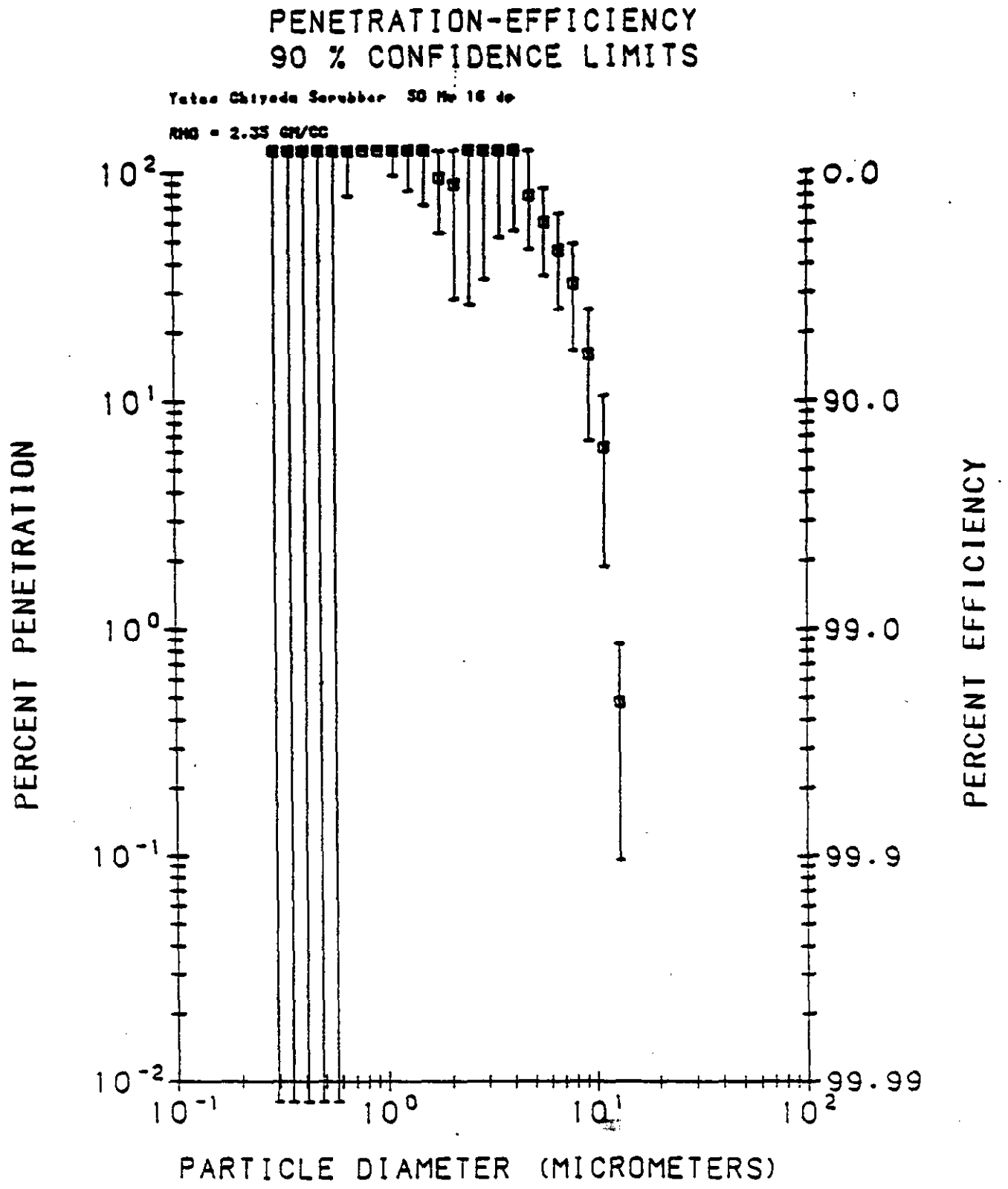

Figure 27. Fractional Collection Efficiency of Chiyoda Scrubber, 50 MW, at 16" ΔP, January 31, 1993.

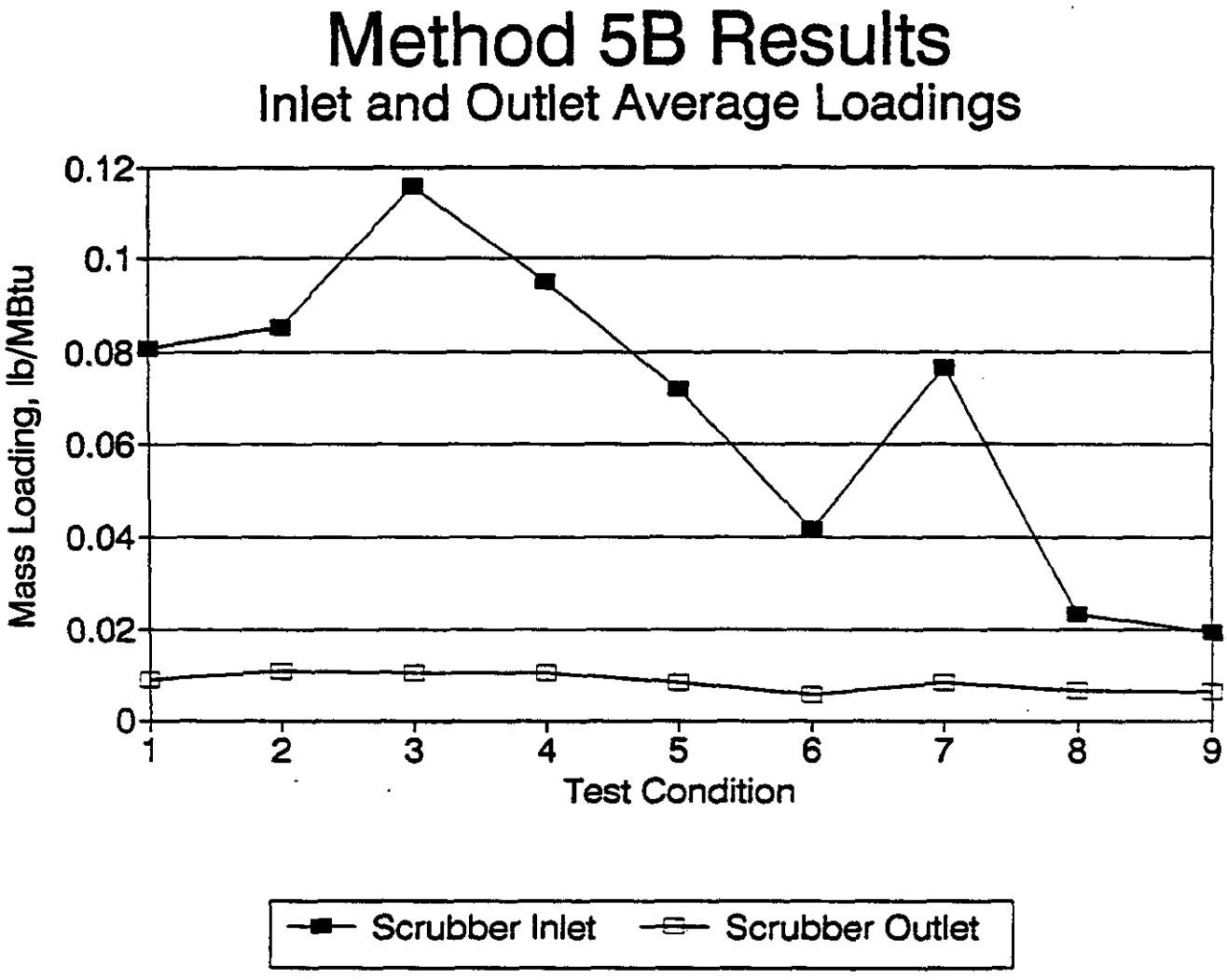

Figure 28. Average Method 5B Results for Each Test Condition, Chiyoda Test Program, January 21-31, 1993.

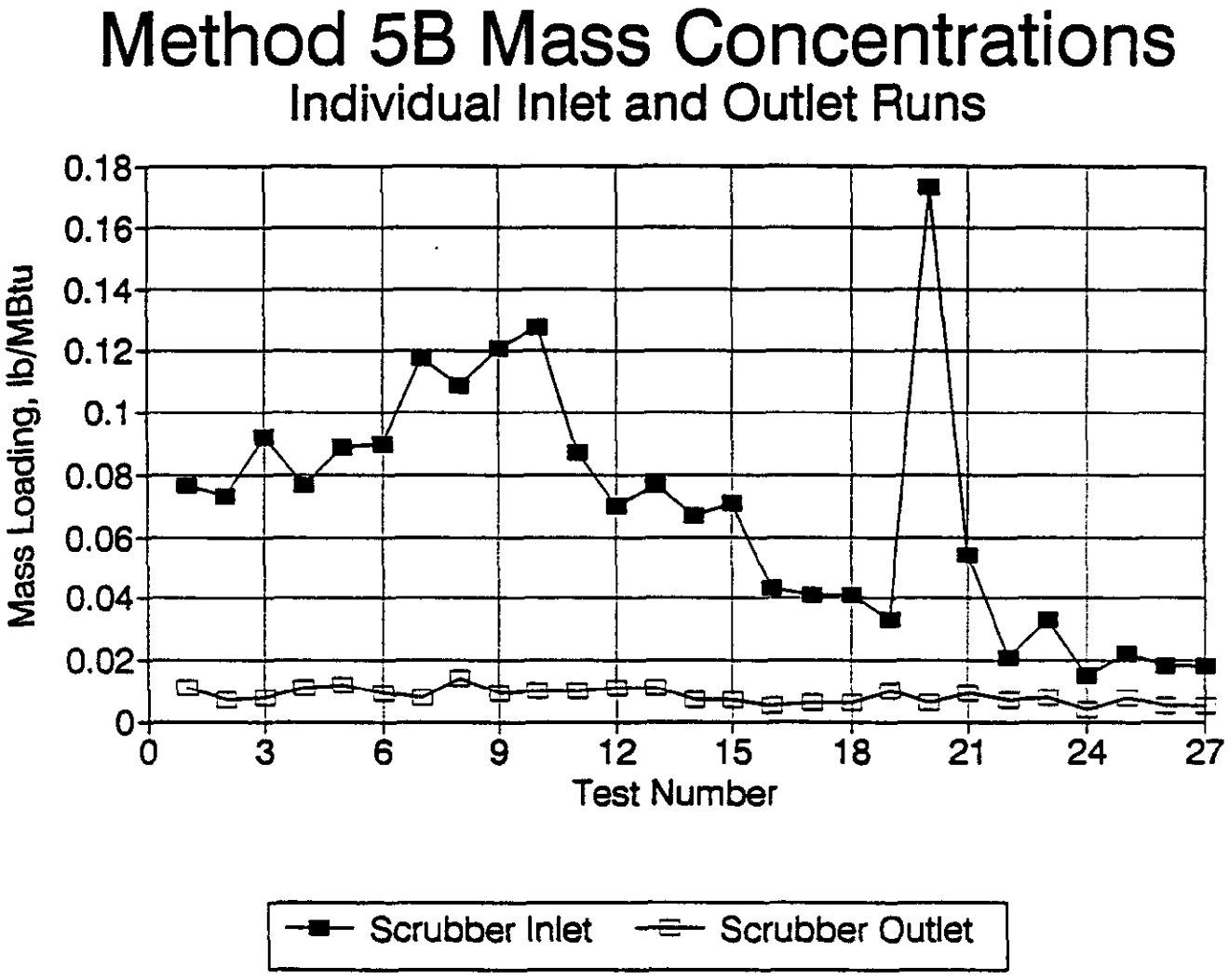

Figure 29. Each Method 5B Result During Chiyoda Test Program, January 21-31, 1993.

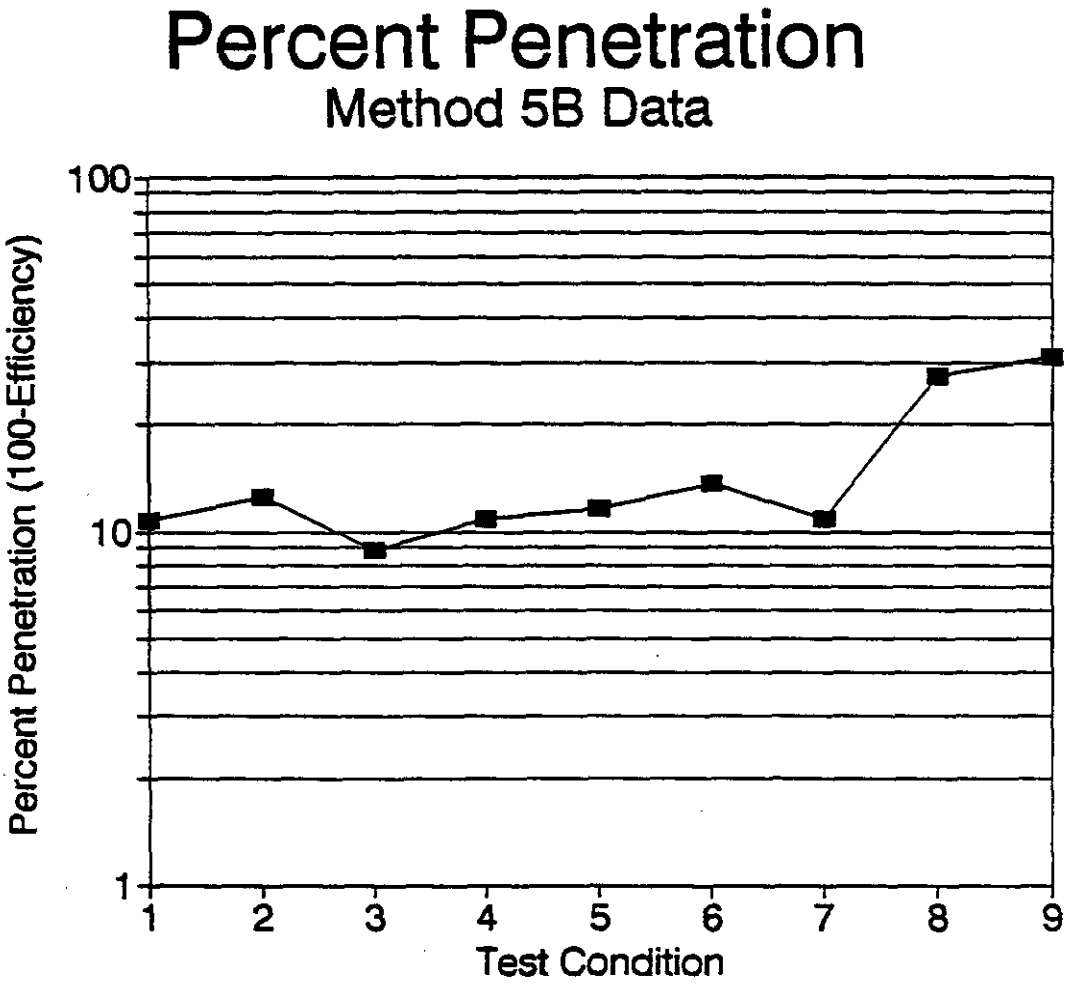

Figure 30. Average Penetration For Each Test Condition, Method 5B Data, Chiyoda Test Program, January 21-31, 1993.

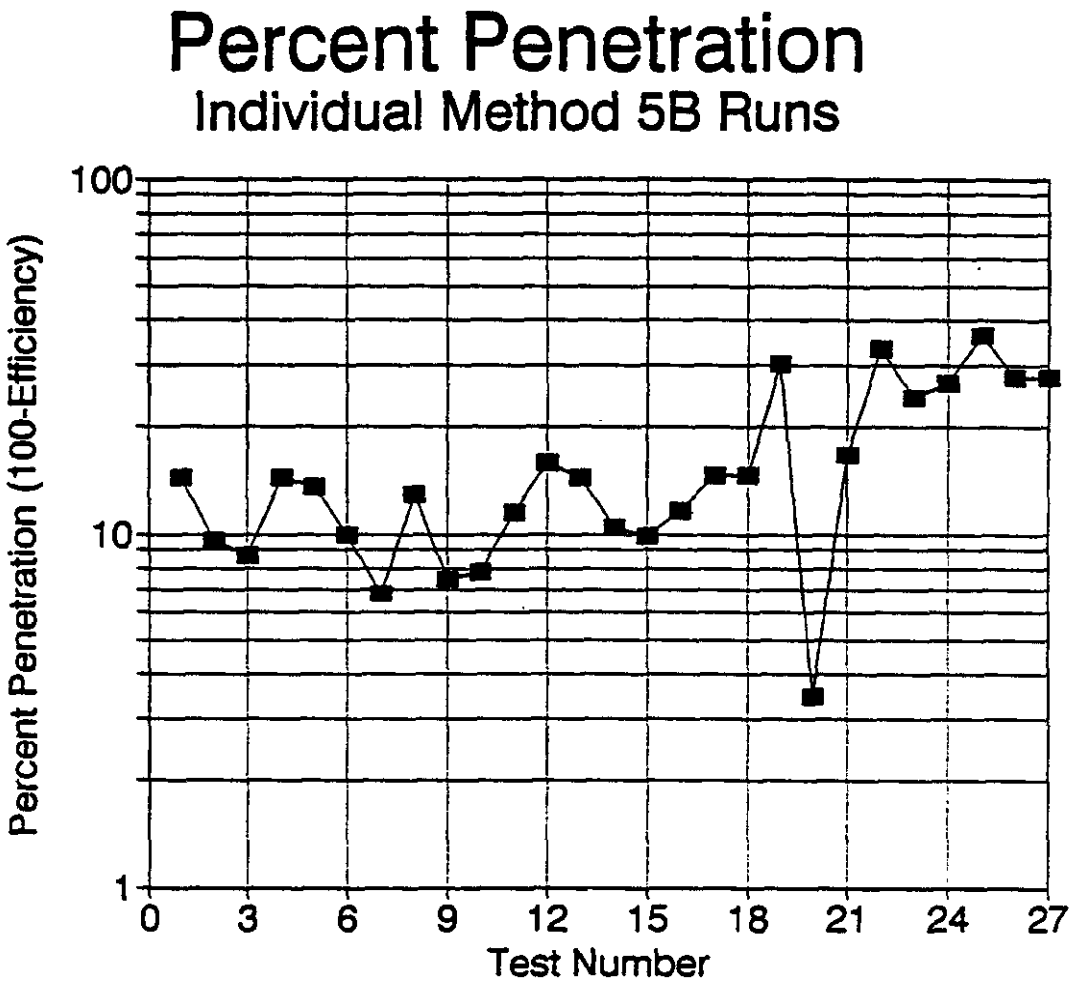

Figure 31. Penetration for Each Method 5B Run Pair, Chiyoda Test Program, January 21-31, 1993.

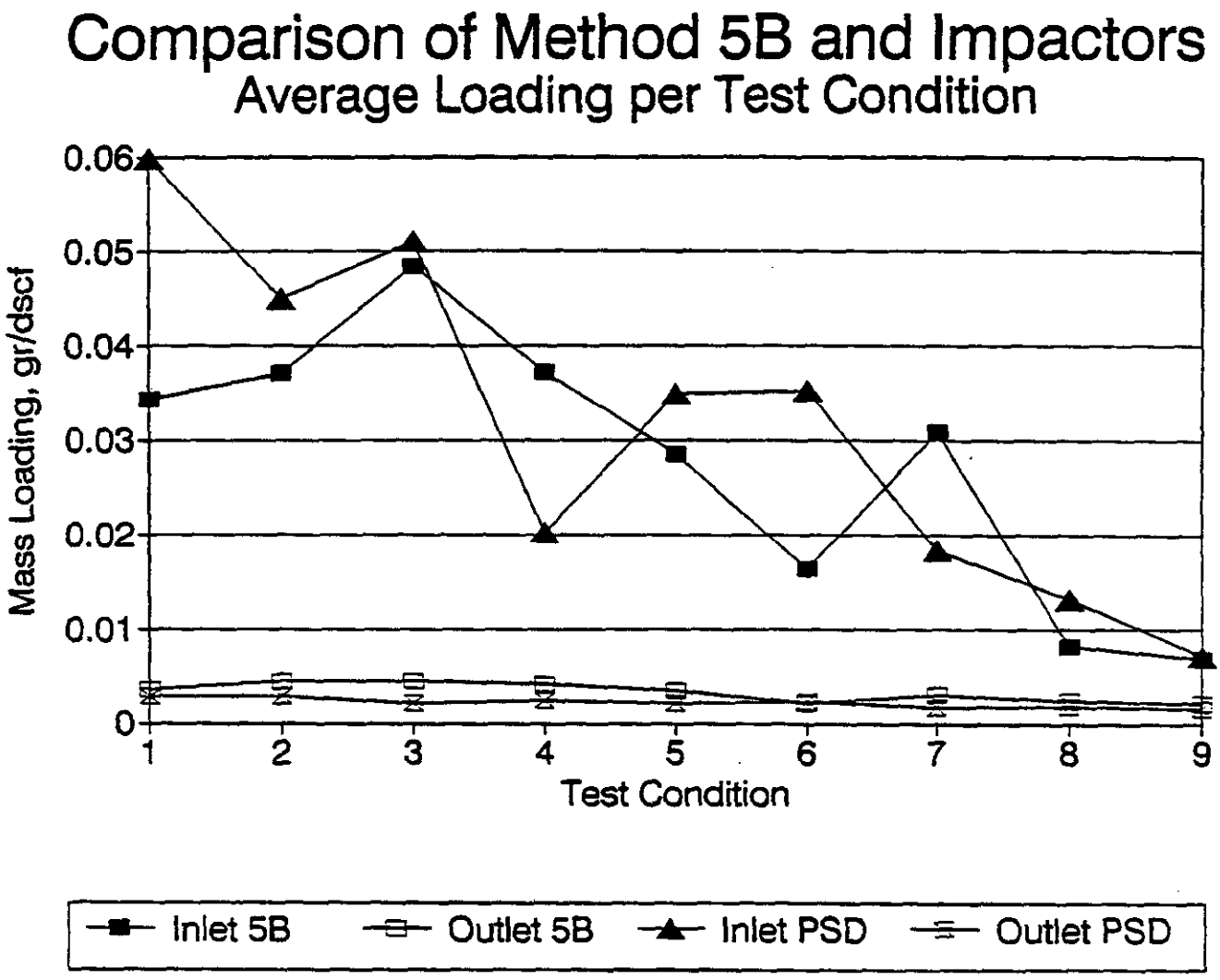

Figure 32. Comparison of Mass Loadings from Method 5B and Impactors -- Inlet and Outlet Sampling Locations, Chiyoda Test Program, January 21-31, 1993

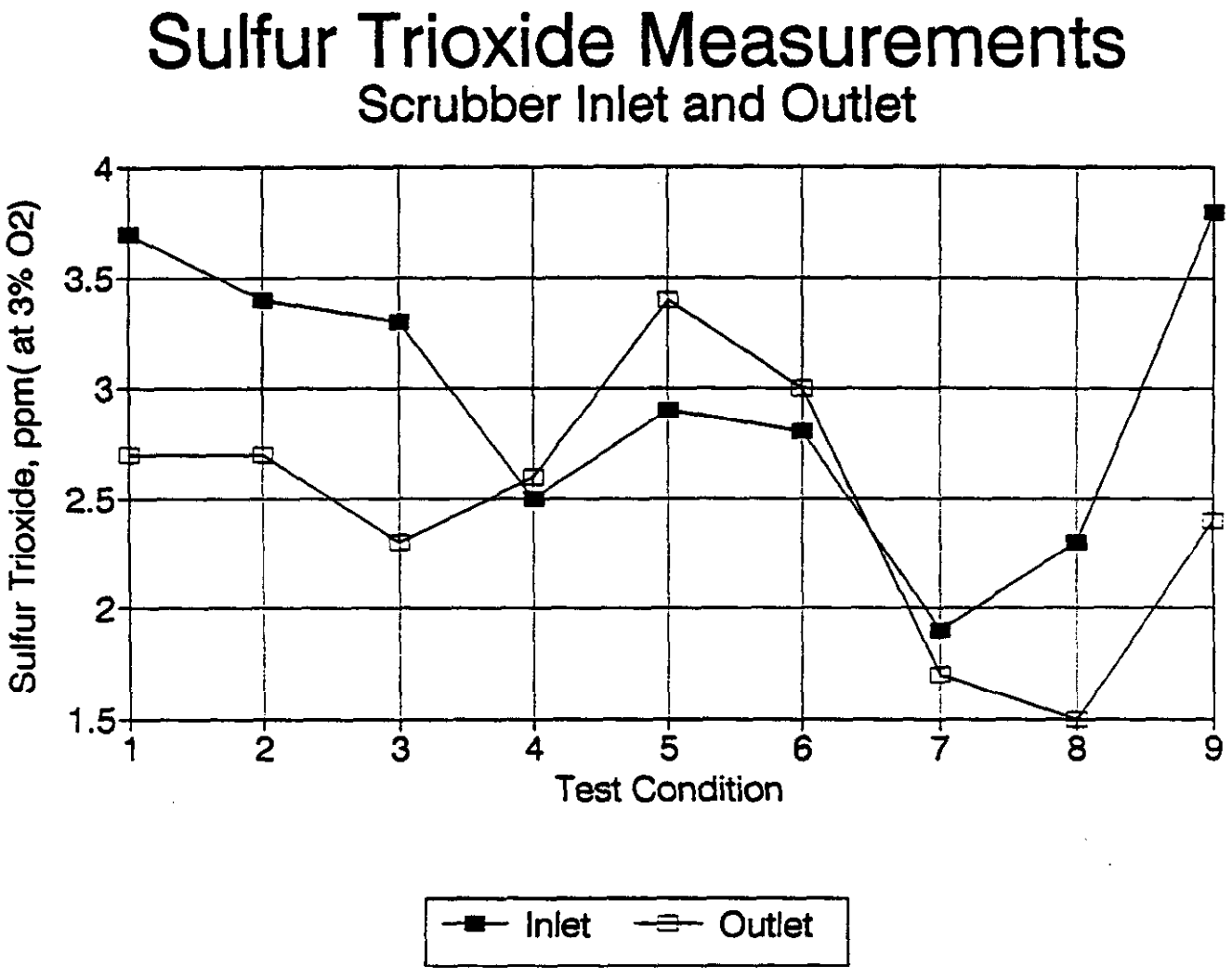

Figure 33. Average Sulfur Trioxide Measurements for Each Test Condition, Chiyoda Test Program, January 21-31, 1993

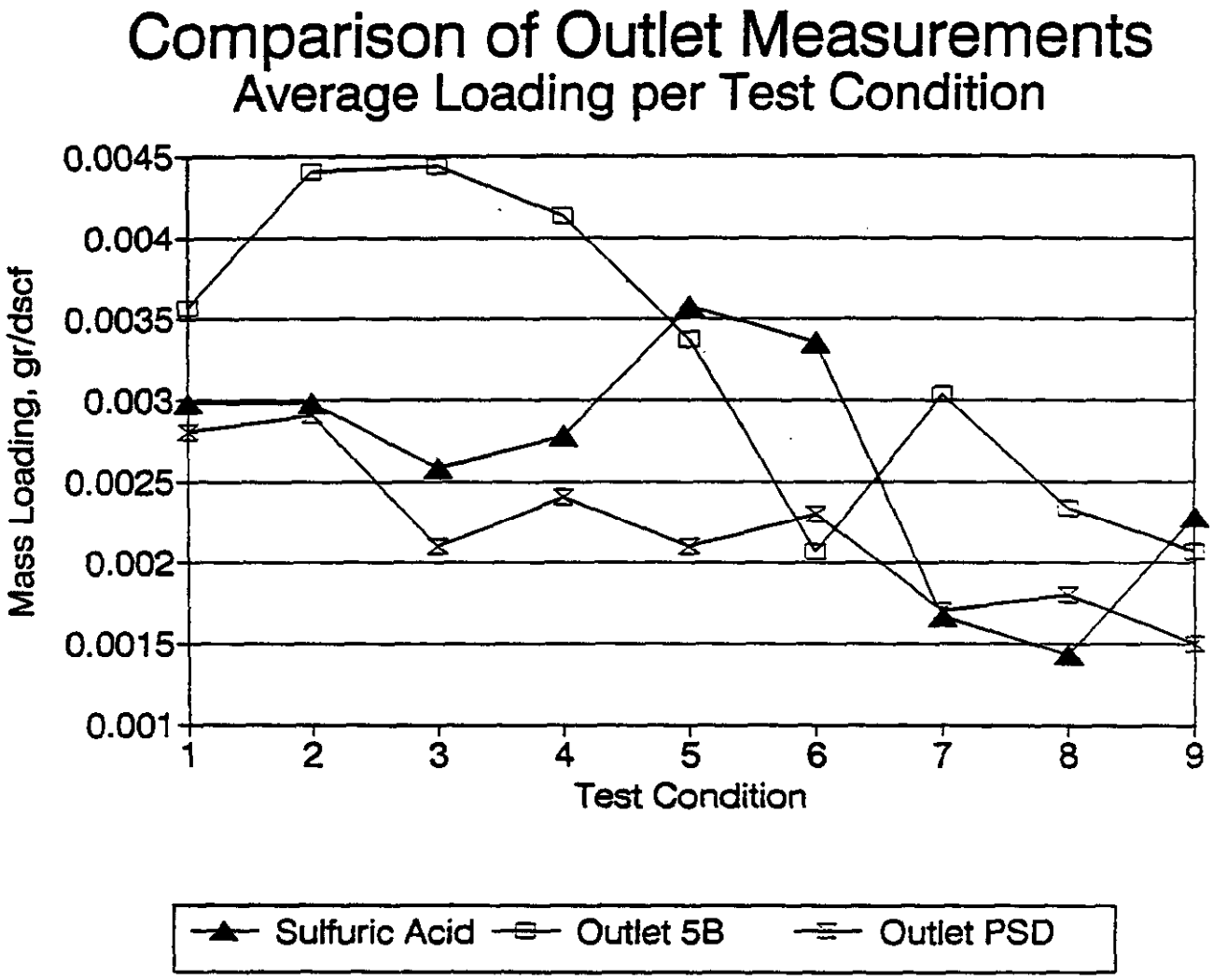

Figure 34. Average Outlet Mass Loading for Each Test Condition, Method 5B, Impactors and Sulfuric Acid (if Particulate). Chiyoda Test Program, January 21-31, 1993

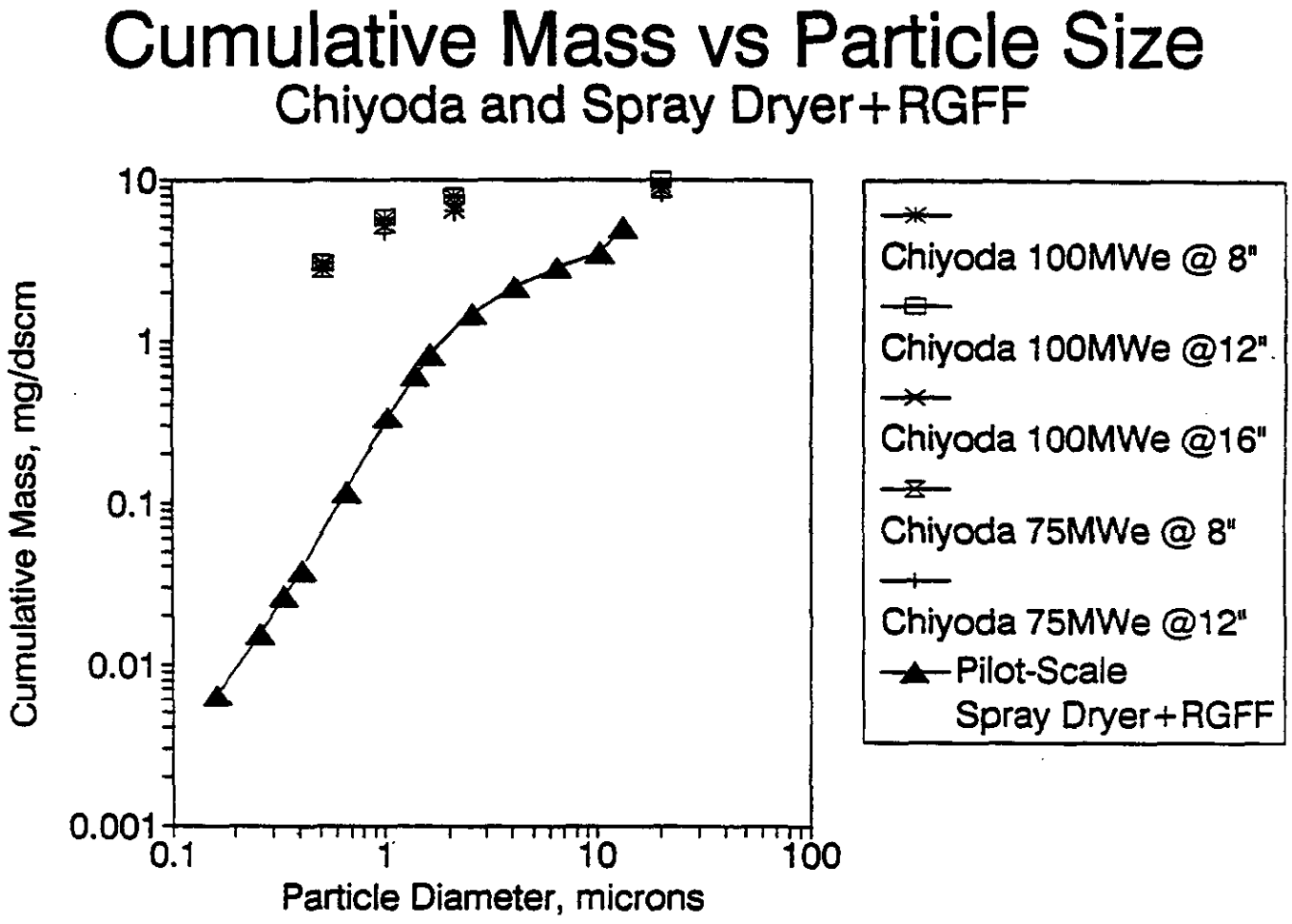

Figure 35. Comparison of Chiyoda Scrubber Test Conditions and a Pilot-Scale Spray Dryer and Fabric Filter Combination. Cumulative Mass for Each on a 3% O_2 Basis.

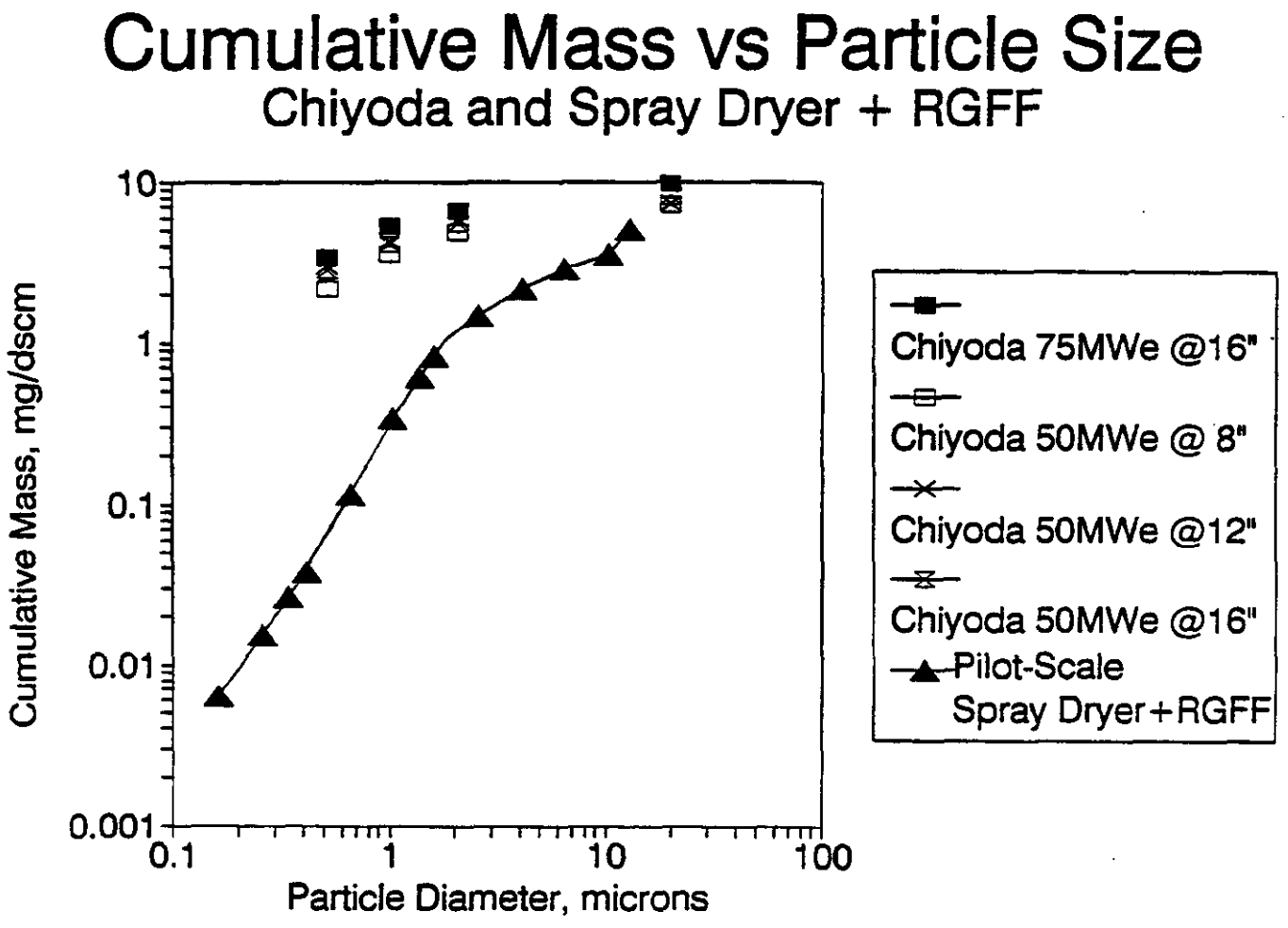

Figure 36. Comparison of Chiyoda Scrubber Test Conditions and a Pilot-Scale Spray Dryer and Fabric Filter Combination. Cumulative Mass for Each on a 3% O_2 Basis.

STAGE 2, D_{50} = 3.18 μm

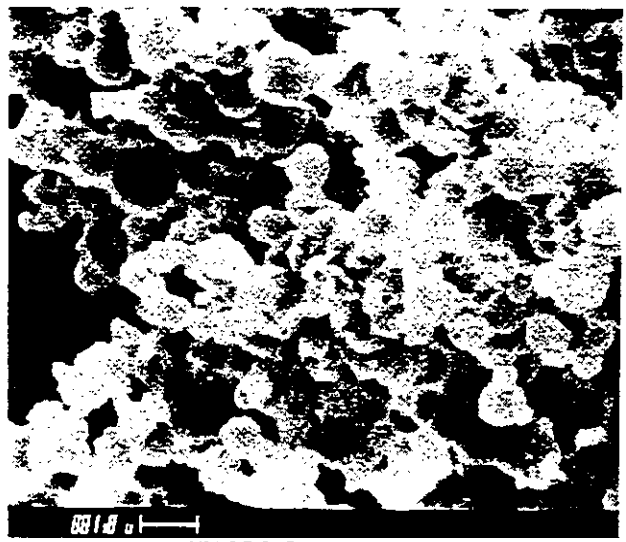

STAGE 3, D_{50} = 1.10 μm

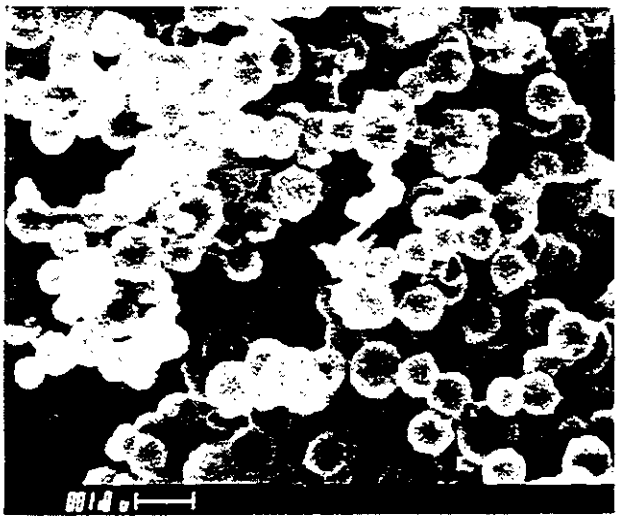

STAGE 4, D_{50} = 0.98 μm

STAGE 5, D_{50} = 0.47 μm

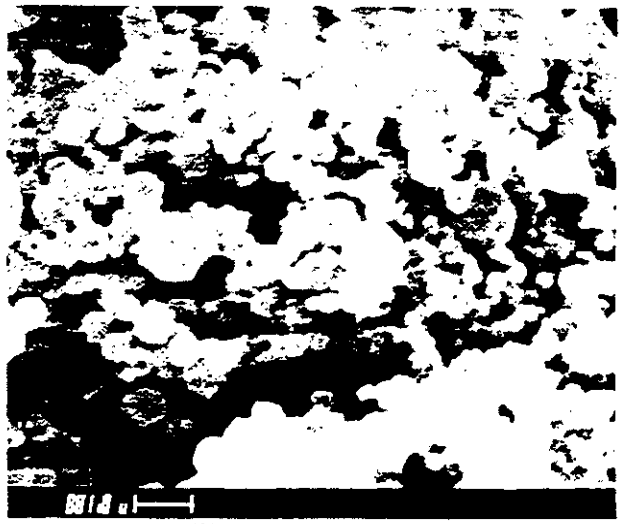

STAGE 6, D_{50} = 0.22 μm

Figure 37. Scanning Electron Microscopy Photomicrographs of Outlet Impactor Stages, Chiyoda Test Condition 2, January 22, 1993.

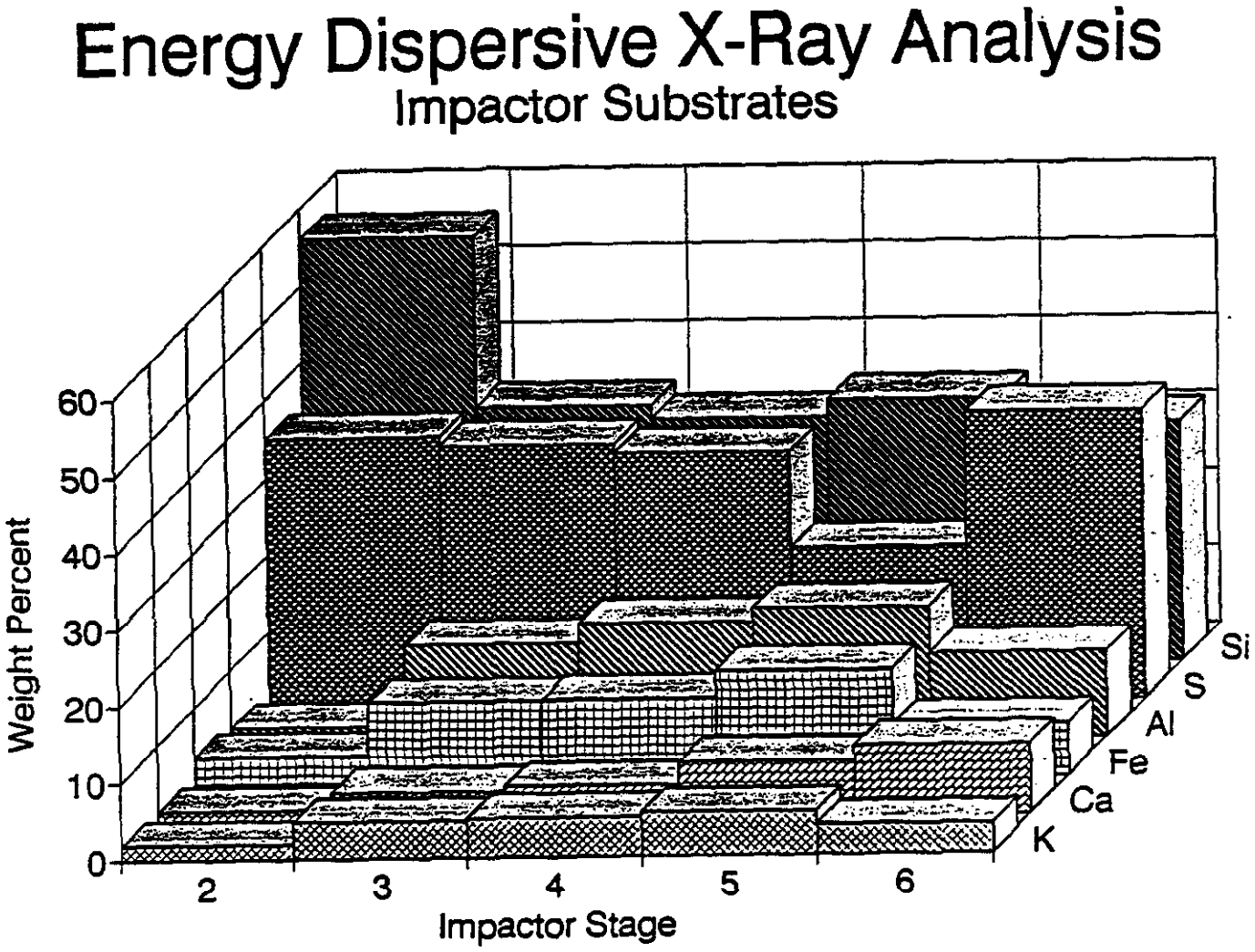

Figure 38. Comparison of Energy Dispersive X-Ray Analysis for Each Impactor Stage in Figure 37.

APPENDIX

IMPACTOR GRAPHS

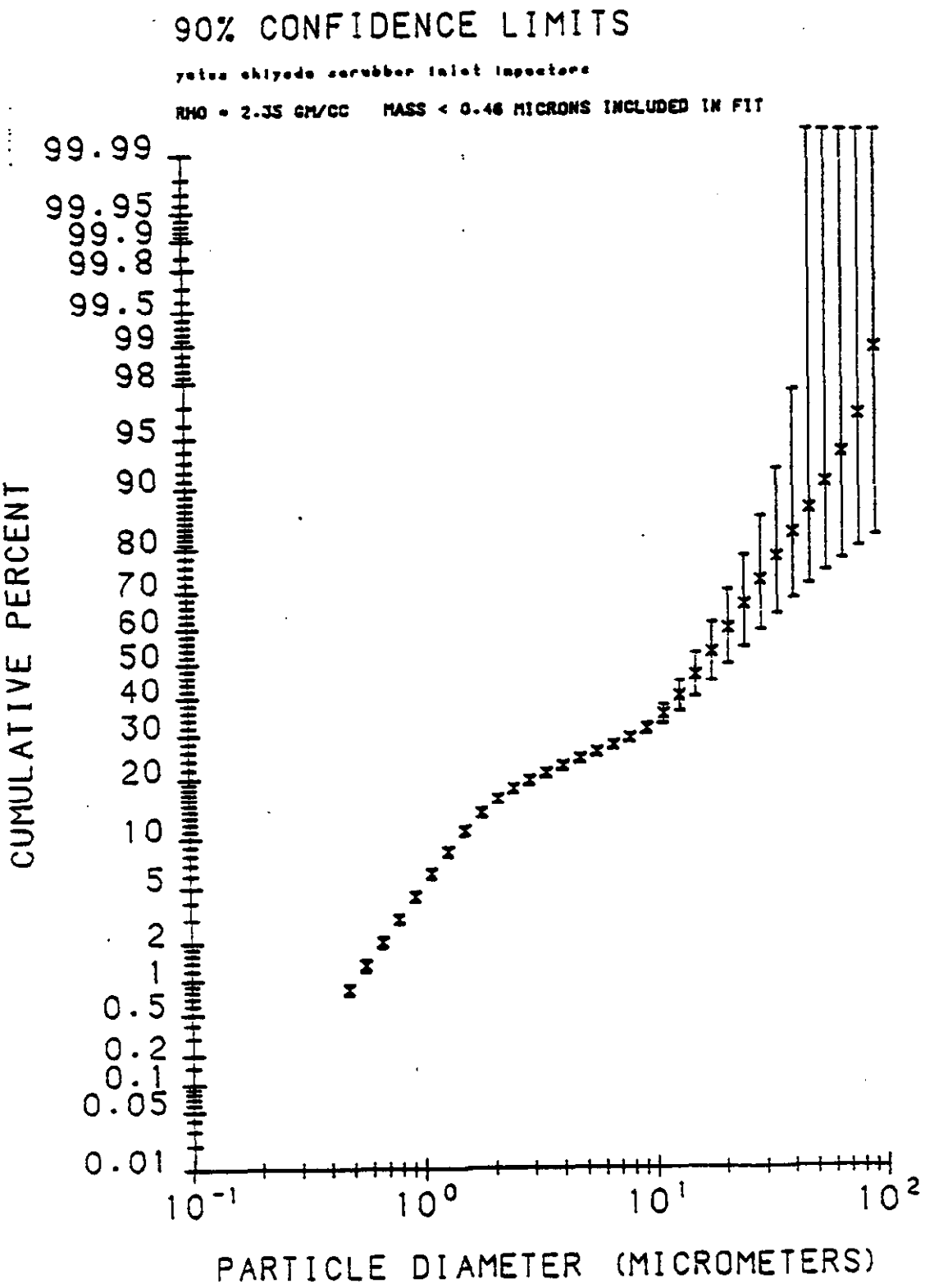

Figure A1. Inlet Cumulative Percent vs Particle Diameter for Chiyoda Scrubber, 100 MW, 8" ΔP, January 21, 1993.

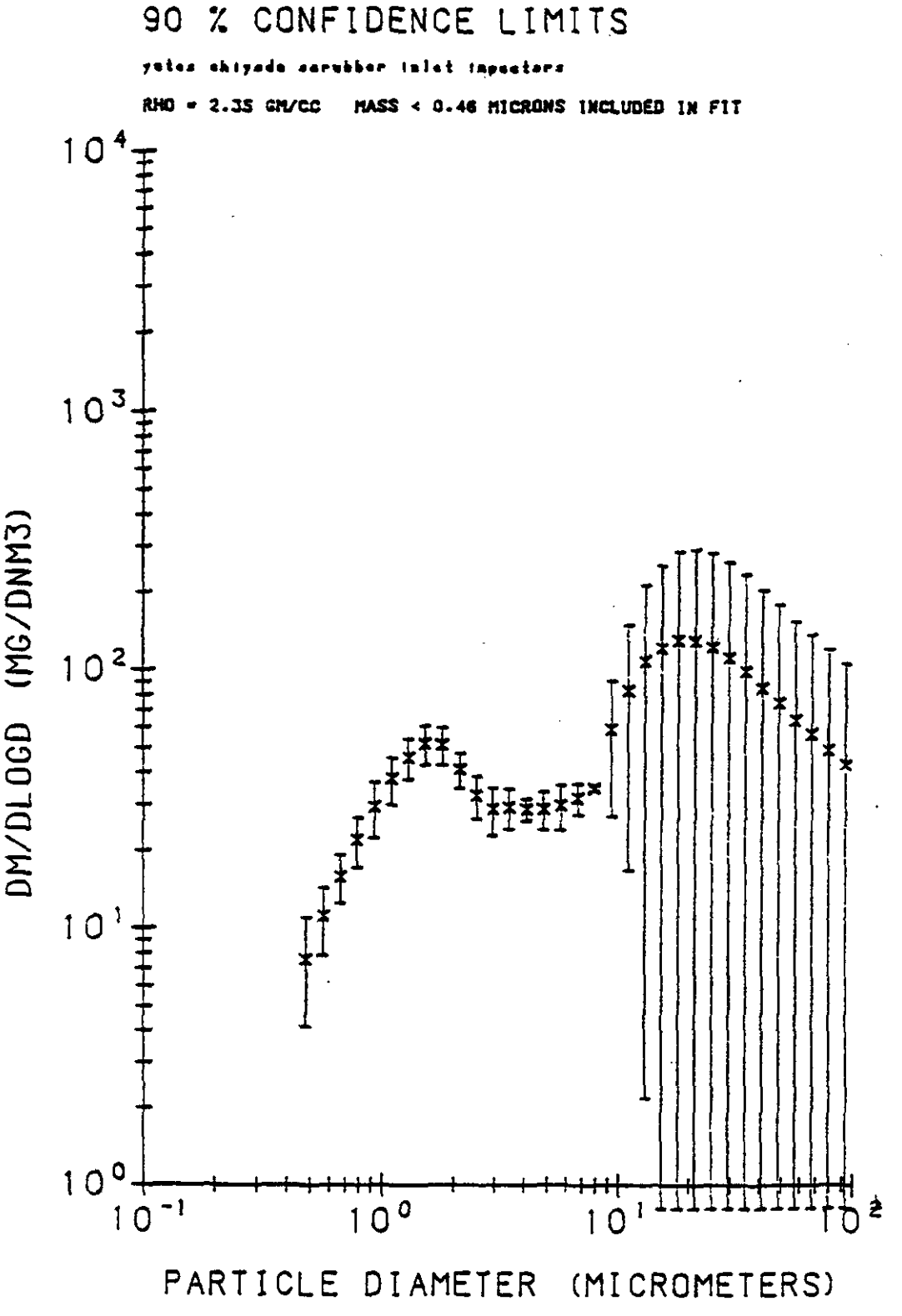

Figure A2. Inlet dM/dlogD vs Particle Diameter for Chiyoda Scrubber, 100 MW$_e$, 8" ΔP, January 21, 1993.

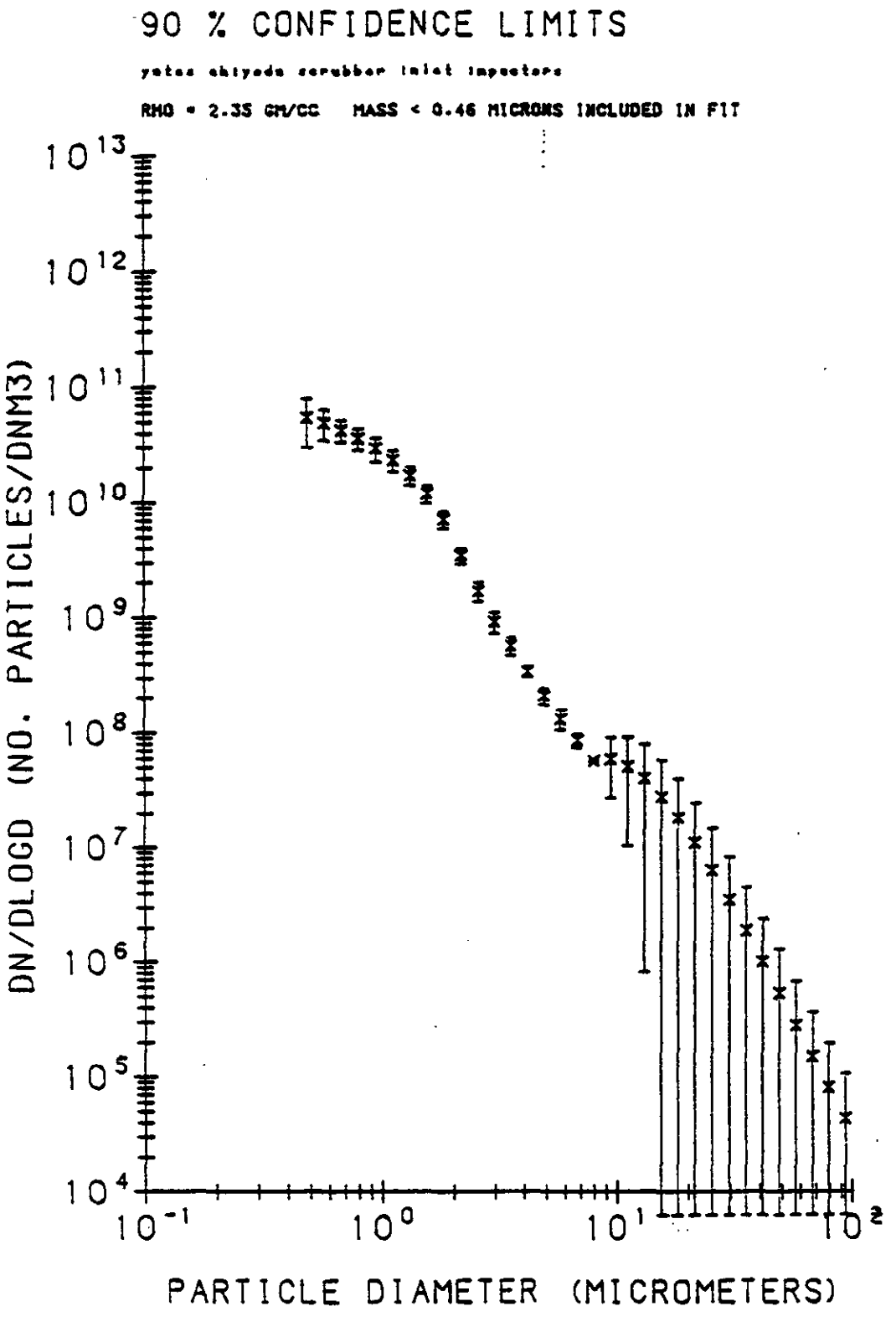

Figure A3. Inlet dN/dlogD vs Particle Diameter for Chiyoda Scrubber, 100 MW, 8" ΔP, January 21, 1993.

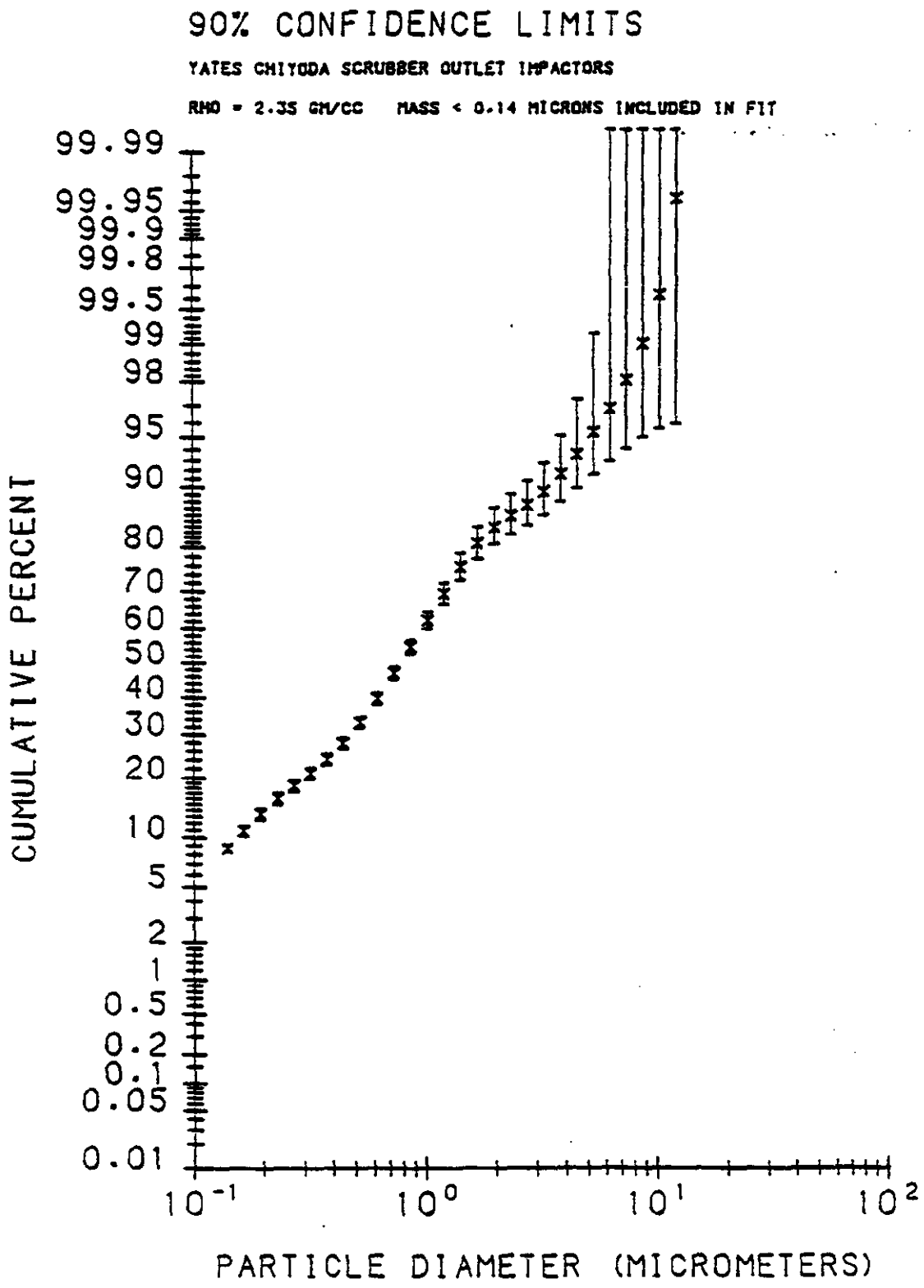

Figure A4. Outlet Cumulative Percent vs Particle Diameter for Chiyoda Scrubber, 100 MW, 8" ΔP, January 21, 1993.

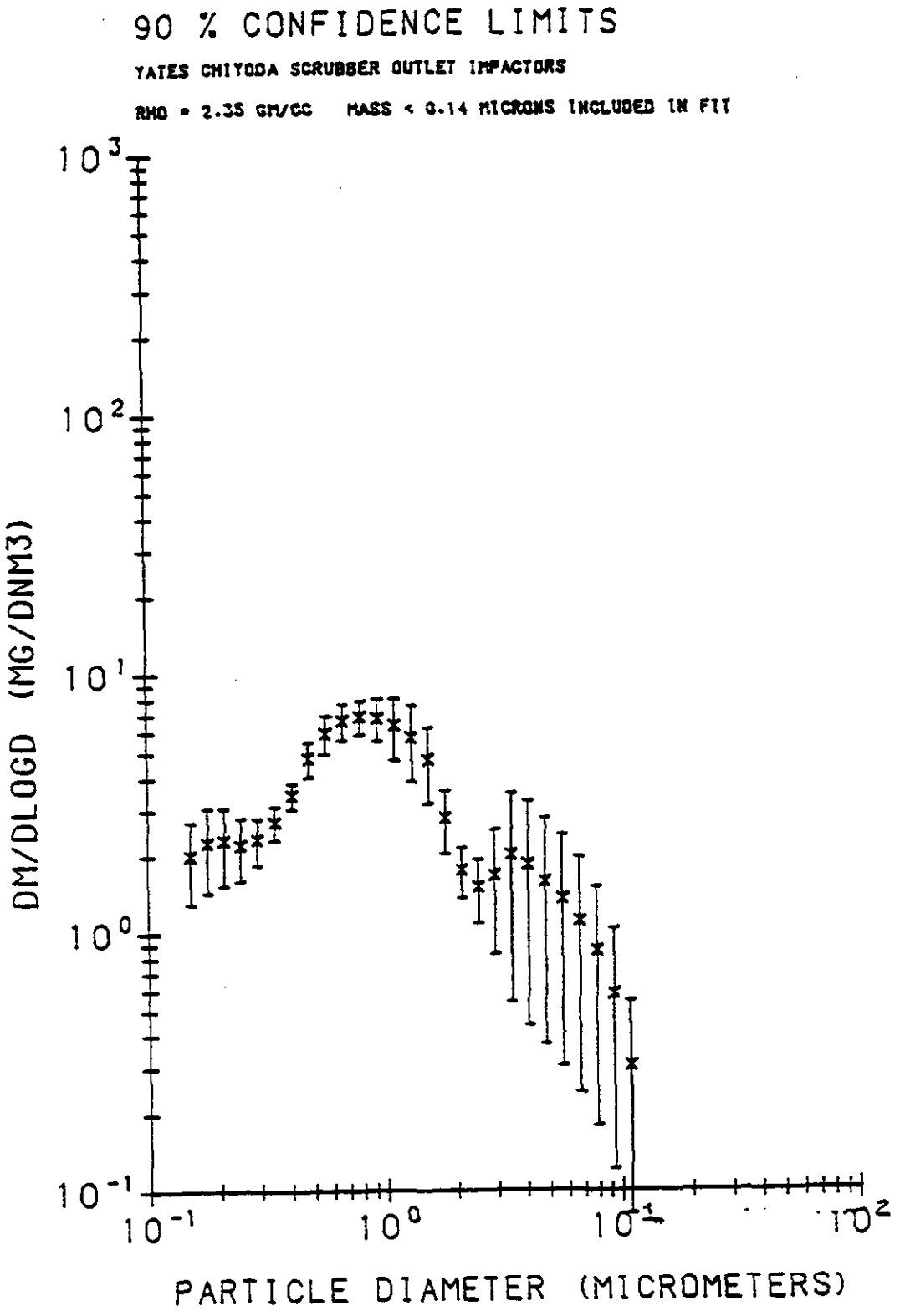

Figure A5. Outlet dM/dlogD vs Particle Diameter for Chiyoda Scrubber, 100 MW, 8" ΔP, January 21, 1993.

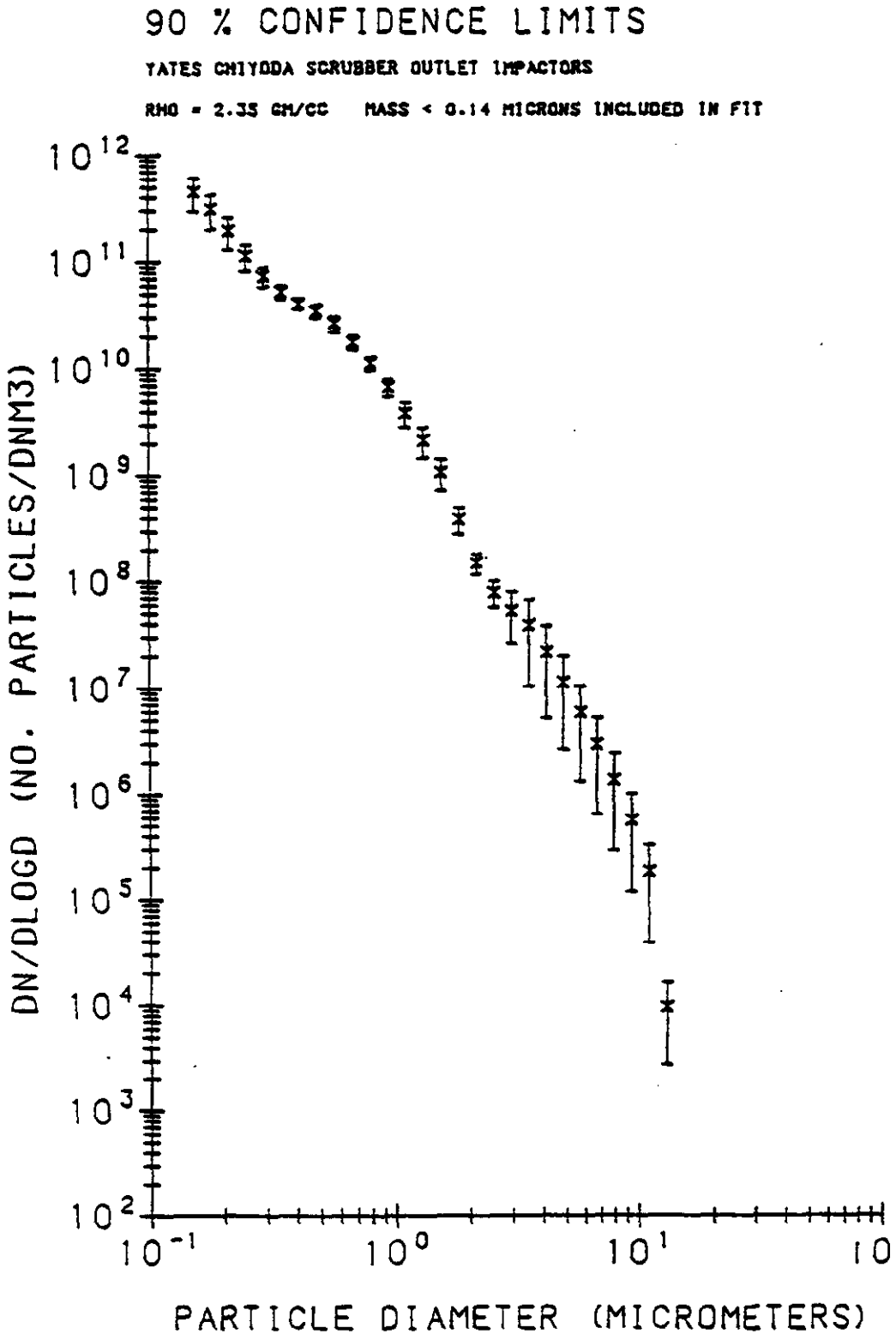

Figure A6. Outlet dN/dlogD vs Particle Diameter for Chiyoda Scrubber, 100 MW, 8" ΔP, January 21, 1993.

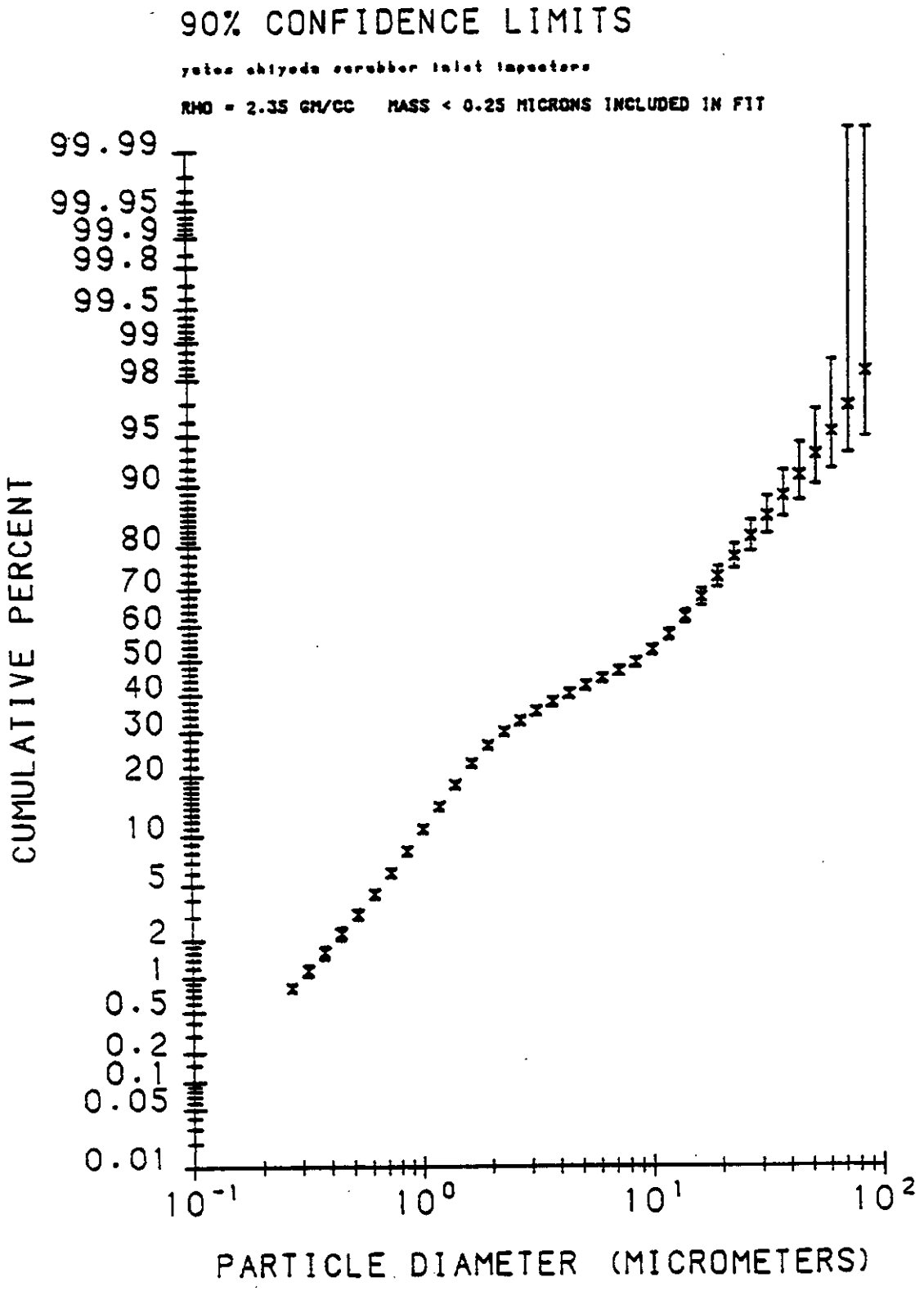

Figure A7. Inlet Cumulative Percent vs Particle Diameter for Chiyoda Scrubber, 100 MW, 12" ΔP, January 22, 1993.

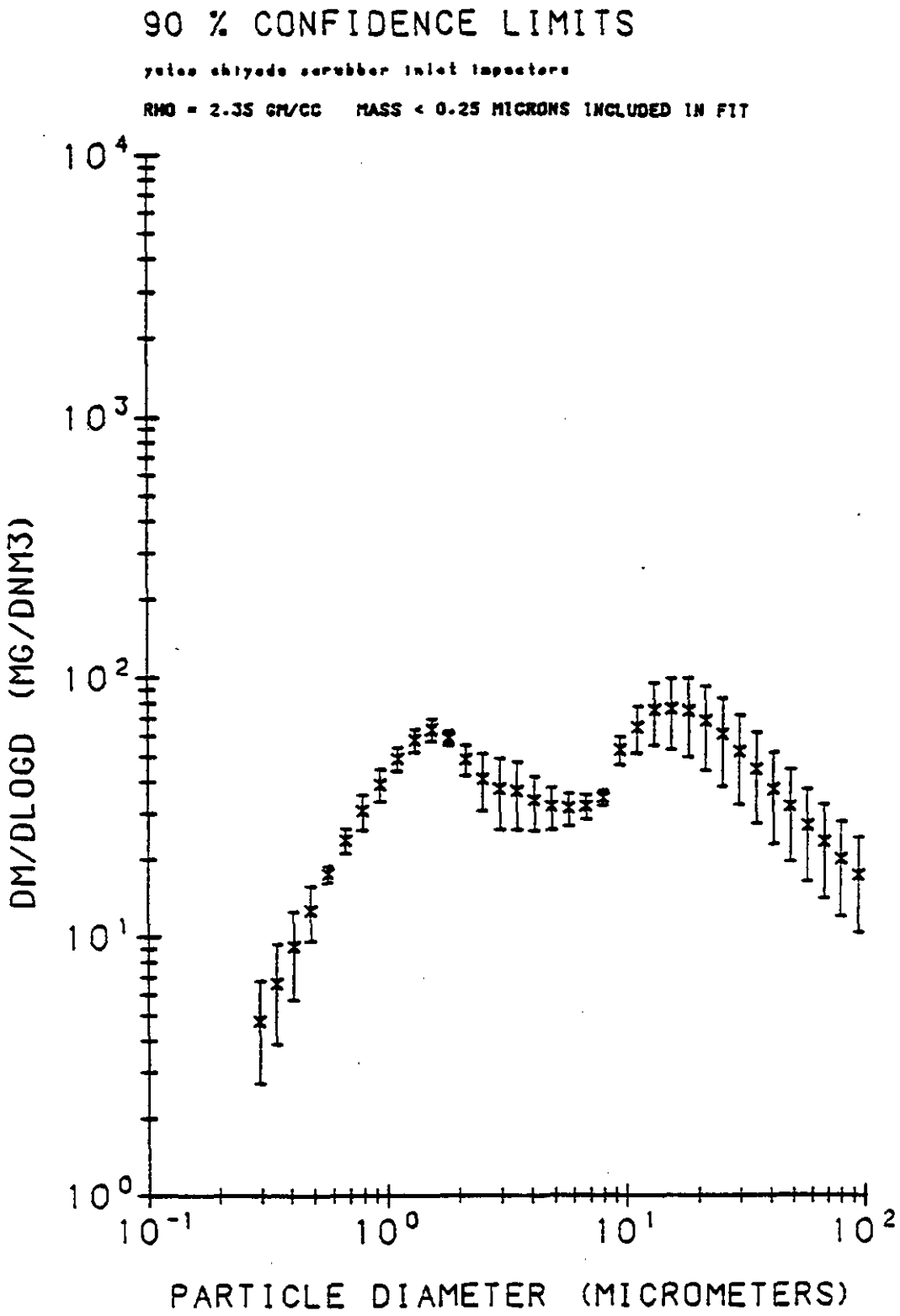

Figure A8. Inlet dM/dlogD vs Particle Diameter for Chiyoda Scrubber, 100 MW, 12" ΔP, January 22, 1993.

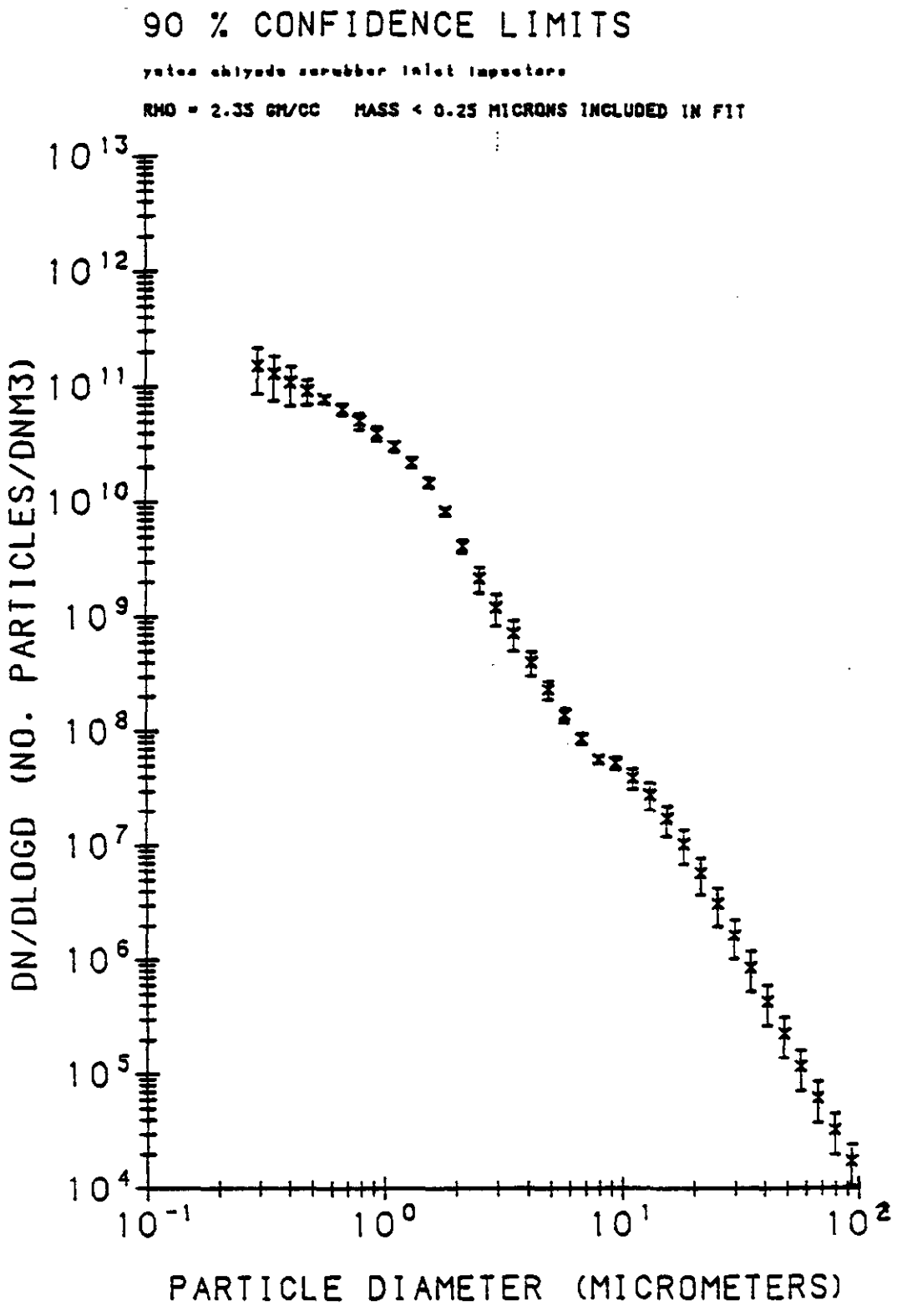

Figure A9. Inlet dN/dlogD vs Particle Diameter for Chiyoda Scrubber, 100 MW, 12" ΔP, January 22, 1993.

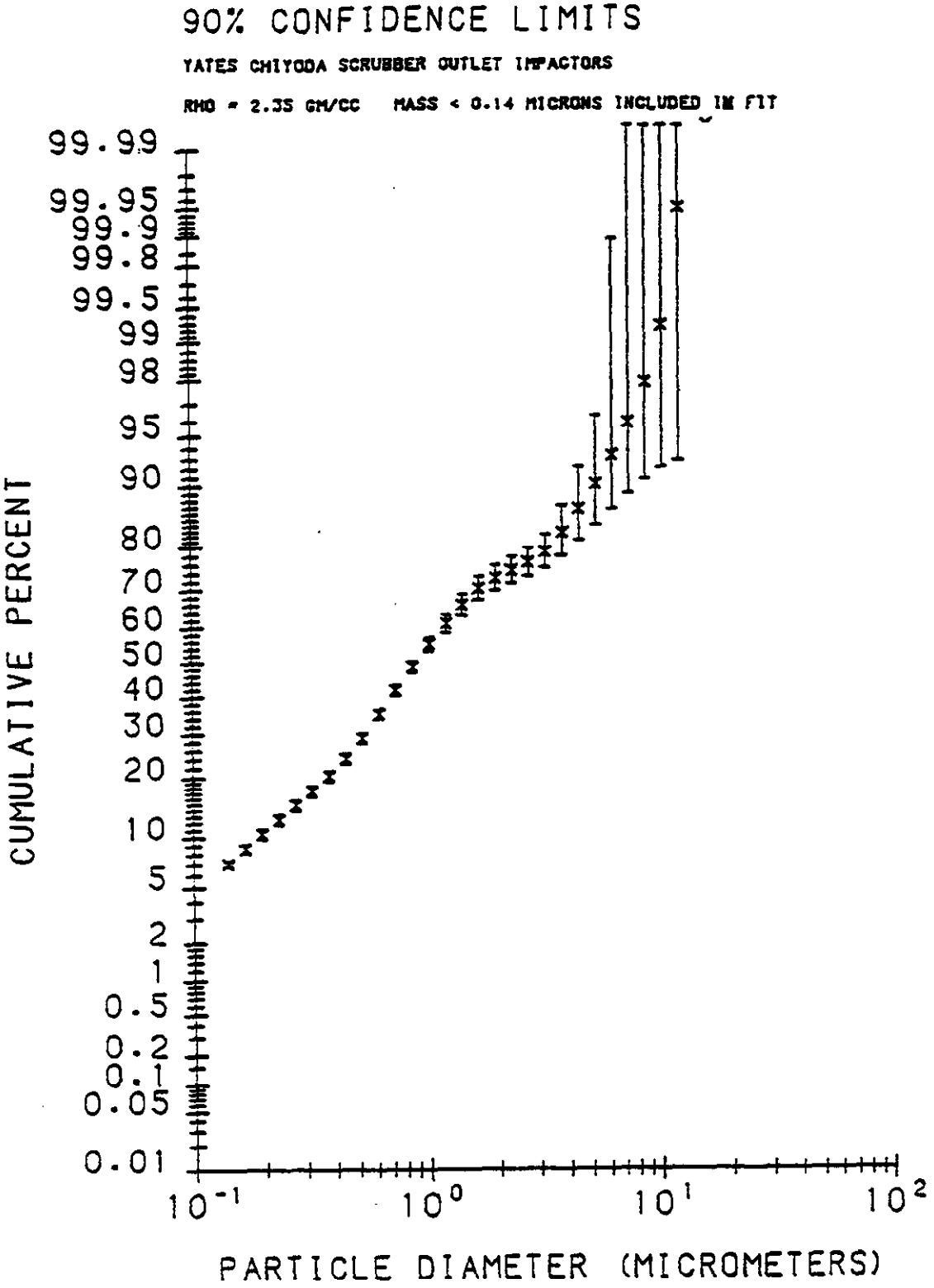

Figure A10. Outlet Cumulative Percent vs Particle Diameter for Chiyoda Scrubber, 100 MW, 12" ΔP, January 22, 1993.

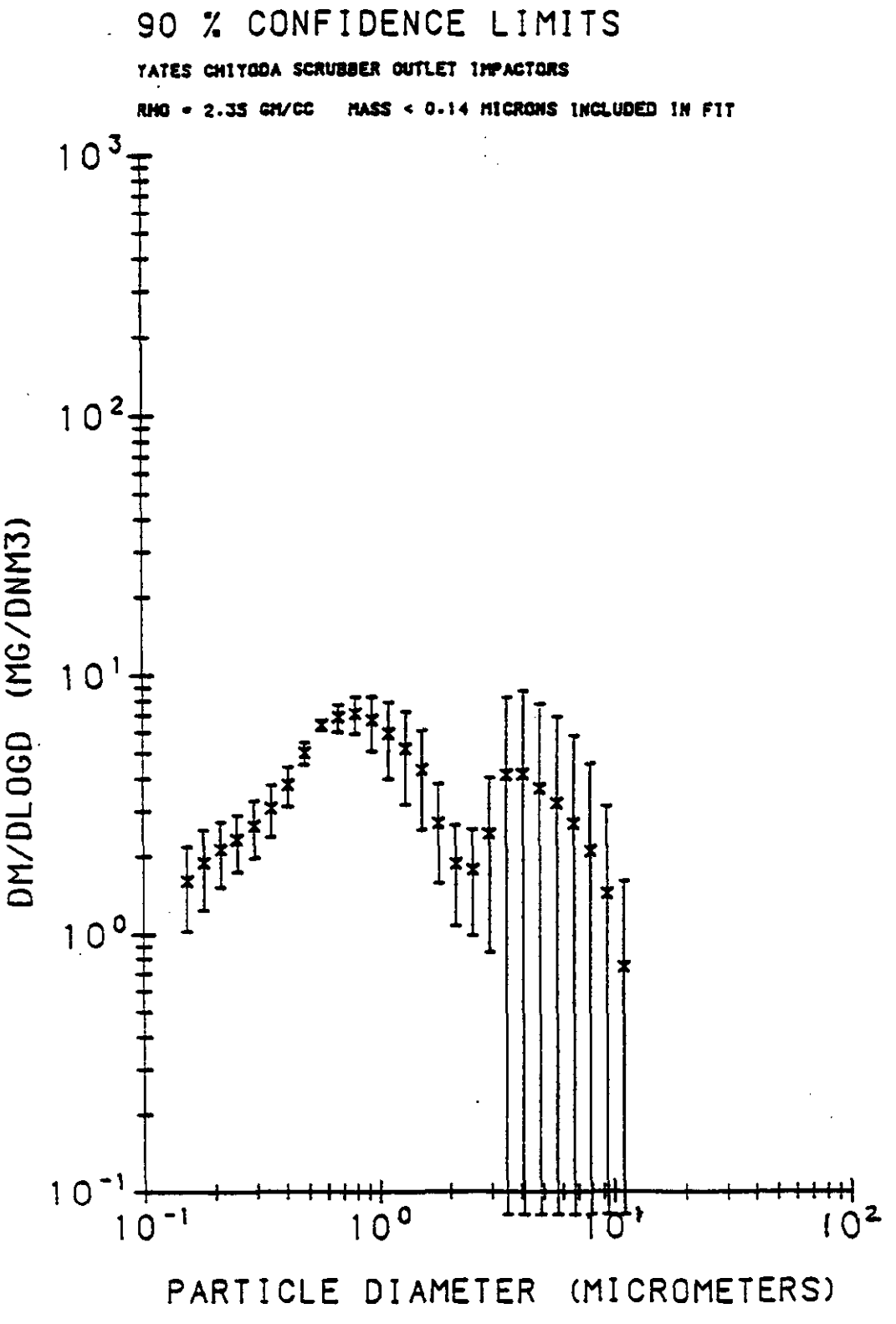

Figure A11. Outlet dM/dlogD vs Particle Diameter for Chiyoda Scrubber, 100 MW, 12" ΔP, January 22, 1993.

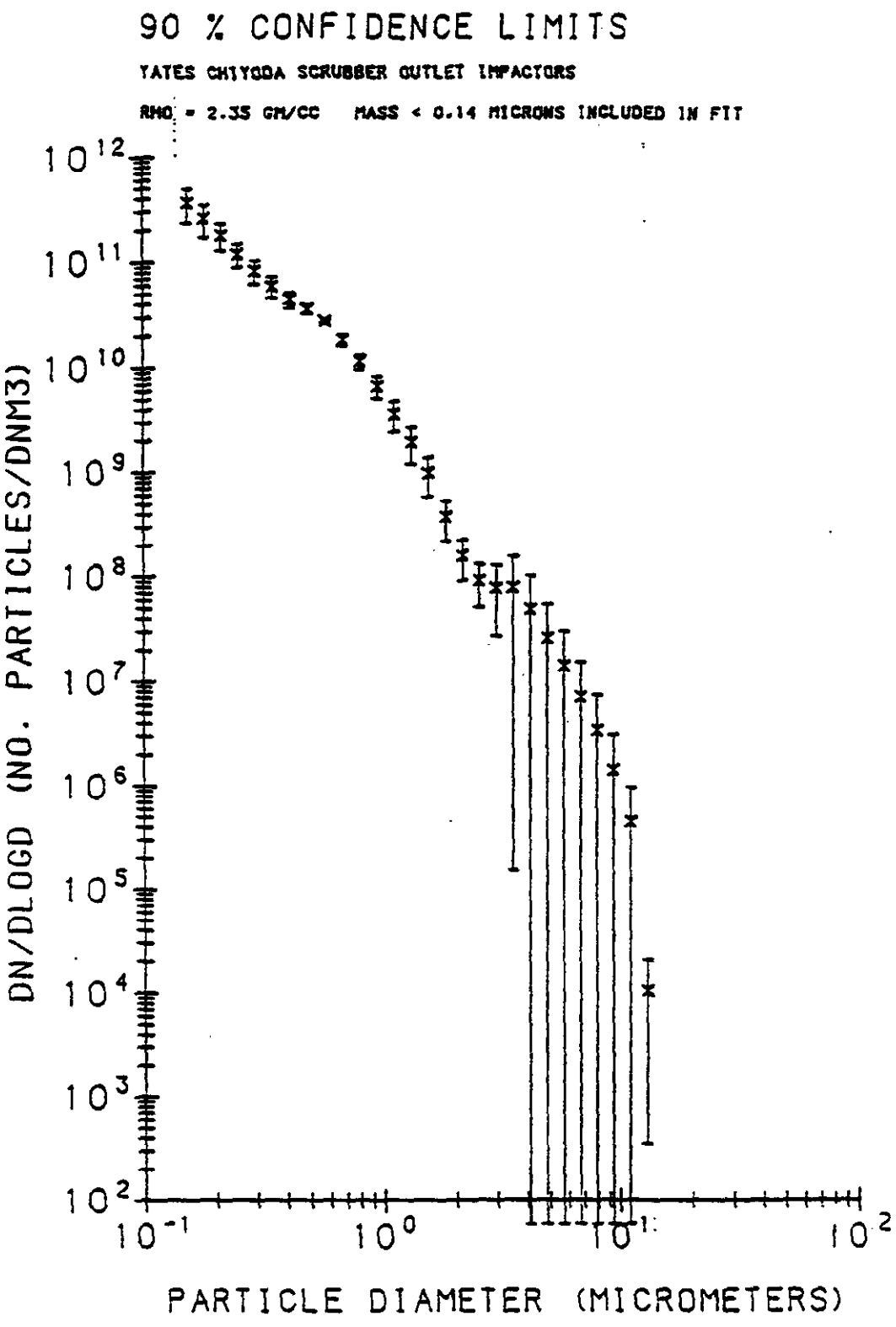

Figure A12. Outlet dN/dlogD vs Particle Diameter for Chiyoda Scrubber, 100 MW, 12" ΔP, January 22, 1993.

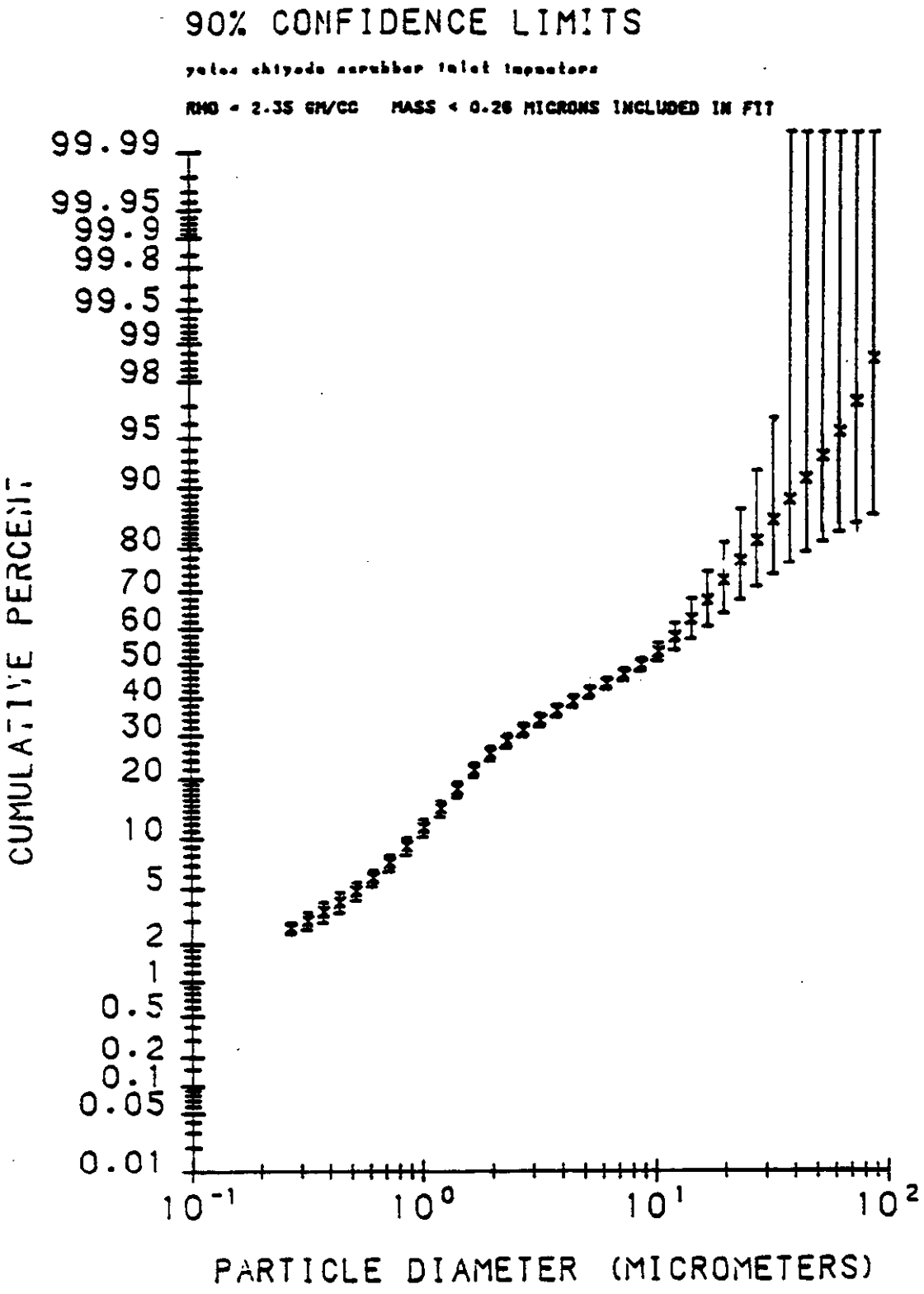

Figure A13. Inlet Cumulative Percent vs Particle Diameter for Chiyoda Scrubber, 100 MW, 16" ΔP, January 23, 1993.

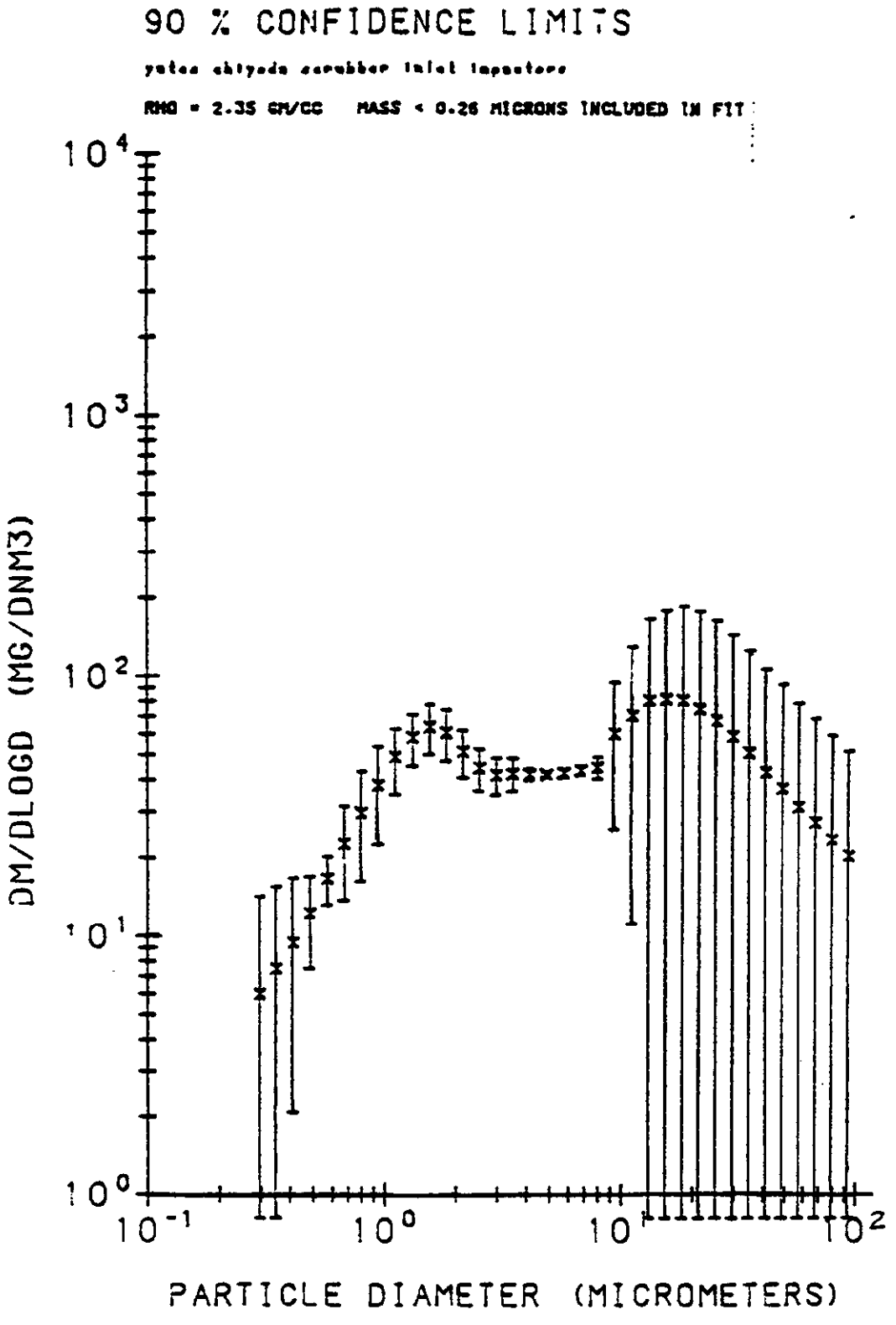

Figure A14. Inlet dM/dlogD vs Particle Diameter for Chiyoda Scrubber, 100 MW, 16" ΔP, January 23, 1993.

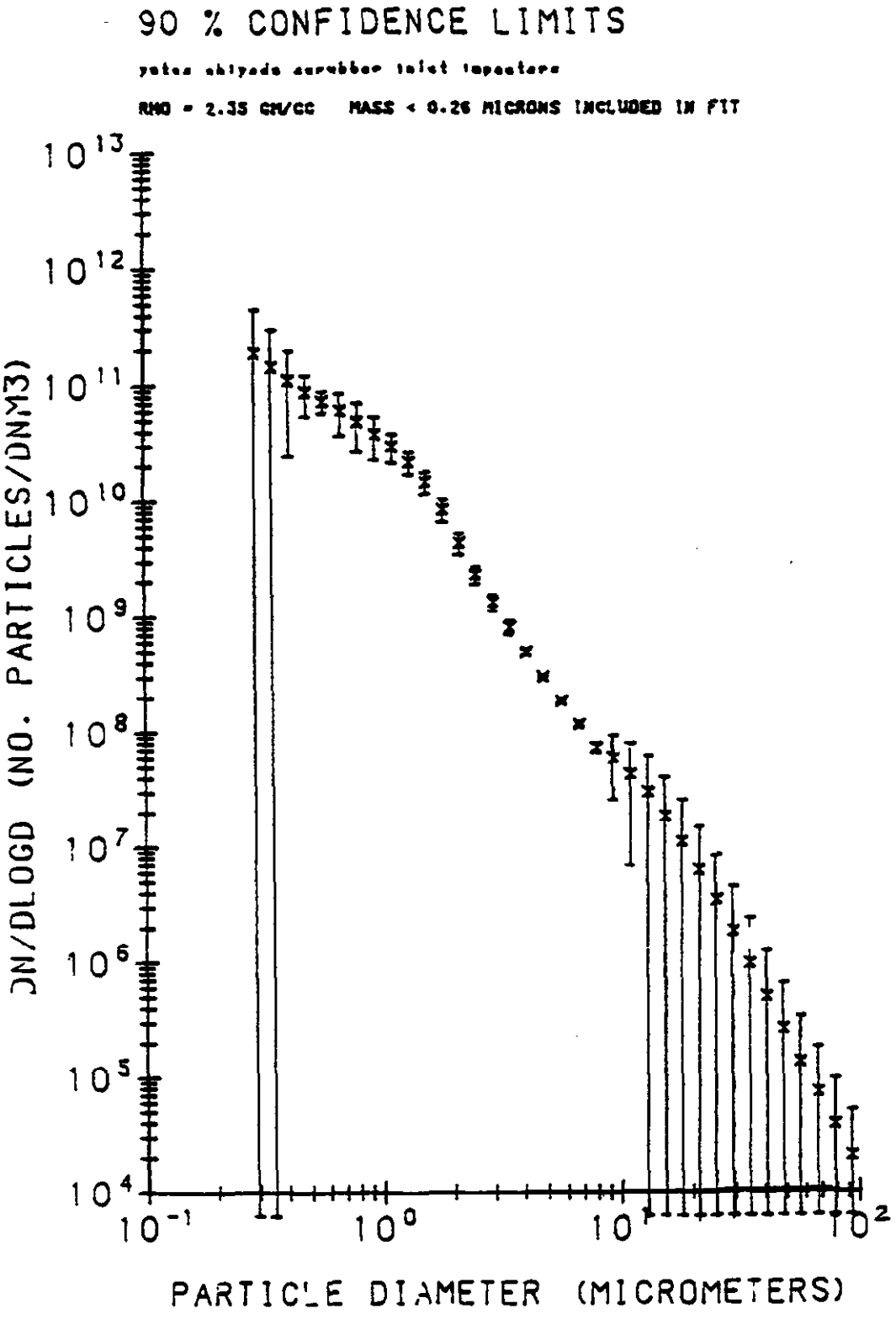

Figure A15. Inlet dN/dlogD vs Particle Diameter for Chiyoda Scrubber, 100 MW, 16" ΔP, January 23, 1993.

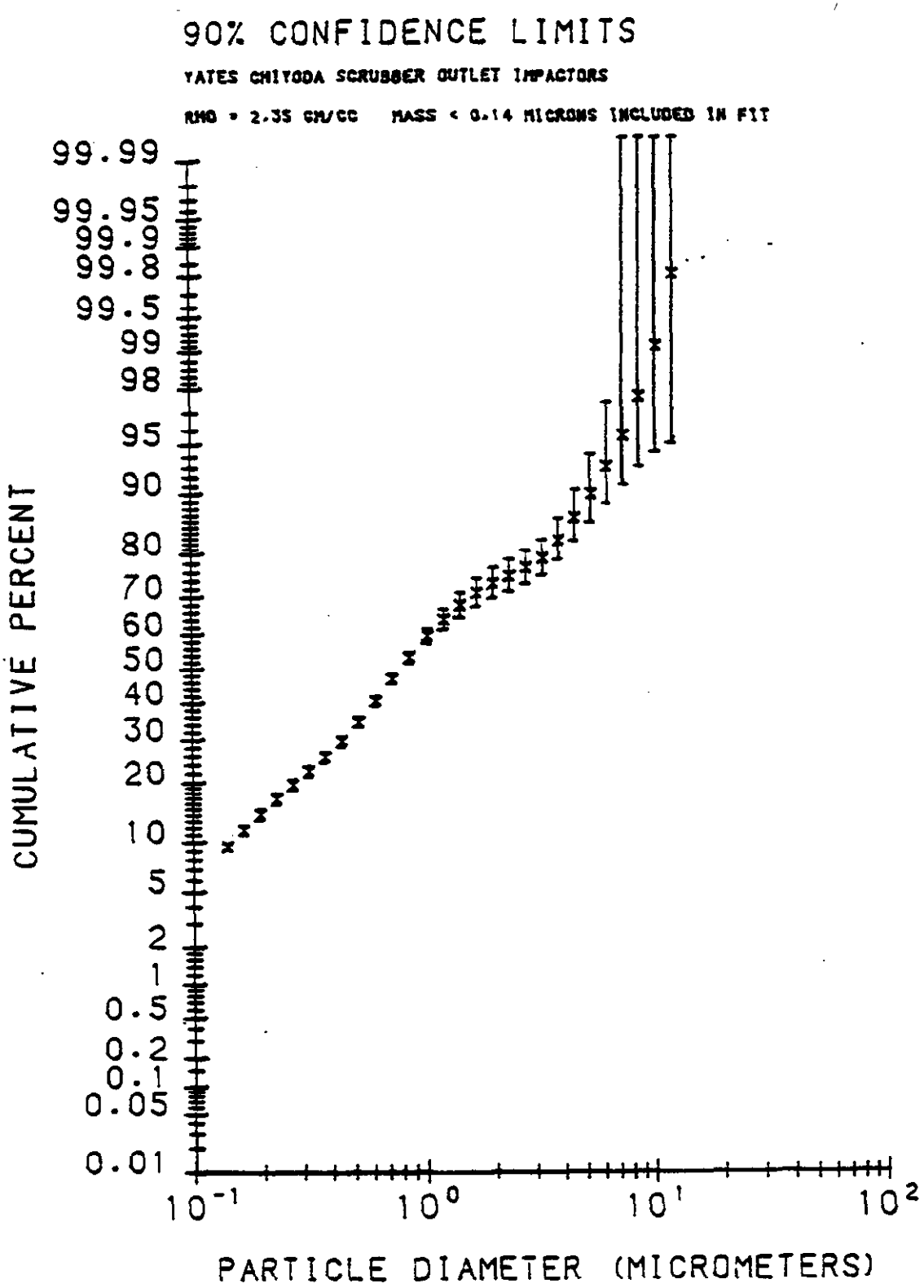

Figure A16. Outlet Cumulative Percent vs Particle Diameter for Chiyoda Scrubber, 100 MW, 16" ΔP, January 23, 1993.

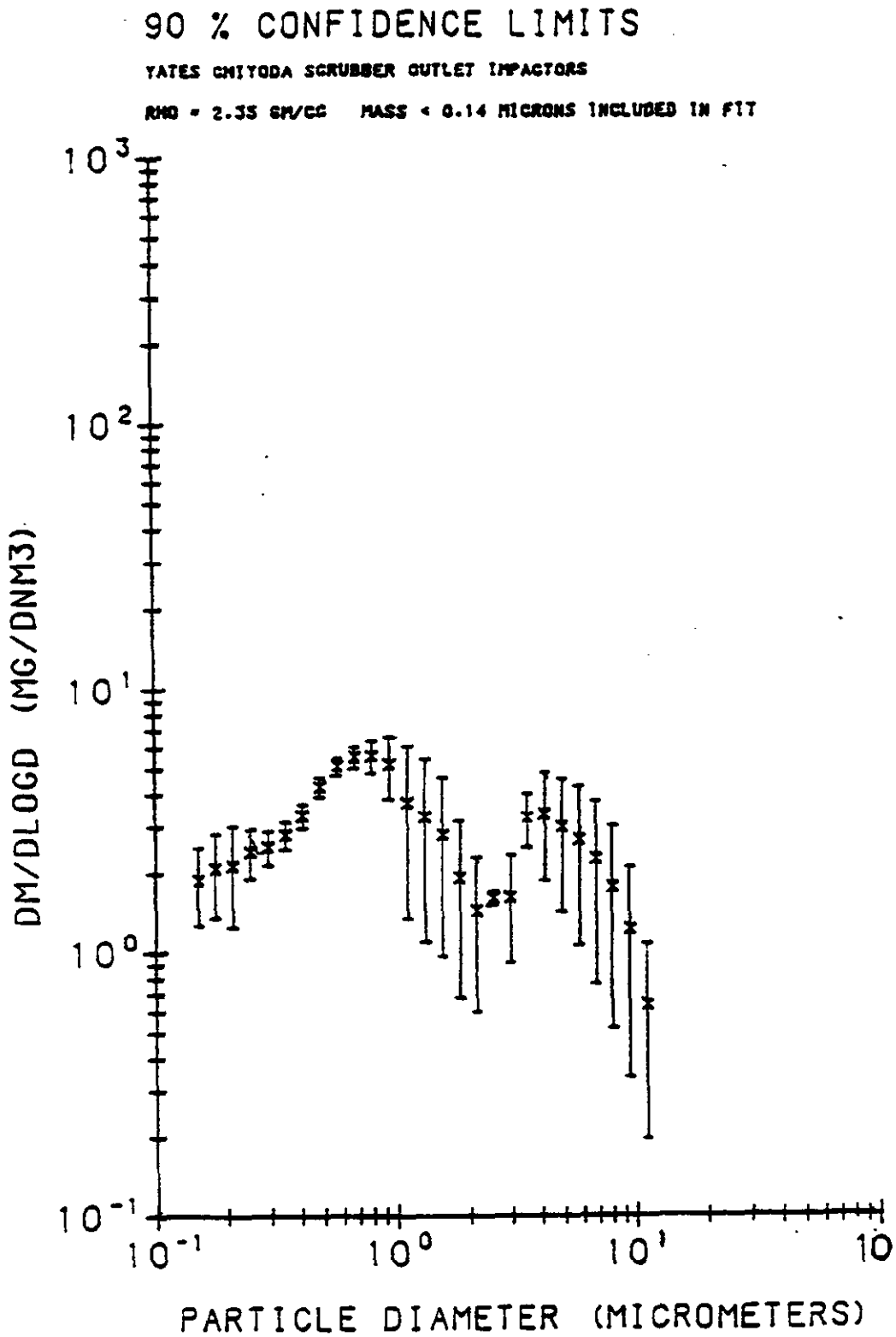

Figure A17. Outlet dM/dlogD vs Particle Diameter for Chiyoda Scrubber, 100 MW, 16" ΔP, January 23, 1993.

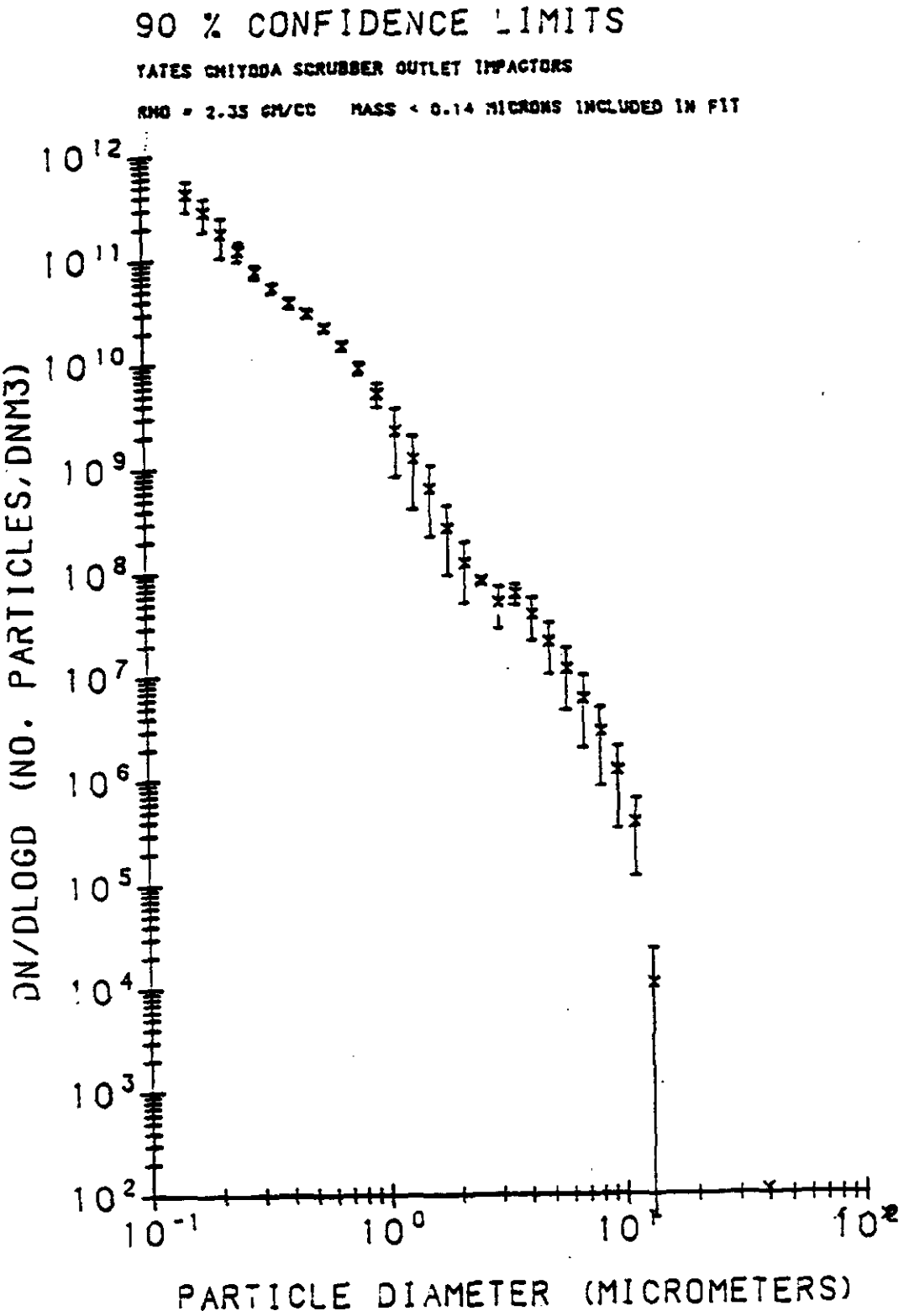

Figure A18. Outlet dN/dlogD vs Particle Diameter for Chiyoda Scrubber, 100 MW, 16" ΔP, January 23, 1993.

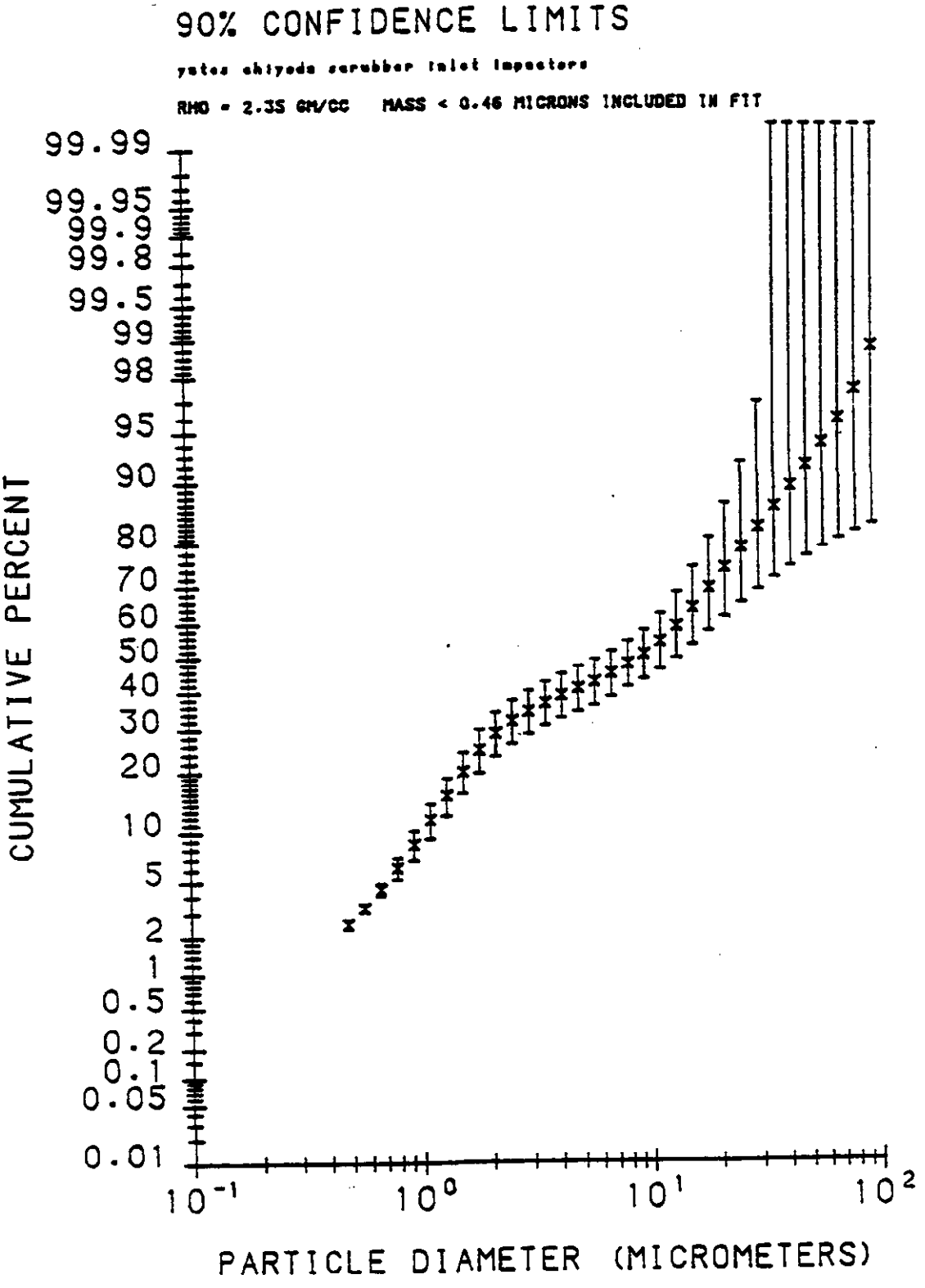

Figure A19. Inlet Cumulative Percent vs Particle Diameter for Chiyoda Scrubber, 75 MW, 8" ΔP, January 25, 1993.

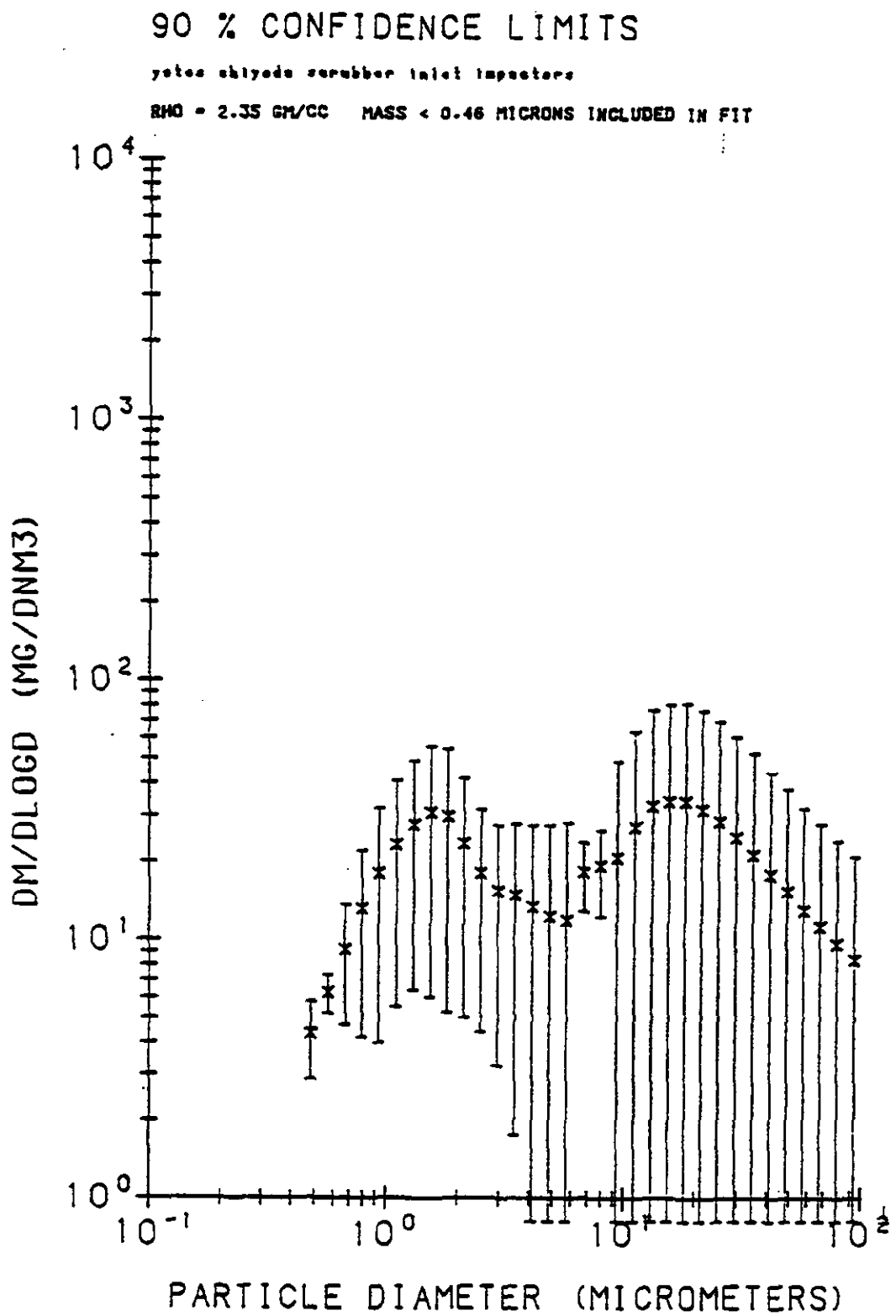

Figure A20. Inlet dM/dlogD vs Particle Diameter for Chiyoda Scrubber, 75 MW, 8" ΔP, January 25, 1993.

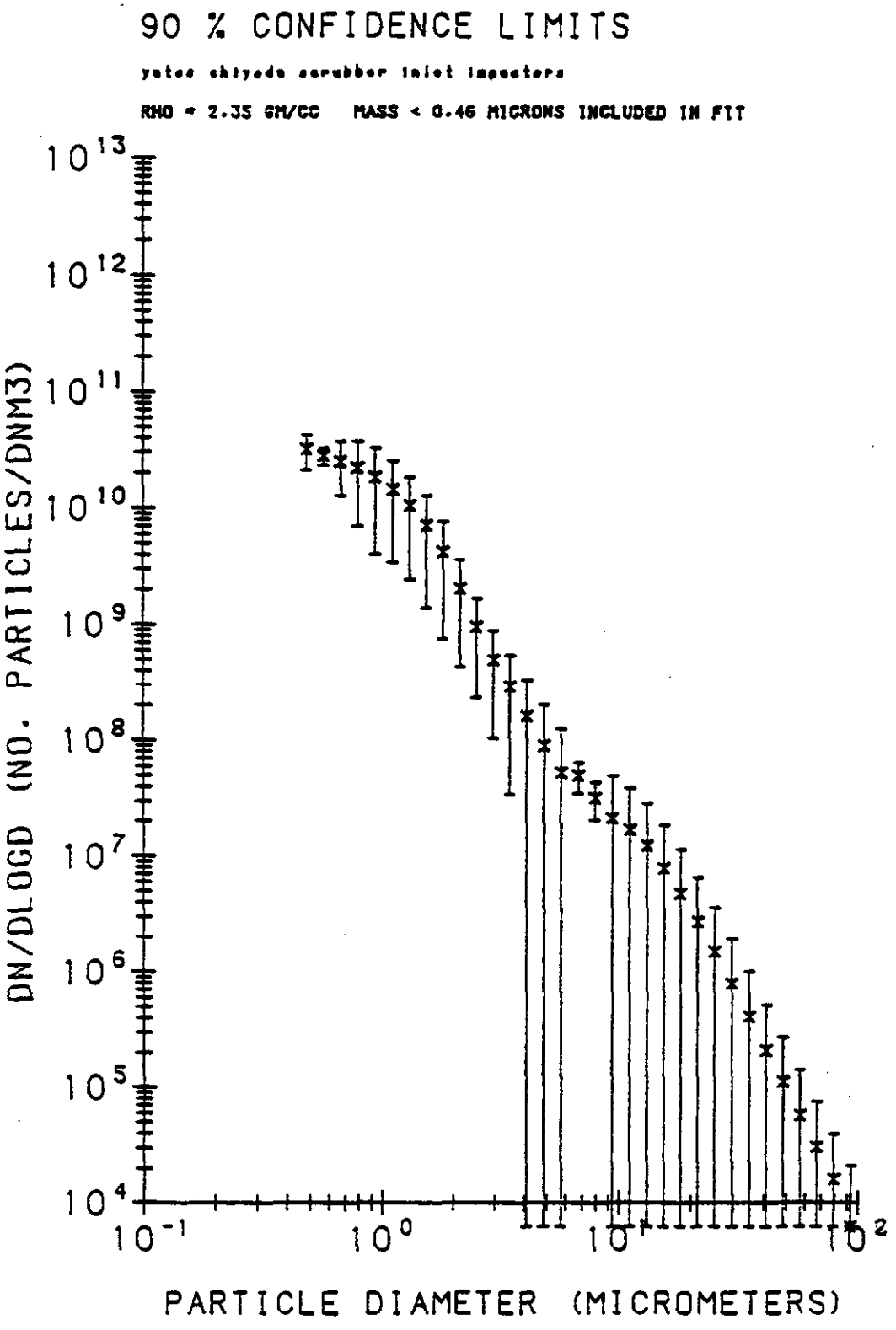

Figure A21. Inlet dN/dlogD vs Particle Diameter for Chiyoda Scrubber, 75 MW, 8" ΔP, January 25, 1993.

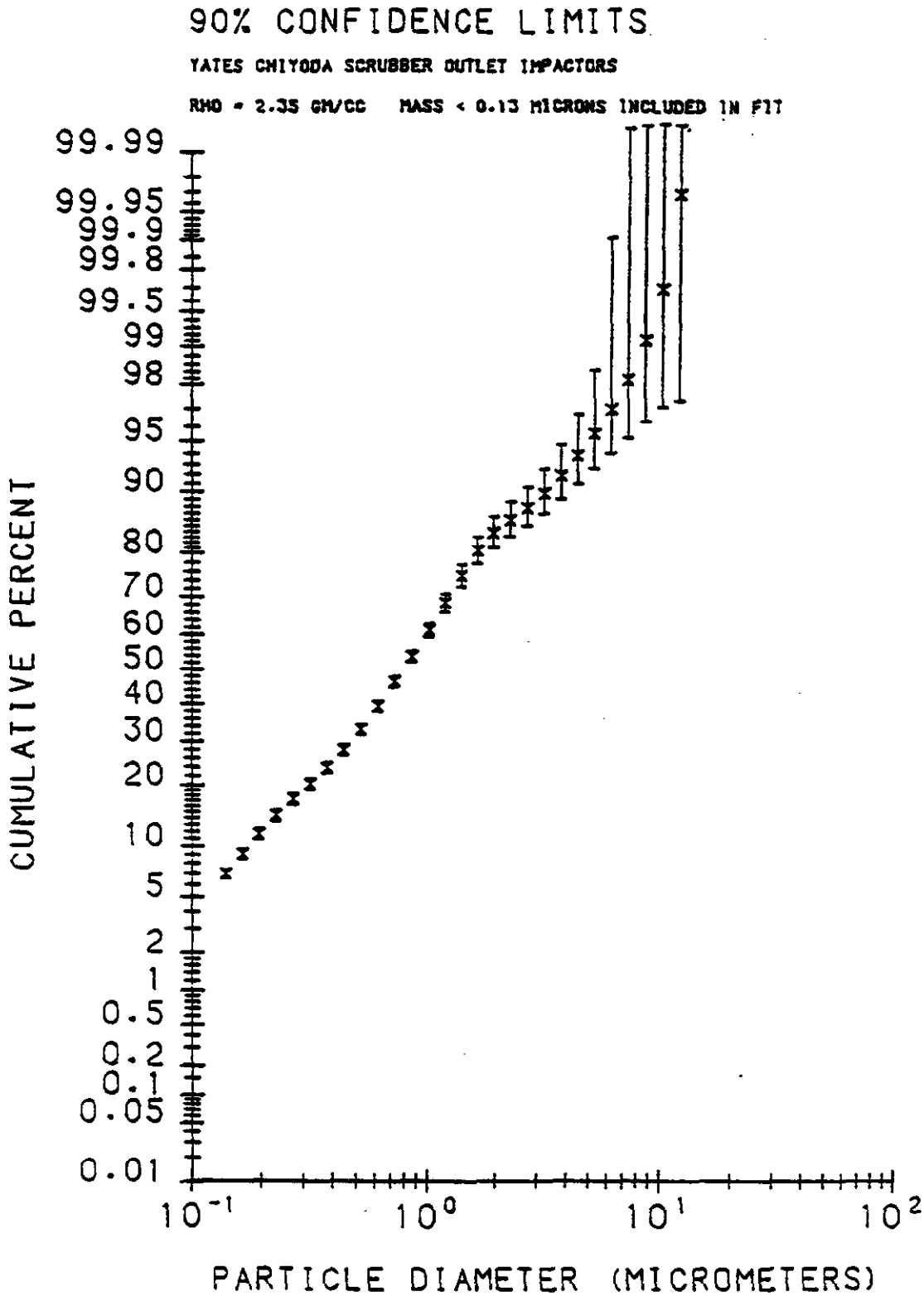

Figure A22. Outlet Cumulative Percent vs Particle Diameter for Chiyoda Scrubber, 75 MW, 8" ΔP, January 25, 1993.

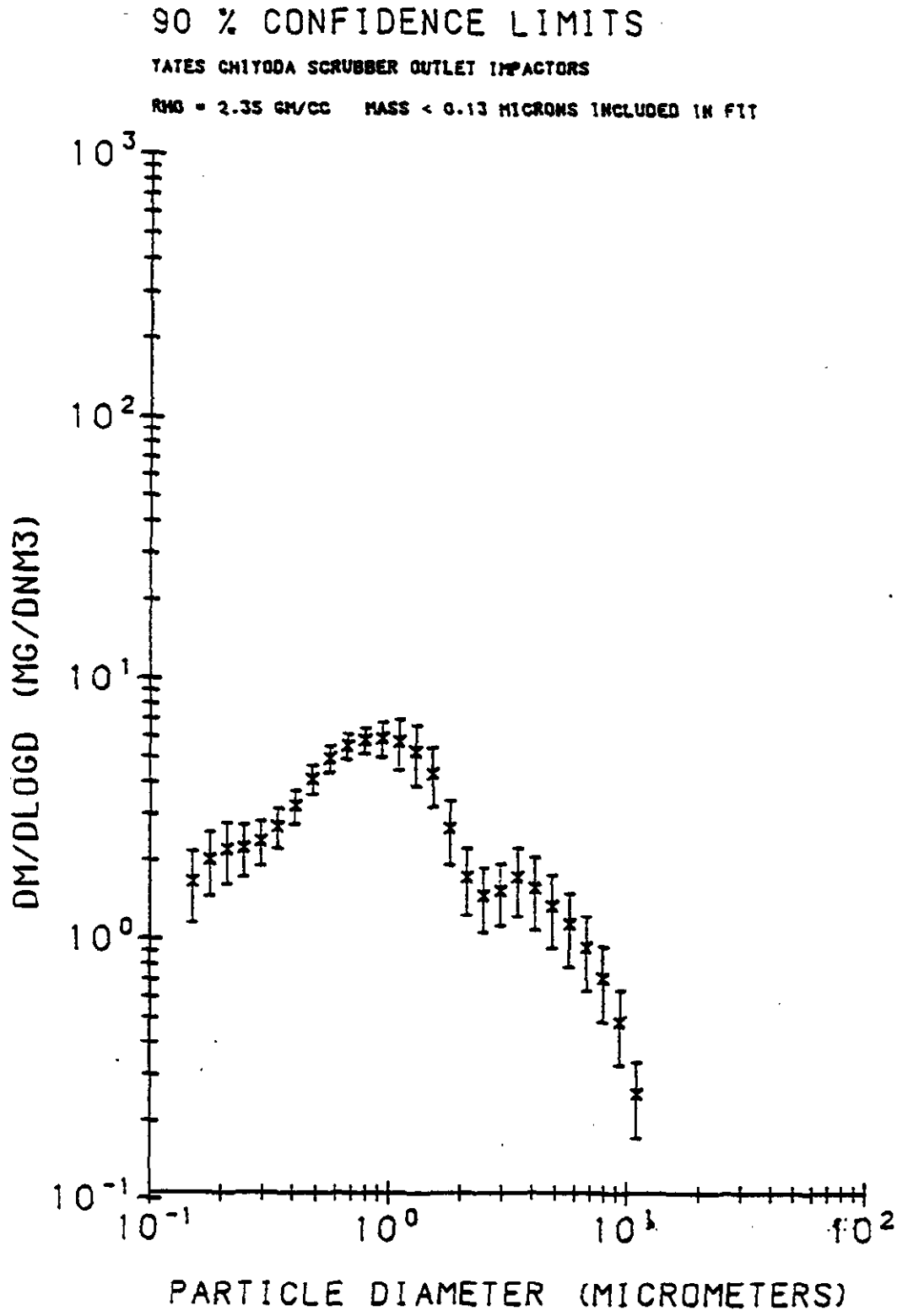

Figure A23. Outlet dM/dlogD vs Particle Diameter for Chiyoda Scrubber, 75 MW, 8" ΔP, January 25, 1993.

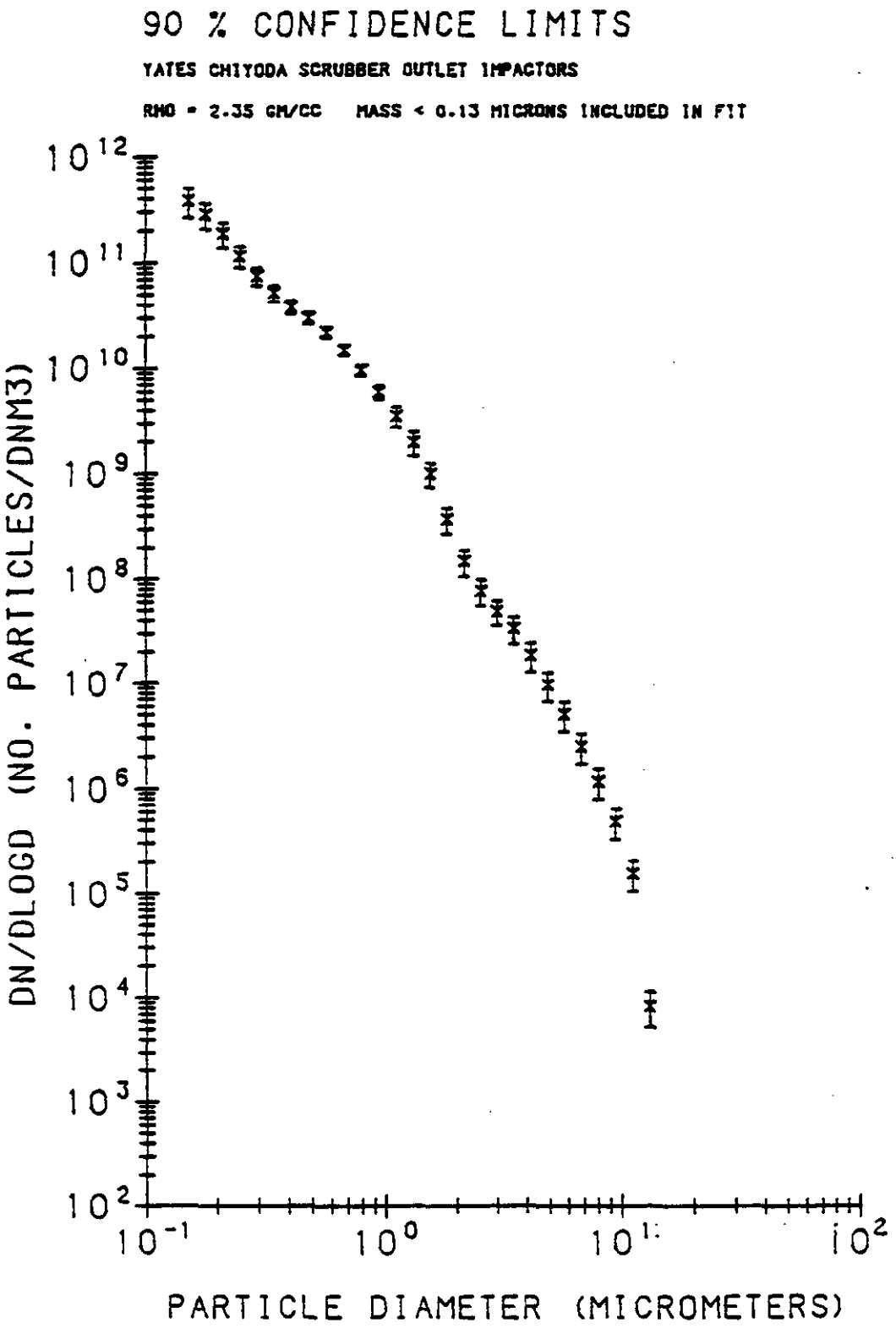

Figure A24. Outlet dN/dlogD vs Particle Diameter for Chiyoda Scrubber, 75 MW_e 8" ΔP, January 25, 1993.

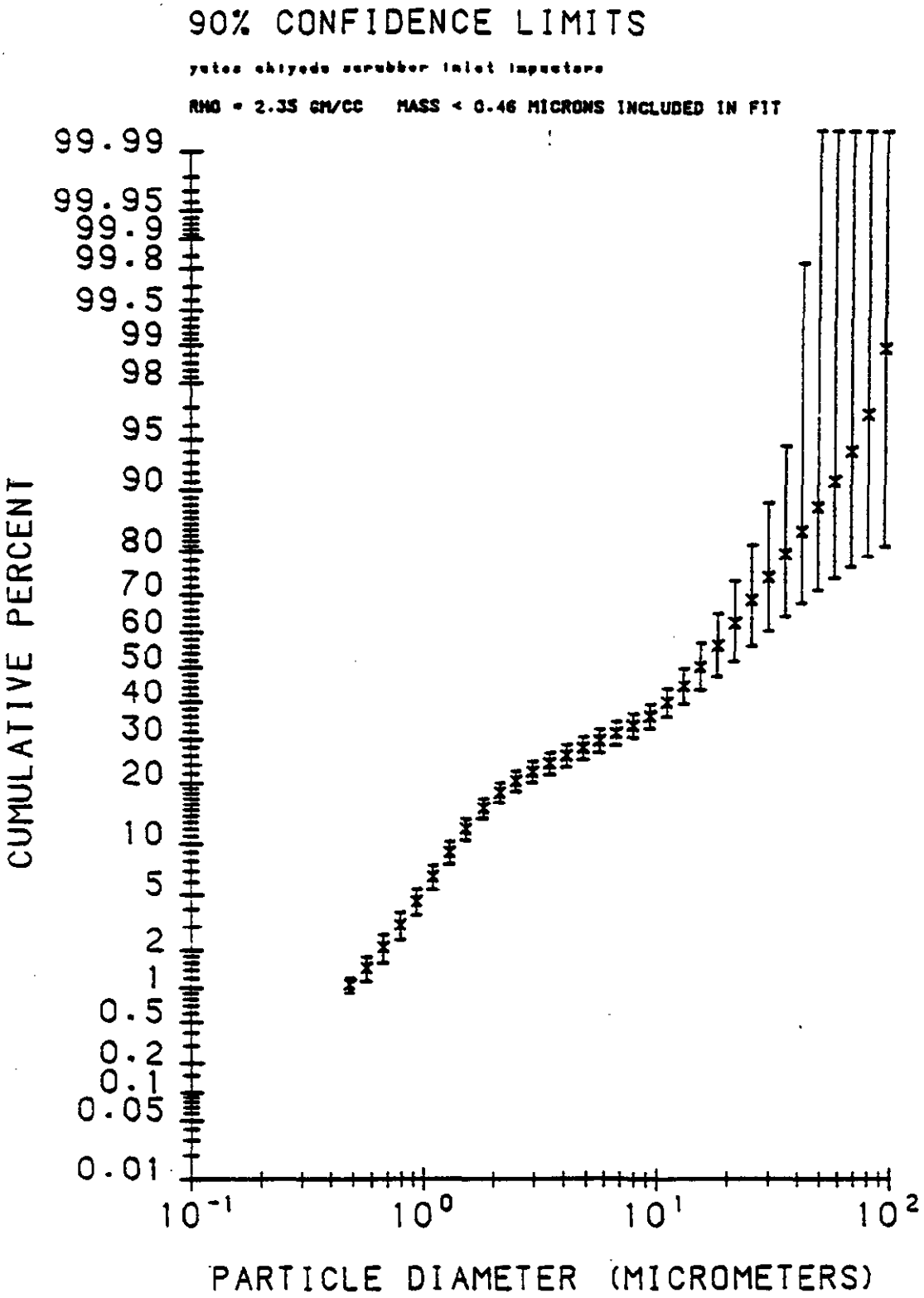

Figure A25. Inlet Cumulative Percent vs Particle Diameter for Chiyoda Scrubber, 75 MW, 12" ΔP, January 26, 1993.

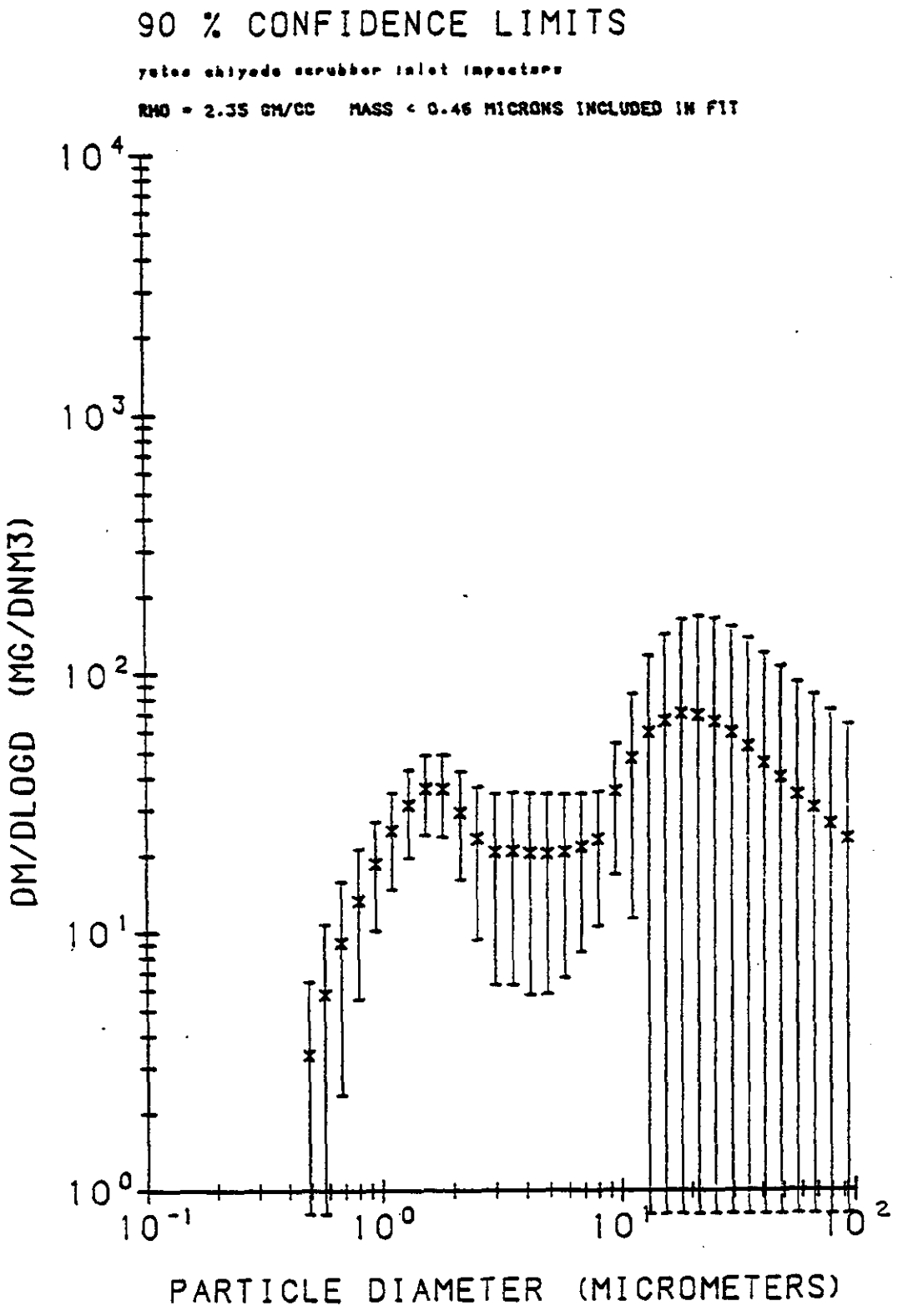

Figure A26. Inlet dM/dlogD vs Particle Diameter for Chiyoda Scrubber, 75 MW, 12" ΔP, January 26, 1993.

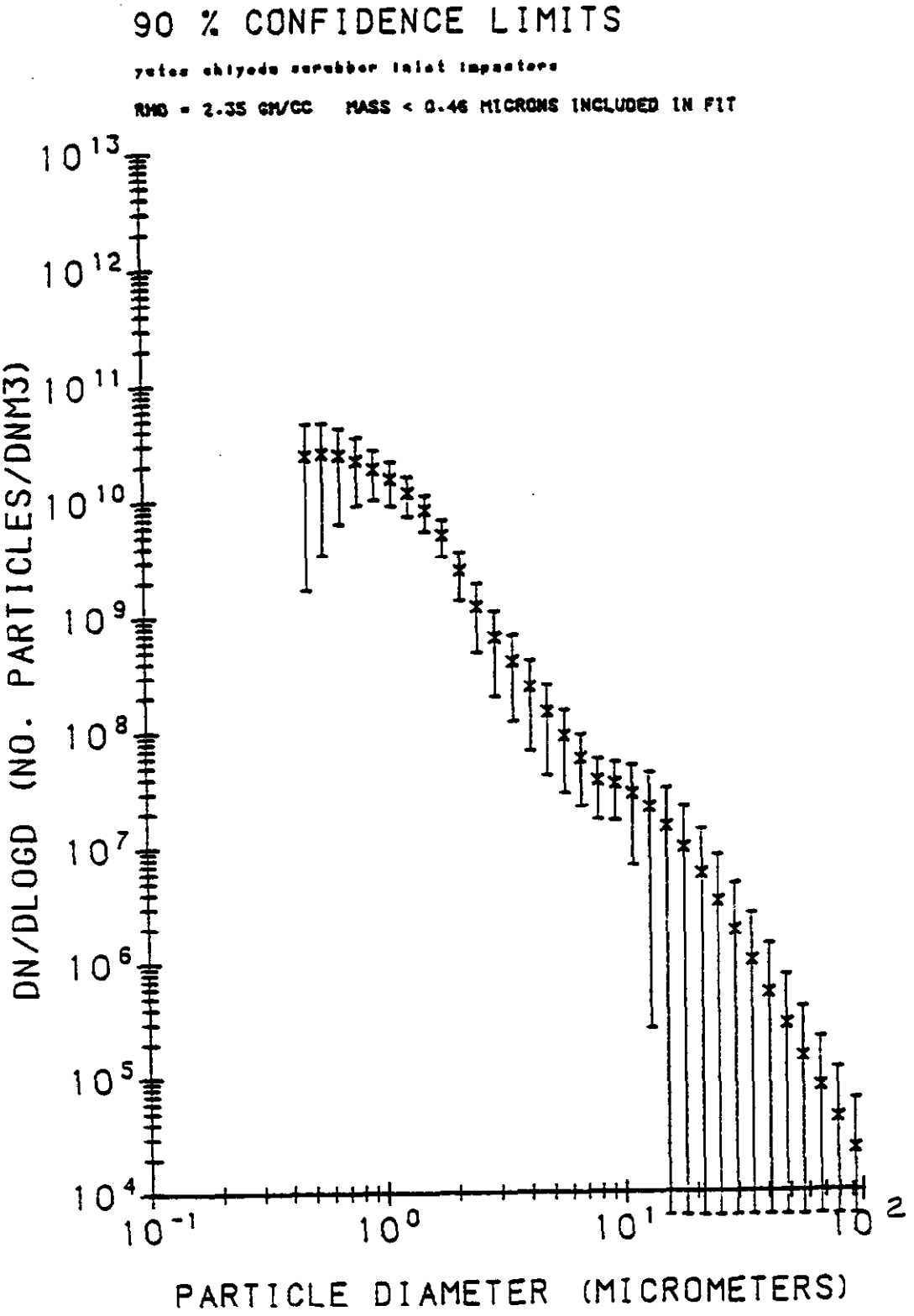

Figure A27. Inlet dN/dlogD vs Particle Diameter for Chiyoda Scrubber, 75 MW, 12" ΔP, January 26, 1993.

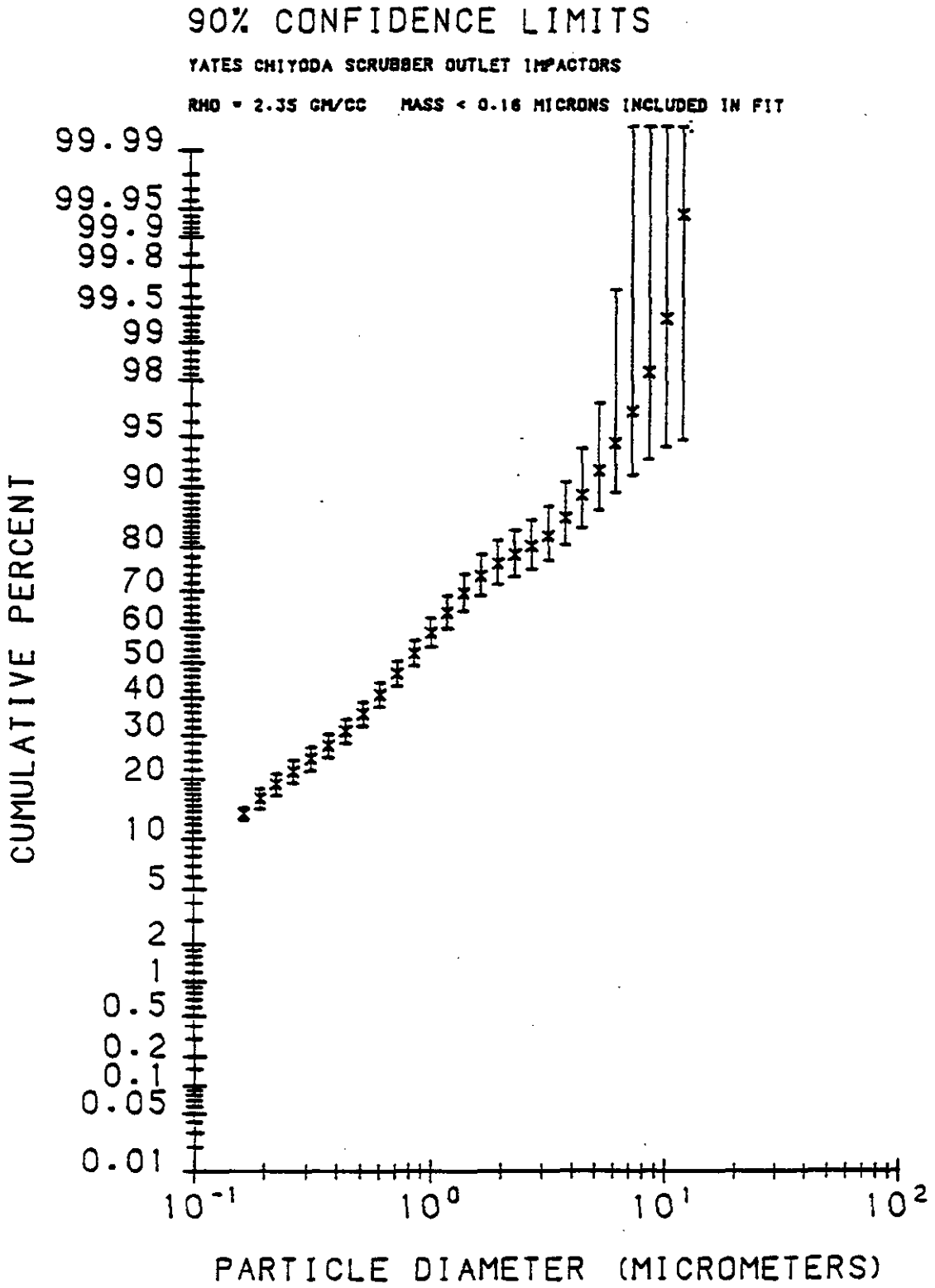

Figure A28. Outlet Cumulative Percent vs Particle Diameter for Chiyoda Scrubber, 75 MW, 12" ΔP, January 26, 1993.

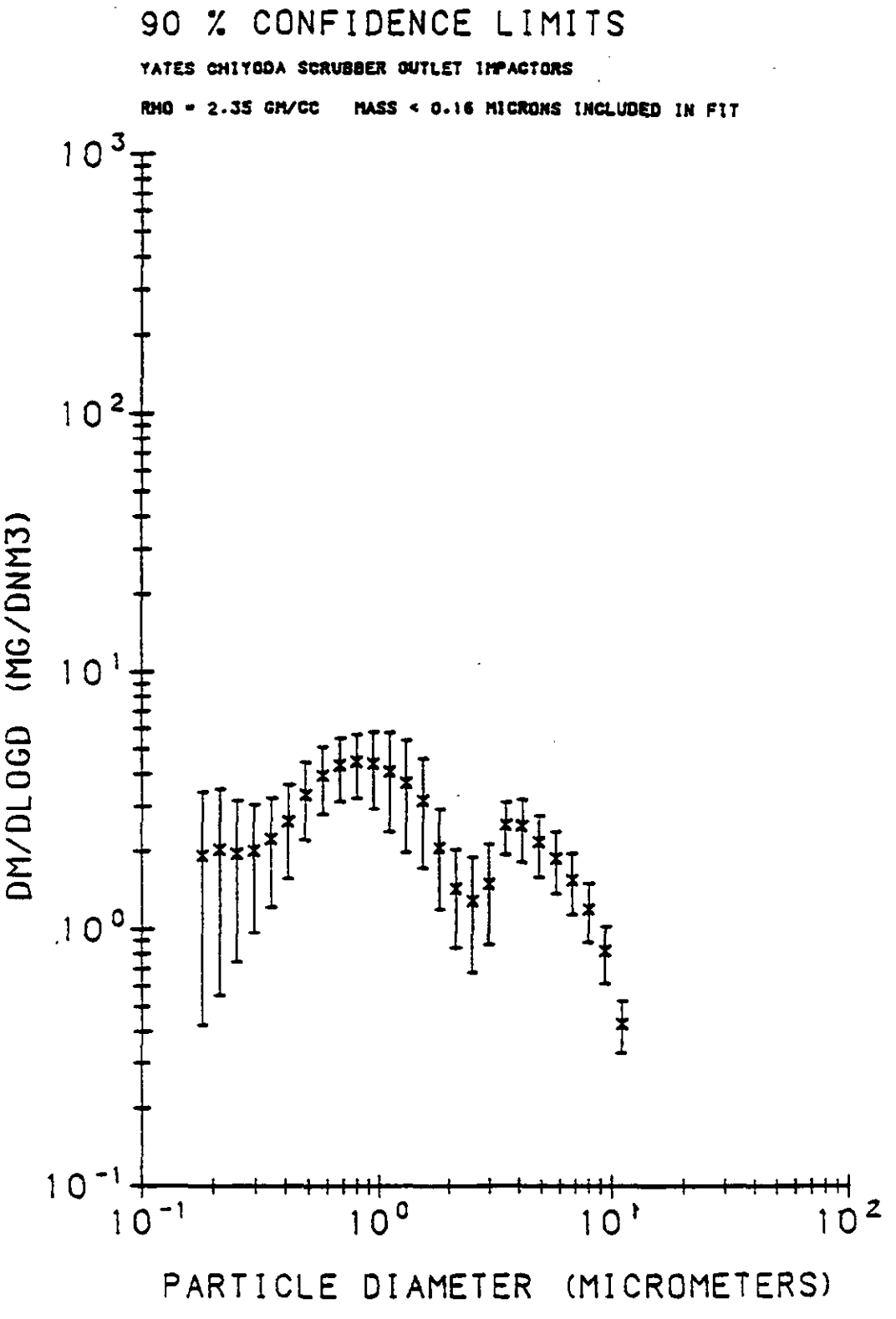

Figure A29. Outlet dM/dlogD vs Particle Diameter for Chiyoda Scrubber, 75 MW, 12" ΔP, January 26, 1993.

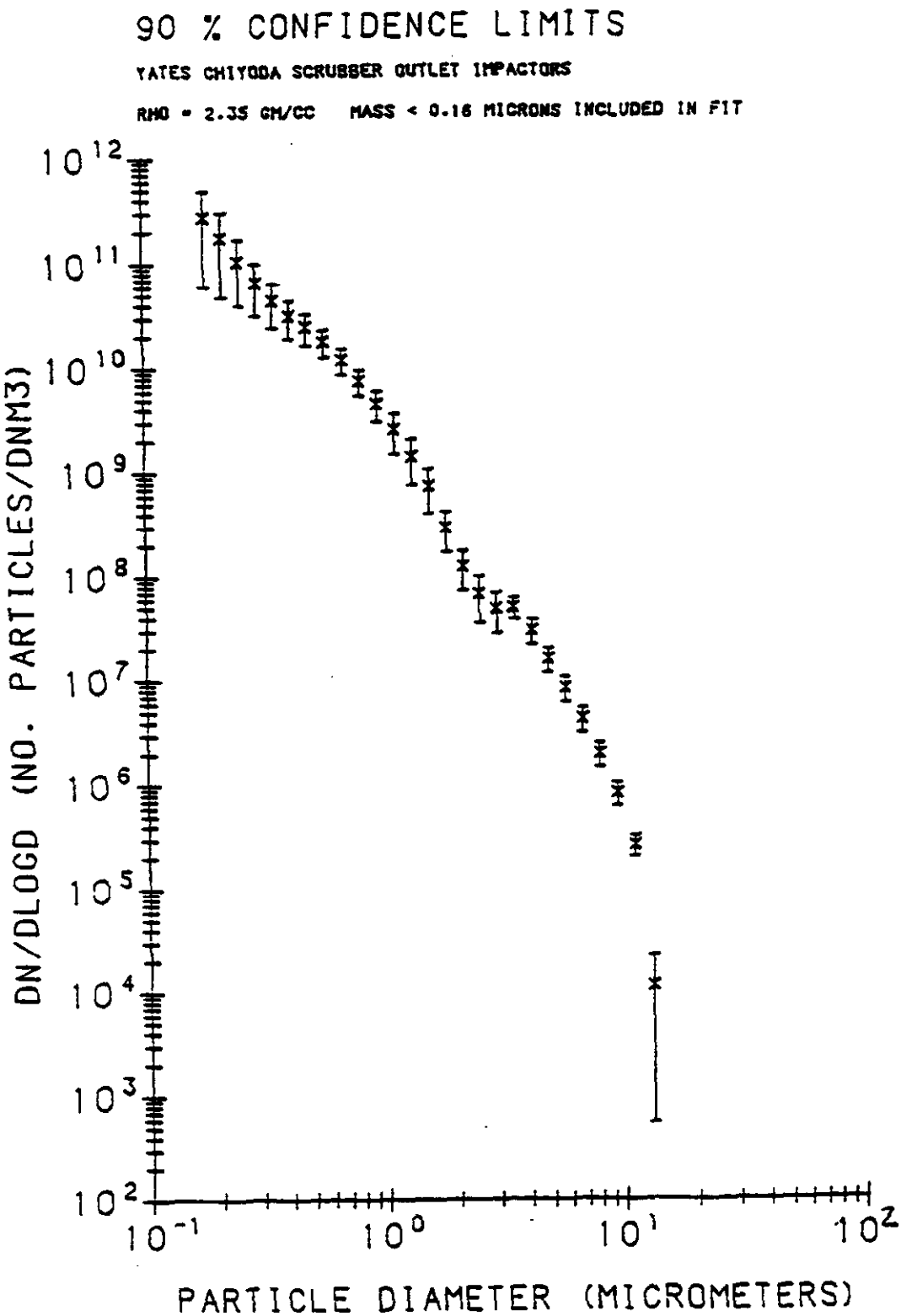

Figure A30. Outlet dN/dlogD vs Particle Diameter for Chiyoda Scrubber, 75 MW, 12" ΔP, January 26, 1993.

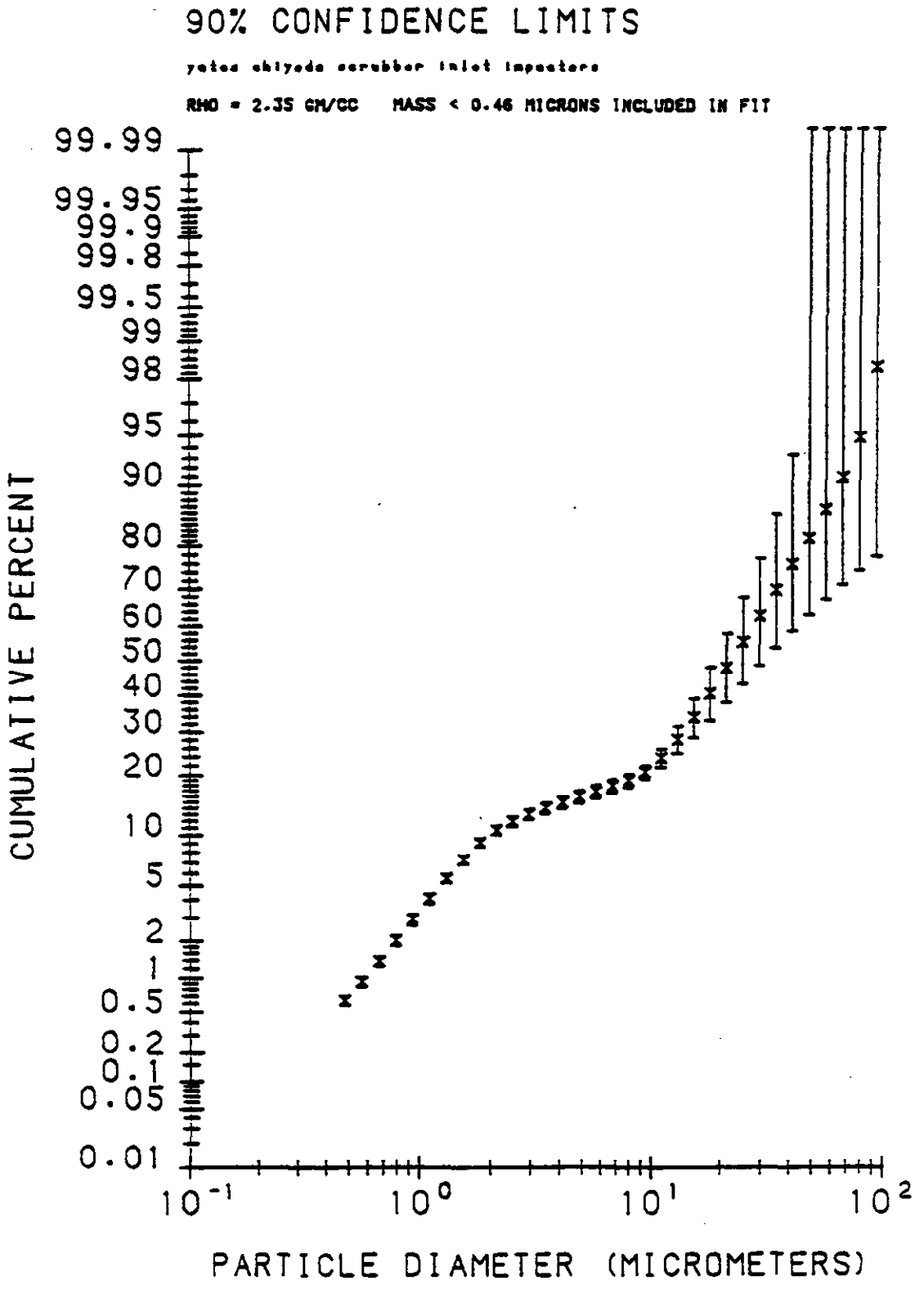

Figure A31. Inlet Cumulative Percent vs Particle Diameter for Chiyoda Scrubber, 75 MW, 16" ΔP, January 27, 1993.

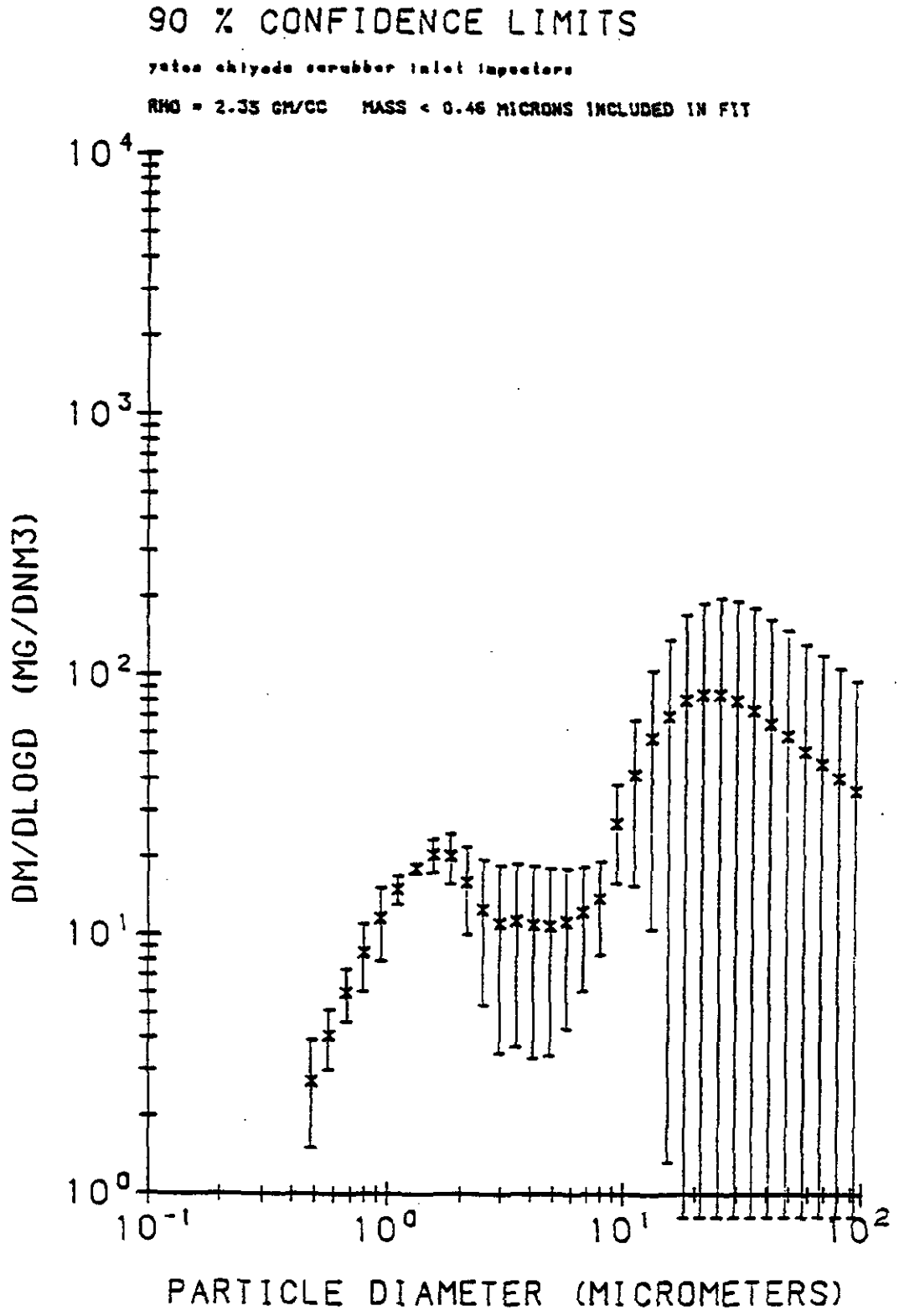

Figure A32. Inlet dM/dlogD vs Particle Diameter for Chiyoda Scrubber, 75 MW, 16" ΔP, January 27, 1993.

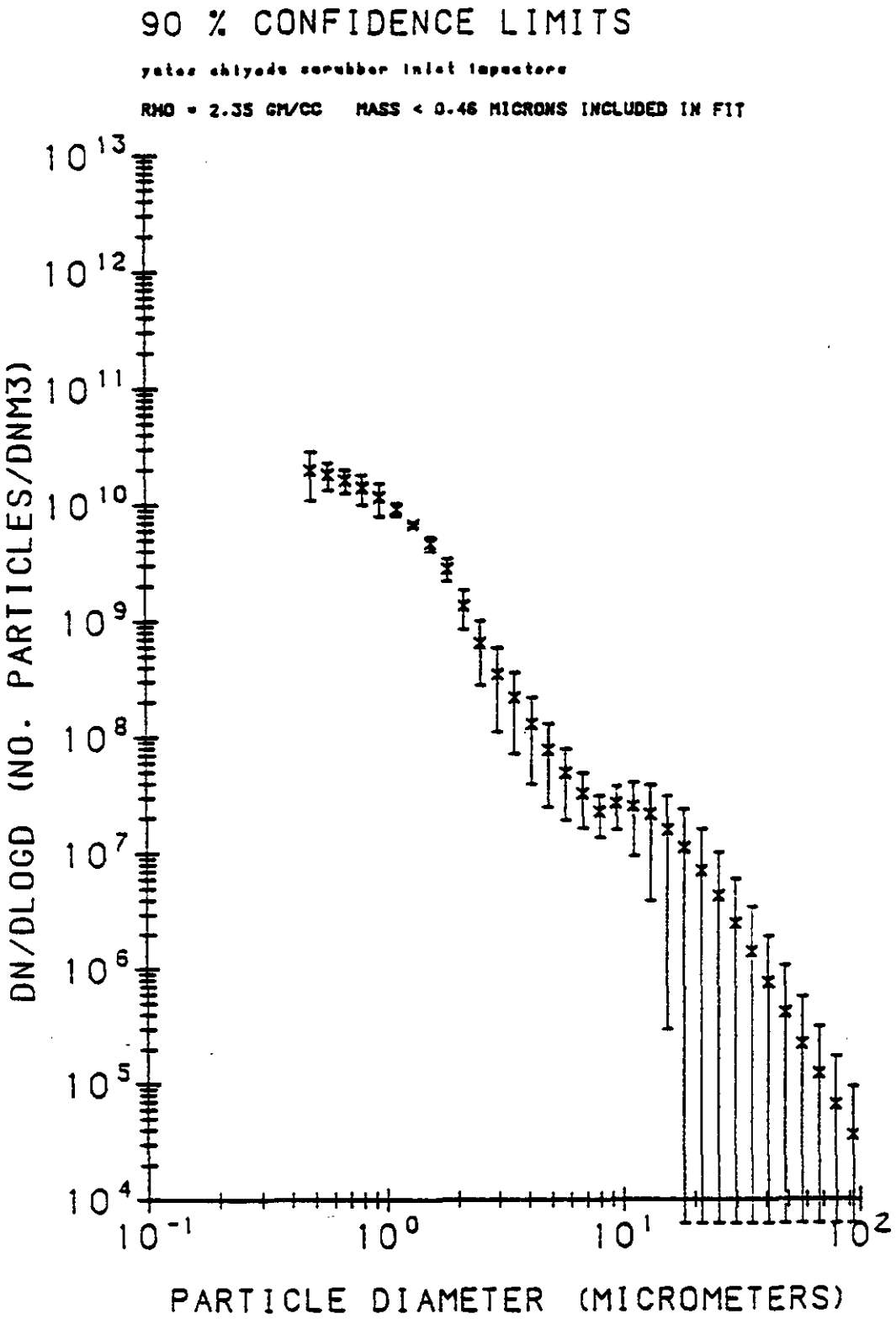

Figure A33. Inlet dN/dlogD vs Particle Diameter for Chiyoda Scrubber, 75 MW, 16" ΔP, January 27, 1993.

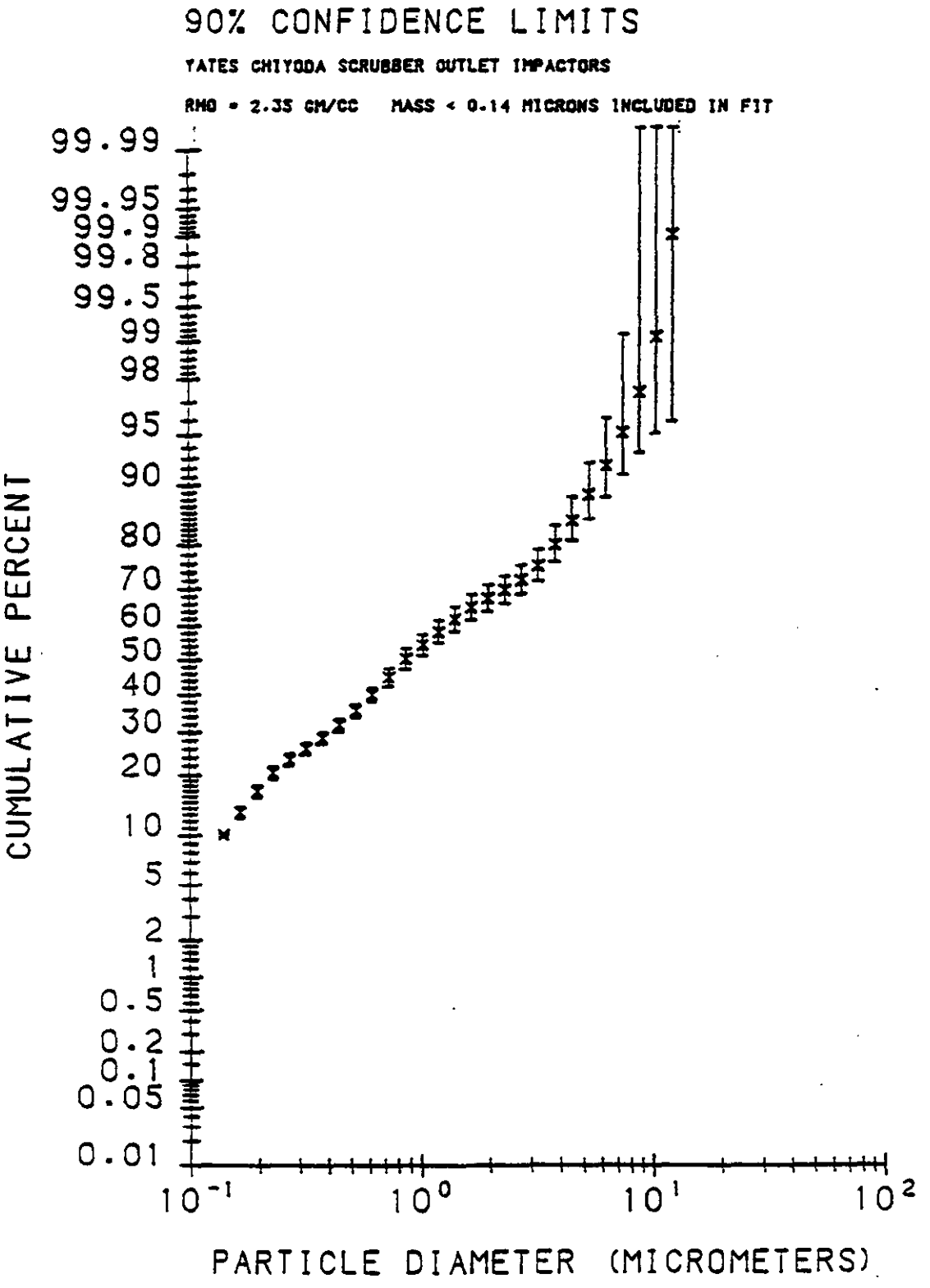

Figure A34. Outlet Cumulative Percent vs Particle Diameter for Chiyoda Scrubber, 75 MW, 16" ΔP, January 27, 1993.

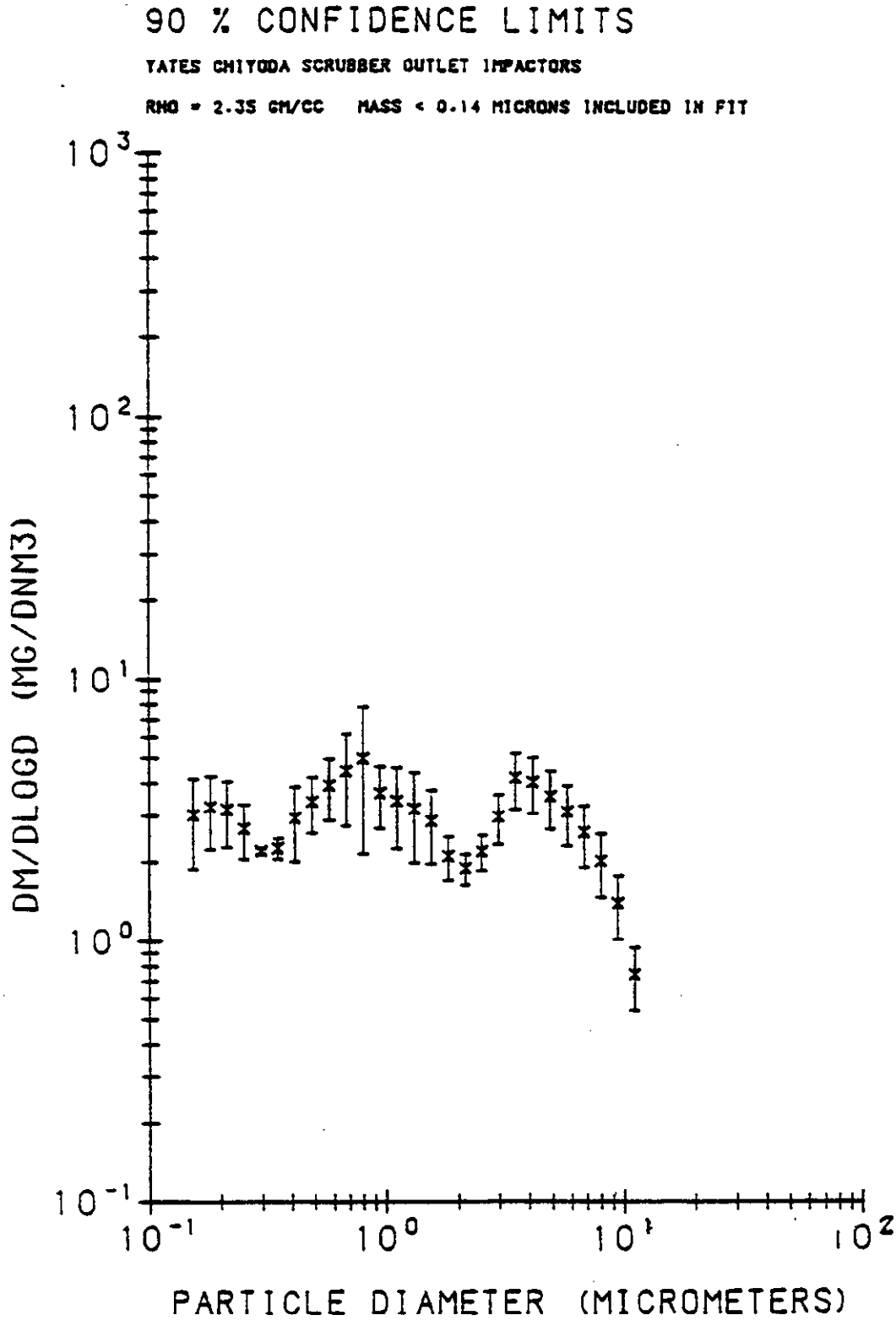

Figure A35. Outlet dM/dlogD vs Particle Diameter for Chiyoda Scrubber, 75 MW, 16" ΔP, January 27, 1993.

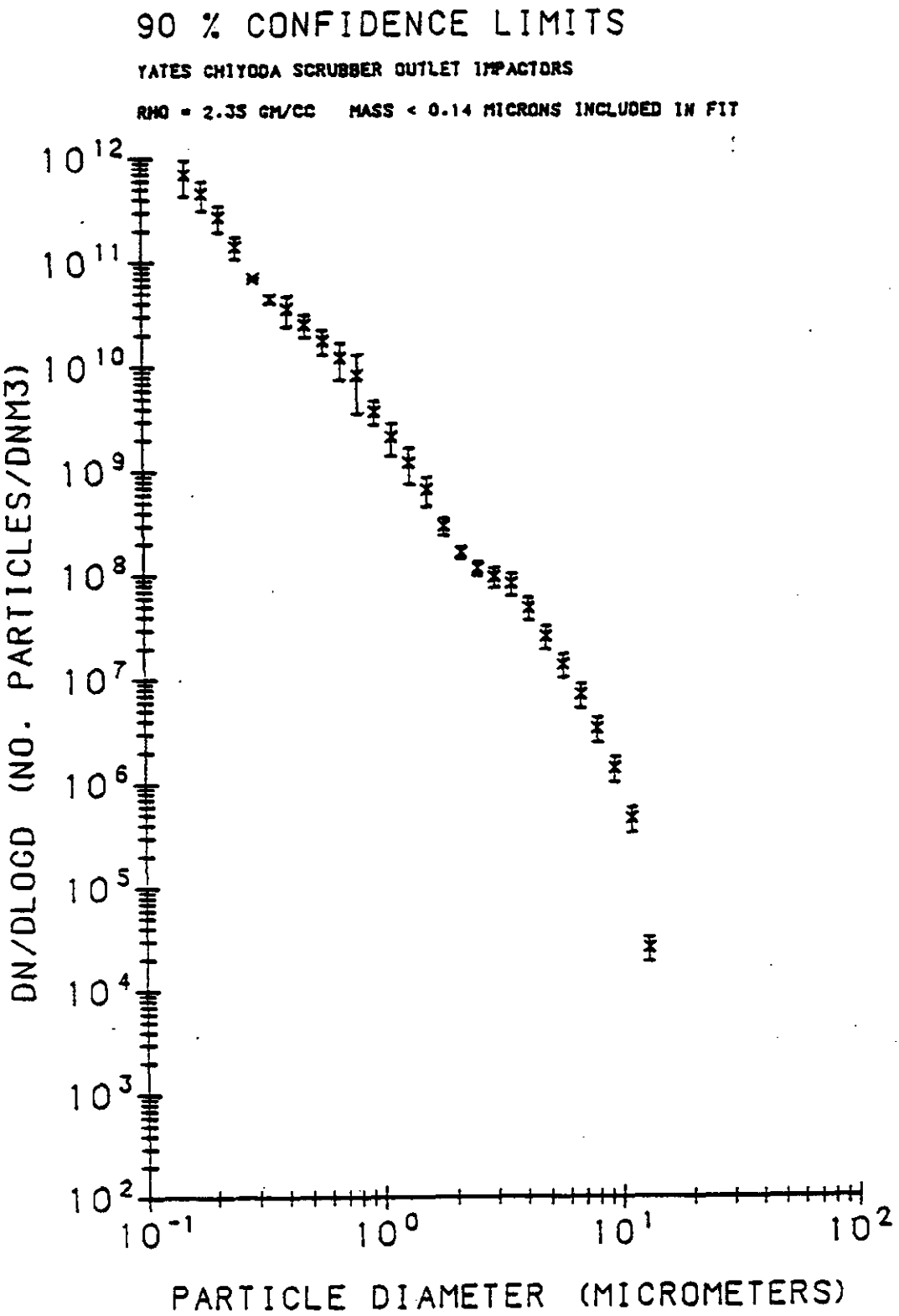

Figure A36. Outlet dN/dlogD vs Particle Diameter for Chiyoda Scrubber, 75 MW, 16" ΔP, January 27, 1993.

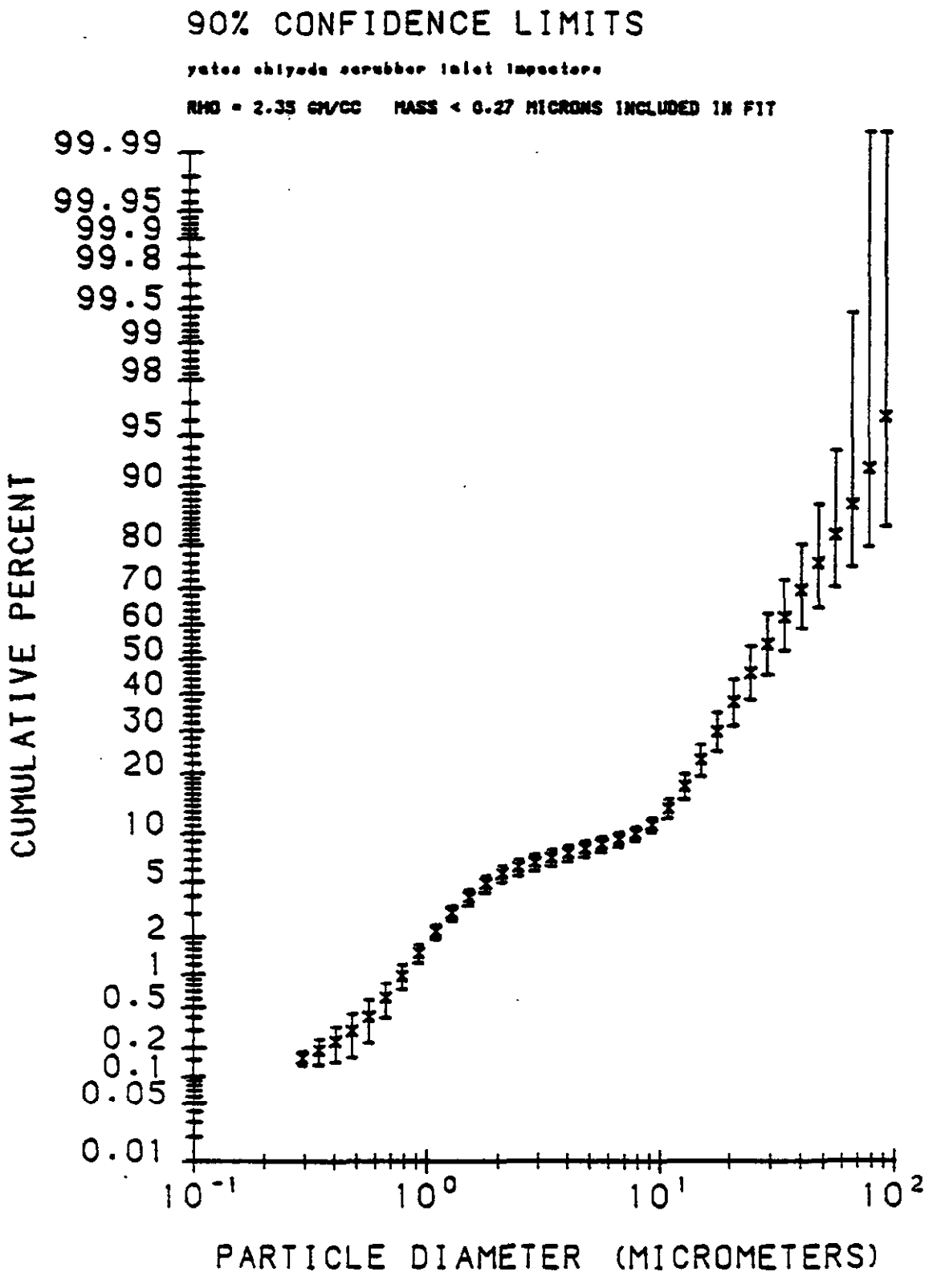

Figure A37. Inlet Cumulative Percent vs Particle Diameter for Chiyoda Scrubber, 50 MW, 8" ΔP, January 29, 1993.

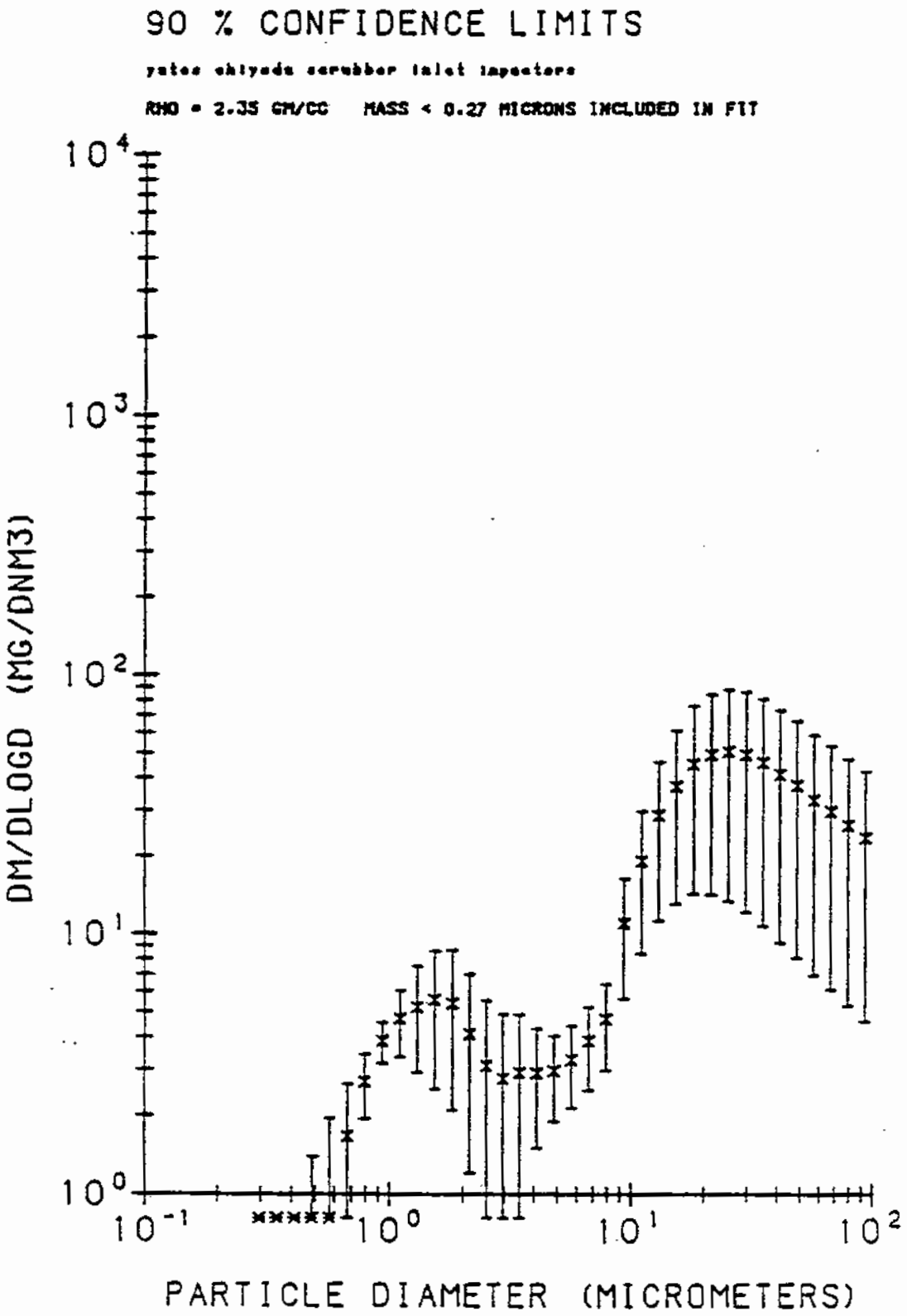

Figure A38. Inlet dM/dlogD vs Particle Diameter for Chiyoda Scrubber, 50 MW_e 8" ΔP, January 29, 1993.

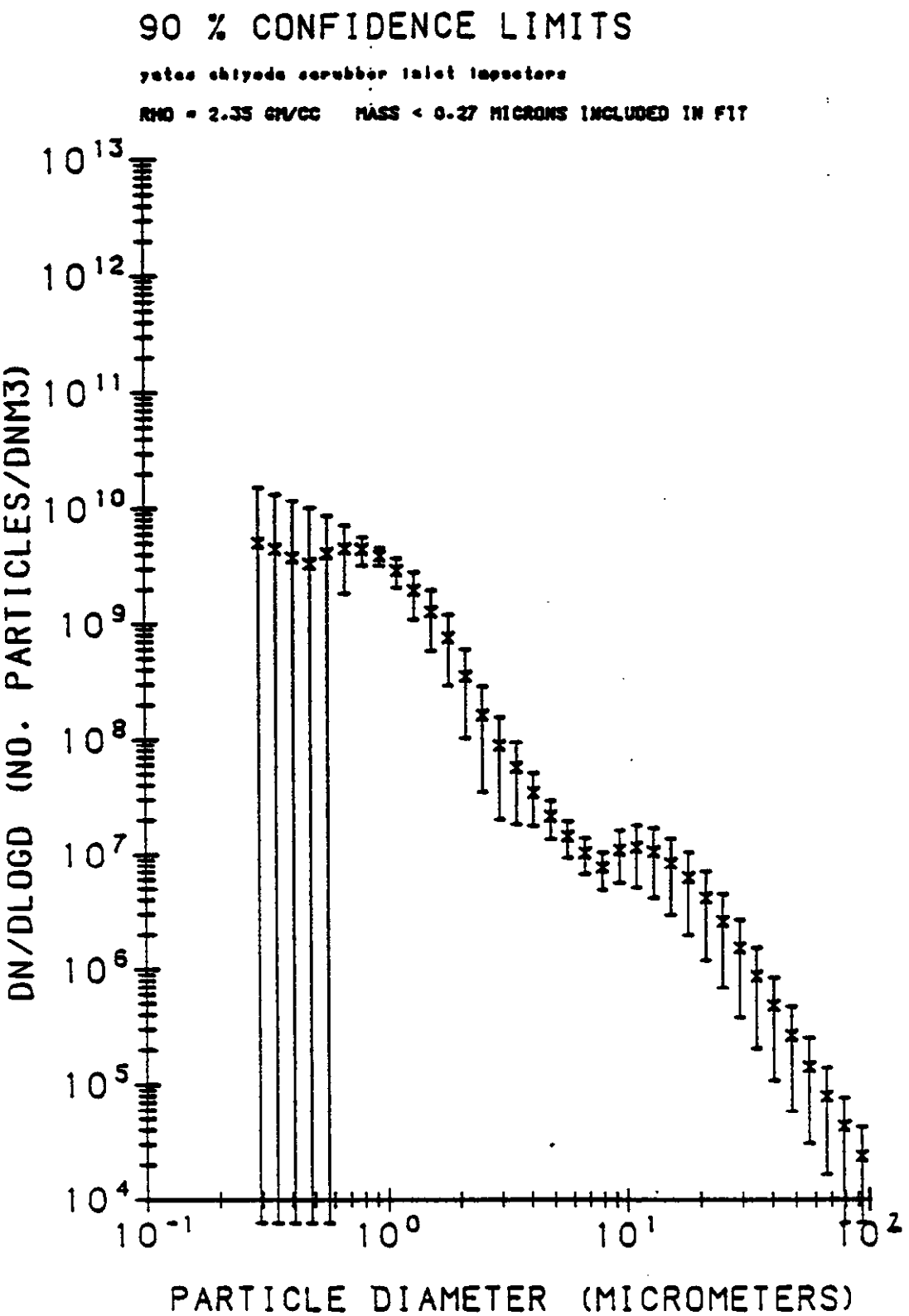

Figure A39. Inlet dN/dlogD vs Particle Diameter for Chiyoda Scrubber, 50 MW, 8" ΔP, January 29, 1993.

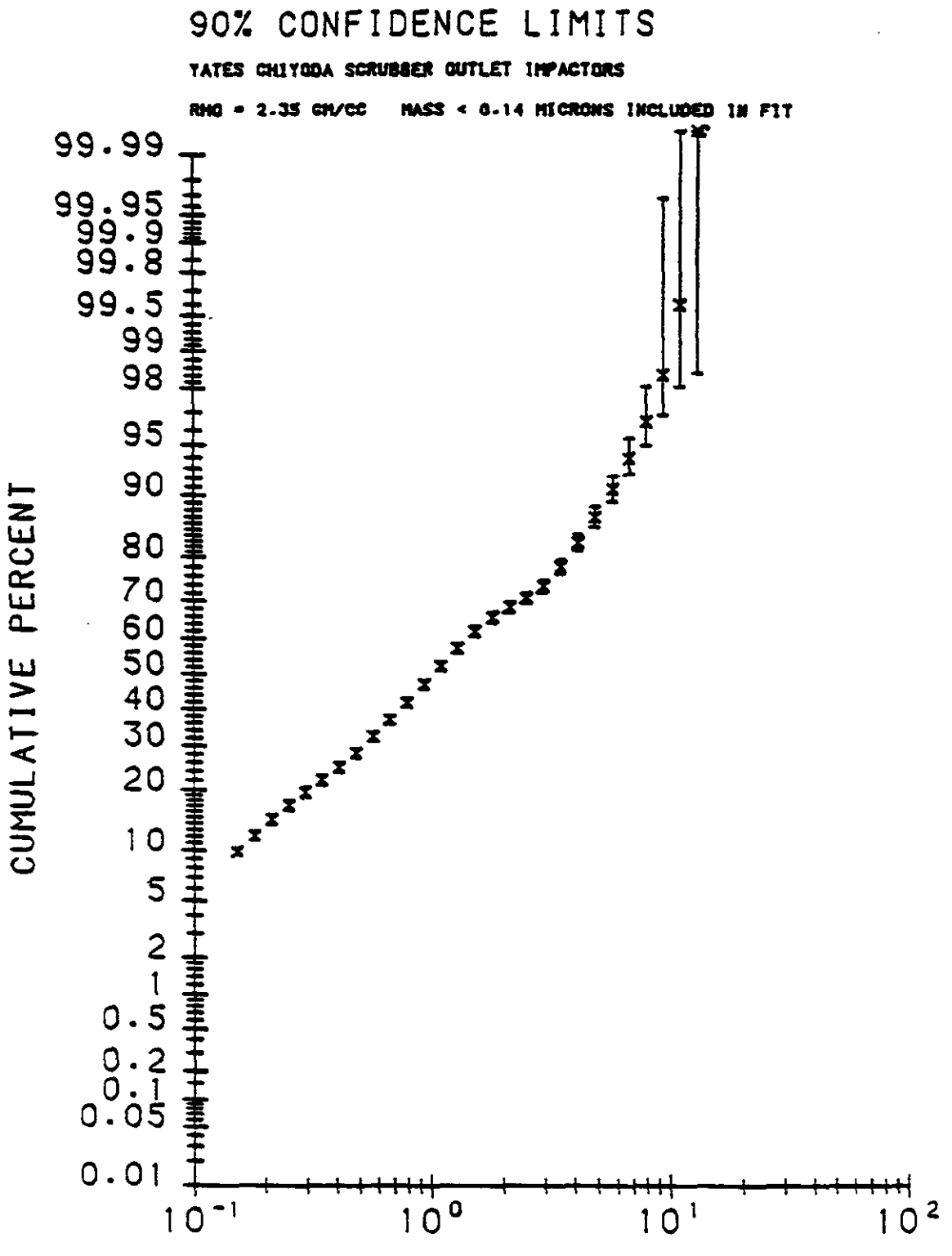

Figure A40. Outlet Cumulative Percent vs Particle Diameter for Chiyoda Scrubber, 50 MW, 8" ΔP, January 29, 1993.

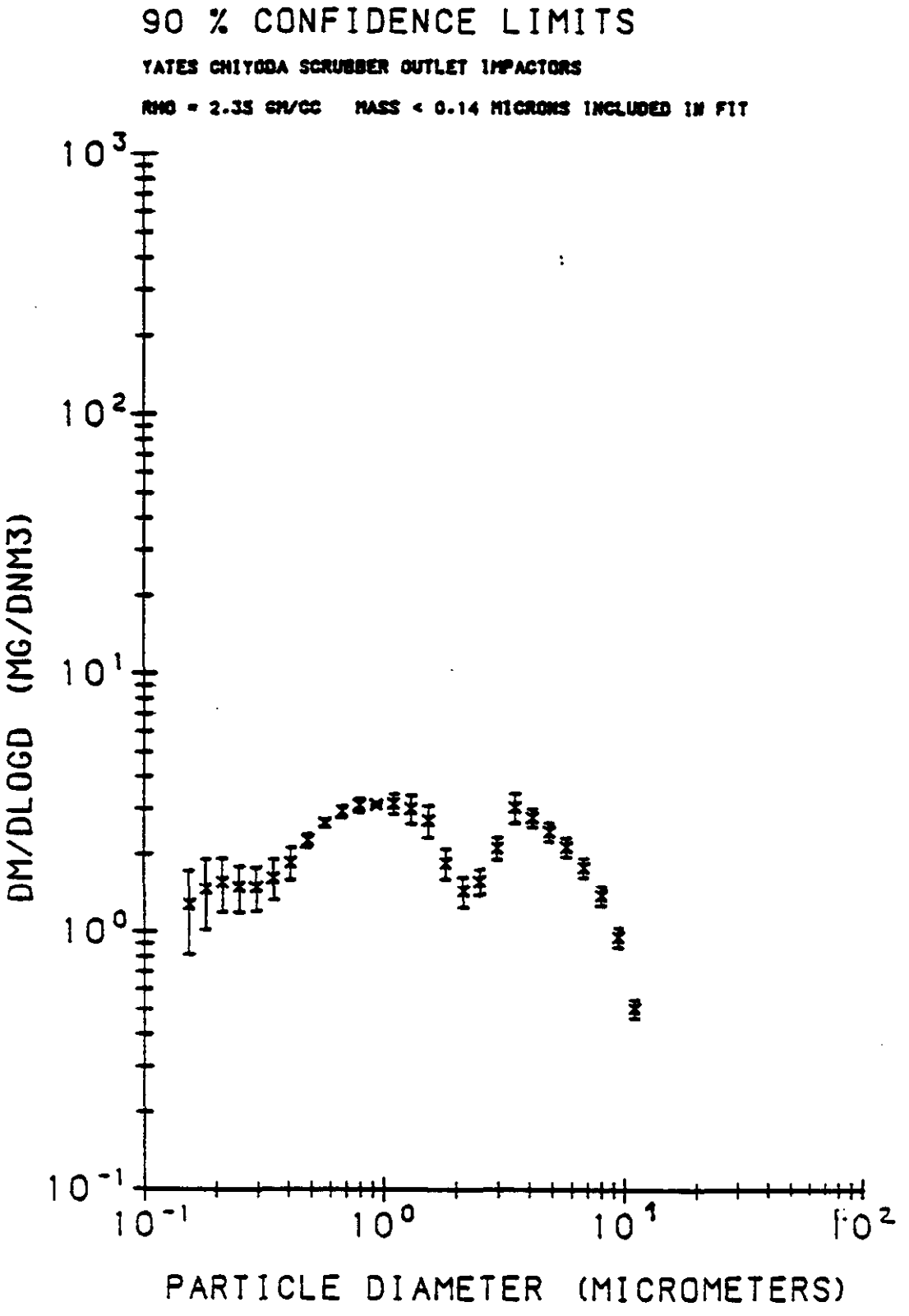

Figure A41. Outlet dM/dlogD vs Particle Diameter for Chiyoda Scrubber, 50 MW, 8" ΔP, January 29, 1993.

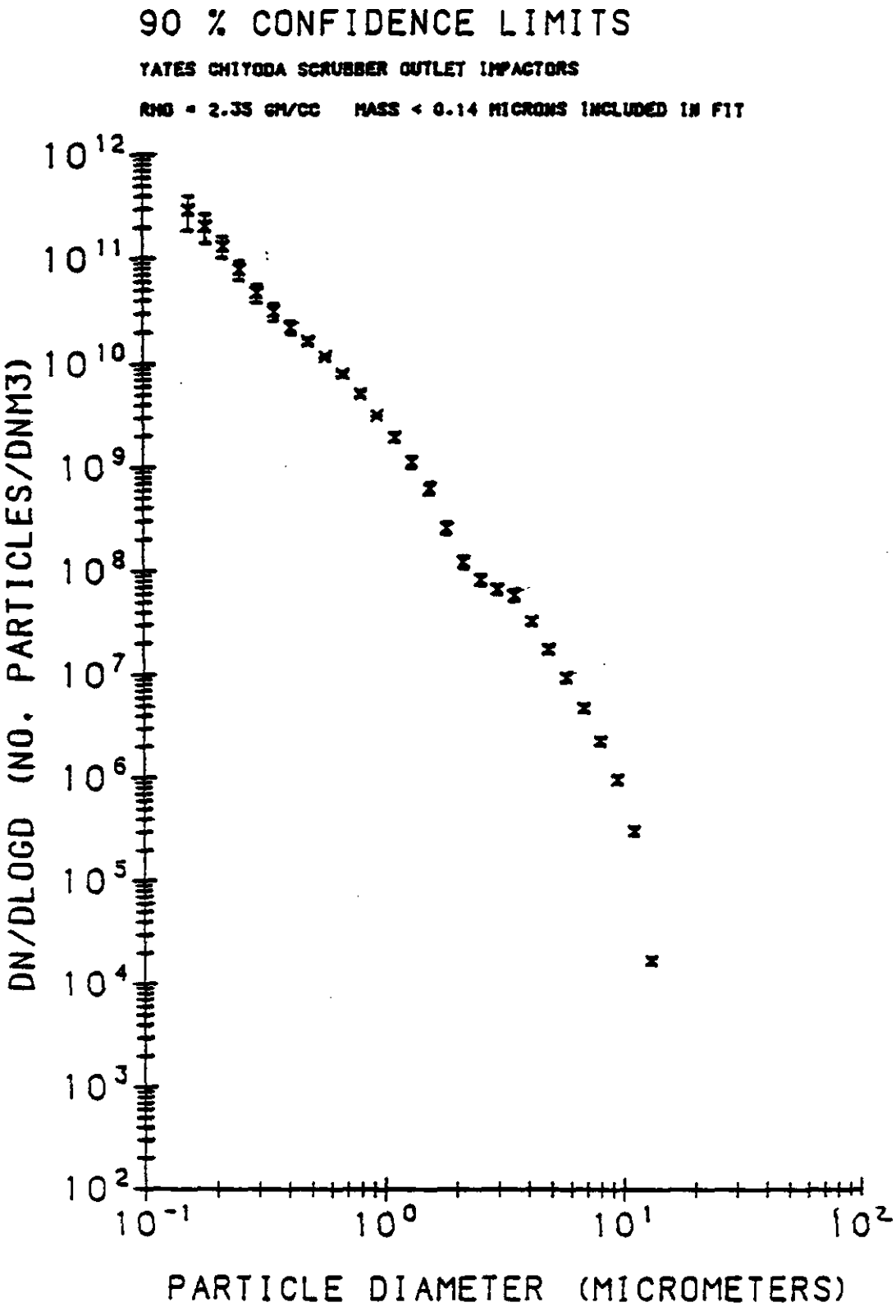

Figure A42. Outlet dN/dlogD vs Particle Diameter for Chiyoda Scrubber, 50 MW, 8" ΔP, January 29, 1993.

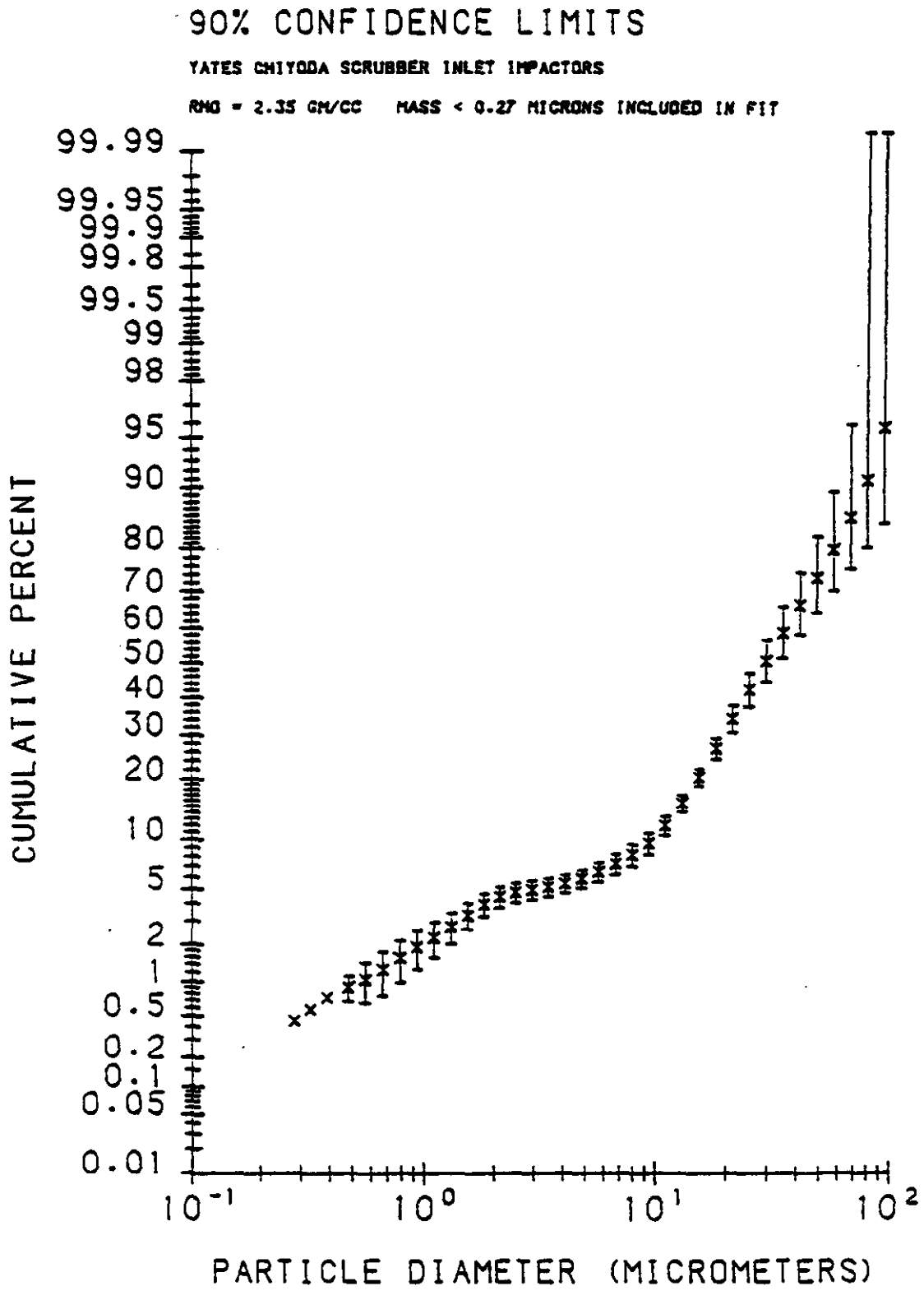

Figure A43. Inlet Cumulative Percent vs Particle Diameter for Chiyoda Scrubber, 50 MW, 12" ΔP, January 30, 1993.

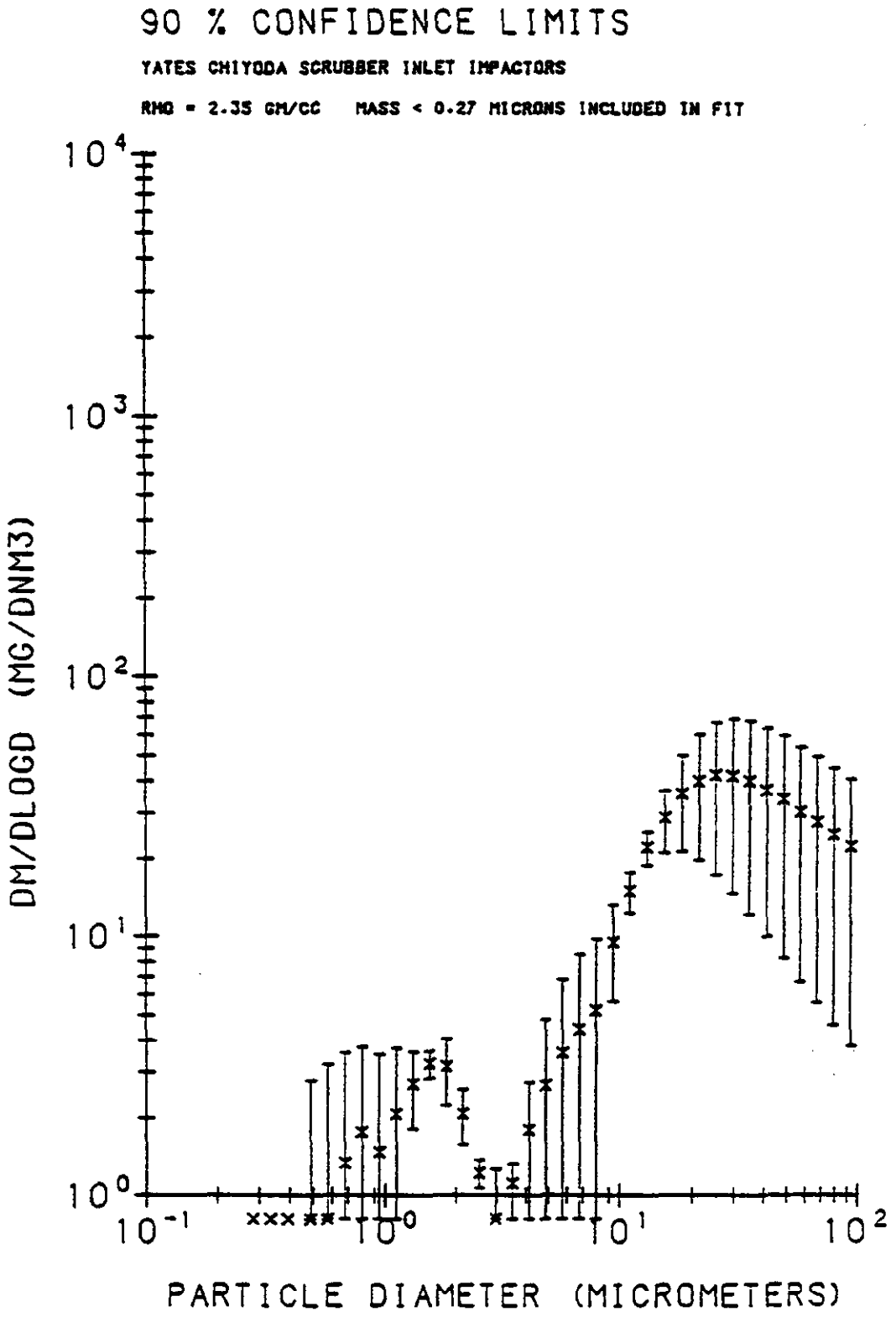

Figure A44. Inlet dM/dlogD vs Particle Diameter for Chiyoda Scrubber, 50 MW, 12" ΔP, January 30, 1993.

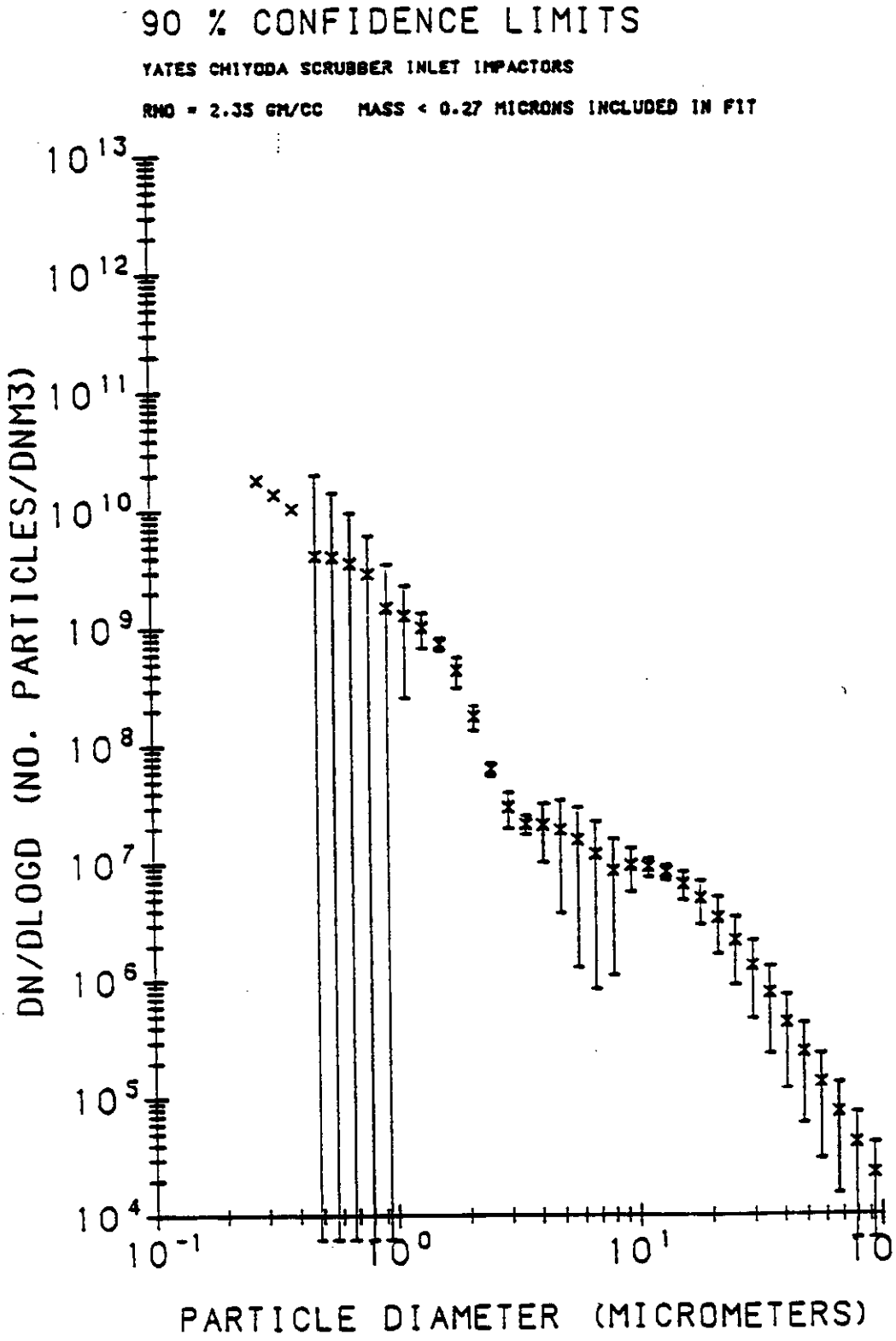

Figure A45. Inlet dN/dlogD vs Particle Diameter for Chiyoda Scrubber, 50 MW, 12" ΔP, January 30, 1993.

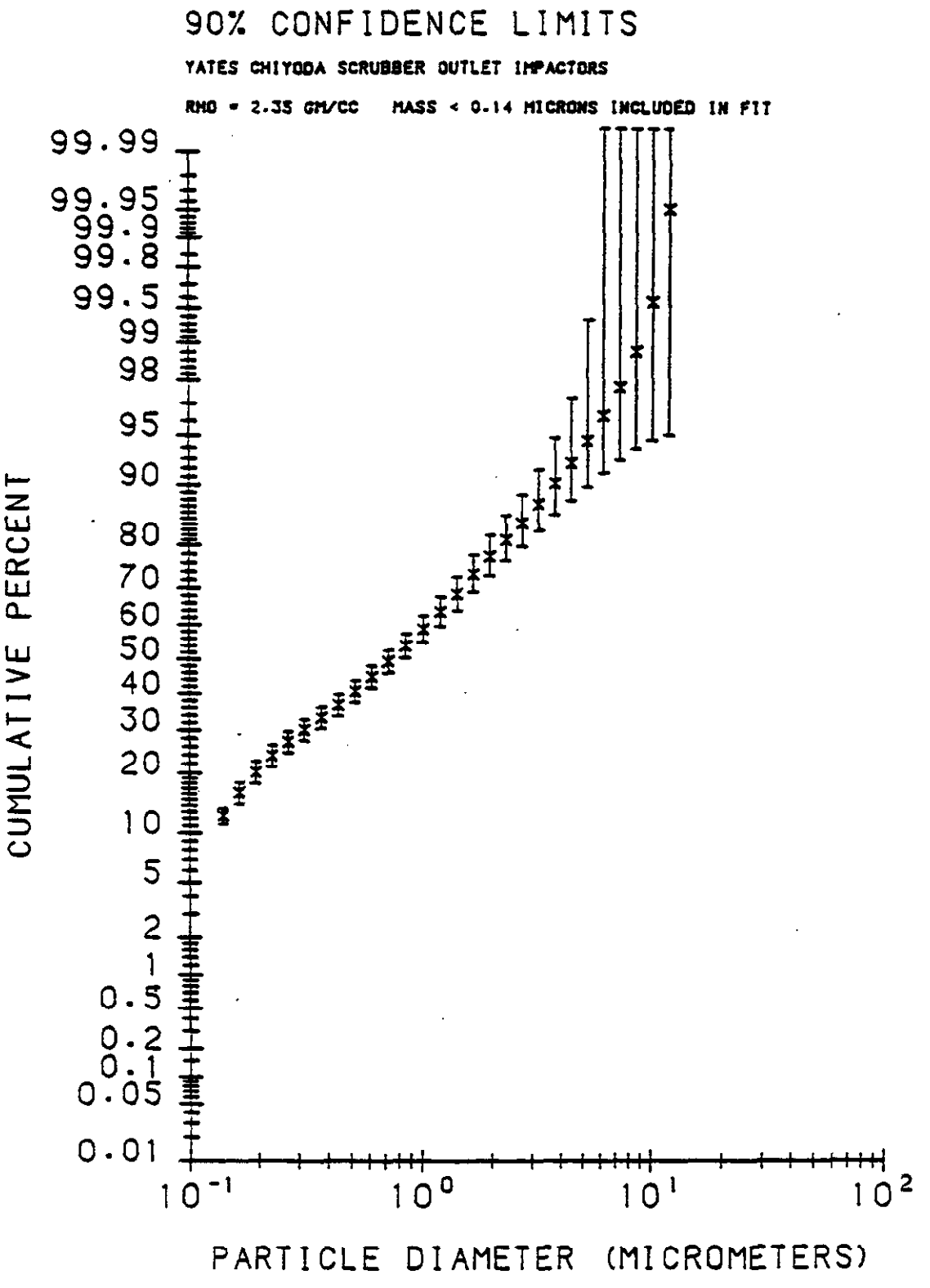

Figure A46. Outlet Cumulative Percent vs Particle Diameter for Chiyoda Scrubber, 50 MW, 12" ΔP, January 30, 1993.

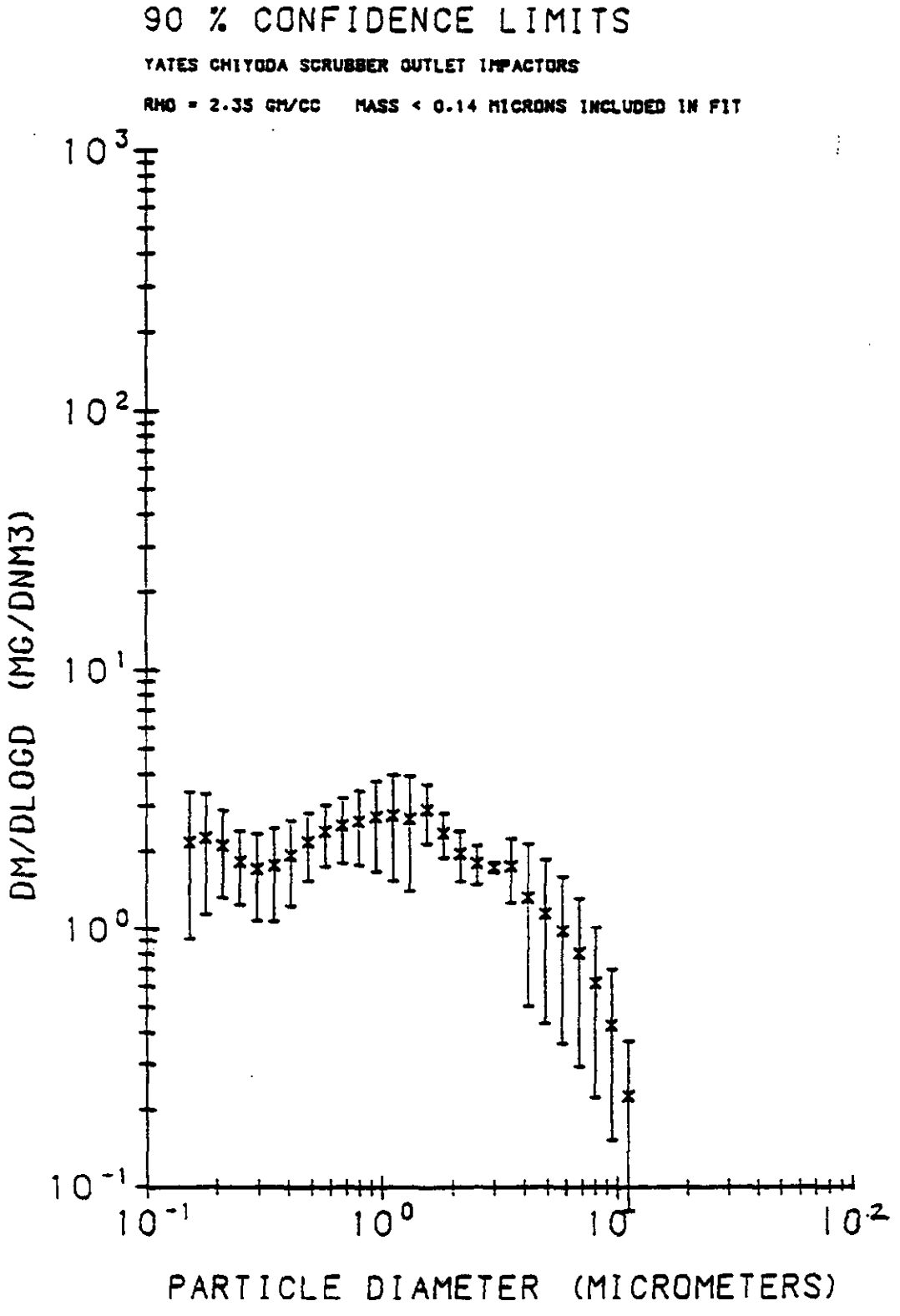

Figure A47. Outlet dM/dlogD vs Particle Diameter for Chiyoda Scrubber, 50 MW, 12" ΔP, January 30, 1993.

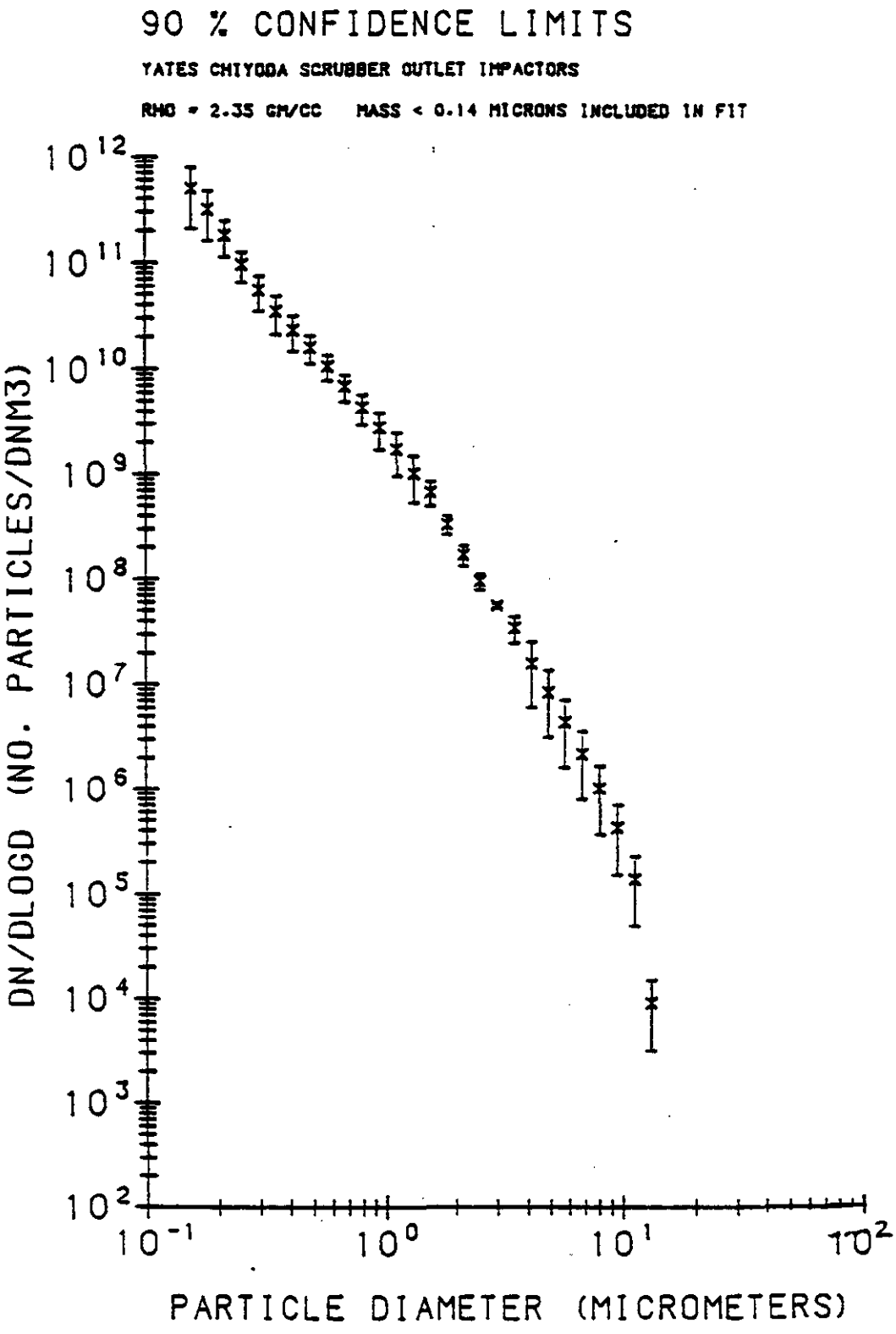

Figure A48. Outlet dN/dlogD vs Particle Diameter for Chiyoda Scrubber, 50 MW, 12" ΔP, January 30, 1993.

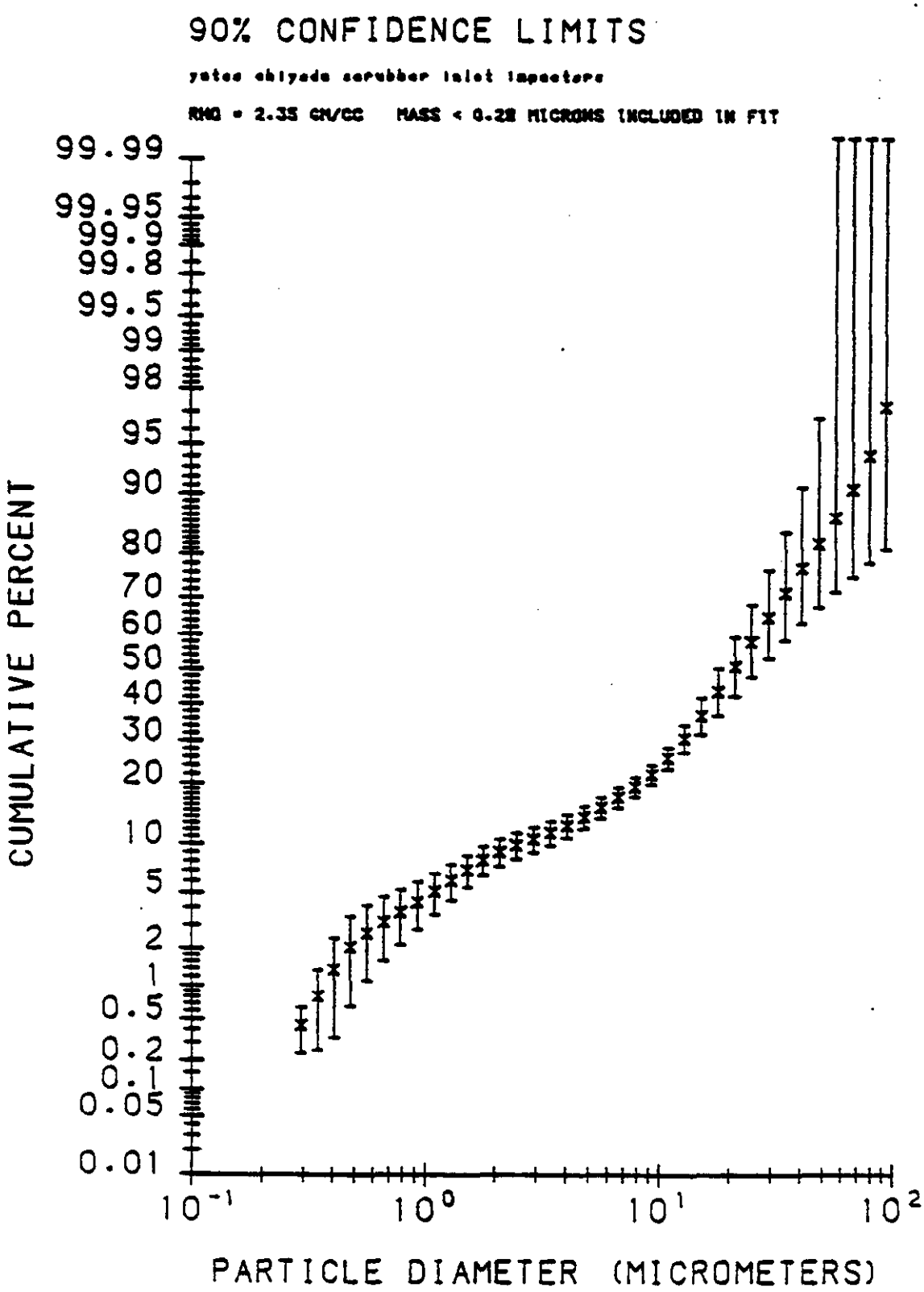

Figure A49. Inlet Cumulative Percent vs Particle Diameter for Chiyoda Scrubber, 50 MW, 16" ΔP, January 31, 1993.

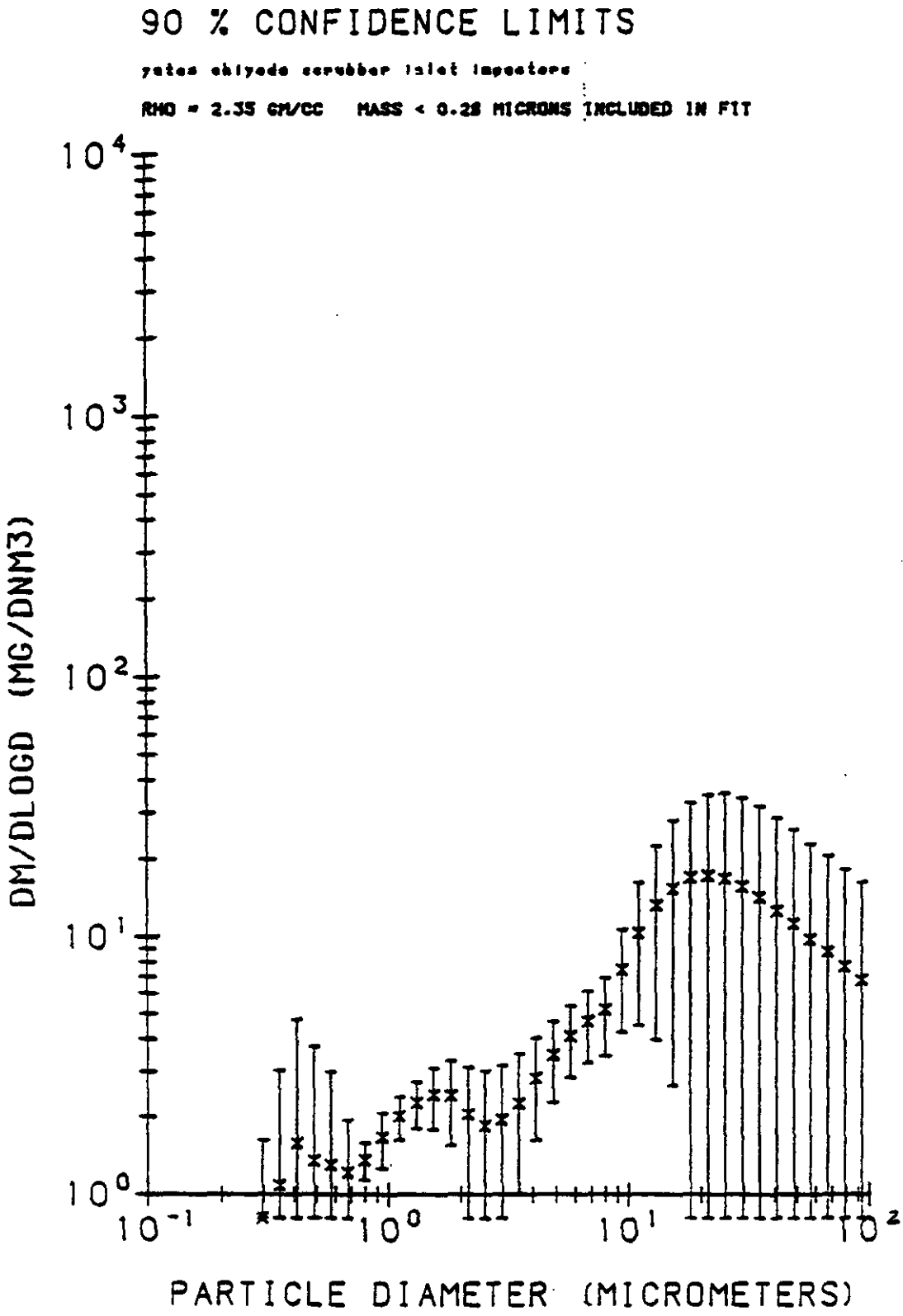

Figure A50. Inlet dM/dlogD vs Particle Diameter for Chiyoda Scrubber, 50 MW, 16" ΔP, January 31, 1993.

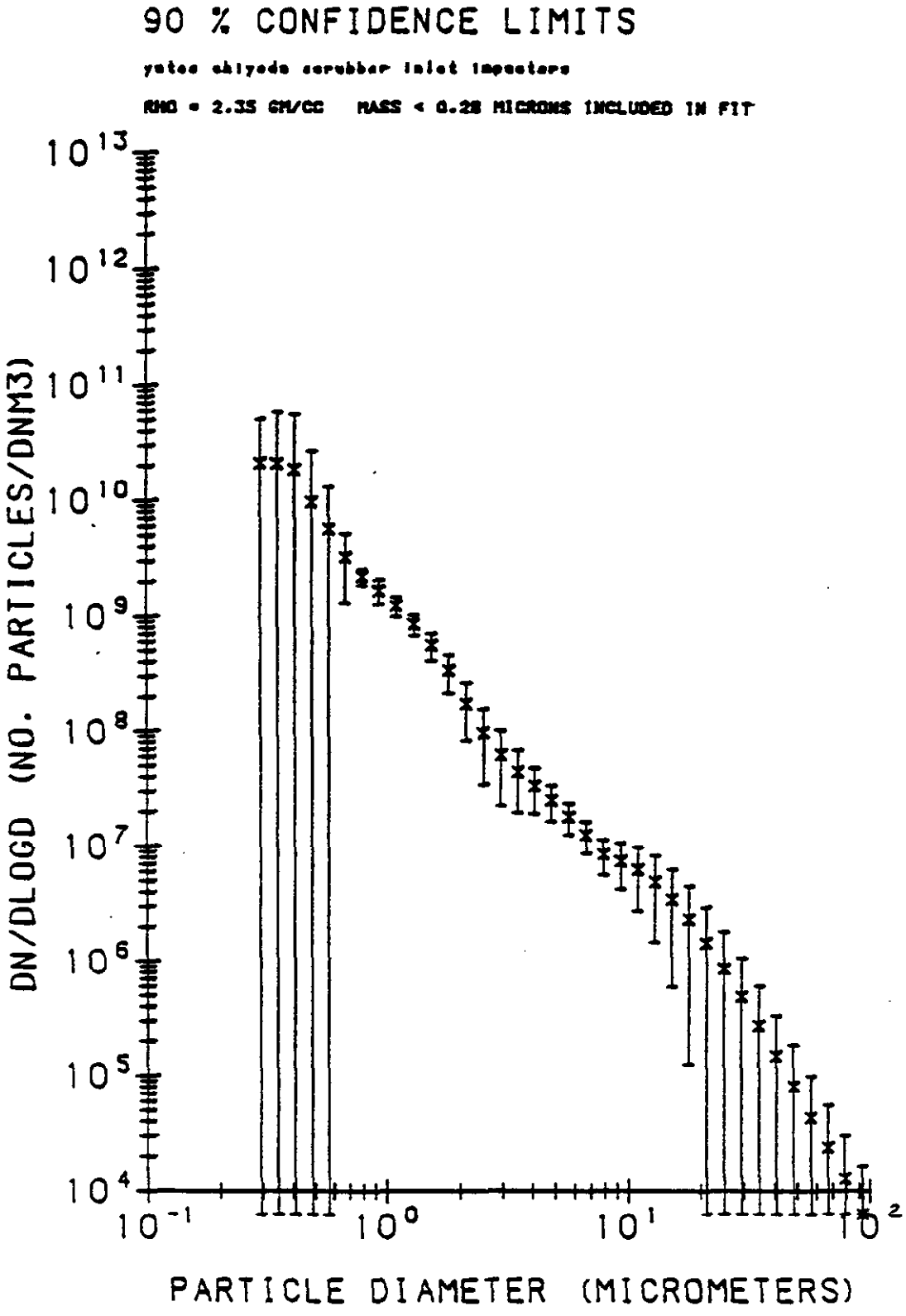

Figure A51. Inlet dN/dlogD vs Particle Diameter for Chiyoda Scrubber, 50 MW, 16" ΔP, January 31, 1993.

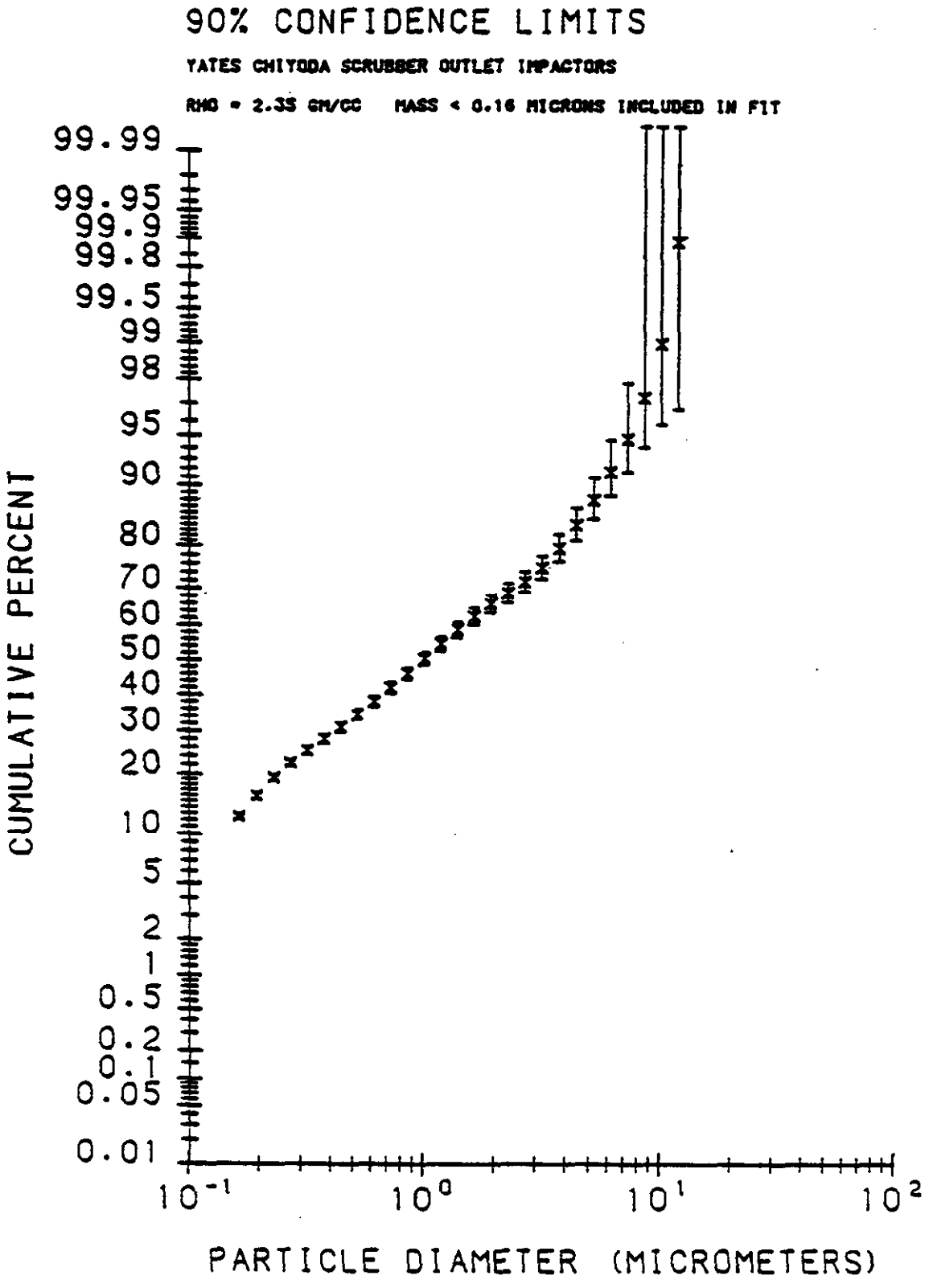

Figure A52. Outlet Cumulative Percent vs Particle Diameter for Chiyoda Scrubber, 50 MW, 16" ΔP, January 31, 1993.

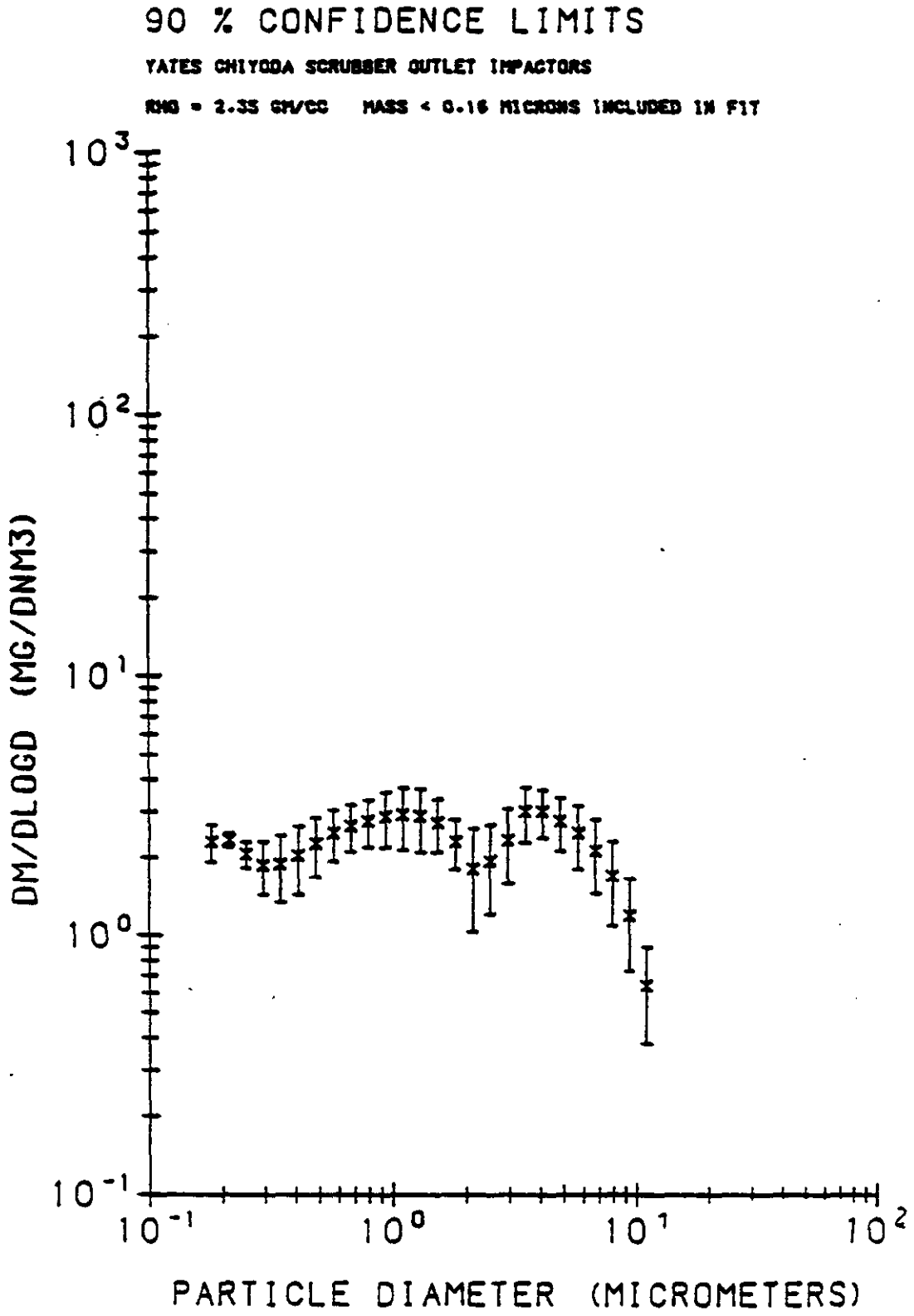

Figure A53. Outlet dM/dlogD vs Particle Diameter for Chiyoda Scrubber, 50 MW, 16" ΔP, January 31, 1993.

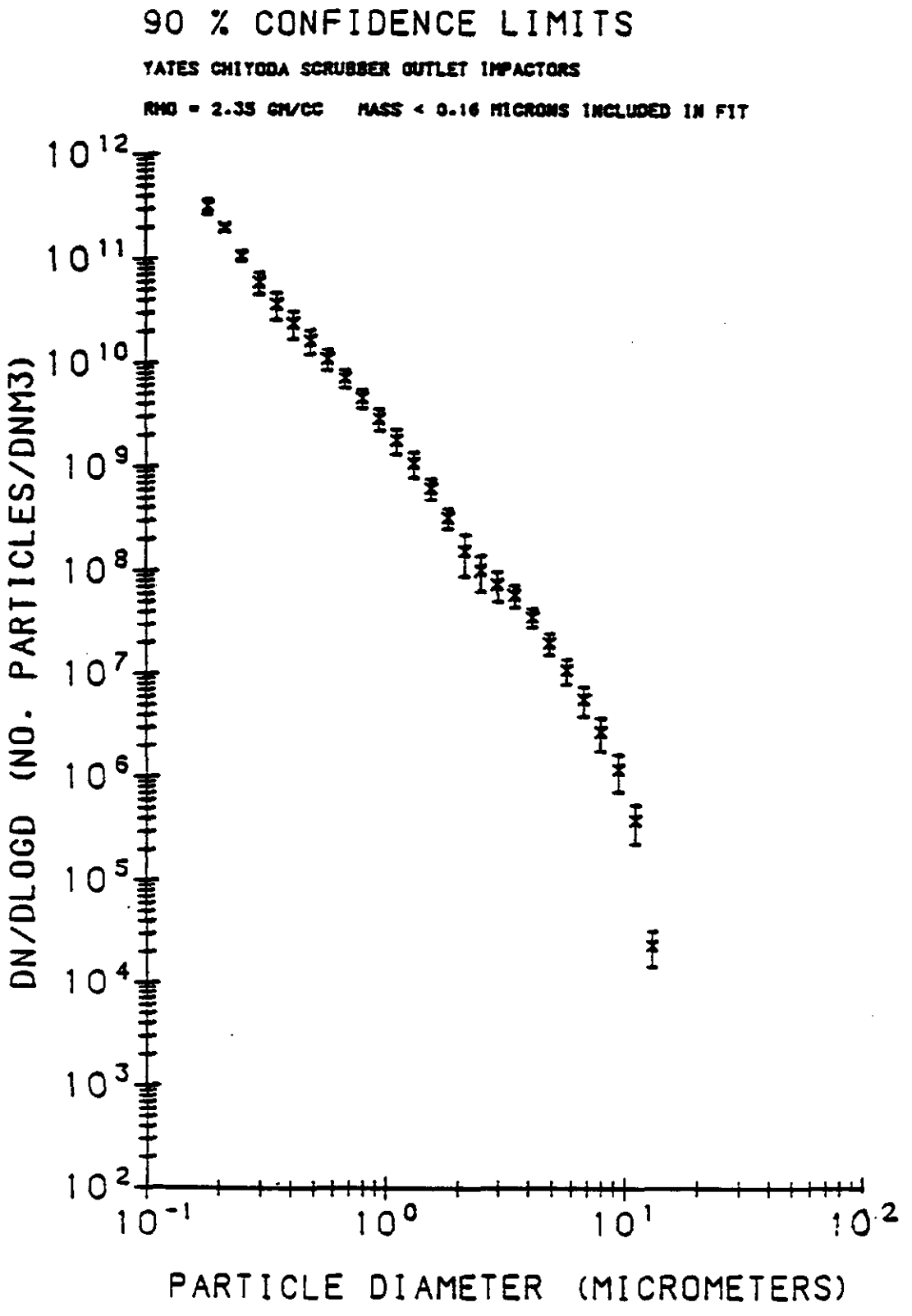

Figure A54. Outlet dN/dlogD vs Particle Diameter for Chiyoda Scrubber, 50 MW, 16" ΔP, January 31, 1993.

"Particulate Sampling of Chiyoda CT-121 Jet Bubbling Reactor
Georgia Power Company Plant Yates Unit 1 - Increased Mass Loading Test Phase"

Southern Research Institute

PARTICULATE SAMPLING OF CHIYODA CT-121 JET BUBBLING REACTOR GEORGIA POWER COMPANY PLANT YATES UNIT 1

Prepared for:
Southern Company Services
800 Shades Creek Parkway
Birmingham, AL 35209

David Burford
Project Manager

SRI-ENV-94-497-7872.2F

July 13, 1994

Southern Research Institute

PARTICULATE SAMPLING OF CHIYODA CT-121 JET BUBBLING REACTOR GEORGIA POWER COMPANY PLANT YATES UNIT 1

INCREASED MASS LOADING TEST PHASE

MARCH 17 THROUGH 27, 1994

PREPARED BY:

SOUTHERN RESEARCH INSTITUTE
2000 Ninth Avenue South
Birmingham, AL 35205

FOR

SOUTHERN COMPANY SERVICES
800 Shades Creek Parkway
Birmingham, AL 35209

July 13, 1994

SRI-ENV-94-497-7872.2F

LIST OF TABLES

LIST OF FIGURES

LIST OF FIGURES (CONT.)

PARTICULATE SAMPLING OF CHIYODA CT-121 JET BUBBLING REACTOR GEORGIA POWER COMPANY PLANT YATES UNIT 1

INTRODUCTION

As part of the Innovative Clean Coal Technology (ICCT) program, funded primarily by Southern Company Services and the U. S. Department of Energy, a Chiyoda CT-121 Jet Bubbling Reactor (JBR) was installed at Georgia Power Company's Plant Yates Unit 1. As part of the two-year demonstration of this innovative process for Flue Gas Desulfurization (FGD), Southern Research Institute was contracted to determine the particulate mass removal efficiency, SO_3/H_2SO_4 mist removal efficiency, and particle fractional collection efficiency of the JBR. The test program, which this report covers, was conducted with the electrostatic precipitator installed ahead of the JBR in reduced collection efficiency modes and de-energized.

This test program was designed to evaluate the operations of the JBR under increased inlet mass loadings. Table 1 presents the nine different test conditions which were evaluated. The second, third, and fourth fields of the ESP were de-energized for all test conditions in Table 1. During each day of testing, three EPA Method 5B measurements were obtained at the inlet and outlet sampling locations, as well as, SO_2/SO_3 and particle size distribution measurements.

MEASUREMENTS

Mass Measurements

At the outlet (stack) sampling location, EPA Method 5B, [Determination of Nonsulfuric Acid Particulate Matter From Stationary Sources (40CFR60)] was used. This Method was also used at the inlet sampling location to limit possible method bias in calculating the overall mass collection efficiency of the JBR. Table 2 presents a summary of all Method 5B mass loading results, as pounds-per-million Btu (lb/MBtu), for each test condition.

Table 3 presents the inlet mass loading data for the 50 MW test during which the first field of the ESP was energized (Conditions 1 and 2). Table 4 presents the outlet mass data for these conditions. Tables 5 and 6, respectively, present the inlet and outlet mass loading data for the 100 MW test during which the first field of the ESP was energized (Conditions 3 and 4).

Mass loadings and additional data from Method 5B tests for Condition 5, 100 MW with first field of the ESP detuned, are presented as Table 7. Variations in ESP outlet mass loadings (Chiyoda inlet loadings) were due to soot blowing in the furnace, air heaters, and/or ESP rappers. These events were not logged by Unit 1 operating personnel.

Tables 8 and 9 present the inlet and outlet Method 5B results for the tests at 100 MW with the ESP de-energized (Conditions 6 and 7), while Tables 10 & 11 present these data for the 50 MW, de-energized ESP tests (Conditions 8 and 9).

SO_2/SO_3 Measurements

The Controlled Condensation Method for SO_2/SO_3 determinations was used at each sampling location. These data are presented in Tables 12 through 16 for the various unit load and ESP operating conditions. The shaded data in Tables 12 and 13 are considered to be anomalous since they were considerably higher than the other results from the same day and were therefore not used in calculating the averages. These differences were not experienced during the first Chiyoda scrubber test program in January, 1993.

Particle Size Measurements

Since this test program was designed for higher inlet mass loadings to the Chiyoda scrubber, modified Brink Cascade Impactors were operated at the inlet sampling location for determinations of inlet particle size distributions. University of Washington (UW) Cascade Impactors were operated at the outlet sampling location as during the previous test program--January 1993. A "Blank Impactor" (an impactor preceded by a filter) was operated at each sampling location, each day, to evaluate impactor substrates weight gains or losses.

A Brink impactor was operated in each port at the inlet sampling location at the average isokinetic flow-rate for that port. The inlet impactors were grouped into five groupings for evaluating the inlet size distribution for the different conditions. These groupings were: Group 1, Test days 1 and 2; Group 2, Test days 3 and 4; Group 3, Test day 5; Group 4, Test days 6 and 7; and Group 5, Test days 7 and 8.

The UW impactors were heated to approximately 300°F and each impactor traversed one port at the average isokinetic flow-rate for that port. The outlet impactors from each test day were averaged together to produce the outlet size distribution for the condition tested on that day. After the data for each impactor run were reduced and groupings determined, the data were input into a

cascade data reduction program that was originally developed for EPA by SRI. Several changes in the cascade impactor data reduction program have been recently made, and this revised program was used to reduce the impactor data collected for this report. These changes result in a more user friendly program, improved calculation of stage cutpoints, improved assessment of stage overlap, and an improved curve fit that also includes downward extrapolation to a minimum particle diameter.

The cascade impactor data reduction program calculated the size distributions for the respective locations and groupings as cumulative mass, cumulative percent, differential mass per differential-log-diameter (dM/dlogD), and differential number per differential-log-diameter (dN/dlogD). It then used the dM/dlogD data for each assigned grouping to calculate and plot the fractional collection efficiency of the Chiyoda scrubber for each test condition. All of the impactor graphs include 90% confidence intervals for each data point.

The cumulative mass vs particle diameter for the five (5) different inlet conditions are presented in Figures 1 through 5. The outlet cumulative mass vs particle diameter for the nine (9) test conditions are presented in Figures 6 through 14. Figures 15 through 23 present the fractional collection efficiency calculated from the inlet and outlet groupings for each condition. The remaining size distribution curves, cumulative percent and dM/dlogD, are in the Appendix.

DISCUSSION OF RESULTS

Mass Measurements and Chemical Analyses

The mass loading data in Table 2 are graphically presented as Figure 24. The inlet mass loading data for each Method 5B test are presented in Figure 25 along with the average inlet impactor loadings used for the different test conditions. There were three Method 5B tests for each condition and five average inlet impactor groupings during this test phase. The agreement in mass loading between the impactors and Method 5B data is considered to be reasonable since the impactors operate at an average flow rate in a port and the Method 5B system samples isokinetic at all sample points at the location being tested.

Figure 26 presents the outlet mass data for each Method 5B test and average impactor loadings for each test day/condition. The average outlet loading for the impactors and Method 5B system remained below 0.017 lb/MBtu, while only the first field of the ESP remained energized. With the ESP de-energized, the highest outlet loading was 0.063 lb/MBtu from the impactor data

of condition 6 and 0.061 lb/MBtu from outlet run #3 for condition 8 (see Table 11).

The mass data in Figures 25 and 26 were used to calculate the particulate collection efficiency for each test condition and are presented as Figure 27. The particulate efficiency of the Chiyoda scrubber remained above 93% for all conditions.

The average sulfur trioxide data in Tables 12 through 16 are plotted in Figure 28. The higher average outlet numbers reported for the first three test conditions caused a negative collection efficiency for SO_3 for these conditions. Although we believe these numbers to be representative of the gases sampled, there is no way to know if the SO_3 concentrations were stratified at either location from day to day or if there was excessive scrubber carryover that was sampled, etc. The SO_3 data are reported to a second decimal place, and it is felt that these measurements are not more accurate than ± 0.025 ppm with the lower detection limit being 0.20 ppm.

The SO_2 collection efficiency (see Tables 12 through 16) of the scrubber was greater than 80% for all test conditions with the exception of Test Condition 6 (Table 15, March 24). This was the first test after the ESP had been turned off, and the scrubber may not have reached a stable operating condition. The ESP was turned off the evening of March 22, and testing for Condition 6 began the morning of March 24, 1994.

Selected filters, solids, and acetone probe and nozzle washes were analyzed in SRI's lab for selected elements and soluble calcium and sulfates. Samples were selected for analyses from the five test conditions where the JBR was operated at sixteen (16) inches delta P (Table 1). The results of the chemical analyses are presented in Table 17 for filters and solids from the inlet and outlet Method 5B samples, while Table 18 presents soluble calcium and sulfate results from acetone washes.

Table 17 indicates that the outlet solids increased in calcium only slightly. The soluble data show that there are higher percentages of soluble calcium and sulfates at the outlet than the inlet, and these percentages decrease as the outlet mass loading increases, as expected. The high soluble sulfates on 3/18, 3/20 and 3/22 for the outlet solids suggest that sulfuric acid is a predominant factor in the outlet mass loadings for these days. Table 18 indicates that as the mass loading increased, the fraction of soluble calcium and sulfate increased in the probe washes. This suggests that the larger particles escaping the scrubber, and settling out in the probe, have come in contact with scrubber liquid or have provided additional surface area for SO_3 uptake.

Impactor substrates from three of the sixteen-inch delta P test days, Conditions 4, 5, & 7, were analysed for soluble calcium and sulfates. These data are presented in Tables 19, 20, and 21. The impactor substrate material used during these tests was ultrapure quartz. The fourth impactor, which was run during these conditions, was carbon coated and subjected to scanning electron microscopy (SEM) energy dispersive x-ray analysis (EDAX). Figure 29 presents the SEM photographs for Condition 4 impactor substrates, while Figure 30 presents the EDAX data from these photographs. Figure 31 and 32 present the SEM and EDAX data, respectively, for Condition 5 impactor, while Figures 33 and 34 present these for Condition 7. The EDAX data suggest that the electron beam sees primarily fly ash in all cases, with perhaps slightly higher amounts of Ca and S (perhaps gypsum) in the Condition 4 samples (the lowest mass loading case). The data in Tables 19 through 21 indicate that sulfuric acid makes up most of the mass of stages 2 and 3 (three micron and larger) of Conditions 4 and 5.

Particle Size Measurements

Comparing Figures 1 through 5, inlet cumulative size distributions, we see that with only one field of the ESP on, the cumulative mass loading to one micron is 13 mg/dncm (Figures 1 and 2). This occurred while Unit 1 was operating at 50 and 100 megawatts, inlet impactor groupings 1 and 2, respectively. The inlet impactor loading increased by a factor of two (180 mg/dncm to 364 mg/dncm) from inlet grouping 1 to 2 due to the reduced efficiency of the ESP when the unit load was increased. Figure 3 shows that the cumulative mass at one micron increased to 25 mg/dncm when the first field of the ESP was detuned and the inlet loading increased to 755 mg/dncm.

When the ESP was de-energized completely, the cumulative mass of one micron particulate increased to 103 mg/dncm, while the inlet impactor mass loading increased to 6420 mg/dncm (Conditions 7 and 8). When the unit load was reduced for Conditions 8 and 9, the cumulative mass of one-micron particles decreased to 80 mg/dncm, and the average impactor inlet mass loading decreased to 5320 mg/dncm (Figure 5).

From the outlet cumulative mass size distributions, Figures 6 through 14, it is not apparent that changing from 10 to 16 inches delta P across the scrubber has a very noticeable change in the outlet emissions. The change in outlet loading can best be seen in Figure 26 where the second day at a condition (Method 5B tests 4,5,6; 10,11,12; 19,20,21; and 25,26,27), results in lower impactor mass loadings. For the conditions when the ESP was totally de-energized, 99% of the particulate exiting the scrubber was less than 4 microns.

Figures 15 through 23, fractional collection efficiency graphs, show that in all cases one-micron particles are collected with at least 82% collection efficiency. There is also a 99% collection of 2.5 micron and larger particles for Conditions 3 through 9. Under Conditions 1 and 2, 99% collection occurred for particles larger than 5 and 6.3 microns, respectively.

With the ESP partially energized, the Chiyoda CT-121 scrubber never exceeded an average outlet mass loading of 0.02 lb/MBtu. At these lower outlet mass concentrations, sulfuric acid is a predominate contributor, even though EPA Method 5B was used. When the ESP was not energized at all, the Chiyoda CT-121 scrubber never exceeded the Georgia allowable emissions rate of 0.24 lb/MBtu, and, in fact, never exceeded 0.062 lb/MBtu for any of the 12 Method 5B tests that were conducted during Conditions 6 through 9.

Table 1

CHIYODA CT-121 TEST CONDITIONS

March 1994

Date	Test Number or Condition	JBR ΔP (in. WC)	Boiler Load (MW)	First Field of ESP Status
3/17	1	10	50	ON
3/18	2	16	50	ON
3/19	3	10	100	ON
3/20	4	16	100	ON
3/22	5	16	100	Detuned
3/24	6	10	100	OFF
3/25	7	16	100	OFF
3/26	8	10	50	OFF
3/27	9	16	50	OFF

Table 2

CHIYODA SCRUBBER

SRI METHOD 5B MASS LOADING SUMMARY

March 1994

CONDITION	Average Inlet, lb/MBtu	Average Outlet, lb/MBtu	Part. Removal Efficiency, Percent
Condition 1 50 MW First field only	0.196	0.013	93.61
Condition 2 50 MW First field only	0.168	0.011	93.45
Condition 3 100 MW First field only	0.434	0.017	95.99
Condition 4 100 MW First field only	0.525	0.010	98.16
Condition 5 100 MW First field detuned	0.819	0.015	98.18
Condition 6 100 MW ESP off	5.778	0.049	99.14
Condition 7 100 MW ESP off	5.293	0.042	99.21
Condition 8 50 MW ESP off	5.046	0.056	98.88
Condition 9 50 MW ESP off	4.927	0.048	99.02

TABLE 3

CHIYODA SCRUBBER, 50 MEGAWATTS

ONLY FIRST FIELD OF ESP ON

METHOD 5B MASS LOADING

INLET

Run ID	IMT-1-1	IMT-1-2	IMT-1-3	IMT-2-1	IMT-2-2	IMT-2-3
Date	3/17/94	3/17/94	3/17/94	3/18/94	3/18/94	3/18/94
Sample time	0957-1113	1251-1406	1538-1653	0810-0927	1115-1226	1512-1625
Gas analysis, %						
O2 (dry)	9.4	10.4	10.0	9.6	9.6	9.6
CO2 (dry)	8.6	8.8	8.4	9.8	9.8	9.8
H2O	7.9	8.1	7.2	6.4	7.4	6.6
Ambient pressure, in Hg	29.26	29.26	29.26	29.03	29.03	29.03
Static pressure, in H2O	-5.4	-4.8	-4.8	-4.4	-4.4	-4.2
Stack Temperature, F	227	233	238	231	237	239
Velocity, ft/sec	34.9	33.0	34.1	32.4	32.8	32.5
Gas volume flow,						
Kacfm	269	254	263	250	253	251
Kdscfm	184	172	178	171	170	170
Mass loading,						
gr/acf	0.0398	0.0455	0.0643	0.0433	0.0435	0.0459
gr/dscf	0.0583	0.0673	0.0948	0.0630	0.0647	0.0678
lb/MBtu	0.148	0.187	0.254	0.163	0.167	0.175

TABLE 4

CHIYODA SCRUBBER, 50 MEGAWATTS

ONLY FIRST FIELD OF ESP ON
METHOD 5B MASS LOADING

OUTLET

Run ID	OMT-1-1	OMT-1-2	OMT-1-3	OMT-2-1	OMT-2-2	OMT-2-3
Date	3/17/94	3/17/94	3/17/94	3/18/94	3/18/94	3/18/94
Sample time	1007-1121	1256-1415	1542-1822	0815-925	1115-1233	1513-1704
Gas analysis, %						
O2 (dry)	11.6	11.2	12.2	11.0	10.6	9.8
CO2 (dry)	7.4	7.6	7.6	9.0	9.0	8.8
H2O	8.6	9.3	10.6	11.0	9.3	12.2
Ambient pressure, in Hg	29.19	29.19	29.19	28.95	28.95	28.95
Static pressure, in H2O	-0.2	-0.2	-0.2	-0.2	-0.2	-0.2
Stack Temperature, F	105	110	111	112	114	113
Velocity, ft/sec	29.4	28.3	30.0	27.8	28.2	27.9
Gas volume flow,						
Kacfm	234	225	239	221	225	222
Kdscfm	195	184	192	176	181	174
Mass loading,						
gr/acf	0.0034	0.0037	0.0028	0.0046	0.0024	0.0023
gr/dscf	0.0040	0.0045	0.0034	0.0057	0.0029	0.0030
lb/MBtu	0.013	0.013	0.012	0.017	0.008	0.008

TABLE 5

CHIYODA SCRUBBER, 100 MEGAWATTS

ONLY FIRST FIELD OF ESP ON

METHOD 5B MASS LOADING

INLET

Run ID	IMT-3-1	IMT-3-2	IMT-3-3	IMT-4-1	IMT-4-2	IMT-4-3
Date	3/19/94	3/19/94	3/19/94	3/20/94	3/20/94	3/20/94
Sample time	0941-1049	1324-1457	1550-1706	0840-0949	1104-1216	1333-1504
Gas analysis, %						
O2 (dry)	7.2	6.8	7.4	7.0	7.0	7.0
CO2 (dry)	11.8	12.0	11.8	11.8	11.6	11.6
H2O	7.6	6.6	7.0	7.4	7.2	7.8
Ambient pressure, in Hg	29.15	29.15	29.15	29.21	29.21	29.21
Static pressure, in H2O	-9.1	-9.3	-9.4	-9.0	-8.5	-8.5
Stack Temperature, F	261	266	269	252	252	255
Velocity, ft/sec	52.0	52.1	52.8	50.7	51.1	51.0
Gas volume flow,						
Kacfm	401	401	407	391	394	393
Kdscfm	258	259	261	256	259	256
Mass loading,						
gr/acf	0.1466	0.1300	0.1183	0.1645	0.1720	0.1543
gr/dscf	0.2276	0.2012	0.1846	0.2511	0.2616	0.2372
lb/MBtu	0.485	0.417	0.399	0.528	0.549	0.498

TABLE 6

CHIYODA SCRUBBER, 100 MEGAWATTS

ONLY FIRST FIELD OF ESP ON

METHOD 5B MASS LOADING

OUTLET

Run ID	OMT-3-1	OMT-3-2	OMT-3-3	OMT-4-1	OMT-4-2	OMT-4-3
Date	3/19/94	3/19/94	3/19/94	3/20/94	3/20/94	3/20/94
Sample time	0921-1045	1215-1406	1400-1512	0830-0941	1125-1238	1310-1416
Gas analysis, %						
O2 (dry)	8.0	7.2	7.4	6.8	7.2	7.6
CO2 (dry)	11.0	11.6	11.6	11.4	11.8	11.2
H2O	11.0	13.3	13.2	10.2	13.3	12.5
Ambient pressure, in Hg	29.07	29.07	29.07	29.13	29.13	29.13
Static pressure, in H2O	-0.4	-0.3	-0.3	-0.5	-0.2	-0.2
Stack Temperature, F	117	118	121	115	119	121
Velocity, ft/sec	43.1	41.7	42.5	41.9	41.9	43.1
Gas volume flow,						
Kacfm	343	332	339	334	334	343
Kdscfm	271	255	259	267	257	266
Mass loading,						
gr/acf	0.0066	0.0076	0.0043	0.0033	0.0040	0.0033
gr/dscf	0.0084	0.0099	0.0056	0.0041	0.0052	0.0042
lb/MBtu	0.019	0.021	0.012	0.009	0.011	0.009

TABLE 7

CHIYODA SCRUBBER, 100 MEGAWATTS

ESP FIRST FIELD DETUNED

METHOD 5B MASS LOADINGS

	INLET			OUTLET		
Run ID	IMT-5-1	IMT-5-2	IMT-5-3	OMT-5-1	OMT-5-2	OMT-5-3
Date	3/22/94	3/22/94	3/22/94	3/22/94	3/22/94	3/22/94
Sample time	1026-1136	1238-1356	1456-1605	0818-0928	1112-1220	1257-1405
Gas analysis, %						
O2 (dry)	7.0	7.0	8.0	8.0	7.4	7.6
CO2 (dry)	11.6	11.6	11.0	10.0	12.4	11.0
H2O	8.2	6.4	5.8	11.6	14.0	13.5
Ambient pressure, in Hg	29.31	29.31	29.31	29.24	29.24	29.24
Static pressure, in H2O	-9.2	-8.9	-9.2	-0.5	-0.4	-0.3
Stack Temperature, F	259	262	271	115	117	116
Velocity, ft/sec	52.3	51.6	52.1	42.0	42.7	41.9
Gas volume flow,						
Kacfm	403	398	401	334	340	334
Kdscfm	260	261	261	265	261	259
Mass loading,						
gr/acf	0.3560	0.1712	0.2154	0.0059	0.0055	0.0044
gr/dscf	0.5517	0.2611	0.3308	0.0075	0.0071	0.0056
lb/MBtu	1.159	0.548	0.749	0.017	0.015	0.012

TABLE 8

CHIYODA SCRUBBER, 100 MEGAWATTS

ESP OFF

METHOD 5B MASS LOADINGS

INLET

Run ID	IMT-6-1	IMT-6-2	IMT-6-3	IMT-7-1	IMT-7-2	IMT-7-3
Date	3/24/94	3/24/94	3/24/94	3/25/94	3/25/94	3/25/94
Sample time	0800-0910	1027-1134	1415-1522	0809-0933	1134-1242	1339-1447
Gas analysis, %						
O2 (dry)	6.8	6.8	7.2	7.5	8.2	7.4
CO2 (dry)	11.6	11.6	11.6	11.5	10.6	11.4
H2O	5.5	8.0	7.7	7.7	6.9	7.1
Ambient pressure, in Hg	29.25	29.25	29.25	29.12	29.12	29.12
Static pressure, in H2O	-9.2	-9.2	-9.0	-9.4	-9.4	-9.4
Stack Temperature, F	260	265	257	246	256	258
Velocity, ft/sec	51.8	52.0	51.4	53.7	53.6	53.5
Gas volume flow,						
Kacfm	399	400	396	414	413	412
Kdscfm	264	256	257	271	269	268
Mass loading,						
gr/acf	1.5680	1.7197	2.0841	1.8475	1.4898	1.3492
gr/dscf	2.3689	2.6884	3.2080	2.8170	2.2824	2.0773
lb/MBtu	4.906	5.590	6.838	6.139	5.248	4.493

TABLE 9

CHIYODA SCRUBBER, 100 MEGAWATTS

ESP OFF

METHOD 5B MASS LOADINGS

OUTLET

Run ID	OMT-6-1	OMT-6-2	OMT-6-3	OMT-7-1	OMT-7-2	OMT-7-3
Date	3/24/94	3/24/94	3/24/94	3/25/94	3/25/94	3/25/94
Sample time	0809-0919	1030-1205	1240-1422	0807-0917	1022-1132	1202-1312
Gas analysis, %						
O2 (dry)	7.4	7.4	7.6	7.8	8.2	7.8
CO2 (dry)	11.2	10.8	11.4	11.0	10.8	11.0
H2O	14.7	14.5	14.4	14.5	13.3	14.1
Ambient pressure, in Hg	29.18	29.18	29.18	29.04	29.04	29.04
Static pressure, in H2O	-0.3	-0.5	-0.4	-0.3	-0.5	-0.5
Stack Temperature, F	120	120	121	119	117	115
Velocity, ft/sec	42.8	43.1	43.3	44.0	44.0	43.6
Gas volume flow,						
Kacfm	340	343	345	350	350	347
Kdscfm	258	260	261	265	270	265
Mass loading,						
gr/acf	0.0168	0.0171	0.0178	0.0121	0.0142	0.0163
gr/dscf	0.0222	0.0226	0.0234	0.0160	0.0184	0.0213
lb/MBtu	0.048	0.049	0.051	0.036	0.042	0.048

TABLE 10

CHIYODA SCRUBBER, 50 MEGAWATTS

ESP OFF

METHOD 5B MASS LOADINGS

INLET

Run ID	IMT-8-1	IMT-8-2	IMT-8-3	IMT-9-1	IMT-9-2	IMT-9-3
Date	3/26/94	3/26/94	3/26/94	3/27/94	3/27/94	3/27/94
Sample time	0819-0935	1049-1157	1247-1353	0748-0856	0948-1155	1125-1232
Gas analysis, %						
O2 (dry)	8.0	10.2	9.6	8.8	9.5	9.2
CO2 (dry)	10.0	9.0	9.8	10.2	9.9	10.2
H2O	6.4	6.0	7.7	5.9	7.8	6.2
Ambient pressure, in Hg	29.22	29.22	29.22	29.01	29.01	29.01
Static pressure, in H2O	-4.5	-3.8	-4.1	-3.9	-4.3	-4.1
Stack Temperature, F	236	240	240	243	246	247
Velocity, ft/sec	31.3	31.4	30.6	31.3	31.7	31.5
Gas volume flow,						
Kacfm	241	242	236	241	244	243
Kdscfm	165	166	159	164	161	163
Mass loading,						
gr/acf	1.2250	1.4400	1.3973	1.2939	1.6893	0.9785
gr/dscf	1.7877	2.0988	2.0759	1.9068	2.5560	1.4560
lb/MBtu	4.047	5.728	5.364	4.602	6.547	3.634

TABLE 11

CHIYODA SCRUBBER, 50 MEGAWATTS

ESP OFF

METHOD 5B MASS LOADINGS

OUTLET

Run ID	OMT-8-1	OMT-8-2	OMT-8-3	OMT-9-1	OMT-9-2	OMT-9-3
Date	3/26/94	3/26/94	3/26/94	3/27/94	3/27/94	3/27/94
Sample time	0828-0937	1046-1153	1225-1330	0758-0907	0956-1114	1144-1250
Gas analysis, %						
O2(dry)	10.0	10.2	10.2	9.6	9.8	9.8
CO2 (dry)	8.0	9.0	8.8	9.6	9.4	9.4
H2O	9.1	10.6	11.9	11.5	12.8	12.5
Ambient pressure, in Hg	29.13	29.13	29.13	28.94	28.94	28.94
Static pressure, in H2O	-0.3	-0.2	-0.3	-0.2	-0.2	-0.2
Stack Temperature, F	108	110	114	114	118	116
Velocity, ft/sec	26.1	26.3	26.3	26.7	27.8	27.1
Gas volume flow,						
Kacfm	208	210	210	213	221	216
Kdscfm	171	169	165	167	170	167
Mass loading,						
gr/acf	0.0154	0.0170	0.0177	0.0140	0.0166	0.0126
gr/dscf	0.0187	0.0211	0.0225	0.0178	0.0216	0.0162
lb/MBtu	0.050	0.058	0.061	0.046	0.057	0.043

TABLE 12
SO_2/SO_3 MEASUREMENTS
CHIYODA SCRUBBER, 50 MEGAWATTS
ONLY FIRST FIELD OF ESP ON

DATE	LOCATION	TIME	ppm SO_2	ppm SO_3	% O_2	% H_2O	FLUE GAS TEMP., °F	@ 3% O_2		SCRUBBER SO_2 EFF., @ 3% O_2
								SO_2	SO_3	
3/17/94	INLET	948-1005	1251	3.13	10.5		224	2153		
3/17/94	INLET	1057-1111	1266	0.77	10.5		225	2179	1.33	
3/17/94	INLET	1149-1203	1260	1.01	10.5		227	2169	1.74	
3/17/94	INLET	1242-1256	1242	1.06	10.5	5.1	228	2138	1.82	
AVERAGE			1255	1.19	10.5		226	2160	1.63	
3/17/94	OUTLET	950-1003	129	5.11	10.9		112	231		89.27
3/17/94	OUTLET	1149-1110	137	1.15	11.1		111	250	2.10	88.53
3/17/94	OUTLET	1149-1202	123	1.64	10.9		111	220	2.94	89.86
3/17/94	OUTLET	1242-1255	122	1.73	11.0	9.8	111	221	3.13	89.66
AVERAGE			128	1.51	11.0		111	230	2.72	89.35
3/18/94	INLET	919-935	1392	1.07	10.0		234	2286	1.76	
3/18/94	INLET	1010-1030	1375	0.72	9.5		230	2159	1.13	
3/18/94	INLET	1112-1125	1387	0.88	10.0		230	2278	1.45	
3/18/94	INLET	1153-1206	1384	0.73	10.0	6.5	230	2273	1.20	
AVERAGE			1385	0.85	9.9		231	2249	1.38	
3/18/94	OUTLET	919-933	28	2.92	10.1		113	46		97.99
3/18/94	OUTLET	1017-1030	33	1.29	10.1		114	55	2.14	97.45
3/18/94	OUTLET	1110-1123	31	1.50	10.3		114	52	2.53	97.72
3/18/94	OUTLET	1152-1206	29	1.08	10.2	11.1	115	49	1.81	97.84
AVERAGE			30	1.29	10.2		114	50	2.16	97.78

TABLE 13
SO_2/SO_3 MEASUREMENTS
CHIYODA SCRUBBER, 100 MEGAWATTS
ONLY FIRST FIELD OF ESP ON

DATE	LOCATION	TIME	ppm SO_2	ppm SO_3	% O_2	% H_2O	FLUE GAS TEMP., °F	@ 3% O_2		SCRUBBER SO_2 EFF., @ 3% O_2
								SO_2	SO_3	
3/19/94	INLET	852-904	1645	1.38	8.4		248	2356	1.98	
3/19/94	INLET	943-956	1712	1.57	7.6		256	2304	2.11	
3/19/94	INLET	1049-1102	1739	1.47	7.6		256	2340	1.98	
3/19/94	INLET	1133-1147	1721	1.25	7.4	7.2	257	2282	1.66	
AVERAGE			1704	1.42	7.8		254	2321	1.93	
3/19/94	OUTLET	848-901	296	2.67	8.4		117	427		81.88
3/19/94	OUTLET	941-955	321	2.01	7.6		118	432	2.71	81.25
3/19/94	OUTLET	1047-1100	330	1.88	7.5		119	441	2.51	81.17
3/19/94	OUTLET	1134-1147	329	2.74	7.5	12	119	439	3.66	80.74
AVERAGE			320	2.21	7.8		118	435	2.96	81.26
3/20.94	INLET	905-915	1717	1.14	7.6		255	2311	1.53	
3/20/94	INLET	945-958	1651	1.44	7.4		256	2189	1.91	
3/20/94	INLET	1035-1047	1692	1.34	7.4		257	2243	1.78	
3/20/94	INLET	1118-1130	1690	1.18	7.3	7.8	258	2224	1.55	
AVERAGE			1688	1.28	7.4		257	2242	1.69	
3/20/94	OUTLET	904-914	81	0.69	7.8		120	111	0.94	95.20
3/20/94	OUTLET	944-954	88	0.94	7.7		119	119	1.27	94.56
3/20/94	OUTLET	1033-1047	90	0.76	7.6		119	121	1.02	94.61
3/20/94	OUTLET	116-1130	90	0.62	7.5	12.7	122	120	0.83	94.60
AVERAGE			87	0.75	7.7		120	118	1.02	94.74

TABLE 14

SO_2/SO_3 MEASUREMENT
CHIYODA SCRUBBER, 100 MEGAWATTS
ESP FIRST FIELD DETUNED

DATE	LOCATION	TIME	ppm SO_2	ppm SO_3	% O_2	% H_2O	FLUE GAS TEMP., °F	@ 3% O_2		SCRUBBER SO_2 EFF., @ 3% O_2
								SO_2	SO_3	
3/22/94	INLET	827-844	1652	0.96	7.6		256	2223	1.29	
3/22/94	INLET	913-930	1662	1.20	7.5		256	2220	1.60	
3/22/94	INLET	1016-1033	1665	1.19	7.4		256	2208	1.58	
3/22/94	INLET	1104-1121	1638	1.25	7.7	6.3	256	2221	1.70	
AVERAGE			1654	1.15	7.6		256	2218	1.54	
3/22/94	OUTLET	826-842	87	2.52	7.6		119	117	3.39	94.74
3/22/94	OUTLET	912-928	98	0.60	7.5		120	131	0.80	94.10
3/22/94	OUTLET	1015-1031	94	0.55	7.1		119	122	0.71	94.47
3/22/94	OUTLET	1103-1118	102	0.29	7.5	12.4	119	136	0.39	93.88
AVERAGE			95	0.99	7.4		119	127	1.32	94.27

TABLE 15
SO_2/SO_3 MEASUREMENTS
CHIYODA SCRUBBER, 100 MEGAWATTS
ESP OFF

DATE	LOCATION	TIME	ppm SO_2	ppm SO_3	% O_2	% H_2O	FLUE GAS TEMP., °F	@ 3% O_2		SCRUBBER SO_2 EFF., @ 3% O_2
								SO_2	SO_3	
3/24/94	INLET	843-859	1655	0.89	7.4		259	2194	1.18	
3/24/94	INLET	933-949	1630	1.06	7.3		260	2145	1.40	
3/24/94	INLET	1034-1056	1630	1.17	7.5		261	2177	1.56	
3/24/94	INLET	1125-1143	1639	1.17	7.5	7.8	261	2189	1.56	
AVERAGE			1639	1.07	7.4		260	2176	1.43	
3/24/94	OUTLET	841-856	488	0.52	7.7		122	662	0.71	69.83
3/24/94	OUTLET	931-936	507	0.62	7.5		123	677	0.83	68.44
3/24/94	OUTLET	1038-1053	534	0.26	7.5		123	713	0.35	67.25
3/24/94	OUTLET	1124-1139	533	0.27	7.6	13.4	123	717	0.36	67.25
AVERAGE			516	0.42	7.6		123	692	0.56	68.20
3/25/94	INLET	839-858	1604	0.49	7.8		254	2192	0.67	
3/25/94	INLET	934-951	1618	0.71	7.8		255	2211	0.97	
3/25/94	INLET	1028-1046	1648	0.60	7.2		254	2153	0.78	
3/25/94	INLET	1118-1137	1603	0.81	7.7	7.0	254	2174	1.10	
AVERAGE			1618	0.65	7.6		254	2182	0.88	
3/25/94	OUTLET	834-854	156	0.43	7.9		121	215	0.59	90.19
3/25/94	OUTLET	933-947	185	<0.20	7.8		123	253	<0.2	88.56
3/25/94	OUTLET	1027-1042	189	<0.20	7.8		122	258	<0.2	88.02
3/25/94	OUTLET	1118-1134	194	<0.20	7.6	12.7	122	261	<0.2	87.99
AVERAGE			181	<0.26	7.8		122	247	<0.26	88.68

TABLE 16
SO_2/SO_3 MEASUREMENT
CHIYODA SCRUBBER, 50 MEGAWATTS
ESP OFF

DATE	LOCATION	TIME	ppm SO_2	ppm SO_3	% O_2	% H_2O	FLUE GAS TEMP., °F	@ 3% O_2		SCRUBBER SO_2 EFF., @ 3% O_2
								SO_2	SO_3	
3/26/94	INLET	833-850	1325	0.83	10.1		241	2196	1.38	
3/26/94	INLET	917-934	1343	0.89	10.0		242	2205	1.46	
3/26/94	INLET	1014-1031	1303	1.02	10.2		243	2180	1.71	
3/26/94	INLET	1057-1113	1342	1.04	9.4	5.4	244	2089	1.62	
AVERAGE			1328	0.95	9.9		243	2168	1.54	
3/26/94	OUTLET	832-847	111	<0.20	10.4		112	189	<0.2	91.39
3/26/94	OUTLET	916-931	133	<0.20	10.3		113	225	<0.2	89.80
3/26/94	OUTLET	1013-1028	141	<0.20	10.1		116	234	<0.2	89.27
3/26/94	OUTLET	1056-1111	156	<0.20	10.0	11.0	114	256	<0.2	87.75
AVERAGE			135	<0.20	10.2		114	226	<0.2	89.58
3/27/94	INLET	823-839	1446	0.62	9.5		252	2270	0.97	
3/27/94	INLET	905-921	1435	0.74	9.5		253	2214	1.14	
3/27/94	INLET	949-1006	1406	1.02	9.8		253	2267	1.64	
3/27/94	INLET	1053-1109	1389	1.12	9.4	6.4	255	2162	1.74	
AVERAGE			1419	0.88	9.5		253	2228	1.38	
3/27/94	OUTLET	822-838	63	<0.20	9.6		119	100	<0.2	95.59
3/27/94	OUTLET	904-921	62	0.23	9.6		120	98	0.36	95.57
3/27/94	OUTLET	948-1005	61	0.42	9.6		120	97	0.67	95.72
3/27/94	OUTLET	1052-1108	230	0.38	9.5	11.9	119	361	0.60	83.30
AVERAGE			104	0.31	9.6		120	164	0.41	92.64

Table 17
ANALYSES OF FILTERS AND SOLIDS FROM METHOD 5B TESTS CHIYODA SCRUBBER, MARCH 1994

Date	3/18/94		3/20/94		3/22/94		3/25/94		3/27/94	
Sample	Inlet	Outlet	Inlet	Outlet	Inlet	Outlet	Inlet	Outlet	Inlet	Outlet
Acid Digestion										
Na, %	0.91		0.80	0.79	0.74	0.82	0.58	0.73	0.58	0.98
K, %	2.4		2.2	2.0	2.0	1.9	1.9	2.1	1.9	2.6
Ca, %	1.7		1.6	4.8	1.7	3.7	1.8	3.1	1.7	8.0
Mg, %	0.77		0.66	1.2	0.64	1.1	0.57	0.97	0.54	1.1
Fe, %	7.8		7.2	6.1	7.9	6.3	9.2	6.3	9.4	2.8
Water Extraction										
Soluble, Ca^{+2},%	0.75	6.5	0.67	4.8	0.71	3.6	0.89	2.7	0.91	1.5
Soluble, SO_4^{-2},%	4.27	55.0	2.18	50.2	1.51	43.2	0.93	18.5	2.18	10.5
pH	4.2	3.6	4.9	3.9	5.0	3.7	6.9	3.9	4.9	4.2
Mole ratio, SO_4/Ca	2.37	3.53	1.36	4.36	0.89	5.0	0.45	2.85	1.36	2.92

Table 18

WATER EXTRACTIONS OF PROBE AND NOZZLE ACETONE WASHES METHOD 5B TESTS CHIYODA SCRUBBER, MARCH 1994

Date	3/18/94		3/20/94		3/22/94		3/25/94		3/27/94	
Sample	Inlet	Outlet	Inlet	Outlet	Inlet	Outlet	Inlet	Outlet	Inlet	Outlet
Soluble Ca^{+2}, %	0.79	0.96	0.62	1.4	0.71	2.2	0.85	2.6	0.91	4.1
Soluble SO_4^{-2}, %	3.91	6.35	1.97	12.6	3.80	15.1	0.94	17.9	1.28	23.5
pH	4.1	4.7	4.4	4.4	5.3	4.4	5.1	4.4	4.5	4.1
Mole ratio, SO_4/Ca	2.06	6.61	1.32	3.75	2.23	2.86	0.46	2.87	1.41	2.39

Table 19
CHIYODA SCRUBBER, CONDITION 4
WATER EXTRACTION ANALYSIS OF OUTLET IMPACTOR STAGES

Substrate-stage	Total wt. gain, mg	% Soluble Ca^{+2}	% Soluble SO_4^{-2}	Mole ratio SO_4/Ca
67-3	0.54	3.0	68.2	9.47
67-4	1.4	2.7	19.3	2.98
67-5	3.02	3.2	18.4	2.4
67-6	1.15	5.6	35.9	2.67
68-2	0.41	2.9	80.2	11.5
68-3	0.50	3.2	69.2	9.01
68-4	1.79	2.3	25.8	4.67
68-5	3.33	2.6	20.5	3.29
68-6	0.72	9.2	86.4	3.91
70-2	0.22	3.6	98.6	11.4
70-3	0.36	2.8	72.1	10.7
70-4	0.49	2.9	48.4	6.95
70-5	1.58	2.5	19.0	3.17
70-6	3.05	2.4	12.6	2.19

Table 20
CHIYODA SCRUBBER, CONDITION 5
WATER EXTRACTION ANALYSIS OF OUTLET IMPACTOR STAGES

Substrate-stage	Total wt. gain, mg	% Soluble Ca^{+2}	% Soluble SO_4^{-2}	Mole ratio SO_4/Ca
73-2	0.38	2.6	59.2	9.49
73-3	0.99	2.2	36.8	6.97
73-4	2.6	1.8	20.2	4.68
73-5	4.78	2.2	16.6	3.14
73-6	2.35	3.1	27.8	3.74
74-2	0.56	1.8	53.3	12.3
74-3	0.68	1.8	48.7	11.3
74-4	1.91	1.6	22.3	5.81
74-5	3.87	1.9	17.4	3.82
74-6	2.24	2.9	27.7	3.98
75-2	0.45	1.8	60.2	13.9
75-3	0.51	2.0	55.9	11.6
75-4	0.71	2.0	43	8.96
75-5	2.36	1.4	17.8	5.3
75-6	3.89	2.0	14.8	3.08

Table 21
CHIYODA SCRUBBER, CONDITION 7
WATER EXTRACTION ANALYSIS OF OUTLET IMPACTOR STAGES

Substrate-stage	Total wt. gain, mg	% Soluble Ca^{+2}	% Soluble SO_4^{-2}	Mole ratio SO_4/Ca
84-2	0.22	1.8	38.7	8.96
84-3	0.37	2.2	26.6	5.04
84-4	3.1	0.84	5.78	2.87
84-5	5.56	1.3	5.78	1.85
84-6	3.11	2.4	11.1	1.93
85-2	0.23	2.6	23.4	3.75
85-3	0.44	2.3	16.2	2.93
85-4	2.91	1.1	5.11	1.94
85-5	5.92	1.4	5.75	1.71
85-6	3.16	2.2	9.04	1.71
86-3	0.1	6.0	88.6	6.15
86-4	0.52	1.5	16.4	4.56
86-5	3.4	0.76	5.04	2.76
86-6	6.49	0.89	5.26	2.46

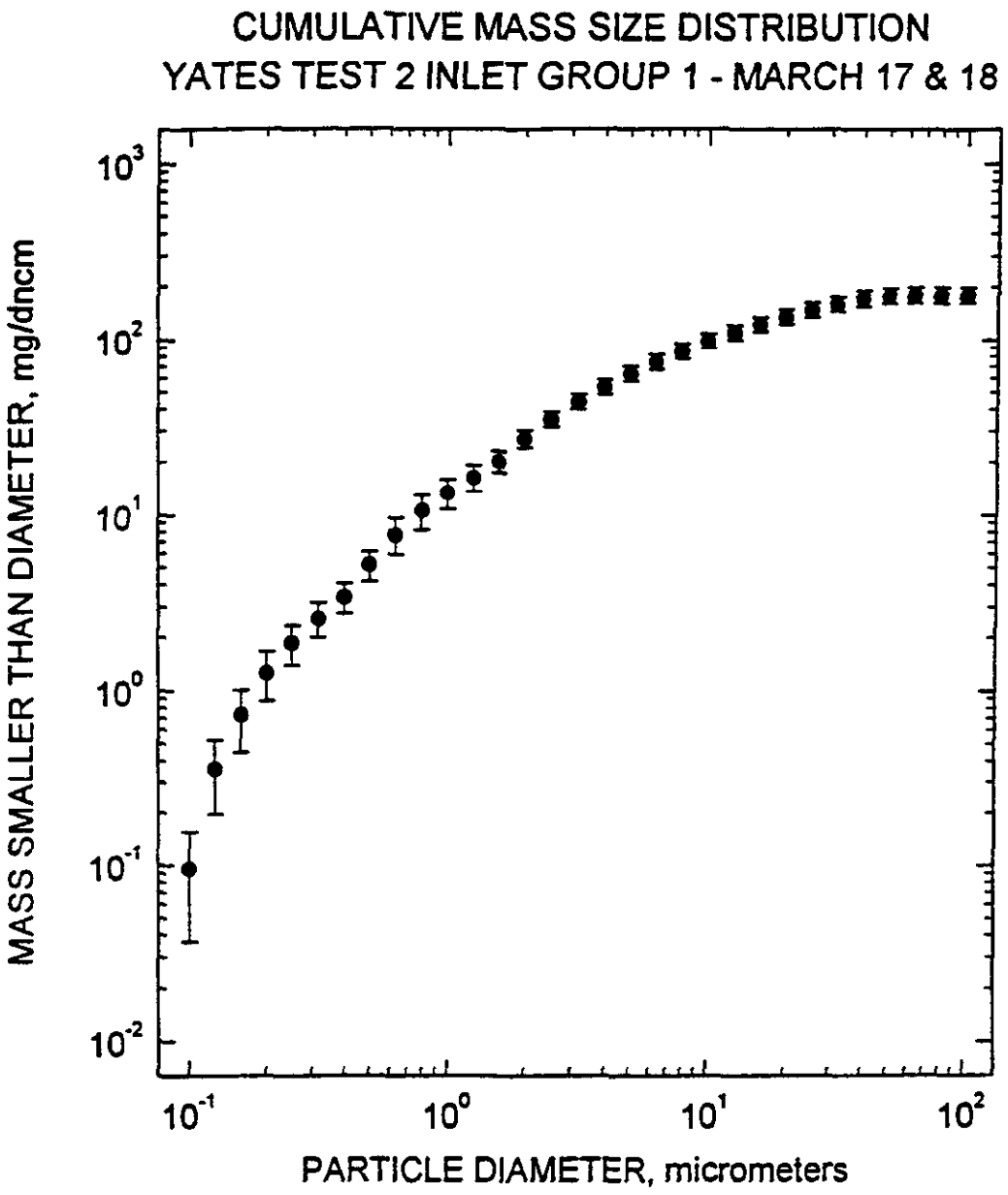

Figure 1. Chiyoda Inlet Cumulative Mass vs Particle Diameter. Group 1, March 17 & 18, 1994.

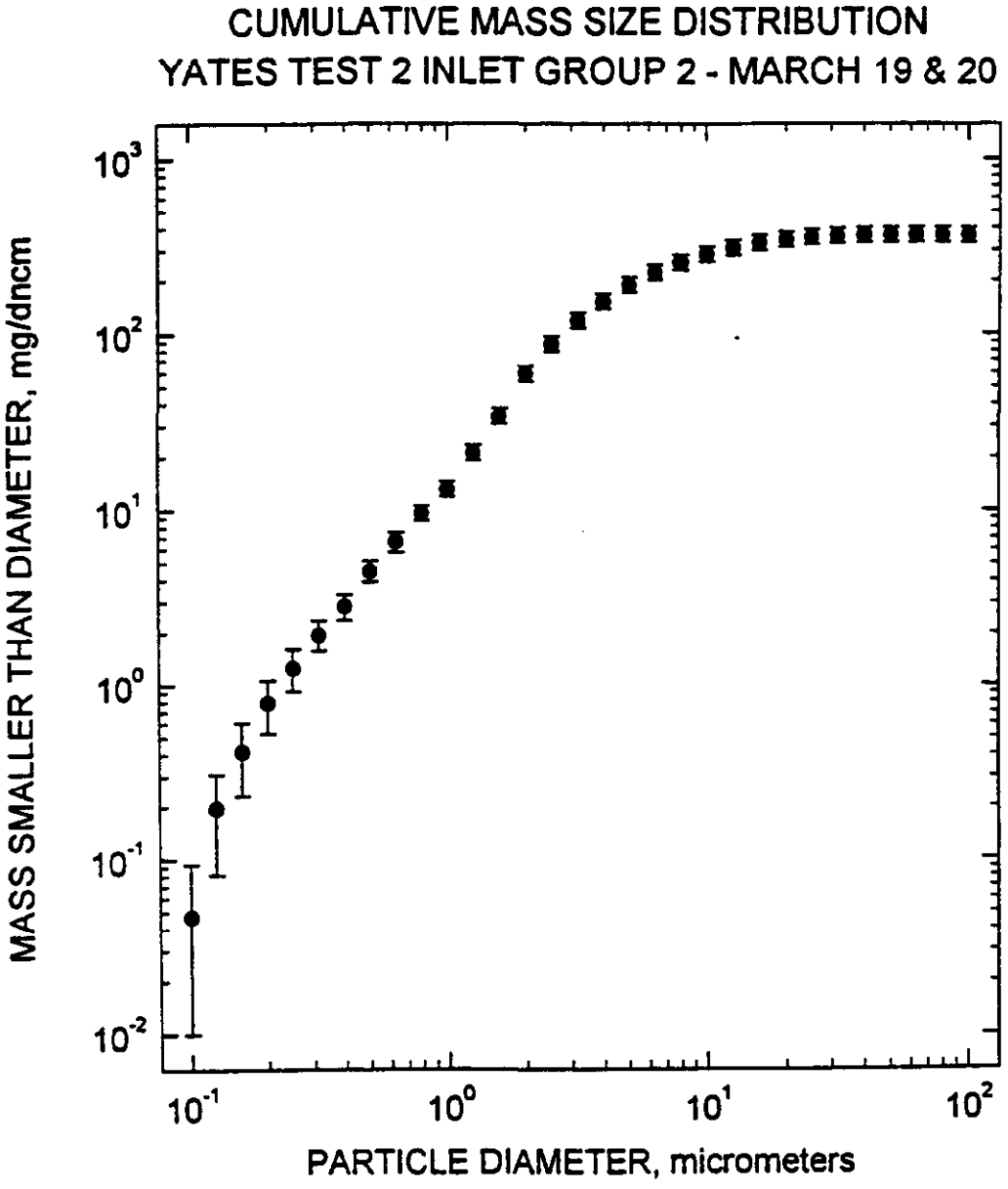

Figure 2. Chiyoda Inlet Cumulative Mass vs Particle Diameter. Group 2, March 19 & 20, 1994.

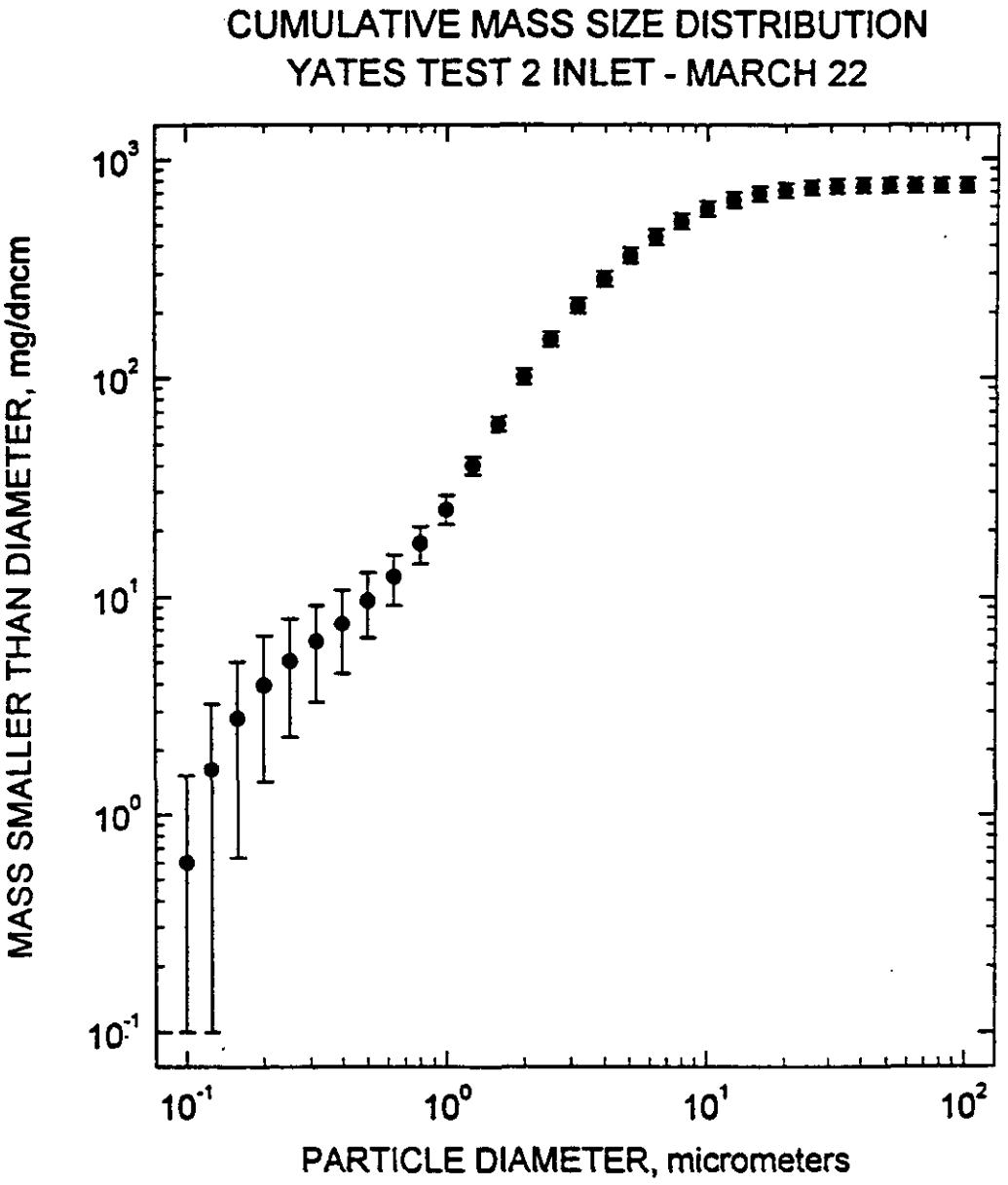

Figure 3. Chiyoda Inlet Cumulative Mass vs Particle Diameter. Group 3, March 22, 1994.

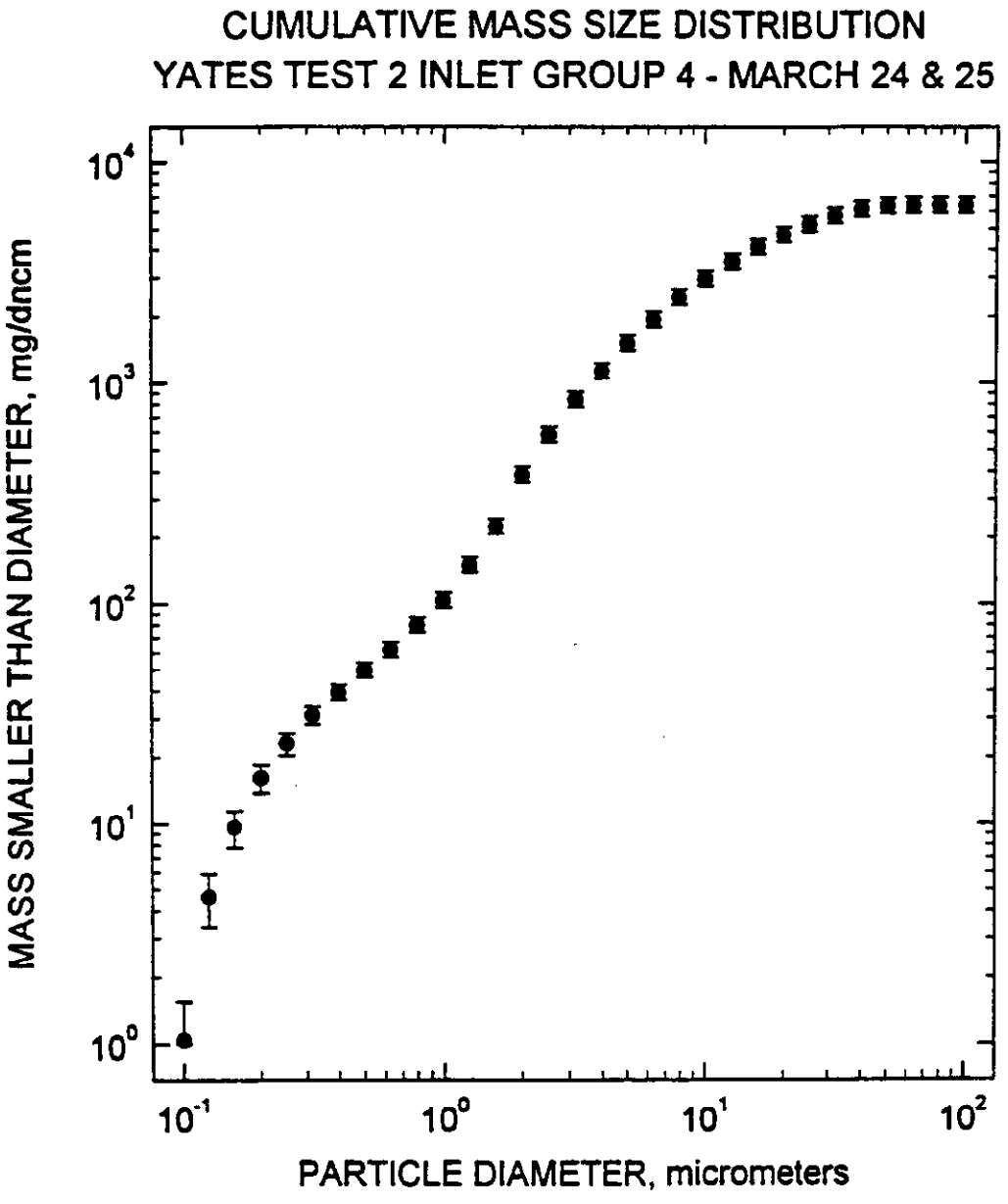

Figure 4. Chiyoda Inlet Cumulative Mass vs Particle Diameter. Group 4, March 24 & 25, 1994.

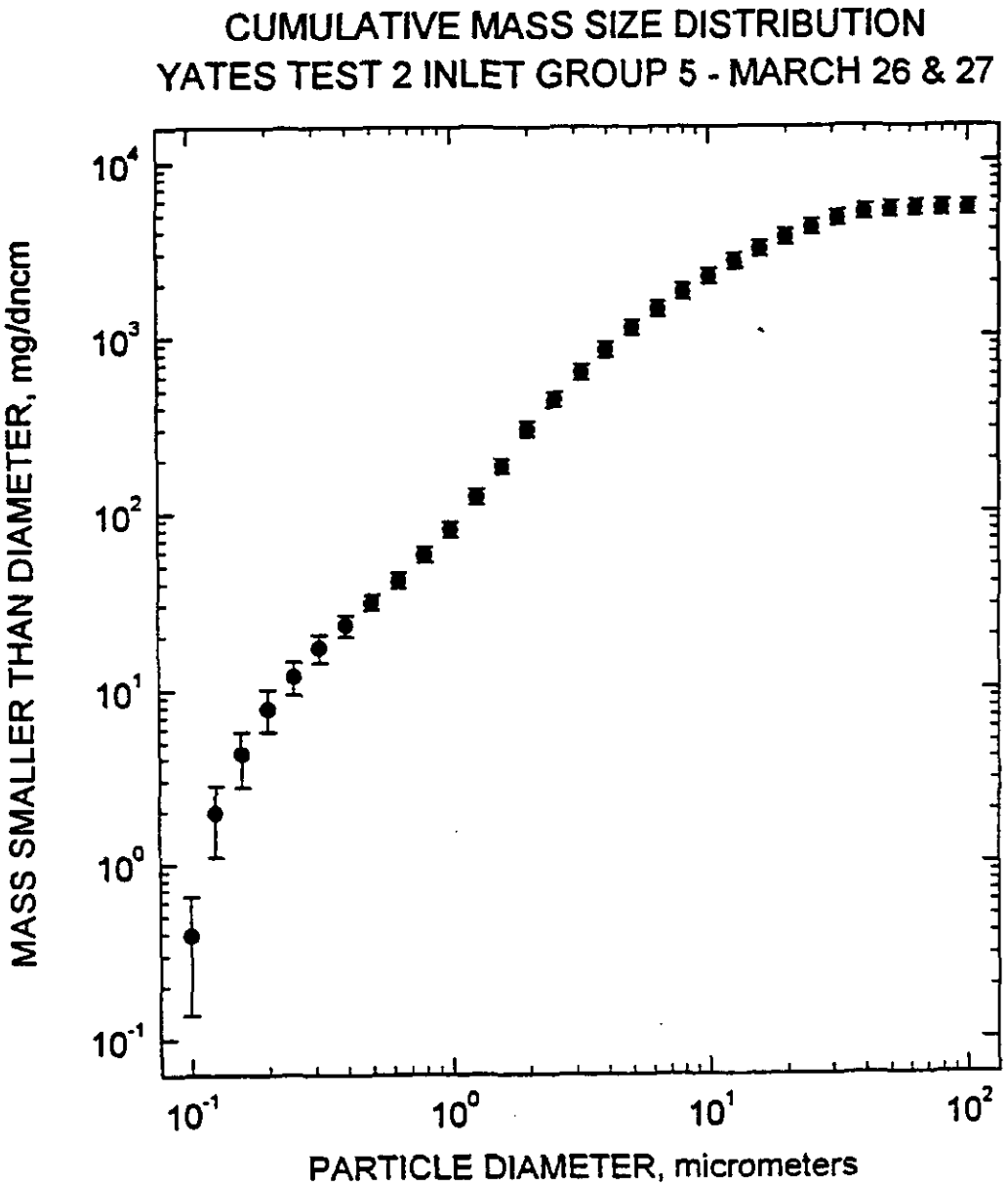

Figure 5. Chiyoda Inlet Cumulative Mass vs Particle Diameter. Group 5, March 26 & 27, 1994.

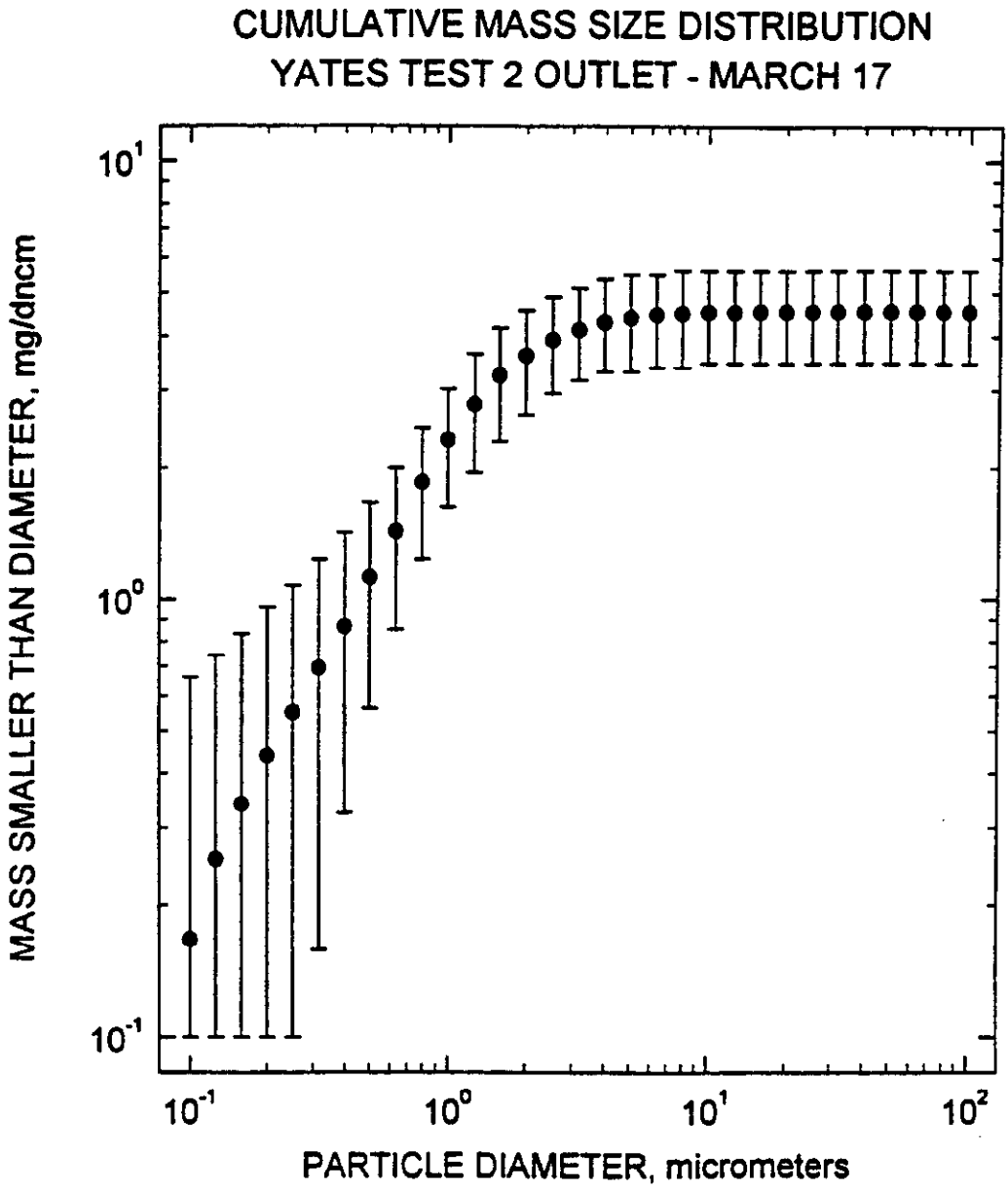

Figure 6. Chiyoda Outlet Cumulative Mass vs Particle Diameter. Condition 1, March 17, 1994.

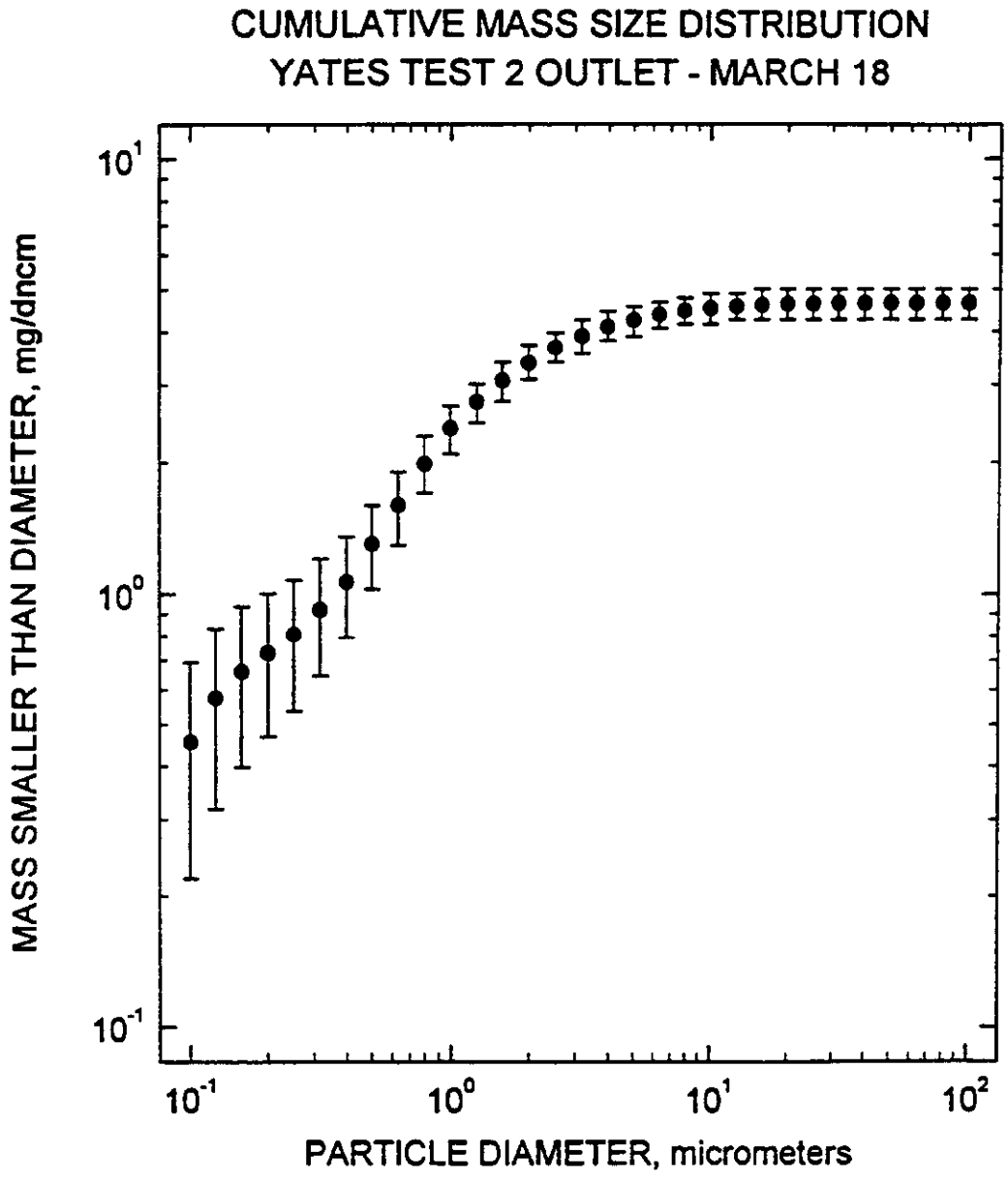

Figure 7. Chiyoda Outlet Cumulative Mass vs Particle Diameter. Condition 2, March 18, 1994.

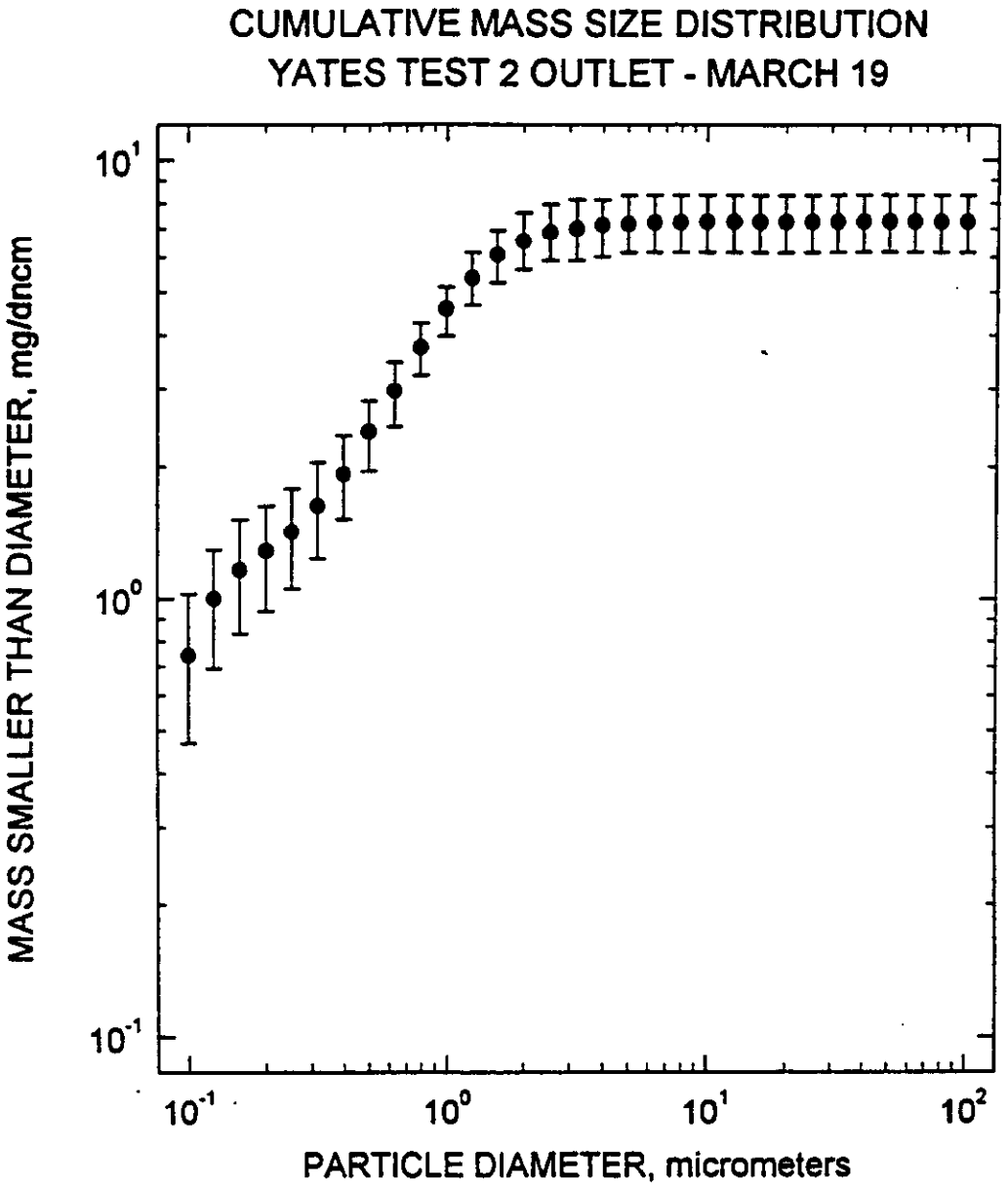

Figure 8. Chiyoda Outlet Cumulative Mass vs Particle Diameter. Condition 3, March 19, 1994.

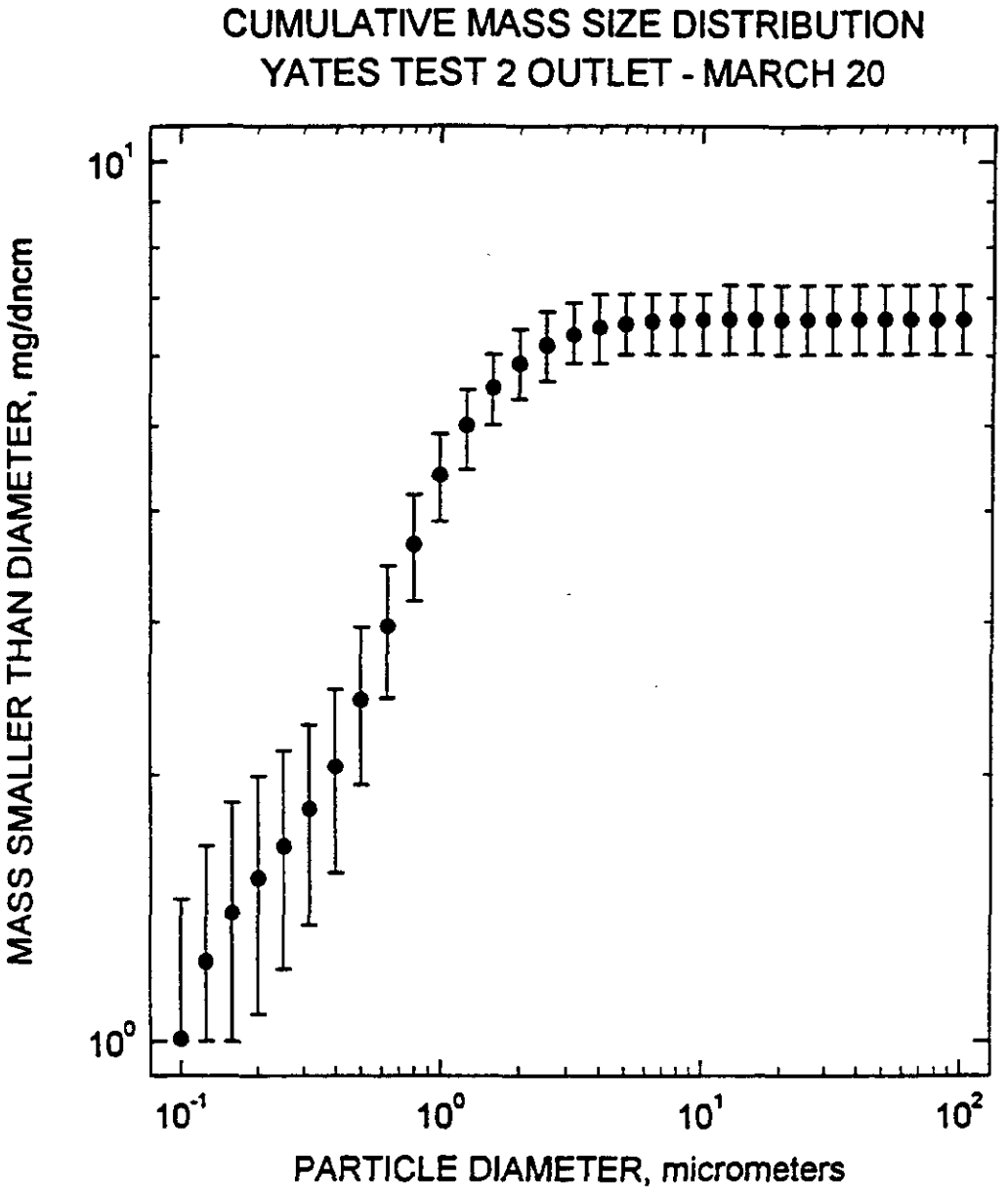

Figure 9. Chiyoda Outlet Cumulative Mass vs Particle Diameter. Condition 4, March 20, 1994.

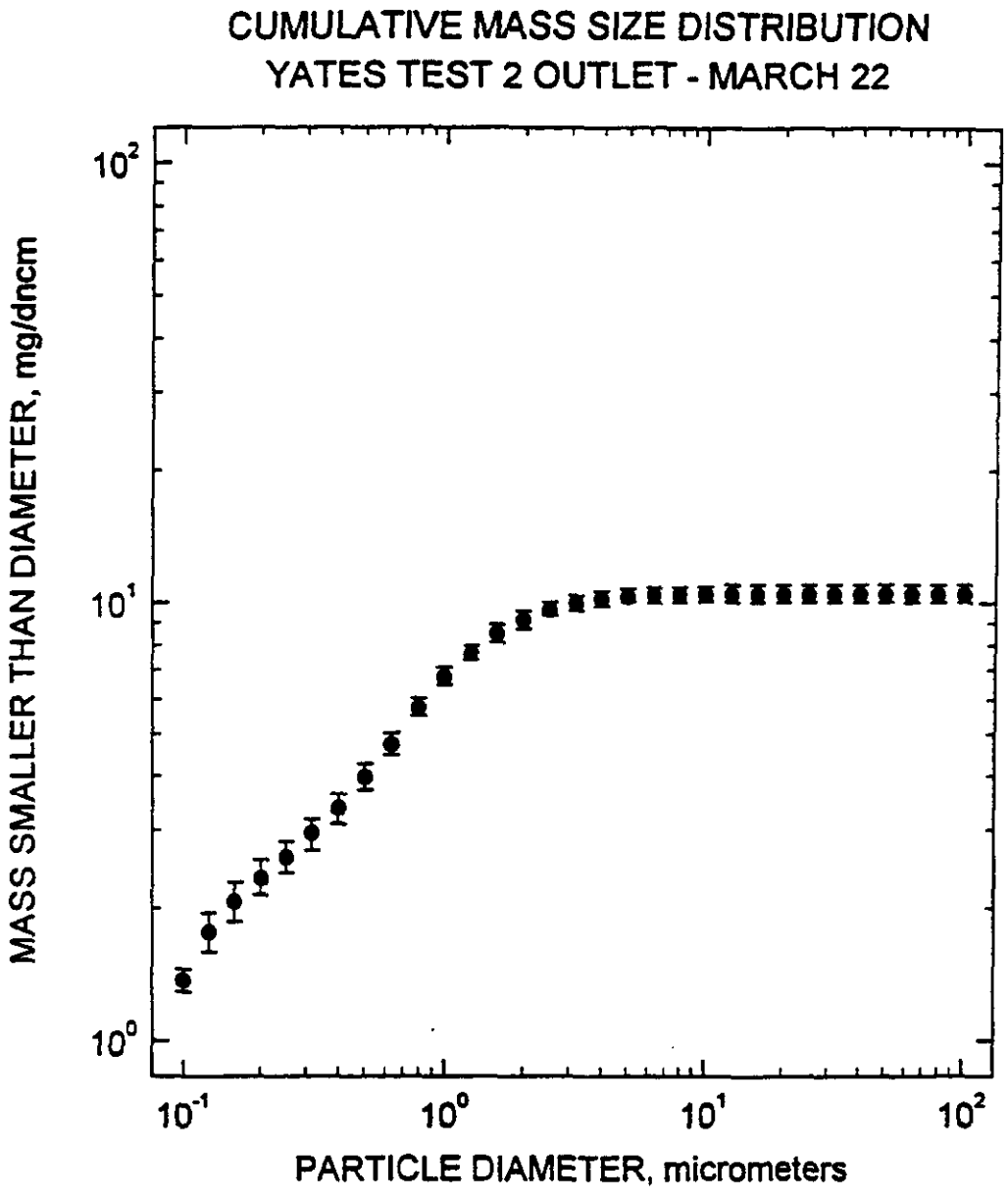

Figure 10. Chiyoda Outlet Cumulative Mass vs Particle Diameter. Condition 5, March 22, 1994.

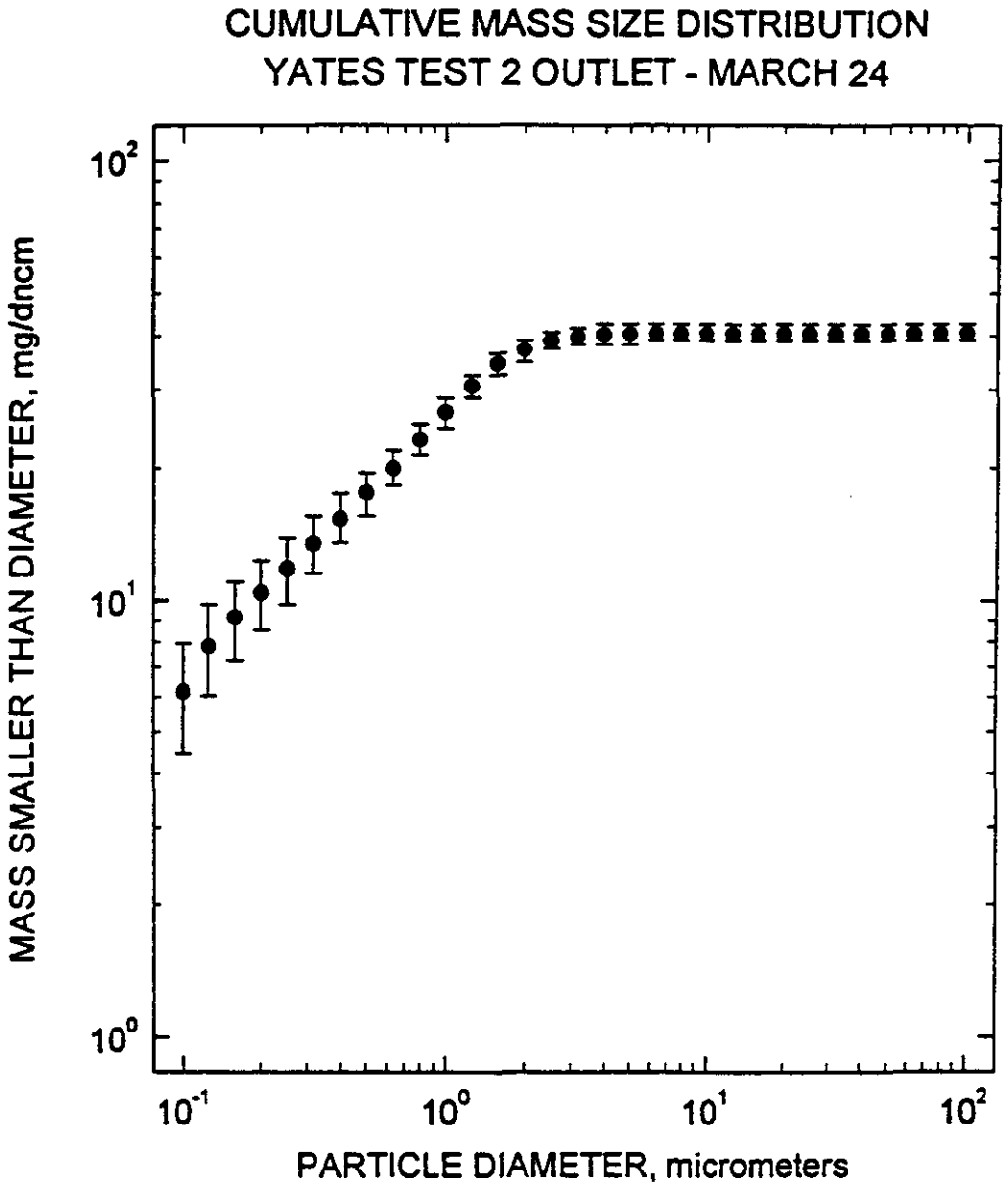

Figure 11. Chiyoda Outlet Cumulative Mass vs Particle Diameter. Condition 6, March 24, 1994.

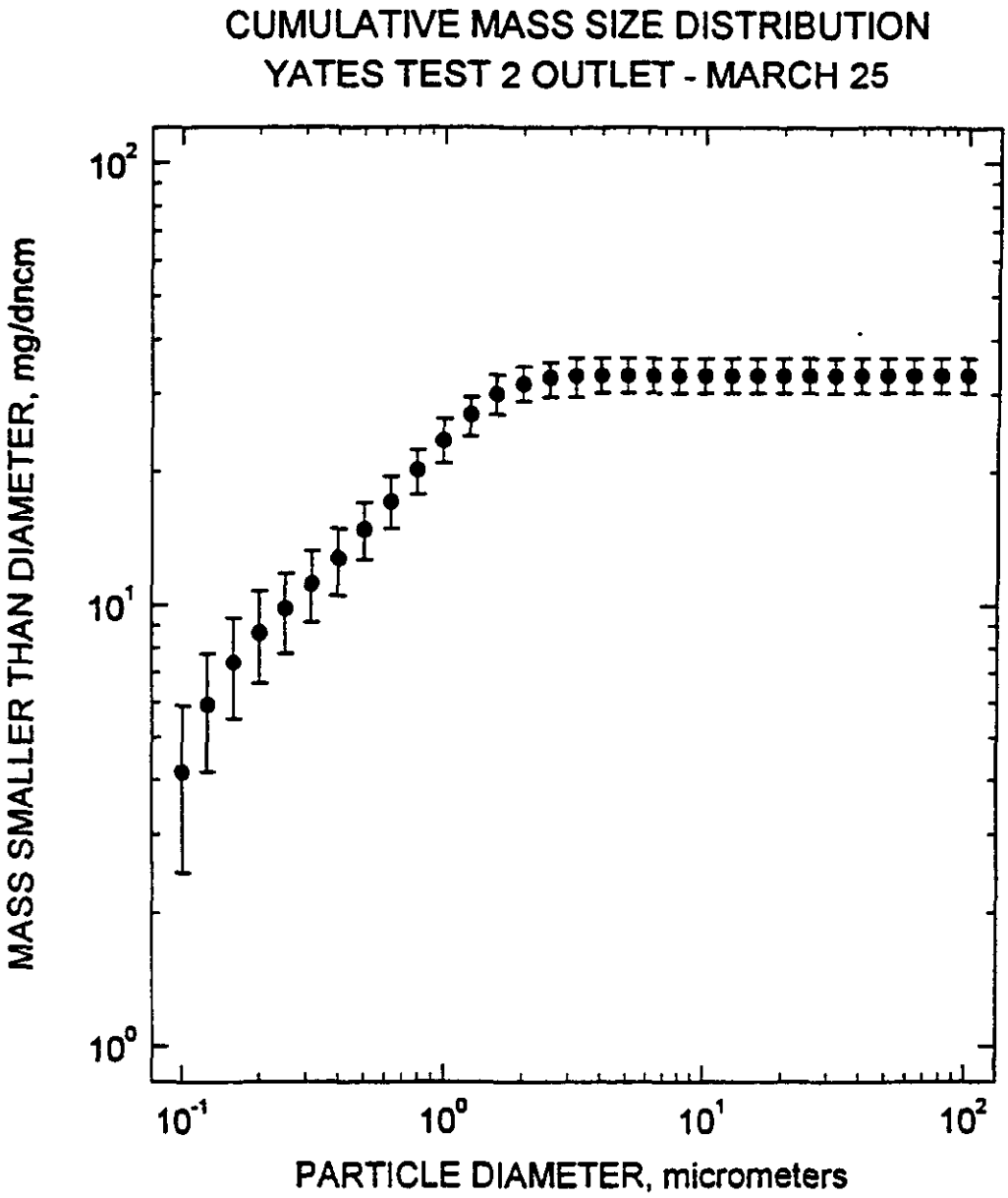

Figure 12. Chiyoda Outlet Cumulative Mass vs Particle Diameter. Condition 7, March 25, 1994.

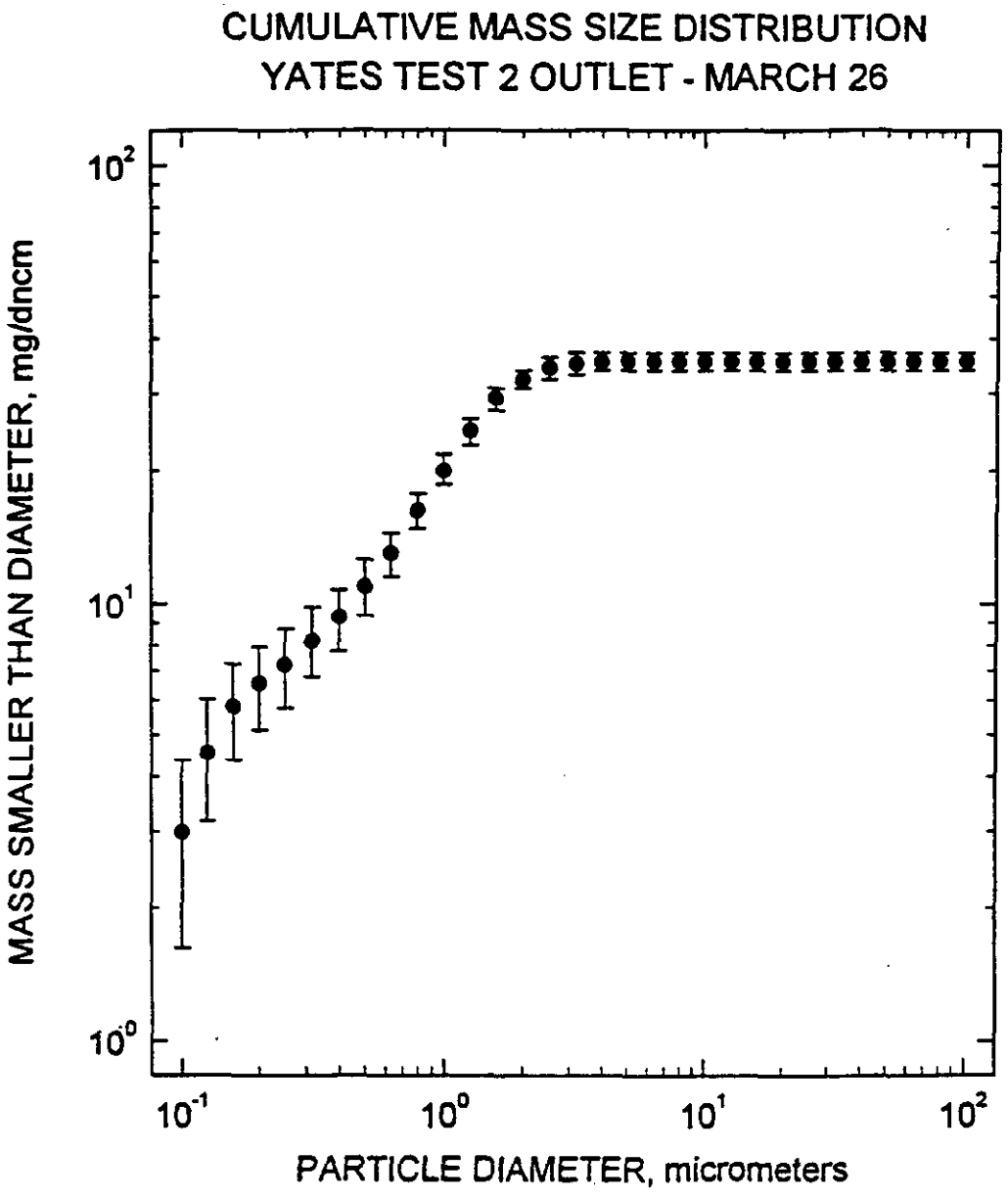

Figure 13. Chiyoda Outlet Cumulative Mass vs Particle Diameter. Condition 8, March 26, 1994.

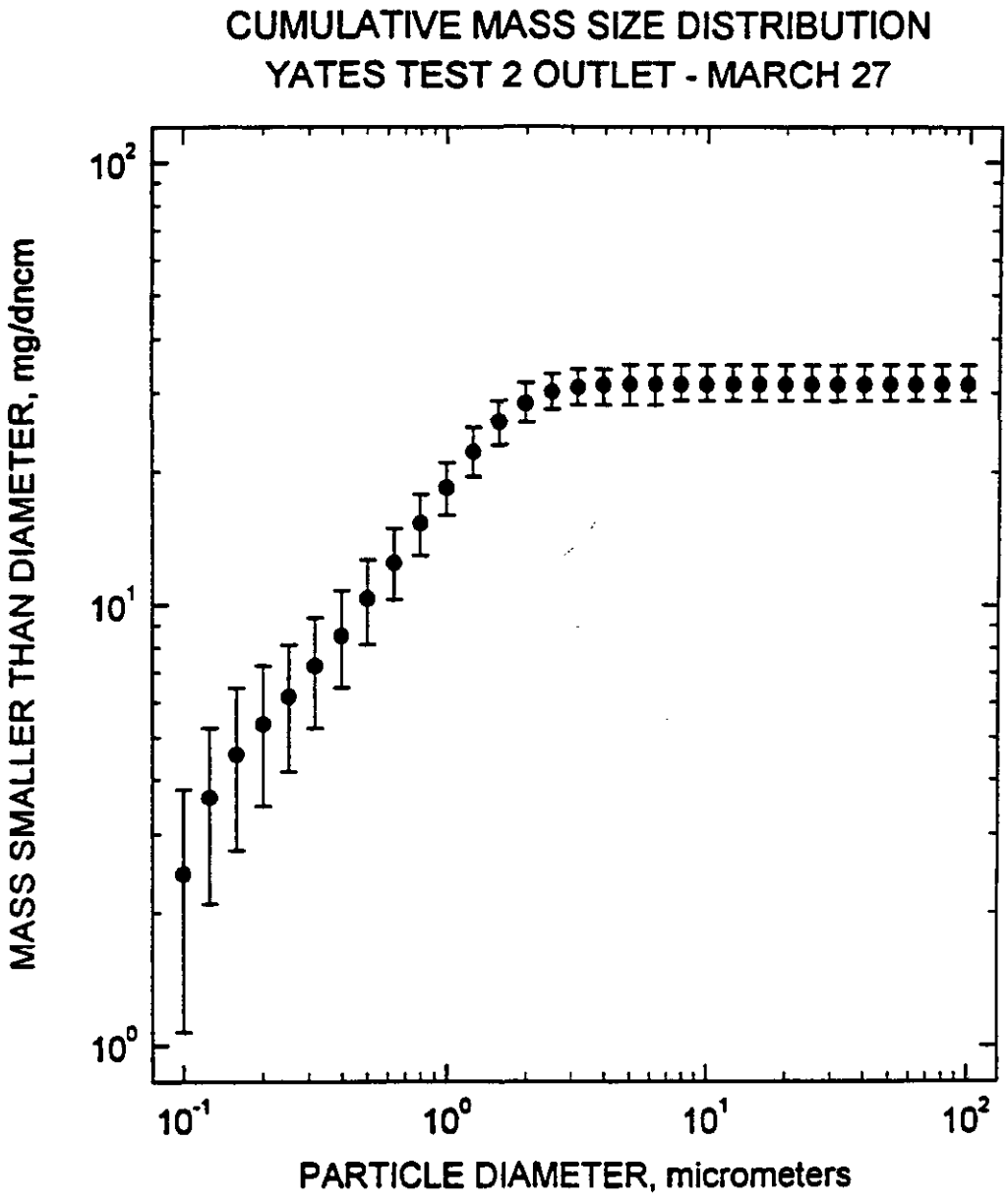

Figure 14. Chiyoda Outlet Cumulative Mass vs Particle Diameter. Condition 9, March 27, 1994.

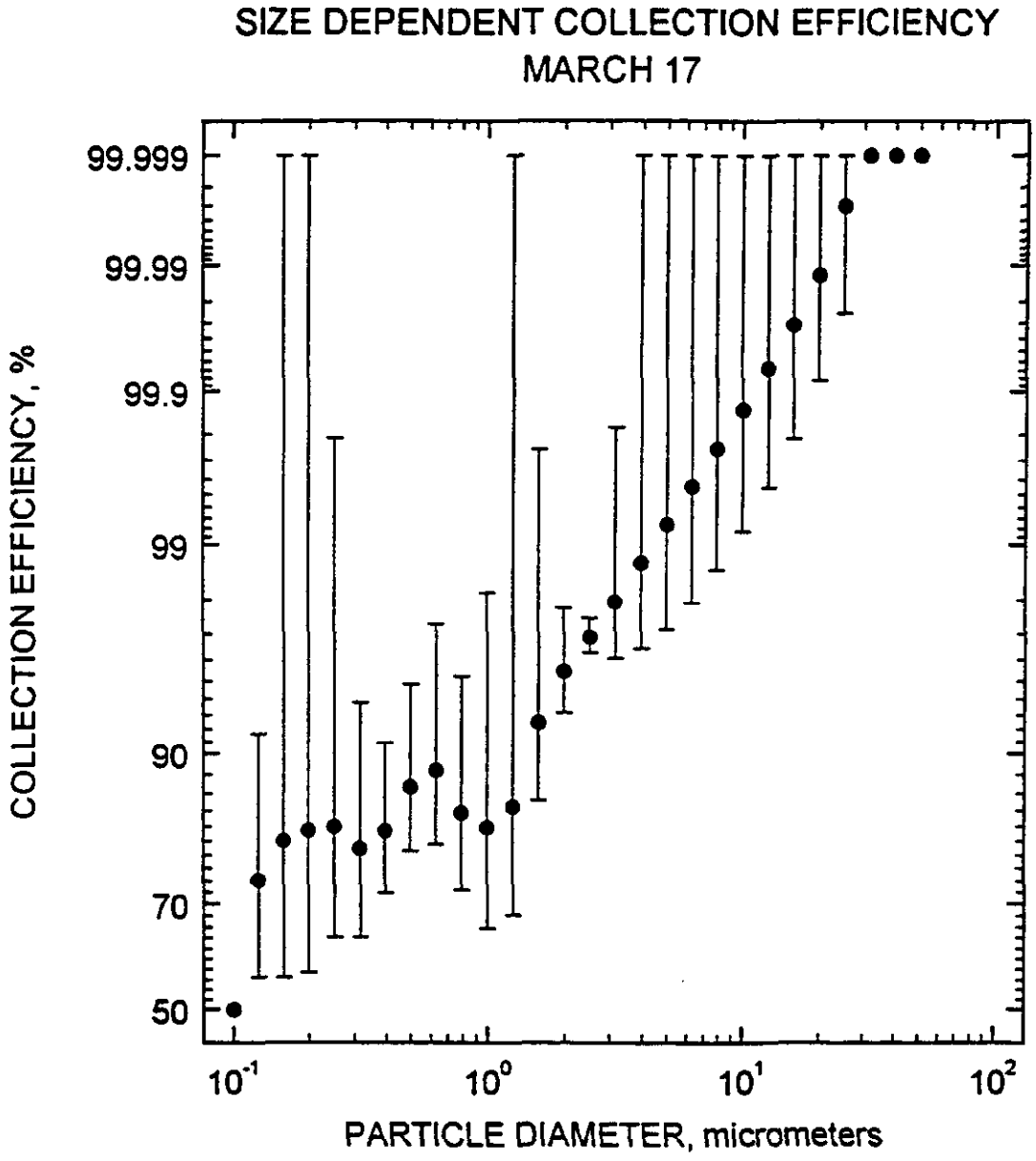

Figure 15. Chiyoda Scrubber Fractional Collection Efficiency. Condition 1, March 17, 1994.

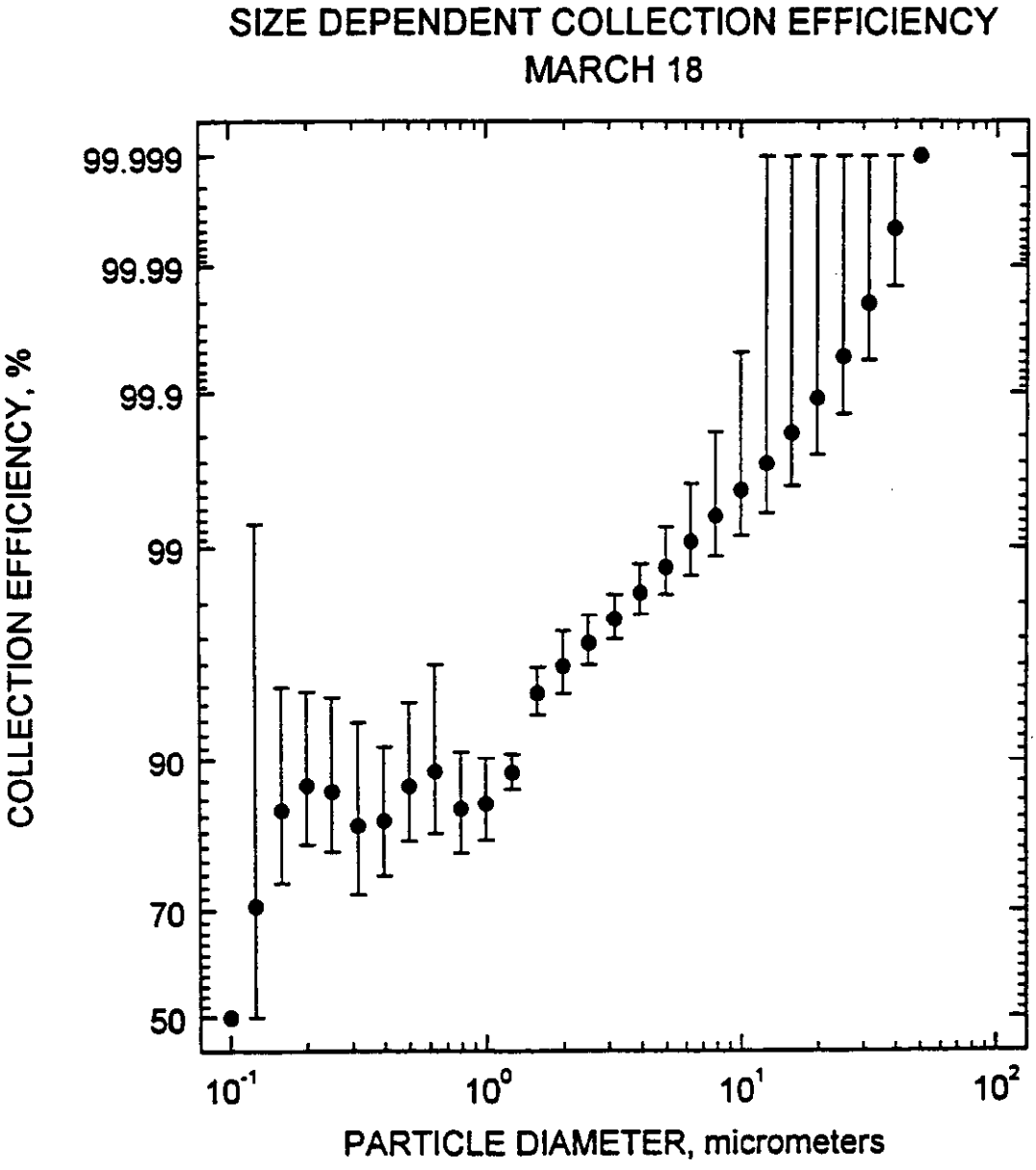

Figure 16. Chiyoda Scrubber Fractional Collection Efficiency. Condition 2, March 18, 1994.

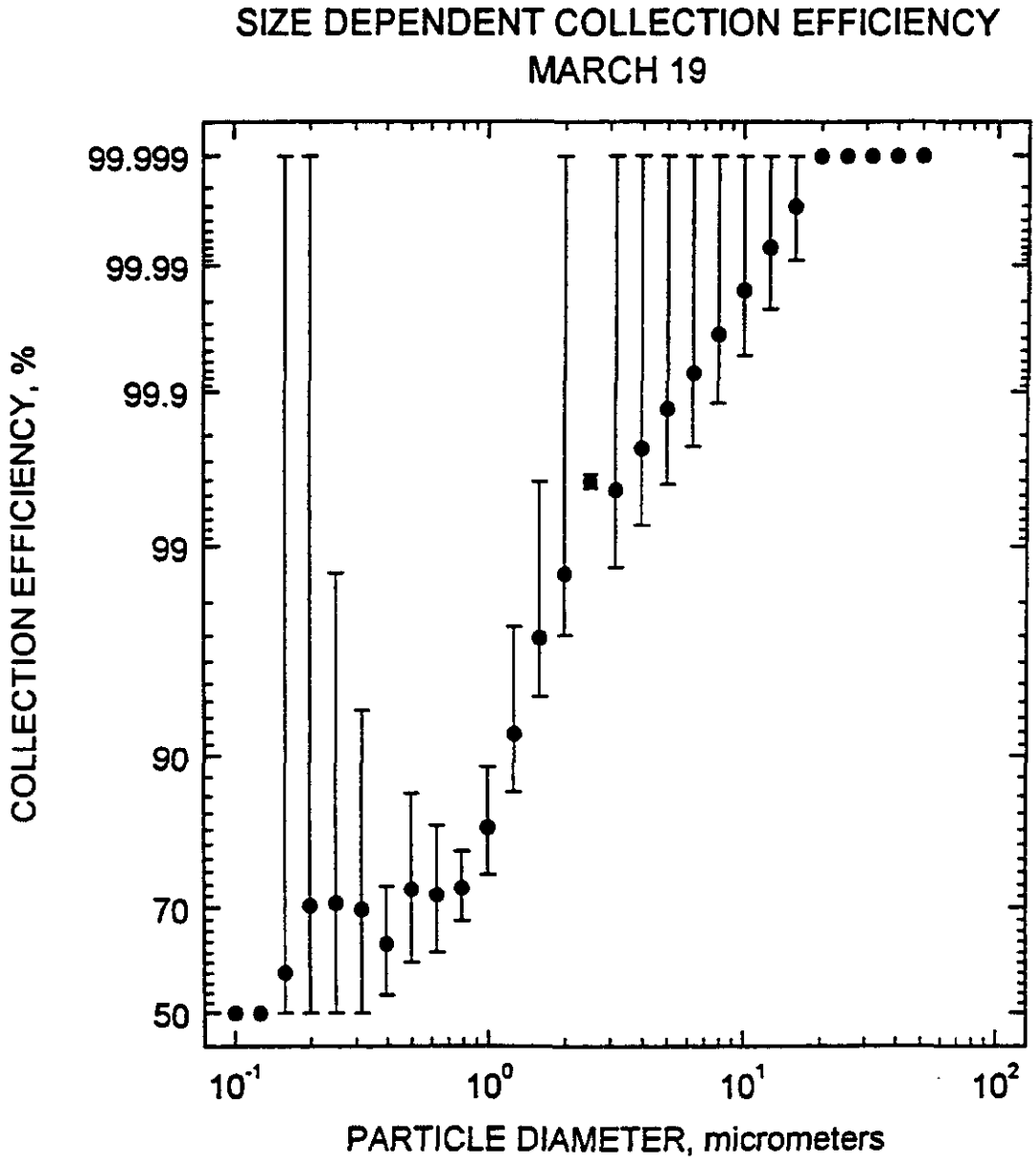

Figure 17. Chiyoda Scrubber Fractional Collection Efficiency. Condition 3, March 19, 1994.

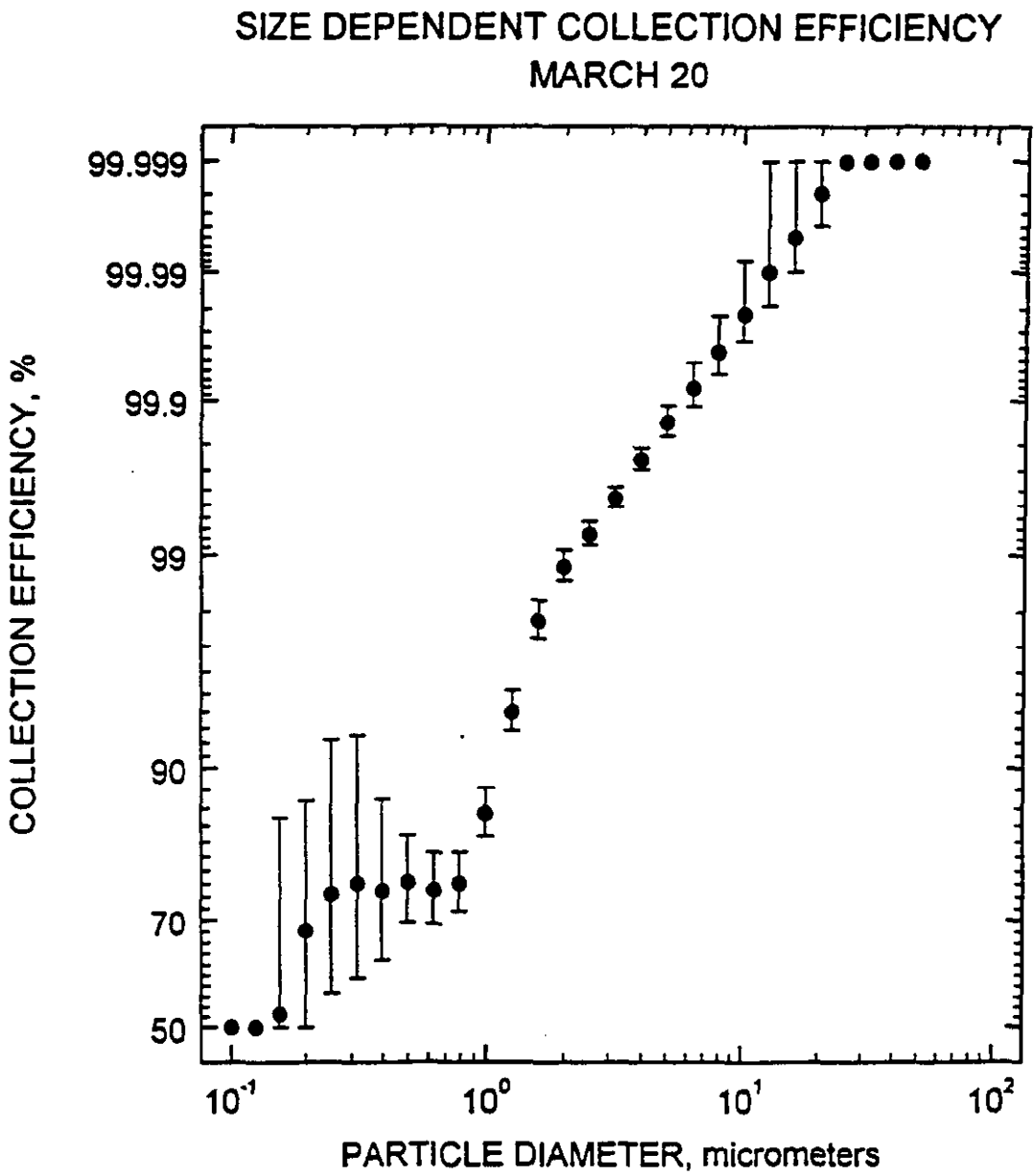

Figure 18. Chiyoda Scrubber Fractional Collection Efficiency. Condition 4, March 20, 1994.

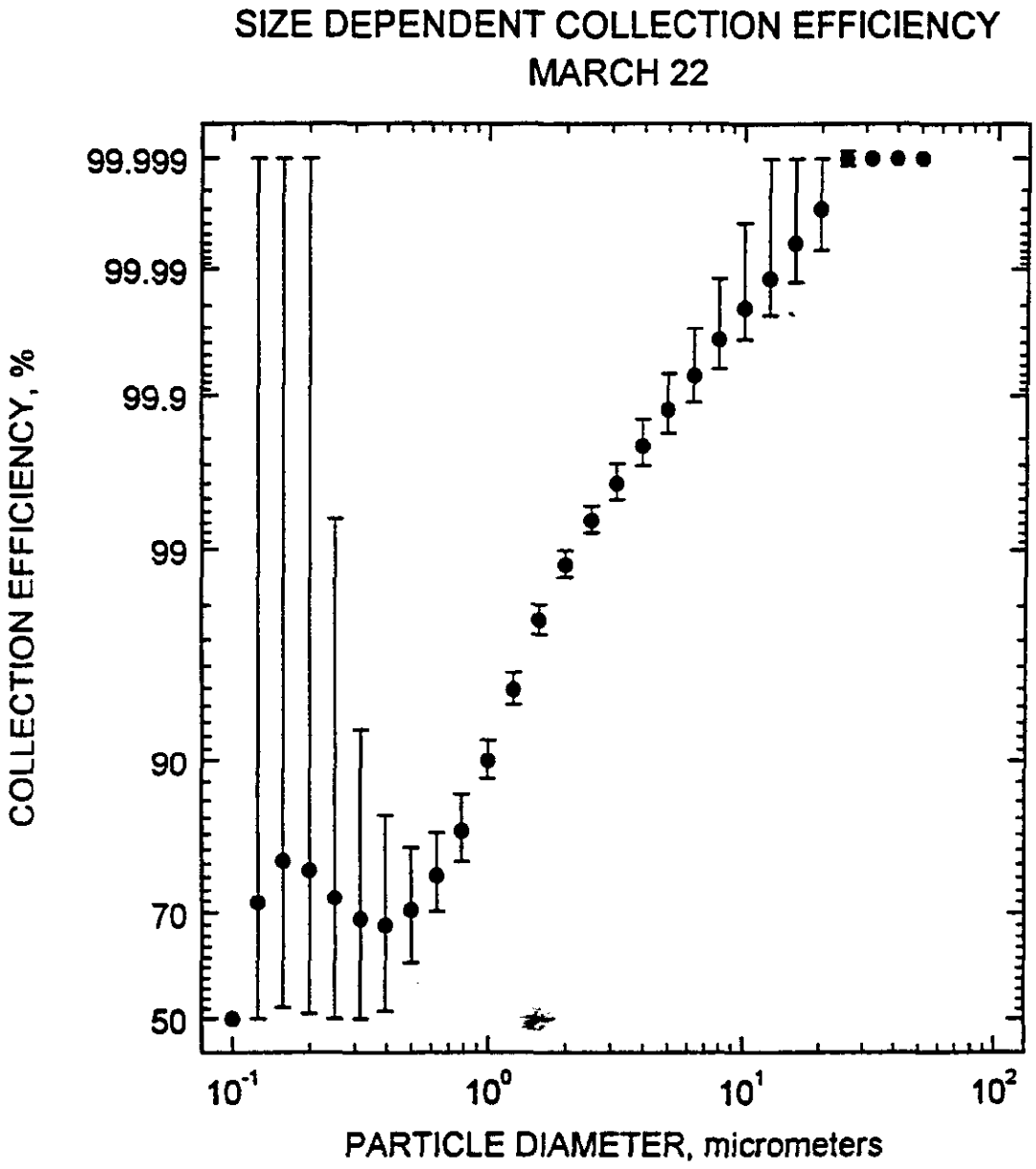

Figure 19. Chiyoda Scrubber Fractional Collection Efficiency. Condition 5, March 22, 1994.

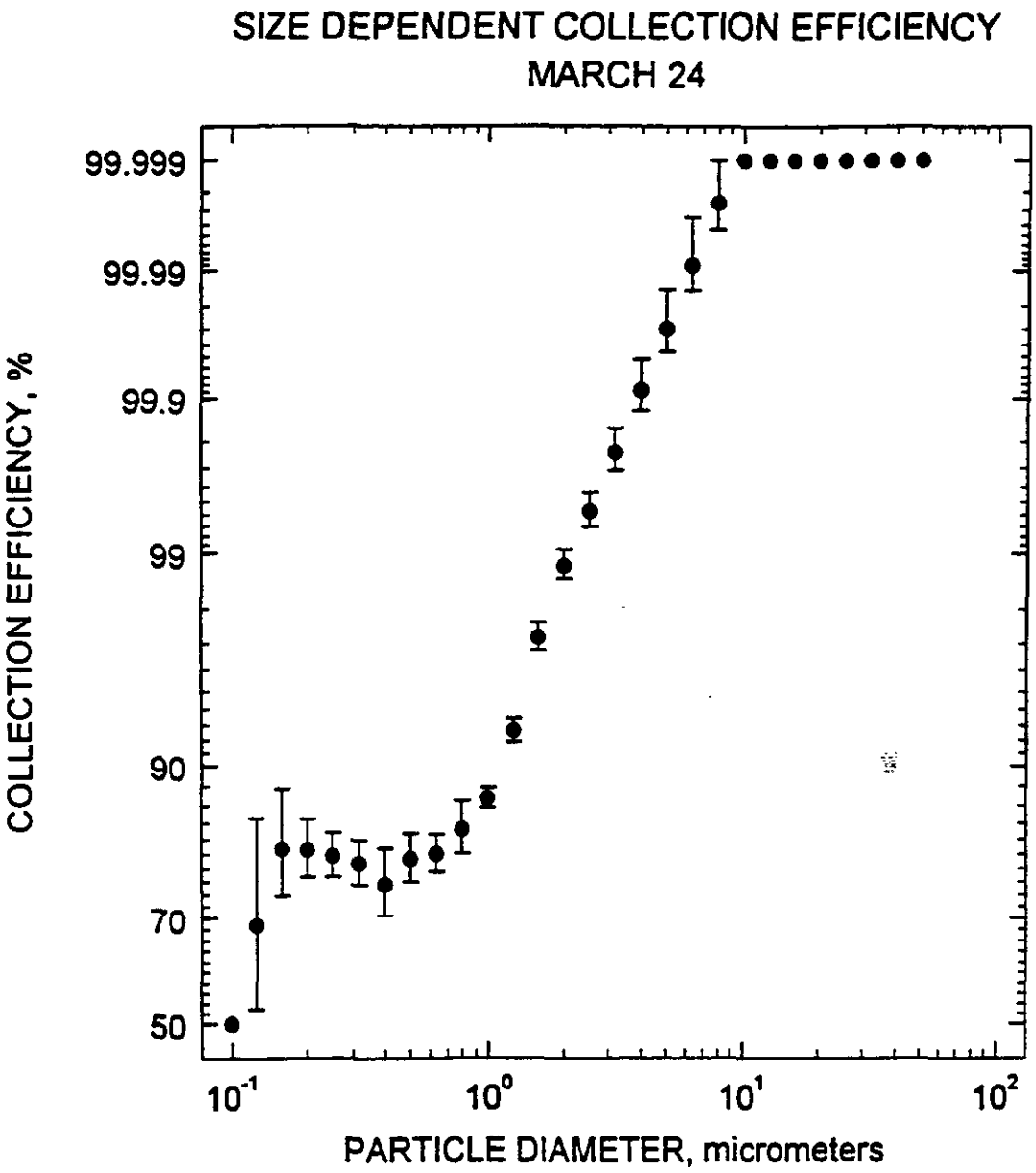

Figure 20. Chiyoda Scrubber Fractional Collection Efficiency. Condition 6, March 24, 1994.

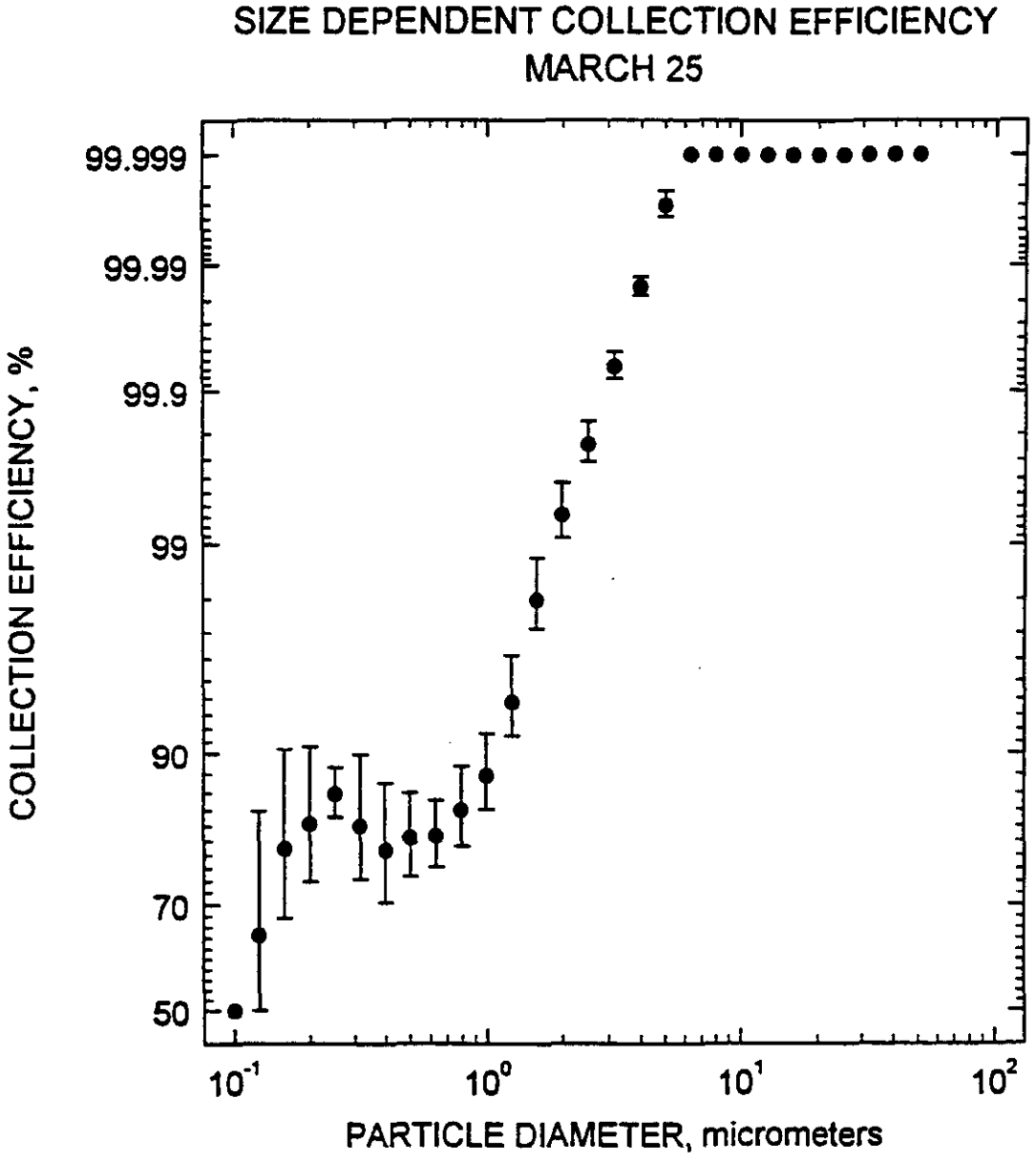

Figure 21. Chiyoda Scrubber Fractional Collection Efficiency. Condition 7, March 25, 1994.

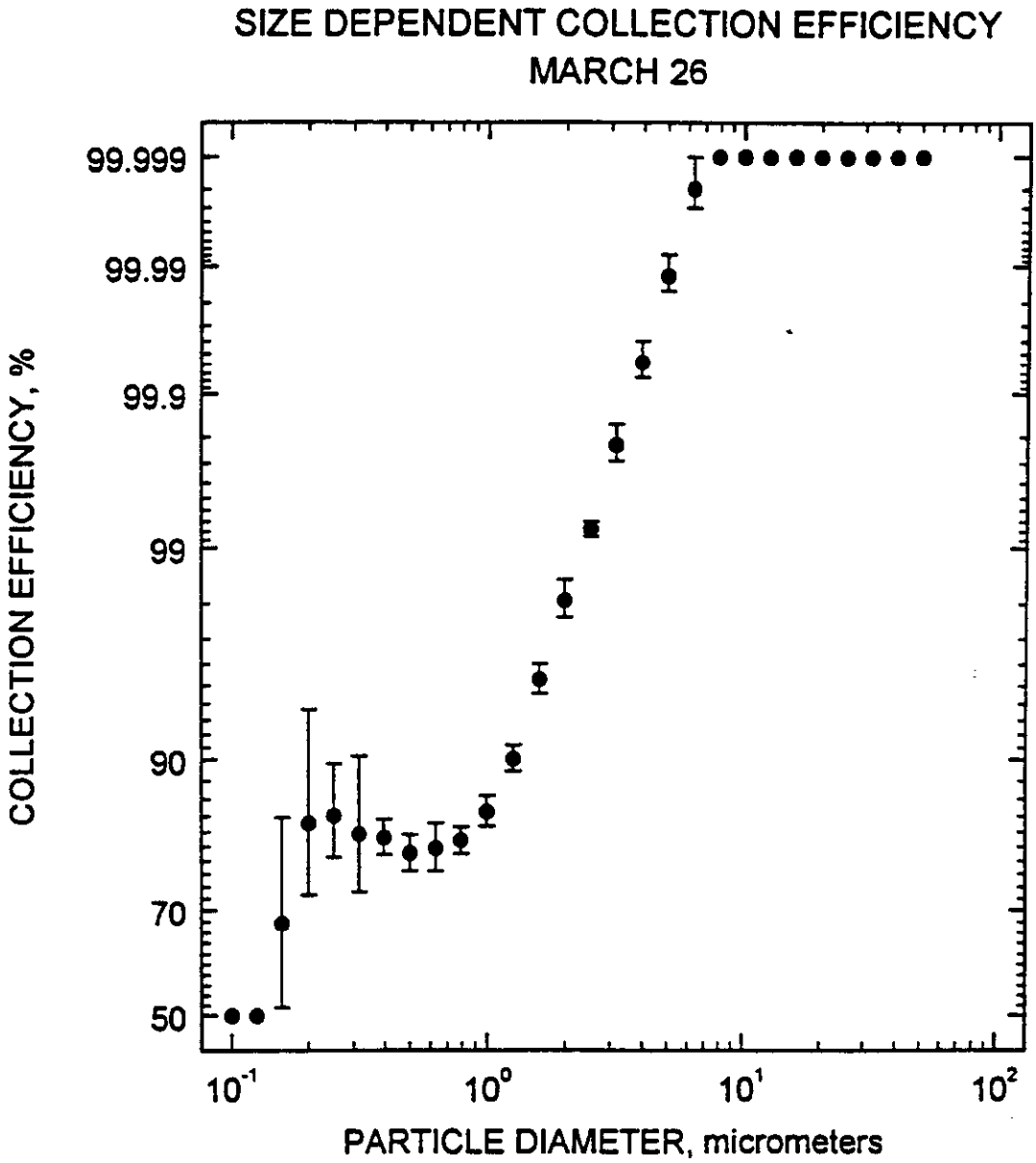

Figure 22. Chiyoda Scrubber Fractional Collection Efficiency. Condition 8, March 26, 1994.

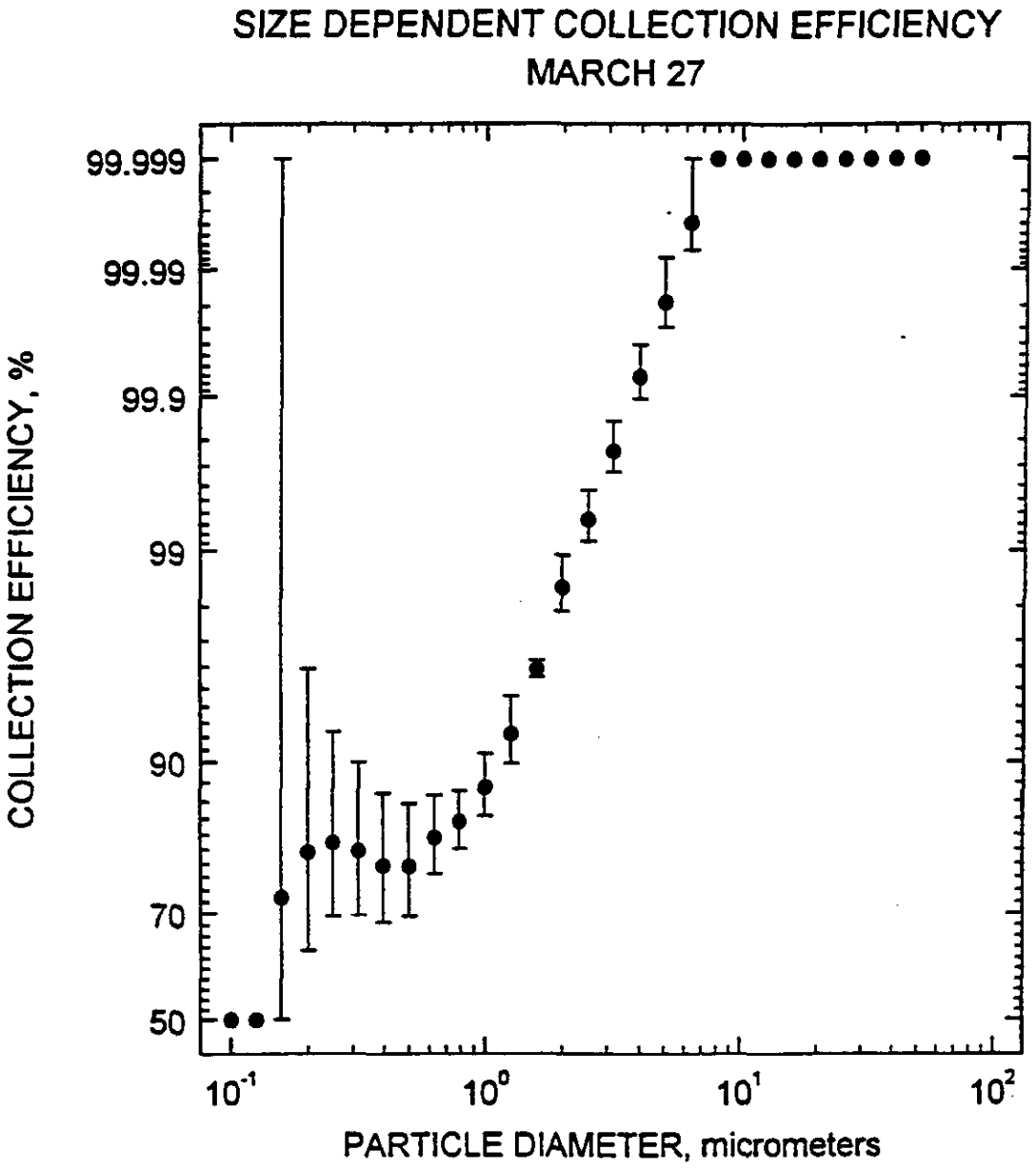

Figure 23. Chiyoda Scrubber Fractional Collection Efficiency. Condition 9, March 27, 1994.

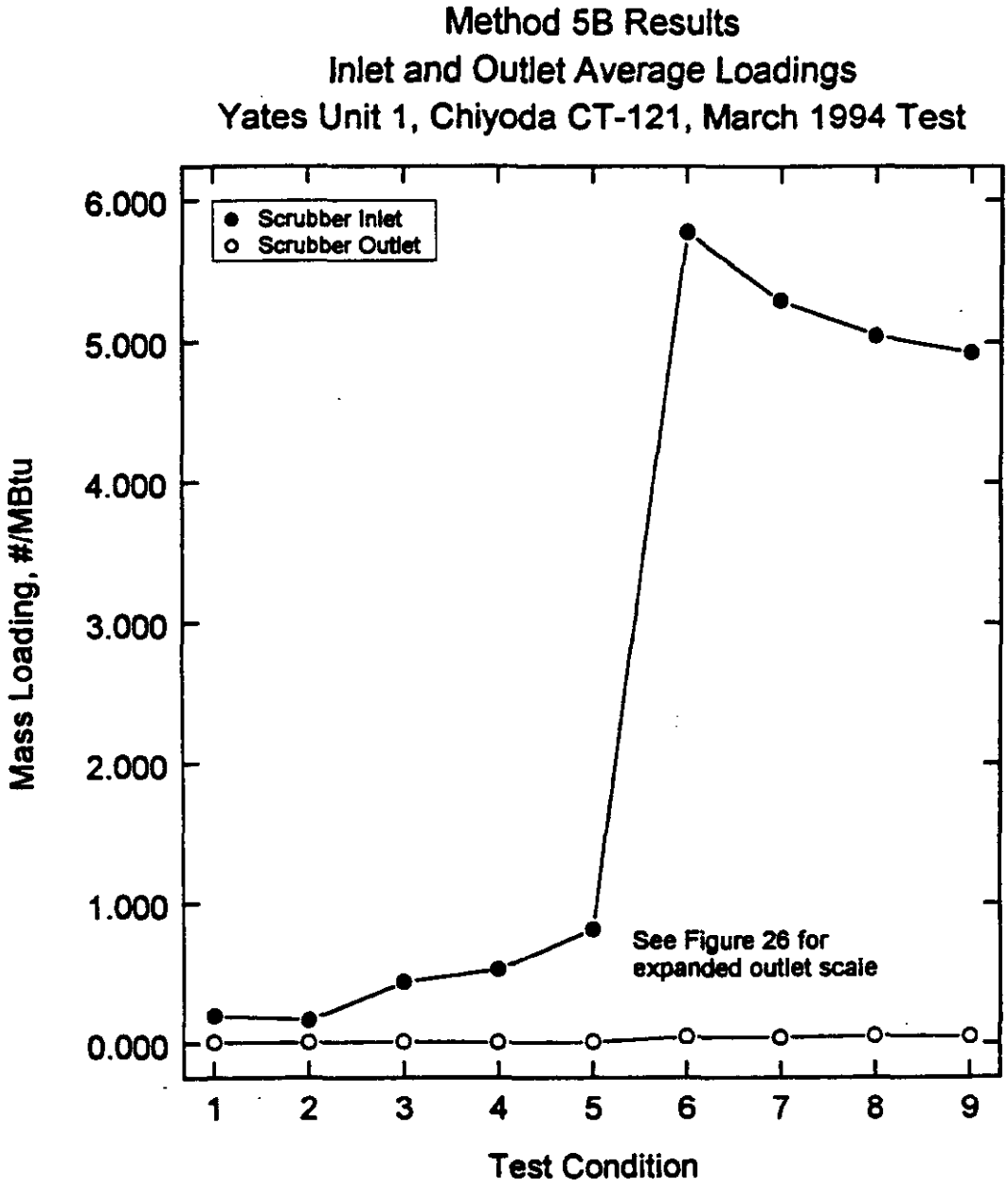

Figure 24. Inlet and Outlet Mass Loadings vs Test Condition for Chiyoda Scrubber Test Program. March 1994.

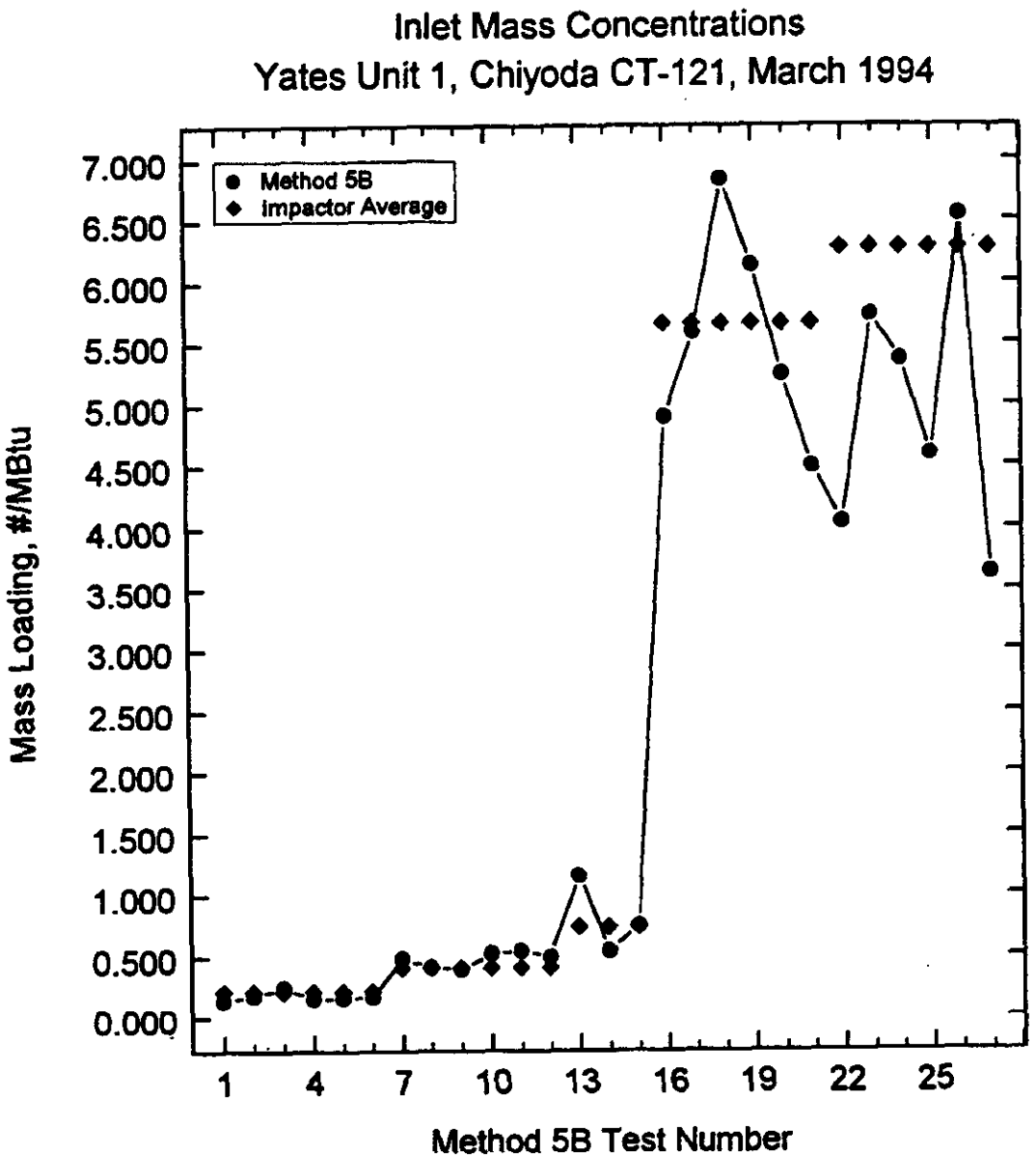

Figure 25. Mass Loading vs Inlet Method 5B Individual Test. Chiyoda Scrubber Test Program, March 1994.

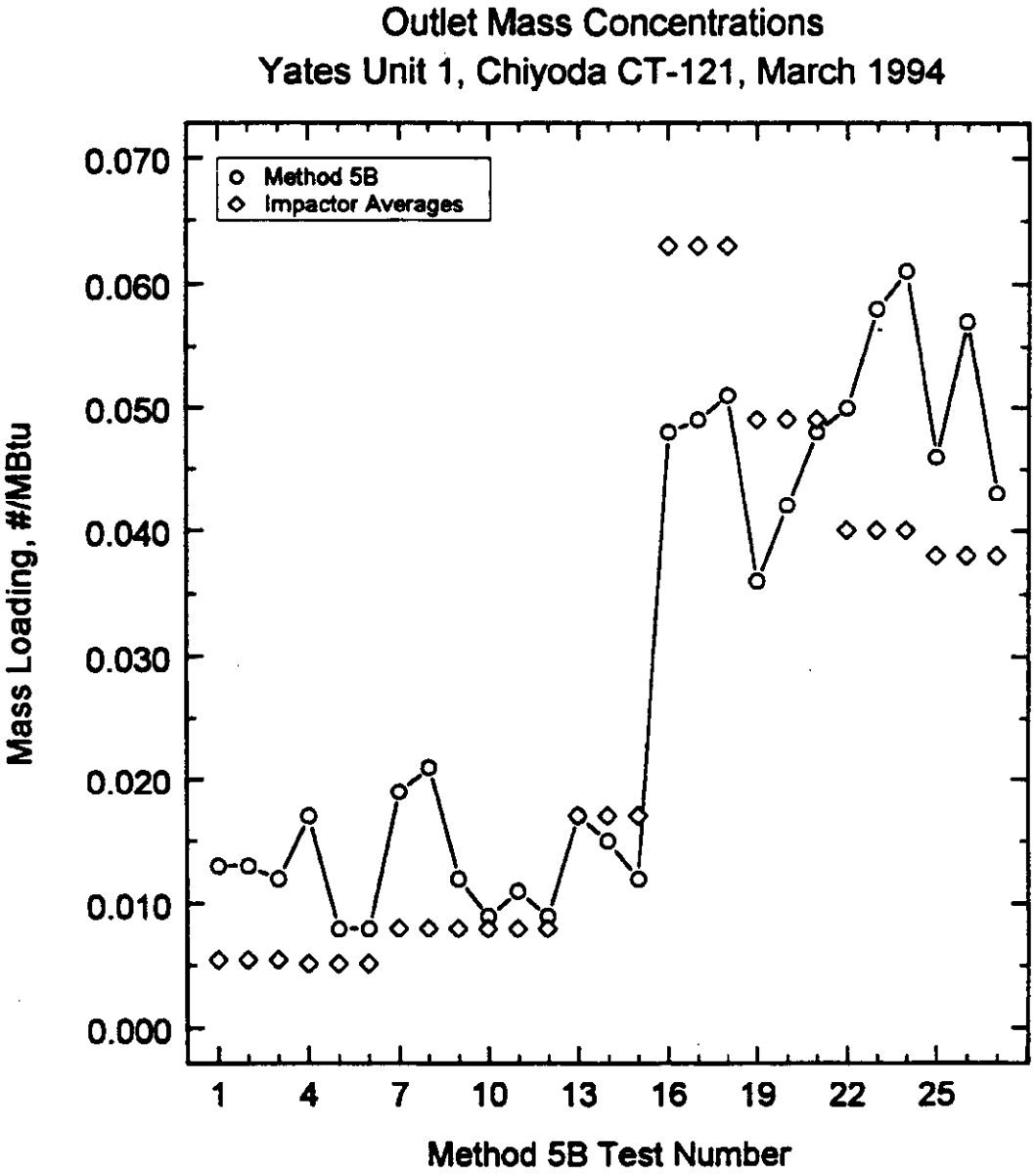

Figure 26. Mass Loading vs Outlet Method 5B Individual Test. Chiyoda Scrubber Test Program, March 1994.

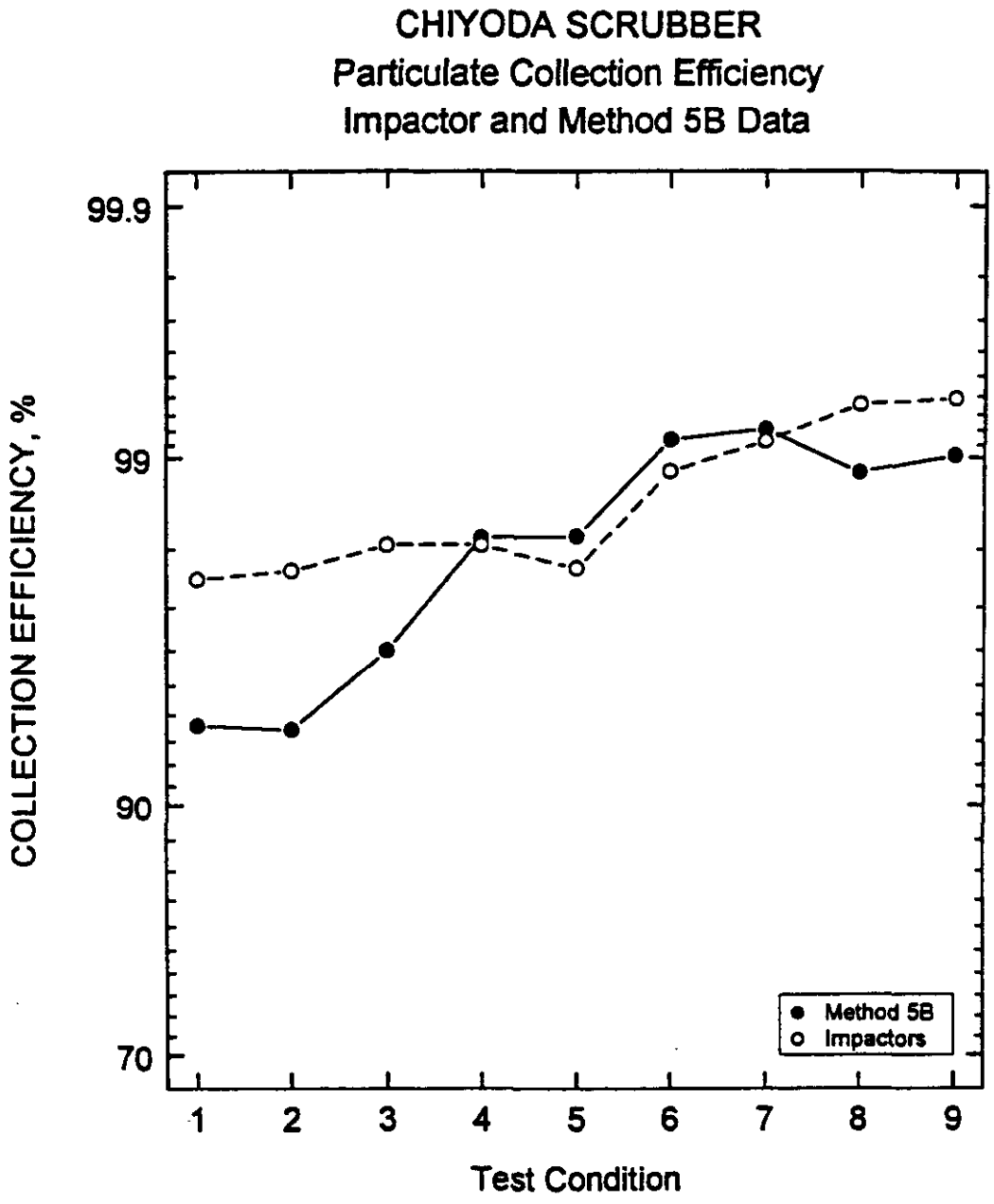

Figure 27. Particulate Collection Efficiency vs Test Condition for Chiyoda Scrubber Test Program, March 1994. Method 5B and Impactor Results.

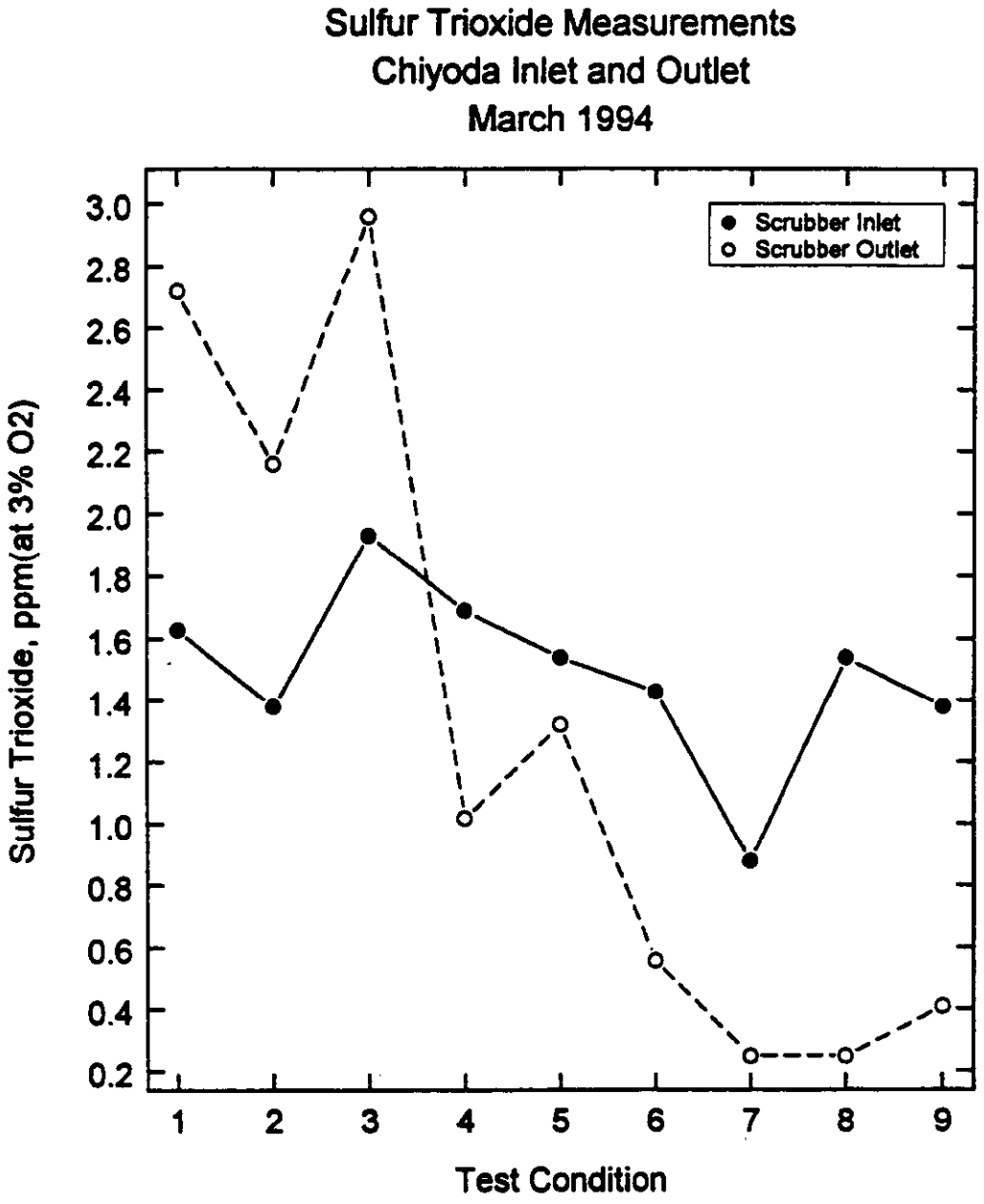

Figure 28. Daily Averages of Inlet and Outlet Sulfur Trioxide Measurements for Each Test Condition.

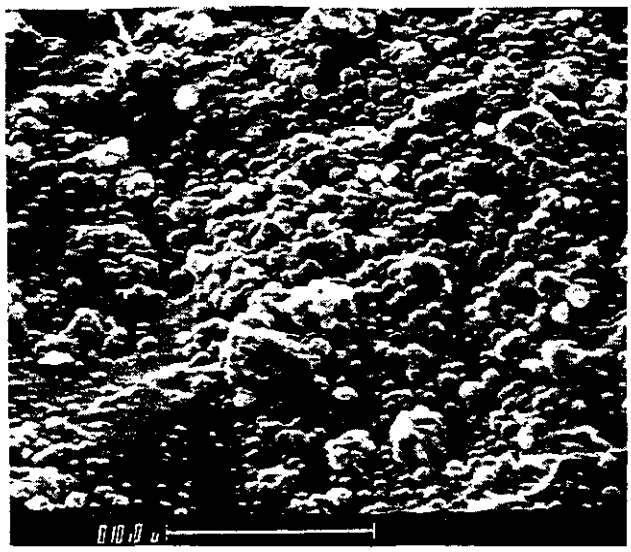

STAGE 3, D_{50} = 3.30 μm

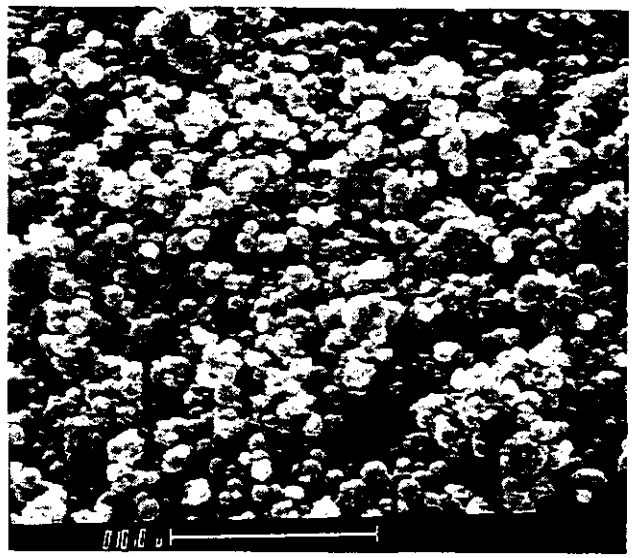

STAGE 4, D_{50} = 1.88 μm

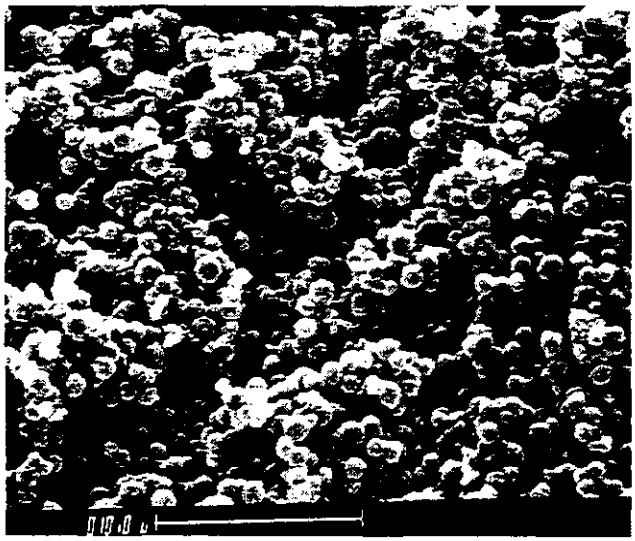

STAGE 5, D_{50} = 1.12 μm

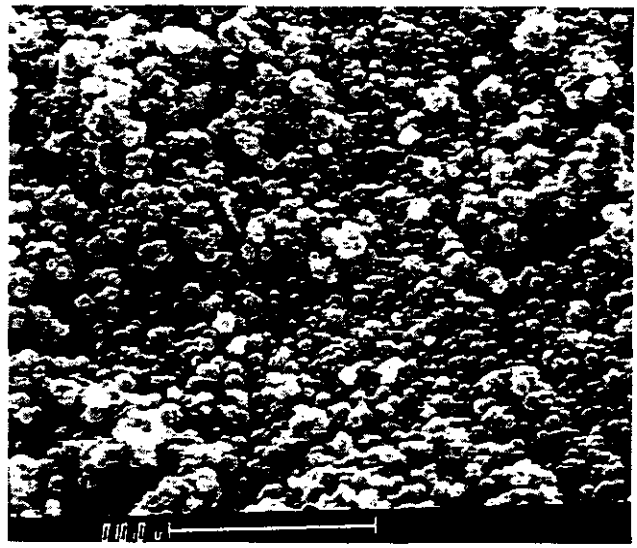

STAGE 6, D_{50} = 0.54 μm

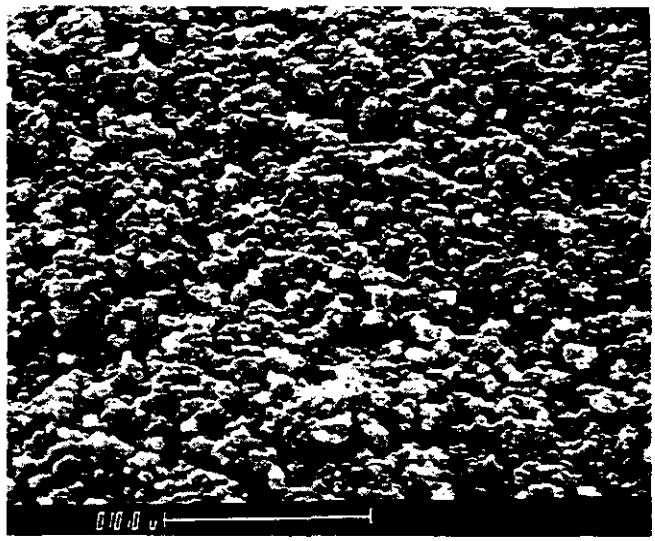

STAGE 7, D_{50} = 0.19 μm

Figure 29. SEM Photographs of Outlet Impactor Substrates, Test Condition 4, March 20, 1994.

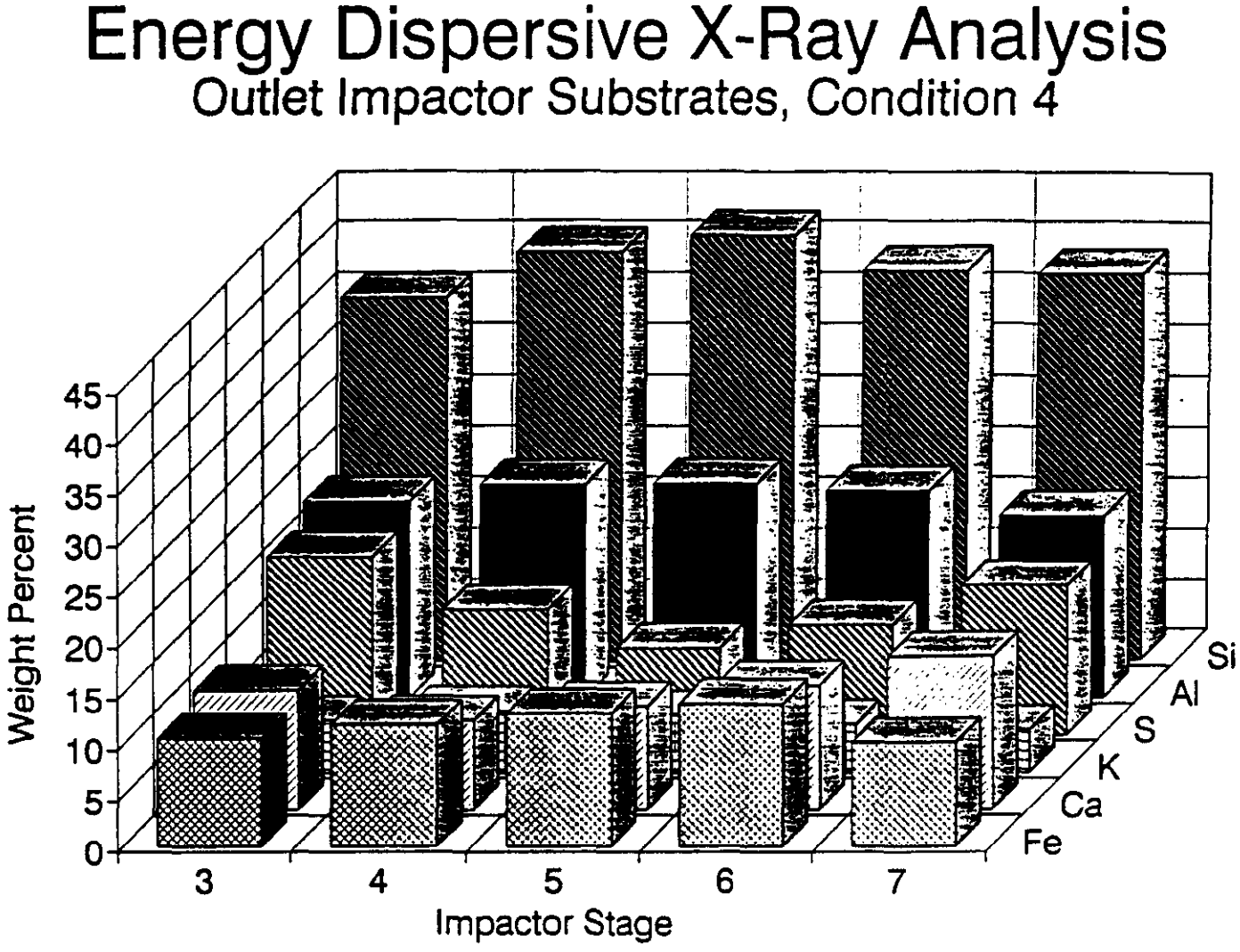

Figure 30. Weight Percent vs Impactor Stage for Selected Elements. Outlet Impactor from Test Condition 4, March 20, 1994.

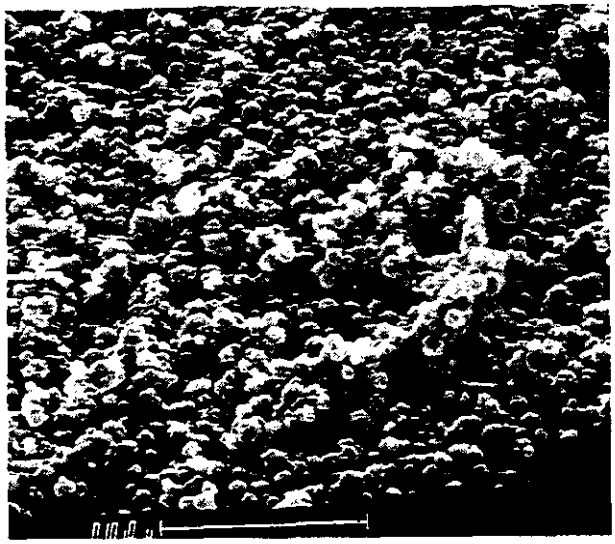

STAGE 3, D_{50} = 3.29 μm

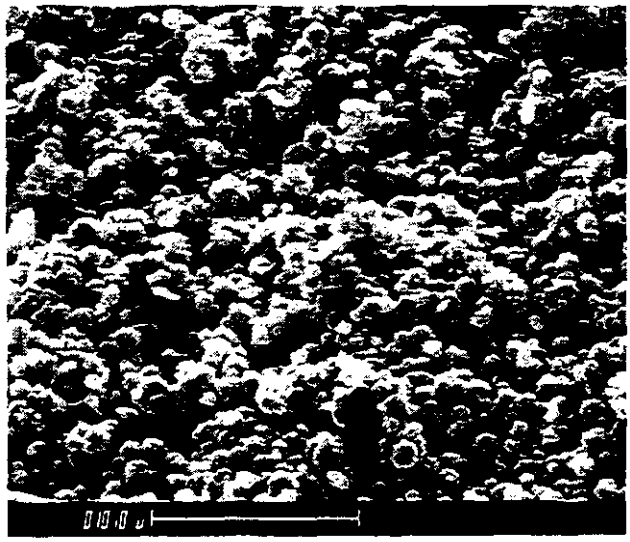

STAGE 4, D_{50} = 1.88 μm

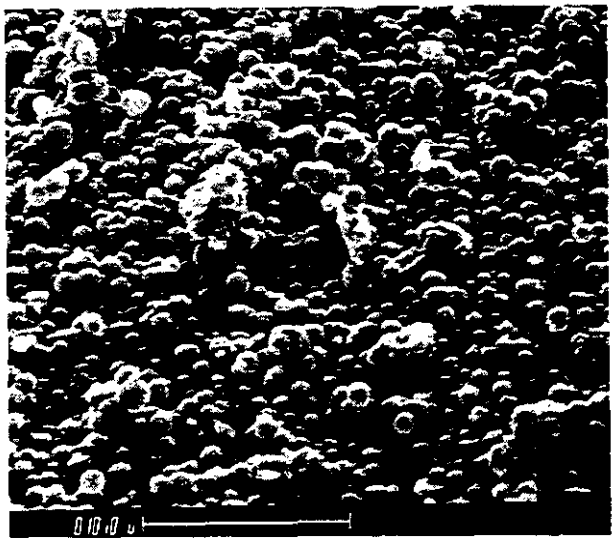

STAGE 5, D_{50} = 1.12 μm

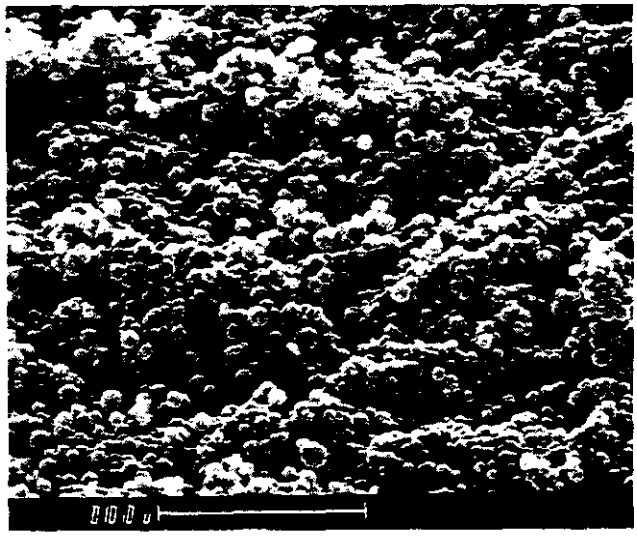

STAGE 6, D_{50} = 0.54 μm

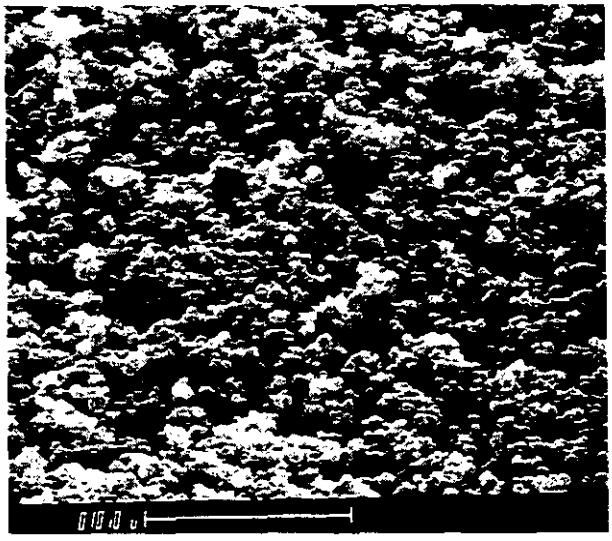

STAGE 7, D_{50} = 0.19 μm

Figure 31. SEM Photographs of Outlet Impactor Substrates, Test Condition 5, March 22, 1994.

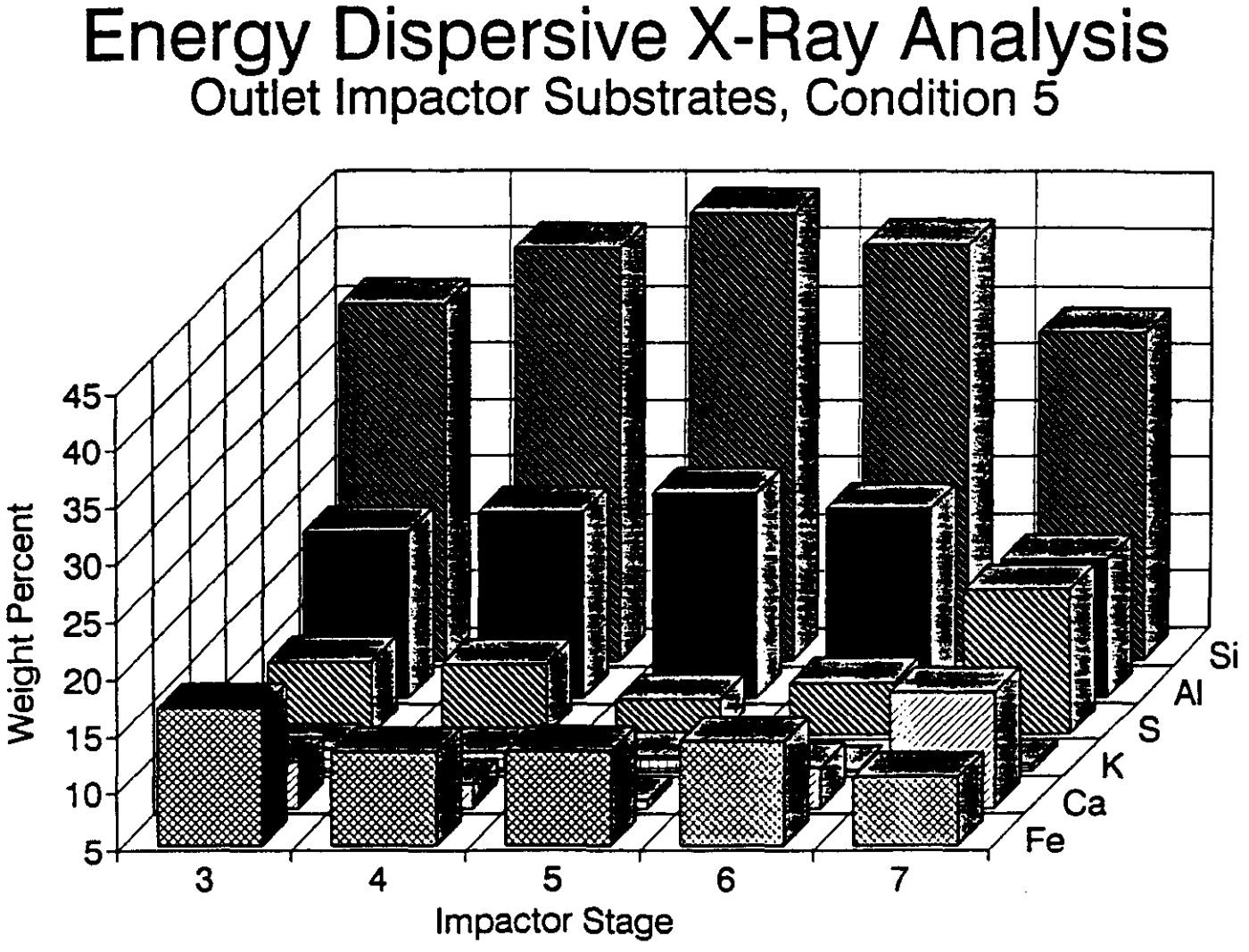

Figure 32. Weight Percent vs Impactor Stage for Selected Elements. Outlet Impactor from Test Condition 5, March 22, 1994.

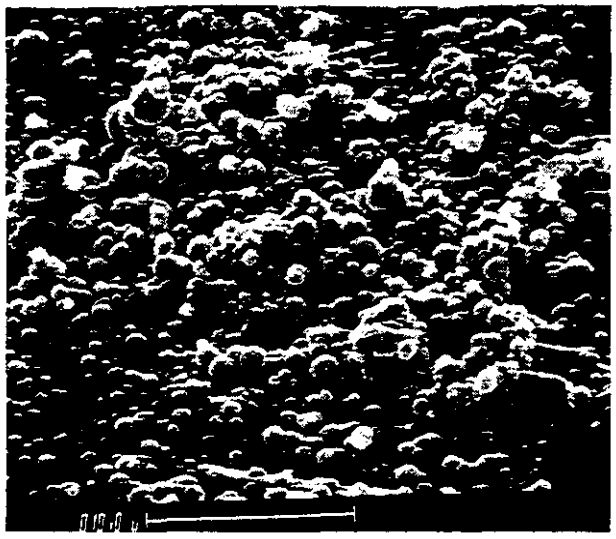

STAGE 3, D_{50} = 3.40 μm

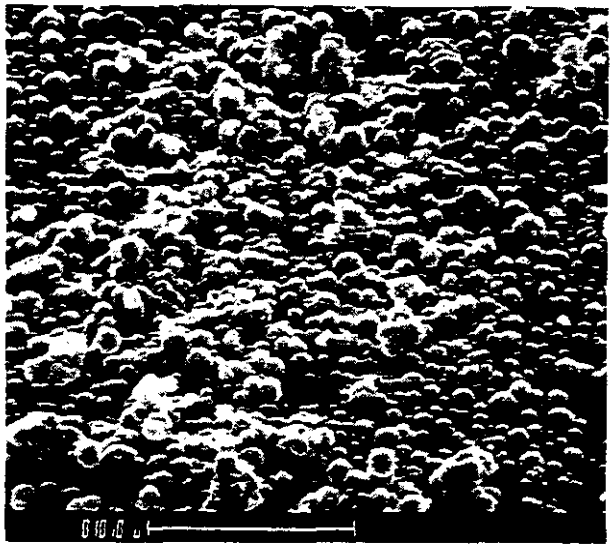

STAGE 4, D_{50} = 1.96 μm

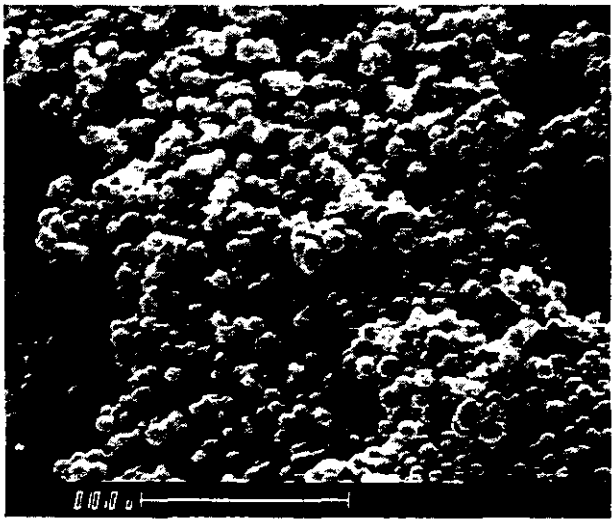

STAGE 5, D_{50} = 1.18 μm

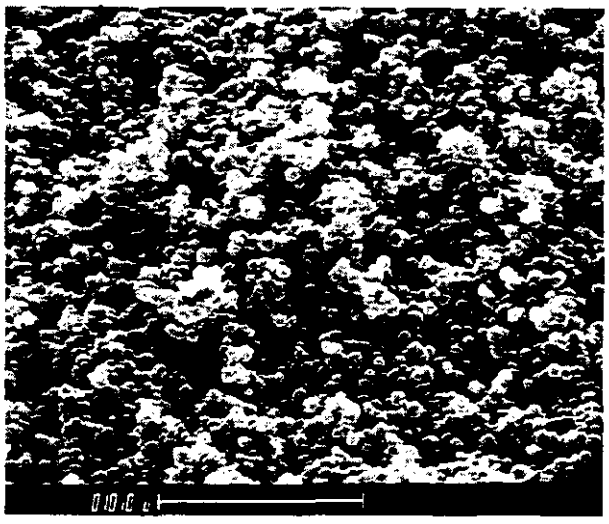

STAGE 6, D_{50} = 0.57 μm

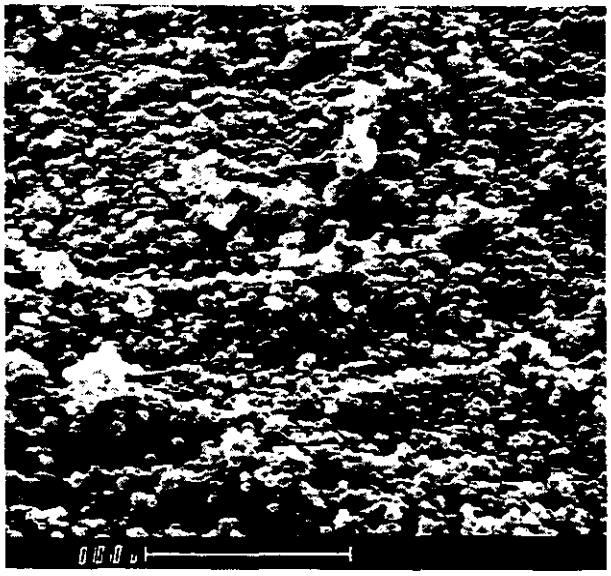

STAGE 7, D_{50} = 0.21 μm

Figure 33. SEM Photographs of Outlet Impactor Substrates, Test Condition 7, March 25, 1994.

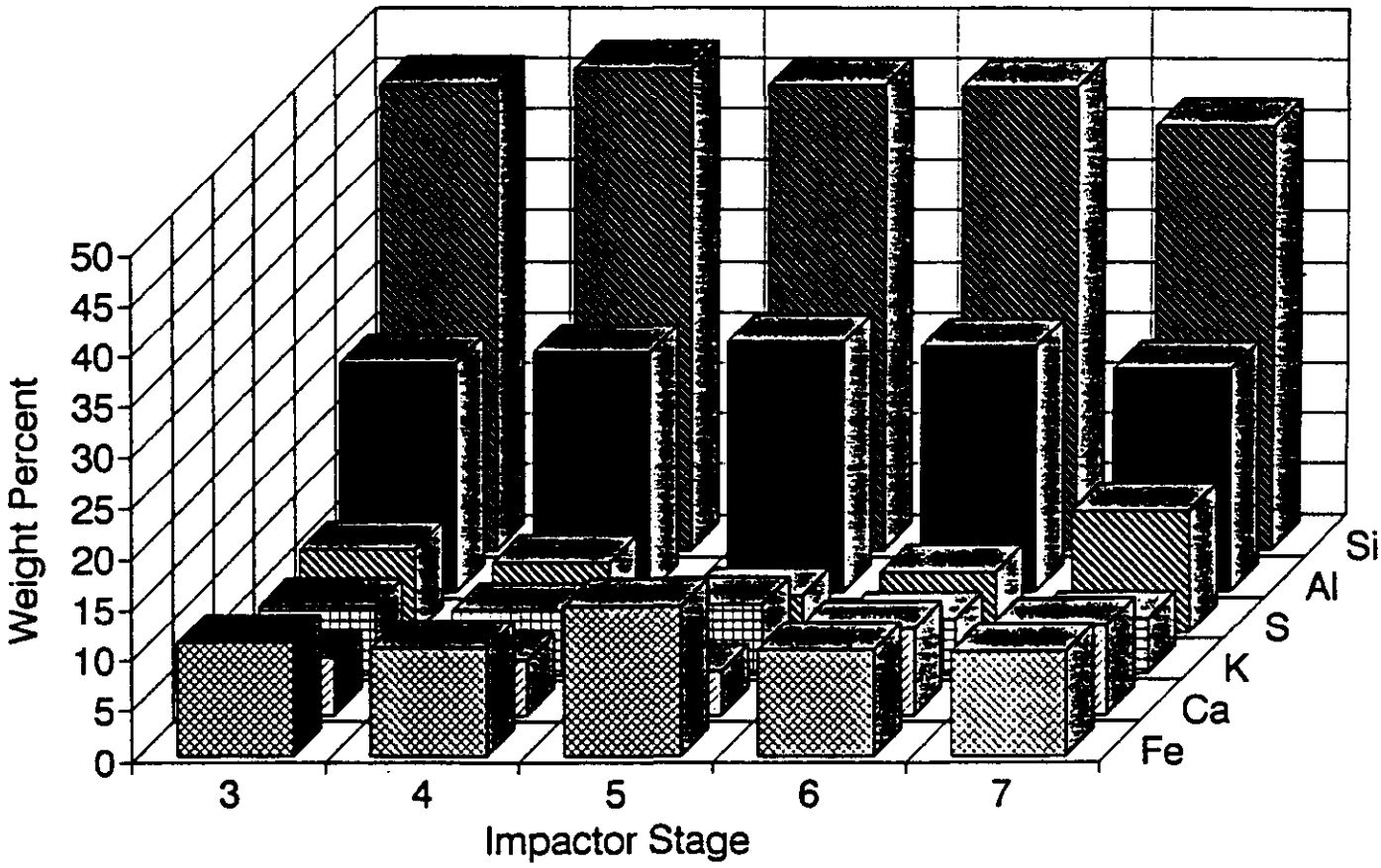

Figure 34. Weight-Percent vs Impactor Stage for Selected Elements. Outlet Impactor from Test Condition 7. March 25, 1994.

APPENDIX

Impactor Graphs

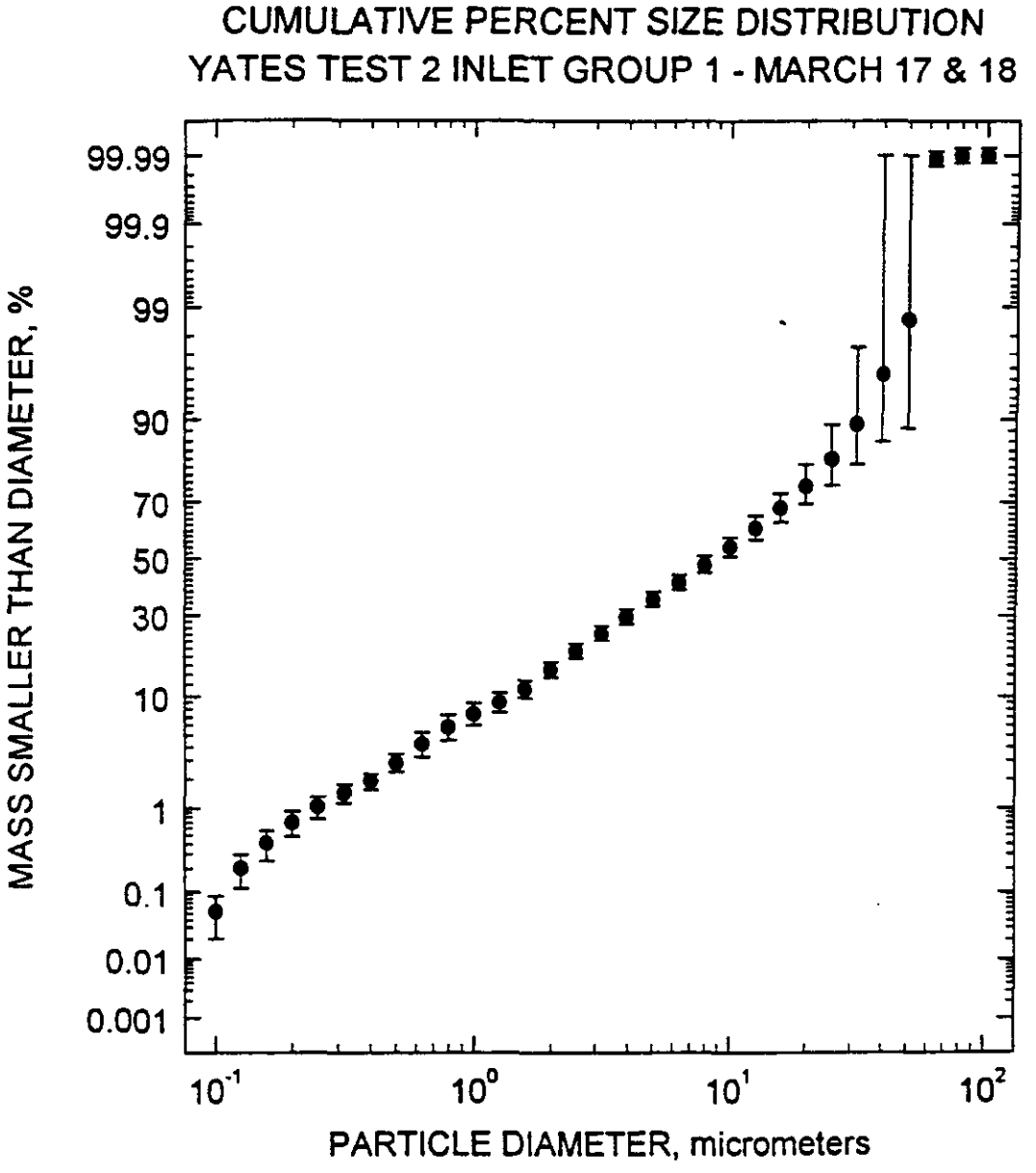

Figure A1. Cumulative Percent vs Particle Diameter, Inlet Impactor Grouping 1 - March 17 & 18, 1994.

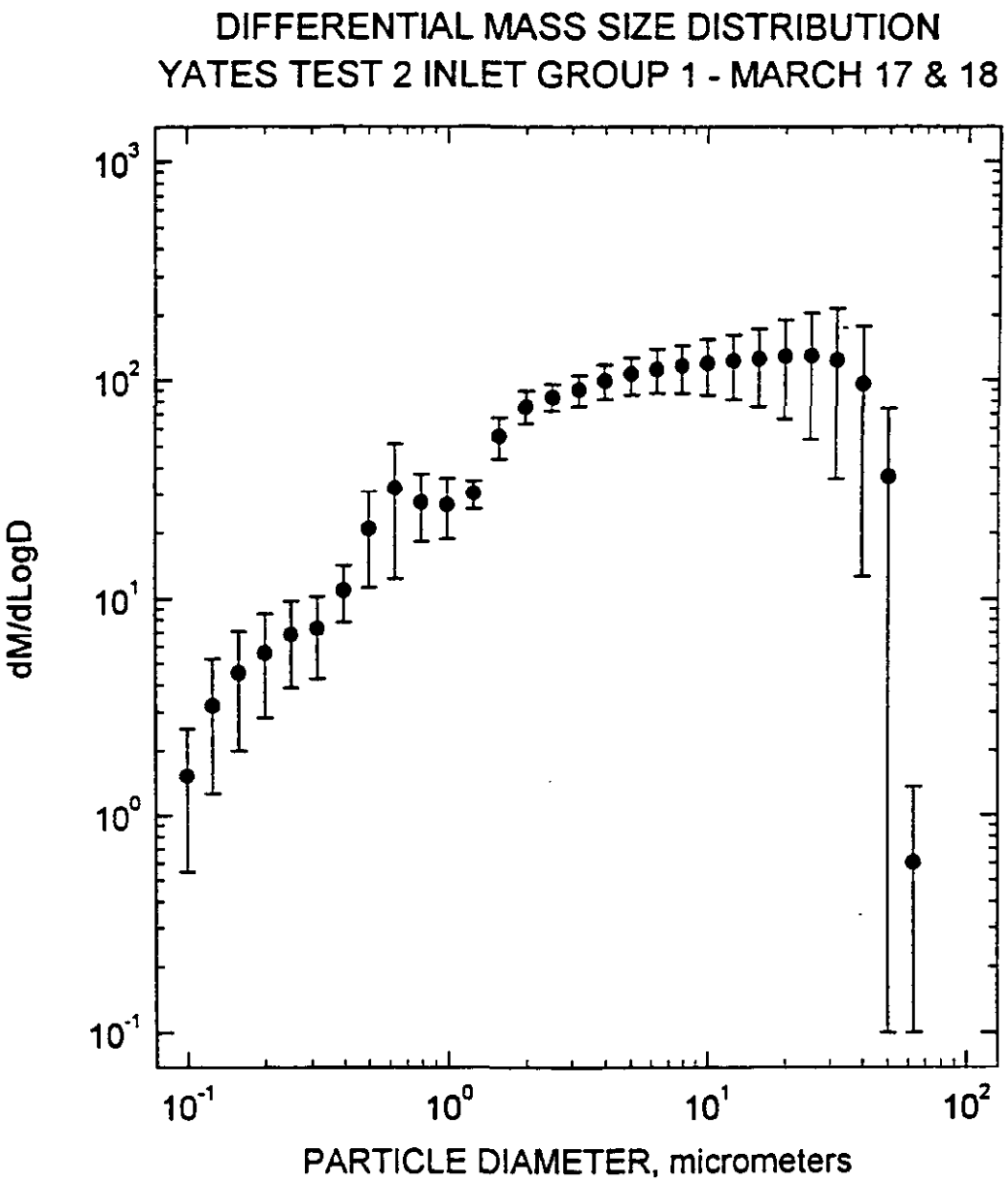

Figure A2. Differential Mass vs Particle Diameter, Inlet Impactor Grouping 1 - March 17 & 18, 1994.

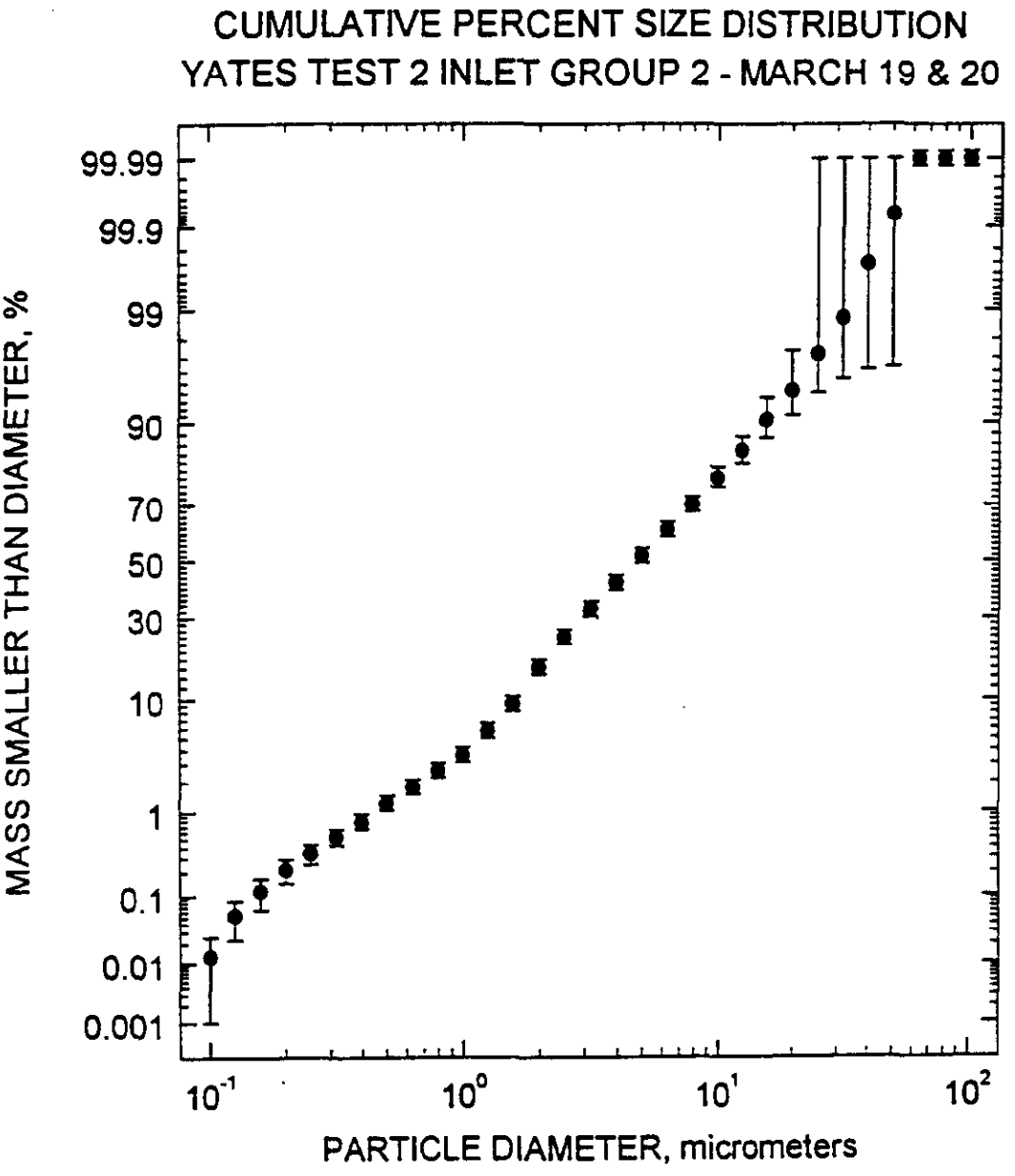

Figure A3. Cumulative Percent vs Particle Diameter, Inlet Impactor Grouping 2 - March 19 & 20, 1994.

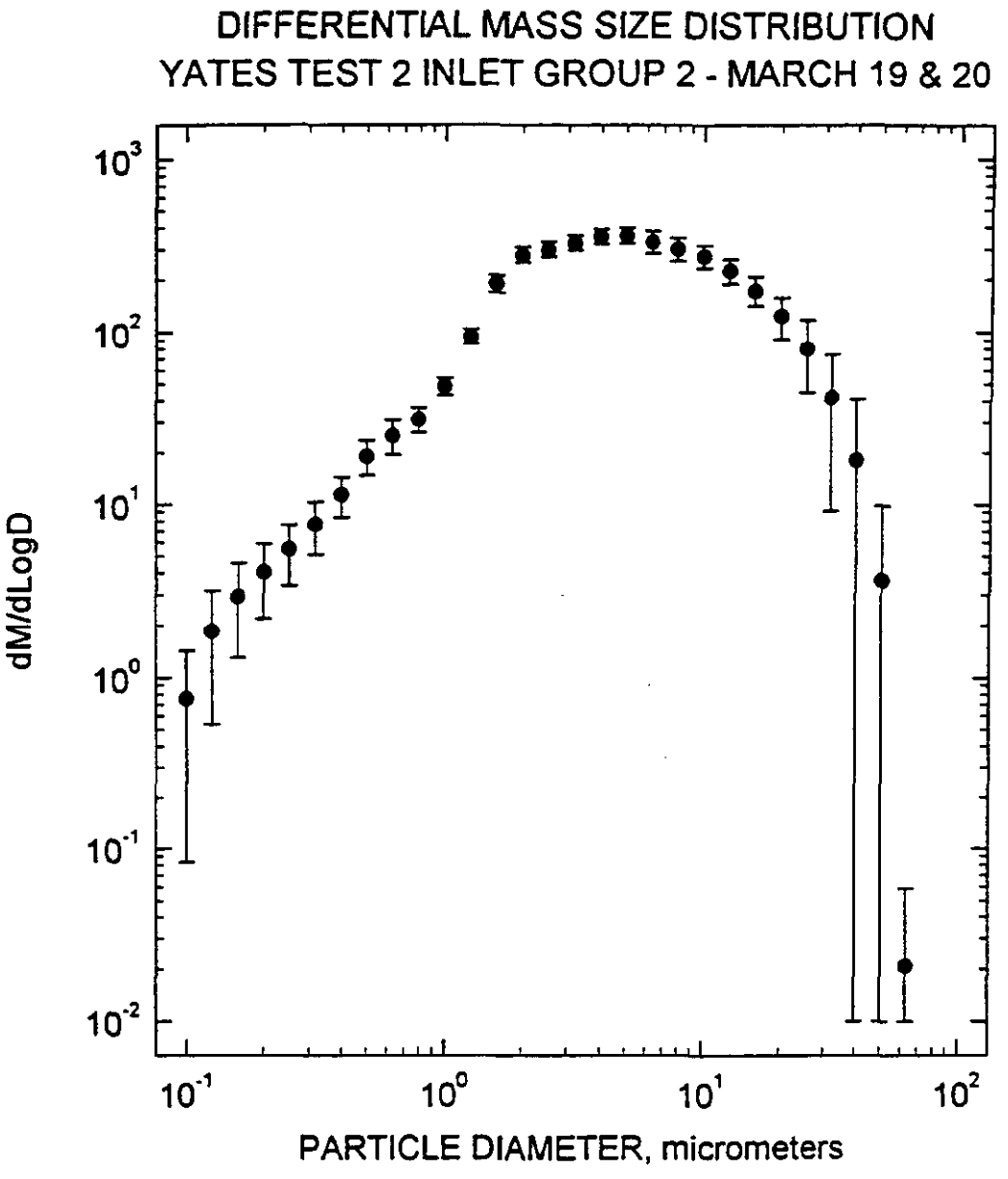

Figure A4. Differential Mass vs Particle Diameter, Inlet Impactor Grouping 2- March 19 & 20, 1994.

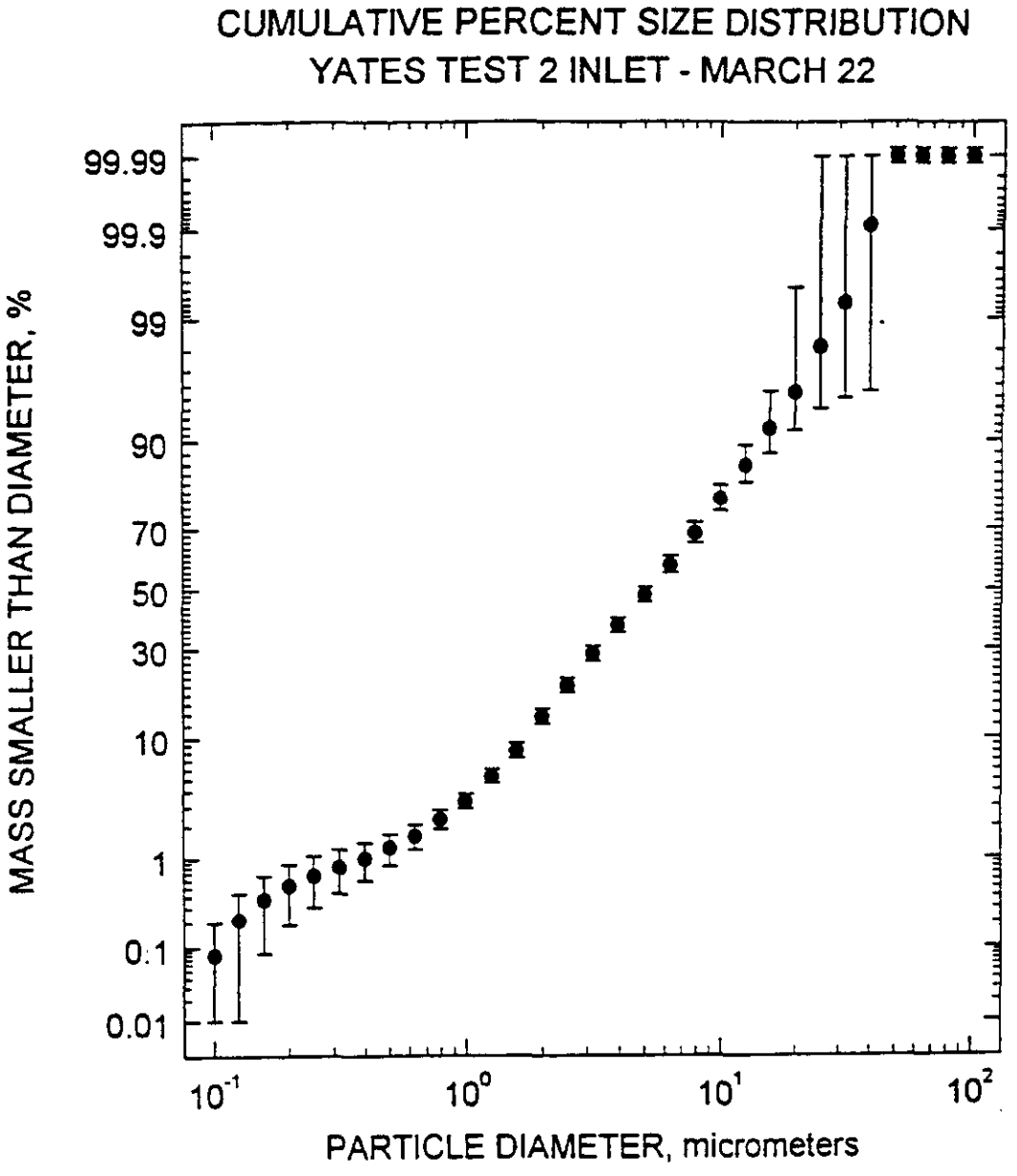

Figure A5. Cumulative Percent vs Particle Diameter, Inlet Impactor Grouping 3 - March 22, 1994.

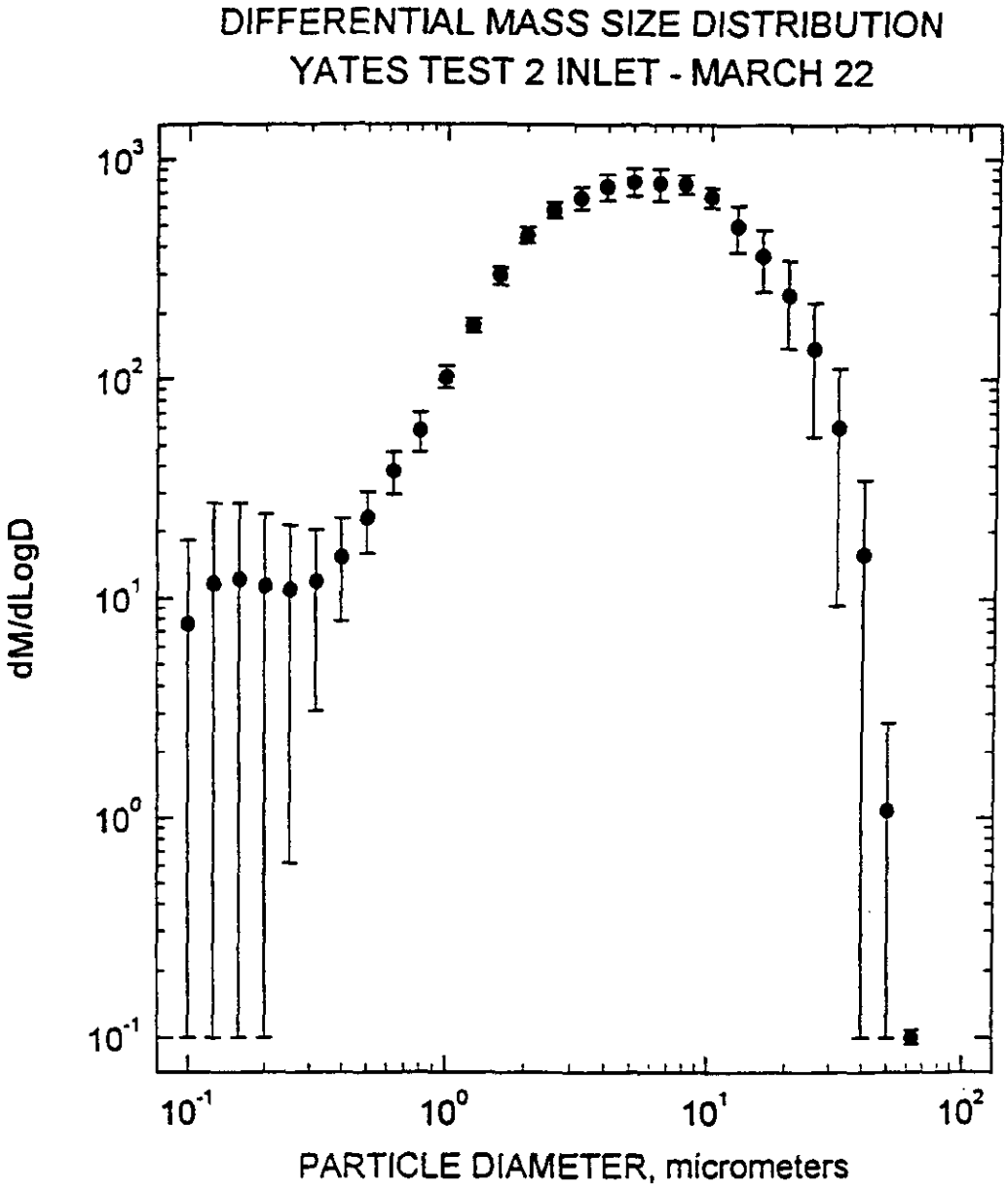

Figure A6. Differential Mass vs Particle Diameter, Inlet Impactor Grouping 3 - March 22, 1994.

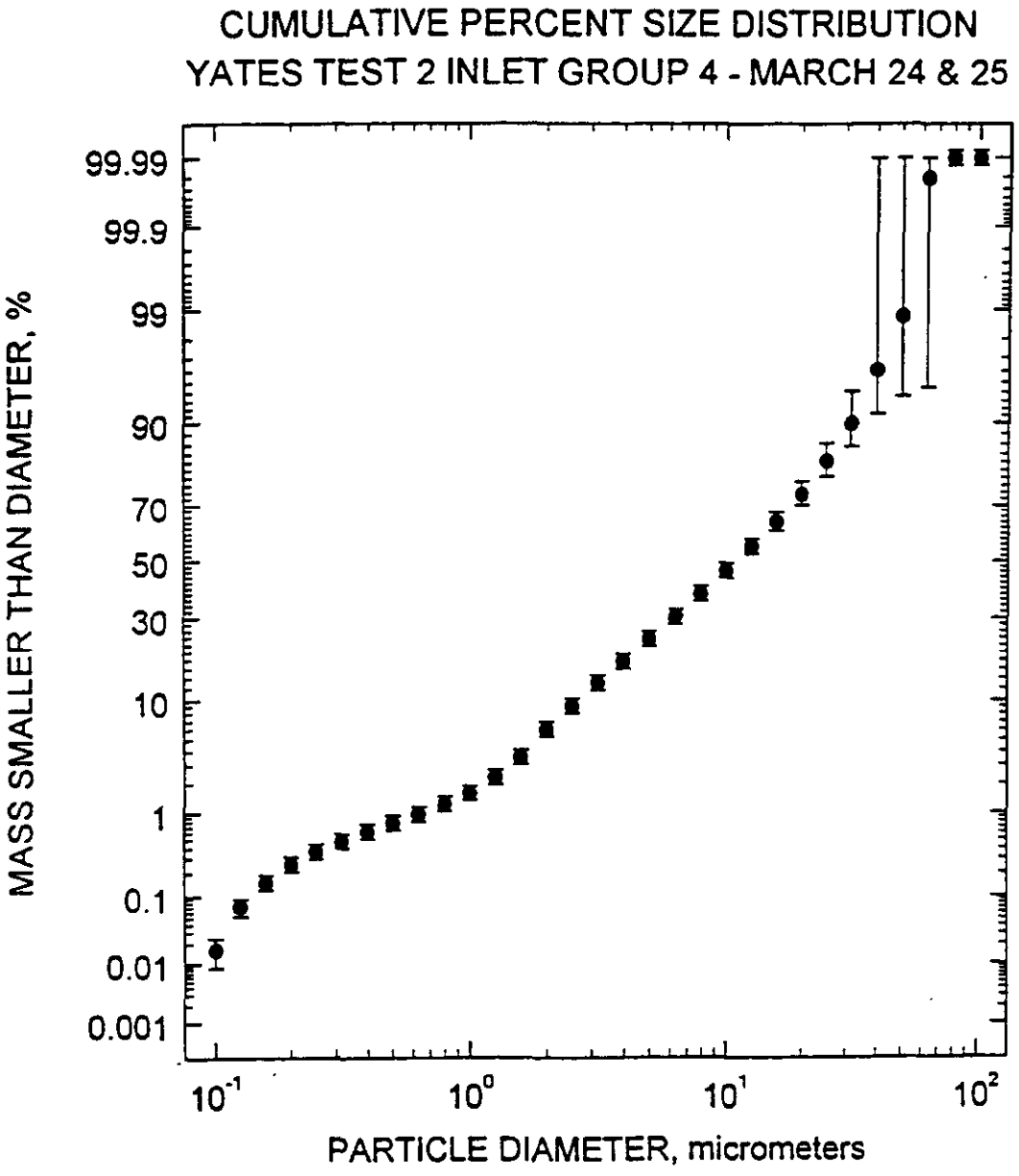

Figure A7. Cumulative Percent vs Particle Diameter, Inlet Impactor Grouping 4 - March 24 & 25, 1994.

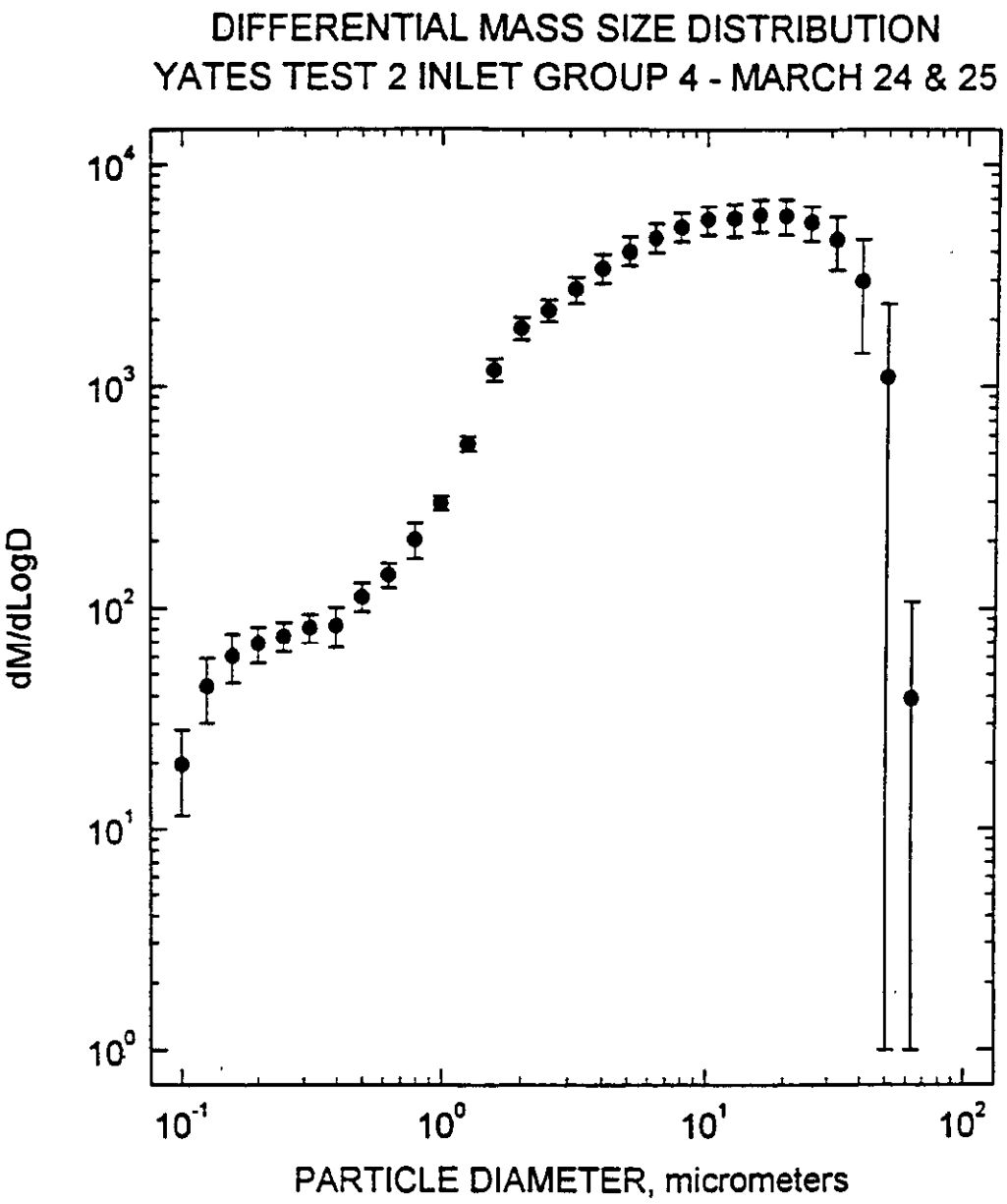

Figure A8. Differential Mass vs Particle Diameter, Inlet Impactor Grouping 4 - March 24 & 25, 1994.

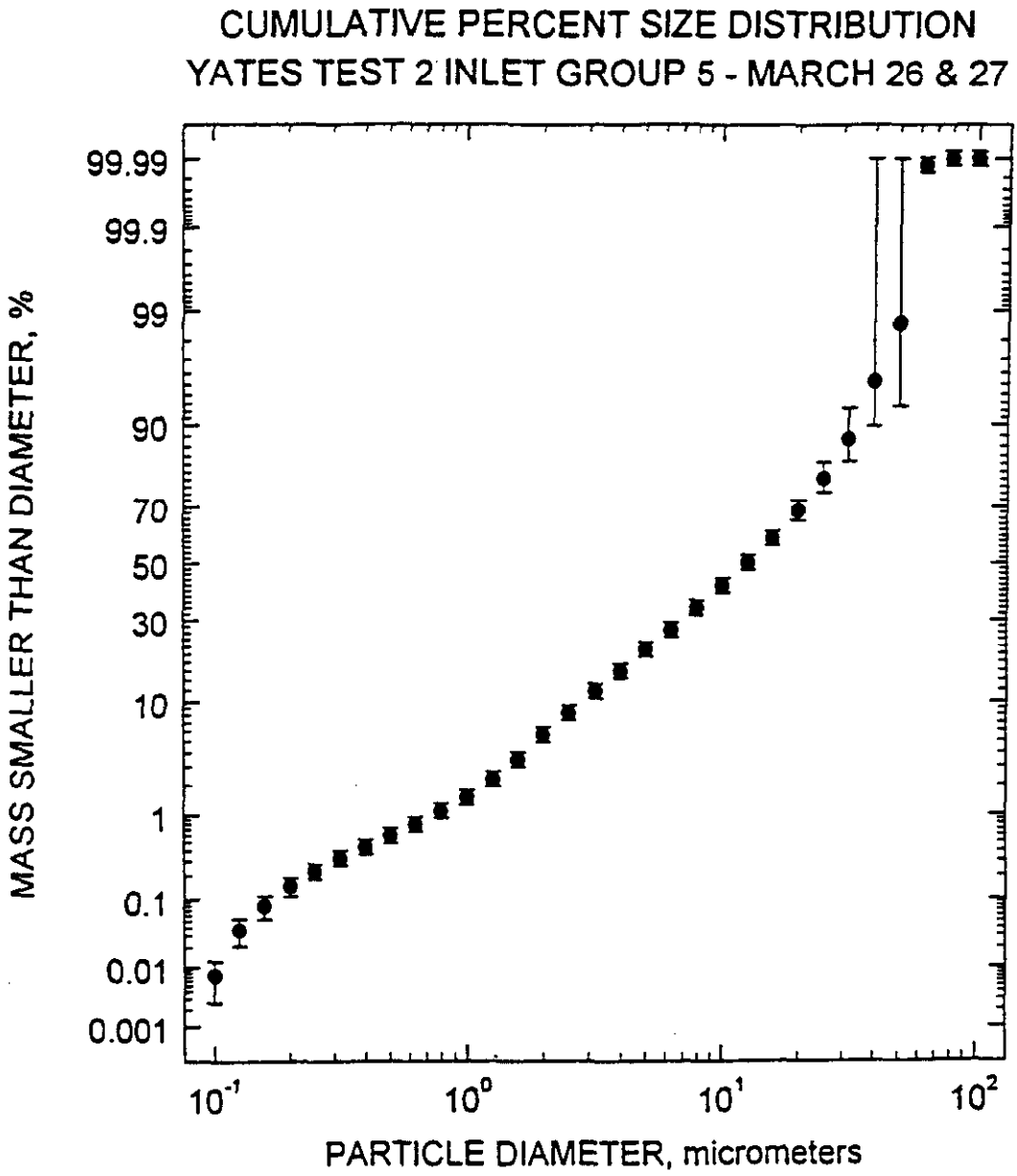

Figure A9. Cumulative Percent vs Particle Diameter, Inlet Impactor Grouping 5 - March 26 & 27, 1994.

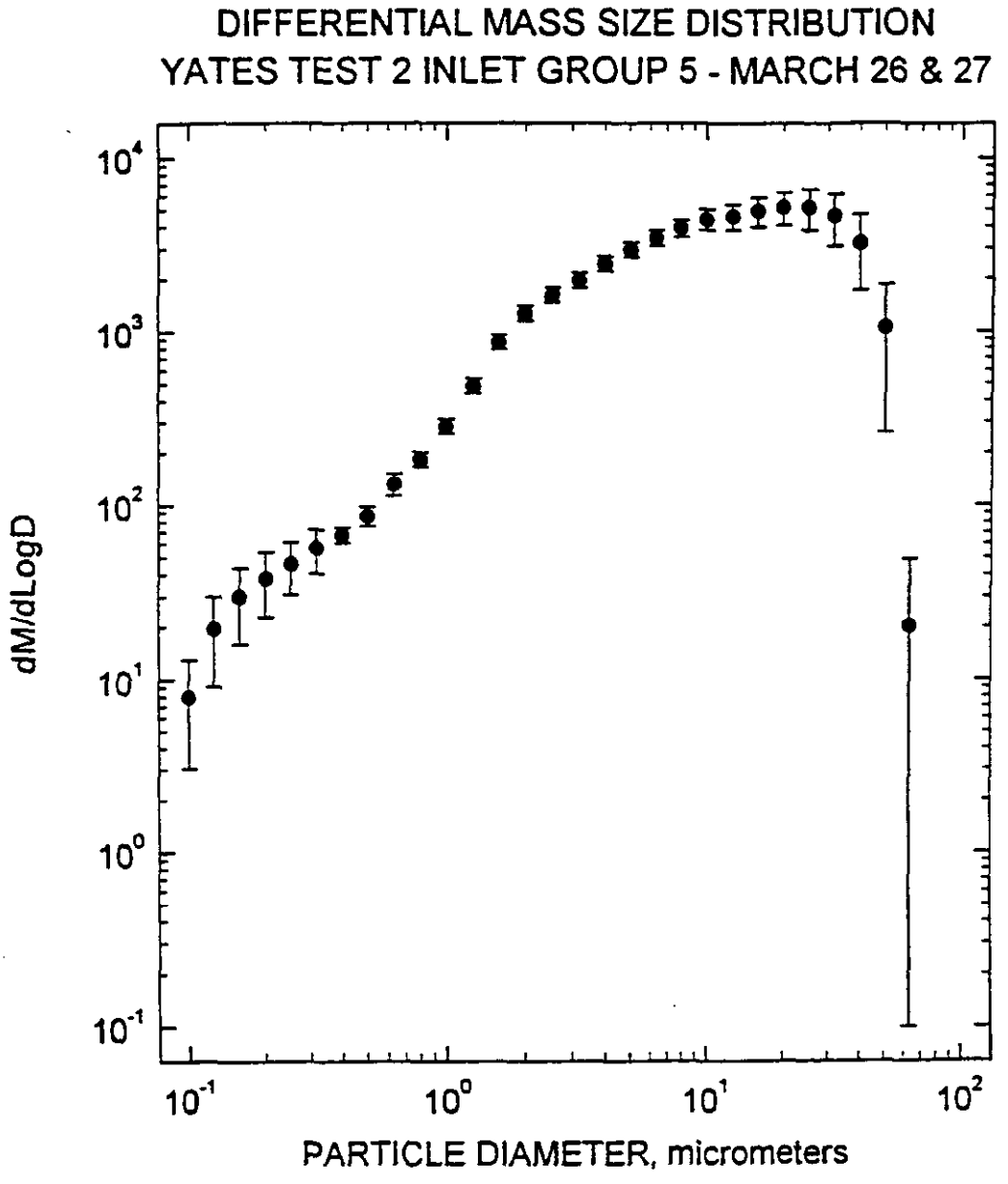

Figure A10. Differential Mass vs Particle Diameter, Inlet Impactor Grouping 5 - March 26 & 27, 1994.

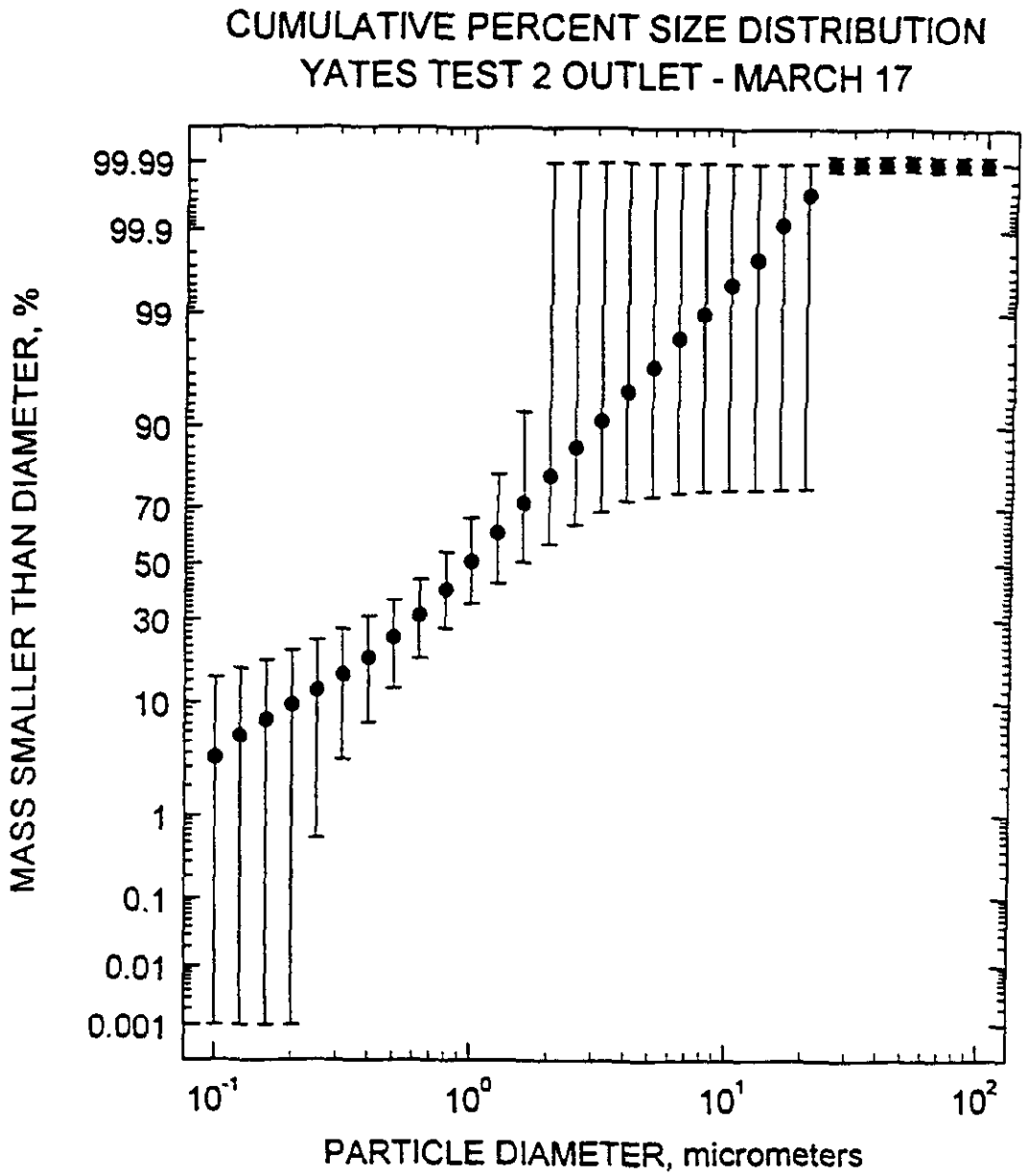

Figure A11. Cumulative Percent vs Particle Diameter, Outlet Impactors - March 17, 1994.

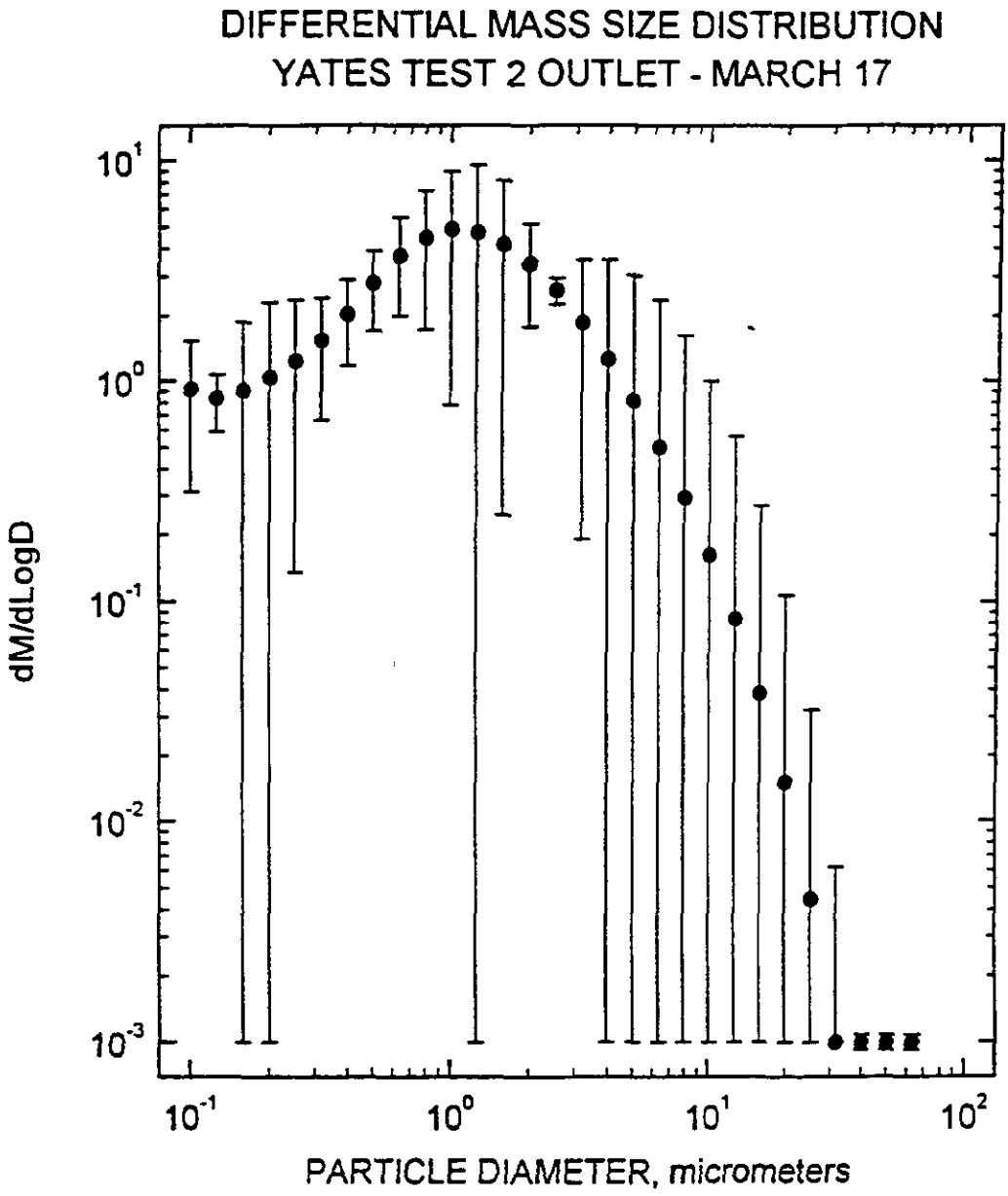

Figure A12. Differential Mass vs Particle Diameter, Outlet Impactors - March 17, 1994.

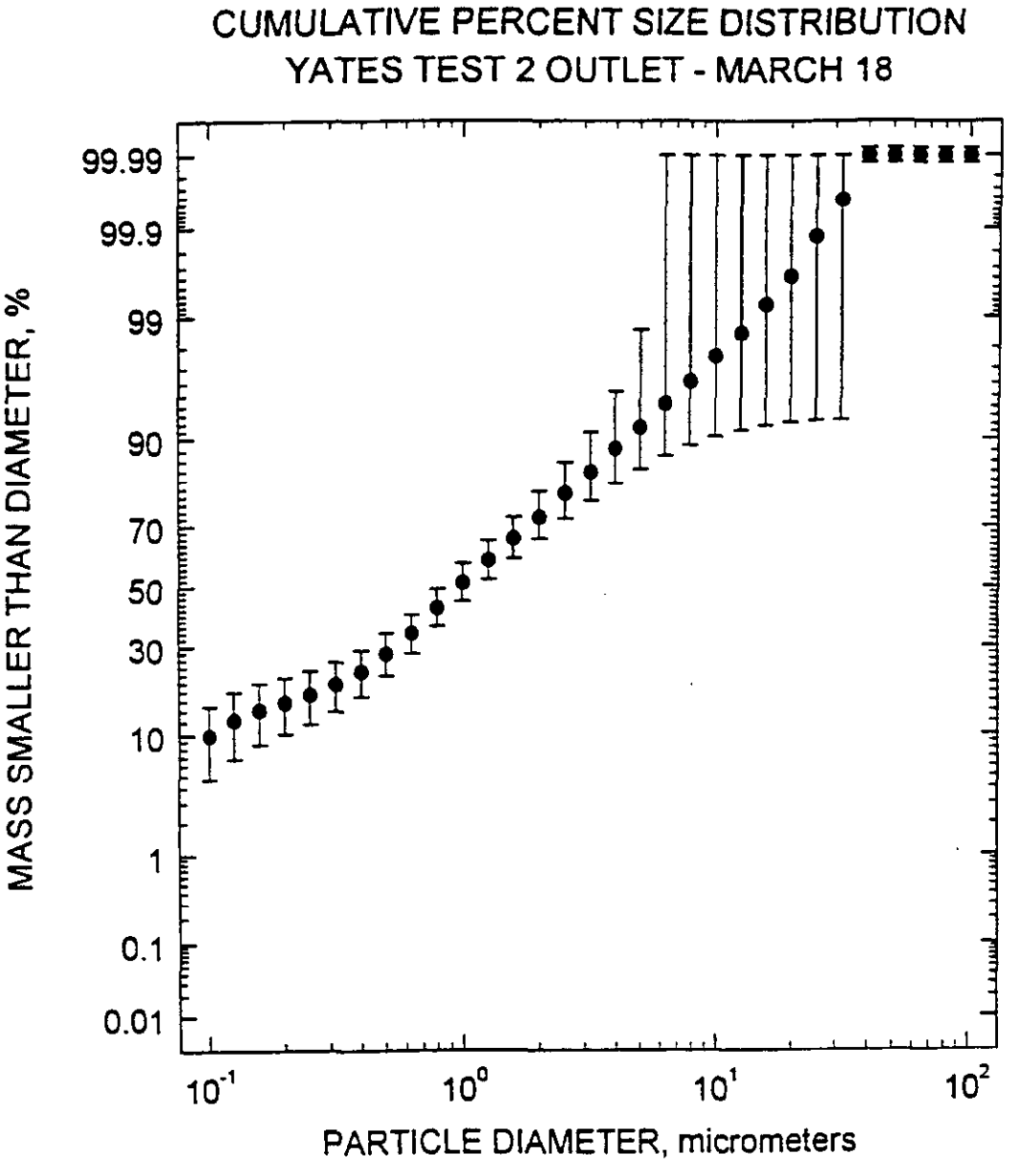

Figure A13. Cumulative Percent vs Particle Diameter, Outlet Impactors - March 18, 1994.

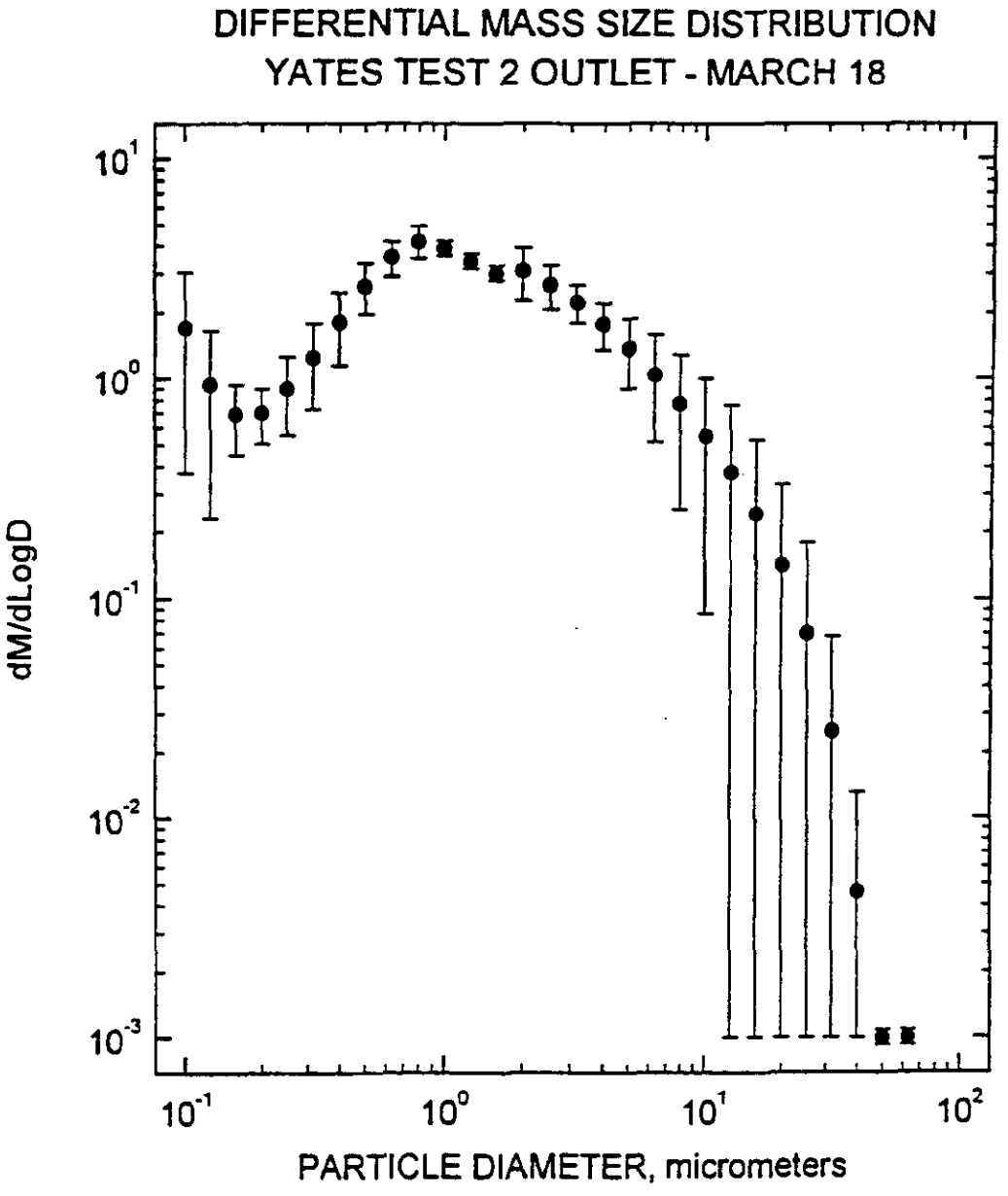

Figure A14. Differential Mass vs Particle Diameter, Outlet Impactors - March 18, 1994.

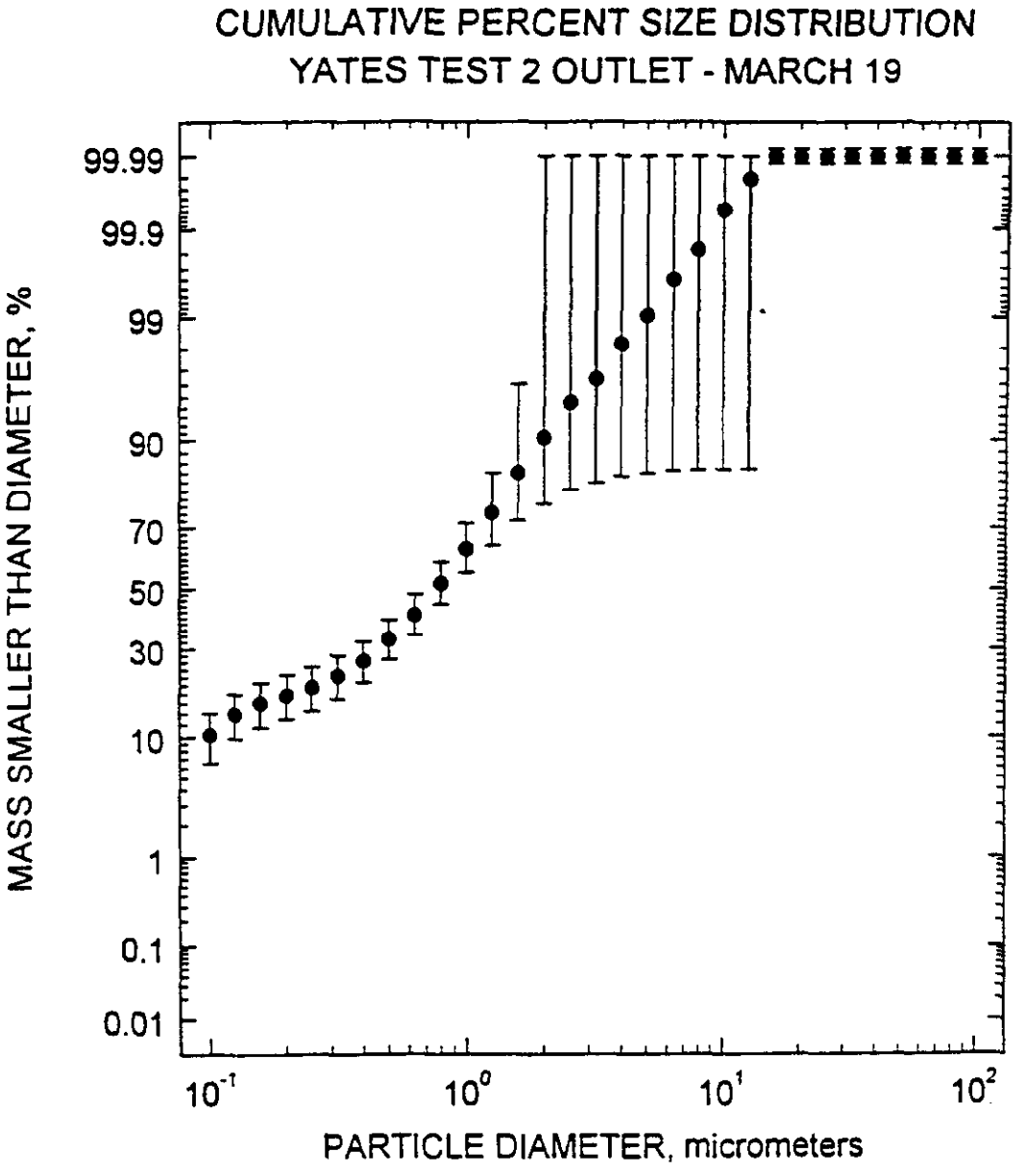

Figure A15. Cumulative Percent vs Particle Diameter, Outlet Impactors - March 19, 1994.

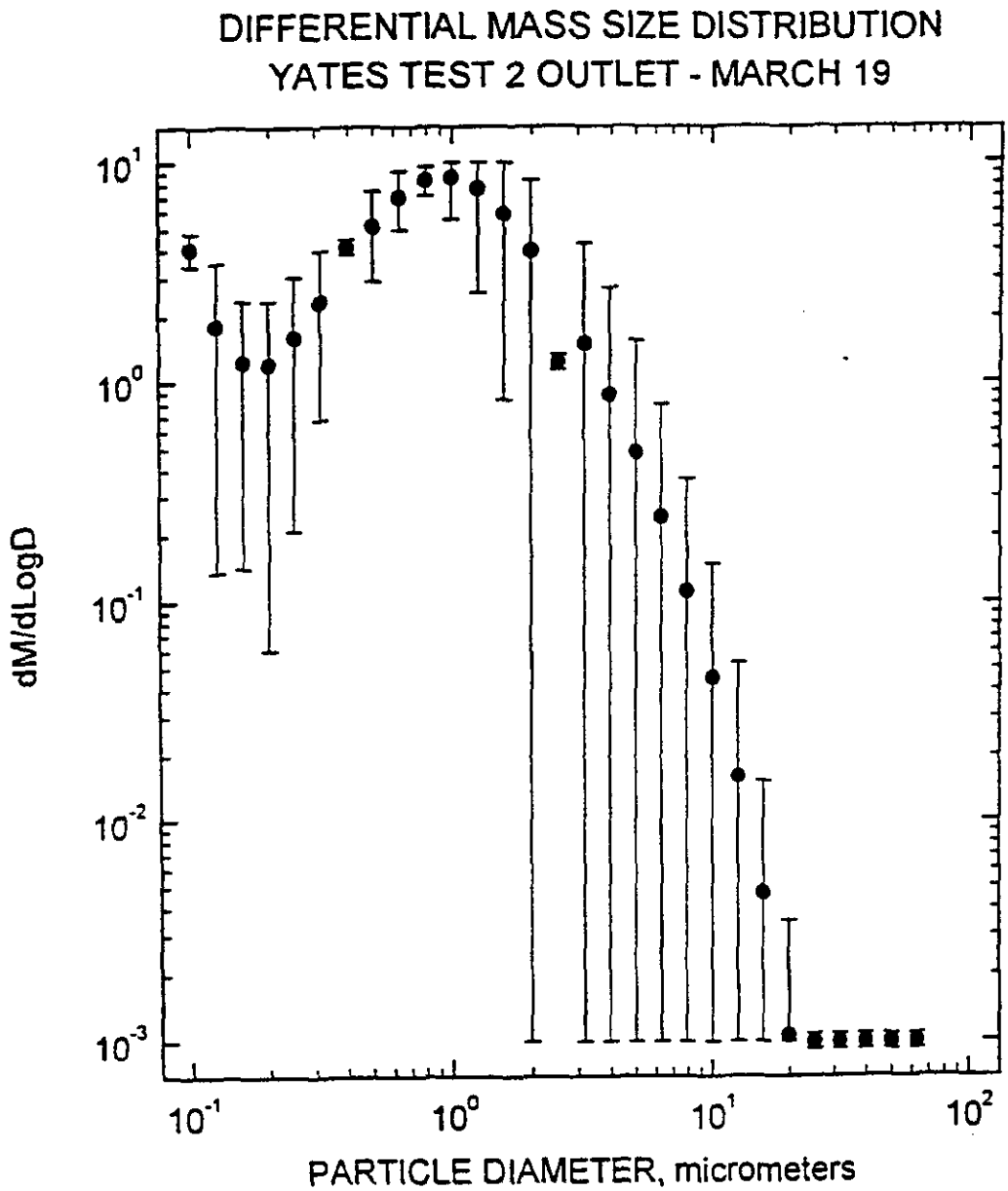

Figure A16. Differential Mass vs Particle Diameter, Outlet Impactors - March 19, 1994.

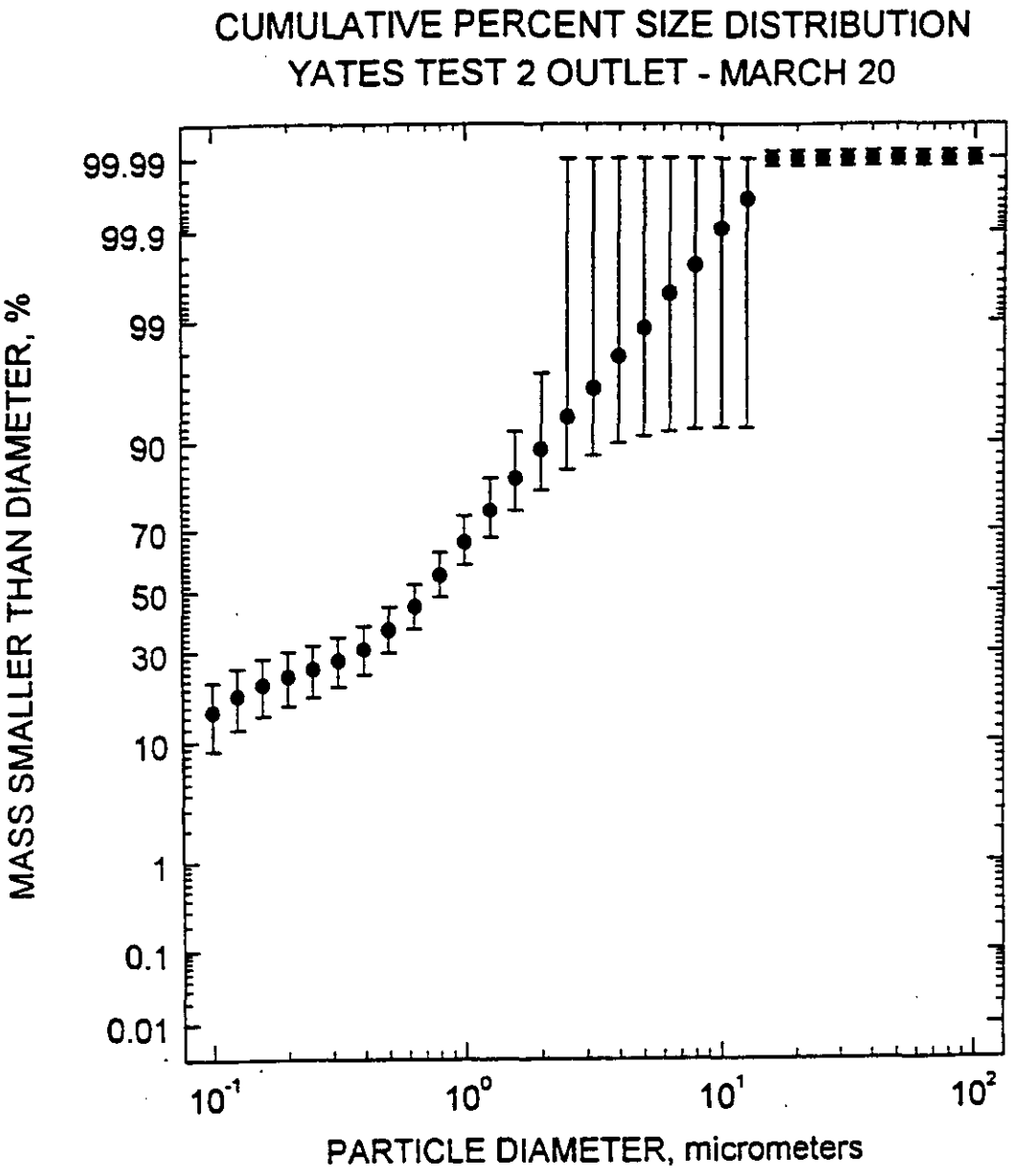

Figure A17. Cumulative Percent vs Particle Diameter, Outlet Impactors - March 20, 1994.

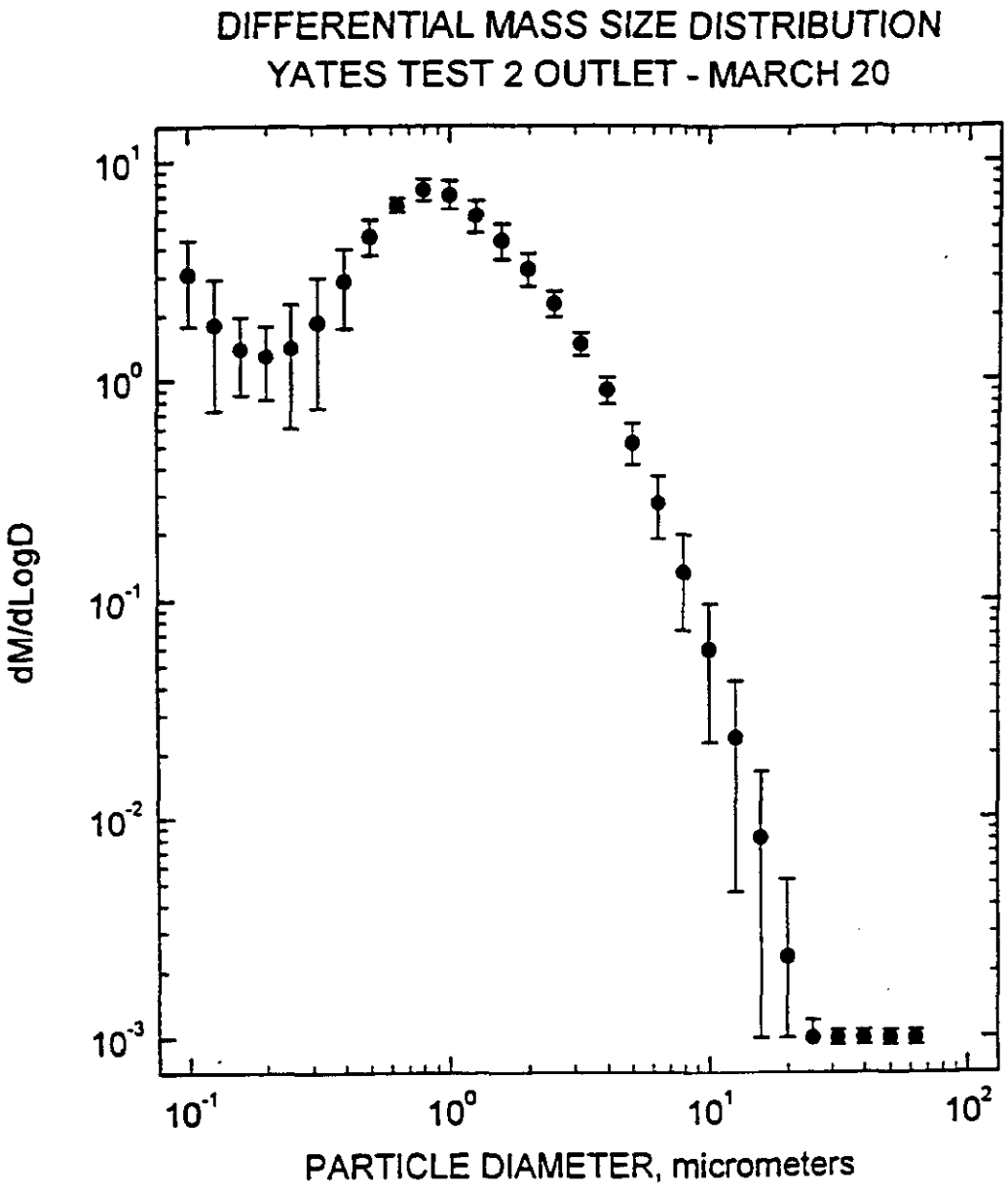

Figure A18. Differential Mass vs Particle Diameter, Outlet Impactors - March 20, 1994.

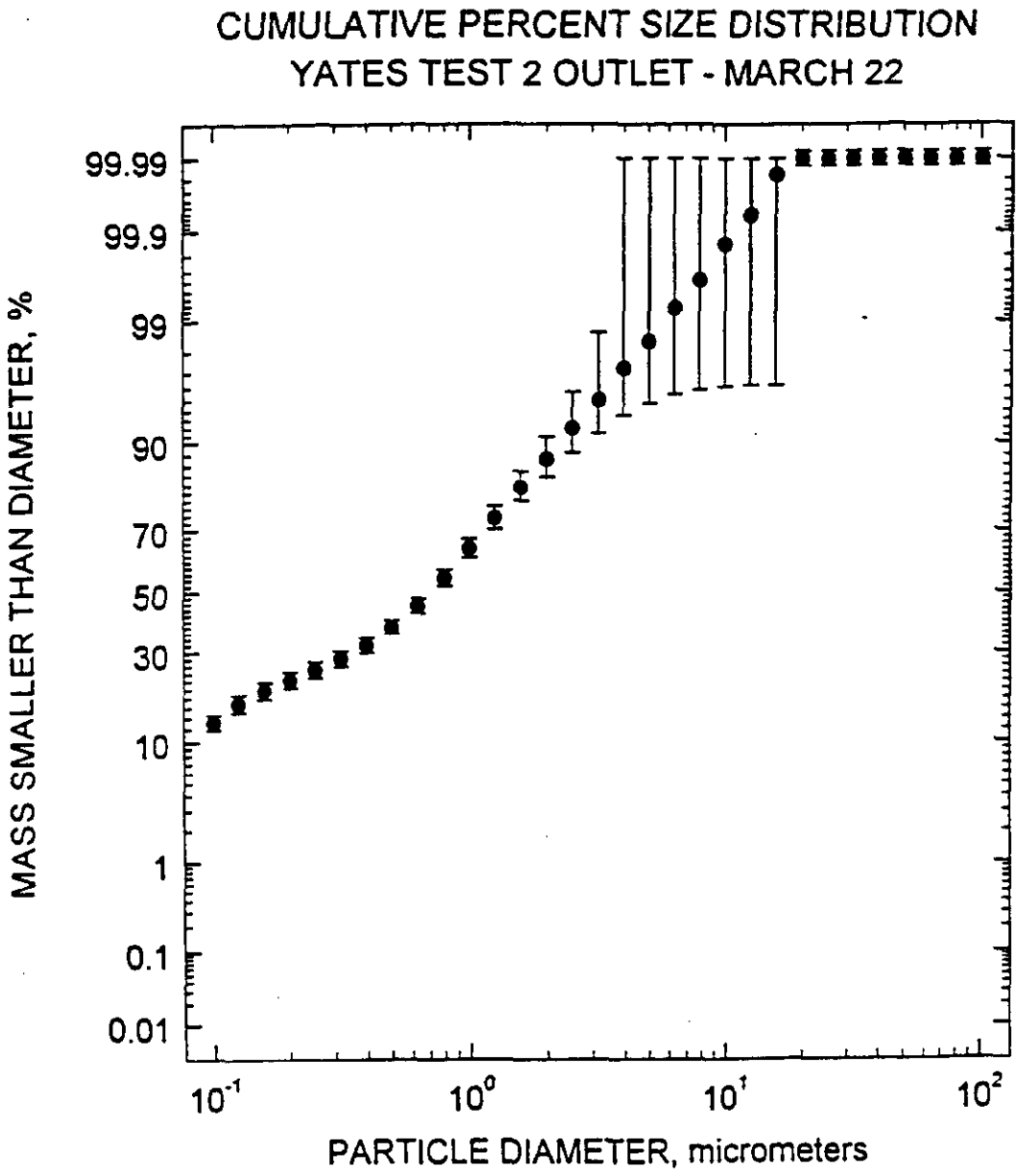

Figure A19. Cumulative Percent vs Particle Diameter, Outlet Impactors - March 22, 1994.

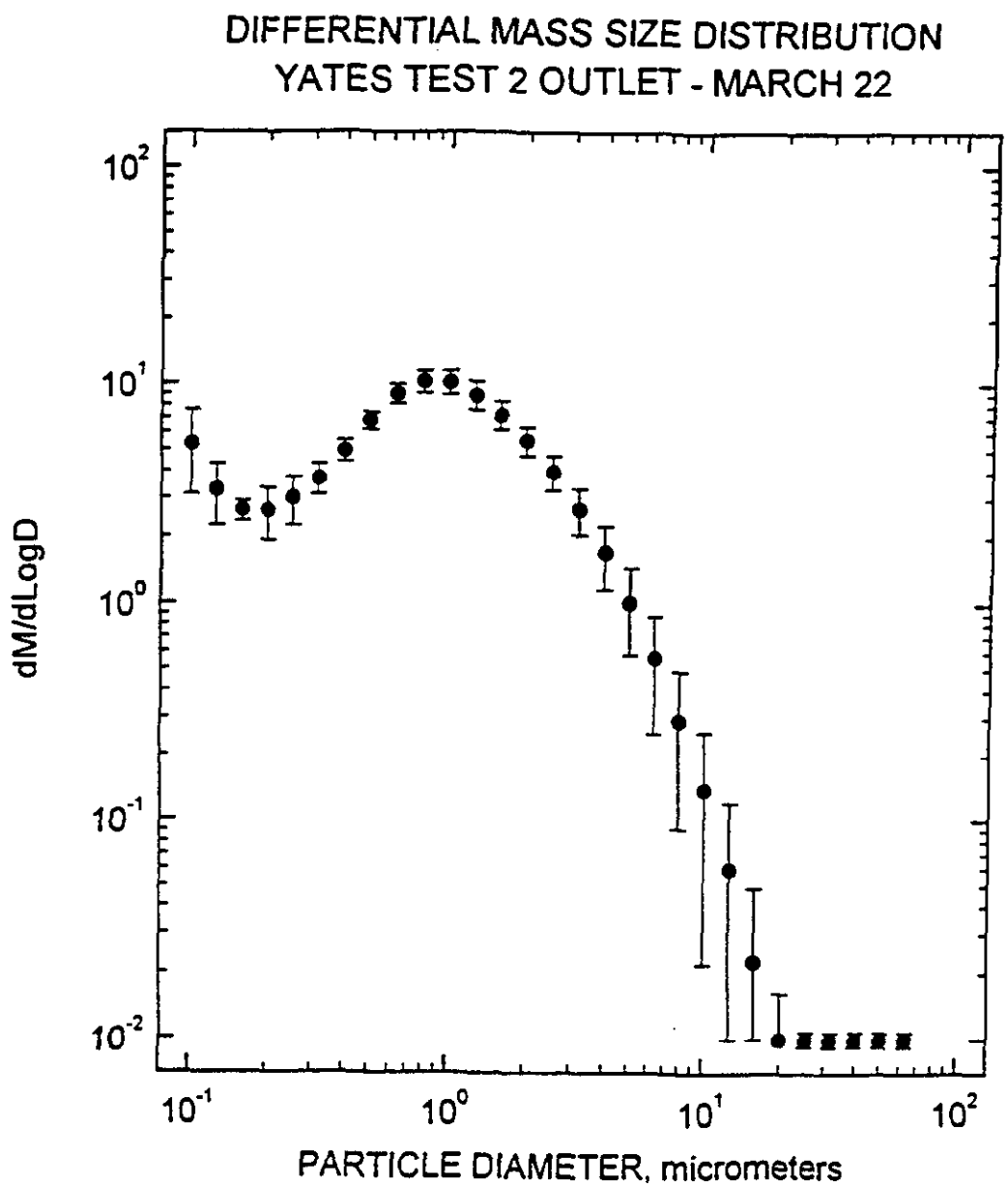

Figure A20. Differential Mass vs Particle Diameter, Outlet Impactors - March 22, 1994.

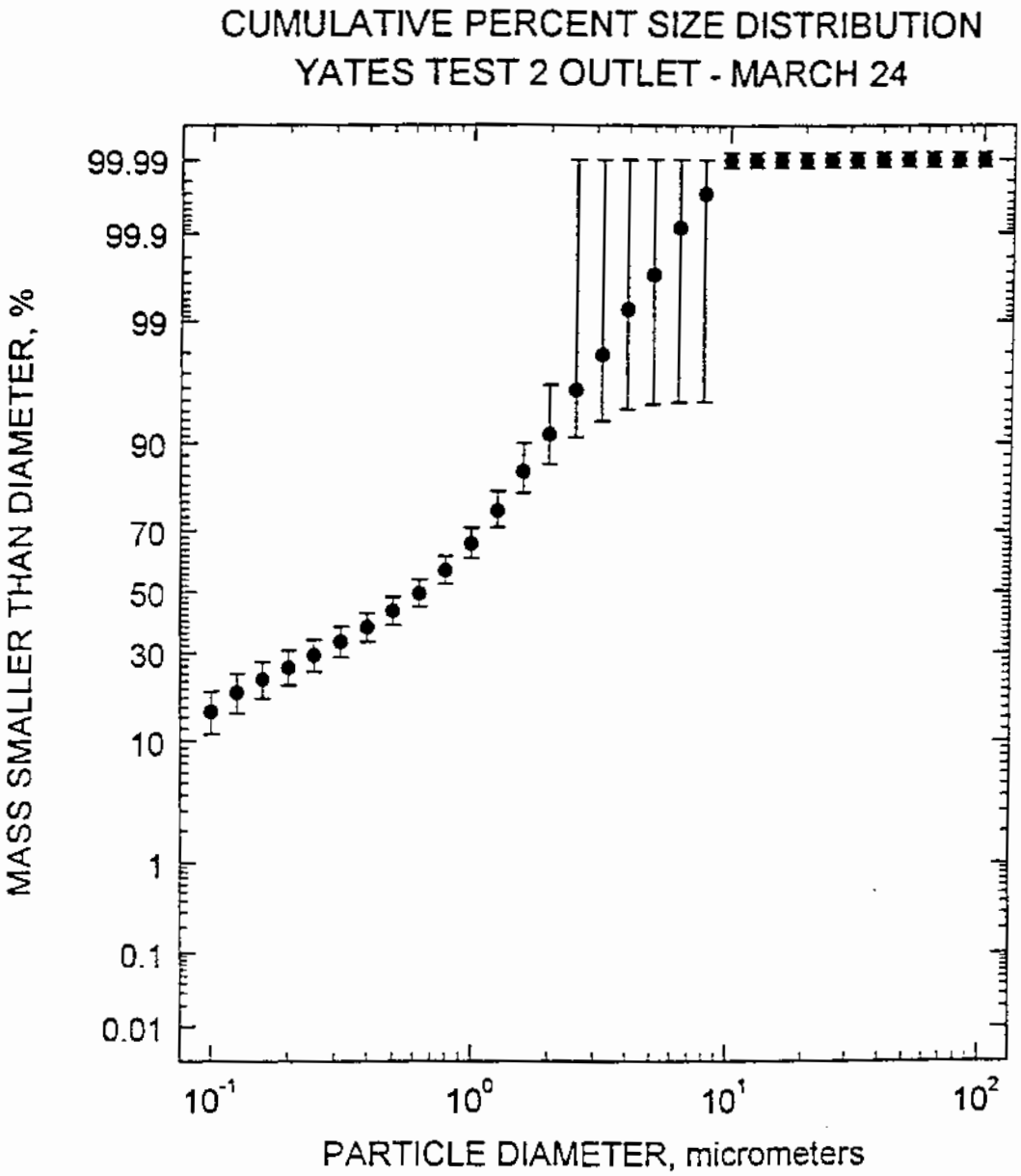

Figure A21. Cumulative Percent vs Particle Diameter, Outlet Impactors - March 24, 1994.

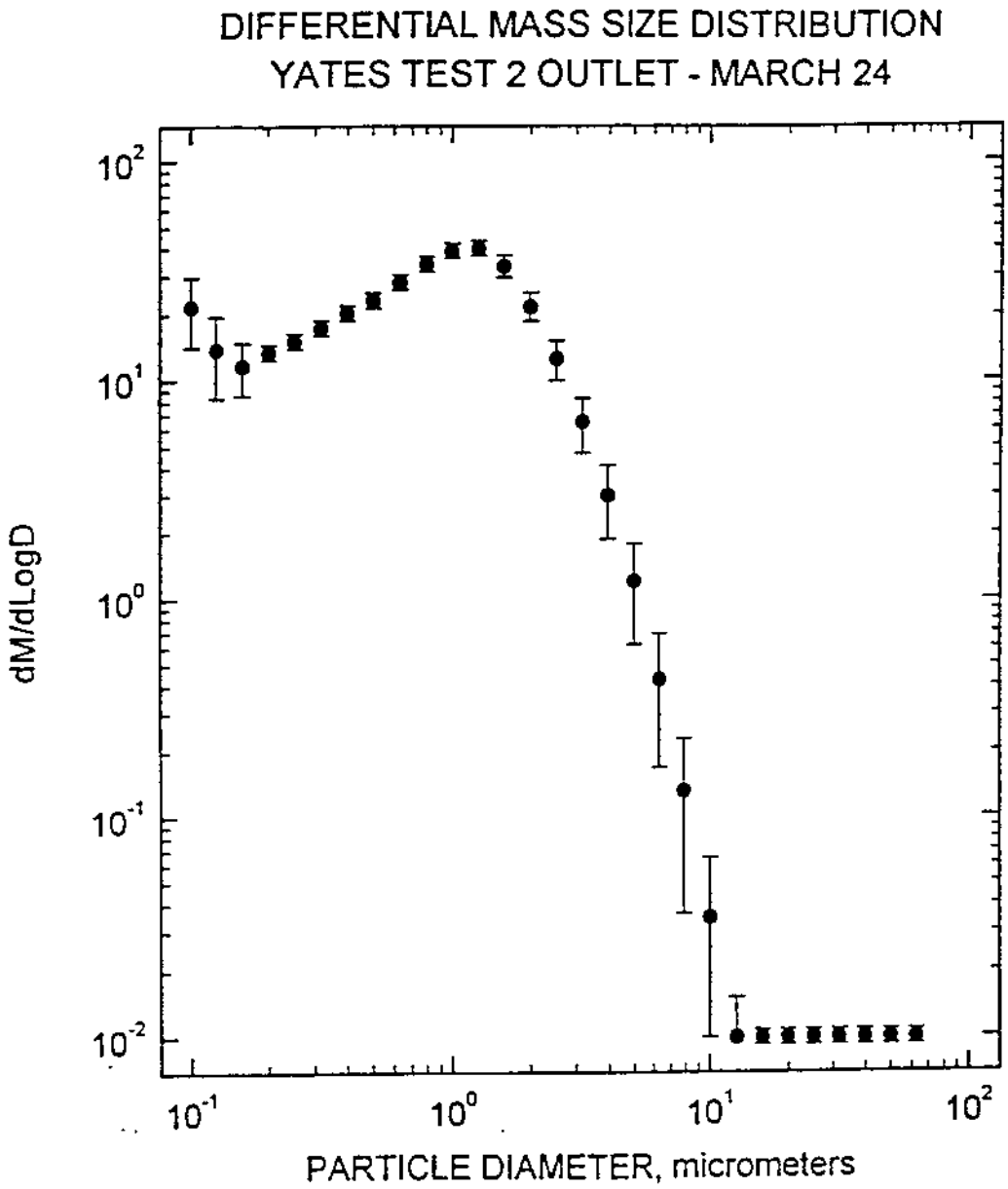

Figure A22. Differential Mass vs Particle Diameter, Outlet Impactors - March 24, 1994.

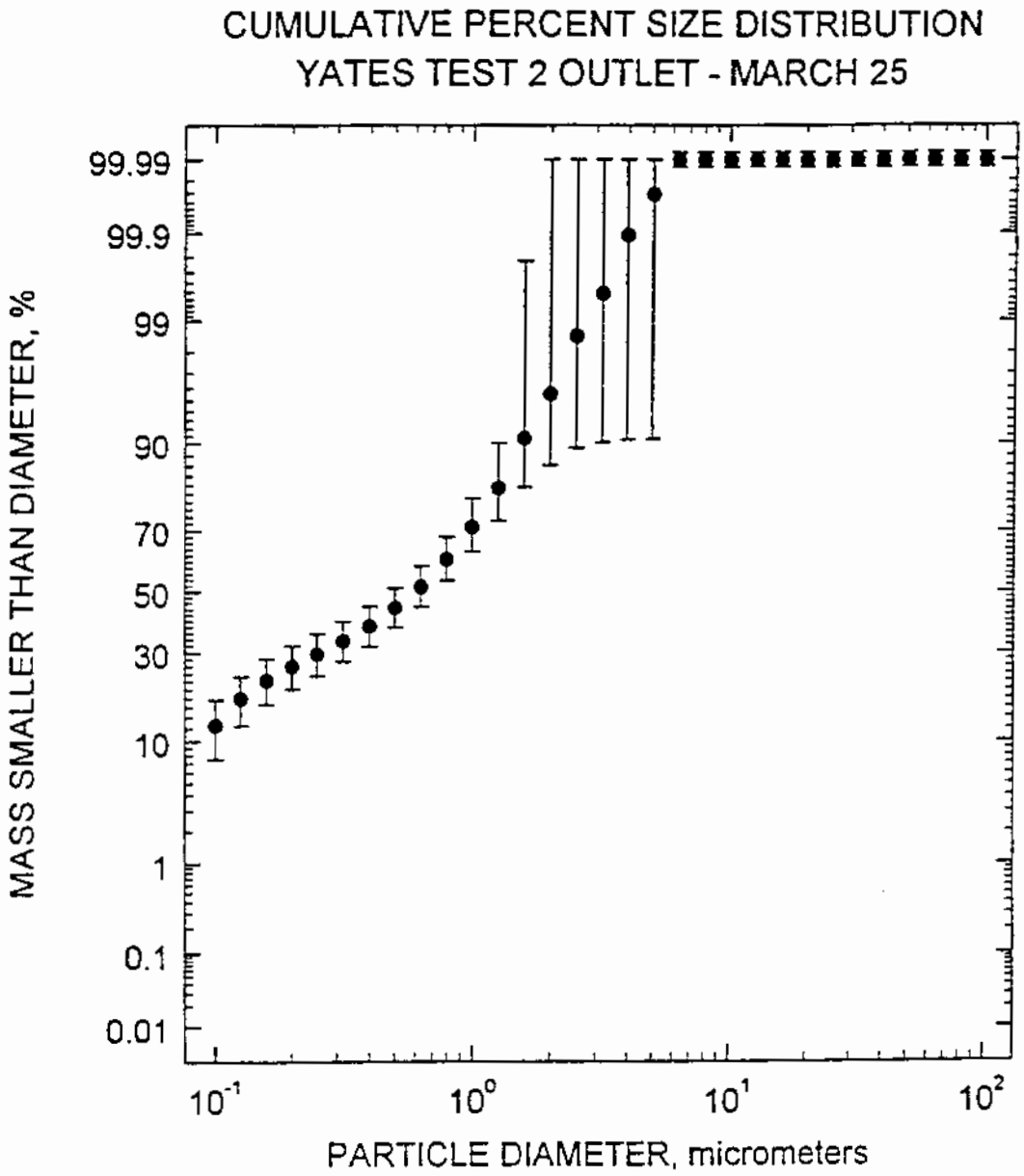

Figure A23. Cumulative Percent vs Particle Diameter, Outlet Impactors - March 25, 1994.

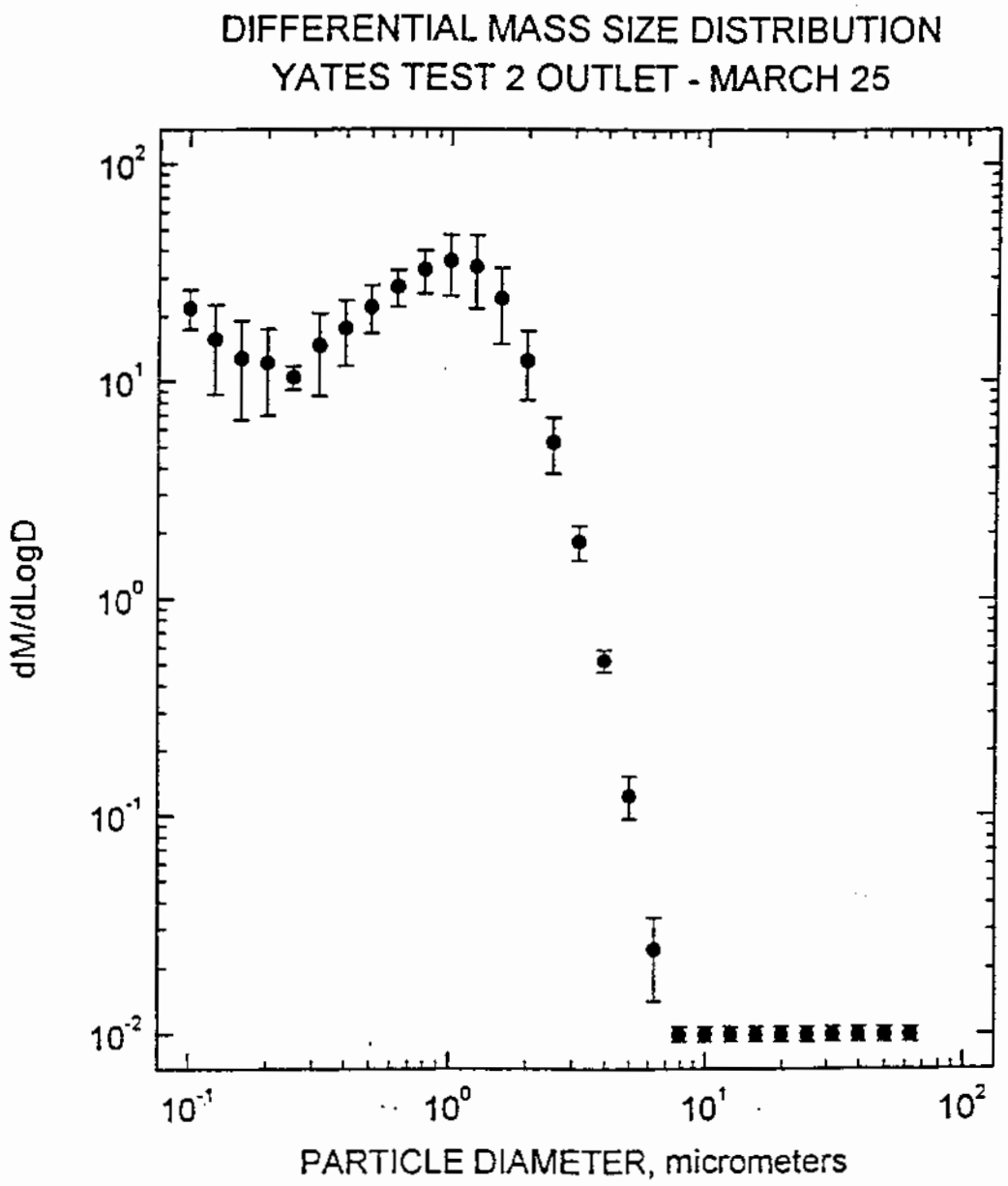

Figure A24. Differential Mass vs Particle Diameter, Outlet Impactors - March 25, 1994.

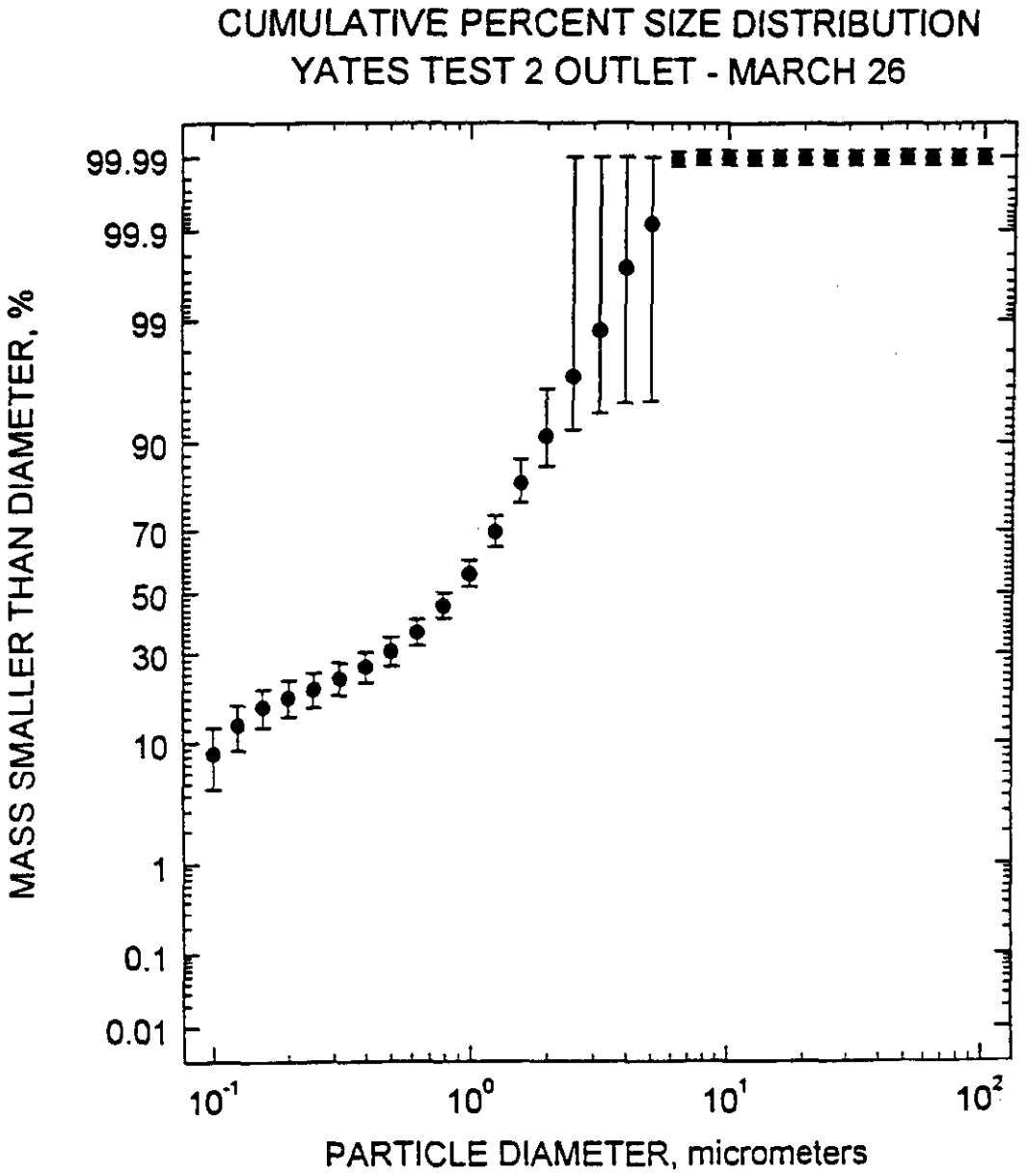

Figure A25. Cumulative Percent vs Particle Diameter, Outlet Impactors - March 26, 1994.

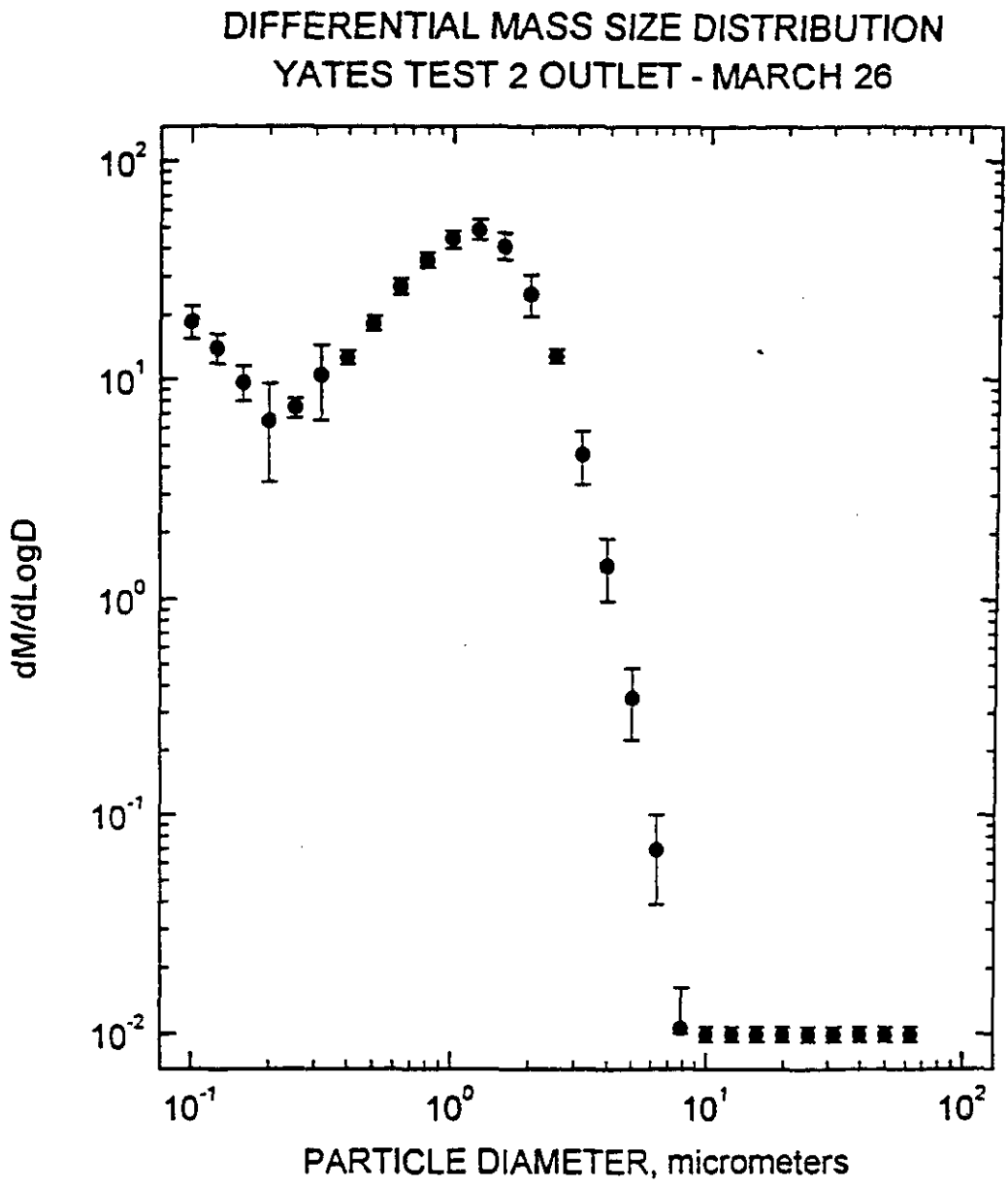

Figure A26. Differential Mass vs Particle Diameter, Outlet Impactors - March 26, 1994.

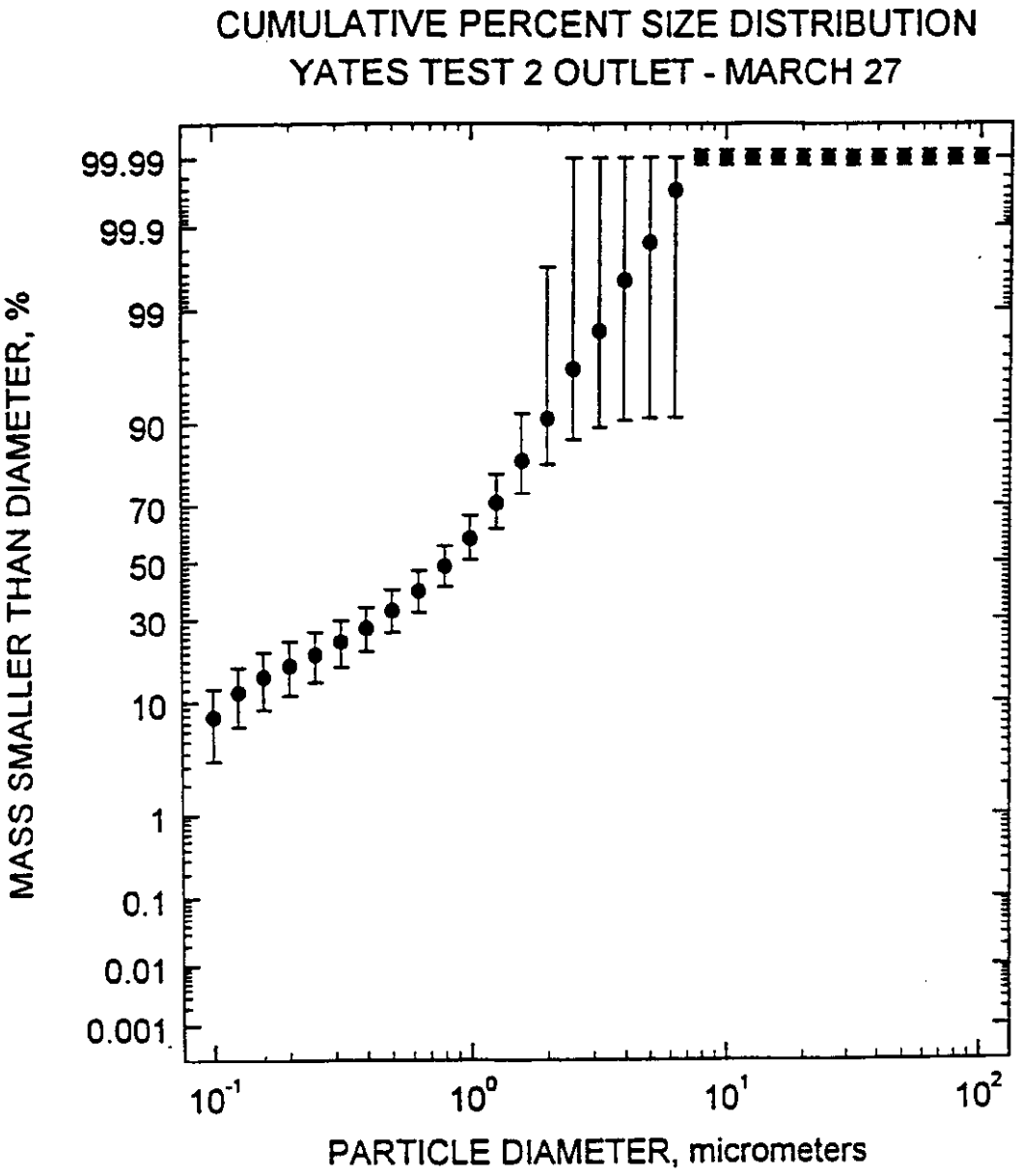

Figure A27. Cumulative Percent vs Particle Diameter, Outlet Impactors - March 27, 1994.

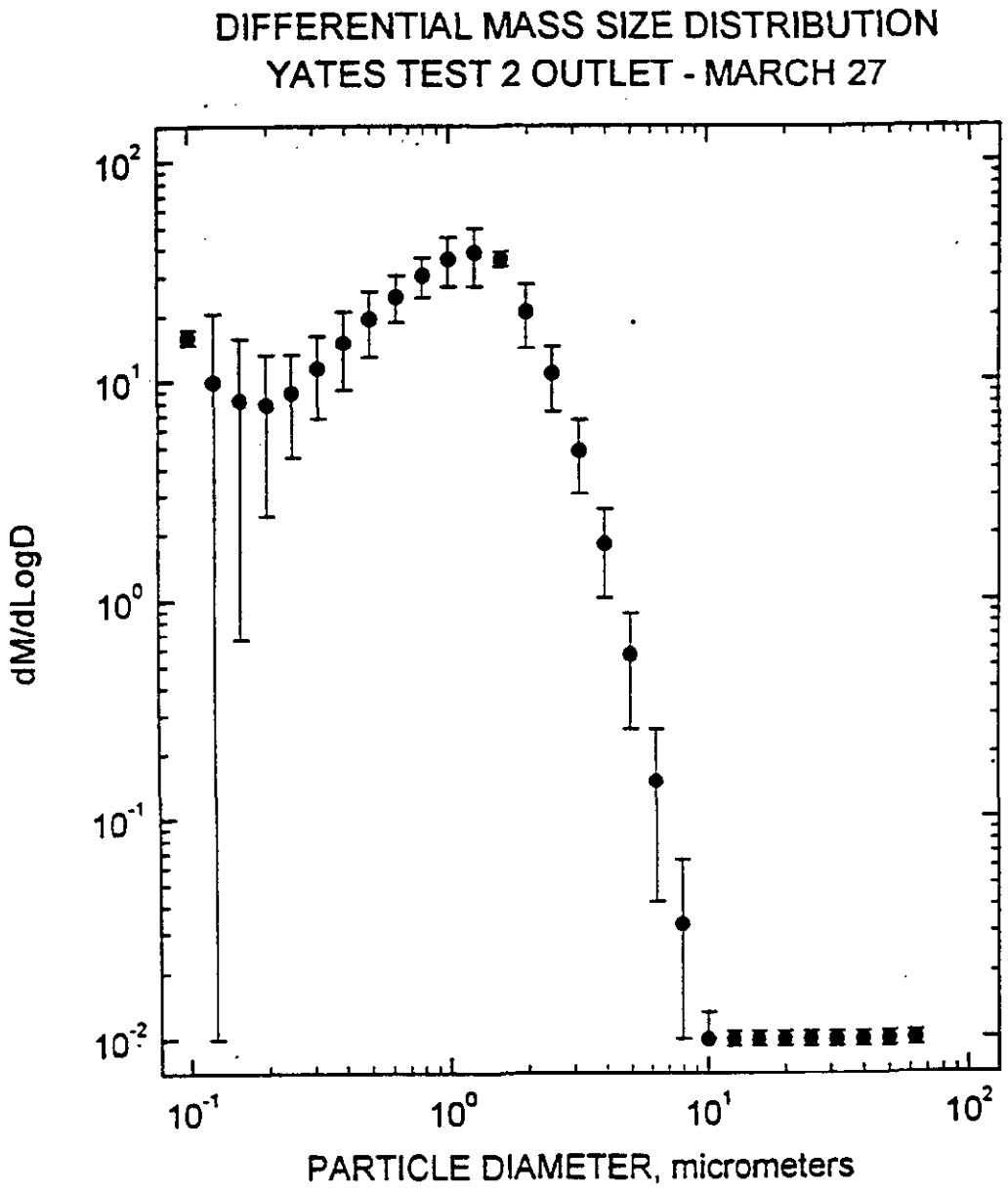

Figure A28. Differential Mass vs Particle Diameter, Outlet Impactors - March 27, 1994.

"Particulate Testing Around the Yates CT-121 Scrubber,
While Simulating a Marginally Performing ESP"

Radian Corporation

Draft Report
DCN 95-642-002-01

Particulate Testing Around the Yates CT-121 Scrubber, While Simulating a Marginally Performing ESP

Prepared by:

Radian Corporation
P.O. Box 201088
Austin, Texas 78720-1088

Submitted to:

Southern Company Services, Inc.
800 Shades Creek Parkway
Birmingham, Alabama 35209

April 28, 1995

TABLE OF CONTENTS

LIST OF FIGURES

LIST OF TABLES

1.0 INTRODUCTION

This document presents the results of a test measurement program performed by Radian Corporation for Southern Company Services at the CT-121 Scrubber Project at Plant Yates. Particulate removal efficiency by the JBR has been previously measured under low- and high-ash loading conditions. For this test program ash loading was set to simulate a marginally performing ESP. Although the ESP was completely energized, the particulate removal efficiency of the ESP was approximately 90% (vs. 99% normally) due to the low sulfur content of the coal. Burning low sulfur coal can result in reduced ash resistivity and decreased collection efficiency in the ESP. As a result, the ESP efficiency was roughly equivalent to that achieved with higher sulfur coals and partially energized ESPs.

Characterization of the dust emissions at Plant Yates was complicated due to the conditions of the wet stack. Sorting out what mass was attributable to dust, sulfuric acid mist, and scrubber carryover was not feasible using a typical sampling approach, so Radian characterized the particulate effluent by source apportionment. This involved chemically characterizing the emitted fly ash, the inlet fly ash, and the scrubber liquor. Radian used a computerized data analysis and reduction routine to apportion the mass of material in the stack effluent to each of it's respective sources. In addition, Radian collected samples for air toxics analysis (metals) from the stack during the 100 megawatt test conditions. Samples were also collected from the JBR inlet and stack for the determination of particle-size distribution (PSD).

The Radian field crew arrived on November 30, 1994, for equipment setup; sample collection began at noon on December 1. Testing was performed during four process operating conditions which are listed in Table 1.

Table 1
Test Conditions

Date	Test Condition	pH	JBR ΔP (inches WC)	Boiler Load (MW)
12/1 - 12/2	1 (AL2-1)	4.0	18 (High)	100
12/3 - 12/4	2 (AL2-2)	4.0	10 (Normal)	100
12/5 - 12/6	3 (AL2-3)	4.0	18	50
12/7 - 12/8	4 (AL2-4)	4.0	10	50

A summary of the types of samples collected at each location during each test condition is shown in Table 2.

Table 2
Summary of Collected Samples

	No. 1: High ΔP 100 MW	No. 2: Normal ΔP 100 MW	No. 3: High ΔP 50 MW	No. 4: Normal ΔP 50 MW
Stack				
Metals by Method 29	3	3		
Loading by Method 5b	3	3	6	6
Particle-Size Distribution	3	2	2	2
JBR Inlet				
Metals by Method 29	3	3		
Loading by Method 5b	3	3	6	6
Particle-Size Distribution by Cascade Impactor	2	2	3	2
Process				
Mist Elim. H_2O			1	
JBR Slurry	1		1	1
Limestone			1	
Pulverized Coal	1	1	1	1

The methodologies used to collect and analyze these samples are described in Appendices A and B, respectively.

Another facet of this program involved a comparison of methods between those of the U.S. EPA and the Japanese Industrial Standards (JIS). Samples collected by EPA Method 5b were also subjected to drying temperatures that adhere to the JIS. A comparison of these methodologies is also presented in this report. Table 3 presents an overall analytical matrix for the collected samples.

Table 3
Analytical Matrix

Location/Type	Analysis
Multi-Metals, (EPA Method 29)	Trace: Sb, As, Ba, Be, Cd, Co, Cu, Cr, Pb, Hg, Mo, Mn, Ni, Se, S, and V. Major: Al, Ca, Fe, K, Mg, Na, and Ti.
Loading, (EPA Method 5b)	For source apportionment: Al, Ca, Fe, K, Mg, Mn, Na, S, and Ti.
Process Grab Samples:	
Mist Eliminator	Al, Ca, Fe, K, Mg, Mn, Na, S, Ti and Cl.
JBR Scrubber Liquor	Cl, Ca, and Mg
JBR Scrubber Solids	Metals
Limestone	Al, Ca, Fe, K, Mg, Mn, Na, S, and Ti.
Pulverized Coal	Ultimate, proximate, and metals.

* Metals = Sb, As, Ba, Be, Cd, Co, Cu, Cr, Pb, Hg, Mo, Mn, Ni, Se, S, V. Al, Ca, Fe, K, Mg, Na, and Ti.

2.0 PROCESS OPERATION

During the test period, Plant Yates was burning a low sulfur, bituminous/subbituminous rank coal. The ESP was operated with only the first field energized, so particulate loading into the JBR was substantially higher than normal operation, but still attenuated from that of the full output of the boiler. As an indicator of process operational stability, the plant output [in megawatts] and the JBR inlet SO_2 during the testing periods have been graphed and are shown in Figure 1. The data represents 15-minute averages taken from the on-line data acquisition system.

Process flow rates during the test periods have been summarized and are presented in Table 4. Coal flow rates are estimated, based upon flow rates measured during previous testing efforts at Plant Yates, under 100 MW load conditions. Also, JBR inlet flow rates, although measured, are calculated based upon flow rates at the stack (wet chimney). The stack flow rates are considered to be the more accurate of the two locations due to the physical geometry of the duct work. The two flow rates should differ only by the amount of oxidation air added in the JBR. Based upon historical operation, the oxidation air was estimated as 4,000 scfm.

Table 4
Flow Rates

	Condition			
	100 MW, High ΔP	**100 MW, Normal ΔP**	**50 MW, High ΔP**	**50 MW, Normal ΔP**
Coal Moisture (%)	8.59	7.5	9.29	7.95
Coal Ash (%, dry)	10.95	10.48	10.86	10.91
Coal heating value (Btu/lb)	13,460	13,395	13,461	13,479
Raw Coal (lb/hr, wet)	91,000	91,000	46,000	46,000
Pulverizer Rejects (lb/hr)	120	120	60	60
Feed Coal (lb/hr, dry)	83,200	84,200	41,700	46,900
JBR Inlet:				
Loading (mg/Nm³)	1,256	1,530	287	301
Loading (gr/scf)	0.512	0.623	0.117	0.123
Flow Rate (dscfm)	295,000	294,000	182,000	181,000
Stack:				
Loading (mg/Nm³)	27	9.4	3.9	4
Loading (gr/scf)	0.0112	0.0038	0.0016	0.0016
Flow Rate (dscfm)	299,000	298,000	186,000	185,000
Emissions (lb/hr)	28.6	9.8	2.6	2.6
Emissions (lb/10^6 Btu)	0.02550	0.00869	0.00463	0.00456

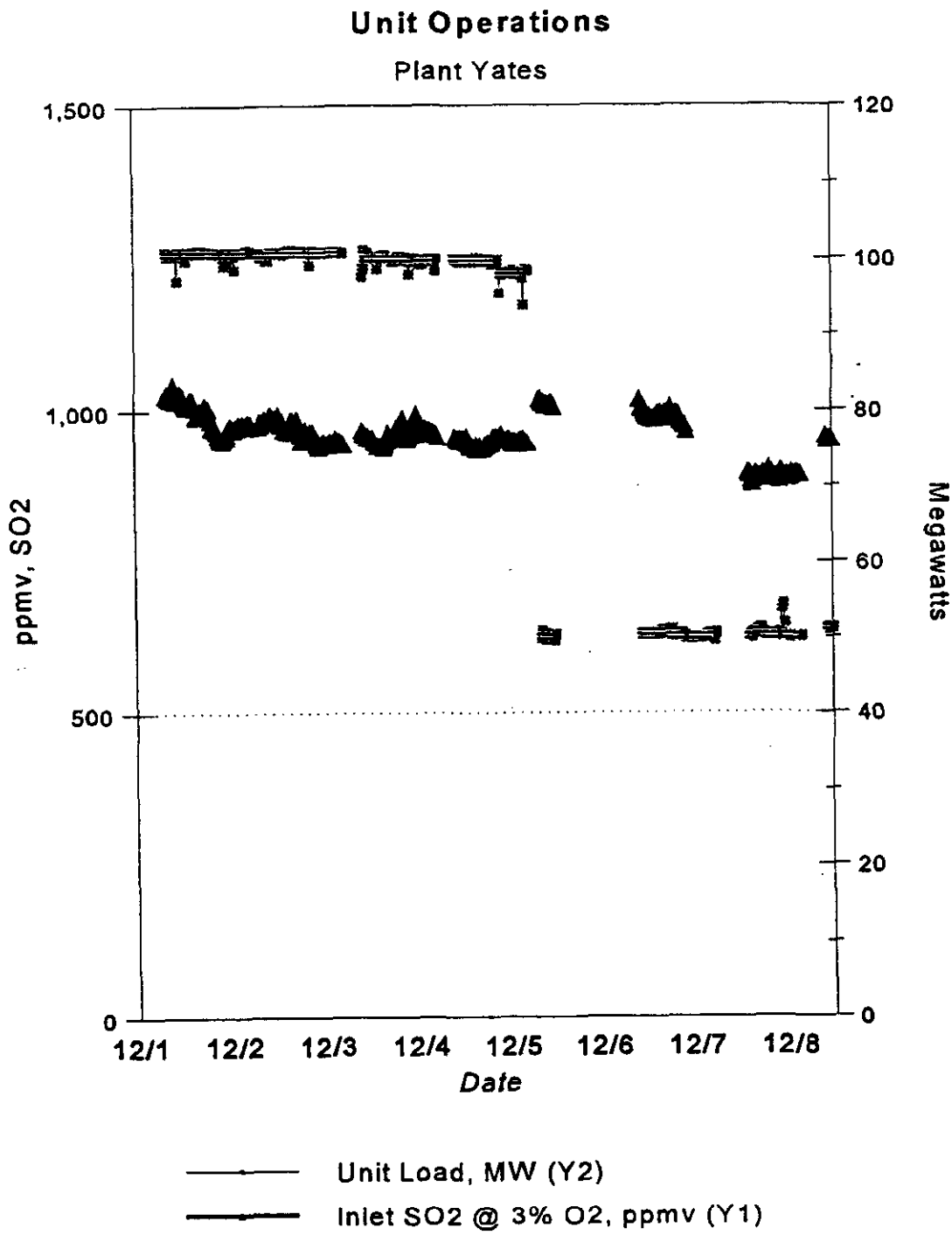

Figure 1. Plant Yates Unit 1 Operations During Testing Periods

3.0 RESULTS

3.1 Loading

Particulate loading was measured at both the JBR inlet and the (wet chimney) stack. The JBR inlet measurements were straightforward, and results from these tests are consistent. Representative loading measurements at the stack were more difficult to obtain due to the conditions of the wet stack. The loading data from the stack shows much greater scatter. Two issues regarding particulate loading have been addressed in this program. The first involves slightly different methodologies applied to determine "nonsulfuric acid mist" loading. The second issue involves separating the stack emissions into their various parts, i.e., particulate (ash), scrubber carryover (JBR scrubber liquor), and sulfuric acid mist. These two issues are discussed in the following sections.

3.1.1 EPA Method 5b and JIS Particulate Loading

Particulate loading at both the JBR inlet and the stack was determined using EPA Method 5b, designed for the collection of "nonsulfuric acid mist" particulate. This method involves the collection of a gaseous sample at temperatures of 160°C, which should be above the dew point of sulfuric acid mist. The equivalent method from the Japanese Industrial Standard (JIS) specifies a sample collection temperature of 250°C. To obtain comparative data, all samples were collected at 160°C, but, following the heating of the samples for six hours at 160°C and the subsequent weighings, the samples were heated to 250°C to simulate the JIS analytical protocol. The results of this methods comparison are inconsistent. As shown in Figure 2, the loading for the JBR inlet is virtually identical for both the EPA Method and the JIS results. However, the data from the stack are not only significantly different between the two methods, but the particulate loading actually appears to increase with additional heating at 250°C in three of the four test conditions, and the bulk of this increase comes from weight gains in the sample probe and nozzle rinses. The cause for this is not known. For a weight increase to occur, one would assume that there has been a reaction between the residue and either oxygen, moisture, or carbon dioxide in the ambient air. None of these reactions seem likely, even at the higher (250°C) temperature.

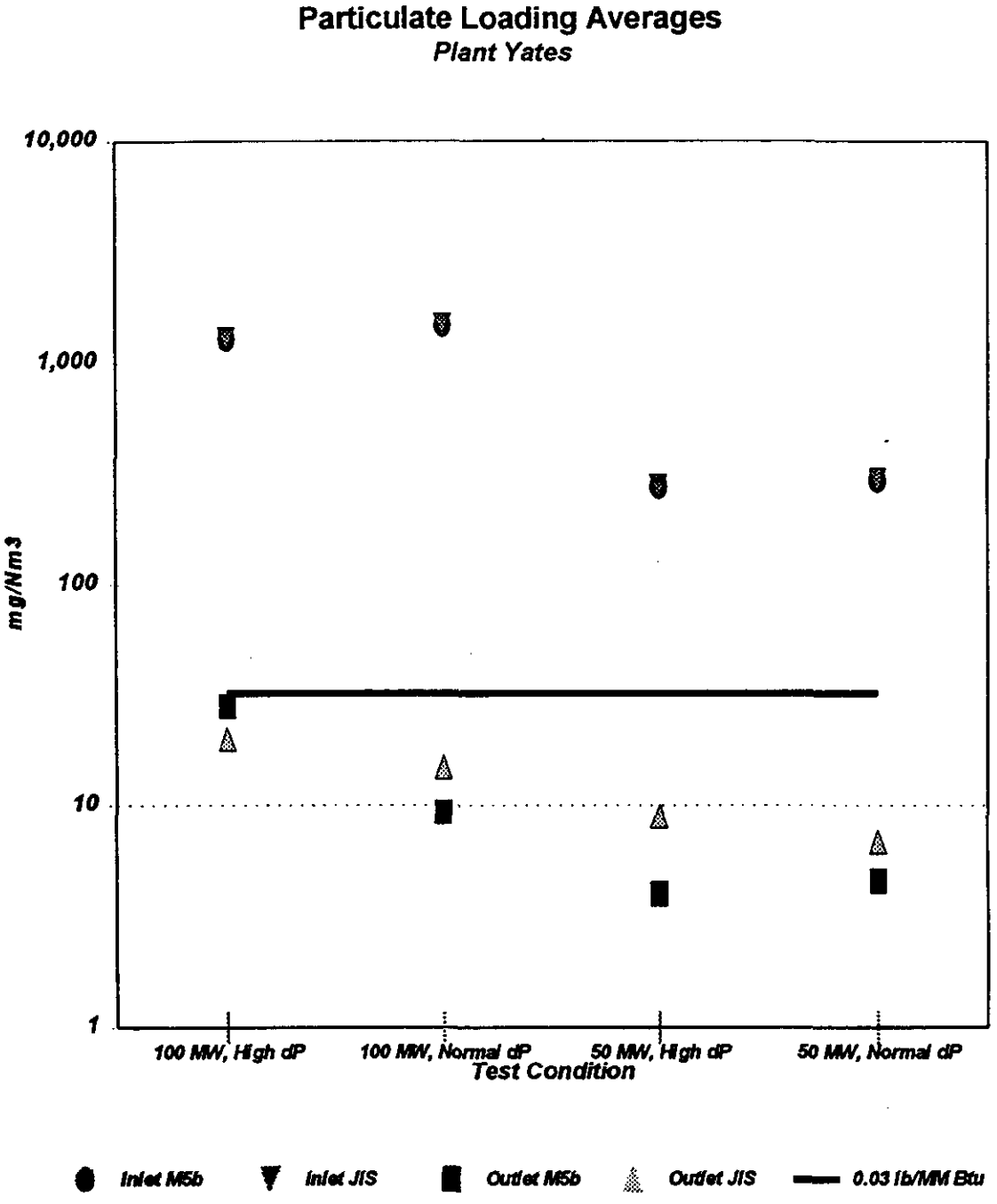

Figure 2. Particulate Loading Summary

It is highly likely that the samples collected from the stack were not entirely free of sulfuric acid mist when collected, since the stack (130°F) is significantly cooler than the target collection temperature (160°C/ 325°F) and below the sulfuric acid dew point. Nevertheless, subsequent drying should remove [unreacted] condensed sulfuric acid mist. One theory for a weight loss in some samples and weight gains in the others could be sulfuric acid mist was driven from some of the samples then condensed on others. However, this could happen only if the samples were heated, then the oven turned off and the samples allowed to cool in the oven. This theory seems unlikely since the samples were removed from the hot oven to cool. Again, the reasons for the apparent weight gains are unknown.

Average values for particulate loading, via Method 5b and the JIS, are presented in Table 5. Loading values for individual runs are located in Appendix E.

Table 5
Particulate Mass Loading Summary, mg/Nm³

	Condition			
	100 MW High ΔP	100 MW Normal ΔP	50 MW High ΔP	50 MW Normal ΔP
Inlet M5b	1300	1500	280	300
Inlet JIS	1300	1500	280	300
Outlet M5b	28	9.4	4	4.6
Outlet JIS	20	15	9	6.9
Removal, M5b (%)	97.8	99.4	98.6	98.5
Removal, JIS (%)	98.5	99	96.8	97.7

For a given boiler load, particulate removal appears to be greater for the high JBR pressure drop operating condition. Although this is not entirely evident from the data in Table 5, an evaluation of the individual data points shows that Condition 1 (100 MW, high ΔP), Runs 1 and 2, are significantly different from Run 3. An analysis of the particulate residue also shows orders of magnitude difference in the sulfur results. This suggests that the first two samples were not entirely free of condensed sulfuric acid, and these two samples are biased high. Taking this into account, the average loading values drop below those obtained during Condition 2. This is discussed further in the following section.

3.1.2 *Source Apportionment*

Measured particulate in the wet stack from the JBR at Plant Yates can consist of mass from three potential sources:

- Condensed sulfuric acid mist;
- JBR scrubber carryover; and
- Particulate [fly] ash.

A technique known as source apportionment was used to determine the ash penetration of the JBR scrubber and the amount of JBR scrubber liquor carryover by chemically analyzing the emitted particulate, then using statistical analysis to calculate the mass resulting from each of the various fractions. The source apportionment was determined using the following relationship:

$$\phi_j^{out} = P\ \phi_j^{in} + C_j\ V + S$$

where:

ϕ_j^{out} = mass flow rate of species j out of scrubber (g/min)
P = penetration fraction of fly ash through scrubber
ϕ_j^{in} = mass flow rate of species j into scrubber (g/min)
C_j = concentration of species j in scrubber liquor (g/mL)
V = volume rate of entrained scrubber liquor (mL/min)
S = volume rate of H_2SO_4 mist, as S (g/min).

The data were reduced using the "effective variance weighted least squares" method and produced the results shown in Table 6. The information presented in Figure 3 shows the individual measured data points for mass loading along with the calculated ash penetration based upon the "P" values from Table 6. The reduction in ash loading, as a function of JBR pressure drop, is supported from the predicted values. An inspection of the coefficient of error for the ash penetration fraction show the data to be highly precise.

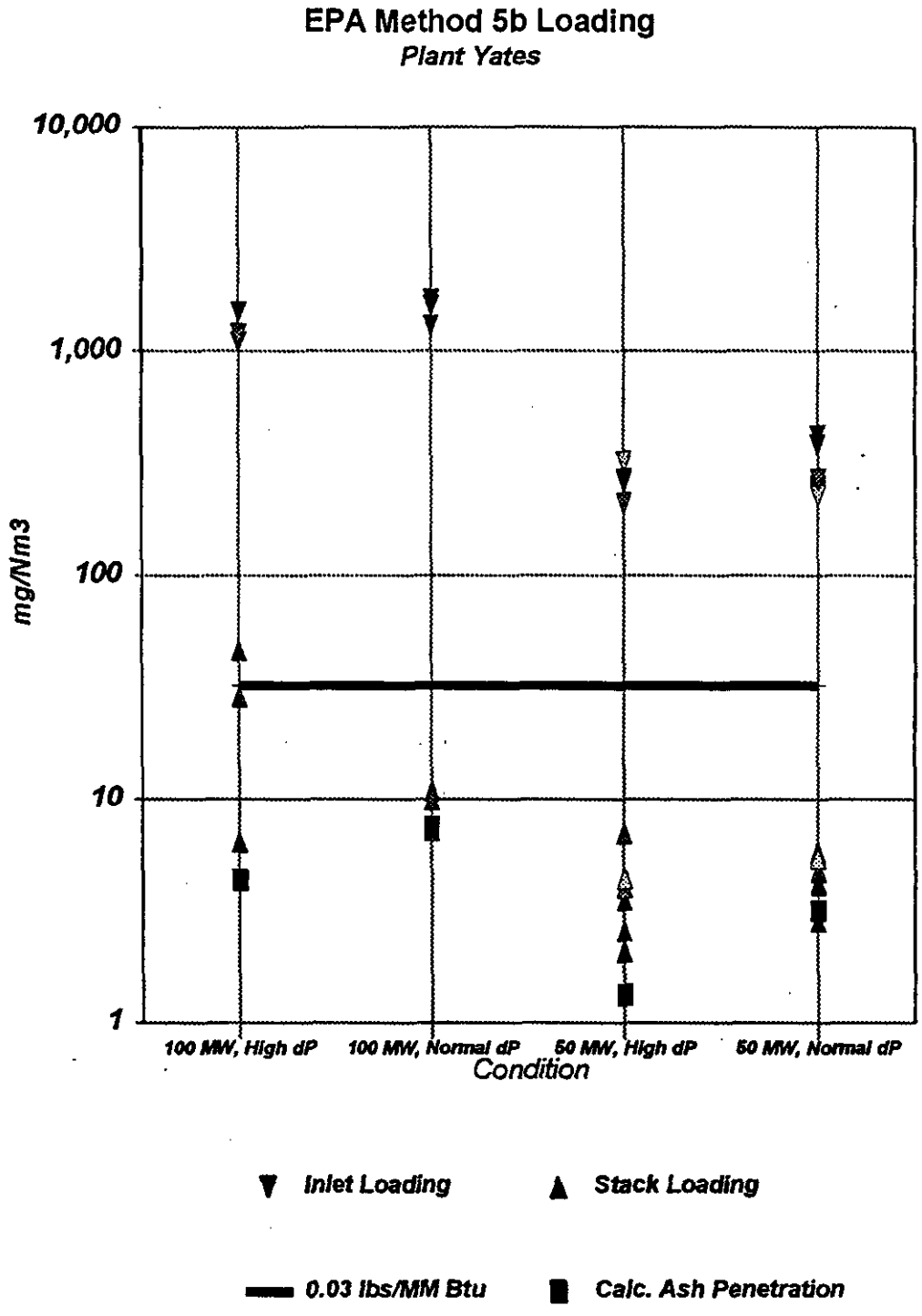

Figure 3. Loading Measurements and Ash Penetration

Table 6
Effective Variance Analysis Summary

Test Condition	Ash Penetration, P (g_{out}/g_{in})		Liquor Entrainment Rate, V (mL/min)		Sulfuric Acid Mist, as S (g/min)	
	Coefficient	Standard Error	Coefficient	Standard Error	Coefficient	Standard Error
100 MW, High ΔP	0.00348	0.000127	37.7	39.1	30.6	8.91
100 MW, Normal ΔP	0.00492	0.000191	36.4	69.3	1.86	17.2
50 MW, High ΔP	0.00472	0.0000516	6.56	2.75	0.050	0.555
50 MW, Normal ΔP	0.0106	0.00037	14.8	22.2	0.183	4.2

The theory that the loading data from condition one (100 MW, High ΔP) is biased high due to sulfuric acid mist is also supported by the source apportionment data. The sulfuric acid coefficient for condition one is 30.6, indicating a much higher level of sulfuric acid present when compared to the other three test conditions. Scrubber carryover appears to be significantly higher under high load condition as compared to low load with the highest value for scrubber carryover equaling approximately 0.6 gph. The standard error for both the scrubber carryover and the sulfuric acid is significant. The results of the source apportionment analysis are shown graphically in Figure 4. The ash, scrubber carryover, and acid mist fractions are shown as percentages of the total calculated emitted mass. The high bias in Condition 1 from sulfuric acid mist is quite evident. Smaller quantities of sulfuric acid also appear to be present in all of the samples.

3.2 Air Toxics

The inlet to the JBR scrubber and the stack were tested for trace metals during full-load (100 MW) conditions. Three samples were collected from each location during high and normal JBR pressure drop conditions. The results of these tests have been summarized and are presented in Table 7. Average values with 95% confidence intervals for both operating conditions are shown. These results for the stack emissions for the two operating conditions are also shown graphically

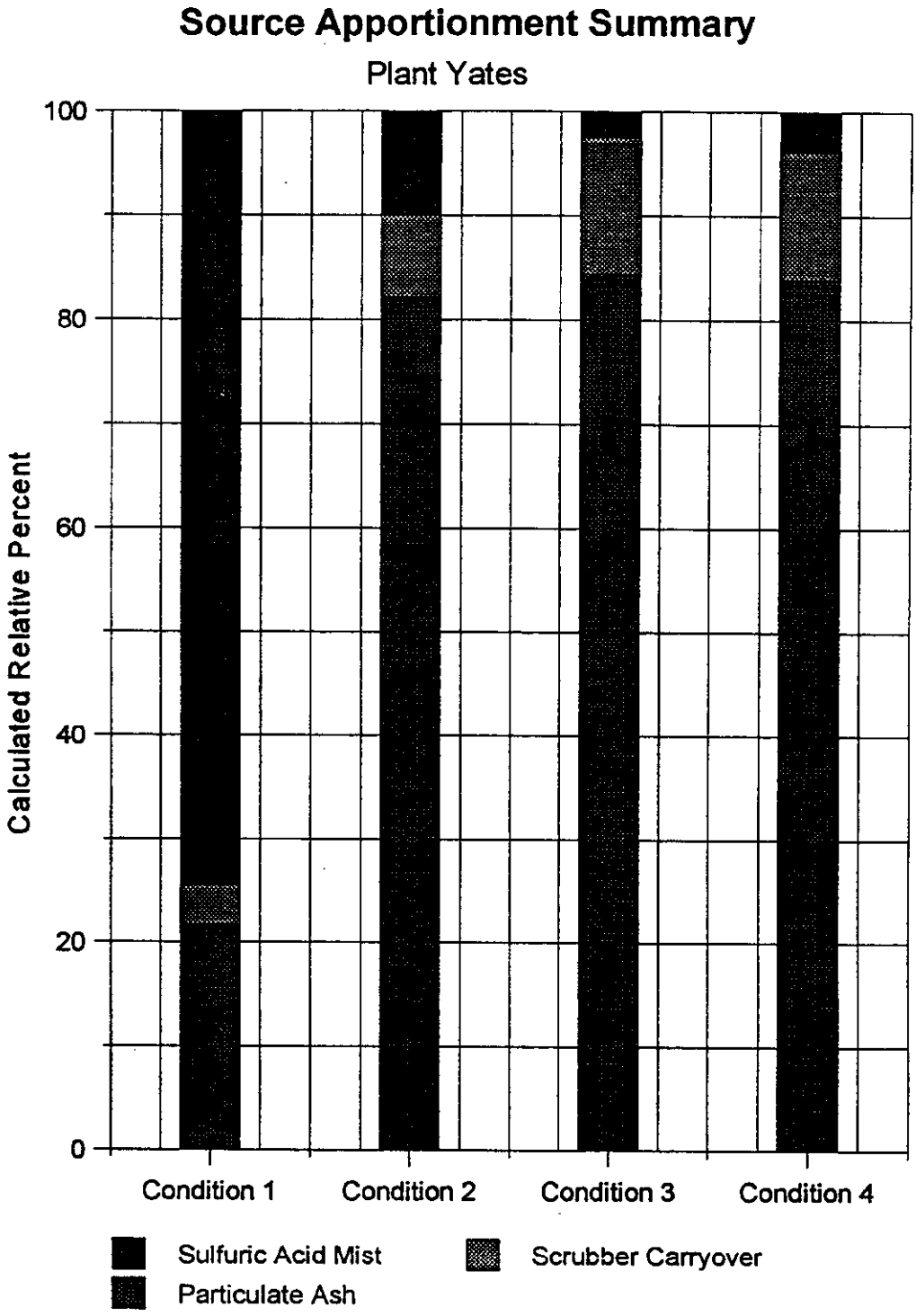

Figure 4. Source Apportionment Results

Table 7
Air Toxics Results Summary

	Condition 1, µg/m³					Condition 2, µg/m³				
	Inlet Conc.		Outlet Conc.		Removal Efficiency	Inlet		Outlet		Removal Efficiency
	Average	95% CI	Average	95% CI		Average	95% CI	Average	95% CI	
Al	144,000	77,000	549	194	99.6%	177,000	45,000	1,180	470	99.3%
Sb	<41.2	--	<8.18	--	79.1%	<45.4	--	<8.83	--	81.1%
As	305	119	23.8	1.7	92.2%	357	97	31.9	7.4	91.1%
Ba	1,610	740	40.3	3.5	97.5%	2,000	620	54.3	9.9	97.3%
Be	28.7	15.4	0.365	0.062	98.7%	35.3	8.7	0.602	0.132	98.3%
Cd	1.99	0.57	0.446	0.102	77.6%	2.66	0.97	0.544	0.246	79.5%
Ca	13,200	7,700	260	62	98.0%	16,800	3,000	335	97	98.0%
Cr	199	104	3.07	0.3	98.5%	262	104	4.57	1.32	98.3%
Co	112	65	2.18	2.85	98.1%	149	52	2.57	2.33	98.3%
Cu	294	161	6.13	2.04	97.9%	382	137	12.6	2.7	96.7%
Fe	65,100	28,800	333	52	99.5%	75,400	16,600	585	184	99.2%
Pb	153	97	17.6	27.3	88.5%	198	72	8.03	10.25	95.9%
Mg	6,250	3,100	63.4	5.2	99.0%	7,650	2,060	97.9	31	98.7%
Mn	203	87	7.74	13.26	96.2%	250	74	14	22.1	94.4%
Hg	6.175	0.457	1.62	2.14	73.8%	6.356	0.181	2.40	0.07	62.2%
Mo	28.4	10.9	7.43	0.74	73.9%	21.7	4.7	8.21	1.49	62.2%
Ni	206	122	4.17	2.58	98.0%	277	102	5.71	4	97.9%
K	24,700	11,900	203	7	99.2%	29,200	6,500	312	52	98.9%
Na	5,970	3,350	209	12	96.5%	6,050	3,050	176	92	97.1%
Se	39.7	22.6	23.6	5.7	40.5%	51.5	30	25.9	12.9	49.7%
S	3,550	2,010	539	457	84.8%	4,500	2,160	568	124	87.4%
Ti	9,720	5,310	51	8.9	99.5%	11,900	2,480	97.4	29	99.2%
V	433	243	8.78	0.97	98.0%	540	112	13.2	1.7	97.6%
Total Particulate, mg/m³	1300	520	28	50	97.8%	1500	520	9.4	4.8	99.4%

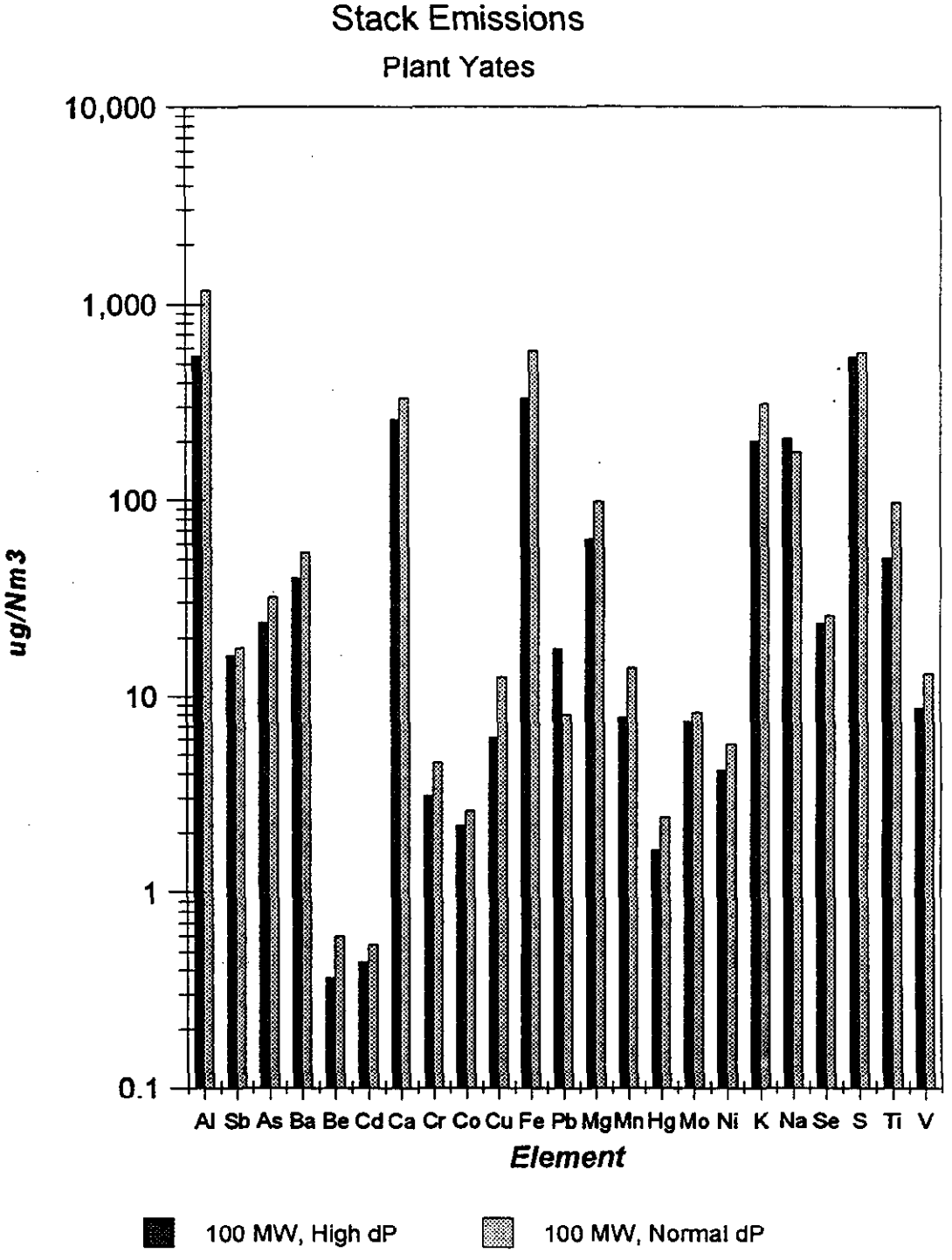

Figure 5. Stack Emissions

in Figure 5. Outlet mass loadings for these metals follow the same trends as that of the particulate loading and are **lower** during the high pressure drop operating condition.

Emission factors for these air toxics species are shown in Table 8 for both high and normal JBR pressure drop. Air toxics emissions were reduced (on average) by 20-30% as a result of operating the JBR at the higher ΔP. Exceptions to these results include emissions for lead and sodium.

Table 8
Emission Factors

lb/10^{12} BTU	High ΔP	Normal ΔP	Ratio; High:Normal
Al	548	1,164	47%
Sb	13	16	83%
As	24	32	76%
Ba	40	54	75%
Be	0.36	0.60	61%
Cd	0.45	0.54	83%
Ca	260	331	79%
Cr	3.07	4.52	68%
Co	2.18	2.54	86%
Cu	6.12	12	49%
Fe	333	579	58%
Pb	18	7.94	221%
Mg	63	97	65%
Mn	7.73	13.79	56%
Hg	1.62	2.38	68%
Mo	7.42	8.12	91%
Ni	4.16	5.65	74%
K	203	308	66%
Na	209	174	120%
Se	24	26	92%
S	539	561	96%
Ti	51	96	53%
V	8.77	13	67%

The emission factors for some of these air toxics species [i.e., arsenic] are significantly higher than those obtained during earlier air toxics testing. The reasons for this are most likely due to the

differences in particulate control devices used during the earlier test program, and particularly the particle removal efficiency in the range of 0.3-1.0 μm.

Some of the more volatile species tend to be very concentrated in the finer particle sizes. As discussed in the next section, particle removal efficiency drops off sharply for particles less than 1 μm in size. These issues will be discussed further in the "Comprehensive Final Report to DOE."

3.3 Particle-Size Distribution

Particle-size distribution was determined at the JBR inlet and at the stack during each of the four operating conditions. Figure 5 shows the average cumulative mass distribution by particle size for the JBR inlet under both 50 and 100 MW boiler loads. This data shows that under high load (100 MW) approximately 30% of the particulate produced is greater than 10 μm in diameter. This compares to only 10-12% of the particulate greater than 10 μm under 50 MW load. As expected, the collection efficiency in the ESP was greater at lower flue gas flow rates. Under both load conditions, the predominance of particles are between 1 and 6 μm.

Figures 6 and 7 show the cumulative mass distribution at the stack for high and low plant load and high and normal JBR ΔP. These data are very similar for all of the test conditions, showing the vast majority (80-90%) of the particulate material to be below 1 μm in size.

The differential particle-size distribution are shown in Figures 8 and 9 for 100 MW and 50 MW respectively. The inlet mass [$dM/d(\log d_{50})$] distribution is plotted along with the stack mass distribution for both high and normal pressure drops across the JBR scrubber. While these graphs cannot be used to determine absolute particle loadings, they are useful to see the *relative* amounts of material in a given particle size range. However, they may also be used to visualize particulate removal by particle size. Each decade (factor of ten) difference between the inlet and stack values on the Y-axis represents a "9" expressed as percent removal. For instance, a one decade difference represents 90% removal. Two decades represents 99% difference and so on. Both graphs show that more than 99% of the particles greater than 2μm are removed in the JBR. Both graphs also show a dramatic reduction in particulate removal between 0.6 and 1.0 μm. There appears to be no removal of particles in the 0.3 - 0.6 μm range, but apparently removal occurs for particles below 0.3 μm. This type of behavior closely resembles the particulate removal characteristics of a venturi scrubber.

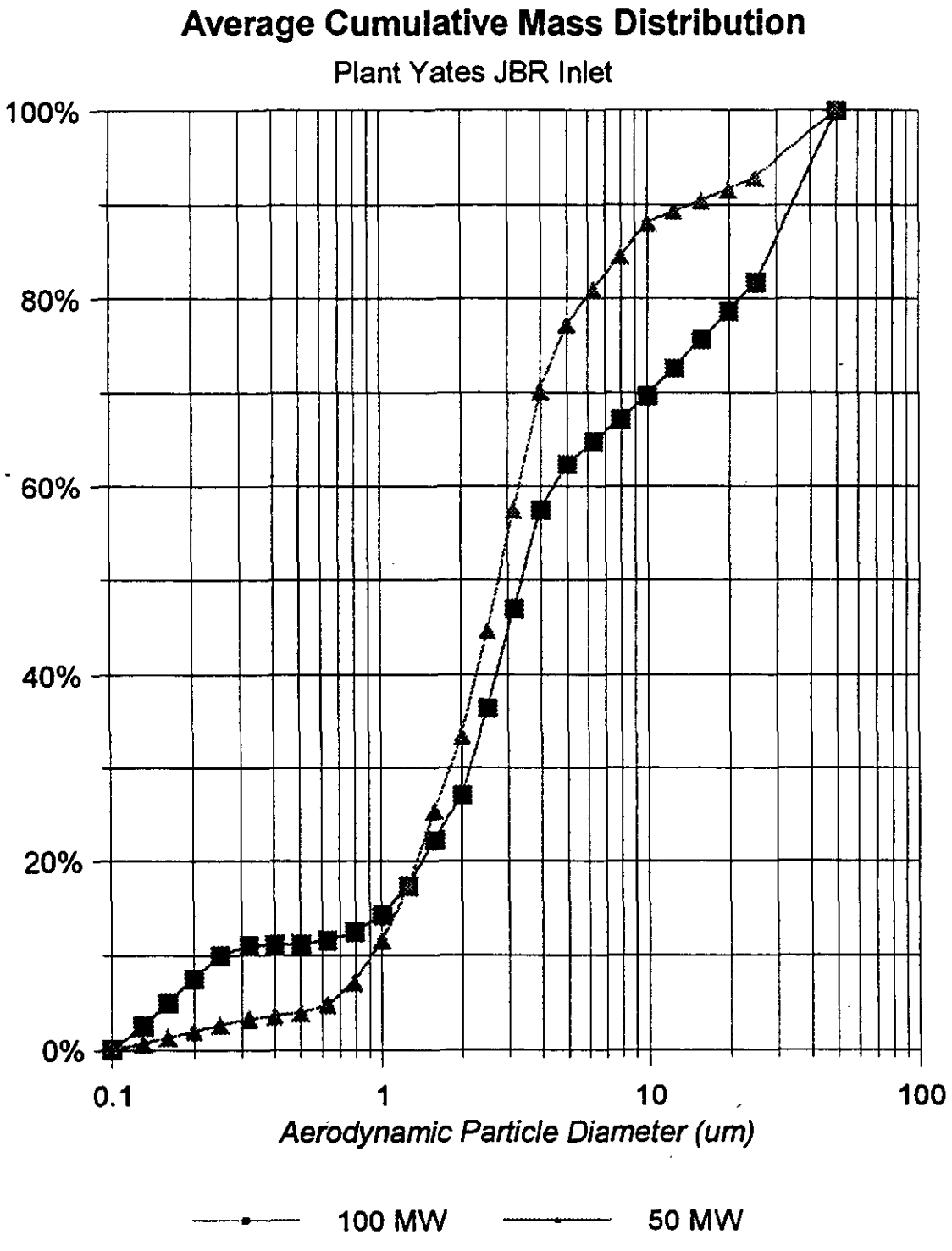

Figure 6. Average Cumulative Mass Distribution, JBR Inlet

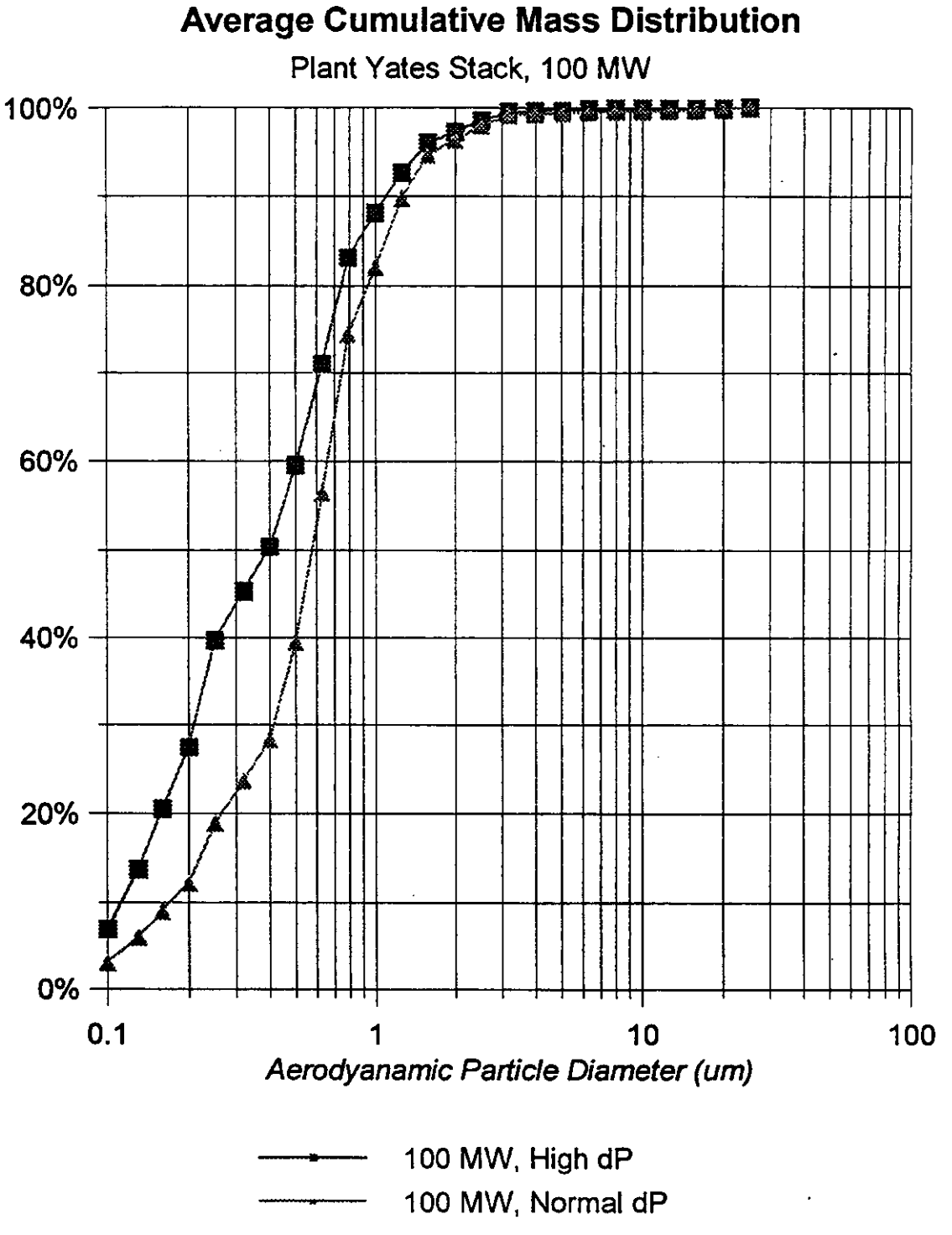

Figure 7. Stack Average Cumulative Mass Distribution, High Load

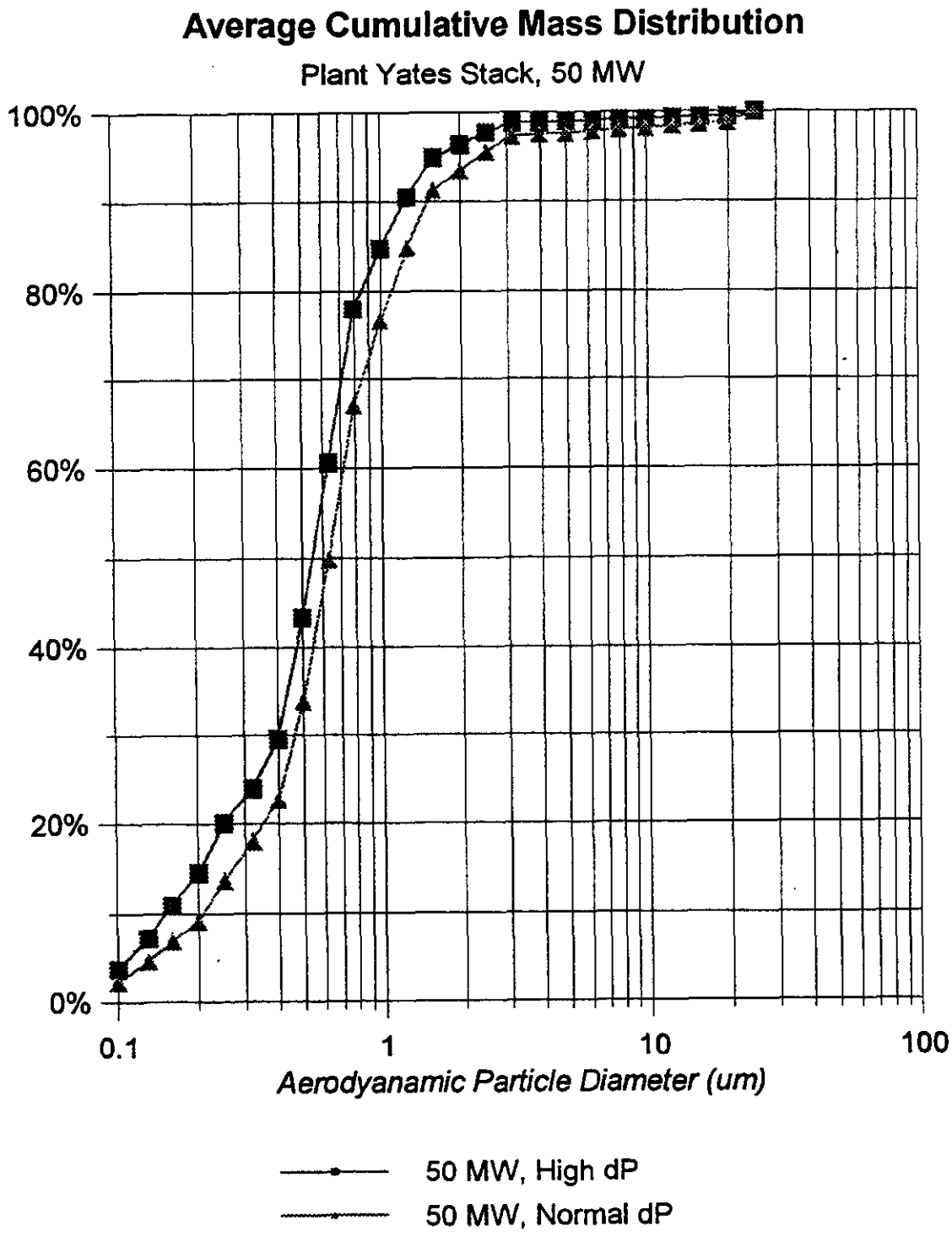

Figure 8. Stack Average Cumulative Mass Distribution, Low Load

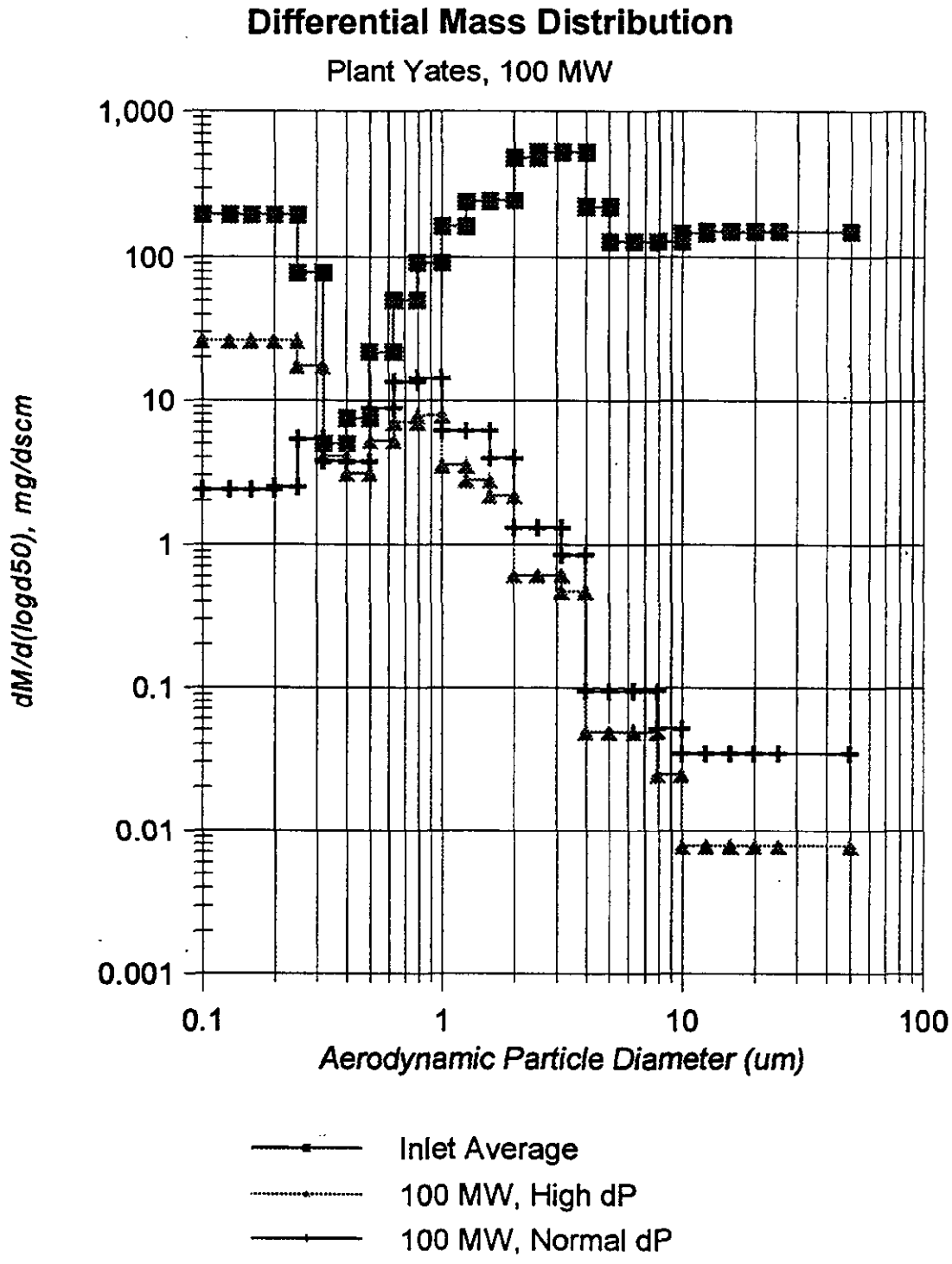

Figure 9. Relative Mass, High Load

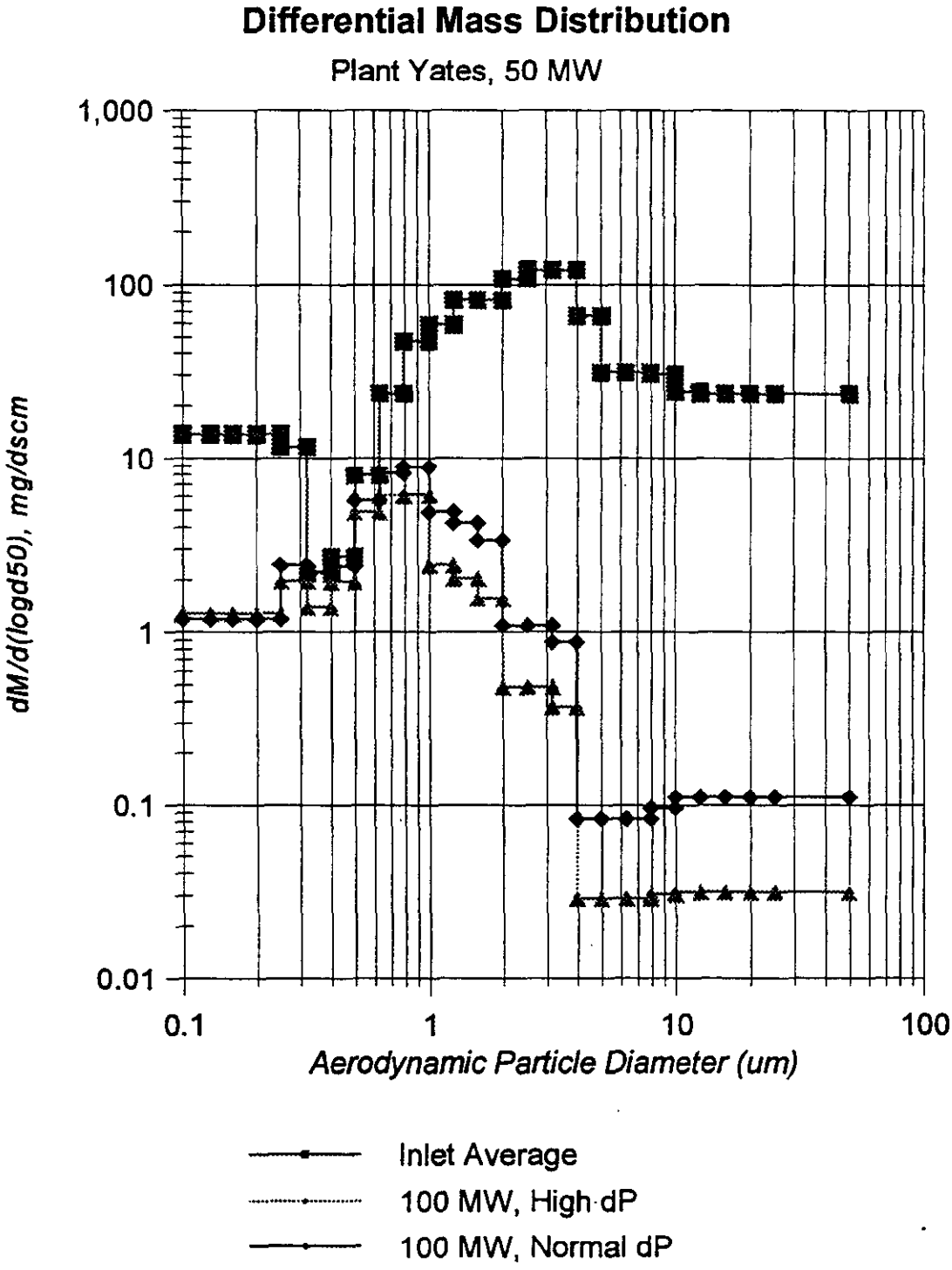

Figure 10. Relative Mass, Low Load

Overall removal efficiency is much better under high load conditions. This may be due primairly because there is more material entering the JBR under high load conditons, however, higher flue gas velocities could improve contacting efficiency in the JBR which could also lead to increased particle removal efficiency.

Average particle removal efficiency for each of the test conditions are presented in Figure 11. The dramatic change in removal efficiency for particles less than 1 μm in diameter is quite evident.

Plots of individual test runs for both cumulative mass distribution and the differential mass distribution are presented in Appendix E.

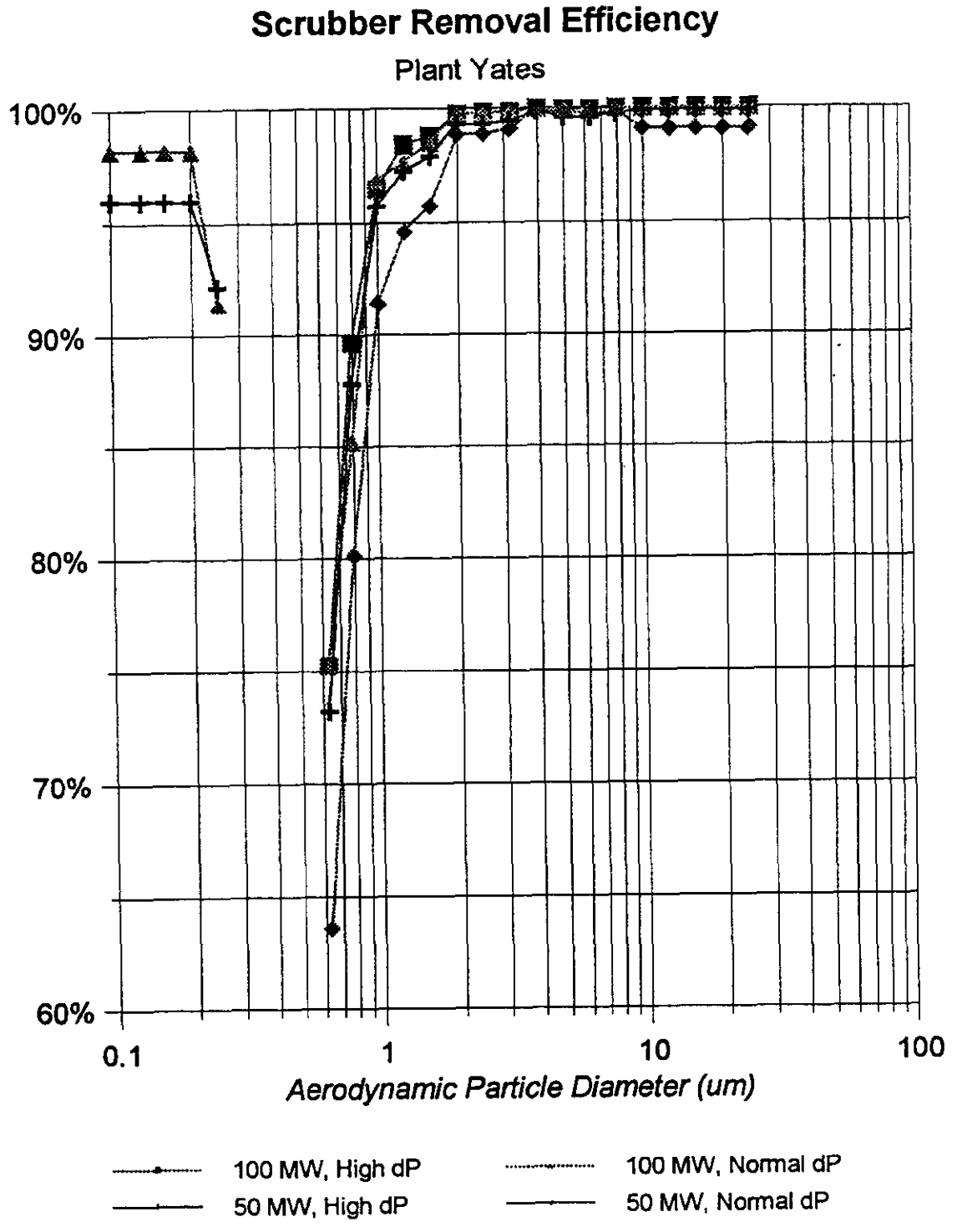

Figure 11. Scrubber Removal Efficiency by Particle Size

APPENDIX A

SAMPLING METHODOLOGIES

1.0 GAS STREAMS

1.1 Particulate Loading

Particulate loading was determined using EPA Reference Method 5b (RM5b). This method allows for an elevated filtration temperature (320°F) to eliminate the bias of sulfuric acid particulate matter. The method was altered to allow for the simultaneous determination of vapor-phase metals in an independent test program supported by EPRI. The modifications included the use of a glass nozzle, glass liner, and quartz-fiber filter in lieu of stainless-steel components and a glass-fiber filter. The condenser assembly was also charged with various absorbing solutions to capture vapor-phase metals.

The RM5b sampling system consisted of a calibrated nozzle, heated probe and filter housing, condenser assembly, and calibrated meter and pump. The isokinetic sampling rate was calculated using preliminary measurements of gas stream conditions at the traverse points determined by EPA Reference Methods 1 and 2.

Upon completion of sampling the particulate matter collected in the nozzle, in the liner, and on the filter were recovered into appropriate containers. The samples were transported to the laboratory, heated to 320°F for 6 hours, cooled in a desiccator for 2 hours, and weighed. To compare RM5b results to the Japanese Industrial Standard (JIS) method for non-sulfuric acid particulate determination, the samples were then heated to 482°F (250°C) for 6 hours, cooled, and weighed. The final weights from both heating levels were used to calculate non-sulfuric acid particulate concentration in the gas streams.

1.2 Particulate Metals and Vapor-Phase Metals

EPA Conditional Method 29 was used for the determination of particulate and vapor-phase metals. The sampling system is identical to the RM5b system described above, with a filtration temperature of 250°F.

Metals-laden particulate matter was collected in the nozzle, in the liner, and on the filter. Vapor-phase metals were collected in a series of impingers (the condenser system). The first impinger was empty to collect condensed moisture. The next two impingers contained a nitric acid and

hydrogen peroxide solution. The fourth impinger was empty. The final two absorbing impingers contained an acidified potassium permanganate solution.

The isokinetic sampling rate and traverse points were determined in the same manner as described above for RM5b. Upon completion of sampling, the particulate matter was recovered in a similar manner to RM5b with the addition of a final dilute nitric acid rinse of the nozzle, liner, and front half of the filter holder. The impinger solutions were recovered into appropriate containers by matrix type, and the individual impingers rinsed with impinger solution to ensure complete recovery. The samples were then transported to the laboratory.

1.3 Particle Size Distribution

The particle size distribution of solids in the gas stream was determined using University of Washington cascade impactors. The impactors classified the particulate matter into ten size fractions (nine impaction stages and a final backup filter) based upon aerodynamic size. The samples were collected at single points of average sample gas velocity as determined by EPA Reference Methods 1 and 2. The samples were collected over representative time periods based on historical data. Upon completion of sampling, the individual impaction stages were recovered into appropriate containers for transportation to the laboratory. The stages were dried to remove uncombined water and weighed. The weight gains were used to determine the particle size distribution.

2.0 PROCESS SOLIDS

Ten kilogram samples of Boiler No. 1 feed coal were collected by plant personnel using an ASTM autosampler located downstream of the primary crusher. The samples were riffle-split to produce a single one-kilogram sample per test condition.

FGD solids were collected once per condition at the slurry discharge pump of the JBR adjacent to the process densitometers. The solids were separated by pressure filtration, dried, and placed in appropriate containers.

3.0 PROCESS LIQUIDS

FGD liquor samples were collected from the froth zone slip stream adjacent to the pH probe locations. The samples were pressure-filtered to remove solids, then transferred to appropriate containers and preserved as a 2% (v/v) HNO_3 diluted filtrate (DF).

Single samples of ash pond water and gypsum pond water were collected per test condition. Ash pond water was collected from one of four sample taps located in the limestone preparation area. Gypsum pond water was collected from the gypsum pond makeup tank. All of the pond water samples were filtered and preserved as HNO_3 DFs as described above.

APPENDIX B

ANALYTICAL METHODOLOGIES

Table B-1

Analytical Methods Summary

Matrix	Analyte	Digestion Method	Analytical Method
Metals in Particulate	ICP-AES Metals[a]	Modified SW3051	SW6010
	GFAA Metals[b]	Modified SW3051	GFAA[c]
	Hg	Modified SW7470	CVAA
Vapor-Phase Metals	ICP-AES Metals	SW3005	SW6010
	GFAA Metals	Modified SW3020	GFAA
	Hg	SW7470	CVAA
Limestone	ICP-AES Metals	Modified SW3050	SW6010
	AA Metals[d]	Modified SW3050	Flame AA
	S (as SO_4)	None	EPA300.0
JBR Solids	ICP-AES Metals	SW3050	SW6010
	GFAA Metals	SW3050	GFAA
	Hg	SW7471	CVAA
	Ca	Modified SW3050	Flame AA
	S (as SO_4)	None	EPA300.0
JBR Liquor / Pond Waters	ICP-AES Metals	SW3005	SW6010
	GFAA Metals	SW3020	GFAA
	Hg	SW7470	CVAA
	Chloride	None	EPA300.0
Coal	ICP-AES Metals	ASTM D3682/D3683	SW6010
	GFAA Metals	ASTM D3682/D3683	GFAA
	Hg		DGAA
	Ultimate	ASTM D3176	ASTM D3176
	Proximate	ASTM D5142	ASTM D5142

Metals[a] = Al, Ba, Be, Ca, Co, Cr, Cu, Ge, K, Mg, Mn, Mo, Na, S, Sb, Ti, and V.

Metals[b] = As, Cd, Ni, Pb, and Se.

GFAA Analyses[c] = As: SW7060, Cd: SW7131, Ni: EPA249.2, Pb: SW7421, and Se: SW7740.

AA Metals[d] = Ca, Mg, and Na.

APPENDIX C

SAMPLING DATA SHEET SUMMARIES

Plant Name Yates
Location JBR Inlet - M5b "B"
Condition 1 - High dP / 100 MW

Run No.	1	2	3	Average
Date	12/1/94	12/2/94	12/3/94	-
Time Start	1314	927	1440	-
Time Finish	1927	1212	1821	-
Operator	CSG/JWH	CSG/JWH	CSG/JWH	-
Initial Leak Rate	.002 @ 15"	.006 @ 16"	.003 @ 15"	-
Final Leak Rate	.002 @ 5"	.003 @ 5"	.001 @ 5"	-
Duct Dimensions (ft)	11.2 x 11.2	11.2 x 11.2	11.2 x 11.2	-
Equivalent Stack Diameter (ft)	12.64	12.64	12.64	-
Pitot Tube Correction Factor (Cp)	0.84	0.84	0.84	-
Dry Gas Meter Calibration (Yd)	0.974	0.974	0.974	-
Nozzle Diameter (inches)	0.1660	0.1660	0.1660	-
Barometric Pressure ("Hg)	30.52	29.54	29.53	-
Static Pressure ("H2O)	-10.5	-10.5	-10.5	-
Meter Volume (acf)	90.171	42.710	44.186	59.022
Average square root of delta p	0.89	0.87	0.86	0.87
Average delta H (" H2O)	0.46	0.42	0.44	0.44
Average Stack Temperature (F)	266	257	262	262
Average DGM Temp (F)	66	58	77	67
Test Duration (minutes)	240.0	120.0	120.0	160.0
Condensed Water (g)	12.1	62.3	65.0	46.5
Filter Weight Gain (g)	2.2936	1.1100	1.4812	1.6283
PNR Weight Gain (g)	0.2511	0.1567	0.1191	0.1756
Impinger Residue (g)	NA	NA	NA	-
% CO2	11.4	11.6	11.6	11.5
% O2	7.9	8.0	8.0	8.0
% N2	80.7	80.4	80.4	80.5
Meter Volume (dscf)	87.654	40.770	40.672	56.365
Meter Volume (Nm3)	2.313	1.076	1.073	1.487
Flue Gas Moisture (%)	0.6	6.7	7.0	4.8
Gas Molecular Weight (Wet) (g/g-mole)	30.1	29.4	29.3	29.6
Absolute Stack Pressure (" Hg)	29.7	28.8	28.8	29.1
Absolute Stack Temperature (R)	726	717	722	722
Average Gas Velocity (f/sec)	57.6	57.6	57.1	57.4
Avg Flow Rate (acfm)	434,000	433,000	430,000	432,000
Avg Flow Rate (dscfm)	312,000	286,000	281,000	293,000
Isokinetic Sampling Rate (%)	98.0	99.2	100.7	99.3
Particulate Concentration (gr/dscf)	0.448	0.480	0.607	0.512
Particulate Concentration (lbs/dscf)	6.40E-05	6.85E-05	8.68E-05	7.31E-05
Particulate Emission (mg/m3)	1,100	1,178	1,491	1,256
Particulate Emission (lbs/hour)	1,198	1,176	1,463	1,279

Plant Name Yates
Location JBR Inlet - M5b "C"
Condition 2 - Norm dP / 100 MW

Run No.	1	2	3	Average
Date	12/3/94	12/4/94	12/4/94	-
Time Start	1227	902	1626	-
Time Finish	1655	1330	2024	-
Operator	CSG/JWH	CSG/JWH	CSG/JWH	-
Initial Leak Rate	.006 @ 18"	.016 @ 16"	.006 @ 15"	-
Final Leak Rate	.001 @ 6"	.004 @ 4"	.002 @ 5"	-
Duct Dimensions (ft)	11.2 x 11.2	11.2 x 11.2	11.2 x 11.2	-
Equivalent Stack Diameter (ft)	12.64	12.64	12.64	-
Pitot Tube Correction Factor (Cp)	0.84	0.84	0.84	-
Dry Gas Meter Calibration (Yd)	0.974	0.974	0.974	-
Nozzle Diameter (inches)	0.1660	0.1500	0.1500	-
Barometric Pressure ("Hg)	28.56	28.51	28.51	-
Static Pressure ("H2O)	-10.5	-10.5	-10.5	-
Meter Volume (acf)	71.134	58.732	61.591	63.819
Average square root of delta p	0.86	0.84	0.88	0.86
Average delta H (" H2O)	0.44	0.29	0.32	0.35
Average Stack Temperature (F)	269	260	269	266
Average DGM Temp (F)	65	74	82	74
Test Duration (minutes)	192.0	192.0	192.0	192.0
Condensed Water (g)	109.6	105.4	116.2	110.4
Filter Weight Gain (g)	2.1501	2.0416	2.2393	2.1437
PNR Weight Gain (g)	0.0949	0.1772	0.1516	0.1412
Impinger Residue (g)	NA	NA	NA	-
% CO2	11.4	11.5	11.5	11.5
% O2	8.2	7.8	7.8	7.9
% N2	80.4	80.7	80.7	80.6
Meter Volume (dscf)	64.715	52.437	54.178	57.1
Meter Volume (Nm3)	1.708	1.384	1.429	1.507
Flue Gas Moisture (%)	7.4	8.7	9.2	8.4
Gas Molecular Weight (Wet) (g/g-mole)	29.3	29.1	29.0	29.1
Absolute Stack Pressure (" Hg)	27.8	27.7	27.7	27.8
Absolute Stack Temperature (R)	729	720	729	726
Average Gas Velocity (f/sec)	58.5	57.0	60.1	58.5
Avg Flow Rate (acfm)	440,000	429,000	453,000	441,000
Avg Flow Rate (dscfm)	274,000	266,000	276,000	272,000
Isokinetic Sampling Rate (%)	102.7	104.9	104.6	104.1
Particulate Concentration (gr/dscf)	5.35E-01	6.53E-01	6.81E-01	6.23E-01
Particulate Concentration (lbs/dscf)	7.65E-05	9.33E-05	9.73E-05	8.90E-05
Particulate Emission (mg/m3)	1,315	1,604	1,673	1,530
Particulate Emission (lbs/hour)	1,258	1,489	1,611	1,453

Plant Name Yates
Location JBR Inlet - M5b "C"
Condition 3 - High dP / 50 MW

Run No.	1	2	3	Average
Date	12/5/94	12/6/94	12/6/94	-
Time Start	1103	930	1525	-
Time Finish	1458	1257	1855	-
Operator	CSG/JWH	CSG/JWH	CSG/JWH	-
Initial Leak Rate	.008 @ 17"	.003 @ 16"	.012 @ 17"	-
Final Leak Rate	.002 @ 5"	.001 @ 7"	.004 @ 6"	-
Duct Dimensions (ft)	11.2 x 11.2	11.2 x 11.2	11.2 x 11.2	-
Equivalent Stack Diameter (ft)	12.64	12.64	12.64	-
Pitot Tube Correction Factor (Cp)	0.84	0.84	0.84	-
Dry Gas Meter Calibration (Yd)	0.974	0.974	0.974	-
Nozzle Diameter (inches)	0.2470	0.2470	0.2470	-
Barometric Pressure ("Hg)	28.57	28.63	28.63	-
Static Pressure ("H2O)	-4.0	-4.0	-4.0	-
Meter Volume (acf)	68.941	70.317	69.378	69.545
Average square root of delta p	0.51	0.51	0.51	0.51
Average delta H (" H2O)	0.77	0.78	0.80	0.78
Average Stack Temperature (F)	247	247	251	248
Average DGM Temp (F)	71	71	78	73
Test Duration (minutes)	144.0	144.0	144.0	144.0
Condensed Water (g)	115.3	109.4	114.8	113.2
Filter Weight Gain (g)	0.4001	0.3284	0.2695	0.3327
PNR Weight Gain (g)	0.1340	0.1200	0.1884	0.1475
Impinger Residue (g)	NA	NA	NA	-
% CO2	10.0	9.7	9.7	9.8
% O2	9.8	9.1	9.1	9.3
% N2	80.2	81.2	81.2	80.9
Meter Volume (dscf)	63.100	64.496	62.807	63.468
Meter Volume (Nm3)	1.665	1.702	1.657	1.675
Flue Gas Moisture (%)	7.9	7.4	7.9	7.8
Gas Molecular Weight (Wet) (g/g-mole)	29.0	29.0	29.0	29.0
Absolute Stack Pressure (" Hg)	28.3	28.3	28.3	28.3
Absolute Stack Temperature (R)	707	707	711	708
Average Gas Velocity (f/sec)	34.0	34.0	34.1	34.0
Avg Flow Rate (acfm)	256,000	256,000	257,000	256,000
Avg Flow Rate (dscfm)	166,000	168,000	166,000	167,000
Isokinetic Sampling Rate (%)	99.5	101.0	99.1	99.8
Particulate Concentration (gr/dscf)	1.31E-01	1.07E-01	1.13E-01	1.17E-01
Particulate Concentration (lbs/dscf)	1.87E-05	1.53E-05	1.61E-05	1.67E-05
Particulate Emission (mg/m3)	321	263	276	287
Particulate Emission (lbs/hour)	186	155	160	167

Plant Name Yates
Location JBR Inlet - M-5b "D"
Condition 3 - High dP / 50 MW

Run No.	1	2	3	Average
Date	12/5/94	12/6/94	12/6/94	-
Time Start	1104	931	1526	-
Time Finish	1455	1258	1856	-
Operator				-
Initial Leak Rate	.012 @ 17"	.006 @ 16"	.006 @ 16"	-
Final Leak Rate	.002 @ 10"	.002 @ 8"	.008 @ 9"	-
Duct Dimensions (ft)	11.2 x 11.2	11.2 x 11.2	11.2 x 11.2	-
Equivalent Stack Diameter (ft)	12.64	12.64	12.64	-
Pitot Tube Correction Factor (Cp)	0.84	0.84	0.84	-
Dry Gas Meter Calibration (Yd)	1.031	1.031	1.031	-
Nozzle Diameter (inches)	0.3082	0.3082	0.3082	-
Barometric Pressure ("Hg)	28.57	28.63	28.63	-
Static Pressure ("H2O)	-4.0	-4.0	-4.0	-
Meter Volume (acf)	98.221	100.505	99.180	99.302
Average square root of delta p	0.50	0.51	0.51	0.51
Average delta H (" H2O)	1.85	1.90	1.82	1.86
Average Stack Temperature (F)	246	246	249	247
Average DGM Temp (F)	70	70	76	72
Test Duration (minutes)	144.0	144.0	144.0	144.0
Condensed Water (g)	169.0	153.6	158.0	160.2
Filter Weight Gain (g)	0.7230	0.4852	0.4912	0.5665
PNR Weight Gain (g)	0.0799	0.0678	0.1971	0.1149
Impinger Residue (g)	NA	NA	NA	-
% CO2	10.0	9.7	9.7	9.8
% O2	9.8	9.1	9.1	9.3
% N2	80.2	81.2	81.2	80.9
Meter Volume (dscf)	95.340	97.764	95.395	96.167
Meter Volume (Nm3)	2.516	2.580	2.517	2.537
Flue Gas Moisture (%)	7.7	6.9	7.3	7.3
Gas Molecular Weight (Wet) (g/g-mole)	29.1	29.1	29.1	29.1
Absolute Stack Pressure (" Hg)	28.3	28.3	28.3	28.3
Absolute Stack Temperature (R)	706	706	709	707.0
Average Gas Velocity (f/sec)	33.3	33.9	34.0	33.7
Avg Flow Rate (acfm)	251,000	255,000	256,000	254,000
Avg Flow Rate (dscfm)	164,000	168,000	167,000	166,000
Isokinetic Sampling Rate (%)	98.2	97.8	95.9	97.3
Particulate Concentration (gr/dscf)	1.30E-01	8.73E-02	1.11E-01	1.10E-01
Particulate Concentration (lbs/dscf)	1.86E-05	1.25E-05	1.59E-05	1.57E-05
Particulate Emission (mg/m3)	319	214	273	269
Particulate Emission (lbs/hour)	183	126	159	156

Plant Name Yates
Location JBR Inlet - M5b "B"
Condition 4 - Norm dP / 50 MW

Run No.	1	2	3	Average
Date	12/7/94	12/7/94	12/8/94	-
Time Start	904	1420	1032	-
Time Finish	1212	1747	1608	-
Operator	CSG/JWH	CSG/JWH	CSG/JWH	-
Initial Leak Rate	.004 @ 15"	.014 @ 17"	.005 @ 16"	-
Final Leak Rate	.002 @ 6"	.008 @ 6"	.003 @ 6"	-
Duct Dimensions (ft)	11.2 x 11.2	11.2 x 11.2	11.2 x 11.2	-
Equivalent Stack Diameter (ft)	12.64	12.64	12.64	-
Pitot Tube Correction Factor (Cp)	0.84	0.84	0.84	-
Dry Gas Meter Calibration (Yd)	0.974	0.974	0.974	-
Nozzle Diameter (inches)	0.2470	0.2470	0.2470	-
Barometric Pressure ("Hg)	29.36	29.36	29.43	-
Static Pressure ("H2O)	-4.0	-4.0	-4.0	-
Meter Volume (acf)	68.937	69.622	71.508	70.022
Average square root of delta p	0.51	0.50	0.52	0.51
Average delta H (" H2O)	0.79	0.78	0.83	0.80
Average Stack Temperature (F)	247	251	255	251
Average DGM Temp (F)	64	75	74	71
Test Duration (minutes)	144.0	144.0	144.0	144.0
Condensed Water (g)	101.4	109.2	99.0	103.2
Filter Weight Gain (g)	0.2639	0.3224	0.6575	0.4146
PNR Weight Gain (g)	0.1482	0.0974	0.0859	0.1105
Impinger Residue (g)	NA	NA	NA	-
% CO2	9.9	9.9	10.6	10.1
% O2	9.8	9.8	9.8	9.8
% N2	80.3	80.3	79.6	80.1
Meter Volume (dscf)	65.726	65.014	67.061	65.934
Meter Volume (Nm3)	1.734	1.715	1.769	1.740
Flue Gas Moisture (%)	6.8	7.3	6.5	6.9
Gas Molecular Weight (Wet) (g/g-mole)	29.2	29.1	29.3	29.2
Absolute Stack Pressure (" Hg)	29.1	29.1	29.1	29.1
Absolute Stack Temperature (R)	707	711	715	711
Average Gas Velocity (f/sec)	33.4	32.9	34.2	33.5
Avg Flow Rate (acfm)	252,000	248,000	257,000	252,000
Avg Flow Rate (dscfm)	170,000	166,000	173,000	170,000
Isokinetic Sampling Rate (%)	101.1	102.8	101.6	101.8
Particulate Concentration (gr/dscf)	9.68E-02	9.97E-02	1.71E-01	1.23E-01
Particulate Concentration (lbs/dscf)	1.38E-05	1.42E-05	2.44E-05	1.75E-05
Particulate Emission (mg/m3)	238	245	420	301
Particulate Emission (lbs/hour)	141	142	254	179

Plant Name Yates
Location JBR Inlet - M5b "D"
Condition 4 - Norm dP / 50 MW

Run No.	1	2	3	Average
Date	12/7/94	12/7/94	12/8/94	-
Time Start	904	1421	1033	-
Time Finish	1213	1748	1633	-
Operator	CSG/JWH	CSG/JWH	CSG/JWH	-
Initial Leak Rate	.002 @ 16"	.018 @ 15"	.004 @ 16"	-
Final Leak Rate	.001 @ 8"	.005 @ 9"	.002 @ 7"	-
Duct Dimensions (ft)	11.2 x 11.2	11.2 x 11.2	11.2 x 11.2	-
Equivalent Stack Diameter (ft)	12.64	12.64	12.64	-
Pitot Tube Correction Factor (Cp)	0.84	0.84	0.84	-
Dry Gas Meter Calibration (Yd)	1.031	1.031	1.031	-
Nozzle Diameter (inches)	0.3023	0.3023	0.3023	-
Barometric Pressure ("Hg)	29.36	29.36	29.43	-
Static Pressure ("H2O)	-4.0	-4.0	-4.0	-
Meter Volume (acf)	99.098	98.528	133.078	110.235
Average square root of delta p	0.52	0.51	0.48	0.50
Average delta H (" H2O)	1.87	1.84	1.39	1.70
Average Stack Temperature (F)	247	250	255	251
Average DGM Temp (F)	62	73	78	71
Test Duration (minutes)	144.0	144.0	216.0	168.0
Condensed Water (g)	152.0	157.8	190.1	166.6
Filter Weight Gain (g)	0.4980	0.4667	1.1890	0.7179
PNR Weight Gain (g)	0.1052	0.2412	0.1389	0.1618
Impinger Residue (g)	NA	NA	NA	-
% CO2	9.9	9.9	10.1	10.0
% O2	9.8	9.8	9.8	9.8
% N2	80.3	80.3	80.1	80.2
Meter Volume (dscf)	100.394	97.757	131.124	109.758
Meter Volume (Nm3)	2.649	2.579	3.460	2.896
Flue Gas Moisture (%)	6.7	7.1	6.4	6.7
Gas Molecular Weight (Wet) (g/g-mole)	29.2	29.1	29.2	29.2
Absolute Stack Pressure (" Hg)	29.1	29.1	29.1	29.1
Absolute Stack Temperature (R)	707	710	715	711
Average Gas Velocity (f/sec)	34.1	33.5	31.6	33.1
Avg Flow Rate (acfm)	257,000	253,000	238,000	249,000
Avg Flow Rate (dscfm)	174,000	170,000	160,000	168,000
Isokinetic Sampling Rate (%)	101.0	100.9	95.6	99.2
Particulate Concentration (gr/dscf)	9.27E-02	1.12E-01	1.56E-01	1.20E-01
Particulate Concentration (lbs/dscf)	1.32E-05	1.60E-05	2.23E-05	1.72E-05
Particulate Emission (mg/m3)	228	274	384	295
Particulate Emission (lbs/hour)	138	163	214	172

Plant Name Yates
Location JBR Inlet - M29 "Std"
Condition 1 - High dP / 100 MW

Run No.	1	2	3	Average
Date	12/1/94	12/2/94	12/2/94	-
Time Start	1313	925	1802	-
Time Finish	1926	1613	2210	-
Operator	CSG/JWH	CSG/JWH	CSG/JWH	-
Initial Leak Rate	.004 @ 15"	.016 @ 15"	.003 @ 15"	-
Final Leak Rate	.002 @ 6"	.006 @ 5"	.004 @ 8"	-
Duct Dimensions (ft)	11.2 x 11.2	11.2 x 11.2	11.2 x 11.2	-
Equivalent Stack Diameter (ft)	12.64	12.64	12.64	-
Pitot Tube Correction Factor (Cp)	0.84	0.84	0.84	-
Dry Gas Meter Calibration (Yd)	1.031	1.031	1.031	-
Nozzle Diameter (inches)	0.1920	0.1920	0.2173	-
Barometric Pressure ("Hg)	30.52	29.53	29.53	-
Static Pressure ("H2O)	-10.5	-10.5	-10.5	-
Meter Volume (acf)	113.079	105.625	112.922	110.542
Average square root of delta p	0.85	0.84	0.89	0.86
Average delta H (" H2O)	0.76	0.75	1.23	0.91
Average Stack Temperature (F)	259	260	264	261
Average DGM Temp (F)	66	66	67	66
Test Duration (minutes)	240.0	240.0	192.0	224.0
Condensed Water (g)	158.0	158.0	167.8	161.3
Filter Weight Gain (g)	2.9731	3.4742	3.8824	3.4432
PNR Weight Gain (g)	0.0133	0.4122	0.2012	0.2089
Impinger Residue (g)	NA	NA	NA	-
% CO2	11.4	11.6	11.6	11.5
% O2	7.9	8.2	8.2	8.1
% N2	80.7	80.2	80.2	80.4
Meter Volume (dscf)	116.355	105.068	112.113	111.2
Meter Volume (Nm3)	3.070	2.772	2.958	2.933
Flue Gas Moisture (%)	6.0	6.6	6.6	6.4
Gas Molecular Weight (Wet) (g/g-mole)	29.4	29.4	29.4	29.4
Absolute Stack Pressure (" Hg)	29.7	28.8	28.8	29.1
Absolute Stack Temperature (R)	719	720	724	721
Average Gas Velocity (f/sec)	55.3	55.7	59.2	56.7
Avg Flow Rate (acfm)	417,000	419,000	445,000	427,000
Avg Flow Rate (dscfm)	286,000	276,000	291,000	284,000
Isokinetic Sampling Rate (%)	105.9	99.1	97.6	100.9
Particulate Concentration (gr/dscf)	3.96E-01	5.71E-01	5.62E-01	5.10E-01
Particulate Concentration (lbs/dscf)	5.66E-05	8.16E-05	8.03E-05	7.28E-05
Particulate Emission (mg/m3)	973	1,402	1,380	1,252
Particulate Emission (lbs/hour)	971	1,351	1,402	1,241

Plant Name Yates
Location JBR Inlet - M29 "Std"
Condition 2 - Norm dP / 100 MW

Run No.	1	2	3	Average
Date	12/3/94	12/4/94	12/4/94	-
Time Start	1228	903	1627	-
Time Finish	1656	1337	2025	-
Operator	CSG/JWH	CSG/JWH	CSG/JWH	-
Initial Leak Rate	.01 @ 18"	.01 @ 15"	.016 @ 15"	-
Final Leak Rate	.006 @ 7"	.002 @ 8"	.012 @ 9"	-
Duct Dimensions (ft)	11.2 x 11.2	11.2 x 11.2	11.2 x 11.2	-
Equivalent Stack Diameter (ft)	12.64	12.64	12.64	-
Pitot Tube Correction Factor (Cp)	0.84	0.84	0.84	-
Dry Gas Meter Calibration (Yd)	1.031	1.031	1.031	-
Nozzle Diameter (inches)	0.2173	0.2173	0.2173	-
Barometric Pressure ("Hg)	28.56	28.51	28.51	-
Static Pressure ("H2O)	-10.5	-10.5	-10.5	-
Meter Volume (acf)	111.924	110.396	114.333	112.218
Average square root of delta p	0.87	0.84	0.88	0.86
Average delta H (" H2O)	1.36	1.22	1.40	1.33
Average Stack Temperature (F)	265	261	266	264
Average DGM Temp (F)	62	72	79	71
Test Duration (minutes)	192.0	192.0	192.0	192.0
Condensed Water (g)	183.4	206.7	216.9	202.3
Filter Weight Gain (g)	3.5661	3.8532	3.8650	3.7614
PNR Weight Gain (g)	0.1825	0.4753	0.4409	0.3662
Impinger Residue (g)	NA	NA	NA	-
% CO2	11.4	11.5	11.5	11.5
% O2	8.2	7.8	7.8	7.9
% N2	80.4	80.7	80.7	80.6
Meter Volume (dscf)	108.403	104.724	107.050	106.726
Meter Volume (Nm3)	2.860	2.763	2.825	2.816
Flue Gas Moisture (%)	7.4	8.5	8.7	8.2
Gas Molecular Weight (Wet) (g/g-mole)	29.3	29.1	29.1	29.2
Absolute Stack Pressure (" Hg)	27.8	27.7	27.7	27.8
Absolute Stack Temperature (R)	725	721	726	724
Average Gas Velocity (f/sec)	59.0	57.0	59.9	58.6
Avg Flow Rate (acfm)	444,000	429,000	451,000	441,000
Avg Flow Rate (dscfm)	278,000	266,000	277,000	274,000
Isokinetic Sampling Rate (%)	98.9	99.8	97.9	98.9
Particulate Concentration (gr/dscf)	5.34E-01	6.38E-01	6.21E-01	5.98E-01
Particulate Concentration (lbs/dscf)	7.62E-05	9.11E-05	8.87E-05	8.54E-05
Particulate Emission (mg/m3)	1,311	1,567	1,524	1,467
Particulate Emission (lbs/hour)	1,272	1,455	1,474	1,400

Plant Name Yates
Location Stack - M5b - "B"
Condition 1 - High dP / 100 MW

Run No.	1	2	3	Average
Date	12/1/94	12/2/94	12/2/94	-
Time Start	1508	1037	1550	-
Time Finish	2051	1322	1820	-
Operator	JWM/MAB	JWM/MAB	JWM/MAB	-
Initial Leak Rate	.01 @ 25"	.003 @ 18"	.008 @ 11"	-
Final Leak Rate	.005 @ 10"	.007 @ 9"	.002 @ 9"	-
Duct Dimensions (ft)	-	-	-	-
Stack Diameter (ft)	13.0	13.0	13.0	13.0
Pitot Tube Correction Factor (Cp)	0.84	0.84	0.84	-
Dry Gas Meter Calibration (Yd)	0.961	0.961	0.961	-
Nozzle Diameter (inches)	0.1940	0.2470	0.2470	-
Barometric Pressure ("Hg)	30.52	29.51	29.53	-
Static Pressure ("H2O)	-0.56	-0.56	-0.56	-
Meter Volume (acf)	104.445	96.660	97.099	99.401
Average square root of delta p	0.77	0.80	0.80	0.79
Average delta H (" H2O)	0.78	2.19	2.21	1.73
Average Stack Temperature (F)	116	117	118	117
Average DGM Temp (F)	60	64	74	66
Test Duration (minutes)	216.0	121.0	120.0	152.3
Condensed Water (g)	266.0	255.6	261.7	261.1
Filter Weight Gain (g)	0.0184	0.0130	0.0141	0.0152
PNR Weight Gain (g)	0.1099	0.0578	0.0011	0.0563
Impinger Residue (g)	NA	NA	NA	-
% CO2	10.9	10.9	10.9	10.9
% O2	8.3	8.3	8.3	8.3
% N2	80.8	80.8	80.8	80.8
Meter Volume (dscf)	103.819	92.188	90.934	95.647
Meter Volume (Nm3)	2.739	2.432	2.399	2.524
Flue Gas Moisture (%)	10.8	11.6	12.0	11.4
Gas Molecular Weight (Wet) (g/g-mole)	28.8	28.7	28.6	28.7
Absolute Stack Pressure (" Hg)	30.5	29.5	29.5	29.8
Absolute Stack Temperature (R)	576	577	578	577
Average Gas Velocity (f/sec)	44.8	47.5	47.5	46.6
Avg Flow Rate (acfm)	357,000	378,000	379,000	371,000
Avg Flow Rate (dscfm)	297,000	301,000	300,000	299,000
Isokinetic Sampling Rate (%)	104.6	100.9	100.8	102.1
Particulate Concentration (gr/dscf)	0.0191	0.0119	0.0026	0.0112
Particulate Concentration (lbs/dscf)	2.72E-06	1.69E-06	3.69E-07	1.60E-06
Particulate Emission (mg/m3)	47	29	6	27
Particulate Emission (lbs/hour)	49	31	7	29

Plant Name Yates
Location Stack - M5b "C"
Condition 2 - Norm dP / 100 MW

Run No.	1	2	3	Average
Date	12/3/94	12/4/94	12/4/94	-
Time Start	1307	1032	1438	-
Time Finish	1547	1301	1730	-
Operator	JWM/MAB	JWM/MAB	JWM/MAB	-
Initial Leak Rate	.013 @ 11"	.004 @ 15"	.008 @ 11"	-
Final Leak Rate	.017 @ 8"	.003 @ 11"	.009 @ 7"	-
Duct Dimensions (ft)	-	-	-	-
Stack Diameter (ft)	13.0	13.0	13.0	-
Pitot Tube Correction Factor (Cp)	0.84	0.84	0.84	-
Dry Gas Meter Calibration (Yd)	0.961	0.961	0.961	-
Nozzle Diameter (inches)	0.2470	0.2470	0.2470	-
Barometric Pressure ("Hg)	28.56	28.51	28.51	-
Static Pressure ("H2O)	-0.56	-0.56	-0.56	-
Meter Volume (acf)	96.775	99.433	99.316	98.508
Average square root of delta p	0.82	0.82	0.82	0.82
Average delta H (" H2O)	2.26	2.28	2.27	2.27
Average Stack Temperature (F)	118	117	120	118
Average DGM Temp (F)	61	74	77	71
Test Duration (minutes)	120.0	120.0	120.0	120.0
Condensed Water (g)	273.1	289.6	302.5	288.4
Filter Weight Gain (g)	0.0214	0.0136	0.0199	0.0183
PNR Weight Gain (g)	0.0040	0.0039	0.0040	0.0040
Impinger Residue (g)	NA	NA	NA	-
% CO2	10.6	10.9	10.9	10.8
% O2	9.1	8.8	8.8	8.9
% N2	80.3	80.3	80.3	80.3
Meter Volume (dscf)	89.836	89.899	89.292	89.676
Meter Volume (Nm3)	2.370	2.372	2.356	2.366
Flue Gas Moisture (%)	12.5	13.2	13.8	13.2
Gas Molecular Weight (Wet) (g/g-mole)	28.5	28.5	28.4	28.5
Absolute Stack Pressure (" Hg)	28.5	28.5	28.5	28.5
Absolute Stack Temperature (R)	578	577	580	578
Average Gas Velocity (f/sec)	49.6	49.7	49.8	49.7
Avg Flow Rate (acfm)	395,000	395,000	397,000	396,000
Avg Flow Rate (dscfm)	301,000	298,000	296,000	298,000
Isokinetic Sampling Rate (%)	99.3	100.0	100.2	99.8
Particulate Concentration (gr/dscf)	4.36E-03	3.00E-03	4.13E-03	3.83E-03
Particulate Concentration (lbs/dscf)	6.23E-07	4.29E-07	5.90E-07	5.48E-07
Particulate Emission (mg/m3)	11	7	10	9
Particulate Emission (lbs/hour)	11	8	10	10

Plant Name Yates
Location Stack - M5b "C"
Condition 3 - High dP / 50 MW

Run No.	1	2	3	Average
Date	12/5/94	12/6/94	12/6/94	-
Time Start	1310	939	1611	-
Time Finish	1610	1428	1945	-
Operator	JWM/MAB	JWM/MAB	JWM/MAB	-
Initial Leak Rate	.002 @ 13"	.004 @ 10"	.003 @ 11"	-
Final Leak Rate	.001 @ 7"	.000 @ 5"	.013 @ 7"	-
Duct Dimensions (ft)	-	-	-	-
Stack Diameter (ft)	13.0	13.0	13.0	-
Pitot Tube Correction Factor (Cp)	0.84	0.84	0.84	-
Dry Gas Meter Calibration (Yd)	0.961	0.961	0.961	-
Nozzle Diameter (inches)	0.2808	0.2808	0.2808	-
Barometric Pressure ("Hg)	28.57	28.63	28.63	-
Static Pressure ("H2O)	-0.24	-0.24	-0.24	-
Meter Volume (acf)	91.653	101.657	106.400	99.903
Average square root of delta p	0.48	0.49	0.53	0.50
Average delta H (" H2O)	1.32	1.40	1.54	1.42
Average Stack Temperature (F)	116	114	116	115
Average DGM Temp (F)	77	77	68	74
Test Duration (minutes)	144.0	156.0	156.0	152.0
Condensed Water (g)	242.9	257.3	269.8	256.7
Filter Weight Gain (g)	0.0056	0.0051	0.0057	0.0055
PNR Weight Gain (g)	0.0000	0.0000	0.0125	0.0042
Impinger Residue (g)	NA	NA	NA	-
% CO2	9.6	9.9	9.9	9.8
% O2	10.0	9.8	9.8	9.9
% N2	80.4	80.3	80.3	80.3
Meter Volume (dscf)	82.644	91.857	97.782	90.761
Meter Volume (Nm3)	2.181	2.424	2.580	2.395
Flue Gas Moisture (%)	12.2	11.7	11.5	11.8
Gas Molecular Weight (Wet) (g/g-mole)	28.5	28.6	28.6	28.6
Absolute Stack Pressure (" Hg)	28.6	28.6	28.6	28.6
Absolute Stack Temperature (R)	576	574	576	575
Average Gas Velocity (f/sec)	29.0	29.5	31.9	30.1
Avg Flow Rate (acfm)	231,000	235,000	254,000	240,000
Avg Flow Rate (dscfm)	177,000	183,000	197,000	186,000
Isokinetic Sampling Rate (%)	99.9	99.7	98.1	99.2
Particulate Concentration (gr/dscf)	1.05E-03	8.57E-04	2.87E-03	1.59E-03
Particulate Concentration (lbs/dscf)	1.49E-07	1.22E-07	4.10E-07	2.27E-07
Particulate Emission (mg/m3)	3	2	7	4
Particulate Emission (lbs/hour)	2	1	5	3

Plant Name Yates
Location Stack - M5b "D"
Condition 3 - High dP / 50 MW

Run No.	1	2	3	Average
Date	12/5/94	12/6/94	12/6/94	-
Time Start	1313	944	1613	-
Time Finish	1612	1419	1941	-
Operator	JWM/MAB	JWM/MAB	JWM/MAB	-
Initial Leak Rate	.006 @ 10"	.003 @ 10"	.006 @ 10"	-
Final Leak Rate	.001 @ 6"	.000 @ 5"	.011 @ 6"	-
Duct Dimensions (ft)	-	-	-	-
Stack Diameter (ft)	13.0	13.0	13.0	-
Pitot Tube Correction Factor (Cp)	0.84	0.84	0.84	-
Dry Gas Meter Calibration (Yd)	0.972	0.972	0.972	-
Nozzle Diameter (inches)	0.2880	0.2880	0.2880	-
Barometric Pressure ("Hg)	28.57	28.63	28.63	-
Static Pressure ("H2O)	-0.24	-0.24	-0.24	-
Meter Volume (acf)	98.322	109.778	109.871	105.990
Average square root of delta p	0.49	0.51	0.51	0.50
Average delta H (" H2O)	1.57	1.63	1.66	1.62
Average Stack Temperature (F)	121	119	119	120
Average DGM Temp (F)	79	79	72	77
Test Duration (minutes)	144.0	156.0	156.0	152.0
Condensed Water (g)	257.0	270.5	270.3	265.9
Filter Weight Gain (g)	0.0086	0.0084	0.0092	0.0087
PNR Weight Gain (g)	0.0000	0.0023	0.0028	0.0017
Impinger Residue (g)	NA	NA	NA	-
% CO2	9.6	9.9	9.9	9.8
% O2	10.0	9.8	9.8	9.9
% N2	80.4	80.3	80.3	80.3
Meter Volume (dscf)	89.339	99.958	101.359	96.886
Meter Volume (Nm3)	2.357	2.637	2.674	2.556
Flue Gas Moisture (%)	12.0	11.3	11.2	11.5
Gas Molecular Weight (Wet) (g/g-mole)	28.5	28.6	28.6	28.6
Absolute Stack Pressure (" Hg)	28.6	28.6	28.6	28.6
Absolute Stack Temperature (R)	581	579	579	580
Average Gas Velocity (f/sec)	29.7	30.8	30.8	30.4
Avg Flow Rate (acfm)	237,000	245,000	245,000	242,000
Avg Flow Rate (dscfm)	181,000	189,000	190,000	187,000
Isokinetic Sampling Rate (%)	100.8	99.2	100.4	100.1
Particulate Concentration (gr/dscf)	1.49E-03	1.65E-03	1.83E-03	0.0
Particulate Concentration (lbs/dscf)	2.12E-07	2.36E-07	2.61E-07	0.0
Particulate Emission (mg/m3)	4	4	4	4
Particulate Emission (lbs/hour)	2	3	3	3

Plant Name Yates
Location Stack - M5b "B"
Condition 4 - Norm dP / 50 MW

Run No.	1	2	3	Average
Date	12/7/94	12/7/94	12/8/94	-
Time Start	953	1455	1033	-
Time Finish	1255	1801	1337	-
Operator	JWM/MAB	JWM/MAB	JWM/MAB	-
Initial Leak Rate	.001 '@ 10"	.001 @ 11"	.002 @ 12"	-
Final Leak Rate	.001 @ 6"	.007 @ 6"	.000 @ 6"	-
Duct Dimensions (ft)	-	-	-	-
Stack Diameter (ft)	13.0	13.0	13.0	-
Pitot Tube Correction Factor (Cp)	0.84	0.84	0.84	-
Dry Gas Meter Calibration (Yd)	0.961	0.961	0.961	-
Nozzle Diameter (inches)	0.2808	0.2808	0.2808	-
Barometric Pressure ("Hg)	29.36	28.62	29.63	-
Static Pressure ("H2O)	-0.24	-0.24	-0.24	-
Meter Volume (acf)	97.964	99.859	102.106	99.976
Average square root of delta p	0.49	0.48	0.50	0.49
Average delta H (" H2O)	1.34	1.36	1.42	1.37
Average Stack Temperature (F)	115	116	114	115
Average DGM Temp (F)	61	73	68	67
Test Duration (minutes)	156.0	156.0	156.0	156.0
Condensed Water (g)	239.5	251.3	252.6	247.8
Filter Weight Gain (g)	0.0071	0.0080	0.0081	0.0077
PNR Weight Gain (g)	0.0000	0.0020	0.0043	0.0021
Impinger Residue (g)	NA	NA	NA	-
% CO2	10.0	9.8	9.8	9.9
% O2	9.8	9.8	9.8	9.8
% N2	80.2	80.4	80.4	80.3
Meter Volume (dscf)	93.566	90.878	97.115	93.853
Meter Volume (Nm3)	2.469	2.398	2.562	2.476
Flue Gas Moisture (%)	10.8	11.5	10.9	11.1
Gas Molecular Weight (Wet) (g/g-mole)	28.7	28.6	28.7	28.6
Absolute Stack Pressure (" Hg)	29.3	28.6	29.6	29.2
Absolute Stack Temperature (R)	575	576	574	575
Average Gas Velocity (f/sec)	29.1	28.9	29.5	29.2
Avg Flow Rate (acfm)	232,000	230,000	235,000	232000
Avg Flow Rate (dscfm)	186,000	178,000	190,000	185000
Isokinetic Sampling Rate (%)	99.6	100.7	100.8	100.4
Particulate Concentration (gr/dscf)	1.17E-03	1.70E-03	1.97E-03	1.61E-03
Particulate Concentration (lbs/dscf)	1.67E-07	2.43E-07	2.82E-07	2.30E-07
Particulate Emission (mg/m3)	3	4	5	4
Particulate Emission (lbs/hour)	2	3	3	3

Plant Name Yates
Location Stack - M5b "D"
Condition 4 - Norm dP / 50 MW

Run No.	1	2	3	Average
Date	12/7/94	12/7/94	12/8/94	-
Time Start	949	1457	1031	-
Time Finish	1251	1803	1333	-
Operator	JWM/MAB	JWM/MAB	JWM/MAB	-
Initial Leak Rate	.003 @ 10"	.004 @ 12"	.003 @ 11"	-
Final Leak Rate	.009 @ 4"	.000 @ 4"	.000 @ 4"	-
Duct Dimensions (ft)	-	-	-	-
Stack Diameter (ft)	13.0	13.0	13.0	-
Pitot Tube Correction Factor (Cp)	0.84	0.84	0.84	-
Dry Gas Meter Calibration (Yd)	0.972	0.972	0.972	-
Nozzle Diameter (inches)	0.2880	0.2880	0.2880	-
Barometric Pressure ("Hg)	29.36	28.62	29.63	-
Static Pressure ("H2O)	-0.24	-0.24	-0.24	-
Meter Volume (acf)	105.795	106.876	112.149	108.273
Average square root of delta p	0.50	0.50	0.52	0.51
Average delta H (" H2O)	1.56	1.54	1.68	1.59
Average Stack Temperature (F)	117	118	118	118
Average DGM Temp (F)	65	75	76	72
Test Duration (minutes)	156.0	156.0	156.0	156.0
Condensed Water (g)	262.1	265.6	277.0	268.2
Filter Weight Gain (g)	0.0115	0.0151	0.0139	0.0135
PNR Weight Gain (g)	0.0000	0.0000	0.0014	0.0005
Impinger Residue (g)	NA	NA	NA	-
% CO2	10.0	10.0	9.8	9.9
% O2	9.8	9.8	9.8	9.8
% N2	80.2	80.2	80.4	80.3
Meter Volume (dscf)	101.424	98.009	106.278	101.904
Meter Volume (Nm3)	2.676	2.586	2.804	2.689
Flue Gas Moisture (%)	10.9	11.3	11.0	11.1
Gas Molecular Weight (Wet) (g/g-mole)	28.7	28.6	28.6	28.7
Absolute Stack Pressure (" Hg)	29.3	28.6	29.6	29.2
Absolute Stack Temperature (R)	577	578	578	578
Average Gas Velocity (f/sec)	29.7	30.2	30.8	30.2
Avg Flow Rate (acfm)	237,000	240,000	245,000	241,000
Avg Flow Rate (dscfm)	189,000	186,000	197,000	191,000
Isokinetic Sampling Rate (%)	100.8	99.2	101.2	100.4
Particulate Concentration (gr/dscf)	1.75E-03	2.38E-03	2.22E-03	2.12E-03
Particulate Concentration (lbs/dscf)	2.50E-07	3.40E-07	3.17E-07	3.02E-07
Particulate Emission (mg/m3)	4	6	5	5
Particulate Emission (lbs/hour)	3	4	4	3

Plant Name Yates
Location Stack - M29 "Std"
Condition 1 - High dP / 100 MW

Run No.	1	2	3	Average
Date	12/1/94	12/2/94	12/2/94	-
Time Start	1453	920	1555	-
Time Finish	1830	1230	1823	-
Operator	JWM/MAB	JWM/MAB	JWM/MAB	-
Initial Leak Rate	.001 @ 27"	.005 @ 13"	.005 @ 16"	-
Final Leak Rate	.004 @ 8"	.005 @ 8"	.001 @ 6"	-
Duct Dimensions (ft)	-	-	-	-
Stack Diameter (ft)	13.0	13.0	13.0	-
Pitot Tube Correction Factor (Cp)	0.84	0.84	0.84	-
Dry Gas Meter Calibration (Yd)	0.972	0.972	0.972	-
Nozzle Diameter (inches)	0.2510	0.2510	0.2510	-
Barometric Pressure ("Hg)	30.52	29.53	29.53	-
Static Pressure ("H2O)	-0.56	-0.56	-0.56	-
Meter Volume (acf)	103.797	101.364	104.192	103.118
Average square root of delta p	0.84	0.82	0.84	0.83
Average delta H (" H2O)	2.53	2.44	2.58	2.52
Average Stack Temperature (F)	119	119	120	119
Average DGM Temp (F)	76	62	72	70
Test Duration (minutes)	120.0	120.0	120.0	120.0
Condensed Water (g)	271.7	273.4	283.7	276.3
Filter Weight Gain (g)				
PNR Weight Gain (g)				
Impinger Residue (g)	NA	NA	NA	-
% CO2	10.9	10.9	10.9	10.9
% O2	8.3	8.3	8.3	8.3
% N2	80.8	80.8	80.8	80.8
Meter Volume (dscf)	101.241	98.222	99.065	99.509
Meter Volume (Nm3)	2.671	2.592	2.614	2.626
Flue Gas Moisture (%)	11.2	11.6	11.9	11.6
Gas Molecular Weight (Wet) (g/g-mole)	28.7	28.7	28.6	28.7
Absolute Stack Pressure (" Hg)	30.5	29.5	29.5	29.8
Absolute Stack Temperature (R)	579	579	580	579
Average Gas Velocity (f/sec)	49.1	48.7	50.0	49.3
Avg Flow Rate (acfm)	391,000	388,000	398,000	392,000
Avg Flow Rate (dscfm)	322,000	308,000	314,000	315,000
Isokinetic Sampling Rate (%)	101.2	102.6	101.4	101.7
Particulate Concentration (gr/dscf)				
Particulate Concentration (lbs/dscf)				
Particulate Emission (mg/m3)				
Particulate Emission (lbs/hour)				

Plant Name Yates
Location Stack - M29 "Std"
Condition 2 - Norm dP / 100 MW

Run No.	1	2	3	Average
Date	12/3/94	12/4/94	12/4/94	-
Time Start	1304	1028	1436	-
Time Finish	1542	1258	1732	-
Operator	JWM/MAB	JWM/MAB	JWM/MAB	-
Initial Leak Rate	.013 @ 16"	.014 @ 10"	.008 @ 10"	-
Final Leak Rate	.008 @ 7"	.003 @ 8"	.014 @ 10"	-
Duct Dimensions (ft)	-	-	-	-
Stack Diameter (ft)	13.0	13.0	13.0	-
Pitot Tube Correction Factor (Cp)	0.84	0.84	0.84	-
Dry Gas Meter Calibration (Yd)	0.972	0.972	0.972	-
Nozzle Diameter (inches)	0.2510	0.2510	0.2510	-
Barometric Pressure ("Hg)	28.56	28.51	28.51	-
Static Pressure ("H2O)	-0.56	-0.56	-0.56	-
Meter Volume (acf)	98.839	101.442	103.634	101.305
Average square root of delta p	0.80	0.82	0.83	0.82
Average delta H (" H2O)	2.32	2.41	2.50	2.41
Average Stack Temperature (F)	120	121	124	122
Average DGM Temp (F)	64	70	74	69
Test Duration (minutes)	120.0	120.0	120.0	120.0
Condensed Water (g)	277.4	293.1	316.0	295.5
Filter Weight Gain (g)				
PNR Weight Gain (g)				
Impinger Residue (g)	NA	NA	NA	-
% CO2	10.6	10.9	10.9	10.8
% O2	9.1	8.8	8.8	8.9
% N2	80.3	80.3	80.3	80.3
Meter Volume (dscf)	92.271	93.465	94.770	93.502
Meter Volume (Nm3)	2.435	2.466	2.500	2.467
Flue Gas Moisture (%)	12.4	12.9	13.6	13.0
Gas Molecular Weight (Wet) (g/g-mole)	28.6	28.5	28.5	28.5
Absolute Stack Pressure (" Hg)	28.5	28.5	28.5	28.5
Absolute Stack Temperature (R)	580	581	584	582
Average Gas Velocity (f/sec)	48.5	49.8	50.6	49.6
Avg Flow Rate (acfm)	386,000	397,000	403,000	395,000
Avg Flow Rate (dscfm)	293,000	299,000	299,000	297,000
Isokinetic Sampling Rate (%)	101.3	100.8	101.9	101.3
Particulate Concentration (gr/dscf)				
Particulate Concentration (lbs/dscf)				
Particulate Emission (mg/m3)				
Particulate Emission (lbs/hour)				

APPENDIX D

DETAILED ANALYTICAL RESULTS

Table D-1

Gaseous Detailed Analyses—JBR Inlet

JBR Inlet					
Condition 1, Vapor Phase, μg/m³					
	Run 1	**Run 2**	**Run 3**	**Avg**	**95% CI**
Al	26	25	26	25	1.63
Sb	<5.57	<7.54	<7.40	<6.84	--
As	<0.05	0.06	<0.06	<0.06	--
Ba	0.53	0.39	0.26	0.39	0.34
Be	<0.04	0.05	<0.05	<0.05	--
Cd	<0.02	0.13	<0.02	0.05	0.17
Ca	140	130	159	143	36.25
Cr	<0.38	0.52	<0.51	<0.51	--
Co	0.69	0.94	1.53	1.05	1.08
Cu	<0.67	0.91	<0.89	<0.89	--
Fe	19	16	24	20	11.00
Pb	1.08	1.48	0.98	1.18	0.66
Mg	<3.52	4.76	<4.67	<4.67	--
Mn	10	1.46	2.14	4.65	12.30
Hg	6.23	5.72	6.00	5.98	0.63
Mo	<0.54	0.73	<0.72	<0.72	--
Ni	0.37	0.74	0.70	0.60	0.49
K	<60	82	<80	<80	--
Na	236	192	234	221	60.91
Se	5.93	8.41	6.02	6.78	3.49
S	0.00	0.00	0.00	0.00	0.00
Ti	1.09	1.62	1.45	1.39	0.67
V	<0.33	0.45	<0.44	<0.44	--
Condition 1, Particulate Phase, μg/m³					
	Run 1	**Run 2**	**Run 3**	**Avg**	**95% CI**
Al	108,950	155,632	167,038	143,873	76,463
Sb	<29	<41	<39	<36	--
As	252	345	318	305	119
Ba	1,265	1,725	1,836	1,608	753
Be	21	33	32	29	15
Cd	2	2	2	2	0.47
Ca	9,533	14,722	14,909	13,055	7,580
Cr	150	223	222	198	104
Co	81	125	126	111	64
Cu	218	332	329	293	161
Fe	51,654	71,086	72,337	65,026	28,812
Pb	108	181	166	152	96
Mg	4,912	6,436	7,399	6,249	3,115

Table D-1 (Continued)

JBR Inlet					
Condition 1, Particulate Phase, $\mu g/m^3$					
	Run 1	**Run 2**	**Run 3**	**Avg**	**95% CI**
Mn	152	217	225	198	100
Hg	0	0	0	0	0.18
Mo	30	31	23	28	11
Ni	150	240	226	205	121
K	19,066	27,060	27,748	24,625	11,990
Na	4,280	6,015	6,958	5,751	3,374
Se	23	38	37	33	20
S	2,646	3,786	4,210	3,547	2,010
Ti	7,247	10,978	10,892	9,706	5,291
V	320	495	485	433	244
Condition 1, Particulate Phase, $\mu g/g$					
	Run 1	**Run 2**	**Run 3**	**Avg**	**95% CI**
Al	112,000	111,000	121,000	114,667	13,683
Sb	<59	<59	<57	<58	--
As	259	246	230	245	36
Ba	1,300	1,230	1330	1,287	127
Be	22	23	23.1	23	1.51
Cd	2	1	1.46	2	0.42
Ca	9,800	10,500	10,800	10,367	1,275
Cr	154	159	161	158	9
Co	83	89	91.4	88	11
Cu	224	237	238	233	19
Fe	53,100	50,700	52,400	52,067	3,066
Pb	111	129	120	120	22
Mg	5,050	4,590	5,360	5,000	963
Mn	156	155	163	158	11
Hg	0	0	0.148	0	0.09
Mo	31	22	16.4	23	18
Ni	154	171	164	163	21
K	19,600	19,300	20,100	19,667	1,004
Na	4,400	4,290	5,040	4,577	1,006
Se	24	27	27	26	4
S	2,720	2,700	3,050	2,823	488
Ti	7,450	7,830	7,890	7,723	593
V	329	353	351	344	33

Table D-1 (Continued)

JBR Inlet					
Condition 1, Total, $\mu g/m^3$					
	Run 1	**Run 2**	**Run 3**	**Avg**	**95% CI**
Al	109,000	156,000	167,000	144,000	76,532
Sb	<29	<82	<79	<63	--
As	252	345	318	305	119
Ba	1,270	1,720	1,840	1,610	747
Be	21.5	32.6	31.9	29	15
Cd	1.73	2.19	2.04	2	1
Ca	9,670	14,900	15,100	13,223	7,649
Cr	150	223	223	199	105
Co	81.4	126	128	112	65
Cu	219	333	329	294	161
Fe	51,700	71,100	72,400	65,067	28,804
Pb	109	182	167	153	96
Mg	4,920	6,440	7,400	6,253	3,107
Mn	162	219	227	203	88
Hg	6.342	5.978	6.205	6	0
Mo	30.6	31.3	23.4	28	11
Ni	150	240	227	206	121
K	19,100	27,100	27,800	24,667	12,008
Na	4,520	6,210	7,190	5,973	3,355
Se	29.4	46.5	43.3	40	23
S	2,650	3,790	4,210	3,550	2,005
Ti	7,250	11,000	10,900	9,717	5,308
V	320	495	485	433	244

Table D-1 (Continued)

JBR Inlet					
Condition 2, Vapor Phase, μg/m³					
	Run 1	**Run 2**	**Run 3**	**Avg**	**95% CI**
Al	34.09	22.55	25.99	28	15
Sb	<7.04	<7.15	<6.80	<7.00	--
As	<0.06	<0.06	<0.06	<0.06	--
Ba	0.67	0.37	0.41	0.48	0.41
Be	<0.05	<0.05	<0.05	<0.05	--
Cd	0.23	0.07	0.17	0.16	0.21
Ca	168.52	162.86	148.70	160	25
Cr	<0.49	<0.49	<0.47	<0.48	--
Co	<0.38	<0.38	<0.36	<0.38	--
Cu	<0.85	<0.86	4.00	2	5
Fe	24.44	18.31	30.55	24	15
Pb	1.23	0.58	1.06	0.96	0.85
Mg	11.57	9.81	8.78	10	4
Mn	9.47	1.38	1.32	4	12
Hg	6.22	5.91	6.06	6.06	0.38
Mo	<0.69	<0.69	<0.66	<0.68	--
Ni	0.79	0.84	1.08	0.91	0.39
K	<76.22	<77.45	<73.46	<76	--
Na	221.66	179.87	173.84	192	65
Se	6.92	8.72	10.30	8.65	4.20
S	0.00	0.00	0.00	0.00	0.00
Ti	1.65	1.54	1.33	1.51	0.41
V	<0.42	<0.43	<0.41	<0.42	--
Condition 2, Particulate Phase, μg/m³					
	Run 1	**Run 2**	**Run 3**	**Avg**	**95% CI**
Al	184,629	191,115	182,937	186,227	10,724
Sb	<44	<45	<45	<45	--
As	368	381	377	375	16
Ba	2,104	2,177	2,104	2,128	106
Be	37	38	36	37	2.14
Cd	3	3	3	2.78	0.39
Ca	17,252	17,858	16,769	17,293	1,356
Cr	283	293	279	285	18
Co	157	163	160	160	7
Cu	396	410	412	406	21
Fe	79,451	82,242	75,004	78,899	9,069
Pb	200	207	220	209	25
Mg	8,172	8,459	7,668	8,100	995
Mn	271	280	242	265	49

Table D-1 (Continued)

JBR Inlet					
Condition 2, Particulate Phase, $\mu g/m^3$					
	Run 1	**Run 2**	**Run 3**	**Avg**	**95% CI**
Hg	0	0	0	0.34	0.05
Mo	21	22	19	20	3.49
Ni	292	302	297	297	13
K	30,116	31,174	30,032	30,441	1,581
Na	4,737	4,903	5,458	5,033	938
Se	54	56	39	50	23
S	5,266	5,451	4,299	5,006	1,538
Ti	12,107	12,532	12,394	12,344	539
V	545	564	567	559	30
Condition 2, Particulate Phase, $\mu g/g$					
	Run 1	**Run 2**	**Run 3**	**Avg**	**95% CI**
Al	119,000	122,000	120,000	120,333	3,795
Sb	<58	<58	<58	<58	--
As	238	243	247	243	11
Ba	1,310	1,390	1,380	1,360	108
Be	24	24	24	24	1
Cd	2	2	2	2	0
Ca	11,800	11,400	11,000	11,400	994
Cr	164	187	183	178	31
Co	95	104	105	101	14
Cu	242	262	270	258	36
Fe	52,600	52,500	49,200	51,433	4,807
Pb	125	132	144	134	24
Mg	5,190	5,400	5,030	5,207	461
Mn	163	179	159	167	26
Hg	0	0	0	0	0
Mo	17	14	12	14	6
Ni	174	193	195	187	29
K	20,000	19,900	19,700	19,867	379
Na	5,510	3,130	3,580	4,073	3,141
Se	26	36	26	29	14
S	2,850	3,480	2,820	3,050	926
Ti	8,160	8,000	8,130	8,097	211
V	372	360	372	368	17

Table D-1 (Continued)

JBR Inlet Condition 2, Total, $\mu g/m^3$					
	Run 1	**Run 2**	**Run 3**	**Avg**	**95% CI**
Al	156,000	191,000	183,000	176,667	45,561
Sb	<75	<91	<89	<85	--
As	312	381	377	357	96
Ba	1,720	2,180	2,100	2,000	611
Be	31	38	37	35	9
Cd	2.22	2.98	2.78	3	1
Ca	15,600	18,000	16,900	16,833	2,985
Cr	215	293	279	262	103
Co	125	163	160	149	52
Cu	318	411	416	382	137
Fe	69,000	82,300	75,000	75,433	16,547
Pb	165	207	221	198	72
Mg	6,810	8,470	7,680	7,653	2,063
Mn	223	282	244	250	74
Hg	6.41	6.27	6.38	6	0
Mo	23	22	20	22	5
Ni	229	303	298	277	103
K	26,300	31,300	30,100	29,233	6,485
Na	7,440	5,080	5,630	6,050	3,068
Se	41	65	49	51	30
S	3,740	5,450	4,300	4,497	2,166
Ti	10,700	12,500	12,400	11,867	2,513
V	488	564	568	540	112

Table D-2

Gaseous Detailed Analyses—Stack

Stack					
Condition 1, Vapor Phase, µg/m3					
	Run 1	**Run 2**	**Run 3**	**Avg**	**95% CI**
Al	<5.63	<5.25	<5.60	<5.50	--
Sb	<8.18	<7.62	<8.15	<7.98	--
As	<0.07	<0.06	<0.07	<0.07	--
Ba	<0.09	0.26	<0.09	0.12	0.31
Be	<0.05	<0.05	<0.05	<0.05	--
Cd	<0.03	<0.02	0.13	0.05	0.17
Ca	41.55	52.09	30.64	41	27
Cr	<0.56	<0.52	<0.56	<0.55	--
Co	<0.44	2.54	1.01	1.26	2.92
Cu	<0.99	<0.92	<0.98	<0.96	--
Fe	7.19	10.23	9.95	9	4
Pb	23.73	2.53	17.64	15	27
Mg	<5.15	<4.80	<5.13	<5.03	--
Mn	4.72	<0.16	10.94	5.25	14
Hg	2.18	2.03	0.62	1.61	2.15
Mo	<0.80	<0.74	<0.79	<0.78	--
Ni	0.69	0.59	0.86	0.71	0.33
K	<88.54	<82.57	<87.99	<86	--
Na	96.21	135.44	75.37	102	76
Se	15.27	18.33	18.98	18	5
S	0.00	0.00	0.00	0.00	0.00
Ti	1.43	1.04	0.47	0.98	1.19
V	<0.49	<0.46	<0.49	<0.48	--
Condition 1, Particulate Phase, µg/m3					
	Run 1	**Run 2**	**Run 3**	**Avg**	**95% CI**
Al	453	587	589	543	193
Sb	<1.10	<1.13	<1.12	<1	--
As	24	23	24	24	2
Ba	39	41	41	40	4
Be	0.28	0.33	0.32	0.31	0.07
Cd	0.45	0.43	0.27	0.39	0.25
Ca	228	227	201	218	38
Cr	2.37	2.56	2.62	2.52	0.32
Co	0.76	0.90	0.90	0.85	0.21
Cu	4.19	5.71	5.59	5.16	2.09
Fe	302	337	334	324	48
Pb	2.86	2.90	3.13	2.96	0.35
Mg	59	60	56	58	6

Table D-2 (Continued)

Stack					
Condition 1, Vapor Phase, µg/m3					
	Run 1	**Run 2**	**Run 3**	**Avg**	**95% CI**
Mn	2.37	2.60	2.43	2.47	0.29
Hg	0.01	0.01	0.01	0.01	0.01
Mo	6.59	6.41	6.96	6.65	0.71
Ni	4.68	2.98	2.70	3.45	2.66
K	113	119	119	117	8
Na	118	73	129	107	73
Se	5.88	5.67	6.70	6.08	1.34
S	749	409	459	539	456
Ti	46	51	54	50	10
V	8.27	7.95	8.68	8.30	0.92
Condition 1, Total, µg/m3					
	Run 1	**Run 2**	**Run 3**	**Avg**	**95% CI**
Al	459	592	595	549	193
Sb	<8.2	<15	<16	<13	--
As	24.3	23	24.2	24	2
Ba	38.7	40.8	41.4	40	4
Be	0.336	0.381	0.377	0.36	0.06
Cd	0.48	0.457	0.401	0.45	0.10
Ca	269	279	232	260	62
Cr	2.94	3.09	3.18	3.07	0.30
Co	1.19	3.44	1.91	2.18	2.85
Cu	5.18	6.63	6.57	6.13	2.04
Fe	309	347	344	333	52
Pb	26.6	5.4	20.8	18	27
Mg	64.3	65	61	63	5
Mn	7.09	2.75	13.38	8	13
Hg	2.19037	2.0416	0.6259	1.62	2.15
Mo	7.38	7.15	7.75	7.43	0.75
Ni	5.37	3.58	3.55	4.17	2.59
K	202	201	207	203	8
Na	214	209	204	209	12
Se	21.2	24	25.7	24	6
S	749	409	459	539	456
Ti	47.1	52	54	51	9
V	8.76	8.4	9.17	8.78	0.96

Table D-2 (Continued)

Stack					
Condition 2, Vapor Phase, µg/m3					
	Run 1	**Run 2**	**Run 3**	**Avg**	**95% CI**
Al	<6.08	<5.31	<5.24	<5.54	--
Sb	<8.83	<7.70	<7.60	<8.04	--
As	<0.08	<0.07	<0.06	<0.07	--
Ba	0.30	0.33	0.59	0.41	0.39
Be	<0.06	<0.05	<0.05	<0.05	--
Cd	<0.03	0.11	<0.02	0.04	0.13
Ca	38.41	35.93	44.39	40	11
Cr	<0.61	<0.53	<0.52	<0.55	--
Co	<0.47	<0.41	1.58	0.67	1.94
Cu	5.22	3.73	2.53	3.82	3.35
Fe	10.52	10.34	5.08	8.64	7.68
Pb	0.69	7.34	<0.20	2.71	10
Mg	15.28	<4.87	<4.80	6.70	18
Mn	2.55	7.66	19.72	10	22
Hg	2.42	2.36	2.38	2.39	0.07
Mo	<0.86	<0.75	<0.74	<0.78	--
Ni	0.63	0.88	1.08	0.86	0.56
K	<95.50	<83.33	<82.18	<87	--
Na	68.60	63.66	47.59	60	27
Se	25.63	16.22	14.12	19	15
S	0.00	0.00	0.00	0.00	0.00
Ti	0.69	0.60	<0.16	0.46	0.82
V	<0.53	<0.46	<0.45	<0.48	--
Condition 2, Particulate Phase, µg/m3					
	Run 1	**Run 2**	**Run 3**	**Avg**	**95% CI**
Al	965	1,326	1,228	1,173	463
Sb	<1.20	<1.19	<1.17	<1	--
As	28	34	33	32	7
Ba	50	58	54	54	10
Be	0.48	0.56	0.60	0.55	0.14
Cd	0.61	0.45	0.42	0.49	0.25
Ca	258	338	289	295	100
Cr	3.35	4.42	4.28	4.02	1.45
Co	1.28	1.97	2.02	1.75	1.03
Cu	8.38	9.08	8.84	8.77	0.89
Fe	513	657	560	577	182
Pb	4.97	5.47	5.40	5.28	0.68
Mg	73	107	88	89	42
Mn	3.40	4.70	3.78	3.96	1.66

Table D-2 (Continued)

Stack					
Condition 2, Particulate Phase, µg/m3					
	Run 1	**Run 2**	**Run 3**	**Avg**	**95% CI**
Hg	0.01	0.01	0.01	0.01	0.00
Mo	7.06	8.15	7.08	7.43	1.55
Ni	3.69	4.46	6.40	4.85	3.47
K	194	247	233	225	69
Na	71	150	126	116	100
Se	6.24	6.73	8.68	7.22	3.20
S	563	620	520	568	125
Ti	83	105	102	97	29
V	12	13	13	13	1.86
Condition 2, Total, µg/m3					
	Run 1	**Run 2**	**Run 3**	**Avg**	**95% CI**
Al	971	1,330	1,230	1,177	460
Sb	<18	<15	<15	<16	--
As	29	34	33	32	7.42
Ba	50	58	55	54	10
Be	0.54	0.62	0.65	0.60	0.13
Cd	0.64	0.56	0.44	0.54	0.24
Ca	297	374	333	335	96
Cr	3.96	4.95	4.80	4.57	1.33
Co	1.75	2.38	3.59	2.57	2.32
Cu	14	13	11	13	3
Fe	524	667	565	585	183
Pb	6	13	6	8	10
Mg	88	112	93	98	31
Mn	5.95	12	24	14	22
Hg	2.43	2.38	2.40	2.40	0.07
Mo	7.92	8.90	7.82	8.21	1.48
Ni	4.32	5.34	7.48	5.71	4.01
K	289	331	315	312	53
Na	140	214	173	176	92
Se	32	23	23	26	13
S	563	620	520	568	125
Ti	84	106	102	97	29
V	12	14	13	13	2

Table D-3

Detailed Analysis—Solids

Coal (µg/g)						
Analyte	**Condition 1**	**Condition 2**	**Condition 3**	**Condition 4**	**Avg.**	**95% CI**
Al	17,000	16,100	17,700	16,900	16,925	911
As	7	7	9	9	8	1.61
Sb	1	1	1	1	1	0
Ba	140	130	140	140	138	6.95
Be	1.7	1.6	1.6	1.5	2	0.11
Cd	<0.5	<0.5	<0.5	<0.5	<0.5	--
Cr	16	16	18	17	17	1.33
Co	7	6	7	5	6	1.33
Cu	22	20	22	22	22	1.39
Ca	1,200	1,200	1,300	1,300	1,250	80
Pb	6.5	7	6	6	6	0.67
Fe	7,600	6,700	7,900	7,300	7,375	712
Hg	0.1	0.09	0.08	0.09	0.090	0.011
Mg	690	660	740	750	710	59
Mn	18	17	20	21	19	2.54
Mo	<3	<3	<3	<3	<3	--
K	2,500	2,500	2,600	2,600	2,550	80
Ni	13	11	13	13	13	1.39
Se	4	4	6	6	5	1.61
Na	280	300	290	290	290	11
Ti	900	870	960	950	920	59
V	36	33	39	37	36	3.48
(prox)						
% Moist.	8.59	7.5	9.29	7.95	8	1.08
% Ash	10.95	10.48	10.86	10.91	11	0.30
% Volatile	33.98	33.97	34.31	64.26	42	21
% C	55.07	55.55	54.83	54.83	55	0.47
Btu/lb	13,460	13,395	13,461	13,479	13,449	51
% S	1.33	1.26	1.35	1.29	1	0.06
MAF Btu	15,115	14,963	15,101	15,130	15,077	107
(ult)						
%Moist.	8.59	7.5	9.29	7.95	8	1.08
% C	76.58	76.47	76.14	76.32	76	0.27
% H	4.78	4.92	4.93	4.91	5	0.10
% N	1.49	1.48	1.48	1.48	1	0.01
% S	1.33	1.26	1.35	1.29	1	0.06
% Ash	10.95	10.48	10.86	10.91	11	0.30
% O_2	4.87	5.39	5.24	5.09	5	0.31

Table D-3 (Continued)

JBR Solids (µg/g)					
Analyte	**Condition 1**	**Condition 3**	**Condition 4**	**Avg.**	**95% CI**
Al	2,600	3,370	2,800	2,923	993
Sb	0.568	1.04	0.687	0.77	0.61
As	26.2	29	25	27	5.10
Ba	85.6	106	88.1	93	28
Be	1.69	1.66	1.71	1.69	0.06
Ca	195,200	220,200	205,400	206,933	31,229
Cd	0.235	0.253	0.228	0.24	0.03
Co	2.41	3.08	2.3	2.60	1.05
Cr	12.6	12.1	11.6	12	1.24
Cu	10.3	15.3	12.8	13	6.21
Fe	3,580	4,060	3,600	3,747	675
Hg	0.766	0.555	0.668	0.66	0.26
K	545	638	635	606	131
Mg	861	1,090	1,010	987	289
Mo	7.14	7.01	2.92	5.69	5.96
Mn	9.15	22.1	17.3	16	16
Na	79.9	135	115	110	69
Ni	5.14	5.3	5.19	5.21	0.20
Pb	5.91	6.41	6.08	6.13	0.63
S	159,300	178,600	170,200	169,367	24,041
Se	18.2	16.3	17	17	2.39
Ti	129	170	148	149	51
V	18.4	26.1	20.2	22	10

Table D-4

Detailed Analyses—Aqueous

	JBR Liquor (mg/L)			Ash Pond (mg/L)	Gypsum Pond (mg/L)		
	Condition 3	Condition 4	Average	Condition 3	Condition 3	Condition 4	Average
Al	35.6	49.9	42.75	0.439	6.25	5.71	5.98
Ca	1,540	2,490	2,015	35.7	1,250	1,100	1,175
Fe	0.0856	0.0954	0.0905	0.859	<0.0226	<0.0226	<0.0226
K	34.9	58	46.45	3.75	25.5	22.9	24.2
Mg	614	982	798	9.02	425	374	399.5
Mn	14.6	23.4	19	0.555	11.5	10.2	10.85
Na	51.6	85.4	68.5	12.1	38	33.4	35.7
S	228	365	296.5	28.6	283	236	259.5
Ti	0.0166	0.0362	0.0264	0.00511	0.0244	0.0129	0.01865
Chloride	4,340	6,570	5,455	53	2,900	2,760	2,830

APPENDIX E

PARTICULATE LOADING PARTICLE-SIZE DISTRIBUTION

Table E-1

Particulate Loading

Test Condition	Run	5b Loading (mg/Nm^3)		JIS Loading (mg/Nm^3)	
		Inlet	Stack	Inlet	Stack
100 MW, High ΔP	1	1,100	46.8	1,106	48.1
	2	1,178	29.1	1,187	4.85
	3	1,491	6.34	1,527	5.88
100 MW, Normal ΔP	1	1,315	10.7	1,328	16.9
	2	1,604	7.38	1,619	12.6
	3	1,673	10.1	1,713	16.1
50 MW, High ΔP	1	321	2.57	322	14.4
	2	263	2.10	271	9.08
	3	276	7.05	292	12.3
	4	319	3.65	320	8.02
	5	214	4.06	220	5.57
	6	274	4.49	273	5.20
50 MW, Normal ΔP	1	238	2.88	249	5.59
	2	245	4.17	258	6.46
	3	420	4.84	430	14.2
	4	228	4.30	228	4.00
	5	274	5.84	271	5.84
	6	384	5.46	382	5.71

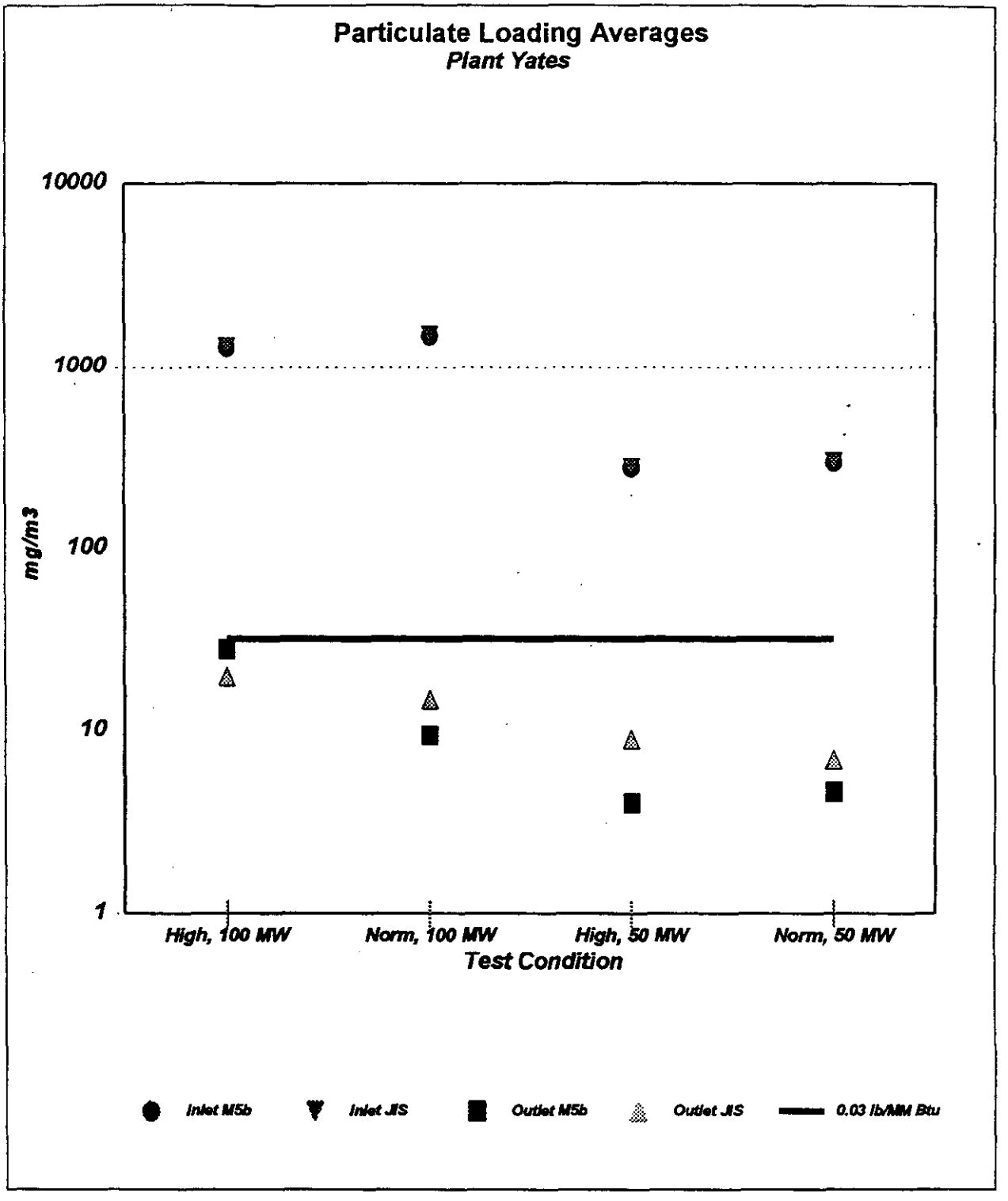

Figure E-1. Average Particulate Loading By Test Condition

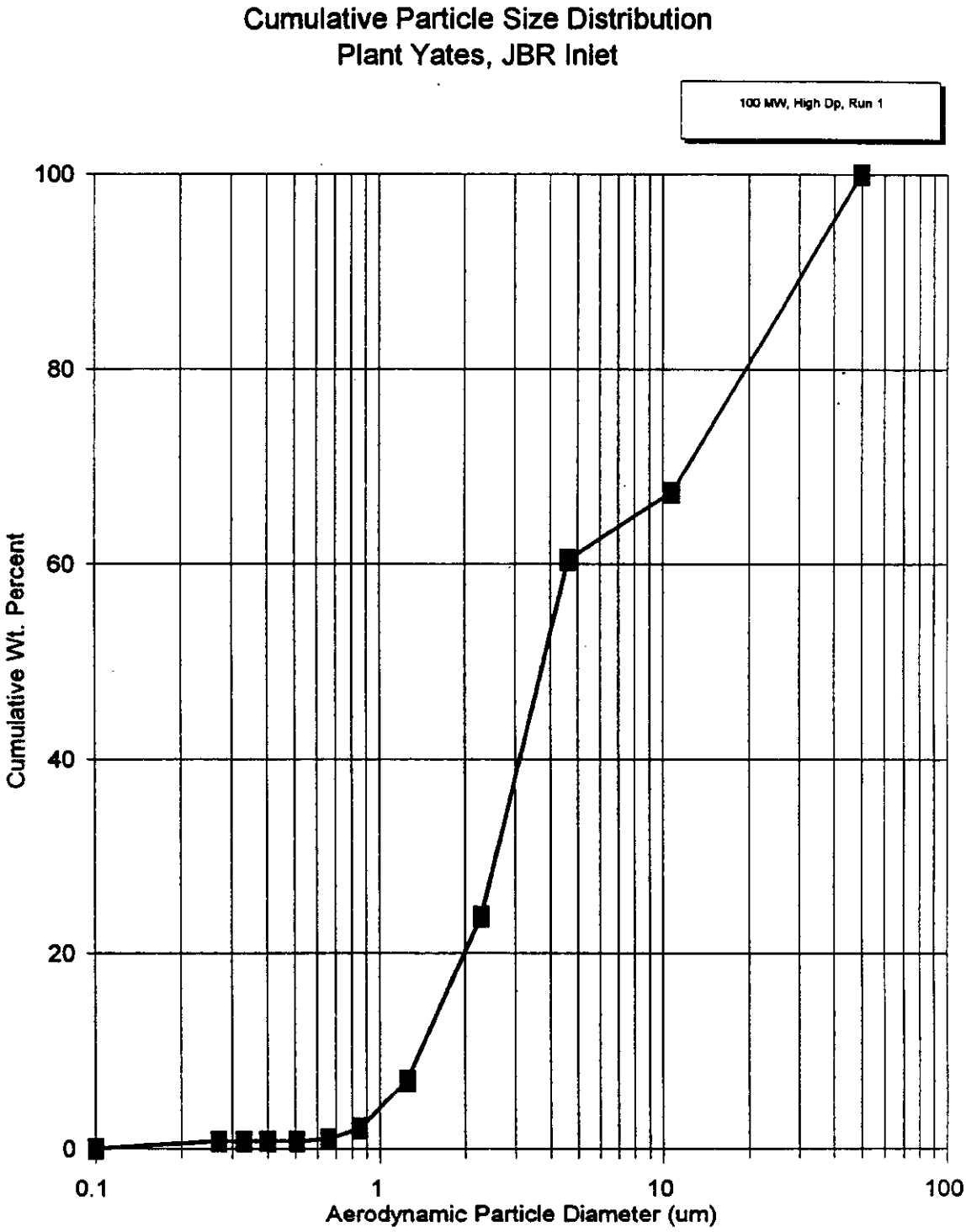
Cumulative Particle Size Distribution
Plant Yates, JBR Inlet
100 MW, High Dp, Run 1
Cumulative Wt. Percent
100
80
60
40
20
0
0.1
1
10
100
Aerodynamic Particle Diameter (um)

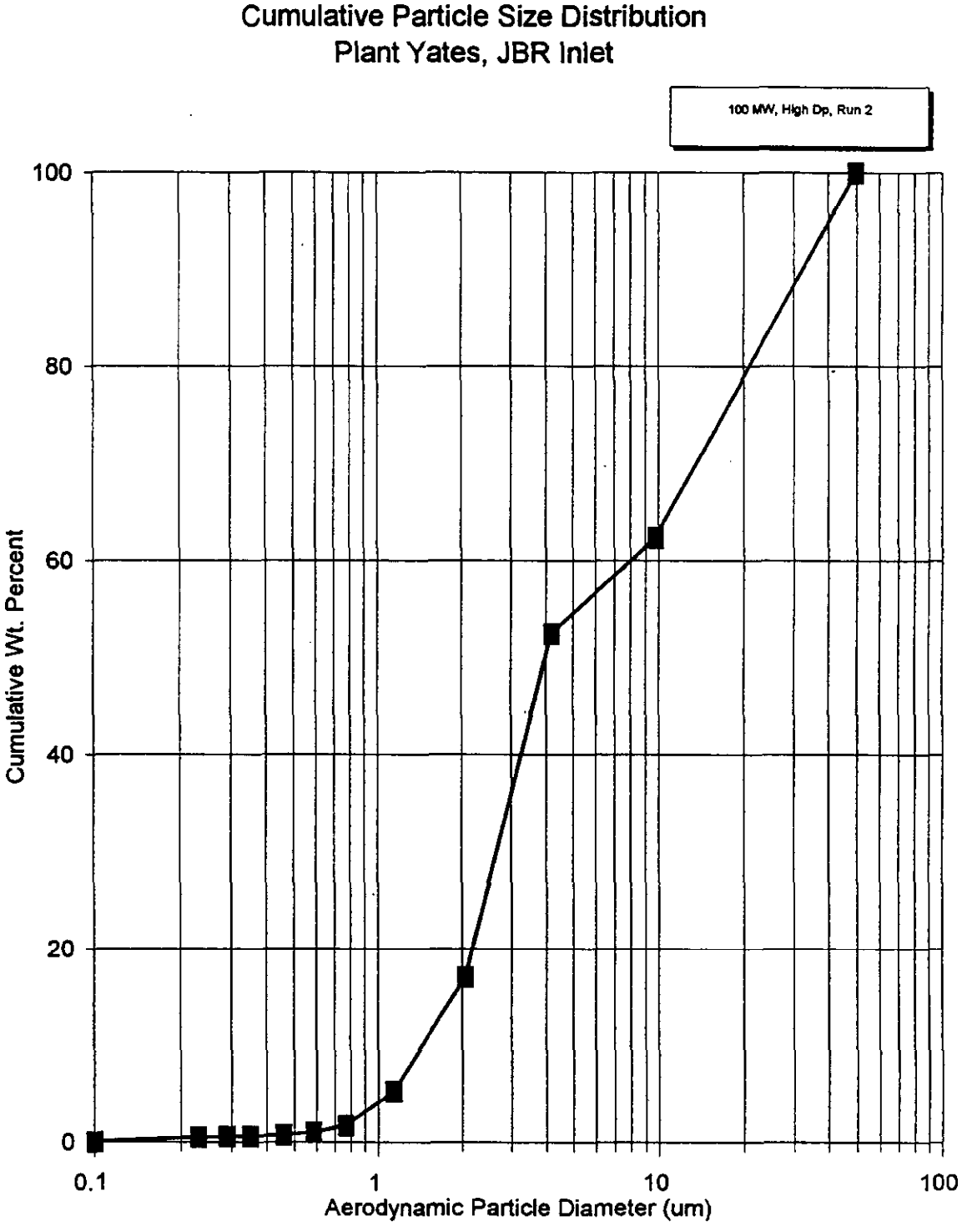
Cumulative Particle Size Distribution
Plant Yates, JBR Inlet
100 MW, High Dp, Run 2
Cumulative Wt. Percent
100
80
60
40
20
0
0.1
1
10
100
Aerodynamic Particle Diameter (um)

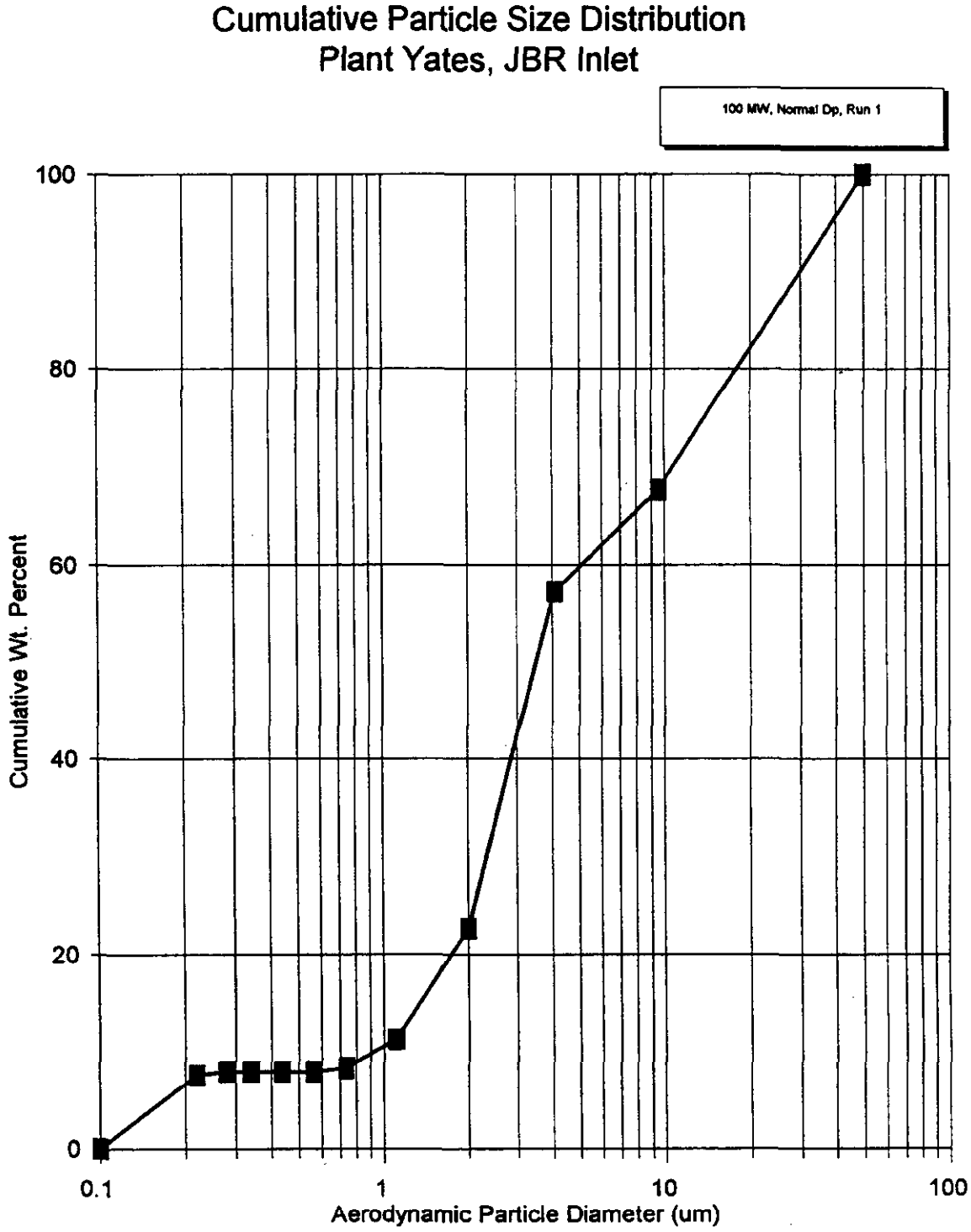
Cumulative Particle Size Distribution
Plant Yates, JBR Inlet
100 MW, Normal Dp, Run 1
Cumulative Wt. Percent
100
80
60
40
20
0
0.1
1
10
100
Aerodynamic Particle Diameter (um)

Cumulative Particle Size Distribution
Plant Yates, JBR Inlet

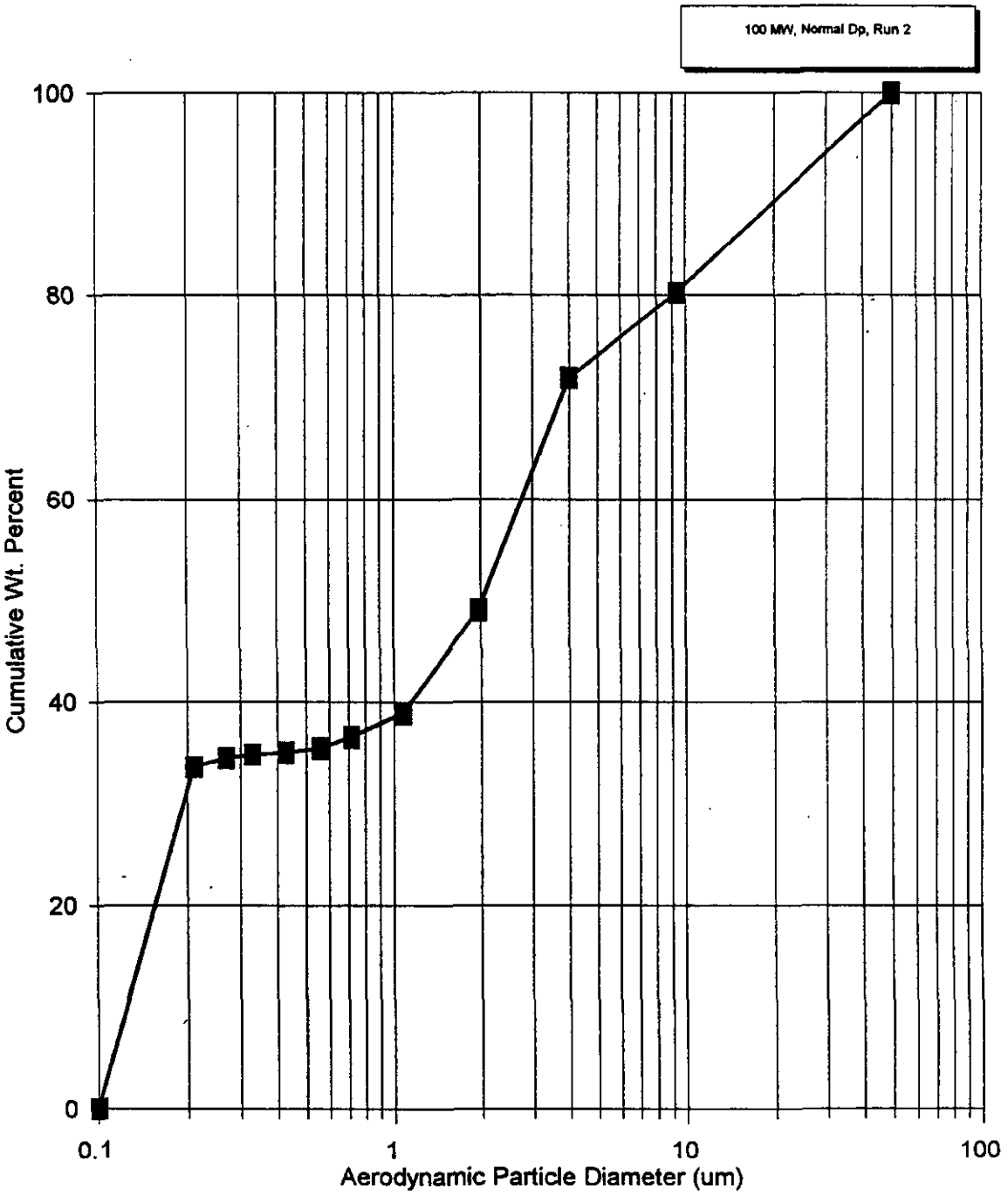

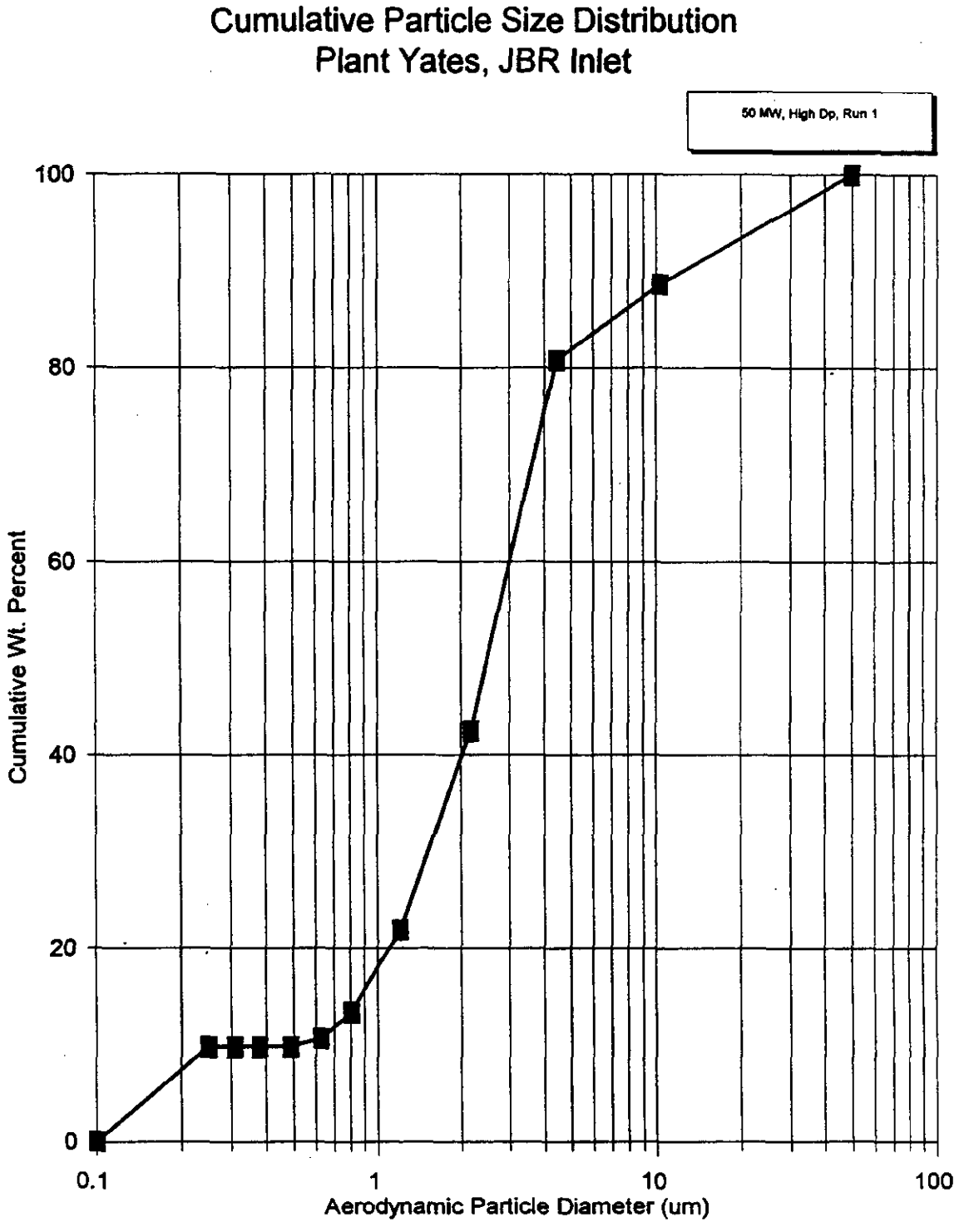
Cumulative Particle Size Distribution
Plant Yates, JBR Inlet
50 MW, High Dp, Run 1
100
80
60
40
20
0
Cumulative Wt. Percent
0.1
1
10
100
Aerodynamic Particle Diameter (um)

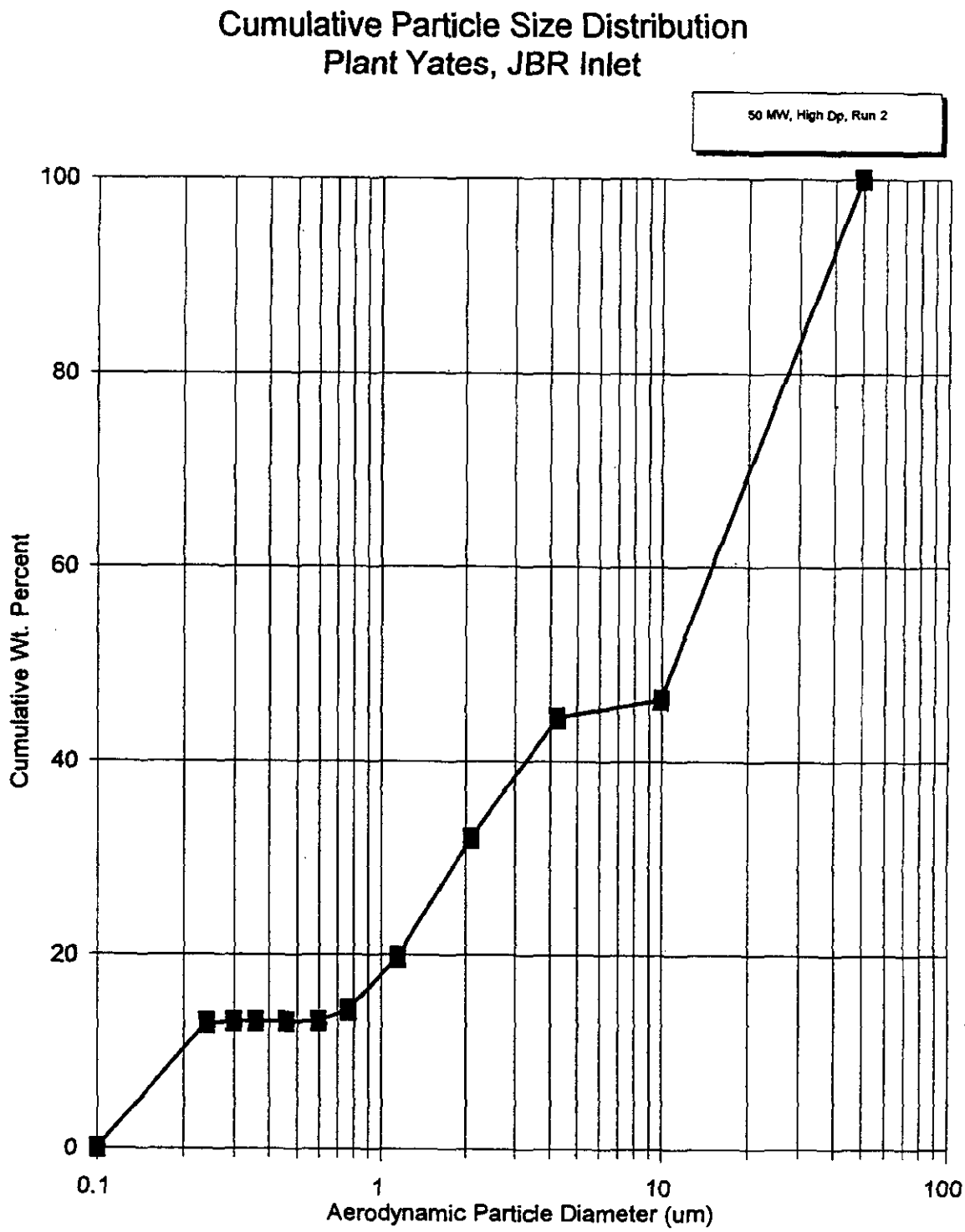
Cumulative Particle Size Distribution
Plant Yates, JBR Inlet
50 MW, High Dp, Run 2
100
80
60
40
20
0
Cumulative Wt. Percent
0.1
1
10
100
Aerodynamic Particle Diameter (um)

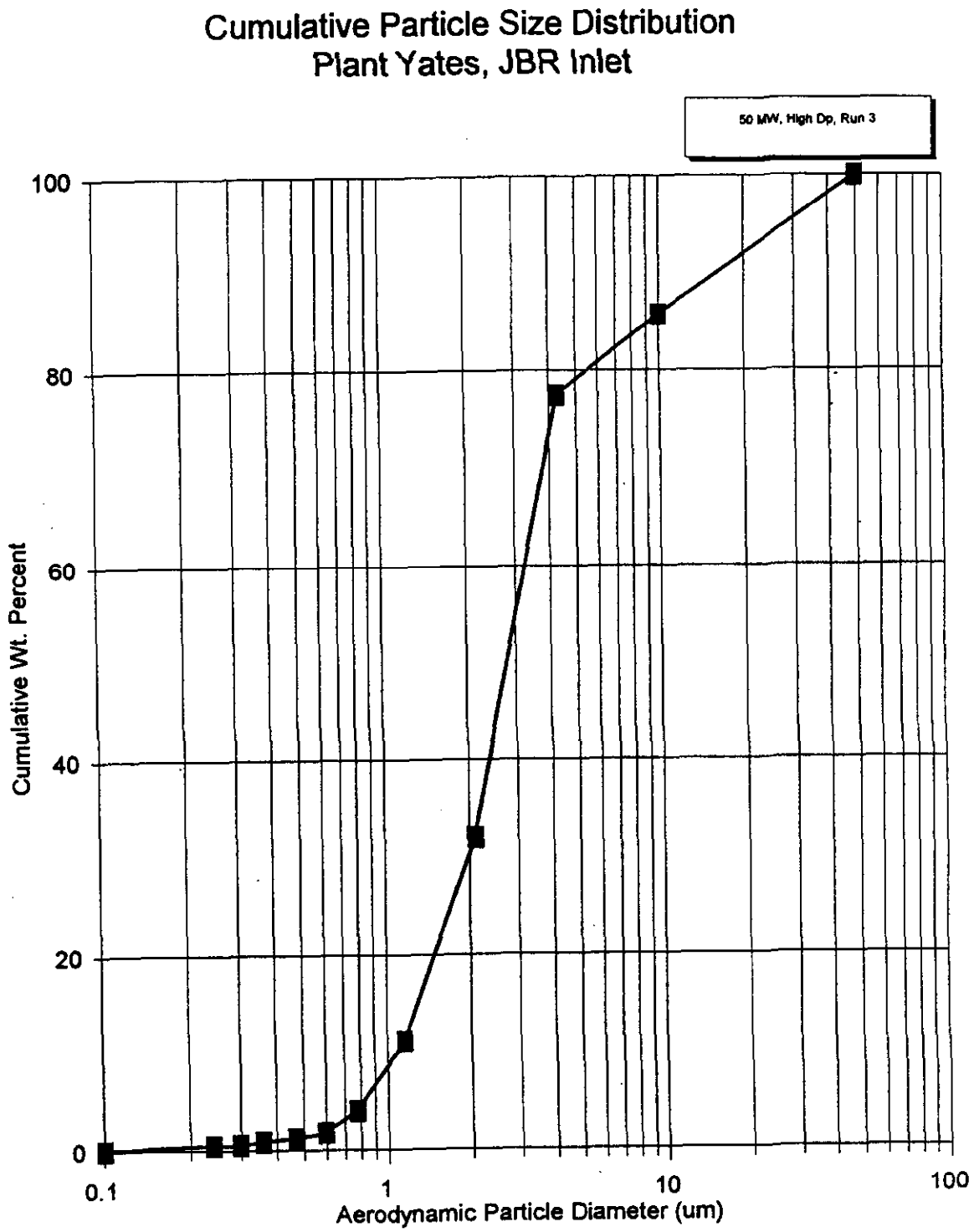
Cumulative Particle Size Distribution
Plant Yates, JBR Inlet
50 MW, High Dp, Run 3
100
80
60
40
20
0
Cumulative Wt. Percent
0.1
1
10
100
Aerodynamic Particle Diameter (um)

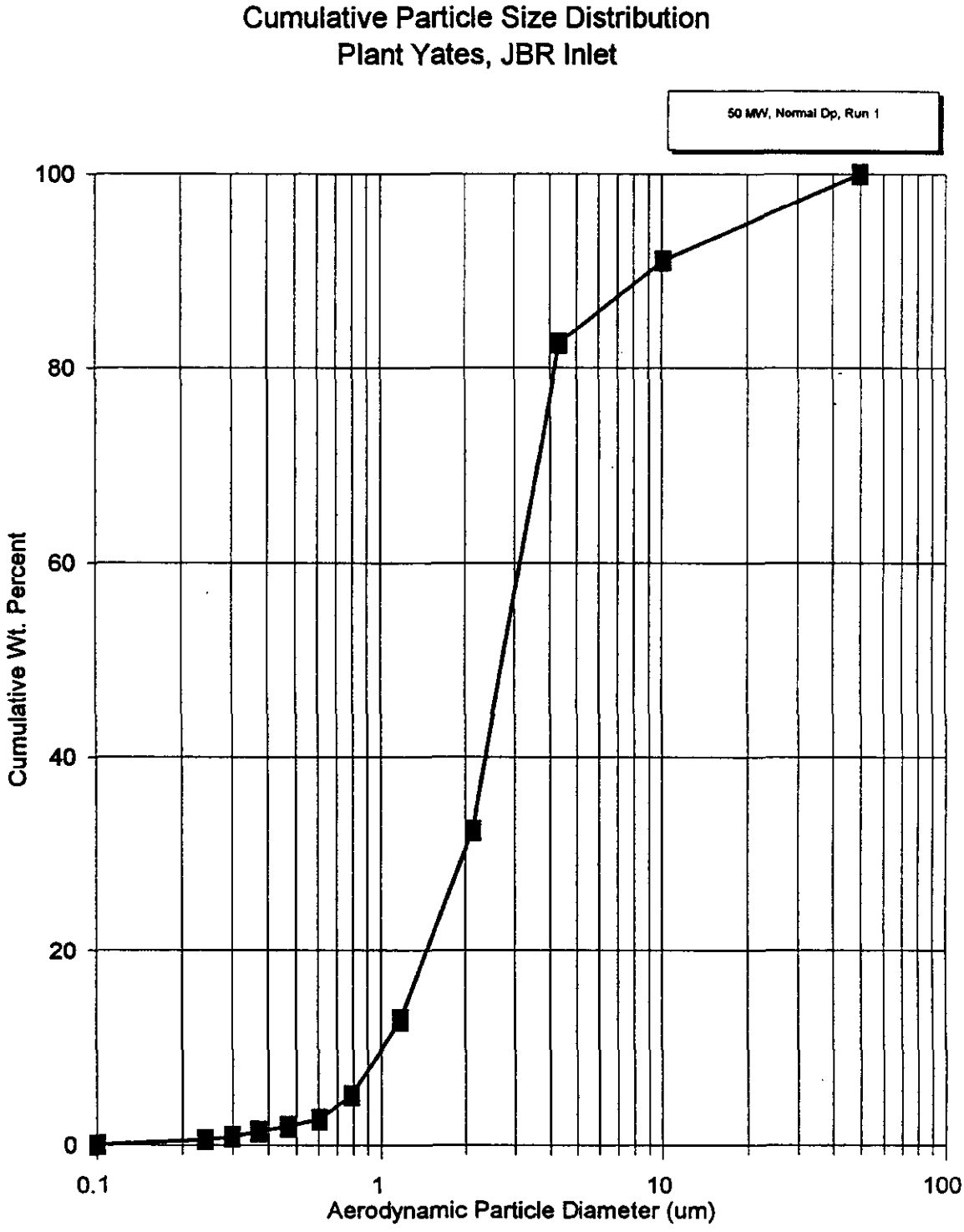
Cumulative Particle Size Distribution
Plant Yates, JBR Inlet
50 MW, Normal Dp, Run 1
100
80
60
40
20
0
Cumulative Wt. Percent
0.1
1
10
100
Aerodynamic Particle Diameter (um)

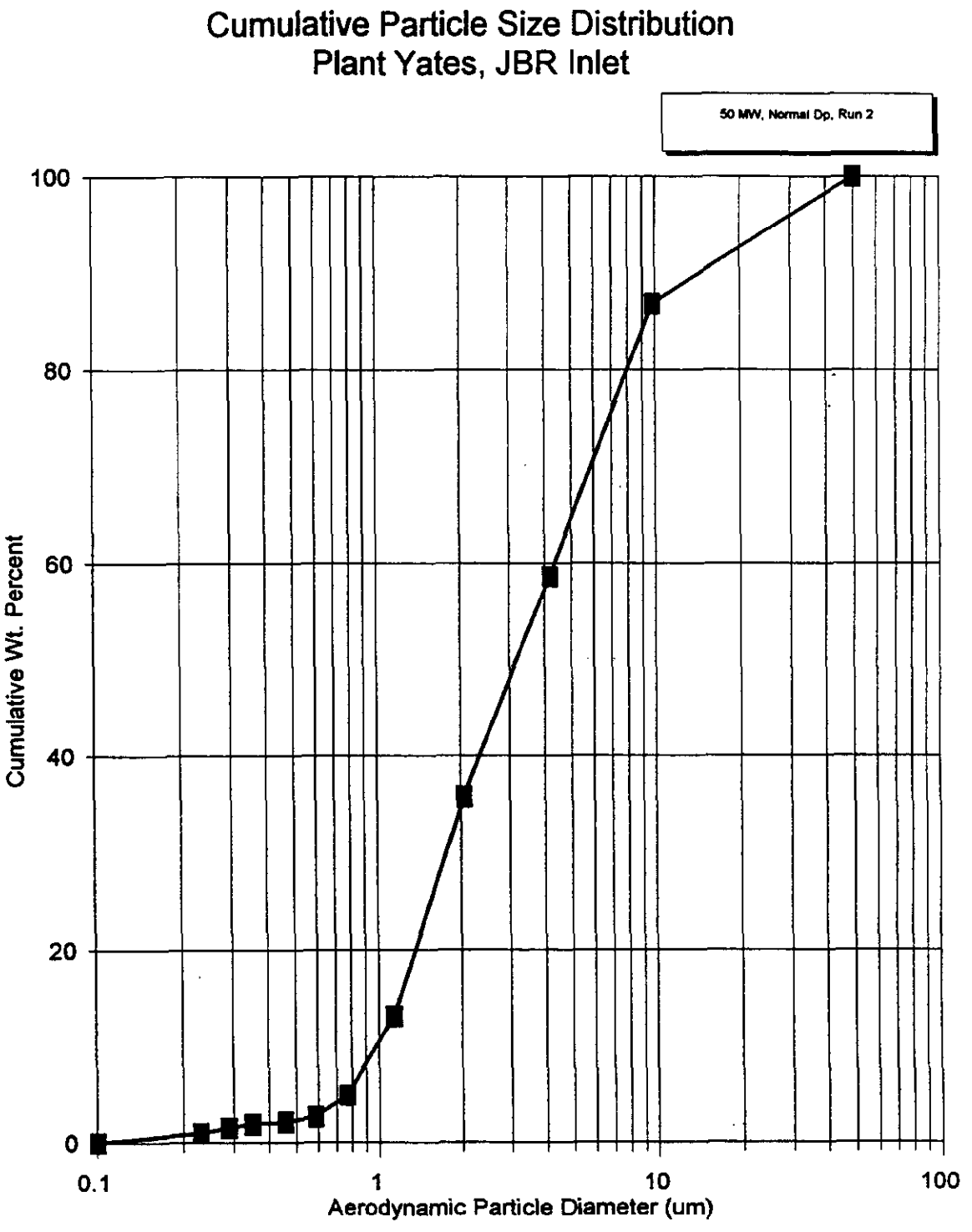
Cumulative Particle Size Distribution
Plant Yates, JBR Inlet
50 MW, Normal Dp, Run 2
100
80
60
40
20
0
Cumulative Wt. Percent
0.1
1
10
100
Aerodynamic Particle Diameter (um)

Differential Size Distribution
Plant Yates, JBR Inlet

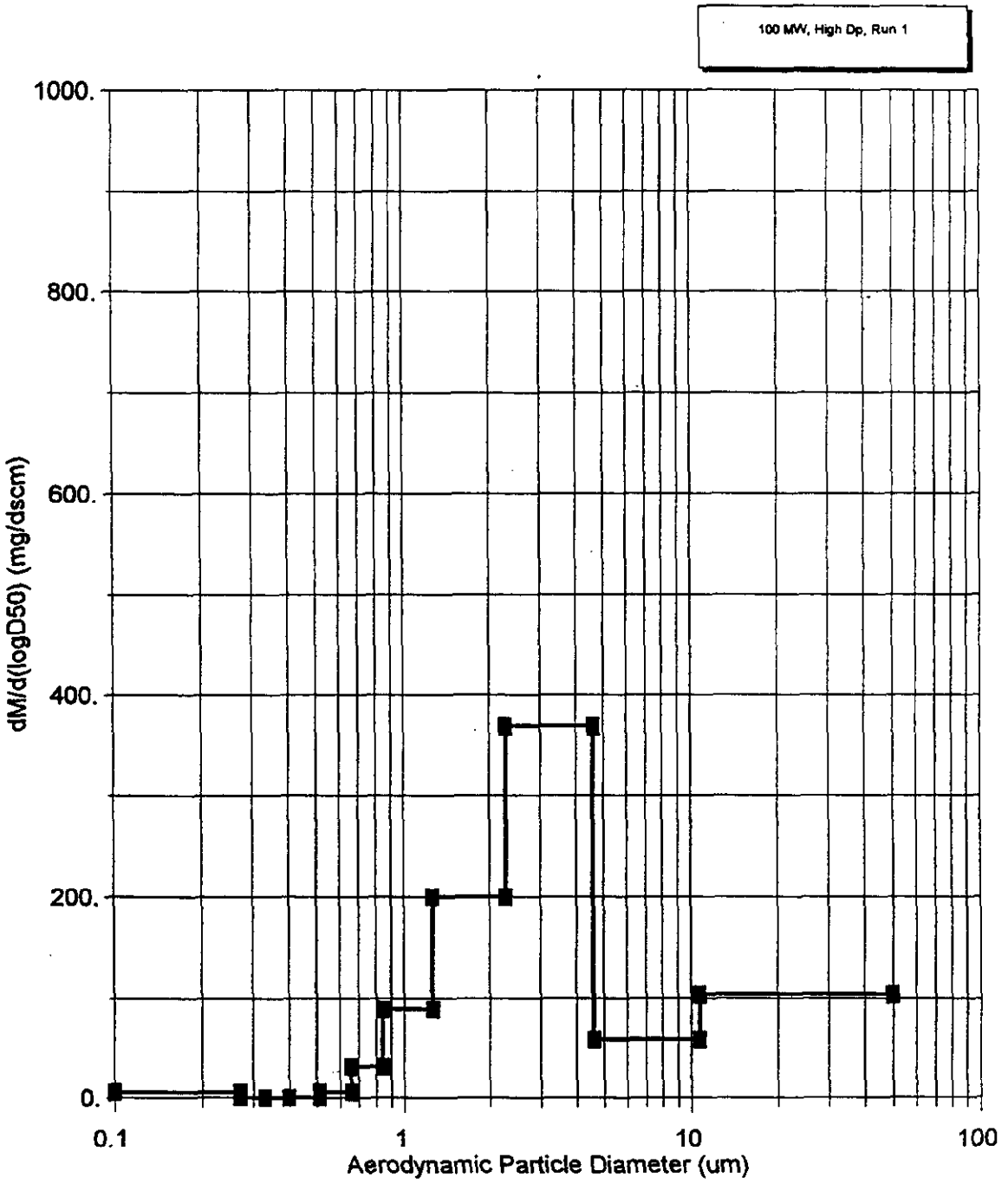

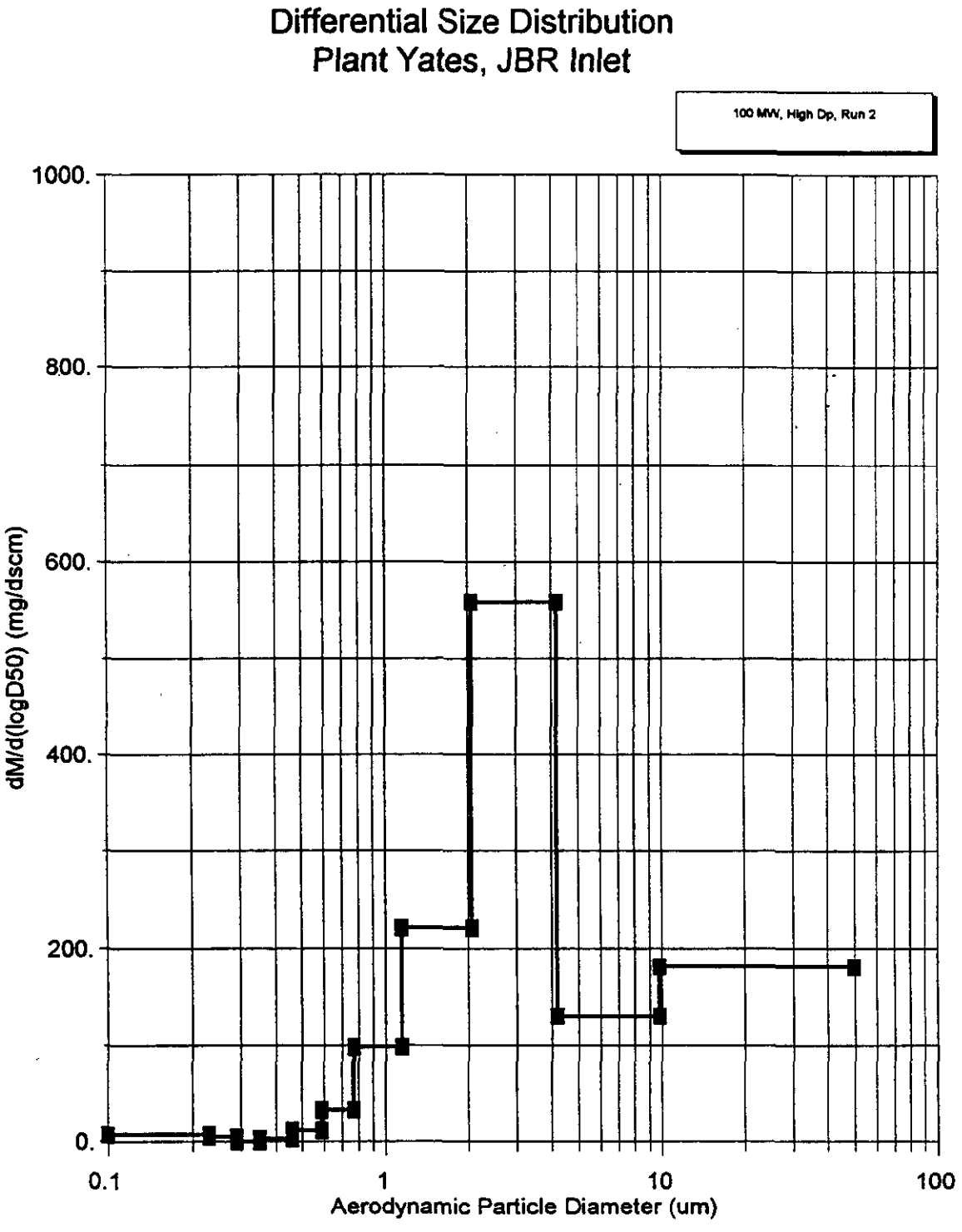
Differential Size Distribution
Plant Yates, JBR Inlet
100 MW, High Dp, Run 2
1000.
800.
600.
400.
200.
0.
dM/d(logD50) (mg/dscm)
0.1
1
10
100
Aerodynamic Particle Diameter (um)

Differential Size Distribution
Plant Yates, JBR Inlet

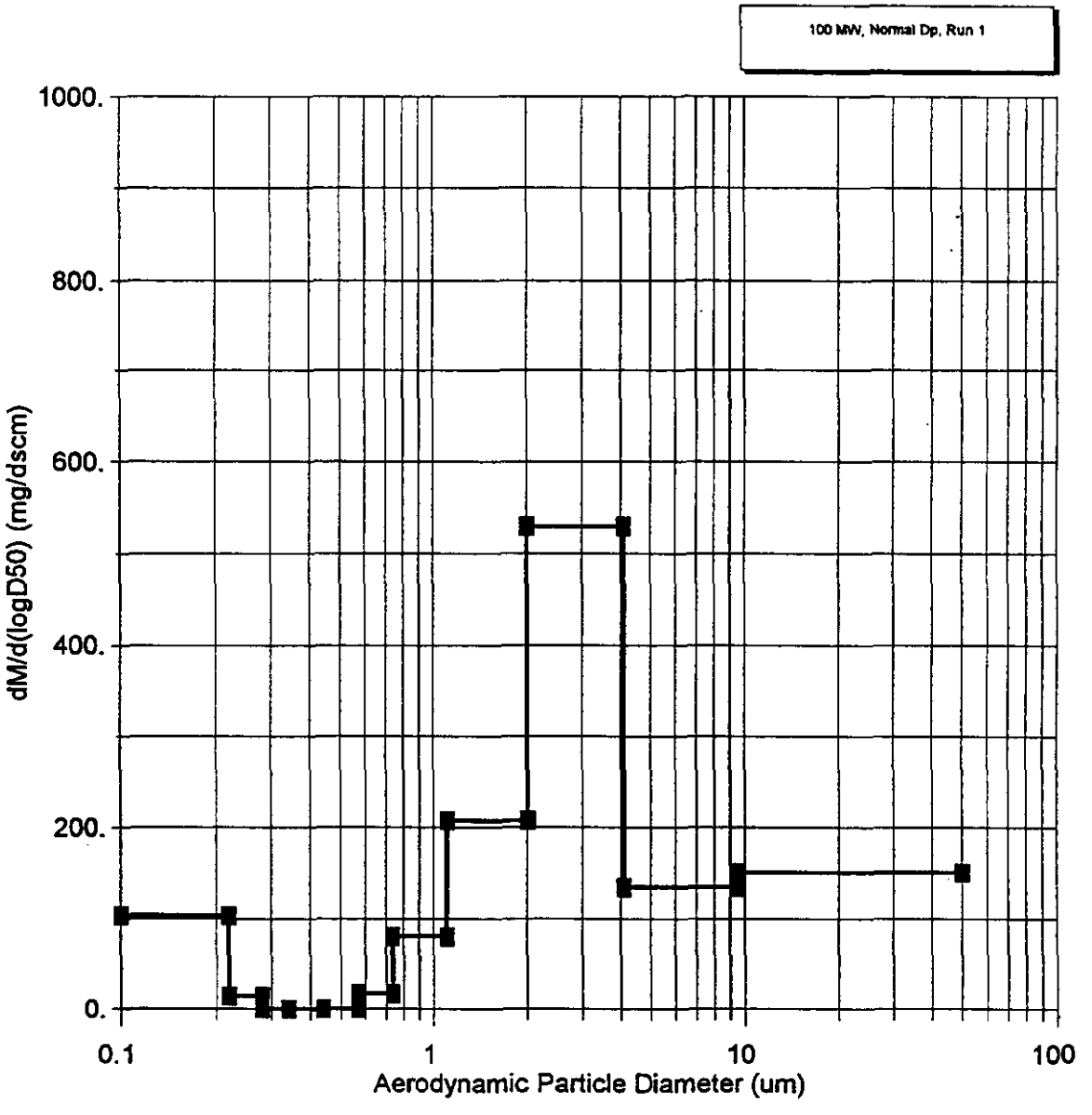

Differential Size Distribution
Plant Yates, JBR Inlet

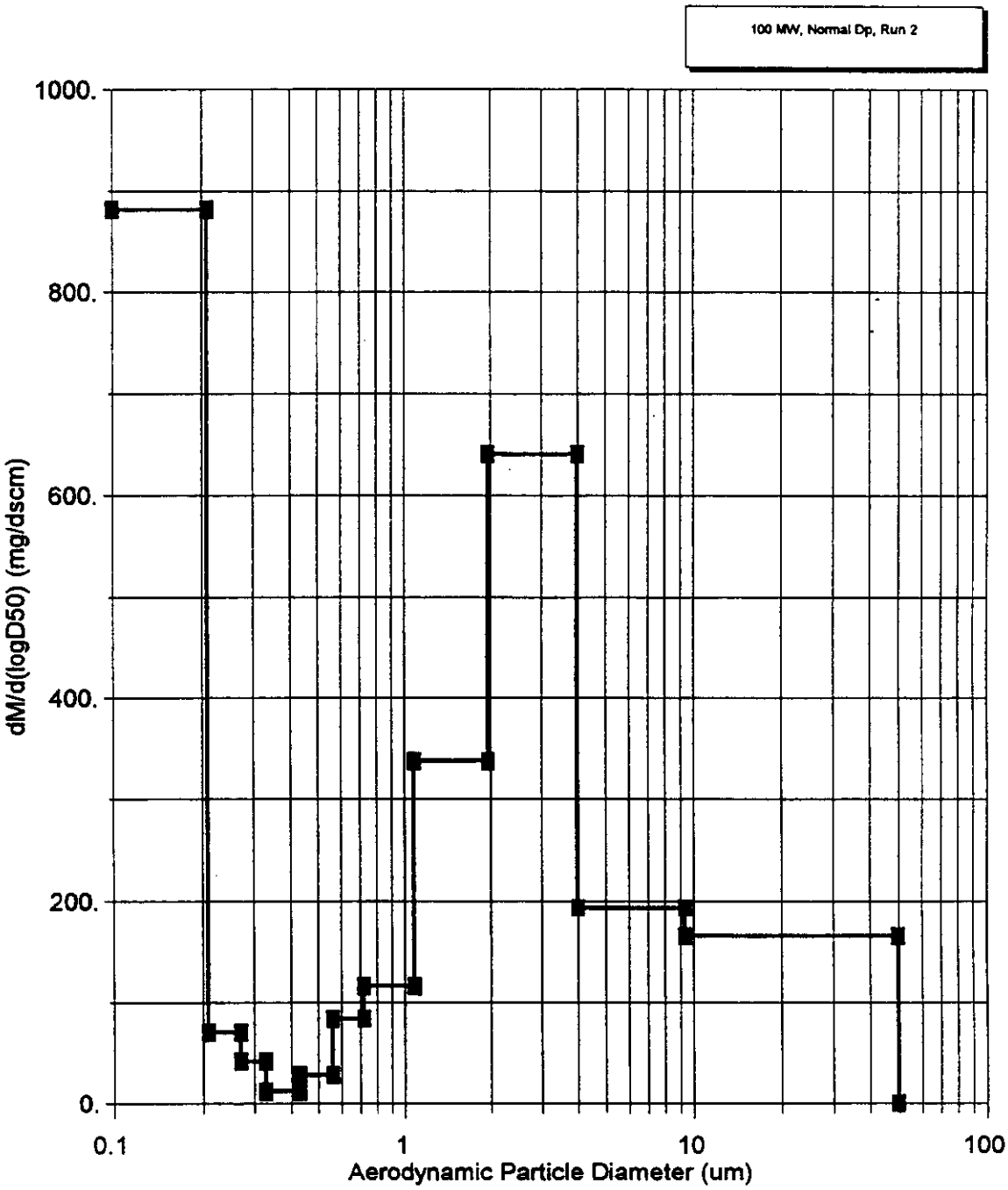

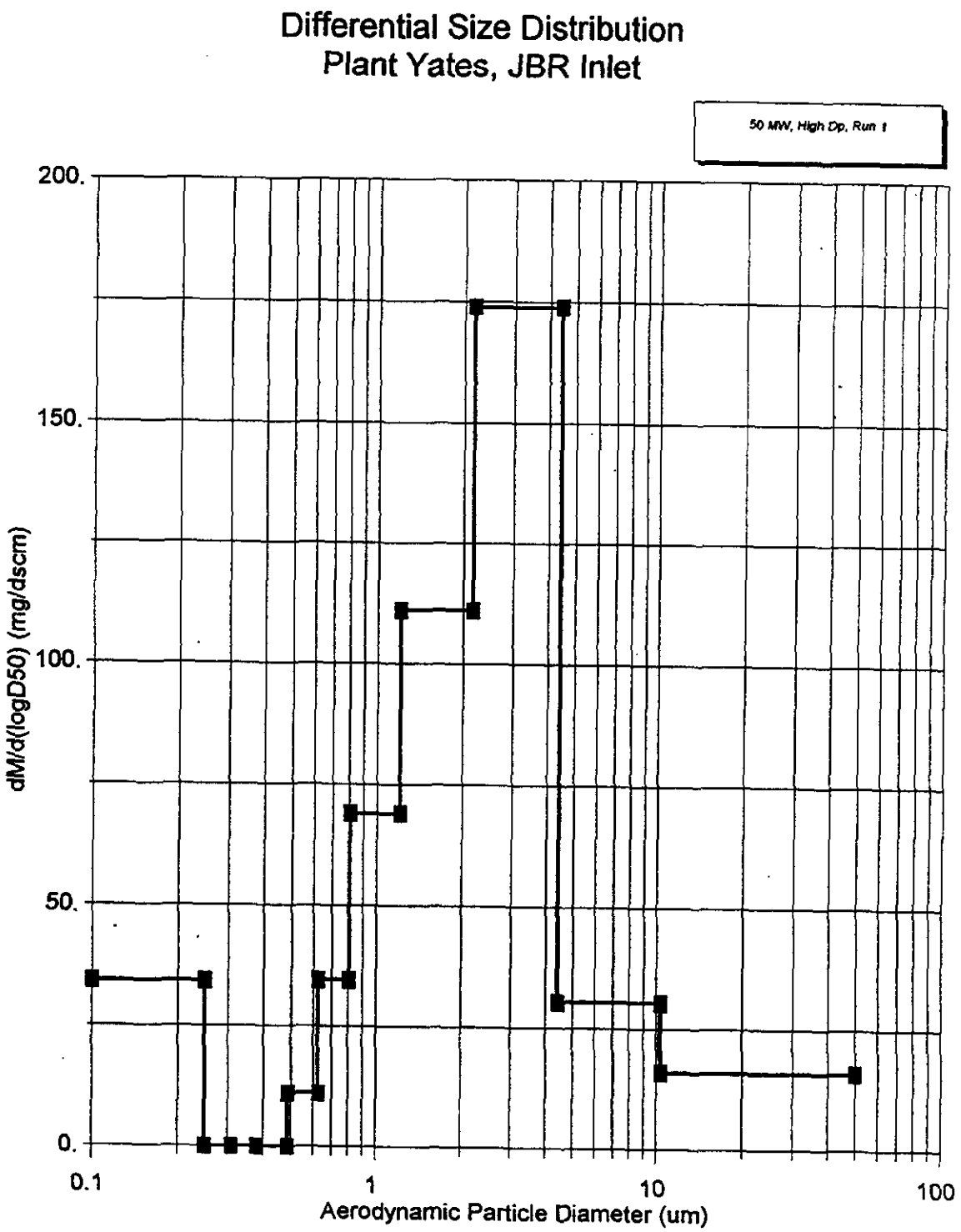
Differential Size Distribution
Plant Yates, JBR Inlet
50 MW, High Dp, Run 1
200.
150.
100.
50.
0.
dM/d(logD50) (mg/dscm)
0.1
1
10
100
Aerodynamic Particle Diameter (um)

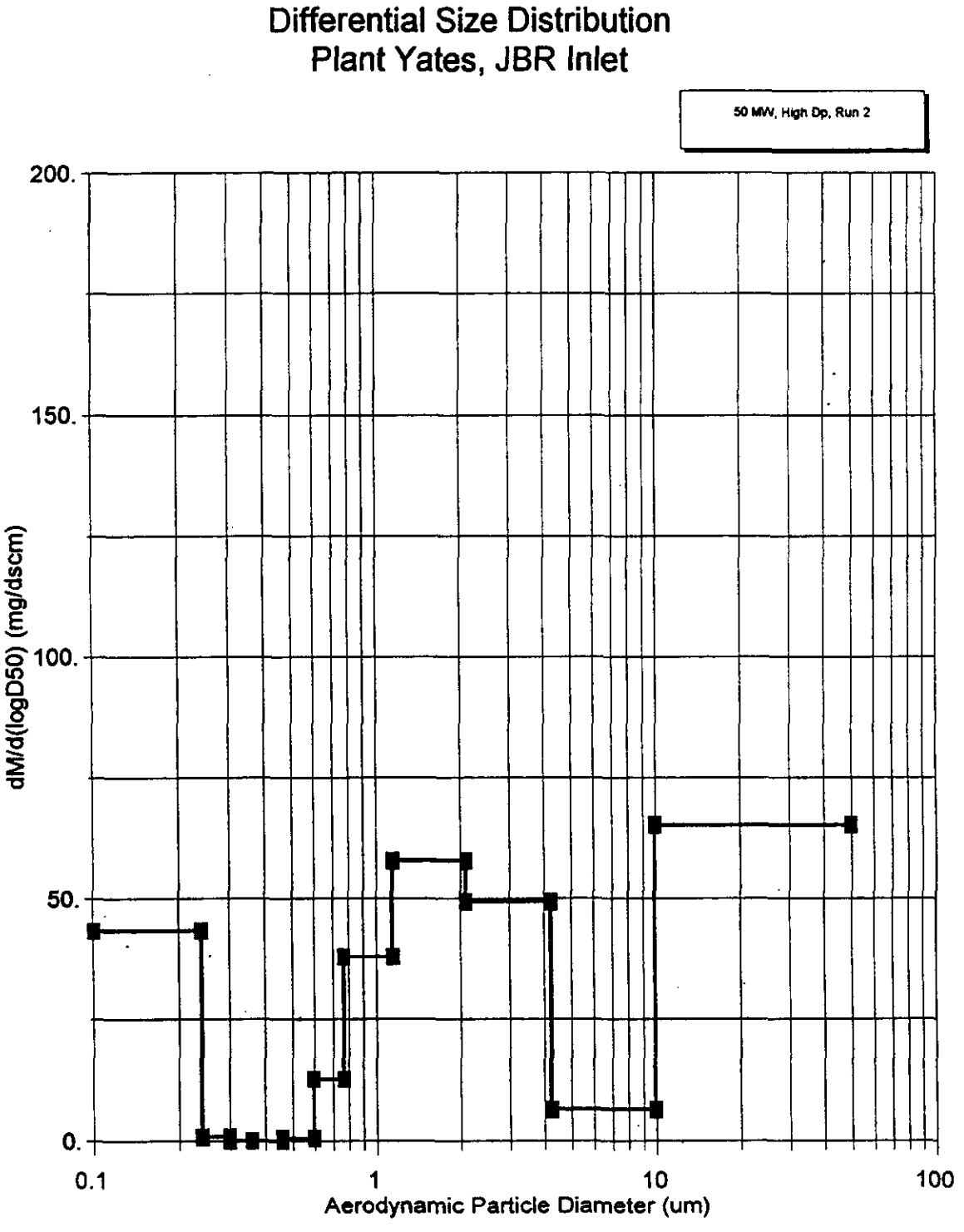
Differential Size Distribution
Plant Yates, JBR Inlet
50 MW, High Dp, Run 2
200.
150.
100.
50.
0.
dM/d(logD50) (mg/dscm)
0.1
1
10
100
Aerodynamic Particle Diameter (um)

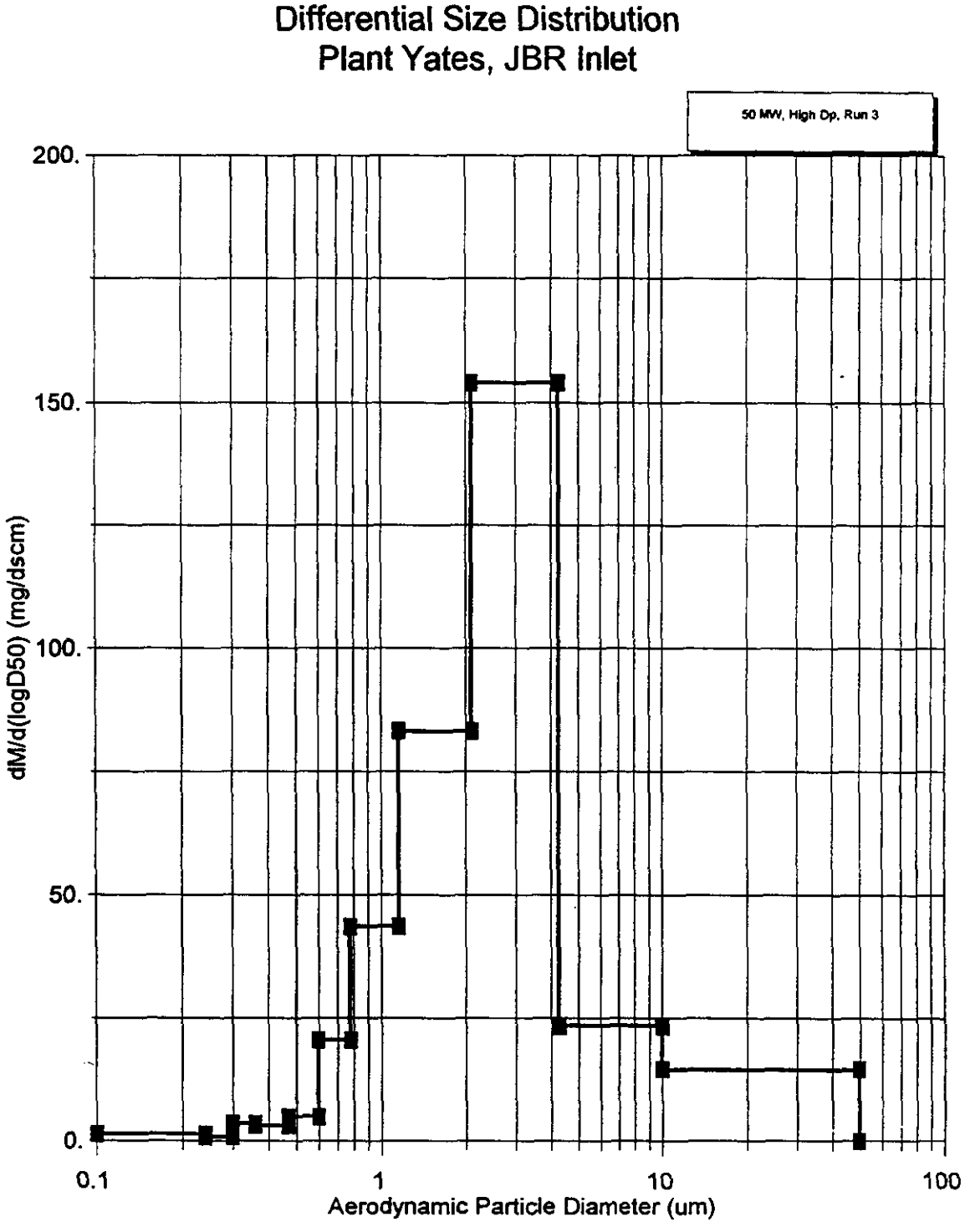
Differential Size Distribution
Plant Yates, JBR Inlet
50 MW, High Dp, Run 3
200.
150.
100.
50.
0.
dM/d(logD50) (mg/dscm)
0.1
1
10
100
Aerodynamic Particle Diameter (um)

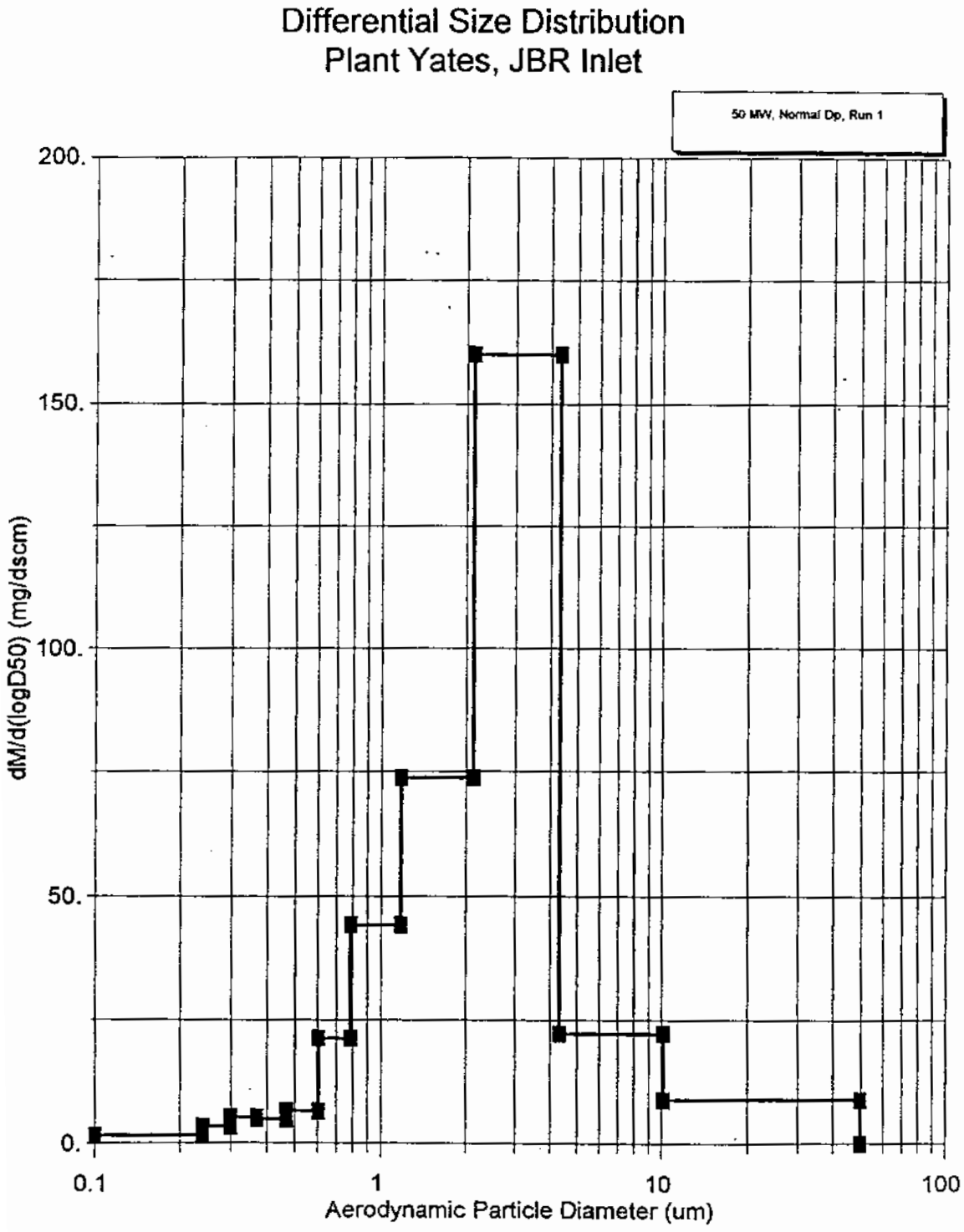
Differential Size Distribution
Plant Yates, JBR Inlet
50 MW, Normal Dp, Run 1
200.
150.
100.
50.
0.
dM/d(logD50) (mg/dscm)
0.1
1
10
100
Aerodynamic Particle Diameter (um)

Differential Size Distribution
Plant Yates, JBR Inlet

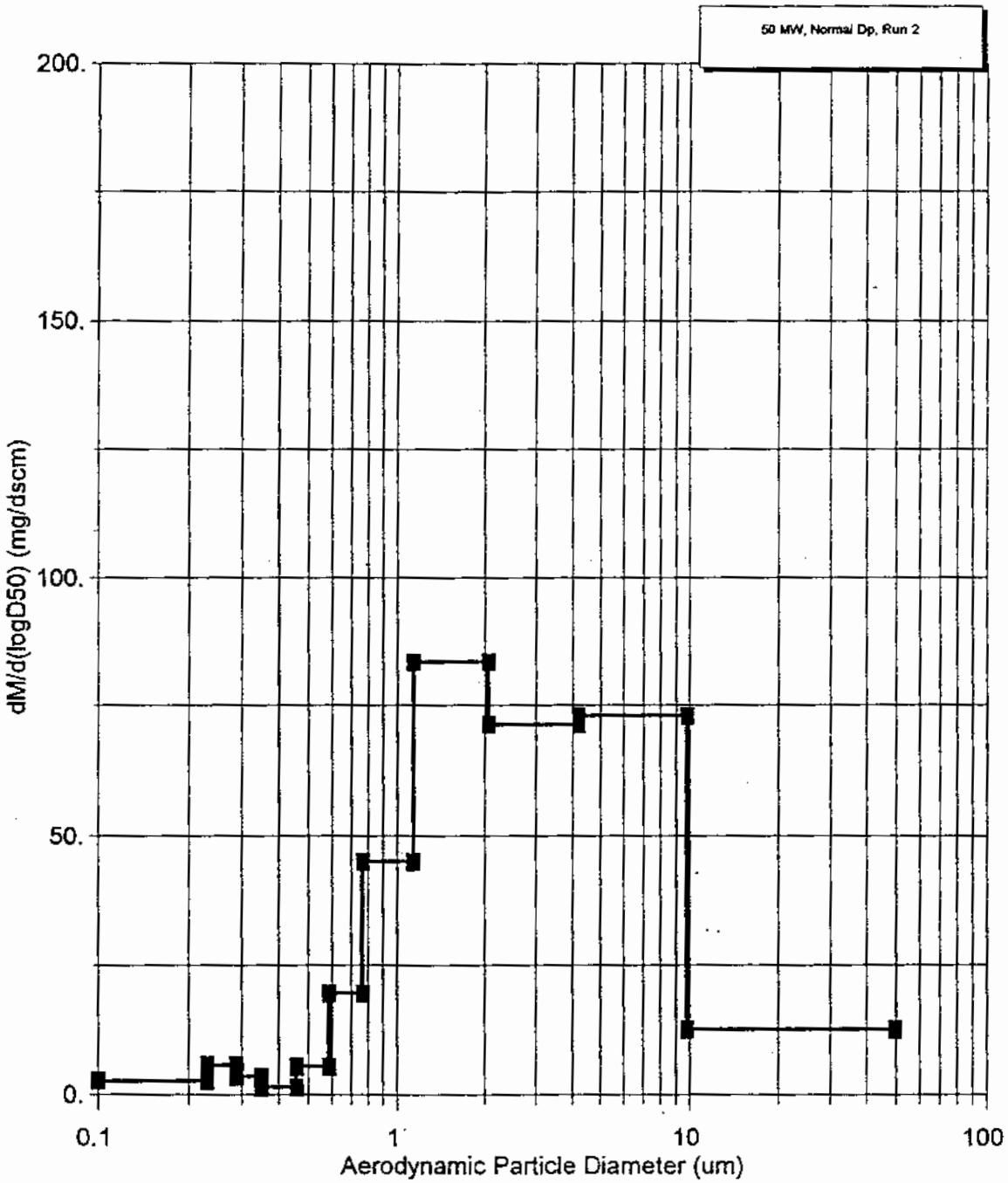

Cumulative Particle Size Distribution
Plant Yates, Stack

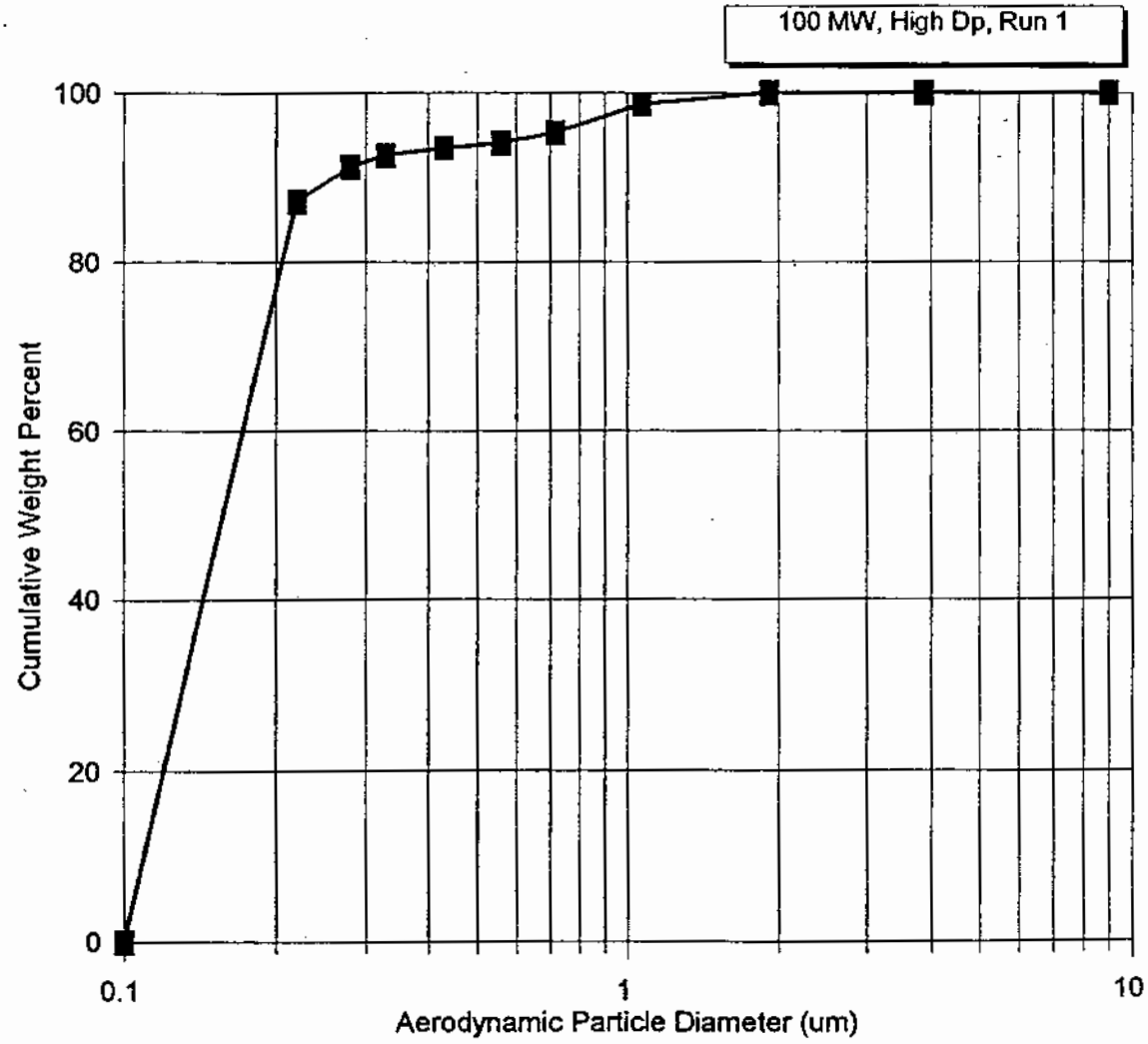

Cumulative Particle Size Distribution
Plant Yates, Stack

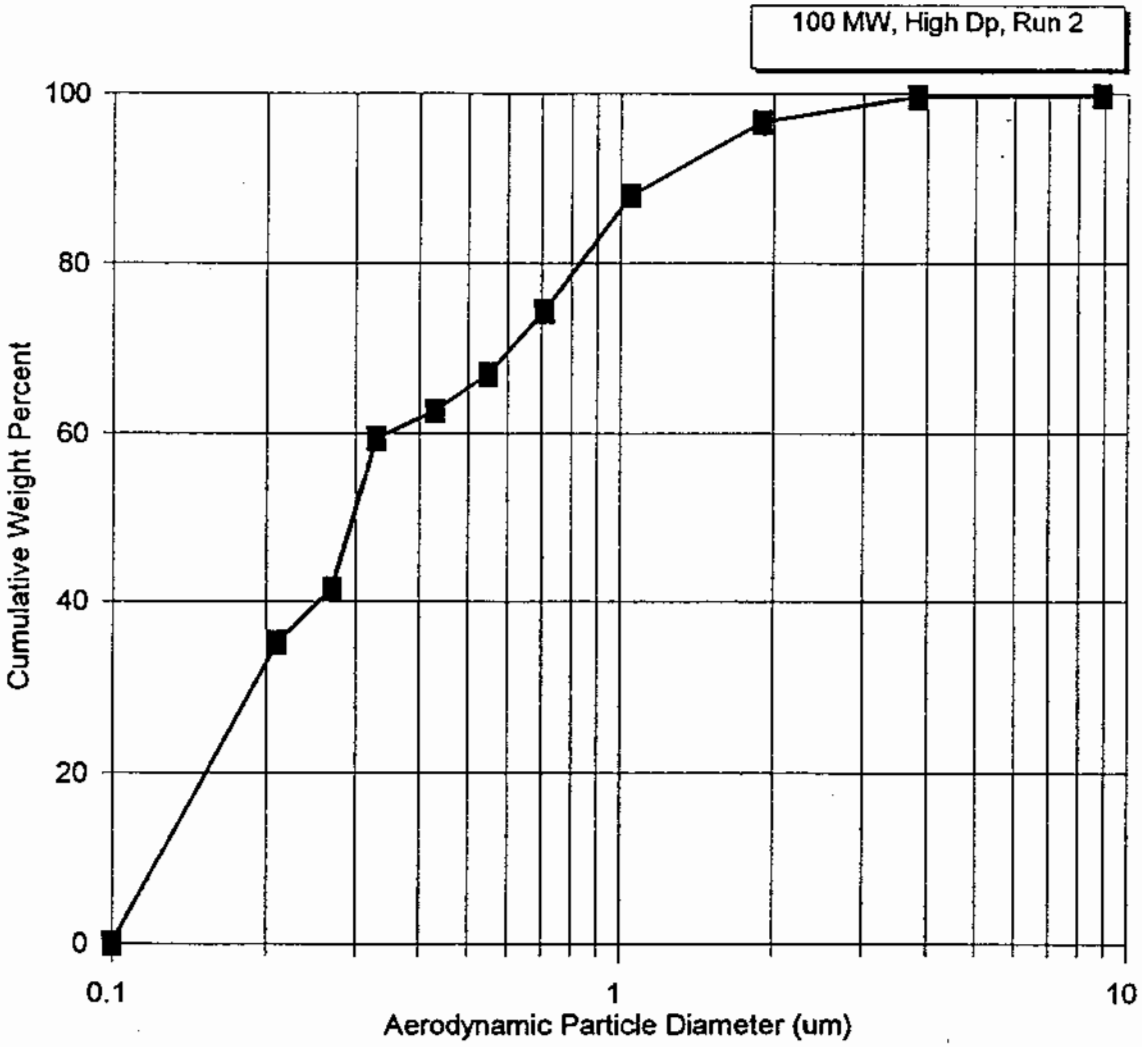

Cumulative Particle Size Distribution
Plant Yates, Stack

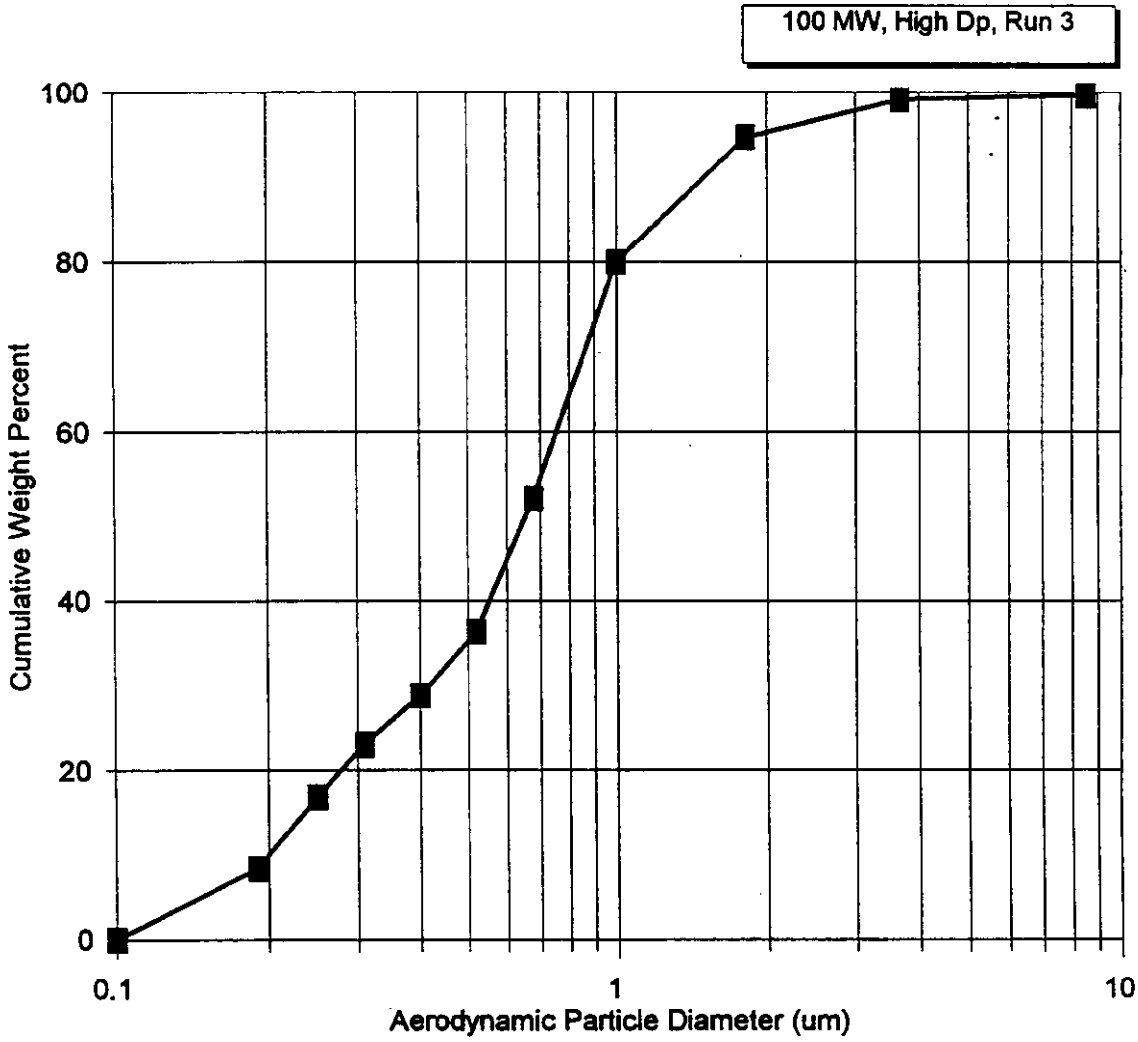

Cumulative Particle Size Distribution
Plant Yates, Stack

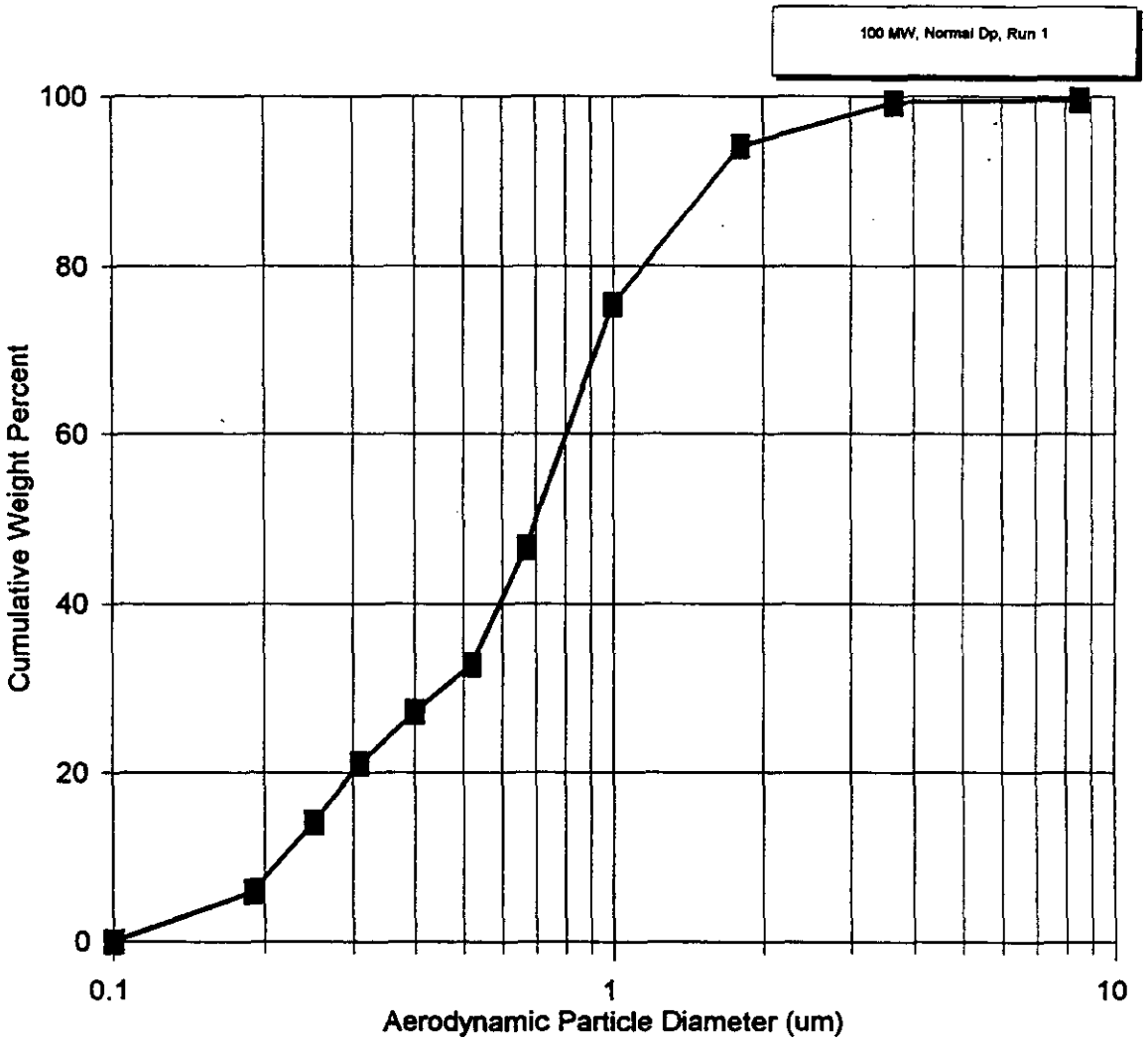

Cumulative Particle Size Distribution
Plant Yates, Stack

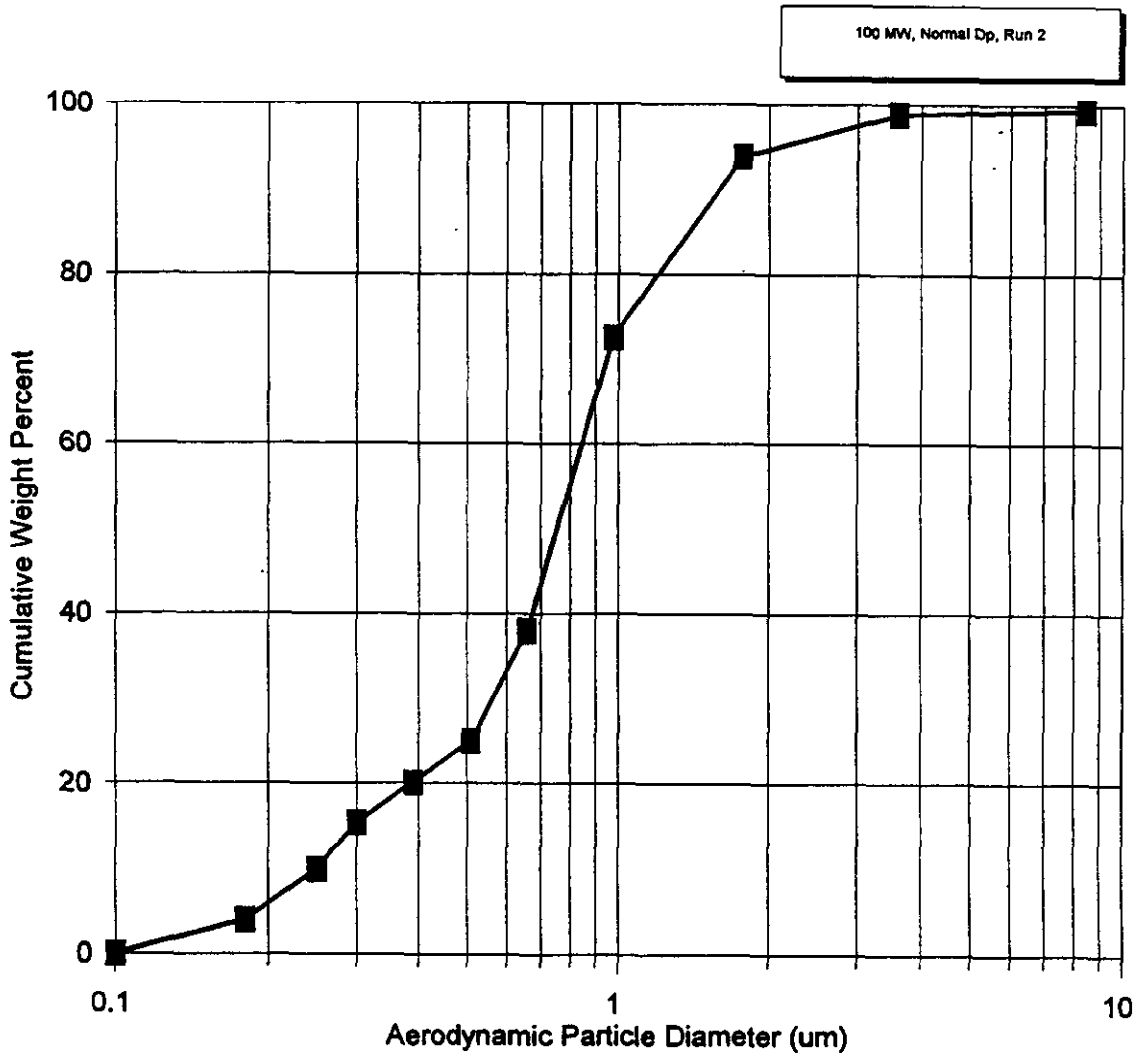

Cumulative Particle Size Distribution
Plant Yates, Stack

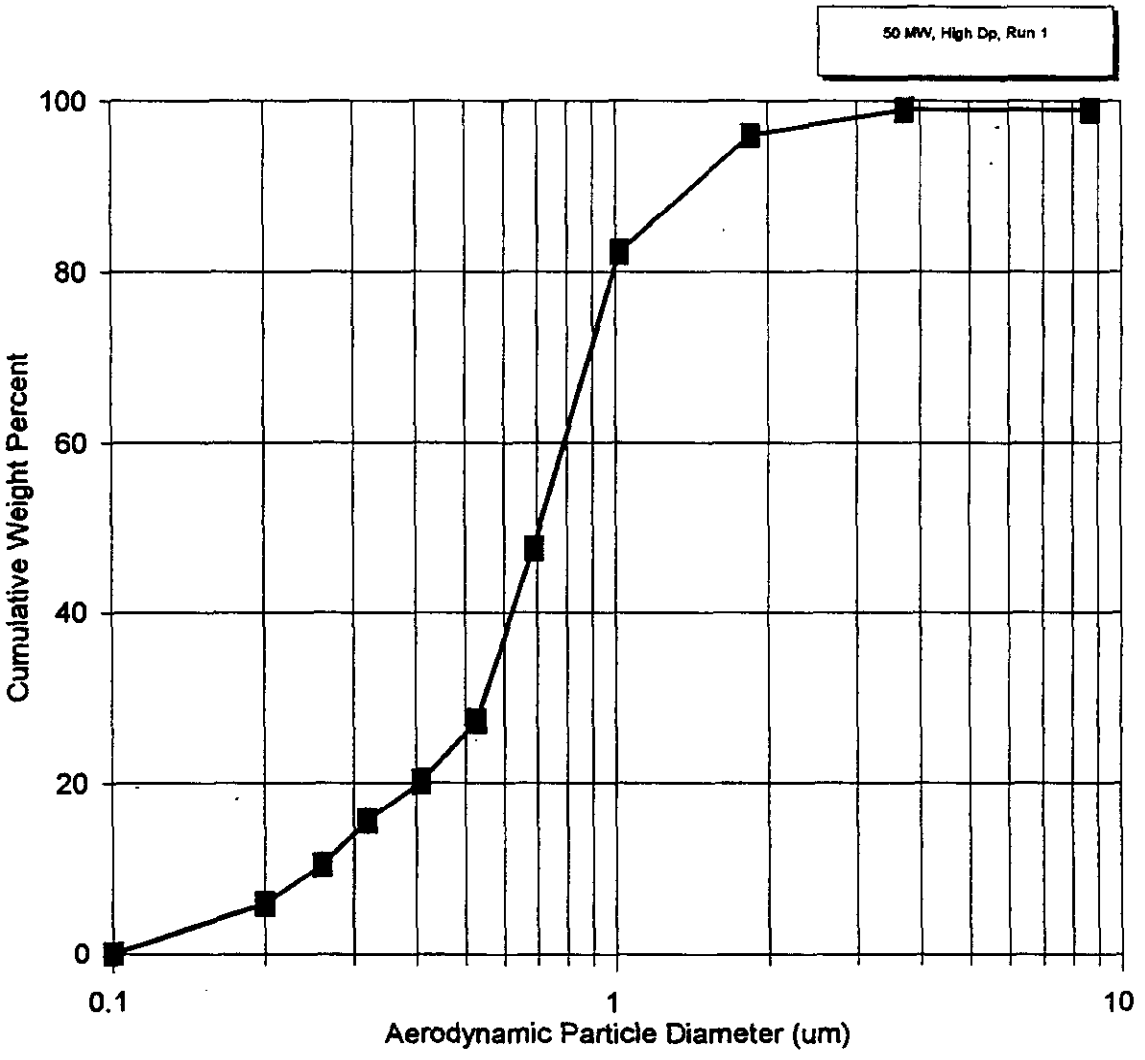

Cumulative Particle Size Distribution
Plant Yates, Stack

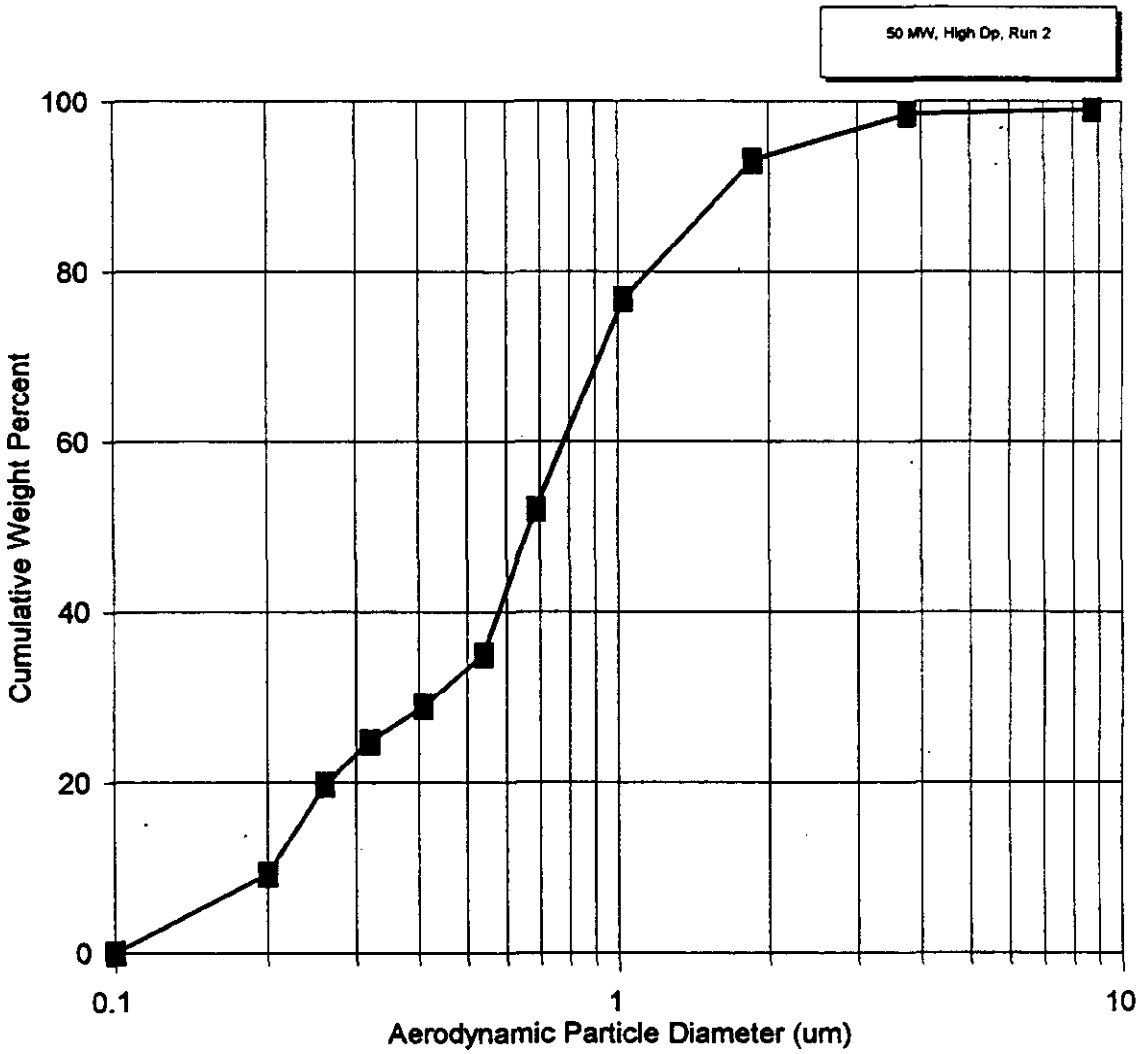

Cumulative Particle Size Distribution
Plant Yates, Stack

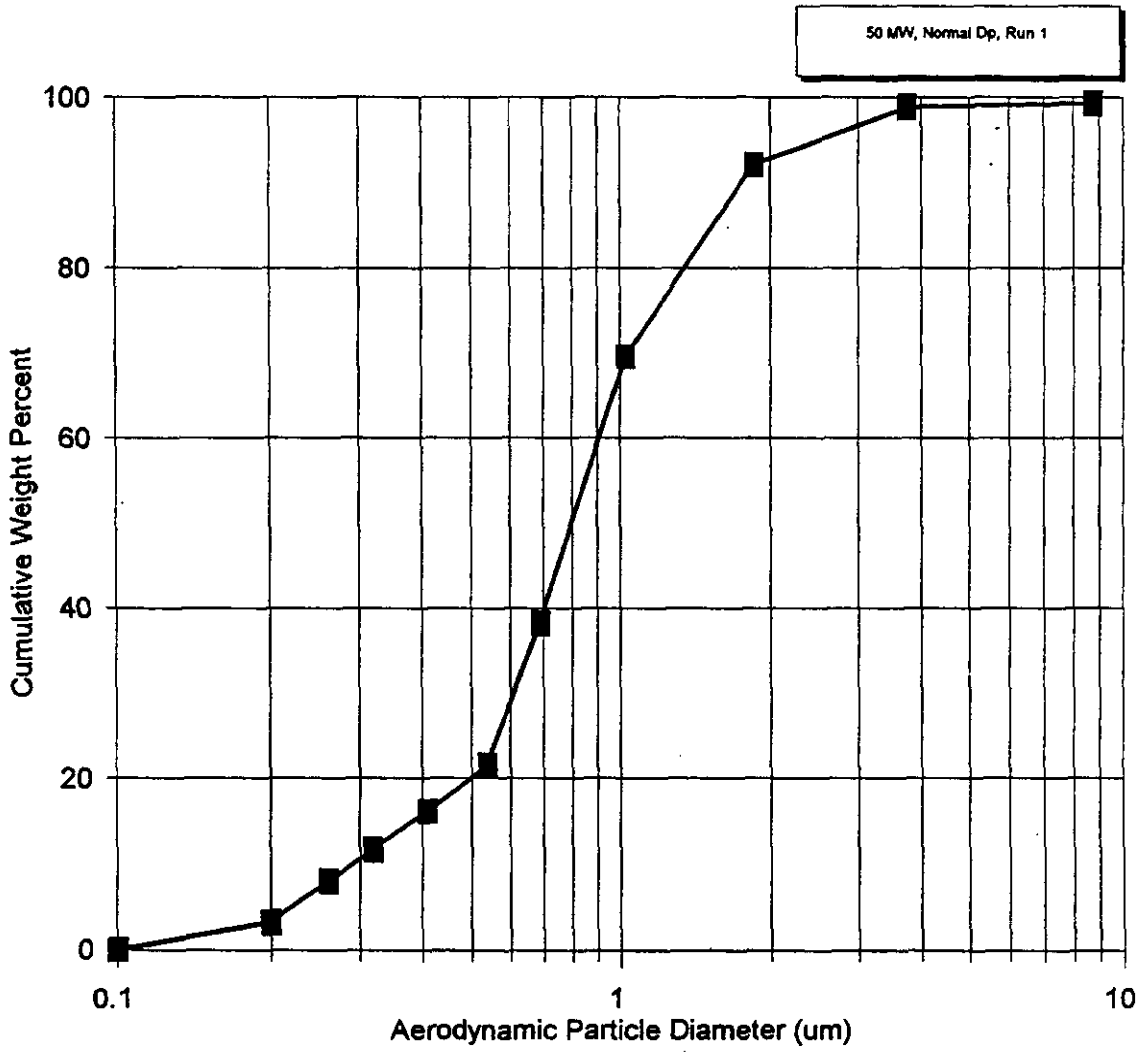

Cumulative Particle Size Distribution
Plant Yates, Stack

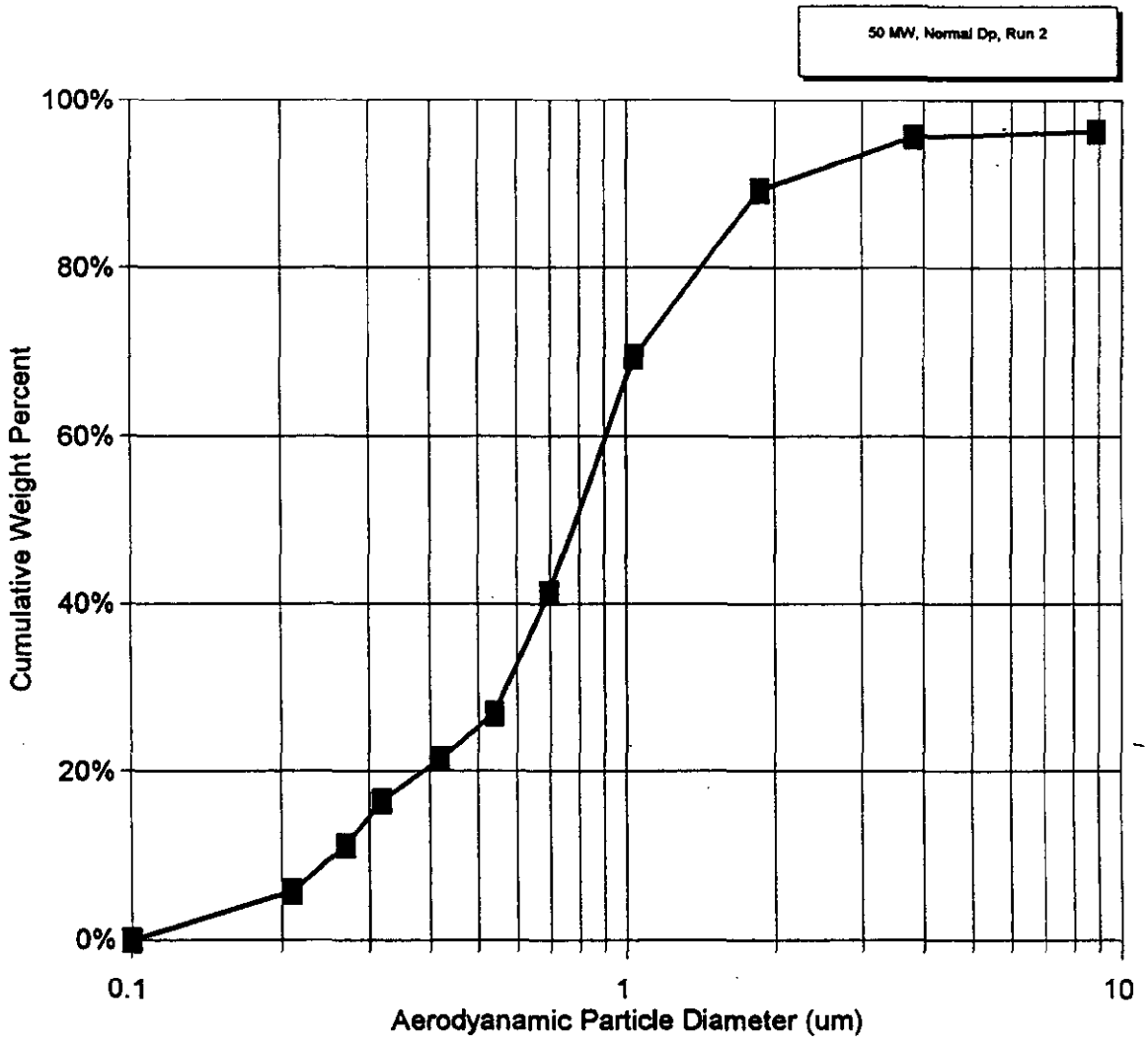

Differential Size Distribution
Plant Yates, Stack

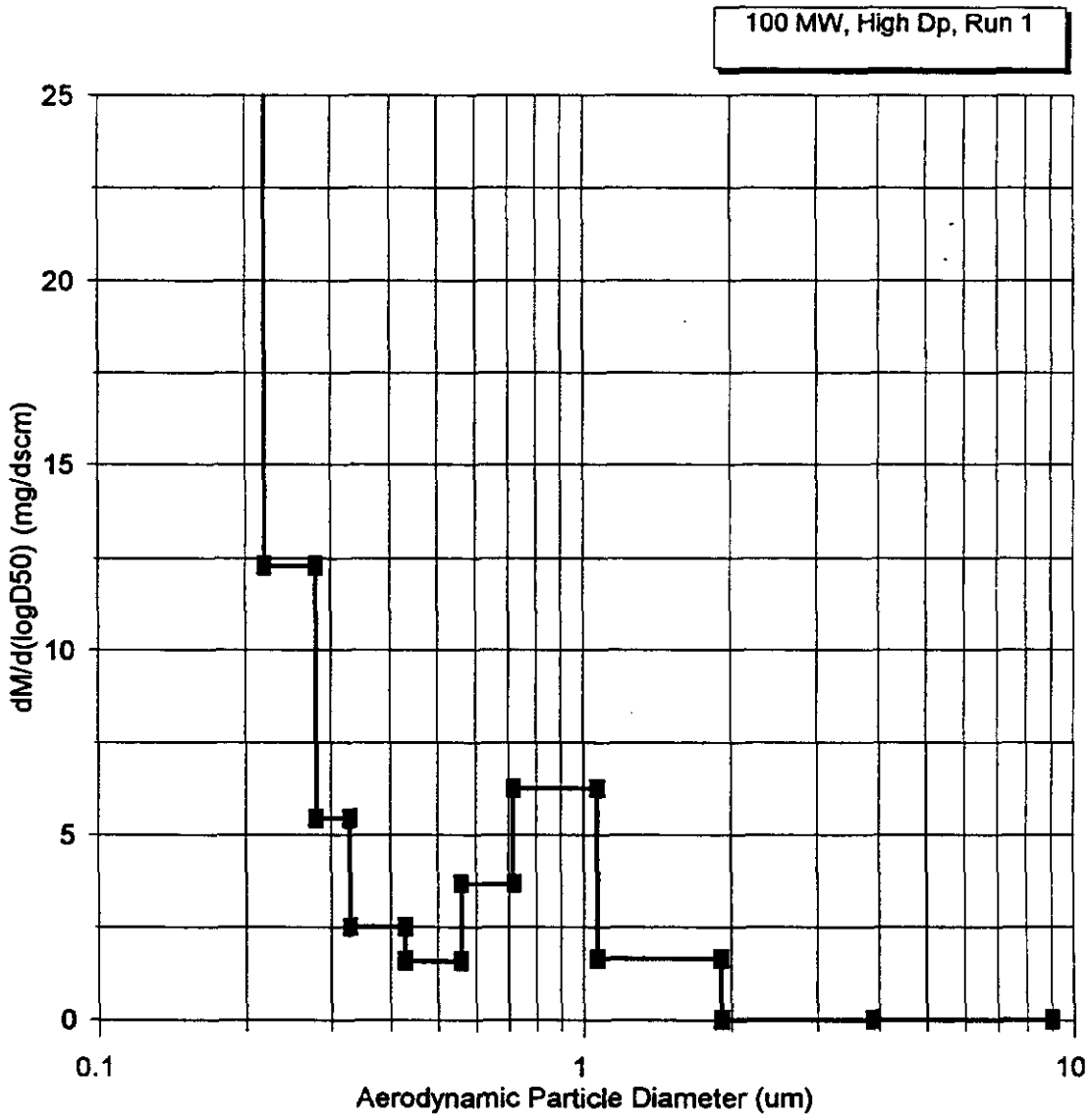

Differential Size Distribution
Plant Yates, Stack

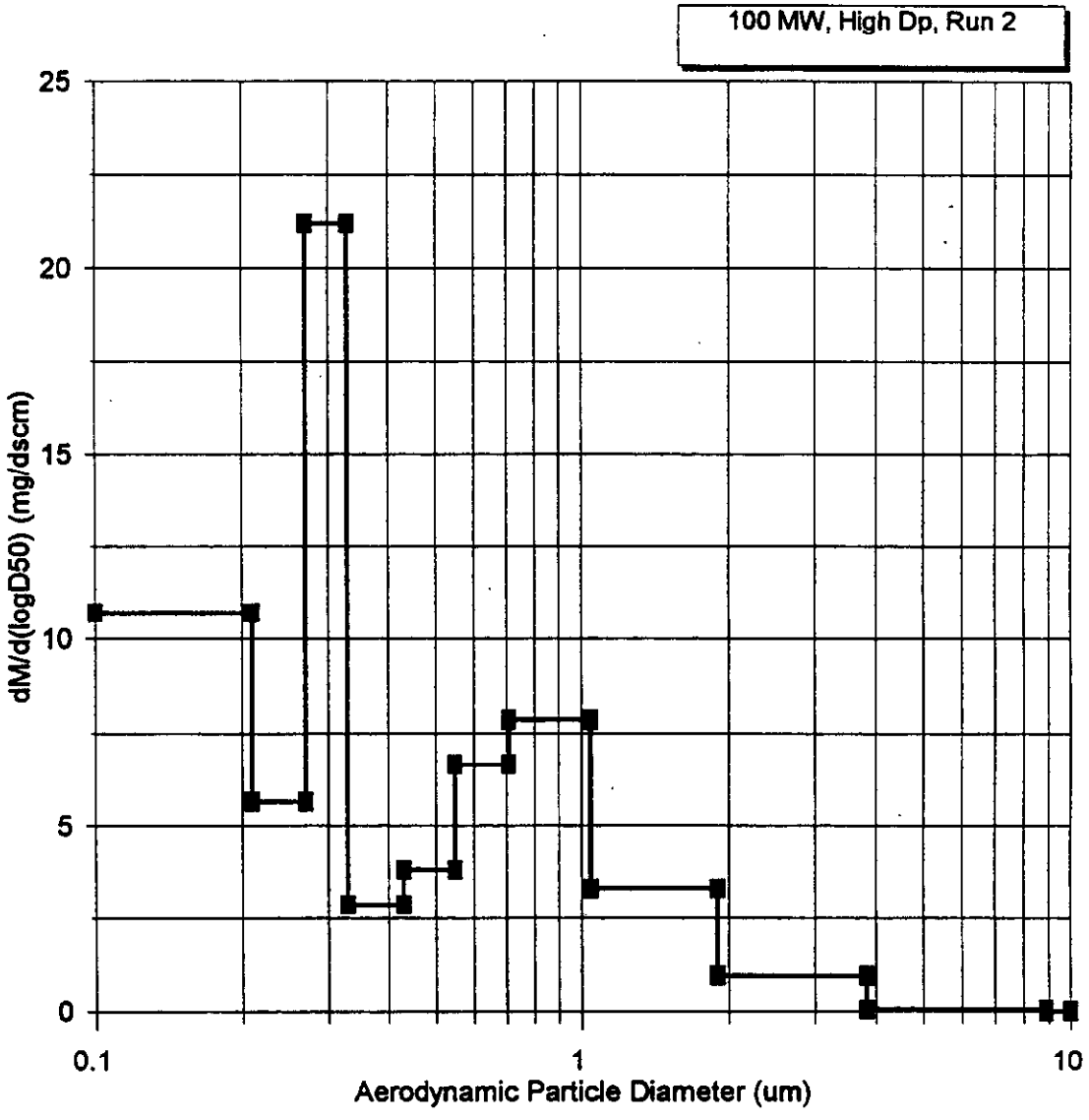

Differential Size Distribution
Plant Yates, Stack

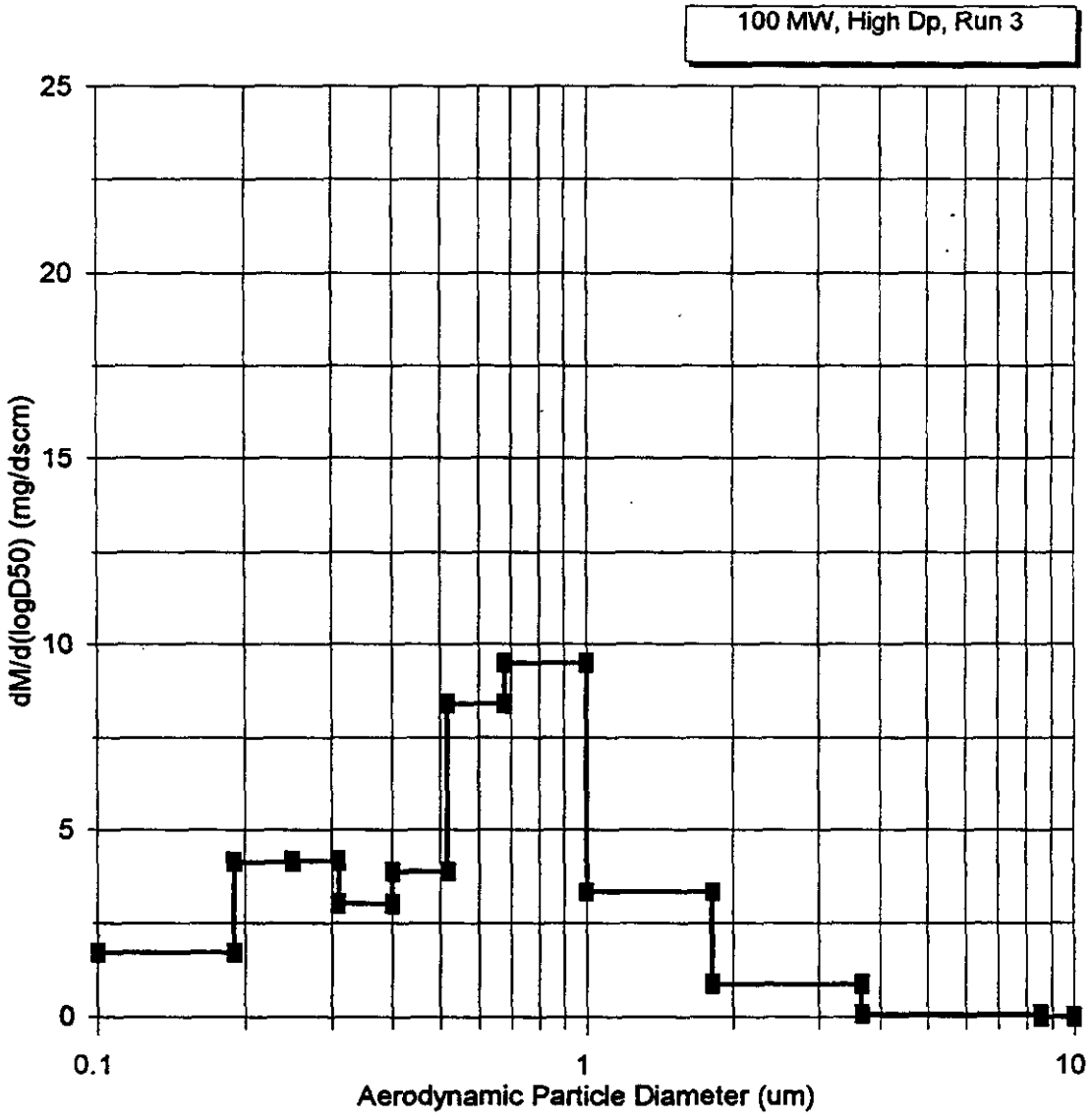

Differential Size Distribution
Plant Yates, Stack

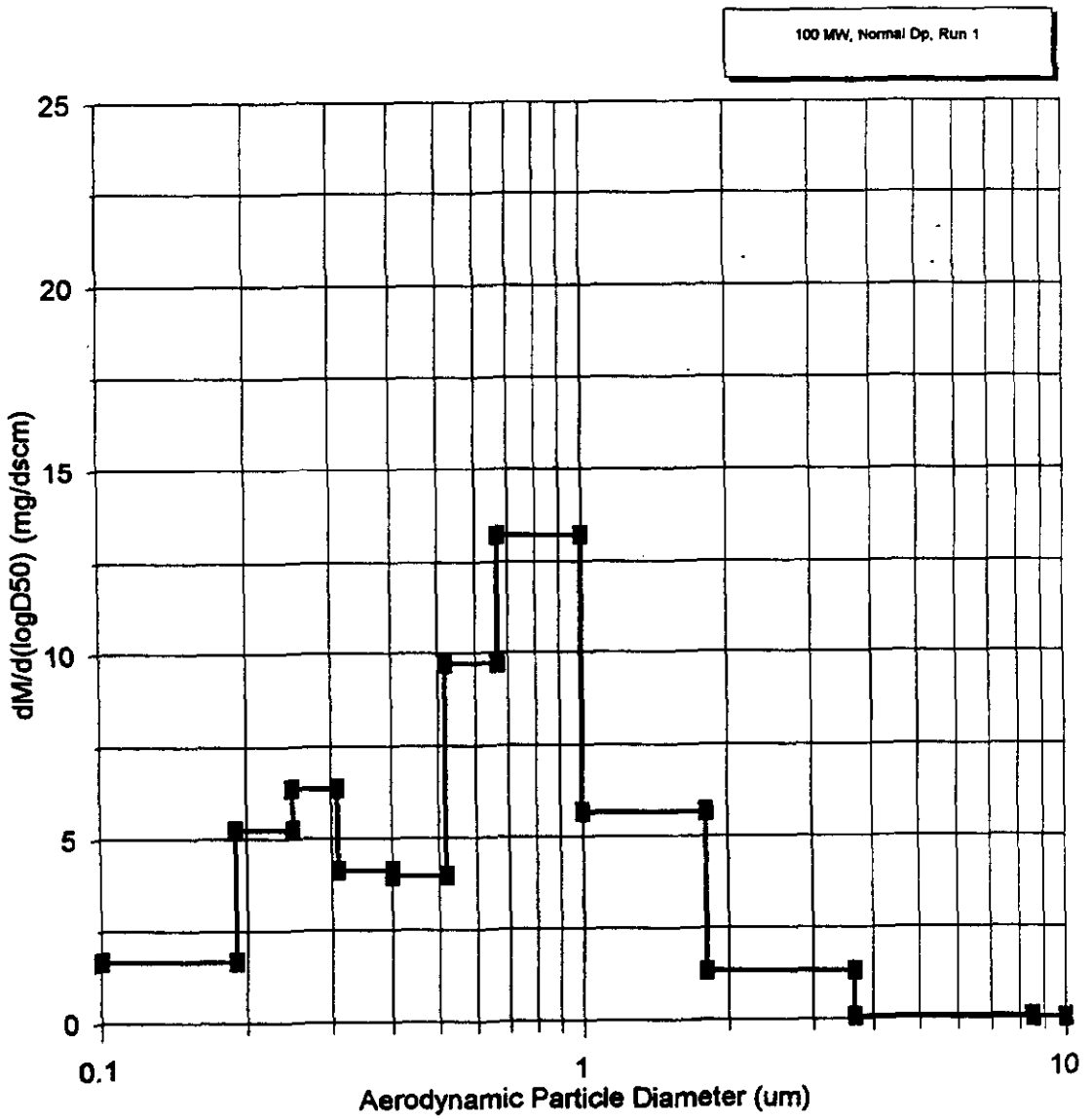

Differential Size Distribution
Plant Yates, Stack

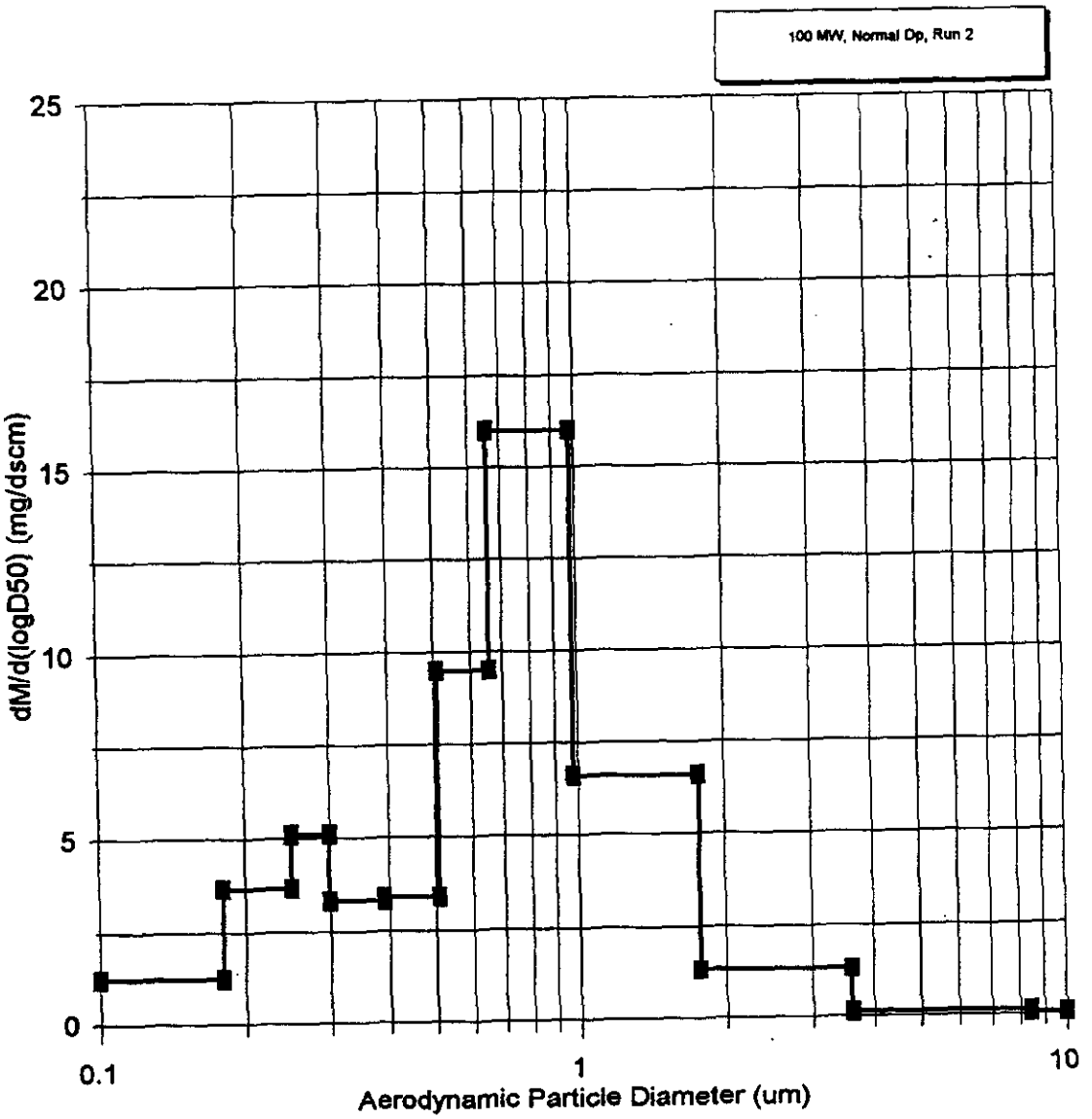

Differential Size Distribution
Plant Yates, Stack

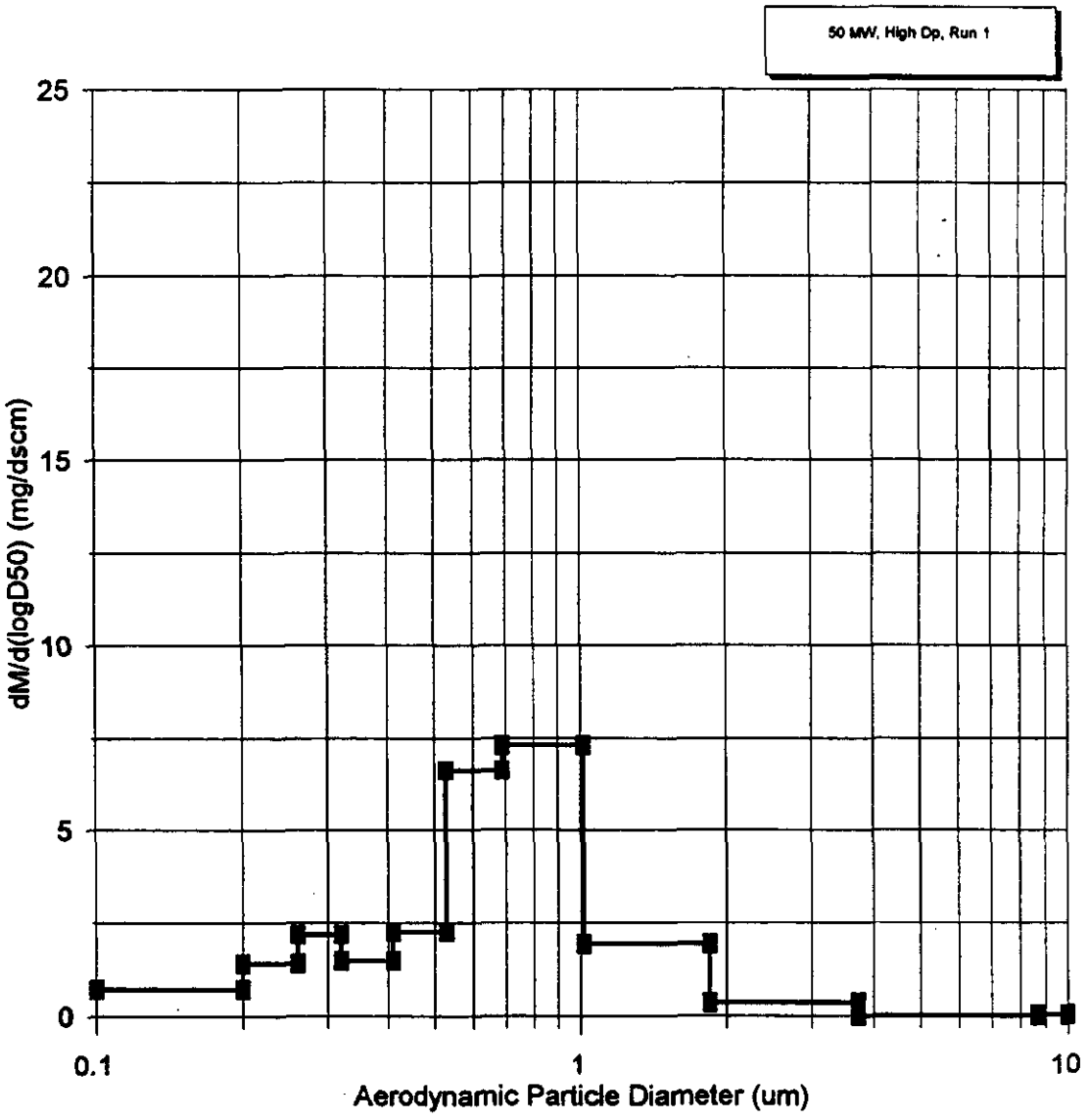

Differential Size Distribution
Plant Yates, Stack

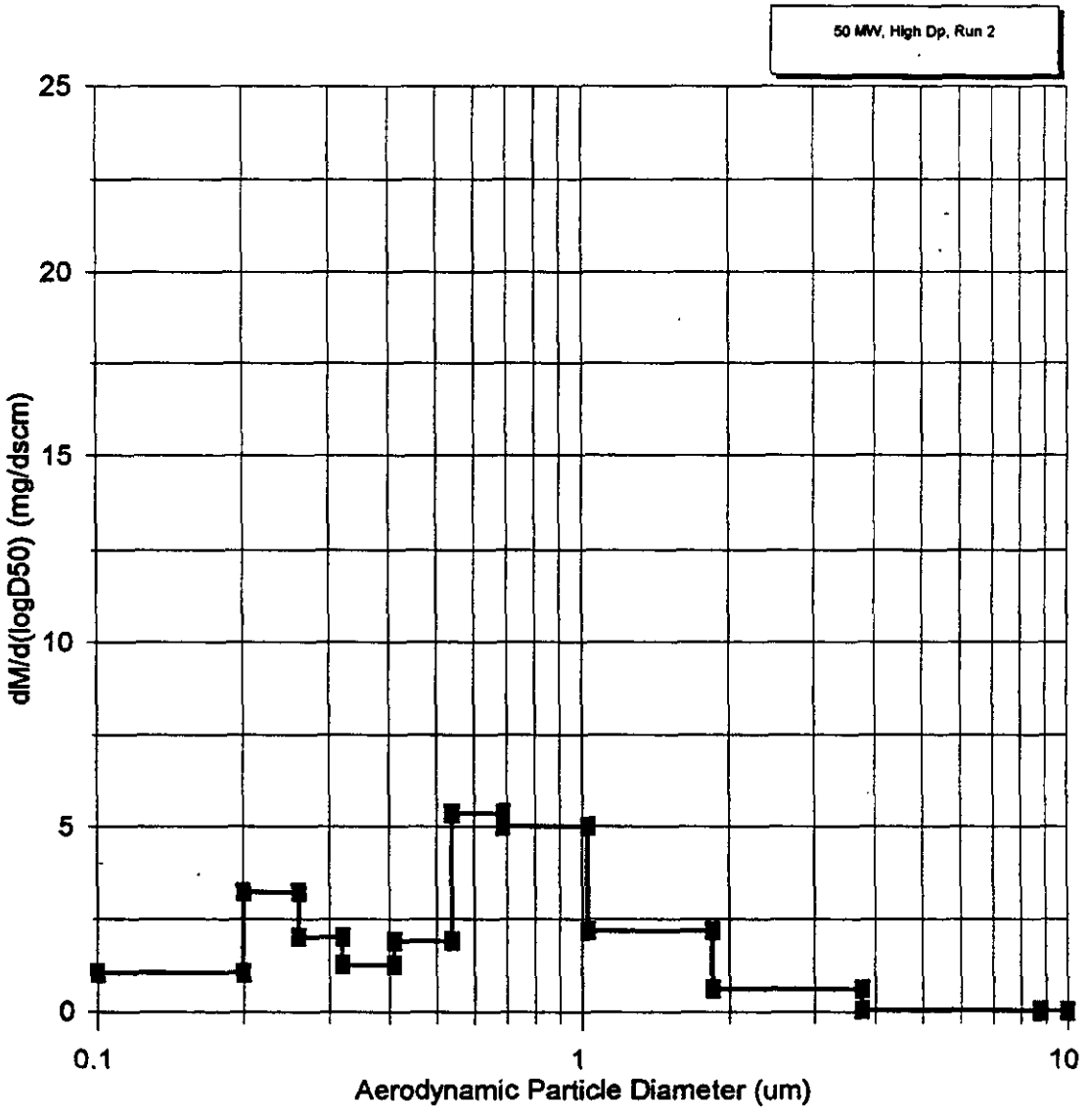

Differential Size Distribution
Plant Yates, Stack

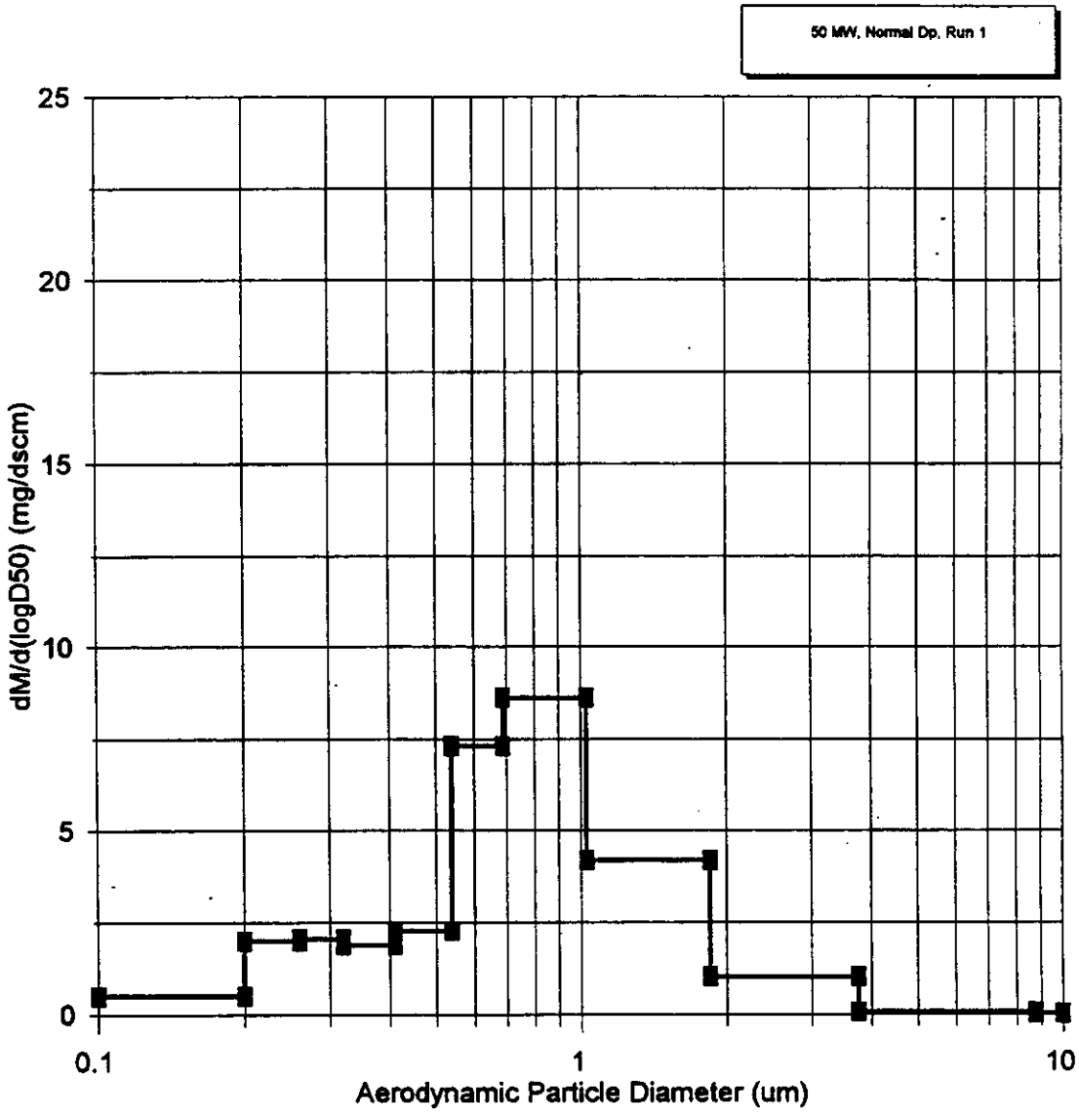

Differential Size Distribution
Plant Yates, Stack